2-10-2017 12:00 AM

Cu-Pd mineralization and exploration geochemistry of the Eastern Gabbro, Coldwell Alkaline Complex, ON, Canada

Yonghua Cao, *The University of Western Ontario*

Supervisor: Robert Linnen, *The University of Western Ontario*

A thesis submitted in partial fulfillment of the requirements for the Doctor of Philosophy degree in Geology

Abstract

The Eastern Gabbro forms the northern and eastern margin of the Coldwell Alkaline Complex. It contains three rock series: the barren meta-basalt, the Layered Series, and the Marathon Series which hosts all known PGE mineralization. The Marathon Series can be distinguished from other Series using the combination of portable X-ray fluorescence (pXRF) and benchtop scanning electron microscope (bSEM). Whole-rock Ba, Mg# (molar Mg/(Mg+Fe)*100), Zr and V/Ti values acquired from pXRF, and Mg#s of olivine and clinopyroxene, and anorthite content (molar Ca/(Ca+Na)*100) of plagioclase acquired from bSEM-EDS are key parameters. The Layered Series generally contains higher Ba and lower V/Ti than the Marathon Series and presents relatively smooth normal and reverse differentiation trends, whereas the Marathon Series exhibits strong compositional changes over short distances.

Reverse and normal lithogeochemical and mineral chemical evolution are observed for the Layered Series at Four Dams and Area 41. Olivine-clinopyroxene Fe/Mg exchange disequilibrium is also observed, and is interpreted to reflect crystallization in an open dynamic system. Geochemical modeling shows that the Layered Series magma is more evolved than the Coubran basalts, but the former contains lower Pd+Pt contents than the latter. Cu-rich & PGE-poor mineralization is also recognized in the Layered Series at Four Dams. This is interpreted to reflect an early sulfide saturation of the Layered Series.

Area 41 is a newly discovered zone of mineralization at the northern edge of the Eastern Gabbro. Three types of mineralization are identified. Type 1 is Cu-rich but PGE-poor mineralization. Type 2 contains PGE mineralization and has mantle-like Cu/Pd ratios, suggesting that it likely formed in a relatively closed system, similar to the Main zone mineralization at the Marathon deposit. Type 3 mineralization is the most PGE-enriched and has low Cu/Pd ratios. This, together with average S/Se

ratios of 1200 is evidence of S loss, which suggests that it formed by multi-stage dissolution upgrading, similar to the W-horizon mineralization at the Marathon deposit. 3D modeling of the igneous stratigraphy and mineralization indicate that Area 41 is a magma conduit, similar to the Marathon deposit. Thus, the Coldwell may also contain additional conduit-related mineralization.

Key word: Coldwell Alkaline Complex, Eastern Gabbro, Cu-Pd mineralization, pXRF, benchtop SEM

Co-Authorship

This thesis consists of six chapters, four of which are in manuscript format. Chapter 3 has been published by Geochemistry: Exploration, Environment, Analysis. Chapters 4, 5, and 6 have yet to be submitted. In each of these manuscripts the thesis advisor R.L. Linnen is the second author. His role in the preparation of these manuscripts consisted of organization of research themes, supply of insightful suggestions and critical evaluations, and discussion of the data and my conclusions. Dr. D.J. Good and I.M. Samson are my thesis committee members, who contributed to the development of research questions and editing, as well as critical evaluation of each manuscript within this thesis. They are listed as the third and forth author, respectively, on any subsequent publications originating from this thesis. R. Epstein was listed as the fifth author in the manuscript of Chapter 3. As a local geologist working on the Coldwell Alkaline Complex, her role in preparation of this chapter included help with rock identification in the field, and critical evaluation pertaining to the geological interpretation part proposed in this manuscript. I collected all of the powders and rock samples used in my thesis during field work in 2013 and 2014, except where noted. Thin section petrography and mineral chemical results including those from benchtop SEM-EDS and electron microprobe were conducted by me. Most whole-rock major and trace element abundances were determined at ALS mineral divisions at Vancouver and Thunder Bay. Additional whole-rock exploration assay data were provided by Stillwater Canada Inc.

Acknowledgements

I would like to express my sincere appreciation to my supervisor, Dr. Robert Linnen. This project would not have been possible without his scientific and financial support and immense knowledge and guidance in my research and writing. My sincere appreciation also goes out to Dr. David Good, who introduced me the Coldwell Alkaline Complex and taught me a lot of knowledges that helped this thesis greatly, without his help this thesis would take way longer. This project was funded by a NSERC grant of Dr. Iain Samson from Windsor, who also acts as my thesis committee member and offers me many insightful suggestions during the course of this thesis study, this deserves a great appreciation. It was great to work with such a dedicated team and I benefited greatly from the variety of backgrounds and specialties each of them possesses. China Scholarship Council (CSC) provided me a funding that covered my 4-year living stipends at Western, which is appreciated as well.

I would like to thank Stillwater Canada Inc. and John McBride for providing me the fieldwork opportunities for two summers, allowing me to gain further experience in exploration geology in addition to gathering samples for this project. I want to thank Rachel Epstein, without her help I am not sure if I would have been able to distinguish between all the gray rocks in Marathon. My thanks also go to Matthew Brzozowski, Ryan Ruthart, and Katrina McLean for assistances during the field work.

I am thankful to Dr. Charles Wu who taught me the principle of XRF technique and trained me how to operate the pXRF instrument at the very beginning of this thesis. I also would like to express my thanks to Marc Beauchamp for assistances of electron microprobe analyses, and to my lab mates Alysha McNeil and Abdullah Aseri for the help and countless discussions when working in the lab. The pXRF

and benchtop SEM-related work received many supports from the Elemental Controls Ltd. and JEOL, both are thanked here.

I would like to extend my gratitude to my parents and sister for their constant love, support, and encouragement. Last, but not least, I want to express my deepest acknowledgement to my dear wife, Xiaolei Liu, for her extreme patience and encouragement during this long time of thesis study.

Table of contents

List of Tables

Table 6-9. PGE assay, Cu/Pd, degree of alteration, and the observed PGM assemblages for representative thin sections.

List of Figures

List of Appendices

List of abbreviations

Ab	albite
Act	actinolite
Act	actinolite
Amph	amphibole
An	anorthite
Ap	apatite
AVG	average
BBC	Beaver Bay Complex
Bio/Bt	biotite
BMS	base metal sulfide
BSE	back-scattered electron
bSEM	benchtop scanning electron microscopy
Cal	calcite
Ccp	chalcopyrite
Chl	chlorite
Cl	chlorine
Cpx	clinopyroxene
EDS	energy dispersive spectroscopy
Elec	electrum
Hbl	hornblende
HFSE	high field strength element
Holl	hollingworthite
ICP-AES	inductively coupled plasma atomic emission spectroscopy
ICP-MS	inductively coupled plasma mass spectroscopy

Ilm	ilmenite
IPGE	iridium-group Platinum group elements
IR	infra-red
Isofe	isoferroplatinum
ISS	intermediate solid solution
K-fsp	K feldspar
Kotu	kotulskite
LILE	large ion lithophile elements
LOD	limit of detection
LREE	light rare earth elements
LS	Layered Series
LST	Lake Shore traps
MC	Mellen Intrusive Complex
Mer	mertierite-II
MIF	Michipicoten Island Formation
MPF	Mamainse Point Formation
MS	Marathon Series
MSS	monosulfide solid solution
Mt	magnetite
N/A	not available
nd	not determined
NVSG	North Shore Volcanic Group
OAM	oxide augite melatroctolite
OG	olivine gabbro
Ol	olivine
Or	orthoclase
OVG	Osler Group

PGE	platinum group elements
PGM	platinum group mineral
Plag/Pl	plagioclase
PLV	Portage Lack Volcanics
PM	primitive mantle
PMG	Powder Mill Group
Pn	pentlandite
Po	pyrrhotite
ppb	parts per billion
PPGE	palladium-group Platinum group elements
ppm	parts per million
PRI	Pigeon River Intrusion
pXRF	portable XRF
Py	pyrite
RD	relative difference
REE	rare earth elements
SCSS	sulfide content at sulfide saturation
SD	standard deviation
SDD	silicon drift detector
Ska	skaergaardite
Sp	sphalerite
Spe	sperrylite
Stil	stillwaterite
Tetra	tetraferroplatinum
WDS	wavelength-dispersive spectrometer
XRF	x-ray fluorescence

Chapter 1
Introduction

1.1 General introduction

The platinum group elements (PGE: Pt, Pd, Ru, Rh, Os, and Ir) are valuable and important in modern society due to their scarcity and use in technological applications. Their stable electrical properties, chemical resistivity, high melting point, as well as other unique physical and chemical prosperities make them ideal for jewelry and indispensable to modern technology and industry. Generally, the uses of PGE (particularly for Pd and Pt) are focused in autocatalyst, electronics, and jewellery, with relatively minor contribution in investment, glass, chemical, petroleum, and other (British Geological Survey Platinum, 2009, www.bgs.ac.uk). Over the last decade, the growing demand for Pt and Pd in industry, e.g., catalytic converters used for cars, led to the dramatic increase in the prices of PGE, from around US$400 per oz for Pt in the 1900's to US$2276 per oz for Pt by March, 2008 (British Geological Survey Platinum, 2009, www.bgs.ac.uk). The increases in prices in turn resulted in a worldwide PGE exploration boom. However, by far, the majority of the worlds supply of PGE is extracted from a few deposits within the Bushveld Complex of South Africa, with smaller contributions from the Stillwater Complex of the United States of America, and the Lac des Iles deposit of Canada, etc. (Maier et al., 2003; Fig.1-1). The question of whether other significant PGE deposits will be found in traditional PGE exploration settings has been increasingly asked by people from both industry and academia.

To aid in the search for other deposits, it is important to understand the processes involved in their deposition. How to explore for PGE in a more efficient and economic manner is another challenge that the mineral exploration industry is facing. The Coldwell Alkaline Complex is an excellent location to investigate mineralization processes and exploration protocols because: 1) the complex hosts several zones of PGE-enriched mineralization, notably the Marathon Cu-PGE

deposit; 2) the geology of the Coldwell Alkaline Complex is relatively well understood; 3) some geochemical exploration tools for the Coldwell Alkaline Complex have been developed (e.g., Good et al., 2015); 4) there is a large database consisting of over 40,000 assays from over 750 drill holes available (Good et al., 2015) for testing hypotheses and generating interpretations; and, 5) the igneous rocks of the complex are relatively pristine and undeformed, offering a good opportunity to study the magmatic process and associated mineralization. There are three main questions that will be addressed in this thesis.

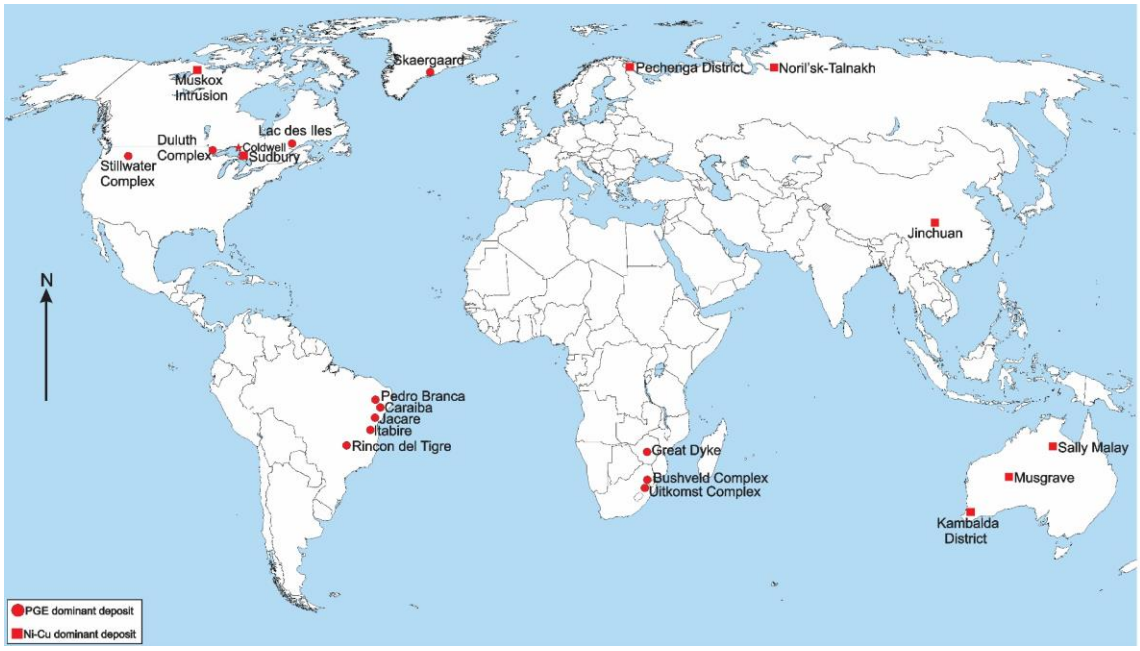

Figure 1-1. Global distribution of major magmatic platinum group elements sulfide deposits, modified after British Geological Survey (2009).

Problem I: One of the key components to mineral exploration at the Coldwell Alkaline Complex is to distinguish between the different series of gabbros because only the Marathon Series is known to host PGE mineralization; whereas other series (e.g., the meta-basalt and the Layered Series) units lack PGE mineralization. However, in the field it is difficult to distinguish between the different series of gabbro units at the Coldwell Alkaline Complex. Particularly, the oxide augite melatroctolite and oxide melatroctolite are petrographically nearly identical, but

only the oxide melatroctolite belongs to the Marathon Series, and is host to some PGE mineralization. The distribution of the different series gabbro units is further complicated by block faults. Using lab-based analyses, Good et al. (2015) demonstrated that different igneous series units are geochemically distinctive, indicating geochemistry is a reliable tool to help distinguish the Marathon Series from other igneous series units. The geochemistry of samples traditionally determined by laboratory-based analyses involves a time delay and a relatively high cost and are therefore not suitable for decision-making in the field. Therefore, there is a need to establish some geochemical methods that can be used directly in the field to distinguish the three series units and help mineral exploration.

Problem II: The Layered Series constitutes the largest part of the Eastern Gabbro of the Coldwell Alkaline Complex, but it has received little scientific scrutiny due to the lack of PGE mineralization in this series. Understanding the characteristics and origin of the Layered Series is significant from at least three perspectives.

First, the PGE-barren nature of the Layered Series at this complex is in contrast to other PGE bearing stratiform or stratabound reefs within layered mafic-ultramafic intrusions, e.g., the Merensky Reef, UG2 chromite of the Bushveld Complex, South Africa (Armitage et al., 2002), the JM reef of the Stillwater Complex, Montana (Todd et al., 1982), etc. It is thus meaningful to investigate why the Layered Series at the Coldwell does not contain PGE mineralization. To answer this question, the genesis of the Layered Series must first be understood.

Second, knowing the characteristics and the origin of this intrusion may help in the interpretation of the early magmatic history of the Coldwell Alkaline Complex. It is, however, not clear what magma chamber processes that generated the Layered Series and their revelances to PGE mineralization. Particularly, Shaw (1997) observed both the normal and reverse evolution of the Layered Series gabbro at the Bamoos and Highway traverses of the Eastern Gabbro, but did not provide a

satisfactory explanation. To understand the genesis of the Layered Series, the origin of the reverse evolution must be explained.

Third, the PGE mineralization related Marathon Series is younger than the Layered Series, but both are petrographically similar and spatially close within the complex. However, it is not clear whether or how the Layered Series and the Marathon Series are genetically related, e.g., the same source, the same parental magma with different modifications, etc.

Problem III: It is unclear whether there is a general exploration model applicable for the whole Coldwell Alkaline Complex. According to previous studies, e.g., Ruthart (2013) and Good et al. (2015), mineralization at the Marathon deposit (the largest deposit within the Coldwell Alkaline Complex) can be explained by a conduit-type setting. It is, however, unclear mineralization elsewhere within the Eastern Gabbro is also conduit related. But knowing mineralization is conduit-related is meaningful because it predicts that mineralization can occur at different stratigraphic horizons and also increases the possibility for extreme PGE concentrations as a result of upgrading by a 'multistage dissolution upgrading' process (Kerr and Leitch, 2005). To investigate this, a relatively newly discovered Cu-Pd zone called Area 41, located at the north edge of the Eastern Gabbro, was examined in Chapter 6, with focuses on its igneous stratigraphy and mineralization processes. All the two perspectives at Area 41 were compared to those at the Marathon deposit to evaluate whether a conduit-type setting is applicable for PGE mineralization in the whole Coldwell Alkaline Complex.

1.2 A review of PGE mineralization

Platinum group elements can be classified into two groups according to their different physical and chemical activities and preferred hosts in natural systems (Naldrett, 1999). The two groups are the iridium-group platinum-group elements (IPGEs: Ru, Ir, Os) and the palladium-group platinum-group elements (PPGEs: Pt, Pd, Rh). All these elements are highly siderophile elements, and also behave as

highly chalcophile elements in base metal sulfide (BMS) liquids. Therefore, they are commonly found in association with magmatic BMS deposits, and are hosted by minerals such as chalcopyrite, pentlandite, bornite, pyrrhotite, which crystallized from the sulfide liquid (Barnes and Ripley, 2016).

Magmatic sulfide deposits can be broadly subdivided into two groups according to metal proportions: Ni-Cu deposits with PGE as a by-product and PGE dominant deposit with Ni and Cu as possible by-products (Li et al., 2001). Owing to the different geochemical behaviours of Ni and Cu versus PGE in igneous processes, particularly their different partition coefficients into segregated sulphides and other silicate phases, the formation of these two groups of magmatic sulfide deposits require some different mechanisms. Cu-Ni-(PGE) deposits are rich in sulfide minerals and require a large tonnage of ore to be economic, whereas the PGE-dominant deposits contain much less sulfide minerals (Naldrett, 1999). It is beyond the scope of this review to fully investigate the differences between these two groups of magmatic sulfide deposits, more details can be found in Li et al. (2001), Cawthorn (2005), and Maier et al. (2011). This chapter focuses on PGE-dominant deposits, in particular the geochemistry of PGE, origins of PGE mineralization, types of PGE deposits and their host units.

1.2.1 Geochemical behaviour of PGE elements

The PGE (plus gold) are often called noble elements because the related metals are resistant to corrosion and oxidation in moist air. These elements also tend to be valuable due to their rarity in the Earth's crust, e.g., 0.4 ppb for Pt (Mungall and Naldrett, 2008). PGE are also chalcophile, which means that they are preferentially enriched in sulfide liquids relative to silicate melts. This is particularly true for PPGE which are normally associated with magmatic sulfide minerals of Fe, Ni and Cu, whereas IPGE may also commonly associated with chromite, as native metal alloys or sulfide minerals as shown by experimental work of Capobianco et al. (1994), Righter et al. (2004), and Brenan et al. (2012). The PGE are also transition

elements that have variable valence states, ranging from 0 to +8. Thus, their chemistry is complex, and they can be bonded with various elements to form different kinds of PGM composites, e.g., oxide minerals, sulfide minerals, etc. The PGE (plus gold) have similar and regularly varying chemical characters. For example, the order of decreasing boiling and melting temperatures of these elements is Os, Ir, Ru, Rh, Pt, Pd, and Au (Barnes et al., 1985). This is also the order of decreasing compatibility in magma systems, which is commonly used when plotting chondrite-normalized abundance of PGE elements (plus gold) analogous to rare earth elements, but with the latter ordered by atomic number.

Of particular interest regarding geochemical behaviour of the PGE elements is their partitioning into sulfide liquids. But before illustrating this, it is necessary to describe the evolution of sulfide liquid because different groups of the PGE elements behave differently at different evolutionary stages of the sulfide liquid. Experimental work (e.g., Kullerud et al. 1969; Dutrizac, 1976; Ebel and Naldrett, 1997; Sinyakova and Kosyakov, 2009) has shown that following the segregation of sulfide liquids from a silicate melt at temperatures of around 1200 ℃, the first phase to crystallize is an Fe-rich monosulfide solid solution (MSS) at around 1000℃. The remaining sulfide liquid is Cu-rich, which crystallizes intermediate solid solution (ISS) when the temperature drops down significantly (<900 ℃). As temperatures drops down to below 650 ℃, the MSS recrystallizes to Fe-rich sulfide minerals such as pyrrhotite and pentlandite whereas the ISS recrystallizes to Cu-rich sulfide minerals such as chalcopyrite (Holwell and McDonald, 2010).

Experimental data of Fleet et al. (1993), Li et al. (1996), Barnes et al. (1997), Mungall et al. (2005), Liu and Brenan (2015), and Brenan et al. (2016) suggest that in sulfur-rich, alloy-poor systems the IPGE and Rh partition into MSS, whereas Pt and Pd will partition into Cu-rich residual liquids after MSS crystallization. Liu and Brenan (2015) suggest that there is a significant effect of oxygen on increasing the activity for IPGE and Rh partitioning into MSS. As a result, IPGE and Rh elements

are preferentially hosted by phases that crystallized from MSS such as pyrrhotite and pentlandite. But for Pt and Pd elements, experimental results of Peregoedova (1998) suggested that they were incompatible with ISS, thus the crystallization phases of ISS such as chalcopyrite would not be favorable hosts to these two elements. Barnes and Ripley (2016) compared PGE contents of the base metal sulfide minerals such as pyrrhotite, pentlandite, chalcopyrite, and pyrite, and found that pentlandite has the highest PGE and the concentrations of all of the PGE are low in chalcopyrite. Rather, work by Helmy et al. (2007) suggested that the Cu-rich residual melt remained liquid after ISS had crystallized, which was transformed into an immiscible semimetal-rich melt where Pd and Pt were concentrated. The semimetal-rich liquid may be enriched in Te, Bi, As, and Sb, thus Pt and Pd are easily combined with these elements to form discrete platinum group minerals (PGM) after the crystallization of the semimetal-rich sulfide liquid. However, it should be noted that at high Pd: semimetal ratios, some excess Pd can not be accommodated by the semimetal-rich sulfide liquid and may partition into MSS (Helmy et al., 2007). This explains the presence of Pd in pentlandite in some ores. However, the mechanism and temperature controls on this are still poorly understood. Nevertheless, the semimetals appear to be the most fundamental factor controlling the mineralogical characteristics of magmatic sulfide-hosted Pt and Pd ores. Barnes and Ripley (2016) suggested that since the major elements of magmatic sulfides have been consumed there is very little semimetal-rich sulfide liquid remaining, thus Pd and Pt may end up being enriched in the ISS cumulate (Cu-rich ore). The schematic cartoon of the partition of PGE elements into different stages of magmatic sulfide liquids is shown in Figure 1-2.

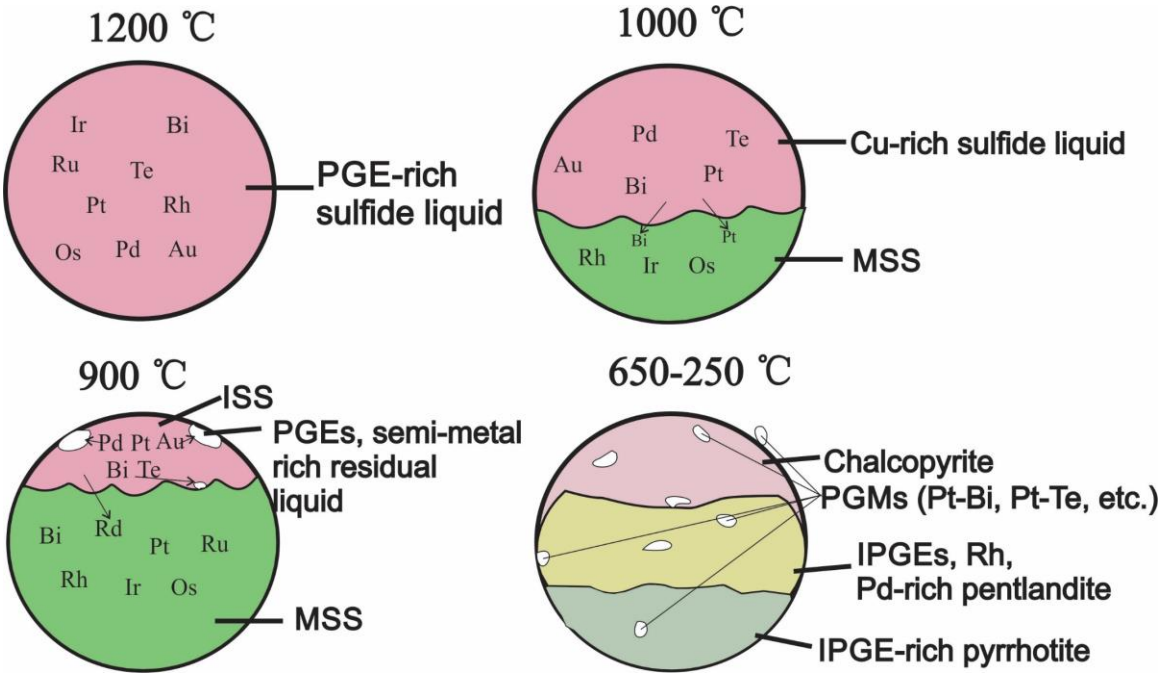

Figure 1-2. Schematic cartoon of a fractionating, platinum group element-rich sulfide droplet, see text for full interpretation, modified after Holwell and McDonald (2010).

1.2.2 Origin of PGE mineralization

Two main genetic models for PGE deposits have been proposed: primary magmatic (also known as orthomagmatic) or concentration of PGE by late fluids. The former model is favored by most authors, who interpret that PGE deposits as having formed by high temperature magmatic processes in mafic-ultramafic igneous rocks, whereas the late fluids are interpreted to be relatively minor significant in terms of PGE mineralization (Naldrett et al., 2008; Maier, 2005).

There are at least three requirements for formation of PGE ores by the primary magmatic sulfide model. The first requirement is for the PGE fertile magma. Although there are several ways in which PGE fertile magmas may be generated, the most generally accepted way that is proposed to be applicable to most known PGE deposits is formation of intraplate picritic magmas from a high degree of partial melting of the mantle (Arndt et al, 2005; Barnes and Lightfoot, 2005). This is because sulfide minerals probably are the main host to PGE elements in the mantle

(see Barnes and Maier, 1999, and references therein) owing to the high partition coefficients of PGE into sulfide liquids (~ 10000 for Pd and Pt, Barnes and Maier, 1999), and only large degrees of mantle melting, e.g., ~ 25% depending on the depth of melting, is ready to dissolve all the sulfides in their mantle source regions (Maier, 2005). However, Botcharnikov et al. (2011) suggest that at least gold-rich magmas can be generated in mantle systems that are sulfide-saturated, as long as they are relatively oxidized.

The next requirement is the saturation of sulfide melt in a fertile magma, which occurs after the magma has ascended to the upper crust. The early sulfide segregation prior to the ascent of PGE fertile magma will inevitably deplete the remaining magma in PGE, thus is considered not favorable for formation of PGE deposits. However, it should be noted that some studies (e.g., Blaine et al., 2011) suggest that it is possible that Pt metal saturation may occur before sulfide saturation if the melt exsolves a chlorine-rich fluid. Once sulfide melt saturation occurred when the magma has emplaced in the crust, PGE elements can be concentrated in the immiscible sulfide melt to form economic ores.

Following the work of Fincham and Richardson (1954) who discussed the solution of S in silicate melts in terms of reaction between base metal oxides and either S^{2-} or SO_4^{2-}, several well-constrained experimental studies have been undertaken to investigate the solubility of sulfur (S^{2-} or SO_4^{2-}) in the magma. When sulfur is present as S^{2-} in the magma, i.e., sulfide liquid, Shima and Naldrett (1995) have referred to this value as the S content at sulfide saturation, which is known as SCSS. Generally, there are four mechanisms that can provoke the sulfide melt saturation. The first mechanism is a large degree of magma fractionation. Since sulfide does enter any silicate phases, during fractionation the concentration of sulfide will progressively increase until reaching SCSS (Mungall and Naldrett, 2008). The second mechanism is the decrease in FeO contents by fractionation of Fe-rich minerals such as olivine, pyroxene, and magnetite. This will reduce the capacity for

the magma to carry dissolved sulfide (Haughton et al., 1974; Li and Ripley, 2005), which in turn triggers the sulfide saturation. The third mechanism is the contamination of the magma by sulfidic country rocks (Ripley, 1999; Lesher and Campbell, 1993). This process is believed to be a very feasible way to provoke sulfide saturation because: 1) country rocks may contain a high amount of sulfur, through the contamination extra S is introduced in the magma, thus triggering the sulfide saturation, 2) the contamination may introduce silica into the magma, decrease the temperature of magma, and increase oxygen fugacity of the magma, all of these will lower the SCSS of the magma (see Li and Naldrett, 1993; Li and Ripley, 2005), 3) the increasing oxygen fugacity by contamination may in turn lead to the fractionation of magnetite and lowering of the FeO content and thus the SCSS of the magma (Li and Ripley, 2005). It is, however, should be noted that this contamination process normally triggers the immiscibility of large amounts of sulfide melts, which is more applicable to formation of Cu-Ni-(PGE) deposits such as Noril'sk of Siberia in Russia and Jinchuan in China (Naldrett, 1997). By contrast, the formation of PGE deposits by such means requires a delicate balance to achieve the right amount (normally a small amount) of excess sulfide in the resulting mixture (Mungall and Naldrett, 2008), thus this process is not favorable for formation of PGE deposits because large amounts of sulfide liquid mean the R-factor (weight fraction of silicate melt/ weight fraction of sulfide liquid) would be small, leading to low PGE concentrations in sulfide liquids. The fourth mechanism is the mixing of compositionally contrasting, sulfur undersaturated magmas. This is illustrated by the work of Li et al. (2001) and Cawthorn (2002) who suggested that mixing of a siliceous melt and a liquid of olivine tholeiite composition can provoke sulfide liquids saturation.

Once the magma became sulfur saturation and immiscible sulfide liquids have formed by mechanisms mentioned above, they must be collected and concentrated in order to produce an economic ore deposit that can be mined, which is the third

requirement for formation of PGE deposits. Normally, the dense sulfide melt droplets segregate to the base of the magma chamber and crystallize to form a sulfide minerals- enriched zone where the highly chalcophile PGE are concentrated. If the immiscible sulfide droplets formed from the magma flowing in a conduit, they may be suspended in the melt, particularly when there is no change in the flowing regime, e.g., the widening of the conduit (Mungall and Naldrett, 2008). The suspended sulfide droplets may react with the later pulses of sulfur undersaturated magma intrusions, and may undergo a 'sulfide dissolution upgrading' process where the PGE tenor of sulfides is progressively upgraded. This process has been successfully modelled by Kerr and Leitch (2005).

There are also numerous studies favoring a role of hydrothermal fluids on PGE mineralization, e.g., hydrothermal veins at Kambalda (Lesher and Keays, 1984), Stillwater J-M reef within the Stillwater Complex in the USA (Boudreau et al., 1986), Sudbury footwall ores at Canada (Farrow and Watkinson, 1999), the Marathon deposit of the Coldwell Alkaline Complex at Canada (Watkinson and Jones, 1996), and footwall ore of Duluth Complex at USA (Benko et al., 2015). Experimental studies of Hsu et al. (1991), Fleet and Wu (1993), and Baker et al. (2001) confirmed that Pd and Pt are highly soluble in chlorine-rich fluids. Blaine et al. (2011) experimentally determined the effect of chlorine on Pt solubility in haplobasaltic melt and found that chlorine-rich fluids can be highly efficient at enriching and transporting Pt in mafic magmatic-hydrothermal ore-forming systems at moderate oxygen fugacities. Hanley et al. (2005) investigated the solubility of platinum and gold in NaCl brines at 1.5 kar and 600-800℃, and proposed that the solubility would be enhanced with increasing fluid salinity. In addition, some studies also suggest that Pt and Pd sulfide minerals are also soluble in aqueous H_2S-rich fluids, but to a lower extent than in chlorine-rich fluids. For example, Pan and Wood (1994) experimentally determined solubility of Pd and Pt sulfide minerals in H_2S-rich aqueous fluids (200-350℃) to be 4-800 ppb for Pt and 1-400 ppb for Pd.

Gammons and Bloom (1993) suggested that the solubility of Pd and Pt sulfide minerals in H_2S-rich aqueous fluids increase with increase in $\sum S^{2-}$ and decrease with increase in temperature particularly between 200 and 300°C.

In this regard, it is plausible that the fluids partially dissolve BMS, and as a consequence, Pd and Pt dissolve into the fluid, which finally precipitated when the physico-chemical conditions change (Barnes and Ripley, 2016). Such a process has been proposed by Mathez (1995) to explain the enrichment of PGE of Merensky Reef pyroxenites at the Bushveld Complex in South Africa, and also is adopted to explain the occurrences of PGE mineralization in faults and shear zones associated with the mafic-ultramafic intrusions (Maier, 2005). In some cases, fluids derived from cooling or metamorphism may result in a change of mineralogy of BMS and PGM. For example, Djon and Barnes (2012) found that pyrrhotite and pentlandite at Lac des Iles in Ontario of Canada were replaced by pyrite and millerite under the influence of fluids, and as a consequence the pyrite was enriched in IPGE and Rh that were initially present in pyrrhotite. Hutchinson and Kinnaird (2005) found that at Platinova reef within the Skaergaard intrusion of Greenland, the PGM assemblage in the altered ores is enriched in arsenic and antimony. Although the evidence for the hydrothermal fluids-related controls on PGE mineralization is well documented by some studies, many researchers have voiced scepticism whether this mechanism could be responsible for formation of most deposits, and many believed the role of hydrothermal fluids on PGE mineralization is only of minor significance for most deposits (e.g., Maier and Barnes, 1999).

There are also some studies proposing a vapor refinement model (also called hydromagmatic model) for the formation of Pt deposits, e.g., the J-M reef of the Stillwater Complex at USA (Boudreau and Meurer, 1999; Boudreau, 2016), Lower and Critical Zones of the Bushveld Complex at South Africa (Willmore et al., 2000), and the Marathon Cu-Pd deposit of the Coldwell Alkaline Complex at Canada (Dahl et al., 2001; Barrie et al., 2002; Samson et al., 2008). In this model, mineralization

is introduced by the interaction between chlorine-rich fluid and silicate melt, e.g., the upward migrating chlorine-rich fluid re-dissolves into the volatile-undersaturated melt. Blaine et al. (2011) suggest that this process possibly would lead to the formation of PGE-bearing phases (e.g., micronuggets) and could allow the bulk PGE content of the magma to increase above the limits imposed by the PGE solubility.

1.2.3 Classification of PGE deposits

The majority of the world's PGE ore deposits are magmatic in origin and occur within mafic and ultramafic portions of large tholeiitic intrusions of late Archean to early Proterozoic age (Maier, 2005). As mentioned earlier, the PGE deposits can be first subdivided into two main types according to whether Ni, Cu, versus PGE are the main economic commodities, they are Ni-Cu-(PGE) deposits and PGE-dominant deposits. More detailed classification of Ni-Cu-(PGE) deposits are proposed by Sutphin and Page (1986), Keays and Lightfoot (2002), Naldrett (2004), and Eckstrand and Hulbert (2007). This chapter only focuses on PGE-dominant deposits. There are two principle subtypes of magmatic PGE-dominant deposits: stratiform or reef deposit and contact deposits (Eckstrand and Hulbert, 2007; Barnes and Ripley, 2016). In addition, depending on the relative roles of magmatism and fluids on PGE mineralization, another type of PGE deposit is late magmatic and/or hydrothermal fluid related (Maier, 2005).

The stratiform or reef type deposits occur in the well layered mafic/ultramafic intrusions, and their ore bodies take the form of laterally extensive layers. Examples of this type of deposits include the UG2 and the Merensky reef of the Bushveld Complex in South Africa, J-M reef of the Stillwater Complex of the USA, and the Main Sulfide Zone of the Great Dyke at Zimbabwe. Various mafic to ultramafic host rocks are generally present for reefs at these different settings. For example, the UG2 reef is hosted by massive chromitite with interstitial orthopyroxene and plagioclase (Barnes and Maier, 2002), the Merensky reef is hosted by rock types

ranging from chromitite, through melanorite, to anorthosite (Barnes and Maier, 2002), the J-M reef is hosted mainly by troctolite, olivine gabbronorite and anorthosite (Barnes and Naldrett, 1985), and host rocks for the Main Sulfide Zone comprise orthopyroxenite or bronzitite (Wilson and Brown, 2005).

The contact-type deposits (also called magmatic breccia type in Eckstrand and Hulbert, 2007) refer to those with ore bodies in variable width. The ore bodies are located at the margins of intrusions, and are in the form of disseminated BMS. Examples of this type of deposits include the Platreef of the Bushveld Complex in South Africa and Lac des Iles deposit in Canada. Note that Platreef, although termed a reef type deposit, essentially belongs to the contact type because it is a relatively wide zone (50-100 m thick) with variable distribution of PGE across the zone (Barnes and Ripley, 2016). Host units of this type deposits vary from pyroxenite to gabbronorite, with minor anorthosite and peridotite (Maier et al., 2008; McDonald and Holwell, 2011).

1.3 Geology of the Coldwell Alkaline Complex

The Coldwell Alkaline Complex is the largest alkaline intrusion in North America. It is associated with the North American Midcontinent Rift (Fig. 1-3) and is one of the largest known intrusions associated with continental rifts in the world (Heaman and Machado, 1992). It intruded the Archean Shreiber-Hemlo greenstone belt along the northern edge of the Midcontinent rift at 1108-1094 Ma, which marked the beginning of the early stage of magmatism related to the Midcontinent rift system (Walker et al., 1993; Heaman et al., 2007; Good et al., 2015). Petrologic and field studies conducted by Puskas (1970), Mitchell and Platt (1978, 1982), Mitchell et al. (1993), and Shaw (1997) recognized three superimposed intrusive centers constituting this complex, from east to west, they are center I, center II, and center III (Fig. 1-4). Center I is composed of syenite, syenodiorite, layered ferroaugite-amphibole syenite, and an outer rim of complicated gabbroic and ultramafic rock units known as the Eastern Gabbro (Fig. 1-4). Most PGE mineralization at the

Coldwell Alkaline Complex is hosted by the Eastern Gabbro. Center II comprises nepheline-bearing alkali biotite gabbro, hastingsite-bearing miaskitic nepheline syenite, and minor lamprophyres and tinguaite dikes. Center III consists of magnesio-hornblendesyenite, ferro-edenite syenite, quartz syenite, and minor granites (Mitchell and Platt, 1978; Mitchell et al., 1991). Paleomagnetic work conducted by Ashley and Kerns (2012) suggests that Centers I and III are the same age but both are older than Center II. It was proposed by Mitchell and Platt (1977, 1978) and Walker et al. (1993) that the emplacement of most rock units in the Coldwell Alkaline Complex was controlled by the faulting during cauldron subsidence at a subvolcanic depth.

The Eastern Gabbro formed by multiple intrusions of basaltic magma with a subalkaline parentage into a partial ring dike structure that cut the Archean country rocks (Shaw, 1994, 1997). Good et al. (2015) identified nine major lithologies that are temporally related through crosscutting relationships. These nine lithologies can be categorized into three major distinctive Magmatic Series by their geochemical character, e.g., different Nb/Zr and Ce/Y ratios (Good et al., 2015). From oldest to youngest, the three magmatic series includes: the meta-basalt (equivalent to fine-grained gabbro in Good et al., 2015), the Layered Series, and the Marathon Series. The relative ages for these units were established from crosscutting relationships, particularly within the numerous units of igneous breccia (Good et al., 2015).

The meta-basalt occurs along the base of the Eastern Gabbro and comprises picritic basalt that underwent pyroxene-hornfels grade metamorphism (Good et al., 2015). It was crosscut by both the Layered Series and the Marathon Series as observed by Good et al. (2015) at the Marathon deposit. The Layered Series constitutes the bulk of the Eastern gabbro and is composed of massive to modally layered olivine gabbro, with a lesser amount of weakly layered oxide augite melatroctolite, and, less commonly, gabbroic anorthosite. Based on drill core logging, the Layered Series at Area 41, Four Dams, and the WD zone (locations are indicated in Fig. 1-4) was

crosscut by numerous thin Marathon Series intrusions. The Marathon Series is the youngest unit and comprises numerous small intrusions composed predominantly of ophitic gabbro, apatitic clinopyroxenite, oxide melatroctolite, as well as small volumes of augite troctolite and wehrlite (Good et al., 2015). Based on compositions and similar textures, the Marathon Series at Area 41, Four Dams, and the WD zone is similar to that at the Marathon deposit. It should be noted that at the Marathon deposit, the most significant Marathon Series rock is the Two Duck Lake gabbro, which is the main host to Cu-Pd mineralization at this deposit (Good et al., 2015). The Two Duck Lake gabbro has an ophitic texture and resembles the ophitic gabbro at Area 41, Four Dams, and the WD zone in terms of textures and geochemical characters (full details will be shown in Chapter 6).

1.4 PGE deposits at the Coldwell Alkaline Complex

There are various mafic to ultramafic Ni-Cu-PGE deposits associated at the margins of the Midcontinent Rift. Most of them contain disseminated-massive sulfide mineralization found within sheet-like gabbro to troctolite intrusions, or are associated with conduit-related smaller, early rift, mafic to ultramafic intrusions (Ripley, 2014). For example, the Partridge River and South Kawishiwi of the Duluth Complex (Ripley, 2014) are sheet-like intrusions that host the basal contact-type Cu-Ni-PGE mineralization. Current Lake deposit (Goodgame et al., 2010), the Eagle deposit (Schulz et al., 2010; Ding et al., 2012), and the Tamarack occurrence (Goldner, 2011) are the Ni-Cu-PGE conduit style mineralization. The Locations of these notable deposits are indicated on Figure 1-3. Another type of PGE-related deposit associated with the Midcontinent Rift is relatively low sulfide and PGE enrichment found as stratiform intervals in well-differentiated tholeiitic layered intrusions (Ripley, 2014). This type of deposits is volumetrically small within the Midcontinent rift system, and some are concentrated within the Coldwell Alkaline Complex, notably the Geordie Lake Cu-PGE deposit and the Marathon Cu-Pd deposit (Fig. 1-4). These two deposits will be reviewed in order to provide

geological context for mineralization at Area 41 (location is indicated in Fig. 1-4), which will be examined in chapter 5.

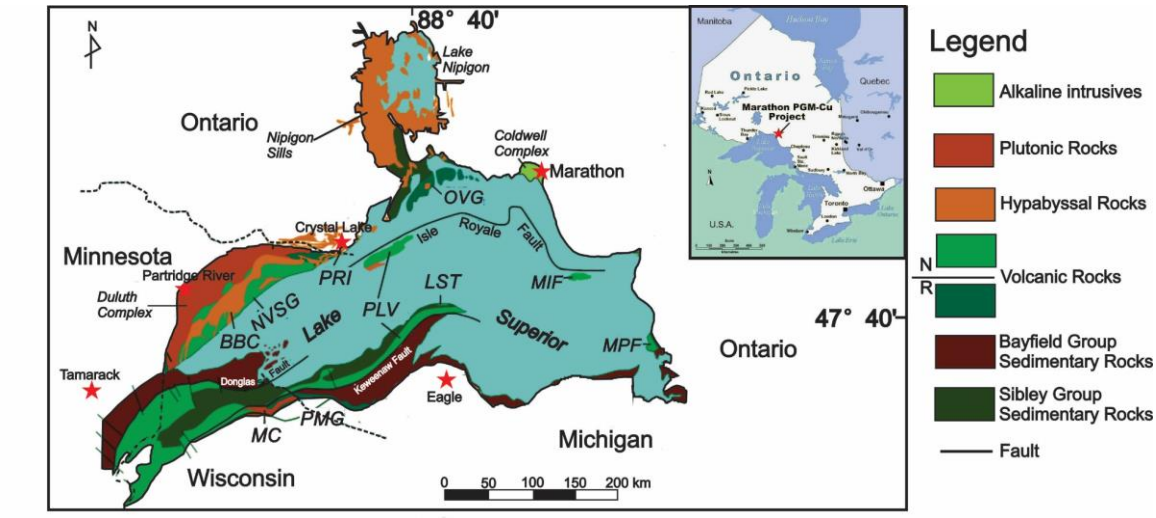

Figure 1-3. Regional map of the Midcontinent rift (modified after Miller and Nicholson, 2013). *BBC* Beaver Bay Complex, *NVSG* North Shore Volcanic Group, *PRI* Pigeon River Intrusion, *OVG* Osler Group, *MPF* Mamainse Point Formation, *MIF* Michipicoten Island Formation, *PLV* Portage Lake Volcanics, *LST* Lake Shore traps, *PMG* Powder Mill Group, *MC* Mellen Intrusive Complex. Notable deposits are indicated using red stars.

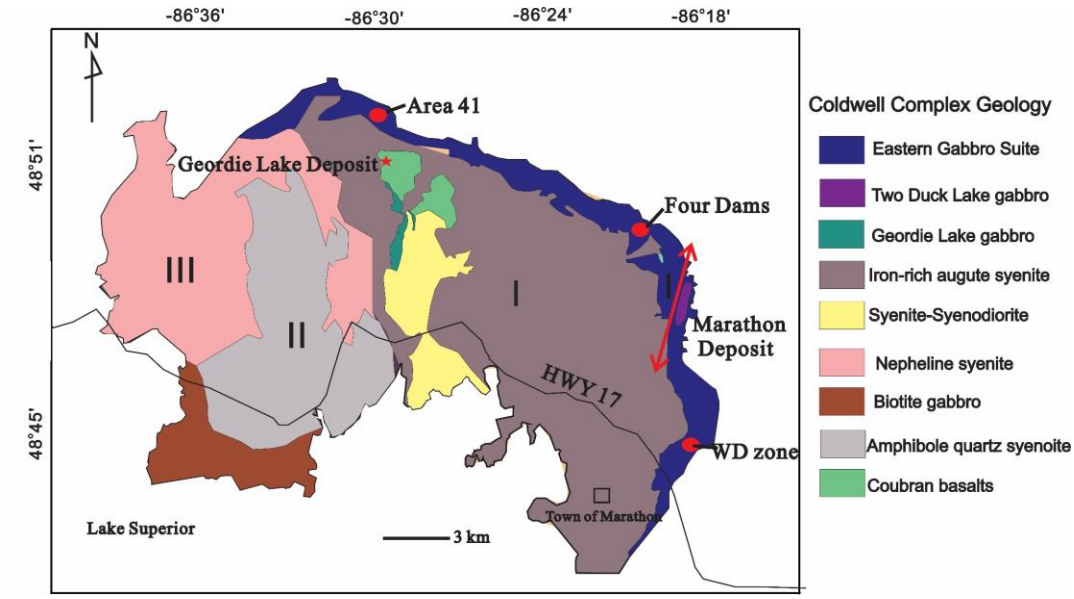

Figure 1-4. Geological map of the Coldwell Alkaline Complex, situated on the northern shore of Lake Superior. Locations of Area 41, Four Dams, and WD zone (these three areas are involved in this thesis study) are represented as three red dots. Locations of the Geordie Lake deposit and Marathon deposit are also indicated using a red star and a double-arrowed red line, respectively (Modified after Walker et al., 1993). The intrusive centers have been shown by Roman numerals (modified after Mulja and Mitchell, 1991).

1.4.1 Geordie Lake Cu-Pd deposit

The Geordie Lake gabbros and troctolites are small mafic, weakly layered, and elongate intrusions located in the central part of the Coldwell Alkaline Complex (Fig. 3). Mineralization in the Geordie Lake intrusion was discovered in 1960 when Ameranium Inc. explored for copper at this area. The subsequent drilling and exploration programs conducted by St. Joe Canada Inc, Gryphon Metals Corporation, Discovery PGM, Marathon PGM. The first resource estimate for the Geordie Lake Deposit by Discovery PGM was 24.4 million tonnes averaging 0.326 % Cu, 0.537 g/t Pd, 0.007 % Co, 0.011 % Ni, 0.030 g/t Pt, 2.52 g/t Ag and 0.04 g/t Au. An additional 5.4 million tonnes are considered inferred at an average grade of 0.36%Cu, 0.626 g/t Pd, 0.007% Co, 0.012% Ni, 0.04 g/t Pt, 3.04 g/t Ag and 0.05 g/t Au (Drennan and Fell, 2010).

Two types of gabbros were recognized at Geordie Lake by Good and Crocket (1994) and Meghji (2016): homogeneous and heterogeneous types, with only the latter contains abundant sulfide and Pd mineralization. Mulja and Mitchell (1991) also studied the petrography of sulfides and PGM at the Geordie Lake intrusion. Sulfide minerals within the Geordie Lake intrusion principally are disseminated chalcopyrite, with less amounts of bornite, pyrite, millerite, cobaltite, sphalerite, and galena. The PGM are dominantly palladium tellurides and arsenides, with rare Pt-PGM such as sperrylite.

Mulja and Mitchell (1991) found that tellurides and PGM were associated primarily with disseminated magmatic chalcopyrite, with rare cases in late-stage massive chalcopyrite. However, Good and Crocket (1994) found that disseminate sulfides and palladium minerals were spatially in close association with albite pods that they interpreted to represent pockets of fluid-rich residual magma. These different observations led to two different emplacement models proposed by the two studies. Mulja and Mitchell (1991) favored a magmatic origin for the Cu-PGE mineralization at the Geordie Lake deposit. They suggested that the mineralization

was associated with the segregation of a relatively evolved sulfide melt from an evolved tholeiitic magma. Factors that induced the sulfide melt segregation include the rapid cooling of the magma and the crystallization of olivine and magnetite. The crystallization of Ti-poor magnetite, tellurides, and PGM from the sulfide melt occurred at <550°C.

On the other hand, Good and Crocket (1994) found that the albite pods had higher abundances of Zr, Hf, Nb, Th, U, and the rare earth elements (REE) than the surrounding Geordie Lake gabbro, but inter-element ratios are similar between the two rock types. They interpreted the albite pods to be representative of pockets of fluid-enriched residual magma, and formed by a two-stage process, including the crystallization of hornblende and plagioclase from the residual magma (stage one) and a hydrous fluid separated from the residual magma and interacted with the plagioclase to form the albite (stage two). The close association of PGM and sulfides with the albite pods thus implies that the PGE mineralization formed from the same fluid with the albite pods, but at different times when the fluid underwent evolution and cooling processes.

Meghji (2016) recently examined the structure and control of Cu-PGE mineralization at the Geordie Lake deposit, and explored how the distribution of Cu-PGE mineralization varied by host lithology, and by various degrees of secondary alteration. He found that the Cu-PGE mineralization at the Geordie Lake deposit was spatially in close association with gabbro and troctolite that present weak to intense actinolite and albite alteration. The similar major element geochemistry between the altered and unaltered samples led Meghji (2016) to propose that sulfide deposition at the Geordie Lake deposit is magmatic, and the interaction with late stage magmatic fluid redistributed some mineralization.

1.4.2 Marathon Cu-Pd deposit

The Marathon Cu-Pd deposit is the largest deposit within the Coldwell Alkaline Complex. It is located approximately at the middle part of the Eastern Gabbro; the

Eastern Gabbro forms the Eastern margin of the Complex (Fig. 4). It is a PGE-relatively rich & sulfide-poor deposit (Ruthart, 2013). The initial exploration of the Marathon deposit was for a large Cu deposit by Anaconda in 1963. Since then, the property has changed hands several times and is currently owned by Stillwater Canada Inc. The latest estimate of the size and grade of the Marathon deposit resource (in-pit, measured plus indicated) are 97.4 million metric tons (Mt) at 0.27% Cu, 0.75 ppm Pd, 0.23 ppm Pt, and 0.09 ppm Au (Puritch et al., 2009).

The major mineralization zones at the Marathon deposit have been divided into Four Zones: the Main Zone, the Footwall Zone, the Hanging Fall Zone, and the W-Horizon. The mineralization of these four zones is mainly hosted by the Two Duck Lake gabbro, with lesser amounts hosted by an apatitic clinopyroxenite and oxide melatroctolite. All of these units belong to the Marathon Series. Sulfide minerals in the Main Zone, the Footwall Zone, the Hanging Fall Zone consist of disseminated chalcopyrite, pyrrhotite, and minor amounts of cubanite, bornite, pentlandite, cobaltite, and pyrite (Good et al., 2015). Only trace amounts of sulfide minerals occur within the mineralized Two Duck Lake gabbro at the W-Horizon, but where sulfide minerals are present they are mainly chalcopyrite and bornite, with minor pyrrhotite and trace amounts of pentlandite and pyrite (Ruthart, 2013).

Approximately 70% of mineral resource is contained within the Main Zone (Good et al., 2015). The Main Zone and the W-Horizon are of the particular interest because they are located at the north and south ends, respectively, of the Two Duck Lake Intrusion and exhibit notably different Cu/Pd ratios (Good et al., 2015). The Main Zone has Cu/Pd ratios typically within 1000-10000 (mantle range; Good et al., 2015), whereas the W-Horizon is characterized by an extremely enrichment of Pd plus Pt relative to Cu and has Cu/Pd<1000 (Ruthart, 2013). In addition, the Main Zone and W-Horizon also differs in terms of PGM hosts and assemblages. Puritch et al. (2009) reported details of the platinum group minerals within the Main Zone and W-Horizon Zone of Marathon Cu-Pd deposit, and found that within the Main

Zone the PGM are dominantly kotulskite-sobolevskite solid solution, hosted by sulfide minerals >hydrous silicate minerals > within plagioclase boundaries whereas within W-Horizon Zone the PGM are dominantly zvyagintsevite-palladinite, hosted by sulfide minerals > plagioclase boundaries > other PGMs > hydrous silicate minerals.

Numerous studies have examined the genesis of the Marathon Cu-Pd deposit and three general models have been proposed to explain the PGE mineralization at this deposit. The first model proposes a hydrothermal origin for mineralization (e.g., Ohnenstetter et al., 1991, Watkinson and Ohnenstetter, 1992, Watkinson and Jones, 1996, Dahl et al. 2001, Barrie et al., 2002, and Brzozowski et al., 2015). In this model, Cu and PGE were initially concentrated by magmatic processes and were remobilized by Cl-rich fluids from the lower parts of the deposit to higher levels when they are deposited. The model explains the commonly observed association of Cu-rich sulfide minerals and PGM with secondary hydrous mineral assemblages, pegmatitic rocks, and Cl-rich minerals in the Main Zone. Another model is related to the zone refining (Dahl et al., 2001; Barrie et al., 2002; Samson et al., 2008). In this model, magmatic sulfides were modified by fluid-rock interaction.

The last and perhaps the most applicable model is related to magmatism, proposed by Good and Crocket (1994) and Good et al. (2015) for sulfide minerals at the Main Zone, and by Ruthart (2013) for mineralization at the W-Horizon. In this model, the Cu-PGE mineralization was mainly controlled by sulfide liquid segregation from the silicate melt, and the compositions of sulfides are governed by partition coefficients of Cu and Pd between silicate melt and sulfide liquid, and by the silicate melt to sulfide liquid ratio (R-factor) (Good et al., 2015). The extreme enrichment of PGE in the W-Horizon was interpreted by Ruthart (2013) to be the result of magmatic ‘multistage dissolution upgrading’ process, similar to the mechanism proposed by Kerr and Leitch (2005).

Barrier et al. (2002) and Miller and Nicholson (2013) defined the Marathon deposit as a contact-type deposit because many of the deposit characteristics match those described for contact-type occurrences. For example, the grades for the Marathon deposit (0.27% Cu, 0.75 g/t Pd, 0.23 g/t Pt, and 0.09 g/t Au) closely match the median values for a total of 37 contact-type ore deposits (0.25%, 0.62, 0.245, and 0.0846 g/t, respectively) as determined by Zientek (2012). By contrast, Good et al., (2015) proposed that this deposit more reasonably belonged to the conduit-type deposits based on: 1) the high proportion of sulfide minerals relative to the host rocks, an important factor in defining conduit systems (Maier et al., 2001), 2) an extrusive volcanic equivalent of the Two Duck Lake Intrusion (the Coubran basalts) is consistent with conduit setting, 3) the shape of the Two Duck Lake gabbro resembles a chonolith rather than a sill-like intrusion, 4) petrological evidence (the replacement of early plagioclase by later more calcic plagioclase) that the Two Duck Lake gabbro formed by multiple intrusions, and, 5) identification of magma pathways along the footwall contact of the Two Duck Lake intrusion.

1.5 References

Armitage P.E.B., McDonald I., Edwards S.J., and Manby G.M. 2002. Platinum-group element mineralization in the Platreef and calcsilicate footwall at Sandsloot, Potgietersrus District, South Africa. *Trans. Inst. Min. Metall. B,* **111**, 36-45.

Arndt, N., Lesher, M., and Czamanske, G. 2005. Mantle-derived magmas and magmatic Ni-Cu-(PGE) deposits. In: Hedenquist J.W., Thompson J.F.H., Goldfarb R.J. and Richards, J.P. (eds.), *Economic Geology 100th Anniversary Volume*, 5-24.

Baker D.R., Barnes S.-J., Simon G., and Bernier F. 2001. Fluid transport of sulfur and metals between sulfide melt and basaltic melt. *Canadian Mineralogist,* **39**, 537-546.

Barnes S.-J. and Lightfoot P.C. 2005. Formation of magmatic nickel-sulfide ore deposits and processes affecting their copper and platinum-group element contents. In: Hedenquist J.W., Thompson J.F.H., Goldfarb R.J., Richards, J.P. (eds.), *Economic Geology 100th Anniversary Volume*, 179-213.

Barnes S.-J.and Maier W.D. 1999. The fractionation of Ni, Cu and the noble metals in silicate and sulphide liquids. In: Keays R.R., Lesher C.M., Lightfoot P.C., Farrow, C.E.G. (eds.), Dynamic Processes in Magmatic Ore Deposits and Their Application to Mineral Exploration, Short Course Notes. Geological Association Canada, **13**, 69–106.

Barnes S.-J. and Maier W. D. 2002. Platinum-group elements and microstructures of normal Merensky Reef from Impala Platinum Mines, Bushveld Complex. *Journal of Petrology*, **43**, 103-128.

Barnes S.-J. and Naldrett A.J. 1985. Geochemistry of the J-M (Howland) reef of the Stillwater Complex, Minneapolis Adit area; 1, Sulfide chemistry and sulfide-olivine equilibrium. *Economic Geology*, **80**, 627−645.

Barnes S.-J. and Ripley E.M. 2016. Highly Siderophile and Strongly Chalcophile Elements in Magmatic Ore Deposits. *Reviews in Mineralogy and Geochemistry*, **81**, 725-774.

Barnes S.-J., Zientek M., and Severson M.J. 1997. Ni, Cu, Au and platinum group element contents of sulfides associated with intraplate magmatism: A synthesis. *Canadian Journal of Earth Sciences*, **34**, 337-351.

Barnes S.-J., Naldrett A.J., and Gorton M.P. 1985. The origin of the fractionation of platinum-group elements in terrestrial magmas. *Chemical Geology*, **53**, 303–323

Barrie C.T., MacTavish A.D., Walford, P.C., Chataway R., and Middaugh R. 2002. Contact-type and magnetitite reef-type Pd-Cu mineralization in ferroan olivine gabbros of the Coldwell Alkaline Complex, Ontario. In: Cabri L.J. (eds.), Can. Inst. Min. Metall. Petrol., Spec. the Geology, Geochemistry, Mineralogy and Mineral Beneficiation of Platinum-group Elements, **54**, 321-338.

Benko Z., Mogessie A., Molnar F., Severson M.J., Hauck S.A., and Raic S. 2015. Partial melting processes and Cu–Ni–PGE mineralization in the footwall of the South Kawishiwi Intrusion at the Spruce Road deposit, Duluth Complex, Minnesota, USA. *Economic Geology*, **110**.

Blaine F.A., Linnen R.L., Holtz F., and Bruegmann G.E. 2011. The effect of Cl on Pt solubility in haplobasaltic melt: Implications for micronugget formation and evidence for fluid transport of PGEs. *Geochimica et Cosmochimica Acta*, 75, 7792-7805.

Botcharnikov R.E., Linnen R.L., Wike M., Holtz F., Jugo P.J., and Berndt J. 2011. High gold concentrations in sulphide-bearing magma under oxidizing conditions. *Nature geoscience*, **4**, 112-115.

Boudreau A.E. and Meurer W. P. 1999. Chromatographic separation of the platinum-group elements, gold, base metals and sulfur during degassing of a compacting and solidifying igneous crystal pile. *Contributions to Mineralogy and Petrology*. **134**, 174–185.

Boudreau A, Mathez E, and McCallum I. 1986. Halogen geochemistry of the Stillwater and Bushveld Complexes: evidence for transport of the platinum-group elements by Cl-rich fluids. *Journal of Petrology*, **27**, 967-986.

Boudreau A.E. 2016. The Stillwater Complex, Montana-Overview and the significance of volatiles. *Mineralogical Magazine*, **80**, 585-637.

Brenan J.M., Finnigan C.F., McDonough W.F., and Homolova V. 2012. Experimental constraints on the partitioning of Ru, Rh, Ir, Pt and Pd between chromite and silicate melt: The importance of ferric iron. *Chemical Geology*, **302-303**, 16-32.

Brenan J.M., Brnnett N.R., and Zajacz Z.2016. Experimental results on fractionation of the highly siderophile elements (HSE) at variable pressures and temperatures during planetary and magmatic differentiation. *Reviews in Mineralogy and Geochemistry*, **81**, 1-87.

Brzozowski M.J., Samson I.M., Gagnon J.E., Linnen R.L., Good D.J., Ames, D.E., and Flemming R.L., 2015. Variation in vein mineralogy and mineral chemistry around the Marathon Cu-Pd deposit, Ontario: Insights into the development of an exploration tool, In: Ames D.E. and Houlé M.G. (eds.), Targeted Geoscience Initiative 4: Canadian Nickel-Copper-Platinum Group Elements-Chromium Ore Systems - Fertility, Pathfinders, New and Revised Models; Geological Survey of Canada, Open File 7856, 245-255.

Capobianco C.H., Hervig R.L., and Drake M. 1994. Experiments on crystal/liquid partitioning of Ru, Rh and Pd for magnetite and hematite solid solutions crystallised from silicate melt. *Chemical Geology*, **113**, 23-43.

Cawthorn R.G. 2002. The role of magma mixing in the genesis of PGE mineralization in the Bushveld Complex: Thermodynamic calculations and new interpretations. *Economic Geology*, **97**, 663-667.

Cawthorn R.G. 2005. Contrasting sulphide contents of the Bushveld and Sudbury Igneous Complexes. *Mineralium Deposita*, **40**, 1-12.

Dahl R., Watkinson, D.H., and Taylor R.P. 2001, Geology of the Two Duck Lake intrusion and the Marathon Cu-PGE deposit, Coldwell Alkaline Complex, northern Ontario. *CIM Exploration and Mining Geology*, **10**, 51-65.

Ding X., Ripley E.M., and Li, C. 2012. PGE geochemistry of the Eagle Ni-Cu-(PGE) deposit, Upper Michigan: Constraints on ore genesis in a dynamic magma conduit. *Mineralium Deposita*, **47**, 89-104.

Djon M.L.N.and Barnes S.-J. 2012. Changes in sulfides and platinum-group minerals with the degree of alteration in the Roby, Twilight, and High Grade Zones of the Lac des Iles Complex, Ontario, Canada. *Mineralium Deposita*, **47**, 875-896.

Drennan M.and Fell M., 2010, Technical Report and Resource Estimate 2010 Update for the Geordie Lake Property Northern Ontario.

Dutrizac J.E. 1976. Reactions in cubanite and chalcopyrite. *Canadian Mineralogist*, 14, 172-181.

Ebel D.S.and Naldrett A.J. 1997. Crystallization of sulfide liquids and the interpretation of ore composition. *Canadian Journal of Earth Sciences*, **34**, 352-365.

Eckstrand O.R.and Hulbert L.J.2007. Magmatic nickel-copper-platinum group element deposits. In: Goodfellow W.D. (eds.) Mineral deposits of Canada-A synthesis of major deposit-types, district metallogeny, the evolution of geological provinces, and exploration methods: Geological Association of Canada, Mineral Deposits Division, Special Publication, **5**, 205-222.

Farrow C.E.G.and Watkinson, D.H. 1999. An evaluation of the role of fluids in Ni-Cu-PGE-bearing, mafic-ultramafic systems: Geological Association of Canada, Short Course Notes, **13**, 31-98.

Fincham C.J.B. and Richardson F.D. 1954. The behaviour of sulphur in silicate and aluminate melts. *Proc R Soc Lond Ser A*, **223**, 40-62.

Fleet M.E.and Wu T.-W. 1993. Volatile transport of platinum-group elements in sulfide-chloride assemblages at 1000 °C. *Geochimica et Cosmochimica Acta*, **57**, 3519-3531.

Fleet M.E., Chryssoulis S.L., Stone W.E., and Weisener C.G. 1993. Partitioning of platinum-group elements and Au in the Fe-Ni-Cu-S system: Experiments on the fractional crystallization of sulfide melt. *Contributions to Mineralogy and Petrology*, **115**, 36-44.

Gammons C.H. and Bloom M.S. 1993. Experimental investigation of the hydrothermal geochemistry of platinum and palladinum: II. The solubility of PtS and PdS in aqueous sulfide solutions to 300°C. *Geochimica et Cosmochimica Acta*, **57**, 2451-2467.

Goldner B.D. 2011. Igneous petrology of the Ni-Cu-PGE mineralized Tamarack intrusion, Aitkin and Carlton Counties, Minnesota. University of Minnesota M.Sc. thesis.

Good D.J.and Crocket J.H.1994. Genesis of the Marathon Cu-platinum group element deposit, Port Coldwell alkalic complex, Ontario: A Midcontinent rift-related magmatic sulfide deposit. *Economic Geology*, **89**, 131-149.

Good D.J., Epstein R., McLean K., Linnen R.L., and Samson I.M. 2015. Evolution of the Main Zone at the Marathon Cu-PGE Sulfide Deposit, Midcontinent Rift, Canada: Spatial Relationships in a Magma Conduit Setting. *Economic Geology*, **110**, 953-1008.

Goodgame V.R., Johnson J.R., MacTavish A.D., Stone W.E., Watkins K.P., and Wilson G.C. 2010. The Thunder Bay North deposit: Chonolith hosted Pt-Pd-Cu-Ni mineralization related to the Midcontinent rift [abs.]: International Platinum Symposium, 11th, 21-24 June 2010, Sudbury, Ontario, Canada, Ontario Geological Survey, Miscellaneous Release-Data, 269.

Hanley J.J., Pettke T., Mungall J.E., and Spooner E.T.C. 2005. The solubility of platinum and gold in NaCl brines at 1.5 kbar, 600 to 800 °C: A laser ablation ICP-MS pilot study of synthetic fluid inclusions. *Geochimica et Cosmochimica Acta*, **69**, 2953-2611.

Haughton D.R., Roeder P.L., and Skinner B.J. 1974. The solubility of sulfur in mafic magmas. *Economic Geology*, **69**, 451-462.

Heaman L. and Machado N. 1992. Timing and origin of midcontinent rift alkaline magmatism, North America: evidence from the Coldwell Alkaline Complex. *Contributions to Mineralogy and Petrology*, **110**, 289-303.

Helmy H.M., Ballhaus C., Berndt J., Bockrath C., and Wohlgemuth-Ueberwasser C. 2007. Formation of Pt, Pd and Ni tellurides: experiments in sulfide-telluride systems. *Contributions to Mineralogy and Petrology*, **153**, 577-591.

Holwell D.A. and McDonald, I. 2010. A Review of the Behaviour of Platinum Group Elements within Natural Magmatic Sulfide Ore Systems. *Platinum Metals Review*, **54**, 26-36.

Hsu J.J., Wang Q.C., Liang L., and Jie H. 1991. Geological evolution of the Neimonides: a working hypothesis. *Eclogae Geol. Helv.*, **84**, 1-31.

Hutchinson D. and Kinnaird J.A. 2005. Complex multistage genesis for the Ni-Cu-PGE mineralisation in the southern region of the Platreef, Bushveld Complex, South Africa. *Trans Inst Min Metall*, **114**, 208-224.

Keays R.R. and Lightfoot P.C. 2002. Exploration for Platinum-Group Element (PGE) Deposits in Mafic and Ultramafic Rocks [ext. abs.]: International Platinum Symposium, 9th, Billings, Montana, 2002, Extended Abstracts, 1-4.

Kerr A. and Leitch A.M. 2005. Self-destructive sulfide segregation systems and the formation of high-grade magmatic ore deposits: *Economic Geology*, **100**, 311-332.

Kullerud G., Yund R.A., and Moh G.H. 1969. Phase relations in the Cu-Fe-S, Cu-Ni-S, and Fe-Ni-S system. *Economic Geology*, **4**, 323-343.

Lesher C.M. and Campbell I.H. 1993. Geochemical and fluid dynamic modeling of compositional variations in Archean komatiite-hosted nickel sulfide ores in Western Australia. *Economic Geology*, **88**, 804-816.

Lesher C.M. and Keays R.R. 1984. Metamorphically and hydrothermally mobilized Fe-Ni-Cu sulphides at Kambalda, Western Australia. In: Buchanan D.L. and Jones, M.J. (eds.), Sulphide Deposits in Mafic and Ultramafic Rocks, Inst. Min. Metall., London, 62-69.

Li C. and Naldrett A.J. 1993. Sulfide capacity of magma: a quantitative model and its application to the formation of sulfide ores at Sudbury, Ontario. *Economic Geology*, **88**, 1253-1260.

Li C. and Ripley E. M. 2005. Empirical equations to predict the sulfur content of mafic magmas at sulfide saturation and applications to magmatic sulfide deposits. *Mineralium Deposita*, **40**, 218-230.

Li C., Mou J., Lan G., Sun Y., Yang Z.X, Tang J., Chen J., Miao F., and Xiao Y. 1996. Origin and Ore-Forming Principals of the Huangshan Cu-Ni Metallogenic Belt, Hami, Xinjiang. *Press of Chengdu University of Sciences and Technology*, **204**. (in Chinese)

Li C., Maier W.D., and de Waal S. A. 2001. The role of magma mixing in the genesis of PGE mineralisation in the Bushveld Complex: Thermodynamic calculations and new interpretations. *Economic Geology*, **96**, 653-662.

Liu Y. and Brenan J. 2015. Partitioning of platinum-group elements (PGE) and chalcogens (Se, Te, As, Sb, Bi) between monosulfide-solid solution (MSS), intermediate solid solution (ISS) and sulfide liquid at controlled fO_2-fS_2 conditions. *Geochimica et Cosmochimica Acta*, **159**, 139-161.

Maier W. D. and Barnes, S.-J. 1999. Platinum-group elements in silicate rocks of the Lower, Critical and Main Zones at Union Section, Western Bushveld Complex. *Journal of Petrology*, **40**, 1647-1671.

Maier W.D., Li C., and de Waal S.A. 2001. Why are there no major Ni-Cu sulfide deposits in large layered mafic-ultramafic intrusions? *Canadian Mineralogist*, **39**, 547-556.

Maier W.D., Barnes S.-J., and Marsh J.S. 2003. The concentrations of the noble metals in Southern African flood-type basalts and MORB: implications for petrogenesis and sulphide exploration. *Contributions to Mineralogy and Petrology*, **146**, 44-61.

Maier W.D., de Klerk L., Blaine J., Manyeruke T., Barnes S.-J, Stevens M.V.A., and Mavrogenes J.A. 2008. Petrogenesis of contact-style PGE mineralization in the northern lobe of the Bushveld Complex: comparison of data from the farms Rooipoort, Townlands, Drenthe and Nonnenwerth. *Mineralium Deposita*, **43**, 255-280.

Maier W.D. 2005. Platinum-group element (PGE) deposits and occurrences: Mineralization styles, genetic concepts, and exploration criteria: *Journal of African Earth Science*, **41**, 165-191.

Mathez E.A. 1995. Magmatic metasomatism and formation of the Merensky Reef, Bushveld Complex. *Contributions to Mineralogy and Petrology*, **119**, 277-286.

Meghji I.M. 2016. The character and distribution of Cu-PGE mineralization at the Geordie Lake Deposit within the Coldwell Alkaline Complex, Ontario. M.Sc. thesis, London, ON, University of Western Ontario.

Miller J. and Nicholson S. 2013. Geology and mineral deposits of the 1.1Ga Midcontinent rift in the Lake Superior region-an overview: Cu-Ni-PGE Deposits of the Lake Superior Region, Precambrian Research Center Professional Workshop Series PRC WS-13-01.

Mulja T. and Mitchell R. 1991. The Geordie Lake Intrusion, Coldwell Alkaline Complex, Ontario; a palladium-and tellurium-rich disseminated sulfide occurrence derived from an evolved tholeiitic magma. *Economic Geology*, **86**, 1050-1069.

Mungall J.E. and Naldrett A.J. 2008. Ore deposits of the Platinum-Group Elements. *Elements*, **4**, 253-258.

Mungall J.E., Andrews D.R.A., Cabri L.J., Sylvester P.J., and Tubrett M. 2005. Partitioning of Cu, Ni, An, and platinum-group elements between monosulfide solid solution and sulfide melt under controlled oxygen and sulfur fugacities. *Geochimical et. Cosmochimical Acta*, **69**, 4349-4360.

Naldrett A.J. 2004. Magmatic sulfide deposits- geology, geochemistry, and exploration. Springer-Verlag, 727pp.

Naldrett A.J., Kinnaird J., Wilson A., and Chunnett G. 2008. The concentration of PGE in the Earth's crust with special reference to the Bushveld Complex. *Earth Science Frontiers*, **15**, 264-297.

Naldrett A.J. 1997. Key factors in the genesis of Noril'sk, Sudbury, Jinchuan, Voisey's Bay and other world-class Ni-Cu-PGE deposits: Implications for exploration. *Australian Journal of Earth Sciences*, **44**, 283-315.

Naldrett A.J. 1999. World-class Ni-Cu-PGE deposits: key factors in their genesis. *Mineralium Deposita*, **34**, 227-240.

Ohnenstetter D., Watkinson D.H., and Dahl R. 1991. Zoned hollingworthite from the Two Duck Lake intrusion, Coldwell Alkaline Complex, Ontario. *American Mineralogist*, **76**, 1694-1700.

Pan P. and Wood S.A. 1994. Solubility of Pt and Pd sulfides and Au metal in aqueous bisulfide solutions: II- results at 200 to 350 ℃ and saturated vapor pressure. *Mineralium Deposita*, **29**, 373-390.

Peregoedova A. 1998. The experimental study of the Pt-Pd-partitioning between monosulfide solid-solution and Cu-Ni-sulfide melt at 900-840°C. 8th Int. Platinum Symp. (Johannesburg), 325-327 (abstr.).

Puritch E.P, Orava D., Armstrong T., Yassa A., Gowans R., Wislesky I., and Jacobs C. 2009. Technical report on the updated mineral resource estimate and feasibility study for the Marathon PGM-Cu project, Marathon, Ontario, Canada: PandE Mining Consultants, Inc., Technical Report NI 43-101.

Righter K, Campbell A.J., Humayun M., and Hervig R.L. 2004. Partitioning of Ru, Rh, Pd, Re, Ir and Au between Cr-bearing spinel, olivine, pyroxene and silicate melts. *Geochimica et Cosmochimica Acta*, **68**, 867-880.

Ripley E.M. 1999. Systematics of sulphur and oxygen isotopes in mafic igneous rocks and related Cu-Ni-PGE mineralization. In: Keays, R.R., Lesher, C.M., Lightfoot, P.C., Farrow, C.E.G., (eds.), Dynamic Processes in Magmatic Ore Deposits and their Application to Mineral Exploration: Geological Association of Canada, Short Course Notes, **13**, 133-158.

Ripley E.M. 2014. Ni-Cu-PGE Mineralization in the Partridge River, South Kawishiwi, and Eagle Intrusions: A Review of Contrasting Styles of Suflide-Rich Occurrences in the Midcontinent Rift System. *Economic Geology*, **109**, 309-324.

Ruthart R. 2013. Characterization of high-PGE, low-sulphur mineralization at the Marathon PGE-Cu deposit, Ontario. M.Sc. thesis, Waterloo, ON, University of Waterloo.

Samson I.M., Fryer B.J., and Gagnon J.E. 2008. The Marathon Cu-PGE deposit, Ontario: Insights from sulphide chemistry and textures [abs.]: Goldschmidt Conference Abstracts, A820.

Schulz K.J., Chandler V.W., Nicholson S.W., Piatak N., Seal R.P., Woodruff L.G., and Zientek M.L. 2010. Magmatic Sulfide-Rich Nickel-Copper Deposits Related to Picrate and (or) Tholeiitic Basalt Dike-Sill Complexes: A Preliminary Deposit Model: USGS Open File Report, U.S. Department of the Interior, U.S. Geological Survey, 31pp.

Shaw C.S.J. 1997. The petrology of the layered gabbro intrusion, Eastern gabbro, Coldwell Alkaline Complex, Northwestern Ontario, Canada: Evidence for multiple phases of intrusion in a ring dyke. *Lithos*, **40**, 243-259

Shima H. and Naldrett A.J. 1995. Solubility of sulfur in ultramafic melt and the relevance of the system Fe-S-O. *Economic Geology*, **70**, 960-967.

Sinyakova E. and Kosyakov V. 2009. Experimental modeling of zonality of copper-rich sulfide ores in copper-nickel deposits. *Dokl Earth Sci*, **427**, 787-792.

Sutphin D.M. and Page N.J. 1986. International strategic minerals inventory summary report-platinum-group metals. U.S. Geological Survey Circular 930-E, 34pp.

Todd S., Keith D., Roy L.L., and Schissel D.1982. The JM platinum-palladium reef of the Stillwater Complex, Montana; I, Stratigraphy and petrology. *Economic Geology*, **77**, 1454-1480.

Walker E.C., Sutcliff R.H., Shaw C.S.J., Shore G.T., and Penczak R.S.1993. Precambrian geology of the Coldwell Alkaline Complex. Ontario Geological Survey Open File Report 5868, 30pp.

Watkinson D. and Jones P.1996. Platinum-group minerals in fluid inclusions from the Marathon deposit, Coldwell Alkaline Complex, Canada. *Mineralogy and Petrology*, **57**, 91-96.

Watkinson D.H. and Ohnenstetter, D. 1992. Hydrothermal origin of platinum- group mineralization in the Two Duck Lake intrusion, Coldwell Alkaline Complex, northwestern Ontario. *Canadian Mineralogist*, **30**, 121-13.

Willmore C.C., Boudreau A.E., and Kruger F.J. 2000. The halogen geochemistry of the Bushveld Complex, Republic of South Africa: Implications for chalcophile element distribution in the Lower and Critical Zones. *Journal of Petrology*, **41**, 1517-1539.

Wilson A.H. and Brown R.T. 2005. Exploration and mining perspective of the Main Sulfide Zone of the Great Dyke, Zimbabwe-case study of the Hartley Platinum Mine. In: Exploration for Platinum Group Element Deposits. In: Mungall J.E., (eds.) Mineralogical Association of Canada, Short Course Notes, **35**, 409-429.

Zientek M.L. 2012. Magmatic ore deposits in layered intrusions-descriptive model for reef-type PGE and contact-type Cu-Ni-PGE deposits: U.S. Geological Survey Open-File Report 2012-1010, 48pp.

Chapter 2
Methodgy

2.1 Sample preparation

2.1.1 Powders

Powdered samples were collected by grinding 1 m-long channels along the drill core approximately 2 mm wide and 1 cm deep using a Thermo Scientific portable grinder (Fig. 2-1 A & B). A typical sample required 2 to 5 minutes to collect and produced ca. 10 to 200 μm of powder. Seven pXRF analyses were made on powders that were re-ground using a motar and pestle, which were compared to pXRF analyses conducted on the the original powders (before re-ground) in order to evaluate the influence from grain size. Results are tabulated in Table 2-1 and compared in Figure 2-2. It shows that the re-ground had little effect on the results.

Samples were taken at intervals of ca. 4.5 m along the length of the drill hole. Cross-contamination was minimized by washing the collection vial, cleaning off the grinder blade, pre-contaminating the vial by grinding some of the sample, shaking the vial to coat the vial with the sample dust and dumping out the vial, and then collecting the powdered sample to be analyzed. All powders were then loaded into PREM-4331 XRF sample cups (powders were packed by hand when they were in cups) capped with 4-μm PREM-F2540 XRF sample cup films for the pXRF analysis (Fig. 2-3).

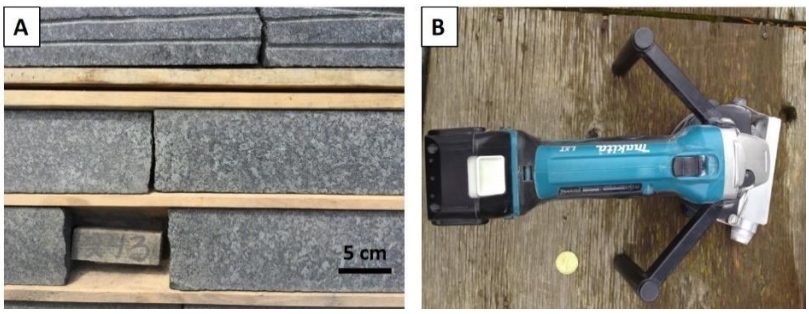

Figure 2-1. Pictures showing the appearance of the drill core after grinding. (A) Drill cores in the box, note the two parallel channels along the length of the top drill core after cutting the core for powders collection; (B) The portable grinder used to cut drill cores for collecting powders.

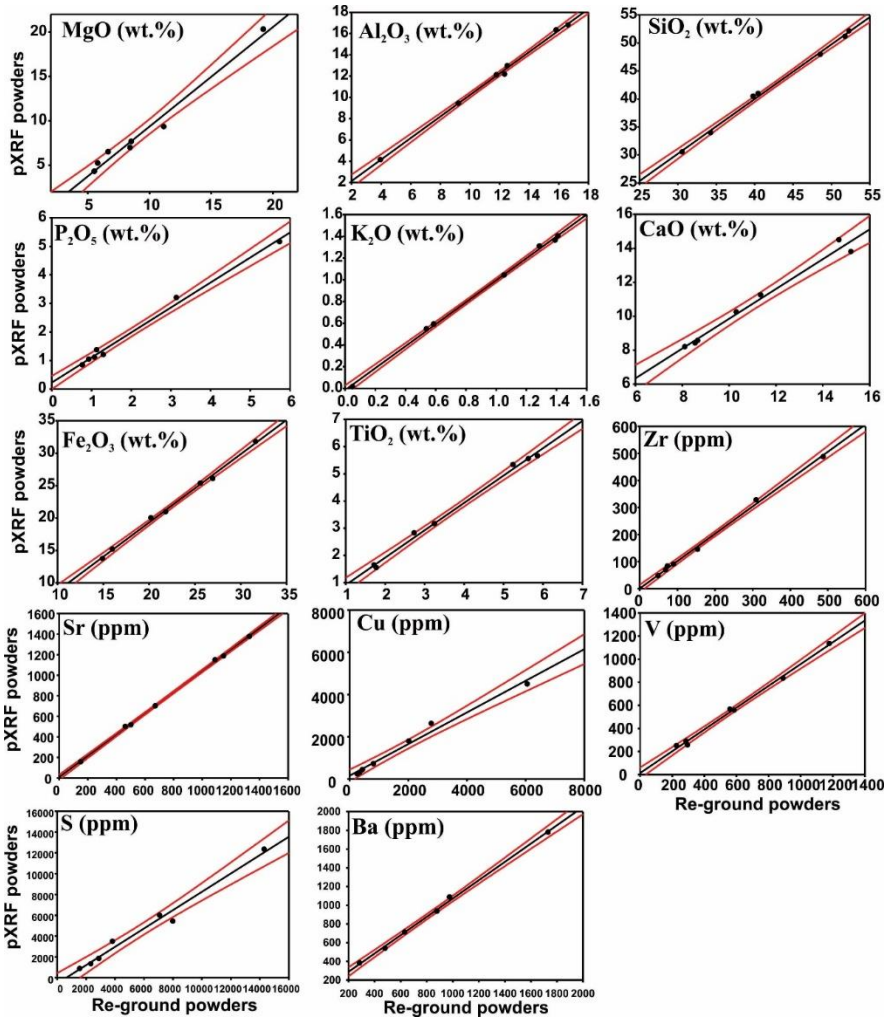

Figure 2-2. The comparison of pXRF whole-rock results determined on powders before and after re-ground. The black line indicates the regression line and the red lines in each diagram represents the 95% confidence interval.

Table 2-1. The comparison of pXRF whole-rock results conducted on powders before and after re-ground. $Fe_2O_3^T$ means total Fe is reported as Fe_2O_3. LOD means limit of detection.

Sample	Powder types	MgO	Al_2O_3	SiO_2	P_2O_5	K_2O	CaO	$Fe_2O_3^T$	TiO_2	Zr	Sr	Cu	V	S	Ba
		wt.%	wt.%	wt.%	wt.%	wt.%	wt.%	wt.%	wt.%	ppm	ppm	ppm	ppm	ppm	ppm
MW-07-08-21.5m	pXRF powders	6.5	13	48.0	1.4	1.4	8	21	3.2	47	1150	309	251	800	1780
MW-07-08-61.5m		4.3	17	52.2	1.1	1.3	9	14	1.6	90	1378	719	257	1300	1086
MW-07-08-65.5m		5.2	16	51.2	1.0	1.4	8	15	1.7	145	1187	2632	289	6000	937
MW-07-06-99.5m		7.0	12	40.5	3.2	1.0	11	26	5.7	328	701	437	567	1800	712
MW-07-06-109.5m		7.7	9	30.5	5.2	0.6	14	32	5.3	69	501	1794	1135	3500	539
MW-07-06-143.5		20.3	4	34.0	0.8	0.0	15	20	5.6	487	156	230	559	12300	<LOD
MW-07-06-155.5m		9.3	12	41.0	1.2	0.5	10	25	2.8	83	517	4498	835	5400	382
MW-07-08-21.5m	Re-ground powders	6.7	13	48.6	1.1	1.4	8	22	3.3	49	1090	343	227	1500	1733
MW-07-08-61.5m		5.5	17	52.3	1.1	1.3	9	15	1.8	90	1330	811	295	2300	976
MW-07-08-65.5m		5.8	16	51.8	0.9	1.4	9	16	1.7	154	1149	2783	287	7000	879
MW-07-06-99.5m		8.4	12	39.8	3.1	1.1	11	27	5.9	310	672	433	560	2800	631
MW-07-06-109.5m		8.5	9	30.6	5.7	0.6	15	32	5.2	69	462	2021	1178	3800	481
MW-07-06-143.5		19.2	4	34.3	0.8	0.0	15	20	5.6	487	150	263	586	14300	<LOD
MW-07-06-155.5m		11.2	12	40.5	1.3	0.5	10	26	2.7	73	502	6059	891	8000	284

Figure 2-3. Powders in cups that are ready for pXRF analysis.

The potential for contamination of Fe, Cr and Ni by the grinder blade was tested by sampling a piece of pure quartz (Fig. 2-4). The pXRF analyses are presented in Table 2-2 and show that grinder blade-related contamination for most elements except Ni is insignificant, with less than 0.1 wt. % for most major elements and lower than the detection limit for trace elements. Approximately 100 ppm of Ni is added to each sample during grinding. A subset of representative powdered samples was further pulverized for laboratory-based whole-rock analyses.

Figure 2-4. A pure quartz prepared to test the contamination during pXRF analysis.

Table 2-2. pXRF analytical results of powders from a pure-quartz pebble, ± values refer to 2σ error determined by repetitive analyses.

MgO (wt. %)	Al_2O_3 (wt. %)	SiO_2 (wt. %)	P_2O_5 (wt. %)	K_2O (wt. %)	CaO (wt. %)	TiO_2 (wt. %)	Fe_2O_3 (wt. %)	Zr (ppm)
2.6±0.72	<LOD	104±0.6	0.08±0.007	<LOD	0.1±0.09	0±0.04	<LOD	<LOD
Sr (ppm)	Cu (ppm)	Ni (ppm)	Mn (ppm)	Cr (ppm)	V (ppm)	Ti (ppm)	S (ppm)	Ba (ppm)
<LOD	<LOD	100±10	<LOD	<LOD	<LOD	<LOD	<LOD	<LOD

LOD, limit of detection

2.1.2 Rock specimens

Drill core samples that are representative of different series' gabbro units with different styles of mineralization (e.g., chalcopyrite-rich, and pyrrhotite-rich) were collected down selected drill holes, with an interval of 5 to 20 meters between every two core samples. Each core sample is about 10 cm in length. After taking pictures and describing the lithology of core samples, thin section blocks were made through cutting core samples using a diamond saw. A subsect of thin section blocks was analyzed by bSEM-EDS in order to test the field portability of this analytical equipment. All thin section blocks were then made into thin sections for petrographic and mineral chemical analyses.

2.2 Analytical equipment

2.2.1 pXRF analysis

A Niton XL3t+ GOLDD+ pXRF analyser equipped with a solid drift detector (SDD), and a high energy, 50kV X-ray Ag anode tube was used in this study. All pXRF measurements were carried out on powders after calibrating the pXRF analyser using a suite of matrix-matched standards, including two U.S. Geological Survey reference materials, BHVO-2 basalt and W-2a diabase, and seven Marathon gabbro internal standards. This suite of standards covers a wide range of concentrations for elements measured in the current work: SiO_2, Al_2O_3, CaO, Fe_2O_3 (as total Fe), TiO_2, K_2O, P_2O_5, MgO, Ba, V, Zr, Sr, Cu, and S. Major elements were determined using the instrument's 'mining mode', with two beams, whereas minor and trace elements were determined using the 'soil mode', with three beams; beam time for both modes

was 60 s. The QA/QC control throughout all analyses was carried out by analyzing two standards after each batch of unknown samples (20 samples typically). A blank standard (98.2 wt. % SiO_2) was analyzed at the beginning and the end of each batch measurement to monitor cross-contamination from the test stand and check for machine drift. Typically, a new calibration was conducted after every two batches of unknown samples. The intent was to acquire the highest quality of results and less-frequent calibration may have yielded a similar result. The analytical error for pXRF analysis with 95% confidence (2σ) was determined through duplicate analyses conducted on the same sample.

2.2.2 Conventional whole-rock analysis

Conventional whole-rock chemical analyses were carried out by ALS Mineral Divisions in Vancouver and Thunder Bay on powders that were initially analyzed by pXRF. Both labs use the same methods for analyzing various elements. After further pulverization, Major elements were analyzed by lithium borate fusion with inductively coupled plasma (ICP)-atomic emission spectroscopy (AES) on a minimum 2 g of pulp samples. Trace elements were analyzed by lithium borate fusion and ICP-mass spectroscopy (MS) on 2 g of sample. Total S was analyzed using a Leco furnace on 1 g of sample. Ferrous Fe was analyzed by H_2SO_4-HF acid digestion and titration on 1 g of sample. Quality-control was conducted based on ALS Chemex quality-control procedures which involve analyses on a wide array of standards, blanks, and duplicates after each batch of samples. The analytical error for conventional whole-rock analysis with 95% confidence (2σ) was determined through duplicate analyses conducted on the same sample. In addition, two different data sets were also prepared, including Stillwater Canada Inc. exploration assays of Cu, S, Ni, Au, Pt, Pd down all included drill holes and 8 high precision S, Se, Pt, Pd, Au, Os, Ru, Ir, and Rh analyses down the PGE-enriched horizon in SL-13-36 (see Chapter 6). The exploration assay data were determined on continuous 2 m sample intervals, and the other data set was collected from eight 2-m-thick, high-grade PGE

intervals at drill hole SL-13-36. Both data sets were analyzed at ALS Thunder, Ontario, by fire assay and mass spectrometer finish (FAMS).

2.2.3 Benchtop SEM-EDS analysis

Major constituents of plagioclase, clinopyroxene, and olivine were determined using a JEOL JMC-600 NeoScope SEM equipped with a JEOL JED-2300 energy dispersive X-ray analyser at Western University. Analyses were conducted using 15 kV accelerating voltage, a high probe current, a working distance of 19 mm, and 30 to 40 μm beam size with standardless ZAF corrections. Unpolished thin section blocks were analyzed under low vacuum mode and carbon-coated polished thin sections were analyzed under high vacuum mode. The analytical precision of bSEM-EDS analyses has been determined by analyzing the same spot 10 times: results are ±0.51 for Mg# of olivine, ±1.0 for Mg# of clinopyroxene, and ±0.63 for anorthite content of plagioclase (1σ standard deviation). The analytical precision (machine error), combing with the nature variation, constitute the sample variability determined through bSEM-EDS analyses on 3-5 grains of each mineral type in each sample.

2.2.4 Electron microprobe analysis

Major and minor constituents of olivine, clinopyroxene, plagioclase, alkali feldspar, and biotite were analyzed using an accelerating voltage of 15 keV and a beam current of 20 nA. The beam was focused to a 1 μm spot for analyzing olivine and clinopyroxene, and to a 5 μm spot for analyzing plagioclase, alkali feldspar, and biotite. The peak counting time was 30 s for all elements and background counts were a total of 30 s. A variety of synthetic and natural standards were used to calibrate different elements during probe analyses. The precision of electron microprobe analyses was determined to be ±0.07 for Mg# of olivine, ±0.30 for Mg# of clinopyroxene, and ±0.15 for plagioclase anorthite content (1σ standard deviation), determined by analysis of the same spot 10 times.

Chapter 3

The application of portable XRF and benchtop SEM-EDS to Cu-Pd exploration in the Coldwell Alkaline Complex, Ontario, Canada

Y.H. Cao[1], R.L. Linnen[1*], D.J. Good[1], I.M. Samson[2], R. Epstein[3]

[1]*University of Western Ontario, London, ON, Canada*
[2]*The University of Windsor, Windsor, ON, Canada*
[3]*P.O. Box 548, Schreiber, ON, Canada*
**Corresponding author (email: rlinnen@uwo.ca)*

3.1 Introduction

Diamond drilling is arguably one of the most important techniques in mineral exploration, and the geochemical analysis of drill core is an essential component of any diamond drilling program. Conventional laboratory geochemical analyses have high accuracy and precision, however, time delays in obtaining results mean that lab-based measurements are not well suited for making rapid decisions in the field. A number of field-portable analytical techniques are designed to collect data with minimal time delay and at low cost. Thus, the mineral exploration industry is increasingly using field portable instruments in modern mineral-exploration campaigns. Portable X-ray fluorescence analysers (pXRF) and benchtop scanning electron microscopes with energy dispersive spectrometers (bSEM-EDS) are two

real-time acquisition instruments that can rapidly collect lithogeochemical and mineral chemical data in the field.

The first pXRF instrument was produced in 1991, following the introduction of cooled Si-PIN diodes and improvements to various components (Nicola et al., 2011). The first media analyzed were simple, with few interferences, e.g., archaeological ceramics and alloys. Since 1991, significant improvements such as the use of silicon drift detectors (SDD) and miniaturised X-ray tubes that can run at higher power, have made the pXRF technique increasingly applicable to the analysis of geological materials. The advantages of pXRF over lab XRF include the smaller size (portability), lower cost, and faster data collection, making it suitable for on-site lithogeochemical analysis. Applications of pXRF initially focused on environmental studies, with few related to mineral exploration. The pioneering work of Potts et al. (1995) provided a preliminary assessment of pXRF in the analysis of silicate rocks. Since then, there have been numerous studies that utilize pXRF in exploration geochemistry, including evaluations of pXRF performance in analyzing geological materials (e.g., Makinen et al., 2006, Morris, 2009, Haffert and Craw, 2009, Hall et al., 2012, 2014) and applications of pXRF to volcanogenic massive sulfide (Ross et al., 2014) and REE deposits (Simandl et al., 2014). Interactive applications of pXRF include using "fit for purpose" data for pathfinder elements in gold exploration (Arne et al., 2014) and the development of a workflow in the mining setting that highlights the importance of QA/QC control (Fisher et al., 2014). There are many other notable publications on the applications of pXRF to mineral exploration, however, it is beyond the scope of this paper to provide a complete review of the subject.

Unlike pXRF lithogeochemical analyses, there are few applications of field-based real-time mineral-chemical analysis. However, the development of benchtop scanning electron microscopes, equipped with energy dispersive spectrometers (bSEM-EDS), offers the possibility of collecting mineral composition data directly

in the field, in contrast with conventional mineral-chemical analysis from lab-based analytical instruments, e.g., scanning electron microscope with energy dispersive spectrometers and electron microprobe. The bSEM-EDS instrument can easily sit on a table in a field setting and samples do not require any preparation, such as polishing or carbon coating, prior to insertion into the instrument. This enables real-time imaging and EDS analysis at the sub-micron scale. Benchtop SEM instruments have been available for several years, but, to our knowledge, this technique has not been applied to mineral exploration. The current study combines pXRF with bSEM-EDS analysis as tools to improve decision-making in the field. In this study, these real-time analytical techniques are applied to Cu-Pd exploration at the Four Dams occurrence in the Eastern Gabbro of the Coldwell Alkaline Complex, northwestern Ontario, and the results are compared to those obtained by conventional laboratory analyses to establish the reliability of these techniques.

3.2 Study Area

3.2.1 Geological Setting

The Coldwell Alkaline Complex is the largest alkaline intrusive complex in North America (25 km diameter, 580 km^2 area) and is part of the Midcontinent Rift (Walker et al., 1993). It intruded the Archean Schreiber-White River greenstone belt at 1108 ±1 Ma (Heaman and Machado, 1992) during the early stages of the Midcontinent Rift (Miller and Nicholson, 2013). The Coldwell Alkaline Complex consists of a margin of ultramafic, gabbroic and meta-volcanic rocks that make up the Eastern Gabbro Suite (Good et al. 2015) and three intrusive centres composed predominantly of syenite and nepheline syenite (Mulja and Platt, 1982; Walker et al., 1993) (Fig. 3-1).

The Eastern Gabbro suite occurs along the outer margin of the Coldwell Alkaline Complex (Fig. 3-1). Good et al. (2015) identified nine major lithologies that were further grouped into three major distinctive magmatic series that were defined, from oldest to youngest, as meta-basalt, the Layered Series and the Marathon Series.

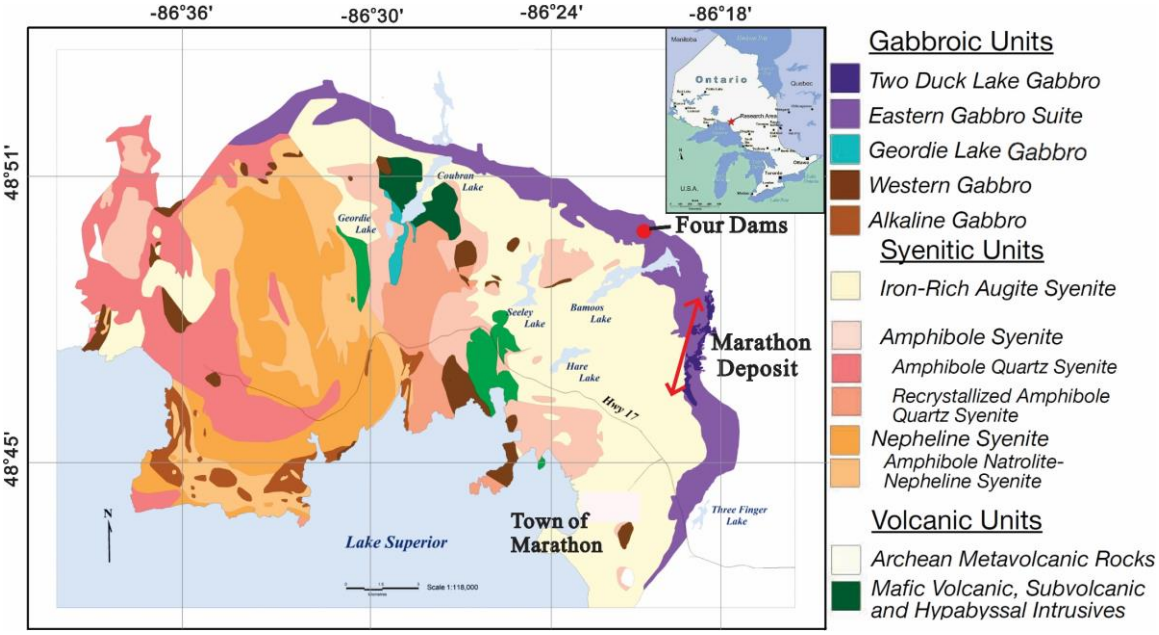

Figure 3-1. Geological map of the Coldwell alkaline complex. The location of Four Dams is represented by the red dot (Modified after Walker et al., 1993 and Good et al., 2015).

Meta-basalt (fine-grained gabbro in Good et al., 2015) occurs at or near the base of the Eastern Gabbro and comprises approximately one fifth to one-third of the volume of the Eastern Gabbro. It consists of pyroxene-hornfels-grade rocks that were intruded by the Layered and Marathon Series. The Layered Series is the next youngest unit and comprises the bulk of the Eastern Gabbro. It consists of massive to modally layered olivine gabbro with lesser amounts of weakly layered oxide augite melatroctolite, and less commonly gabbroic anorthosite. The Marathon Series is the youngest unit. It consists of numerous small intrusions composed predominantly of ophitic gabbro, apatite-bearing olivine clinopyroxenite, apatitic clinopyroxenite, and oxide melatroctolite (Good et al., 2015). The relative ages for these units were confirmed in the field by cross cutting relationships, particularly within the numerous units of igneous breccia.

Most of the copper and all of the known PGE mineralization within the Eastern Gabbro suite are hosted by the Marathon Series. In particular, at the Marathon deposit, the most important sub unit of the Marathon Series is the Two Duck Lake

gabbro, an ophitic gabbro and pegmatitic unit. Because of the significance of the Marathon Series as hosts for Cu-Pd mineralization, it is critical that the entire suite of Marathon Series intrusions can be distinguished from other Eastern Gabbro rocks for mineral exploration, particularly if it is possible to differentiate these units in the field. Note that although some disseminated chalcopyrite and pyrrhotite mineralization does occur in the Layered Series, it is associated with albite-actinolite alteration and contains only trace PGE (<0.005 ppm).

The Eastern Gabbro in the Four Dams area is located approximately 3 km northwest of the Marathon Cu-Pd deposit (Fig. 2-1) and contains units of both the Layered Series and Marathon Series. The Four Dams area is thus an ideal setting to establish whether pXRF and bSEM-EDS can be combined to establish an igneous stratigraphy that could be used to help guide future exploration.

3.2.2 Drill Hole FD-13-34

Drill hole FD-13-34 (Fig. 3-2) was selected because it intersects a complete section of igneous stratigraphy at the Four Dams occurrence, including units of both Layered Series and Marathon Series. The hole was drilled at an azimuth of 32.9º and dip of 69.6º for 375 m. The Layered Series at Four Dams consists of layered olivine gabbro and oxide augite melatroctolite and the Marathon Series consists of apatite-bearing clinopyroxenite, oxide melatroctolite, and a minor amount of ophitic gabbro, similar to the Two Duck Lake gabbro at the Marathon Deposit.

A 70 m thick sequence of oxide-rich units, consisting of, from top to bottom, oxide augite melatroctolite and oxide melatroctolite, separates the Layered Series from the Marathon Series. The oxide melatroctolite exhibits a sharp contact with the overlying Layered Series oxide augite melatroctolite. This contact is important because it forms a 350 m long stratigraphic marker horizon that facilitates interpretation of the local geology. Both oxide units are petrographically similar, but essentially belong to two different igneous series, i.e., the oxide augite melatroctolite is within the PGE barren Layered Series whereas the oxide

melatroctolite is in the Marathon Series and potentially hosts PGE mineralisation. Being able to differentiate both oxide units is important, not only because the oxide melatroctolite is potentially mineralized, but it can help define the contact between the barren Layered Series and the PGE mineralised Marathon Series.

Two types of igneous breccia occur within drill hole FD-13-34 and are representative of breccia units found throughout the Four Dams area. The first type occurs between 47 and 60 m down the hole and consists of xenoliths of meta-basalt rocks cut by Marathon Series intrusions. The second type occurs between 297 and 316 m down the hole and consists of Layered Series units cut by Marathon Series intrusions.

Two types of Cu-Pd mineralization occur in drill hole FD-13-34. The first type occurs within the Layered Series between 13 and 65 m down the hole and contains up to 0.41 % Cu and trace (<0.005 ppm) Pd (unpublished Stillwater Canada Inc. assay). The second type occurs primarily within the Marathon Series apatitic clinopyroxenite unit between 270-278 m and 290-336 m down the hole and contains up to 0.72% Cu and 0.56 ppm Pd (unpublished Stillwater Canada Inc. assay).

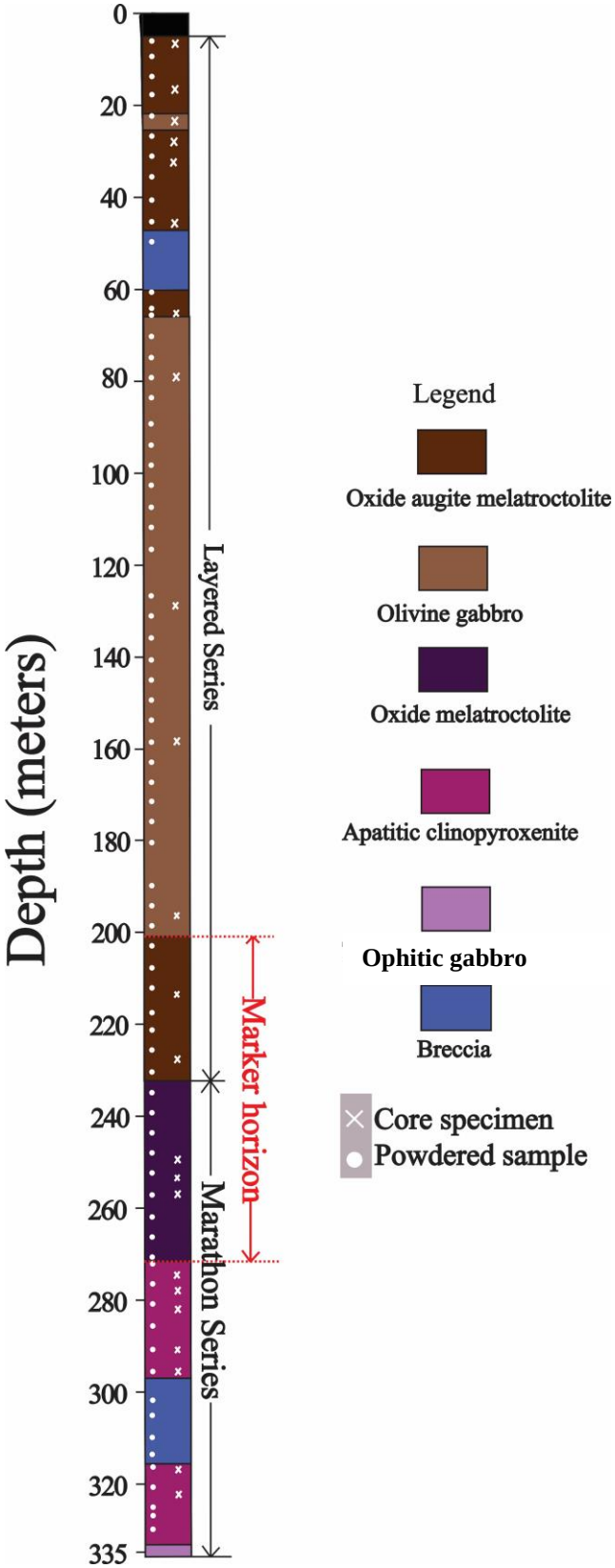

Figure 3-2. Gabbro units and sampling locations for drill hole FD-13-34.

3.2.2.1 Layered Series

The olivine gabbro of the layered series at Four Dams is medium to coarse-grained (1-3 mm) with modal layering defined by a gradational variation in the abundance of plagioclase. The gabbro has an intergranular texture (Fig. 3-3A) and is mainly composed of, in decreasing order of abundance, euhedral plagioclase (40-60 modal%), subhedral clinopyroxene (15-30 modal%), subhedral olivine (10-15 modal%), magnetite (~5 modal%), and less than 6 modal % fine-grained apatite that is typically enclosed in, or interstitial to, olivine and plagioclase.

The oxide augite melatroctolite is medium- to coarse-grained and has similar textures to the layered olivine gabbro. It is distinguished by the presence of abundant (10 to 30 modal %) disseminated magnetite (Fig. 3-3B). The mineral composition of this unit comprises, in approximate decreasing order of abundance, olivine (20-45 modal%), plagioclase (15-30 modal%), clinopyroxene (10-20 modal%), magnetite, and apatite (<10 modal%). Olivine and clinopyroxene are euhedral, and occur between subhedral to anhedral plagioclase clusters. The oxide augite melatroctolite contains disseminated sulfide minerals (2-3 modal %) that are dominated by fine-grained pyrrhotite with trace chalcopyrite.

3.2.2.2 Marathon Series

Where the Marathon Series crosscuts Layered Series rocks in drill hole FD-13-34, intrusive contacts are sharp and lack chilled margins. The oxide melatroctolite and the apatitic (olivine) clinopyroxenite (see below) are interpreted to be part of the Marathon Series because they also commonly occur as thin lenses within the main body of the Two Duck Lake gabbro at the Marathon deposit and typically contain disseminated chalcopyrite and pyrrhotite with elevated PGE concentrations (Good et al., 2015).

The oxide melatroctolite is medium-grained and equigranular, which consists of subhedral magnetite (40-60 modal %), subhedral olivine, clinopyroxene, and plagioclase (the total of the three minerals is less than 30 modal%), and from 2 to

30 modal % euhedral apatite. Between 247.8 and 263.4 m, the oxide melatroctolite becomes coarser grained (2-3 mm) and is characterized by coarse-grained plagioclase laths that vary from 20 to 50 modal % (Fig. 3-3C).

The apatitic (olivine) clinopyroxenite is an apatite-rich rock which consists of up to 30 modal % apatite. It consists mainly of medium- to coarse- grained subhedral olivine (10-20 modal%), clinopyroxene (30-60 modal%), and magnetite (~10 modal%) with interstitial plagioclase (5-10 modal%) and euhedral apatite (Fig. 3-3D), and commonly contains disseminated pyrrhotite and chalcopyrite. Some chalcopyrite occurs intergrown with plagioclase that replaces early plagioclase (Figs. 3-3E and 3F). Chemical (EDS) analyses (discussed later) shows that the late plagioclase is more calcic than the early plagioclase.

The ophitic gabbro is coarse grained (2-4 mm) and is distinguished by an ophitic to subophitic texture. It is composed of, in approximately decreasing order of abundance, subhedral plagioclase (40-70 modal%), subhedral clinopyroxene (15-30 modal%), euhedral to subhedral olivine (5-10 modal%), and less than 10 modal% magnetite and apatite. Although this unit constitutes a major part of the Marathon Series and is the main host to the Cu-PGE mineralization at the Marathon deposit (Two Duck Lake gabbro), it occurs as thin discontinuous intrusions in the Four Dams area.

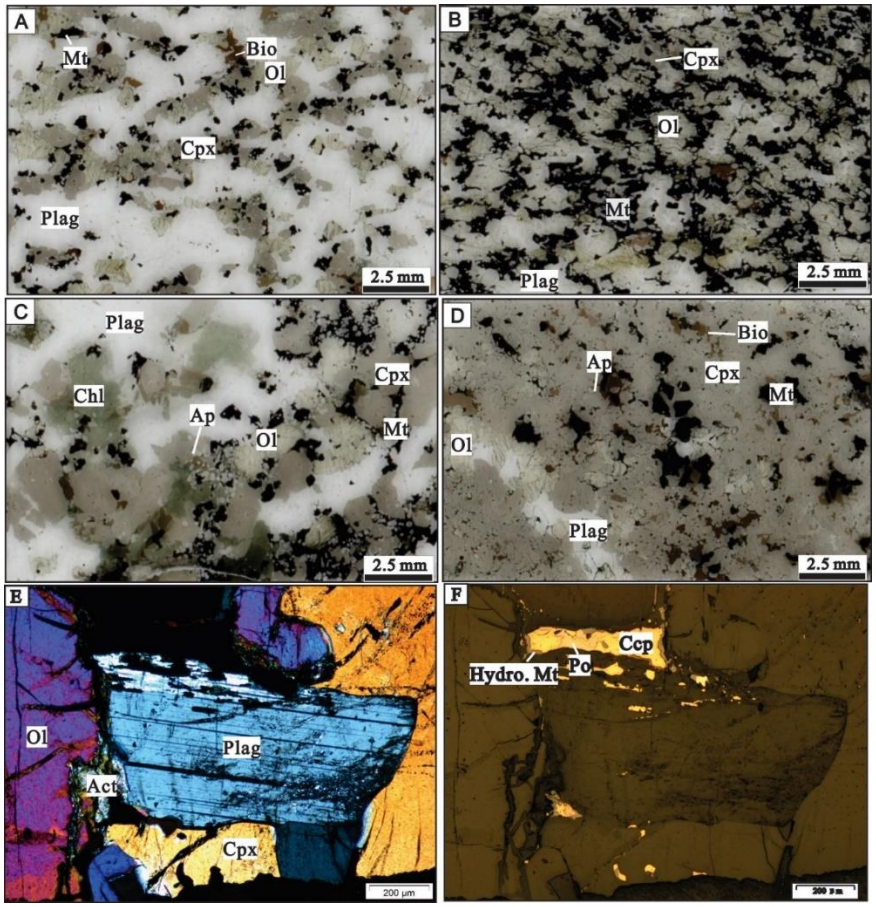

Figure 3-3. Representative thin section scans and photomicrographs from FD-13-34. (A) The Layered Series olivine gabbro with typical equigranular and intergranular texture; (B) The Layered Series oxide augite melatroctolite showing abundant magnetite (25% modal) interstitial to Ol, Cpx, and Plag; (C) The coarse-grained oxide melatroctolite of the Marathon Series within the Marker Horizon, which is relatively enriched in Plag; (D) The apatitic clinopyroxenite of the Marathon Series shows Cpx cumulates with interstitial Plag and Mt; (E) Cross-polarized transmitted light photomicrograph showing early Plag rimmed by late Plag intergrown with Ccp; (F) Reflected-light photomicrograph showing Ccp; some Ccp grains are rimmed by hydrothermal Mt. Abbreviations Ol: olivine; Cpx: clinopyroxene; Plag: plagioclase; Mt: magnetite; Chl: chlorite; Bio: biotite; Ap: apatite; Act: actinolite; Ccp: chalcopyrite; Po: pyrrhotite.

3.3 Methods

3.3.1 Sample preparation

Seventy-two powdered samples were collected by grinding 1 m-long channels along the drill core approximately 2 mm wide and 1 cm deep using a Thermo Scientific

portable grinder. Sample locations for powdered samples are given in Figure 3-2. A typical sample required 2 to 5 minutes to collect and produced ca. 10 to 200 μm of powder. A few pXRF analyses were made on powders that were re-ground, but this had little effect on the results. Samples were taken at intervals of ca. 4.5 m along the length of the drill hole. Cross-contamination was minimized by washing the collection vial, cleaning off the grinder blade, pre-contaminating the vial by grinding some of the sample, shaking the vial to coat the vial with the sample dust and dumping out the vial, and then collecting the powdered sample to be analyzed. All powders were then loaded into PREM-4331 XRF sample cups capped with 4-μm PREM-F2540 XRF sample cup films for the pXRF analysis.

The potential for contamination of Fe, Cr and Ni by the grinder blade was tested by sampling a piece of pure quartz. The pXRF analyses are presented in Table 2-2 and show that grinder blade-related contamination for most elements except Ni is insignificant, with less than 0.1 wt. % for most major elements and lower than the detection limit for trace elements. Approximately 100 ppm of Ni is added to each sample during grinding.

Twenty-three polished thin section blocks that were representative of the different gabbro units and styles of mineralization (e.g., chalcopyrite-rich, bornite-rich, and pyrrhotite-rich) were cut from drill core FD-13-34 (Fig. 3-2) for petrographic and bSEM-EDS analysis.

3.3.2 pXRF analysis

A Niton XL3t+ GOLDD+ pXRF analyzer equipped with a SDD, and a high energy, 50kV X-ray Ag anode tube was used in this study. All pXRF measurements were carried out on powders after calibrating the pXRF analyser using a suite of matrix-matched standards, including two U.S. Geological Survey reference materials, BHVO-2 basalt and W-2a diabase, and seven Marathon gabbro internal standards. This suite of standards covers a wide range of concentrations for elements measured in the current work: SiO_2, Al_2O_3, CaO, Fe_2O_3 (as total Fe), TiO_2, K_2O, P_2O_5, MgO,

Ba, V, Zr, Sr, Cu, and S. Major elements were determined using the instrument's 'mining mode', with two beams, whereas minor and trace elements were determined using the 'soil mode', with three beams; beam time for both modes was 60 s, as suggested by Hall et al. (2014) and Fisher et al. (2014). The QA/QC control throughout all analyses was carried out by analyzing two standards after each batch of unknown samples (20 samples typically). A blank standard (98.2 wt. % SiO_2) was analyzed at the beginning and the end of each batch measurement to monitor cross-contamination from the test stand and check for machine drift. Typically, a new calibration was conducted after every two batches of unknown samples. The intent was to acquire the highest quality of results and less-frequent calibration may have yielded a similar result.

3.3.3 Conventional whole-rock analysis

Whole-rock chemical analyses were carried out by the ALS Mineral Division in Vancouver on powders that were initially analyzed by pXRF. After further pulverization, major and trace elements were determined by ICP-AES and ICP-MS, after lithium borate fusion on a minimum 2 g of pulp samples. Total S was determined using a Leco combustion furnace on 0.01 to 0.1 g of sample, in which the sample is heated to roughly 1350°C in an induction furnace. SO_2 is produced through a reaction with oxygen and is measured by an infra-red detector. Ferrous Fe was determined by H_2SO_4-HF acid digestion and titration on 1 g of sample. Quality-control was achieved by analysing a wide array of standards, blanks, and duplicates after each batch of samples, in accordance with ALS geochemical quality-control procedures. Some additional data from Stillwater Canada Inc. is also used to compare S and Cu values. These were also analyzed by ALS; S by Leco, as above, and Cu by aqua regia dissolution and ICP-AES analysis.

3.3.4 Benchtop SEM-EDS analysis

The major constituents of plagioclase, clinopyroxene, and olivine were determined using a JEOL JMC-600 NeoScope SEM equipped with a JEOL JED-2300 energy

dispersive X-ray analyser at Western University. Analyses were conducted using 15 kV accelerating voltage, a high probe current, a working distance of 19 mm, and 30 to 40 μm beam size with standardless ZAF corrections. Unpolished thin section blocks were analyzed under low vacuum mode and carbon-coated polished thin sections were analyzed under high vacuum mode.

3.3.5 Electron microprobe analysis

Electron microprobe analyses were carried out using a JEOL JXA-8530F field emission probe at Western University. Microprobe analyses were conducted on the same carbon-coated polished thin sections that were analyzed by bSEM-EDS. Analyses were conducted using a 15 kV, 20 nA beam. The beam was focused to a 1 μm spot for analyzing olivine and clinopyroxene, and to a 5 μm spot for analysing plagioclase. The peak counting time was 30 s for all elements and background counts were a total of 30 s. A variety of synthetic and natural standards were used to calibrate different elements during probe analyses.

3.4 Comparison of field portable results to lab-based analyses

3.4.1 pXRF

All major and trace element concentrations determined by pXRF and by ICP-AES, ICP-MS and IR are provided in Table 3-1. The down-hole profile of pXRF data relative to lab-based data (Fig. 3-4) shows that the pXRF data broadly replicate the lithogeochemical patterns defined by the conventional data. The correlation coefficients have R^2 values of > 0.9 for all elements, except for MgO (Table 3-2). Mg is the lightest element and thus should have the poorest precision and accuracy by pXRF. However, the MgO R^2 value is 0.77, which is still a reasonable correlation between these two methods. Therefore, pXRF is able to provide analyses comparable to lab-based analyses for the elements included in the current study.

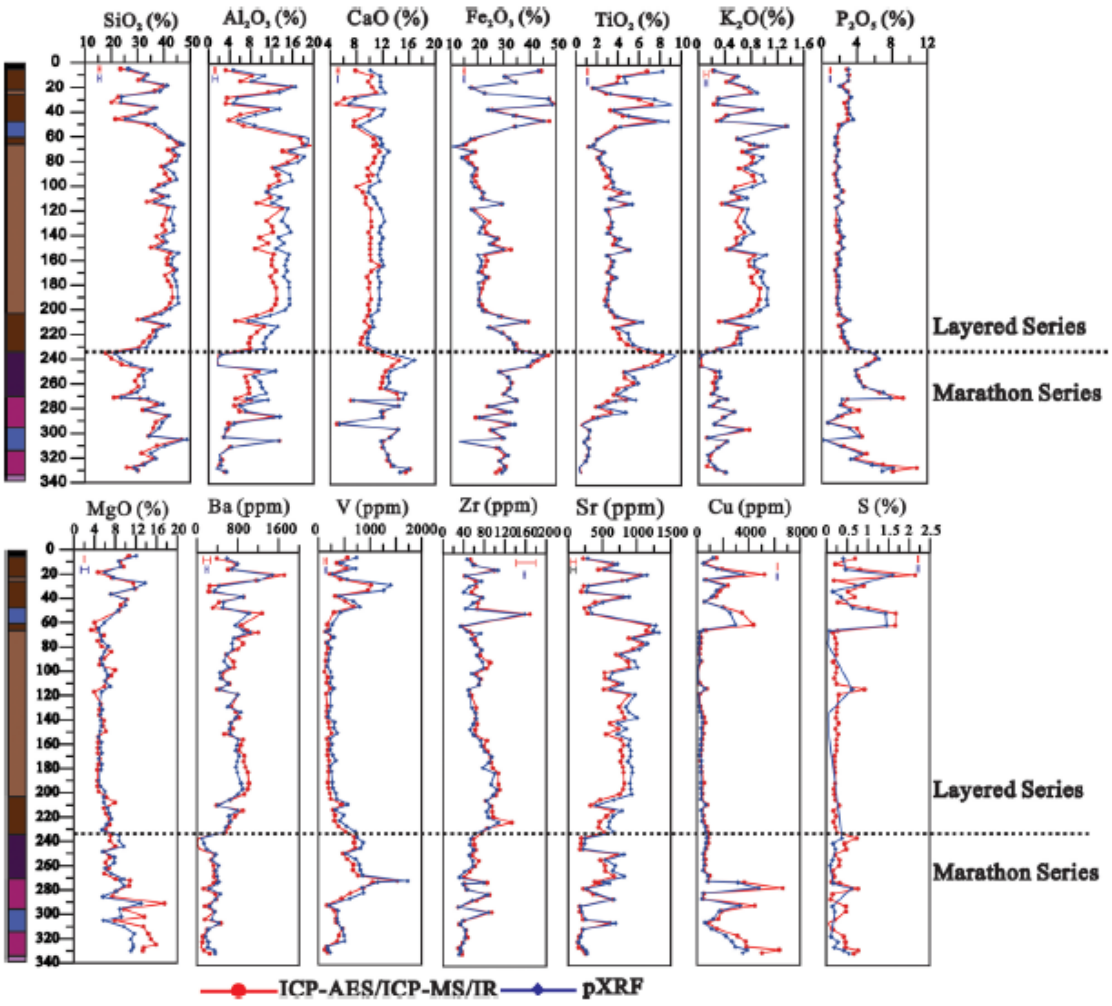

Figure 3-4. Down-hole comparisons between pXRF and ICP-AES/ICP-MS/IR whole-rock analyses, error bar (top of each diagram) represents error with 95% confidence (2σ) determined through repetitive analyses. Legend as in Figure 3-2.

To further illustrate the accuracy of the pXRF analyses, the differences of pXRF results relative to lab-based results (RD) are shown on whisker-box diagrams (Fig. 3-5). pXRF results for major elements, excluding Al_2O_3, generally have an accuracy in the range of ±20 % RD (in the 25 to 75 percentile range); accuracy for pXRF Al_2O_3 is between 10% and 35% RD (in the 25 to 75 percentile range), which is inferior to that for other major elements. For minor and trace elements, Ba, Sr and Zr have better accuracy than other elements, with the majority of RD values within ±20% (in the 25 to 75 percentile range). By contrast, the accuracy for pXRF S, V,

and Cu is inferior, and most of their RD values are outside the ±20% range (in the 25 to 75 percentile range). Since there are excellent correlations between pXRF and ICP-AES/ICP-MS/IR Al_2O_3, V, Cu, and S analyses, recalibration can be applied to improve data accuracy. Figure 3-6 shows the improvement of accuracy for pXRF Cu and S analyses after such recalibration. The pXRF data accuracy and precision reported here are similar to those evaluated by previous studies of Hall et al. (2014), Piercey and Devine (2014), and Ross et al. (2014).

Table 3-1. Comparisons of pXRF analyses with ICP-AES, ICP-MS and IR analysis for major oxides and trace elements. $Fe_2O_3^T$ means the total Fe is reported as Fe_2O_3, 95% confidence errors (2σ) are listed in brackets. RD represents relative differences between pXRF and ICP-AES, ICP-MS and IR analyses. LOD means limit of detection, nd means not determined, N/A=not available.

Depth/m	Lithology	SiO_2 (wt. %)			Al_2O_3 (wt. %)			Fe_2O_3T (wt. %)			CaO (wt. %)		
		ICP-AES (0.4)	pXRF (0.6)	RD	ICP- AES (0.3)	pXRF (0.5)	RD	ICP- AES (0.3)	pXRF (0.3)	RD	ICP- AES (0.2)	pXRF (0.09)	RD
5	Oxide augite melatroctolite	24	27	10%	3	5	47%	44	43	-2%	8	10.1	28%
9.5	Oxide augite melatroctolite	34	34	0%	8	11	30%	31	30	-1%	10	11.6	12%
14	Oxide augite melatroctolite	30	32	7%	6	8	33%	35	35	0%	10	11.7	19%
18.5	Oxide augite melatroctolite	40	41	3%	16	17	4%	18	17	-4%	10	11.7	13%
23	Olivine gabbro	37	39	4%	11	14	18%	23	23	0%	11	12.4	13%
27.5	Oxide augite melatroctolite	23	24	4%	4	5	54%	47	47	-1%	6	7.8	26%
32	Oxide augite melatroctolite	20	24	18%	3	5	47%	50	49	-3%	5	6.9	38%
36.5	Oxide augite melatroctolite	36	37	4%	11	14	21%	26	24	-6%	11	12.2	16%
41	Oxide augite melatroctolite	31	33	7%	6	9	48%	35	34	-3%	10	11.8	19%
45.5	Oxide augite melatroctolite	22	25	15%	4	6	44%	47	45	-4%	8	10.0	30%
50	Mixed olivine gabbro	34	37	8%	7	9	33%	34	35	1%	8	8.4	11%
60	Olivine gabbro	42	42	1%	18	19	9%	19	18	-7%	11	11.6	8%
64.5	Olivine gabbro	45	46	3%	18	19	6%	16	15	-7%	11	11.9	7%
66	Olivine gabbro	47	47	1%	20	18	-6%	11	10	-6%	11	11.7	10%
70.5	Olivine gabbro	42	43	3%	14	16	10%	19	18	-5%	12	12.9	12%
75	Olivine gabbro	44	46	4%	17	18	8%	16	14	-12%	11	12.2	13%
79.5	Olivine gabbro	43	45	4%	15	17	13%	18	17	-7%	11	12.0	13%
84	Olivine gabbro	39	40	3%	12	13	4%	20	19	-3%	10	11.6	20%
89.5	Olivine gabbro	41	44	7%	13	16	16%	20	18	-9%	11	11.2	7%
94.5	Olivine gabbro	42	45	7%	14	16	18%	19	18	-9%	10	11.6	15%
99	Olivine gabbro	38	40	6%	12	13	13%	21	19	-8%	8	10.0	25%
103.5	Olivine gabbro	36	35	-2%	11	11	-2%	22	23	2%	9	9.9	10%

108	Olivine gabbro	39	42	7%	12	14	16%	22	22	-3%	9	10.7	14%
112.5	Olivine gabbro	34	37	8%	9	12	32%	29	30	2%	9	11.1	18%
117	Olivine gabbro	42	44	5%	14	15	8%	19	18	-5%	10	11.7	15%
127	Olivine gabbro	41	42	3%	11	14	26%	25	23	-8%	10	12.3	19%
131.5	Olivine gabbro	40	44	9%	12	15	24%	23	22	-4%	10	11.7	14%
136	Olivine gabbro	41	44	7%	12	16	27%	24	21	-12%	10	11.5	16%
140.5	Olivine gabbro	37	40	7%	10	13	37%	28	27	-2%	10	12.0	18%
145	Olivine gabbro	40	41	3%	11	14	26%	26	25	-5%	10	11.6	15%
149.5	Olivine gabbro	35	38	8%	9	13	45%	33	30	-9%	10	11.7	16%
154	Olivine gabbro	43	46	8%	12	15	23%	23	20	-12%	10	11.6	15%
158.5	Olivine gabbro	41	43	4%	12	15	23%	24	22	-9%	10	11.8	16%
163	Olivine gabbro	41	43	4%	12	15	22%	23	21	-7%	12	12.1	5%
167.5	Olivine gabbro	44	45	3%	13	15	16%	22	20	-7%	10	11.3	10%
172	Olivine gabbro	41	43	7%	12	14	21%	24	24	-2%	10	11.3	18%
176.5	Olivine gabbro	42	45	7%	12	15	24%	22	20	-9%	10	11.7	16%
181	Olivine gabbro	43	45	5%	13	15	19%	22	21	-5%	10	11.4	15%
190	Olivine gabbro	43	45	5%	13	15	18%	21	21	0%	10	11.6	14%
194.5	Olivine gabbro	42	46	8%	13	16	22%	22	21	-6%	10	11.4	16%
199	Olivine gabbro	41	43	4%	12	15	22%	23	22	-4%	10	11.3	13%
203.5	Oxide augite melatroctolite	37	39	6%	9	12	29%	29	28	-3%	10	10.2	5%
208	Oxide augite melatroctolite	30	32	7%	5	8	49%	39	38	-3%	9	10.4	13%
212.5	Oxide augite melatroctolite	40	42	6%	11	13	25%	25	24	-3%	10	10.6	5%
217	Oxide augite melatroctolite	36	37	3%	9	12	30%	30	29	-2%	9	9.9	5%
221.5	Oxide augite melatroctolite	35	37	6%	8	11	38%	32	32	1%	9	9.7	10%
226	Oxide augite melatroctolite	32	35	7%	8	11	36%	35	34	-2%	9	9.7	13%
230.5	Oxide augite melatroctolite	31	34	9%	8	11	38%	35	34	-3%	10	11.0	11%
235	Oxide melatroctolite	18	21	19%	2	3	32%	47	45	-4%	12	14.0	17%

239.5	Oxide melatroctolite	20	23	16%	2	2	0%	43	41	-4%	15	16.8	16%
244	Oxide melatroctolite	24	28	15%	2	2	-15%	40	39	-3%	14	15.4	14%
248.5	Oxide melatroctolite	32	35	9%	10	13	34%	29	28	-2%	12	13.1	6%
253	Oxide melatroctolite	31	32	5%	7	9	23%	32	32	1%	12	12.8	6%
257.5	Oxide melatroctolite	29	33	12%	7	10	34%	33	33	-1%	12	13.0	9%
262	Oxide melatroctolite	30	33	8%	8	10	33%	32	33	2%	12	12.4	6%
266.5	Oxide melatroctolite	28	30	8%	8	11	42%	30	30	1%	14	15.5	9%
271	Oxide melatroctolite	21	24	13%	5	7	43%	35	35	0%	14	15.1	5%
272	Apatitic clinopyroxenite	31	34	10%	8	11	40%	35	35	1%	7	7.6	7%
276.5	Apatitic clinopyroxenite	37	40	6%	5	6	22%	24	25	3%	14	14.5	1%
281	Apatitic clinopyroxenite	32	33	4%	6	7	19%	31	33	6%	12	11.8	-2%
285.5	Apatitic clinopyroxenite	41	42	3%	12	14	11%	19	21	7%	12	11.9	-1%
291	Apatitic clinopyroxenite	37	40	6%	4	5	29%	32	34	6%	5	5.5	10%
295.5	Apatitic clinopyroxenite	36	38	7%	4	3	-8%	25	26	3%	14	14.4	1%
302	Breccia	34	35	1%	3	3	0%	29	30	3%	13	13.2	1%
305	Breccia	47	49	4%	14	13	-1%	13	13	0%	12	11.8	-2%
310	Breccia	37	41	8%	4	4	7%	27	28	4%	12	12.1	1%
316	Breccia	32	35	11%	2	2	0%	31	32	4%	13	12.8	0%
320.5	Apatitic olivine clinopyroxenite	36	37	3%	3	2	-12%	28	28	0%	13	13.0	2%
325	Apatitic olivine clinopyroxenite	32	33	2%	2	2	35%	31	30	-2%	13	13.7	2%
327.5	Apatitic olivine clinopyroxenite	26	29	11%	2	1	-18%	29	31	7%	16	15.9	-2%
330	Apatitic wehrlite	30	30	-1%	3	3	10%	27	29	8%	16	14.7	-5%

Table 3-1 continued

Depth/ m	MgO (wt. %)			K_2O (wt. %)			TiO_2 (wt. %)			P_2O_5 (wt. %)			S (wt. %)		
	ICP- AES (0.04)	pXRF (0.72)	RD	ICP- AES (0.03)	pXRF (0.02)	RD	ICP- AES (0.04)	pXRF (0.04)	RD	ICP- AES (0.01)	pXRF (0.07)	RD	IR (0.01)	pXRF (0.02)	RD

5	10.7	12	13%	0.2	0.2	0%	6.8	8.3	22%	2.8	3.0	7%	0.7	0.4	-43%
9.5	9.0	9	-4%	0.6	0.6	0%	4.0	4.6	15%	3.1	2.9	-6%	0.2	<LOD	N/A
14	9.6	9	-6%	0.4	0.5	25%	3.9	4.8	23%	3.0	3.0	0%	0.8	0.5	-38%
18.5	4.6	6	30%	0.7	0.8	14%	1.6	1.7	6%	2.3	2.0	-13%	2.1	1.6	-24%
23	7.3	8	5%	0.8	0.9	13%	2.9	3.3	14%	3.0	2.8	-7%	0.2	<lod	N/A
27.5	11.5	14	20%	0.3	0.3	0%	6.0	7.5	25%	3.2	3.3	3%	0.9	0.7	-22%
32	11.9	12	-3%	0.2	0.3	50%	7.2	9.1	26%	2.6	3.0	15%	0.5	0.2	-60%
36.5	7.2	7	-1%	0.9	1.0	11%	3.3	3.6	9%	2.8	3.0	7%	0.7	0.4	-43%
41	10.3	10	-2%	0.4	0.5	25%	4.4	5.0	14%	2.9	3.2	10%	0.3	<lod	N/A
45.5	9.0	10	11%	0.3	0.3	0%	7.5	8.8	17%	3.0	3.5	17%	1.0	0.6	-40%
50	8.7	9	-2%	1.3	1.4	8%	3.7	4.2	14%	1.9	2.3	21%	1.7	1.4	-18%
60	4.0	6	48%	0.6	0.6	0%	2.0	2.1	5%	1.7	1.5	-12%	1.7	1.5	-12%
64.5	4.4	5	9%	0.8	0.8	0%	1.7	1.7	0%	1.7	1.5	-12%	0.3	0.1	-67%
66	3.3	5	45%	1	1.0	0%	1.2	1.3	8%	1.5	1.5	0%	0.2	<lod	N/A
70.5	5.9	5	-12%	0.7	0.7	0%	2.6	2.7	4%	1.9	1.9	0%	0.2	<lod	N/A
75	4.6	5	17%	0.8	1.0	25%	2.1	2.2	5%	1.6	1.7	6%	0.2	<lod	N/A
79.5	5.3	7	26%	0.8	0.9	13%	2.4	2.5	4%	1.5	1.6	7%	0.2	<lod	N/A
84	7.3	6	-19%	0.6	0.7	17%	2.6	3.3	27%	1.9	2.0	5%	0.2	<lod	N/A
89.5	5.9	5	-10%	0.8	1.0	25%	3.1	3.2	3%	1.4	1.6	14%	0.2	<lod	N/A
94.5	4.9	6	12%	0.9	1.0	11%	3.4	3.6	6%	1.6	1.7	6%	0.3	<lod	N/A

99	8.0	6	-24%	0.6	0.8	33%	2.8	3.6	29%	1.7	1.9	12%	0.2	<lod	N/A
103.5	7.3	7	-10%	0.5	0.5	0%	4.3	5.1	19%	2.4	2.2	-8%	0.2	<lod	N/A
108	6.1	6	-2%	0.6	0.7	17%	3.4	3.2	-6%	1.5	1.7	13%	0.2	<lod	N/A
112.5	5.9	7	19%	0.4	0.4	0%	4.7	5.3	13%	2.3	2.3	0%	0.9	0.6	-33%
117	3.9	5	36%	0.7	0.7	0%	3.1	2.9	-6%	1.6	1.6	0%	0.3	<lod	N/A
127	5.2	5	-4%	0.6	0.7	17%	3.4	3.5	3%	1.6	2.1	31%	0.3	<lod	N/A
131.5	4.9	6	12%	0.6	0.8	33%	3.1	3.4	10%	1.6	1.8	13%	0.3	0.1	-67%
136	4.9	5	4%	0.7	0.8	14%	3.2	3.0	-6%	1.7	2.0	18%	0.2	<lod	N/A
140.5	5.9	5	-12%	0.6	0.7	17%	3.8	4.2	11%	2.2	2.5	14%	0.3	<lod	N/A
145	5.6	5	-5%	0.6	0.6	0%	3.6	3.8	6%	1.9	2.1	11%	0.2	<lod	N/A
149.5	6.2	5	-19%	0.4	0.5	25%	4.9	5.2	6%	2.4	2.5	4%	0.3	0.1	-67%
154	4.7	5	2%	0.9	1.0	11%	3.1	2.9	-6%	1.6	1.8	13%	0.2	<lod	N/A
158.5	4.7	5	13%	0.8	0.8	0%	3.4	3.6	6%	1.8	2.1	17%	0.2	<lod	N/A
163	4.6	5	11%	0.8	0.8	0%	3.3	3.5	6%	1.9	2.1	11%	0.2	<lod	N/A
167.5	4.6	5	17%	0.9	1.0	11%	3.0	3.1	3%	1.5	1.6	7%	0.2	<lod	N/A
172	5.0	5	-4%	0.8	0.9	13%	3.4	3.9	15%	1.6	1.9	19%	0.2	<lod	N/A
176.5	4.7	5	13%	0.8	1.0	25%	3.2	3.0	-6%	1.7	1.9	12%	0.2	<lod	N/A
181	4.5	5	16%	0.9	1.0	11%	3.0	3.2	7%	1.8	2.0	11%	0.2	<lod	N/A
190	4.5	5	7%	0.9	1.0	11%	2.8	3.0	7%	1.7	1.8	6%	0.2	<lod	N/A
194.5	4.6	5	11%	0.9	1.0	11%	3.0	2.8	-7%	1.7	1.8	6%	0.2	<lod	N/A
199	4.8	6	25%	0.8	0.9	13%	3.3	3.4	3%	2.0	2.0	0%	0.2	<lod	N/A
203.5	6.3	6	-8%	0.7	0.8	14%	3.7	4.0	8%	1.8	2.2	22%	0.2	<lod	N/A
208	7.9	6	-27%	0.3	0.4	33%	5.5	6.3	15%	2.8	3.2	14%	0.3	<lod	N/A

212.5	5.8	7	12%	0.8	0.9	13%	3.5	3.9	11%	1.9	2.2	16%	0.2	<lod	N/A
217	6.2	7	10%	0.6	0.6	0%	4.1	4.9	20%	2.3	2.4	4%	0.2	<lod	N/A
221.5	6.9	7	6%	0.6	0.6	0%	4.2	5.0	19%	2.2	2.5	14%	0.2	<lod	N/A
226	6.9	6	-9%	0.5	0.6	20%	4.9	5.4	10%	2.7	2.9	7%	0.2	<lod	N/A
230.5	6.1	5	-11%	0.3	0.3	0%	6.0	6.9	15%	3.1	3.3	6%	0.3	<lod	N/A
235	7.1	9	23%	nd	nd	nd	8.2	9.5	16%	6.0	6.0	0%	0.7	0.4	-43%
239.5	7.0	9	24%	nd	nd	nd	7.8	8.8	13%	6.1	6.5	7%	0.4	0.2	-50%
244	8.0	10	20%	nd	nd	nd	6.5	7.3	12%	5.1	5.3	4%	0.5	0.2	-60%
248.5	5.9	6	-5%	0.3	0.3	0%	4.6	4.7	2%	3.9	3.8	-3%	0.2	<lod	N/A
253	6.9	8	14%	0.3	0.3	0%	4.6	5.6	22%	4.1	3.9	-5%	0.3	0.1	-67%
257.5	6.1	8	28%	0.2	0.3	50%	5.5	5.9	7%	4.4	4.3	-2%	0.3	0.1	-67%
262	6.7	6	-10%	0.3	0.3	0%	4.0	4.8	20%	4.9	4.7	-4%	0.1	<lod	N/A
266.5	5.9	7	22%	0.2	0.2	0%	3.6	3.9	8%	6.6	7.0	6%	0.2	<lod	N/A
271	8.1	10	20%	0.4	0.4	0%	4.8	5.7	19%	9.2	7.8	-15%	0.1	<lod	N/A
272	10.9	9	-18%	0.3	0.3	0%	3.0	3.8	27%	2.9	2.3	-21%	0.3	0.2	-33%
276.5	10.7	10	-9%	0.2	0.2	0%	1.9	2.2	16%	2.4	2.1	-13%	0.8	0.6	-25%
281	8.2	8	-1%	0.5	0.5	0%	3.3	4.7	42%	4.2	3.2	-24%	0.2	<lod	N/A
285.5	7.4	6	-24%	0.4	0.4	0%	1.6	2.1	31%	2.3	1.8	-22%	0.1	<lod	N/A
291	17.6	13	-26%	0.3	0.2	-33%	0.5	0.6	20%	0.7	0.7	0%	0.5	0.1	-80%

295.5	9.6	9	-7%	0.8	0.7	-13%	1.3	1.3	0%	4.0	3.2	-20%	0.5	0.2	-60%
302	13.7	9	-34%	0.1	0.1	0%	1.2	1.1	-8%	4.6	4.2	-9%	0.2	<lod	N/A
305	7.9	6	-28%	0.4	0.4	0%	0.8	0.8	0%	0.2	0.2	0%	0.1	<lod	N/A
310	13.5	10	-28%	0.3	0.3	0%	1.2	1.2	0%	2.5	2.2	-12%	0.2	<lod	N/A
316	14.4	12	-19%	0.2	0.1	-50%	1.1	1.2	9%	5.1	4.6	-10%	0.4	0.1	-75%
320.5	14.9	11	-26%	0.2	0.2	0%	0.9	0.9	0%	3.8	3.3	-13%	0.5	0.3	-40%
325	15.9	12	-28%	0.1	0.2	100%	0.4	0.4	0%	7.0	5.7	-19%	0.5	0.2	-60%
327.5	13.5	11	-16%	0.3	0.3	0%	0.4	0.3	-25%	10.8	8.1	-25%	0.8	0.4	-50%
330	13.4	11	-18%	0.4	0.4	0%	0.5	0.4	-20%	8.1	6.9	-15%	0.7	0.5	-29%

Table 3-1 continued.

Depth	Ba (ppm)			Sr (ppm)			V (ppm)			Zr (ppm)			Cu (ppm)		
	ICP-MS (69)	pXRF (22)	RD	ICP-MS (43)	pXRF (36)	RD	ICP-MS (30)	pXRF (22)	RD	ICP-MS (19)	pXRF (2)	RD	ICP-MS (10)	pXRF (44)	RD
5	392	590	50%	220	286	30%	559	738	32%	53	47	-12%	1505	1245	-17%
9.5	786	798	2%	650	719	11%	353	422	20%	60	58	-3%	580	454	-22%
14	611	681	11%	441	532	21%	543	724	33%	99	107	8%	1935	1547	-20%
18.5	1710	1475	-14%	1050	1146	9%	221	274	24%	42	44	5%	5220	3604	-31%
23	1155	1206	4%	788	862	9%	427	561	31%	63	75	18%	702	545	-22%
27.5	248	434	75%	227	293	29%	1020	1403	38%	64	51	-21%	2410	2076	-14%
32	233	337	45%	193	271	41%	963	1263	31%	55	40	-28%	1740	1489	-14%
36.5	913	898	-2%	799	888	11%	323	399	23%	74	77	4%	1490	1193	-20%
41	432	519	20%	392	507	29%	513	675	32%	67	58	-13%	555	559	1%

45.5	307	503	64%	238	312	31%	686	804	17%	66	44	-34%	2050	1933	-6%
50	1270	1017	-20%	283	346	22%	304	421	39%	168	158	-6%	3480	2570	-26%
60	866	757	-13%	1185	1280	8%	169	266	58%	37	33	-10%	4370	2978	-32%
64.5	985	914	-7%	1140	1239	9%	197	227	15%	52	47	-9%	686	455	-34%
66	1200	1038	-13%	1230	1323	8%	128	147	15%	56	73	30%	241	194	-20%
70.5	791	720	-9%	882	956	8%	257	301	17%	61	54	-12%	280	179	-36%
75	906	687	-24%	1075	1152	7%	150	173	15%	65	62	-5%	263	176	-33%
79.5	800	702	-12%	947	1039	10%	189	249	32%	74	75	1%	207	134	-35%
84	570	588	3%	698	771	10%	154	214	39%	71	65	-8%	176	146	-17%
89.5	699	532	-24%	862	968	12%	141	195	38%	89	76	-14%	265	244	-8%
94.5	723	629	-13%	884	1015	15%	152	170	12%	84	78	-7%	164	97	-41%
99	508	455	-11%	530	648	22%	116	236	104%	64	55	-14%	103	86	-16%
103.5	488	468	-4%	538	605	12%	178	259	45%	73	71	-3%	117	108	-8%
108	630	612	-3%	719	792	10%	157	224	43%	69	69	0%	180	109	-39%
112.5	394	445	13%	517	617	19%	229	302	32%	50	49	-2%	770	622	-19%
117	796	804	1%	886	977	10%	146	226	55%	55	51	-7%	188	133	-30%
127	680	602	-12%	743	841	13%	173	247	43%	64	56	-13%	231	174	-25%
131.5	763	858	12%	786	883	12%	161	206	28%	63	62	-1%	346	233	-33%
136	828	759	-8%	821	1006	23%	161	190	18%	63	64	2%	532	365	-31%
140.5	656	667	2%	609	726	19%	198	310	57%	66	59	-11%	621	419	-33%
145	704	643	-9%	731	846	16%	207	297	43%	62	52	-15%	418	299	-29%
149.5	532	649	22%	552	716	30%	254	367	44%	62	59	-5%	505	389	-23%
154	901	814	-10%	770	904	17%	164	226	38%	85	73	-15%	420	283	-33%
158.5	859	785	-9%	807	877	9%	197	264	34%	79	74	-6%	344	279	-19%
163	824	761	-8%	764	911	19%	185	232	25%	86	81	-6%	329	253	-23%
167.5	929	827	-11%	795	908	14%	175	274	57%	92	94	3%	241	206	-15%
172	914	790	-14%	765	869	14%	207	340	64%	93	89	-5%	264	328	24%

176.5	946	763	-19%	799	929	16%	206	230	11%	96	77	-20%	312	261	-16%
181	995	792	-20%	807	934	16%	196	253	29%	107	100	-7%	350	271	-23%
190	1015	866	-15%	819	900	10%	183	271	48%	107	93	-13%	542	289	-47%
194.5	995	897	-10%	802	912	14%	199	283	42%	109	104	-5%	352	277	-21%
199	927	803	-13%	750	926	23%	224	338	51%	102	97	-5%	439	327	-26%
203.5	649	639	-2%	468	663	42%	239	352	47%	83	84	2%	349	279	-20%
208	385	415	8%	324	408	26%	448	563	26%	94	91	-3%	796	655	-18%
212.5	897	802	-11%	649	786	21%	285	327	15%	95	85	-11%	367	309	-16%
217	745	626	-16%	559	651	16%	320	488	53%	97	87	-10%	493	419	-15%
221.5	643	656	2%	461	601	30%	309	405	31%	133	107	-20%	521	362	-30%
226	616	559	-9%	446	587	32%	383	542	42%	86	89	3%	758	631	-17%
230.5	561	531	-5%	533	678	27%	522	709	36%	75	62	-17%	855	665	-22%
235	37	83	124%	192.5	251	31%	708	751	6%	58	53	-8%	881	759	-14%
239.5	15.8	139	700%	189	240	27%	691	865	25%	60	52	-14%	893	700	-22%
244	55.3	190	240%	178.5	223	25%	716	815	14%	63	59	-6%	715	626	-12%
248.5	348	372	7%	714	816	14%	474	519	10%	56	51	-9%	549	446	-19%
253	275	292	6%	469	544	16%	554	722	30%	69	58	-16%	646	498	-23%
257.5	323	423	31%	538	691	28%	680	793	17%	61	58	-5%	610	542	-11%
262	340	372	9%	542	650	20%	670	813	21%	52	42	-20%	517	444	-14%
266.5	333	399	20%	668	818	22%	765	852	11%	41	32	-23%	984	847	-14%
271	388	434	12%	389	510	31%	1530	1730	13%	85	79	-7%	883	800	-9%
272	327	398	22%	457	602	32%	1050	1154	10%	42	39	-8%	3660	3173	-13%
276.5	128.5	240	87%	220	268	22%	874	842	-4%	46	46	1%	6640	4781	-28%
281	361	458	27%	365	415	14%	621	872	40%	90	86	-5%	545	438	-20%
285.5	384	363	-6%	646	671	4%	447	607	36%	65	57	-13%	486	364	-25%
291	150.5	246	63%	172.5	182	5%	163	211	30%	29	30	3%	4480	3312	-26%
295.5	342	349	2%	173	199	15%	314	381	21%	94	88	-7%	1920	1753	-9%

302	151.5	289	91%	216	261	21%	341	363	6%	41	38	-7%	1635	1235	-24%
305	465	429	-8%	607	693	14%	344	374	9%	31	34	9%	880	592	-33%
310	203	226	11%	211	221	5%	463	455	-2%	44	43	-1%	1535	1132	-26%
316	115	168	46%	165.5	183	11%	396	495	25%	47	43	-9%	3130	2231	-29%
320.5	109.5	224	104%	143	153	7%	367	506	38%	38	40	4%	3760	2711	-28%
325	80.7	213	164%	157	214	36%	157	177	12%	29	33	13%	3840	2960	-23%
327.5	139.5	343	146%	224	261	17%	118	184	56%	36	35	-4%	6370	3904	-39%
330	250	356	42%	255	275	8%	178	232	30%	37	31	-17%	5030	3539	-30%

Table 3-2. Comparison of pXRF analyses and ICP-MS/ICP-AES/IR analyses. Shown are the lineation equations correlating pXRF results (y) with ICP-MS results (x), and their respective coefficients of determination (R^2).

Elements/oxide	Mode	Equation	R^2
SiO_2	Mining	y=0.9578x+3.587	0.98
Al_2O_3	Mining	y=1.0628x+0.947	0.95
CaO	Mining	y=0.8514x+2.678	0.90
Fe_2O_3T	Mining	y=1.0067x-0.767	0.98
TiO_2	Mining	y=1.195x-0.2626	0.98
K_2O	Mining	y=1.0954x-0.0002	0.96
P_2O_5	Mining	y=0.8136x+0.4919	0.95
MgO	Mining	y=0.6456x+2.4318	0.78
Ba	Soil	y=0.7439x+145.01	0.94
V	Soil	y=1.1373x+44.61	0.97
Zr	Soil	y=0.906x+1.6914	0.92
Sr	Soil	y=1.0678x+52.782	0.98
Cu	Soil	y=0.7065x+61.577	0.98
S	Soil	y=0.8683x-0.1606	0.96

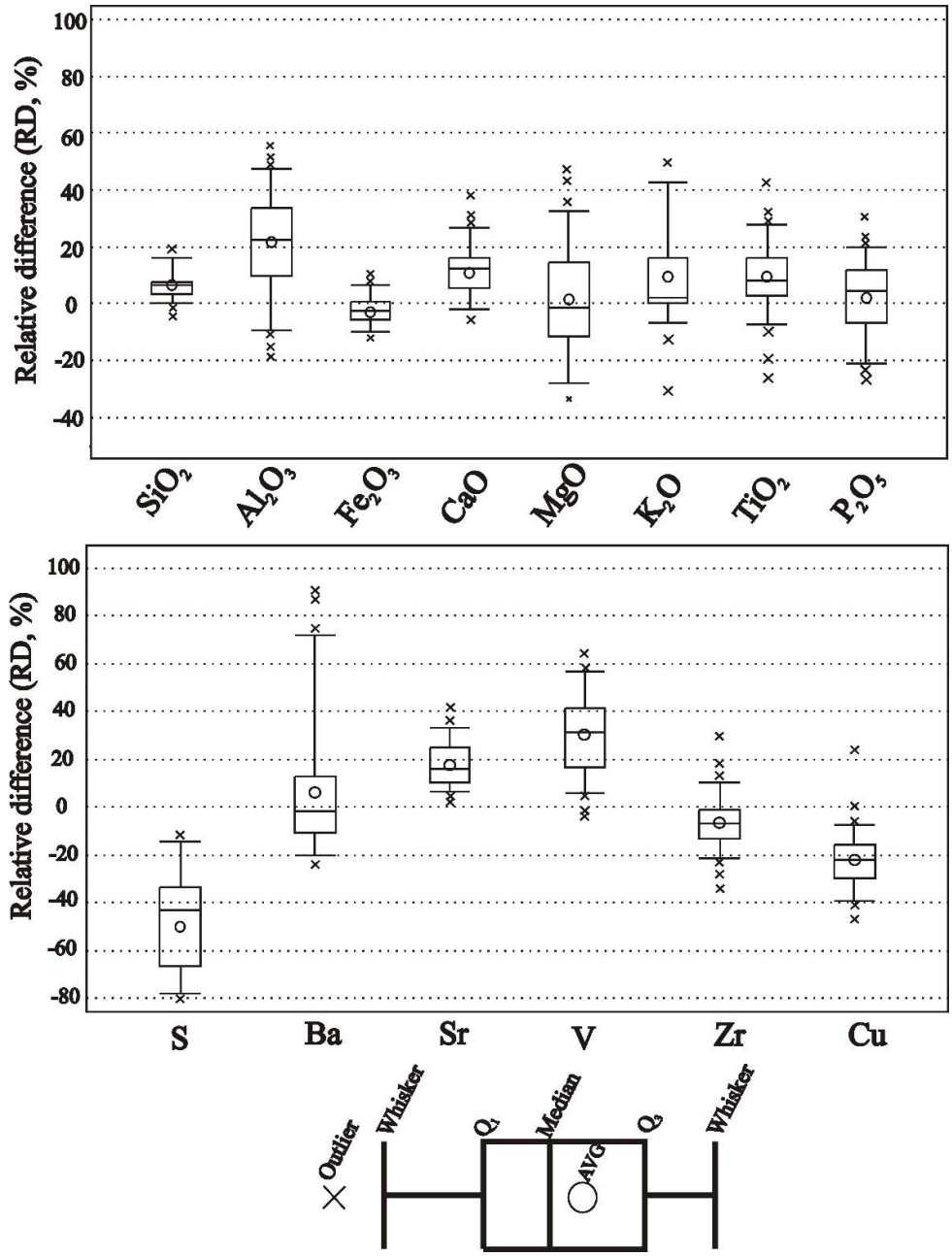

Figure 3-5. Box-and-whisker diagram showing relative differences between pXRF and ICP-AES/ICP-MS/IR whole-rock analyses for selected major and trace elements. Box and whisker plots are uniform in their use of the box: the bottom and top of the box are always the 25th and 75th percentile (the lower and upper quartiles, respectively), and the band near the middle of the box is always the 50th percentile (the median). The small circle is the average and the lines on the ends are the minimum and maximum values, crosses are outliers.

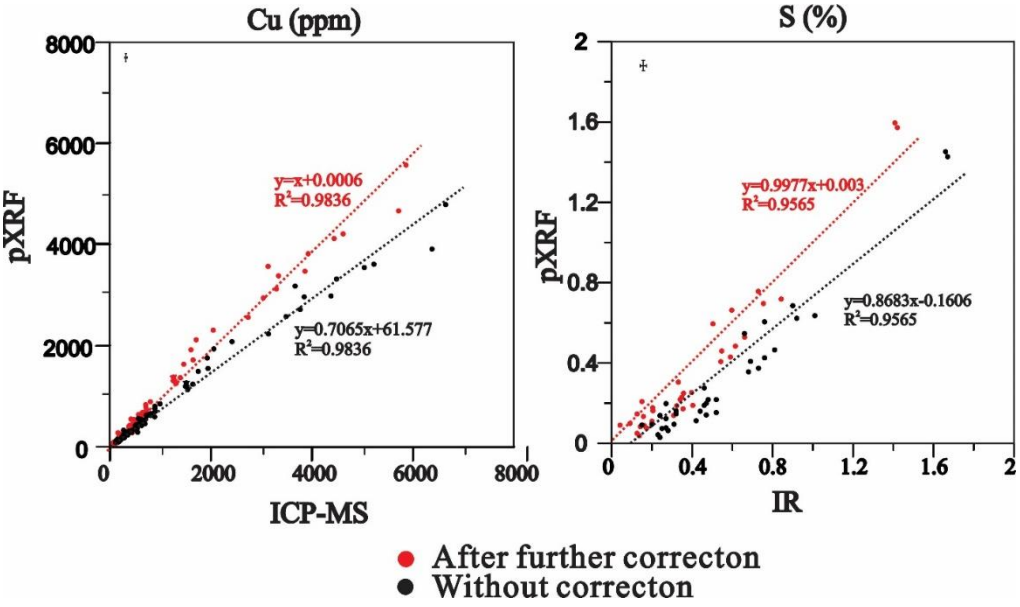

Figure 3-6. Binary diagrams correlating pXRF analyses with ICP-MS/IR whole-rock analyses for Cu and S before and after further corrections.

3.4.2 Benchtop SEM

It is not possible to carry out a full calibration and ZAF correction with matrix-matched materials using the bSEM-EDS. However, mineral ratios rather than absolute concentrations are commonly used to examine mineral chemical variations in suites of magmatic rocks. In this study the Mg#s (molar MgO/(MgO+FeO)*100) of olivine and clinopyroxene, and the An% (molar Ca/(Ca+Na)*100) of plagioclase were determined, because these are useful indices for assessing magma evolution and mechanisms for forming magmatic PGE mineralization (Barnes, 2004; Mungall and Naldrett, 2008). The highest quality bSEM-EDS data will be obtained from carbon-coated polished thin sections, but unpolished cut blocks were also analyzed to establish field portability. Consequently, Mg#s of olivine and clinopyroxene, and An% of plagioclase determined by bSEM-EDS for carbon-coated polished thin sections and unpolished blocks are compared to electron microprobe data (Table 3-3 and Figure 3-7).

The precision of electron microprobe analyses was determined by analyzing the same spot 10 times: results are ±0.07 for Mg# of olivine, ±0.30 for Mg# of

clinopyroxene, and ±0.15 for plagioclase An% (1 sigma standard deviation). These standard deviations (machine error) are well below the sample variability that were determined through wavelength-dispersive spectrometer (WDS) analyses conducted on 3 or 4 grains of each mineral type in each sample (Table 3-3). Machine error for bSEM-EDS analyses of carbon coated polished thin sections are 0.51 for Mg# of olivine, ±1.0 for Mg# of clinopyroxene, and ±0.63 for An% of plagioclase (1 sigma standard deviation). These values are higher than those for the electron microprobe. The sum of the standard deviation of natural variation of all three minerals (determined from 3 or 4 grains per sample) and the machine error for the electron microprobe analyses is < ±1 to ±3, compared to ±1 to ±4 for bSEM-EDS analysis for carbon coated polished thin sections (Table 3-3, Figure 3-7).

For the bSEM-EDS analysis of unpolished blocks it is necessary to use the low vacuum mode to reduce charge build-up from electrons accumulated on non-carbon coated surfaces, but nevertheless it is possible to measure a mineral directly in the field. Considering that rough surfaces will diffract X-rays from the detector, which results in artificially low measured concentrations (Morros, 2009; Fisher et al, 2014), it is difficult to make accurate measurements on unpolished blocks. Whereas data accuracy may be lower for unpolished blocks, the data may still be of sufficient quality to aid decision making in the field. To evaluate this, we first determined the machine error of Mg#s for olivine and clinopyroxene and An% for plagioclase by repeat analysis of single grains in the unpolished blocks. These errors are ±1.9 for Mg# of olivine, ±1.7 for Mg# for clinopyroxene and ±2.0 for An% (1 sigma standard deviation). As anticipated, the errors are higher than those from carbon coated polished thin sections, but they are still of high enough precision to be useful for mapping igneous stratigraphy. Next, the bSEM-EDS analyses of 11 unpolished blocks are compared to their probe counterparts conducted on corresponding carbon-coated polished thin sections (Table 3-3 and Fig. 3-7). The correlation between bSEM-EDS and probe analyses is excellent (R^2>0.9) for Mg#s of olivine

and clinopyroxene, and reasonable (R^2=0.69) for An% of plagioclase, indicating bSEM-EDS analyses of unpolished blocks are comparable to their probe counterparts. However, where unpolished blocks were analyzed, repeated measurements of different mineral grains in each sample show higher variability compared to analyses of carbon-coated polished thin sections. Standard deviation values of the above ratios for unpolished blocks (combination of machine error and natural variability) are typically between 3 and 8. However, the analysis of unpolished blocks is of sufficient precision to aid exploration geologists with decision- making in the field and it should be possible to improve analyses from cut blocks by polishing them in the field.

We have also compared bSEM-EDS analyses of carbon-coated polished thin sections to microprobe analyses, with both sets of analyses conducted on the same grains (Table 3-3 and Fig. 3-7). The correlations between bSEM-EDS and electron microprobe analyses are excellent for Mg# of olivine (R^2=0.90) and An content of plagioclase (R^2=0.85), and reasonable for Mg# of clinopyroxene (R^2=0.73).

In addition, sample precision for bSEM-EDS analyses of carbon-coated polished thin sections are improved substantially when compared to bSEM-EDS analyses of unpolished blocks (Table 3-3 and Fig. 3-7). Figure 3-8 compares down-hole variations in Mg#s of olivine and clinopyroxene, and An% of plagioclase between probe analyses and bSEM-EDS of unpolished blocks and carbon-coated polished thin sections. The carbon-coated polished thin sections (bSEM-EDS) and probe analyses methods display broadly similar down-hole variations throughout the igneous stratigraphy, including both the Layered Series and the Marathon Series, indicating interpretations regarding the igneous stratigraphy based on bSEM-EDS analyses will be comparable to their probe counterparts. Fewer data points were collected from unpolished blocks, but the downhole variation is similar to bSEM-EDS analyses from carbon-coated polished thin sections. However, it must be kept in mind that bSEM-EDS analysis in the current work is semi-quantitative, without

calibration using standards, and, in addition, peak overlaps (e.g., overlaps for Cr, Ti, V) are common issues for EDS analysis. The data quality of bSEM-EDS analysis will therefore inevitably be less accurate and precise than those determined from WDS analysis on an electron microprobe, particularly with respect to data accuracy.

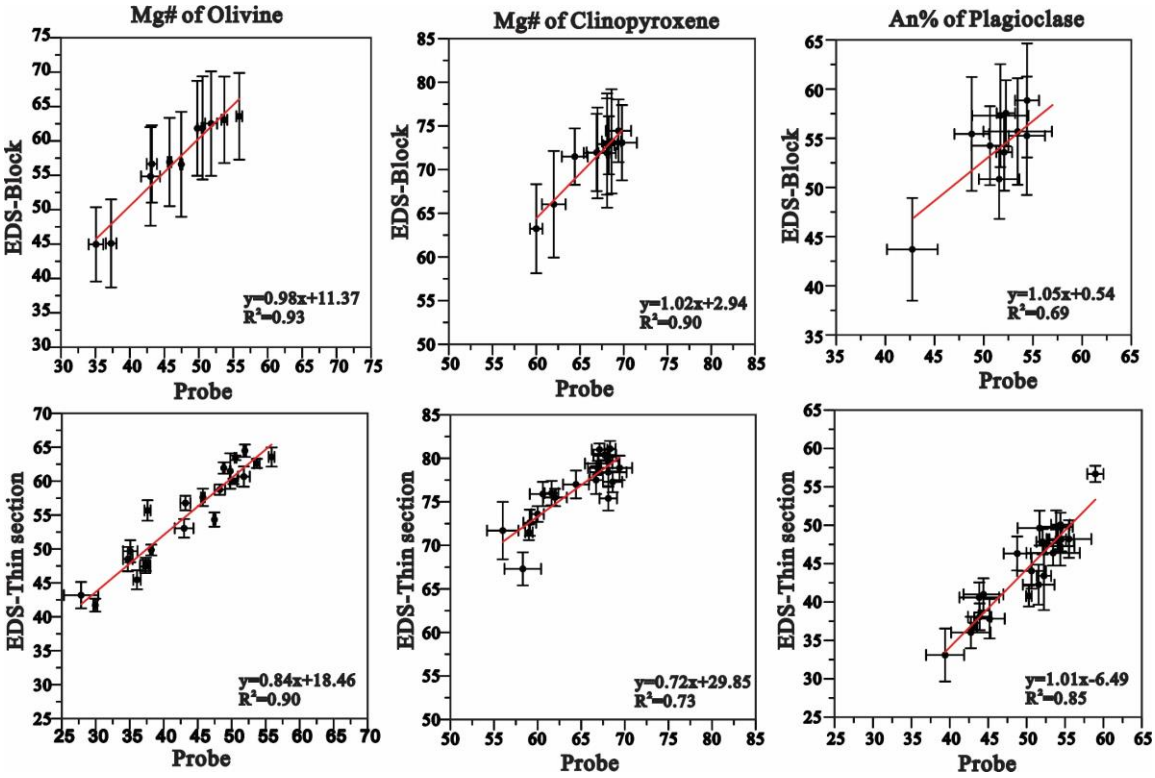

Figure 3-7. Correlation between bSEM-EDS and probe analyses, EDS analyses were conducted on unpolished blocks and carbon-coated polished thin sections separately. The red line represents the best-fit regression line correlating EDS analyses with probe analyses. Error bars represents 1σ sample errors determined through EDS analyses conducted on 3 or 4 grains of each mineral type in each sample, and multiple spot analyses were conducted on each mineral grain. Average values are correlated in this figure.

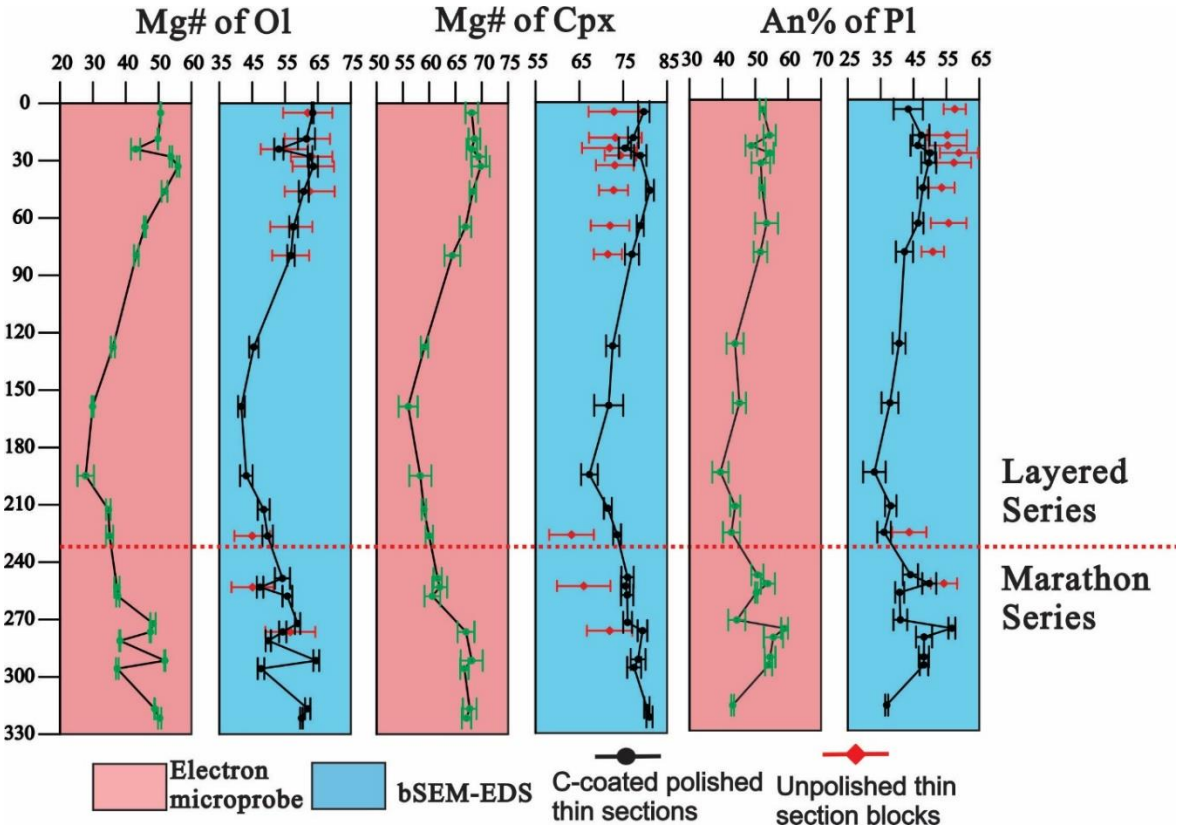

Figure 3-8. Down-hole comparisons between bSEM-EDS (unpolished thin section blocks and carbon-coated polished thin sections) and WDS electron microprobe analyses.

Table 3-3. Comparison of mineral chemical data from electron microprobe with bSEM-EDS analyses of carbon-coated polished thin sections and unpolished offcut blocks, nd means not determined, AVG means average values, SD means 1 σ sample errors determined through EDS analyses conducted on 3 or 4 grains of each mineral type in each sample, and multiple spot analyses were conducted on each mineral grain.

Depth/m	Lithology	Probe						bSEM-EDS-polished thin section						bSEM-EDS-offcut block					
		Mg# of Ol		Mg# of Cpx		An% of Pl		Mg# of Ol		Mg# of Cpx		An% of Pl		Mg# of Ol		Mg# of Cpx		An% of Pl	
		AVG	SD	AVG	SD	AVG	SD	AVG	SD	AVG	SD	AVG	SD	AVG	SD	AVG	SD	AVG	SD
5	Oxide augite melatroctolite	50.6	0.1	68.1	1.2	52.3	0.9	63.4	0.3	79.7	1.3	43.4	4.5	61.9	7.5	72.9	5.8	57.5	3.7
18.6	Oxide augite melatroctolite	49.8	0.1	68.6	1.1	54.4	1.8	61.5	2.6	77.3	1.2	47.3	2.5	61.8	6.9	73.2	6	55.3	6.0
24	Olivine gabbro	43	1.4	68.1	1	48.8	1.8	53.1	1.4	75.4	1.4	46.3	2.2	54.8	7.2	71.9	6.3	55.4	5.8
27.9	Oxide augite melatroctolite	53.7	0.4	69.4	1.4	54.4	1.2	62.6	0.7	78.9	1.4	50.1	1.6	63.1	6.3	74.4	3.6	58.8	5.8
33	Oxide augite melatroctolite	55.9	0.4	69.8	1.7	51.7	2.9	63.6	1.4	nd	nd	49.6	2.3	63.6	6.3	73.1	4.3	57.3	5.2
46.1	Oxide augite melatroctolite	51.8	0.9	68.3	0.6	52.1	0.8	60.7	1.5	81.1	0.9	47.8	1.6	62.5	7.6	72.8	3.3	53.6	3.9
64.6	Oxide augite melatroctolite	45.8	0.3	66.9	1.1	53.4	3.5	57.6	1.3	78.9	0.8	46.4	1.6	56.9	6.4	72	4.4	55.7	5.4
79.6	Olivine gabbro	43.2	0.7	64.4	1.5	51.6	2.1	56.8	1.1	77	1.6	42.3	2.6	56.7	5.6	71.5	3.2	50.9	3.4
127.5	Olivine gabbro	36.1	0.6	59.1	0.7	43.8	2.6	45.5	1.4	72.6	1.5	40.6	2.0	nd	nd	nd	nd	nd	nd
158.6	Olivine gabbro	29.9	0.3	56	1.8	45.2	2.0	41.7	1	71.7	3.3	37.8	2.6	nd	nd	nd	nd	nd	nd
194.8	Olivine gabbro	27.8	2.5	58.3	2.1	39.4	2.5	43.2	1.9	67.3	1.9	33.1	3.4	nd	nd	nd	nd	nd	nd
212.5	Oxide augite melatroctolite	34.7	0.7	59	0.4	43.9	1.5	48.5	1.8	71.5	0.9	38.1	1.7	nd	nd	nd	nd	nd	nd
226.3	Oxide augite melatroctolite	35.1	1.1	60	0.7	42.7	2.6	49.7	1.6	73.6	0.9	36.0	2.1	45	5.4	63.2	5.1	43.7	5.2
248.5	Oxide melatroctolite	nd	nd	61.6	0.8	50.6	1.9	54.2	2.3	76	1.4	44.0	2.3	nd	nd	nd	nd	nd	nd
253.1	Oxide melatroctolite	37.3	0.8	62	1.4	53.9	2.1	47.4	1	75.5	1	49.8	2.1	45.1	6.4	66	6.1	54.2	4.0
257.8	Oxide melatroctolite	37.6	0.5	60.6	1.5	50.3	0.4	55.7	1.5	75.9	1.4	40.8	1.4	nd	nd	nd	nd	nd	nd
272.1	Apatitic clinopyroxenite	48.3	0.8	nd	nd	44.4	2.6	58.8	0.8	76	1	41.0	2.1	nd	nd	nd	nd	nd	nd
276.5	Apatitic clinopyroxenite	47.5	0.2	67	1.6	58.9	1.1	54.3	1.1	79.4	1.1	56.7	1.1	56.6	7.6	71.9	5.2	nd	nd

281.1	Apatitic clinopyroxenite	38.2	0.2	nd	nd	55.5	2.9	49.9	0.8	nd	nd	48.2	2.4	nd	nd	nd	nd	nd	nd
291.5	Apatitic clinopyroxenite	51.9	0.2	68.1	2.1	54.5	1.7	64.5	0.9	78.4	1.7	48.1	1.6	nd	nd	nd	nd	nd	nd
295.7	Apatitic clinopyroxenite	37.4	0.4	66.7	0.8	54.1	1.1	47.7	1	77.5	1.6	48.2	1.3	nd	nd	nd	nd	nd	nd
316.7	Apatitic olivine clinopyroxenite	48.8	0.1	67.7	1.3	43.1	0.4	61.9	0.8	80.4	0.6	36.8	0.4	nd	nd	nd	nd	nd	nd
321.6	Apatitic olivine clinopyroxenite	50.3	0.5	67.1	0.9	nd	nd	60	0.4	81	0.7	43.4	4.5	nd	nd	nd	nd	nd	nd

3.5 Geochemistry of igneous stratigraphy

3.5.1 Lithogeochemistry

As shown above, the variation of the molar Mg#s for olivine and clinopyroxene is important. However, it is difficult to estimate this ratio for whole-rock compositions because of the presence of magnetite. However, most of the whole-rock TiO_2 is contained in magnetite. The laboratory analyses include the determination of FeO by titration from which the whole-rock Fe_2O_3 was calculated by difference from total Fe_2O_3. Figure 3-9 shows a linear correlation between laboratory-based Fe_2O_3 and TiO_2. The data was fit by a least square to a linear equation: Fe_2O_3 (wt. %) = 1.3966TiO_2 (wt. %) + 1.2732. This equation was then applied to pXRF TiO_2 data to deduce pXRF Fe_2O_3 concentrations, after which, the pXRF FeO data was calculated by subtracting pXRF Fe_2O_3 from pXRF total Fe_2O_3. This allowed pXRF whole-rock Mg numbers to be calculated: $Mg\#_{WR}$ is molar MgO /(MgO+FeO)*100 (Table 3-4).

Table 3-4. pXRF whole-rock V/Ti, FeO, and $Mg\#_{WR}$ of different rock units down drill hole FD-13-34.

Depth/m	Lithology	V/Ti	2σ error*	FeO (wt. %) (2σ =0.56）	$Mg\#_{WR}$	2σ error
5.00	Oxide augite melatroctolite	0.01	0.000	32	40.6	2.66
9.50	Oxide augite melatroctolite	0.02	0.001	24	39.5	3.60
14.00	Oxide augite melatroctolite	0.03	0.001	28	36.8	3.17
18.50	Olivine gabbro	0.03	0.002	15	42.2	5.59
23.00	Olivine gabbro	0.03	0.001	18	43.2	4.49
27.50	Oxide augite €melatroctolite	0.03	0.001	37	40.4	2.31
32.00	Oxide augite melatroctolite	0.02	0.000	36	37.0	2.47
36.50	Oxide augite melatroctolite	0.02	0.001	19	40.3	4.47
41.00	Oxide augite melatroctolite	0.02	0.001	27	40.4	3.17
45.50	Oxide augite melatroctolite	0.02	0.000	33	35.2	2.72
50.00	Mixed olivine gabbro	0.02	0.001	29	34.9	3.16
60.00	Mixed olivine gabbro	0.02	0.002	15	42.3	5.67
64.50	Oxide augite melatroctolite	0.02	0.002	12	41.5	6.87
66.00	Olivine gabbro	0.02	0.003	8	50.6	8.75

70.50	Olivine gabbro	0.02	0.001	14	39.4	5.99
75.00	Olivine gabbro	0.01	0.002	11	46.8	7.04
79.50	Olivine gabbro	0.02	0.001	13	47.6	5.80
84.00	Olivine gabbro	0.01	0.001	15	42.2	5.64
89.50	Olivine gabbro	0.01	0.001	13	41.5	6.23
94.50	Olivine gabbro	0.01	0.001	13	43.8	6.35
99.00	Olivine gabbro	0.01	0.001	14	43.9	5.78
103.50	Olivine gabbro	0.01	0.001	15	43.5	5.27
108.00	Olivine gabbro	0.01	0.001	17	38.6	5.05
112.50	Olivine gabbro	0.01	0.001	22	36.4	4.01
117.00	Olivine gabbro	0.01	0.001	14	41.2	6.13
127.00	Olivine gabbro	0.01	0.001	18	33.5	5.15
131.50	Olivine gabbro	0.01	0.001	17	37.0	5.26
136.00	Olivine gabbro	0.01	0.001	17	35.7	5.41
140.50	Olivine gabbro	0.01	0.001	21	30.3	4.44
145.00	Olivine gabbro	0.01	0.001	19	32.9	4.79
149.50	Olivine gabbro	0.01	0.001	23	28.6	4.28
154.00	Olivine gabbro	0.01	0.001	16	34.9	5.63
158.50	Olivine gabbro	0.01	0.001	17	36.5	5.36
163.00	Olivine gabbro	0.01	0.001	16	35.6	5.44
167.50	Olivine gabbro	0.01	0.001	16	37.9	5.49
172.00	Olivine gabbro	0.01	0.001	18	32.2	5.16
176.50	Olivine gabbro	0.01	0.001	16	37.4	5.46
181.00	Olivine gabbro	0.01	0.001	16	36.5	5.45
190.00	Olivine gabbro	0.02	0.001	17	34.3	5.52
194.50	Olivine gabbro	0.02	0.001	17	35.8	5.41
199.00	Olivine gabbro	0.02	0.001	17	38.5	5.01
203.50	Oxide augite melatroctolite	0.01	0.001	23	31.5	4.17
208.00	Oxide augite melatroctolite	0.01	0.001	29	26.2	3.39
212.50	Oxide augite melatroctolite	0.01	0.001	19	38.6	4.62
217.00	Oxide augite melatroctolite	0.02	0.001	22	35.5	4.03
221.50	Oxide augite melatroctolite	0.01	0.001	25	34.2	3.60
226.00	Oxide augite melatroctolite	0.02	0.001	26	30.2	3.62

230.50	Oxide augite melatroctolite	0.02	0.001	25	28.5	3.95
235.00	Oxide melatroctolite	0.01	0.000	32	32.9	2.89
239.50	Oxide melatroctolite	0.02	0.000	29	35.1	3.12
244.00	Oxide melatroctolite	0.02	0.001	29	37.5	3.04
248.50	Oxide melatroctolite	0.02	0.001	21	31.8	4.37
253.00	Oxide melatroctolite	0.02	0.001	24	36.9	3.66
257.50	Oxide melatroctolite	0.02	0.001	24	36.5	3.64
262.00	Oxide melatroctolite	0.03	0.001	26	29.4	3.72
266.50	Oxide melatroctolite	0.04	0.001	25	34.3	3.67
271.00	Oxide melatroctolite	0.05	0.001	27	39.4	3.19
272.00	Apatitic clinopyroxenite	0.05	0.001	30	34.8	3.03
276.50	Apatitic clinopyroxenite	0.06	0.002	22	44.8	3.72
281.00	Apatitic clinopyroxenite	0.03	0.001	26	35.7	3.42
285.50	Apatitic clinopyroxenite	0.05	0.002	18	36.0	4.99
291.00	Apatitic clinopyroxenite	0.06	0.008	33	41.1	2.51
295.50	Apatitic clinopyroxenite	0.05	0.003	24	40.1	3.56
302.00	Breccia	0.05	0.004	29	36.5	3.10
305.00	Breccia	0.08	0.006	12	45.7	6.47
310.00	Breccia	0.06	0.004	27	39.6	3.22
316.00	Breccia	0.07	0.004	30	41.1	2.79
320.50	Apatitic olivine clinopyroxenite	0.09	0.005	27	42.2	3.05
325.00	Apatitic olivine clinopyroxenite	0.08	0.014	30	41.0	2.83
327.50	Apatitic olivine clinopyroxenite	0.09	0.016	30	40.6	2.81
330.00	Apatitic wehrlite	0.09	0.011	29	40.9	2.93

*95% confidence error calculated based on the equation $\sigma_{(A/B)}=A/B*((\sigma_A/A)^2+(\sigma_B/B)^2)^{1/2}$

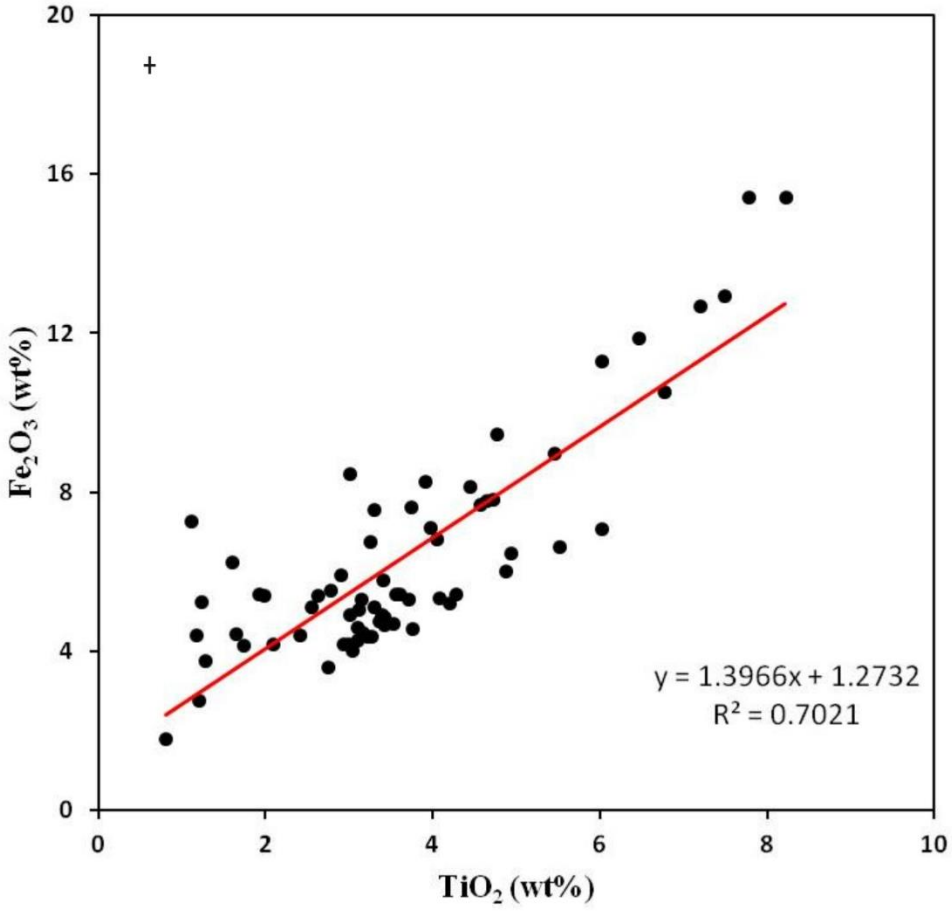

Figure 3-9. The correlation between lab-based whole-rock TiO_2 and Fe_2O_3 contents, by fusion ICP-AES. Error bar represents 2σ analytic precision determined through replicate analyses.

The key pXRF lithogeochemical parameters for defining the different igneous units are $Mg\#_{WR}$, CaO, P_2O_5, Ba, and Zr and the V/Ti ratio (Table 3-1 and Table 3-4). Figure 3-10 shows box and whisker plots of these parameters and their down-hole variations are plotted in Figure 3-11. In Figure 3-10, Layered Series rocks have lower CaO, P_2O_5 and V/Ti ratios, and higher Ba and Zr contents than Marathon Series rocks. However, the $Mg\#_{WR}$ values of the Layered Series rocks are similar to those of the Marathon Series rocks. Good et al. (2015) also observed a lower V/Ti ratio in Layered Series rocks compared to Marathon Series rocks at the Marathon deposit. Thus, the V/Ti ratio seems to be a good discriminant between these two Series throughout the Eastern Gabbro. The higher Ba contents in the Layered Series gabbros is also consistent with the data of Shaw and Penczak (1996) who recognized

Ba-rich biotite in this series. In addition, there is a positive correlation between pXRF K_2O and Ba for samples in this study (Fig. 3-12), indicating that Ba is controlled by biotite (negligible K-feldspar is present in the samples examined in this study, although K-feldspar is observed elsewhere in the Eastern gabbro).

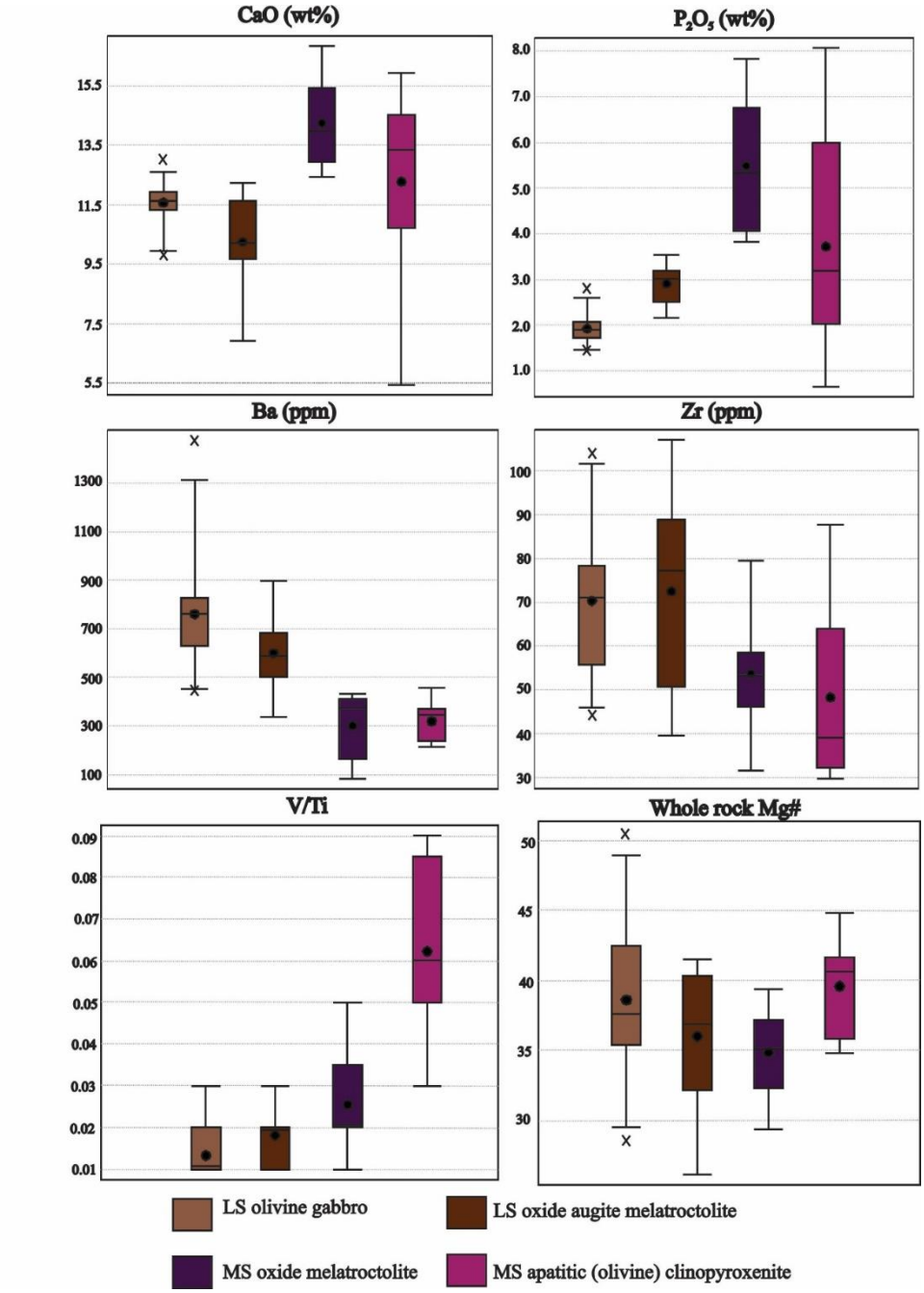

Figure 3-10. Box and whisker plots for pXRF CaO, P_2O_5, Ba, Zr, V/Ti, and $Mg\#_{WR}$ in different rock units at the Four Dams area. LS: Layered Series, MS: Marathon Series.

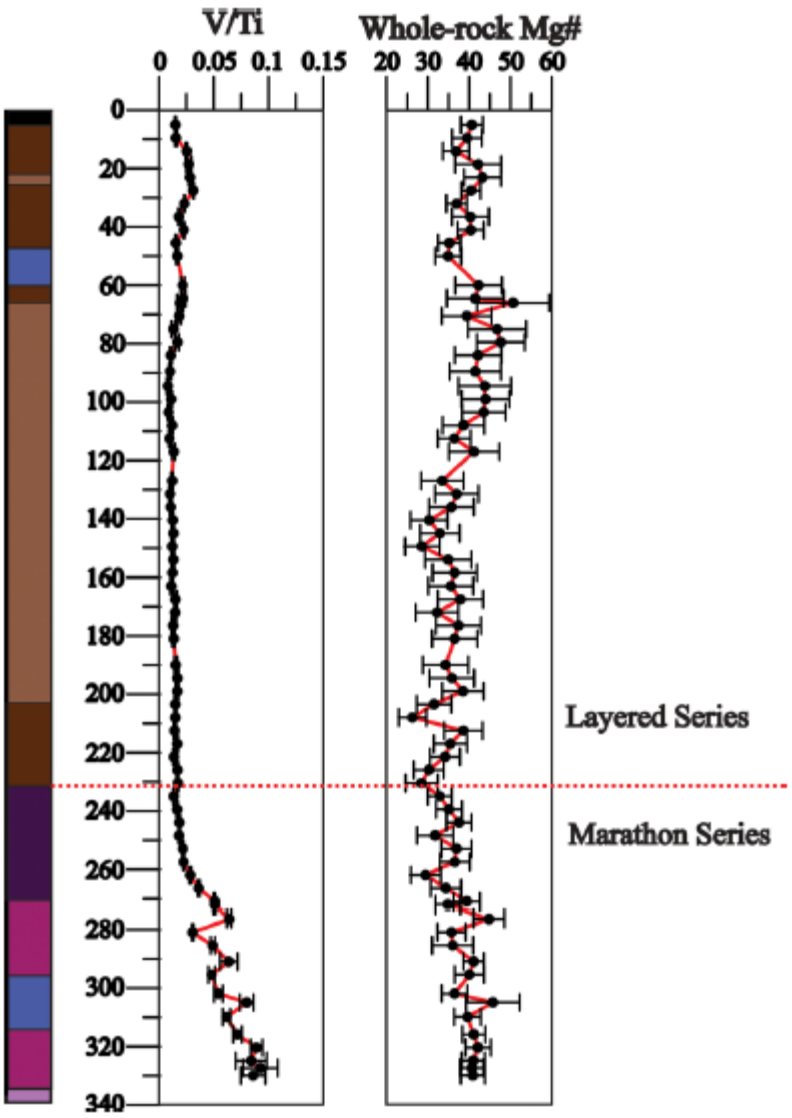

Figure 3-11. Down-hole variations in pXRF whole-rock V/Ti, Mg# $_{WR}$. Note that all data were related to pXRF analyses on powders, the red dashed line indicates the contact, and lithology legend can refer to Figure 3-2.

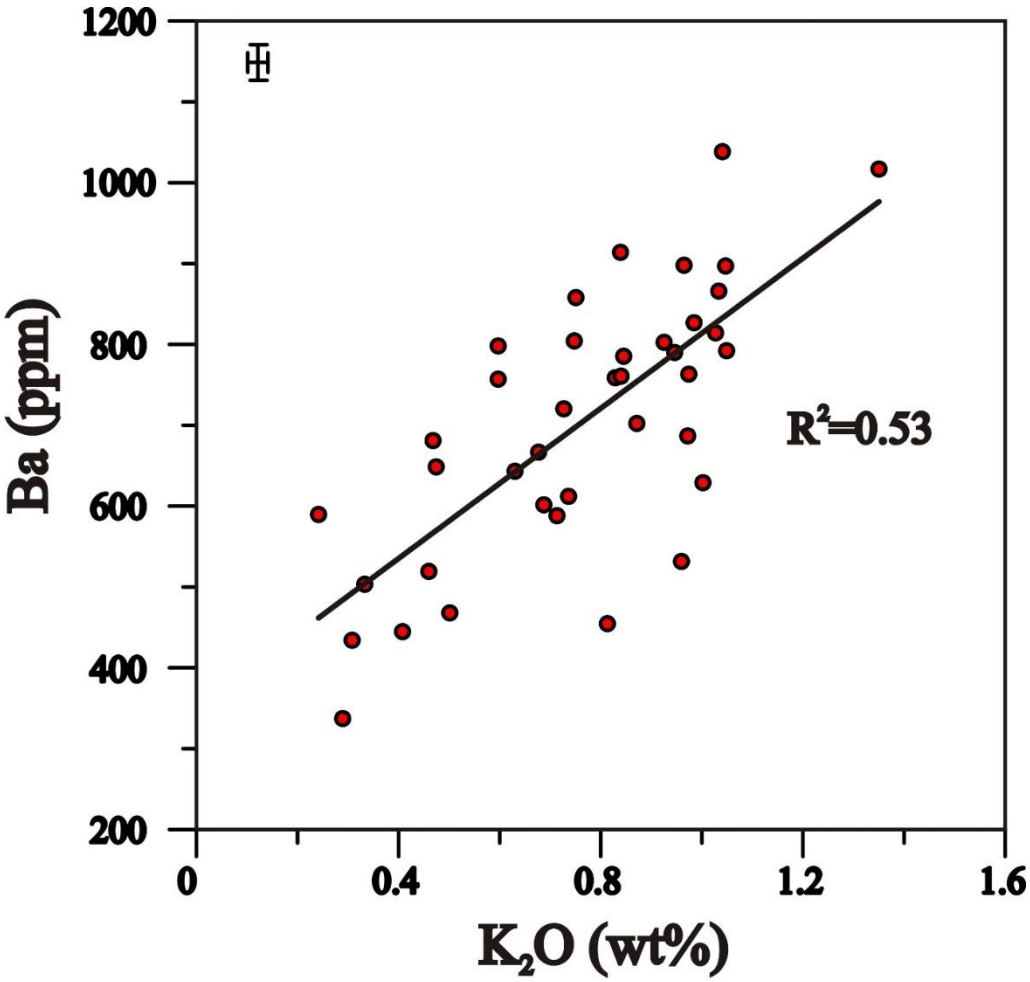

Figure 3-12. Relationship between K_2O and Ba contents as represented by pXRF analysis of powders, all data refer to units in the Layered Series of the Four Dams area. Error bar represents 2σ analytic precision determined through replicate analyses.

Down-hole pXRF whole-rock chemistry can also be used to differentiate between the Layered and Marathon Series rocks. P_2O_5 contents in the Layered Series are nearly constant, whereas the Marathon Series rocks have variable P_2O_5 contents (representing apatite-rich cumulate layers rather than interstitial apatite) that overall increase with depth (Fig. 3-4). Down-hole pXRF variations of Zr contents in the Layered Series are variable but generally increase with depth. By contrast, the Marathon Series rocks have decreasing Zr contents with depth (Fig. 3-4). The down-hole variation in pXRF V/Ti ratio of the Layered Series gabbros is nearly constant at around 0.015, in contrast to that of the Marathon Series rocks where it generally

increases with depth from 0.015 to 0.1 (Fig. 3-11). The $Mg\#_{WR}$, although similar in the Layered and Marathon Series, does show subtle variation. The $Mg\#_{WR}$ decreases with depth in the Layered Series gabbros (reverse differentiation) versus the Marathon Series rocks, which have an increase in $Mg\#_{WR}$ with depth (normal differentiation) (Fig. 3-11).

The concentrations of Hf, Nb, Ta, and Zr in the different rock units from the ICP-MS analyses are given in Table 3-5 and their down-hole variations are shown in Figure 3-13. The Layered Series gabbros contain Hf, Nb, Ta, and Zr concentrations in the range 0.9 to 4.0 ppm, 16 to 73 ppm, 0.7 to 3.0 ppm, and 37 to 168 ppm, respectively, and all of these elements generally increase downward in the Layered Series gabbros. The Marathon Series, by contrast, has variable Hf, Nb, Ta, and Zr contents that overall continually decrease with depth. The down-hole variation in pXRF Zr is included in Figure 3-13 for comparisons, which is broadly similar to down-hole variations of ICP-MS Hf, Nb, Ta, and Zr.

Table 3-5. Concentrations of selected trace elements analyzed by ICP-MS.

Depth/m	Lithology	Hf/ppm	Nb/ppm	Ta/ppm	Zr/ppm
		(0.61)*	(6.7)*	(0.54)*	(19.2)*
5.0	Oxide augite melatroctolite	1.4	27	1.3	53
9.5	Oxide augite melatroctolite	1.4	27	1.3	60
14.0	Oxide augite melatroctolite	2.7	38	1.8	99
18.5	Oxide augite melatroctolite	1.1	17	0.8	42
23.0	Olivine gabbro	1.7	31	1.5	63
27.5	Olivine gabbro	1.6	37	1.8	64
32.0	Oxide augite melatroctolite	1.3	30	1.5	55
36.5	Oxide augite melatroctolite	1.9	27	1.3	74
41.0	Oxide augite melatroctolite	1.8	28	1.4	67
45.5	Oxide augite melatroctolite	1.6	33	1.7	66
50.0	Mixed olivine gabbro	4.0	73	3.0	168
60.0	Mixed olivine gabbro	0.9	16	0.7	37
64.5	Oxide augite melatroctolite	1.3	20	1.0	52

66.0	Olivine gabbro	1.4	20	0.9	56
70.5	Olivine gabbro	1.6	25	1.1	61
75.0	Olivine gabbro	1.6	24	1.1	65
79.5	Olivine gabbro	1.8	31	1.5	74
84.0	Olivine gabbro	1.8	29	1.4	71
89.5	Olivine gabbro	2.1	32	1.5	89
90.0	Olivine gabbro	2.0	33	1.7	92
94.5	Olivine gabbro	1.9	33	1.6	84
99.0	Olivine gabbro	1.5	26	1.2	64
103.5	Olivine gabbro	1.8	33	1.5	73
108.0	Olivine gabbro	1.7	27	1.3	69
112.5	Olivine gabbro	1.4	23	1.1	50
117.0	Olivine gabbro	1.4	19	0.9	55
127.0	Olivine gabbro	1.5	23	1.1	64
131.5	Olivine gabbro	1.7	24	1.2	63
136.0	Olivine gabbro	1.8	31	1.6	63
140.5	Olivine gabbro	1.8	27	1.4	66
145.0	Olivine gabbro	1.8	29	1.5	62
149.5	Olivine gabbro	1.8	38	2.0	62
154.0	Olivine gabbro	2.2	34	1.6	85
158.5	Olivine gabbro	2.1	34	1.8	79
163.0	Olivine gabbro	2.2	41	2.1	86
167.5	Olivine gabbro	2.3	45	2.2	92
172.0	Olivine gabbro	2.4	48	2.1	93
176.5	Olivine gabbro	2.3	49	2.1	96
181.0	Olivine gabbro	2.6	49	2.1	107
190.0	Olivine gabbro	2.6	49	2.1	107
194.5	Olivine gabbro	2.6	53	2.3	109
199.0	Olivine gabbro	2.4	53	2.4	102
203.5	Oxide augite melatroctolite	2.2	50	2.2	83
208.0	Oxide augite melatroctolite	2.5	70	3.2	94
212.5	Oxide augite melatroctolite	2.5	55	2.5	95
217.0	Oxide augite melatroctolite	2.5	64	3.0	97

221.5	Oxide augite melatroctolite	3.1	74	3.3	133
226.0	Oxide augite melatroctolite	2.1	68	3.1	86
230.5	Oxide augite melatroctolite	1.9	73	3.4	75
235.0	Oxide melatroctolite	1.7	48	2.5	58
239.5	Oxide melatroctolite	1.7	47	2.4	60
244.0	Oxide melatroctolite	1.8	43	2.1	63
248.5	Oxide melatroctolite	1.6	39	1.7	56
253.0	Oxide melatroctolite	1.9	42	2.0	69
257.5	Oxide melatroctolite	1.7	49	2.4	61
262.0	Oxide melatroctolite	1.4	36	1.7	52
266.5	Oxide melatroctolite	1.0	36	1.7	41
271.0	Apatitic clinopyroxenite	2.2	51	2.3	85
272.0	Apatitic clinopyroxenite	1.0	28	1.2	42
276.5	Apatitic clinopyroxenite	1.5	11	0.4	46
281.0	Apatitic clinopyroxenite	2.3	47	2.0	90
285.5	Apatitic clinopyroxenite	1.6	20	0.8	65
291.0	Apatitic clinopyroxenite	0.7	7	0.2	29
295.5	Apatitic clinopyroxenite	2.5	24	1.0	94
302.0	Breccia	1.3	15	0.5	41
305.0	Breccia	1.0	6	0.1	31
310.0	Breccia	1.2	12	0.6	44
316.0	Breccia	1.3	15	0.6	47
320.5	Apatitic olivine clinopyroxenite	1.2	9	0.3	38
325.0	Apatitic olivine clinopyroxenite	0.6	7	0.2	29
327.5	Apatitic olivine clinopyroxenite	0.8	12	0.4	36
330.0	Apatitic wehrlite	0.8	12	0.5	37

*2σ precision values are given in brackets

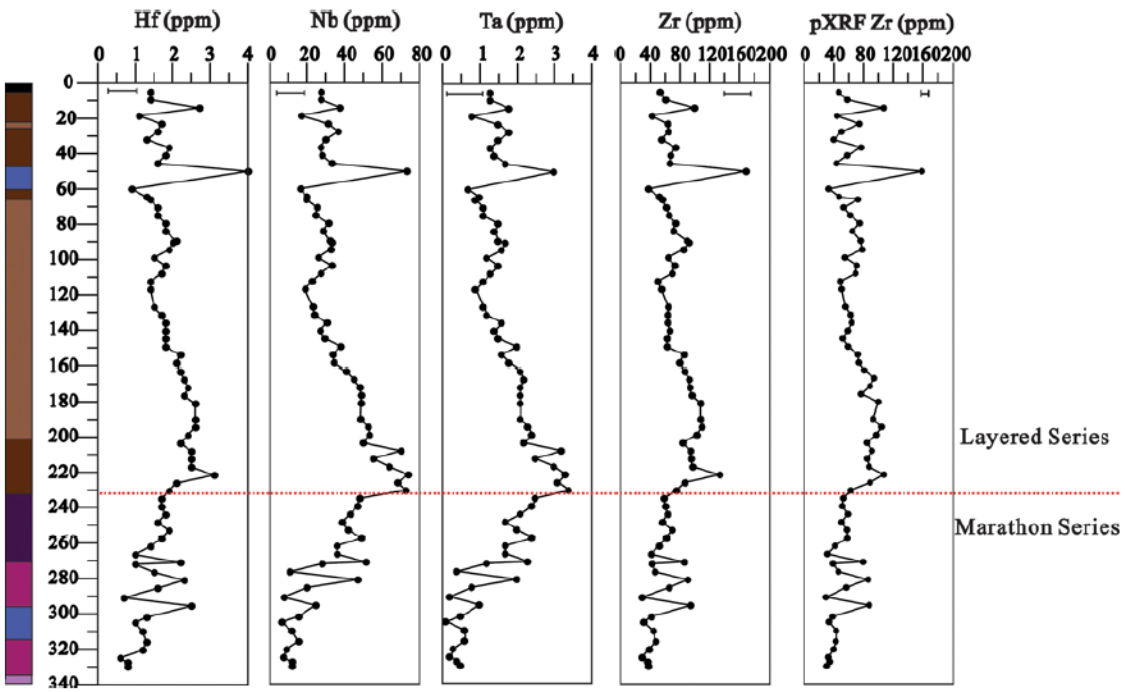

Figure 3-13. Down-hole variation in fusion ICP-MS results for Hf, Nb, Ta, Zr, and pXRF results for Zr. Red dashed line represents the contact between the Layered Series and the Marathon Series. Legend for lithology as in Figure 3-2.

3.5.2 bSEM-EDS mineral chemistry

Down-hole variations in the Mg#s of olivine and clinopyroxene, and the An% of plagioclase are shown in Figure 3-14. The Layered Series gabbros show an overall downward decreasing trend in Mg# of olivine, Mg# of clinopyroxene, and An% of plagioclase. By contrast, the Mg#s of olivine and clinopyroxene, and An% of plagioclase gradually increase downward in both the oxide melatroctolite and the apatitic clinopyroxenite in the Marathon Series.

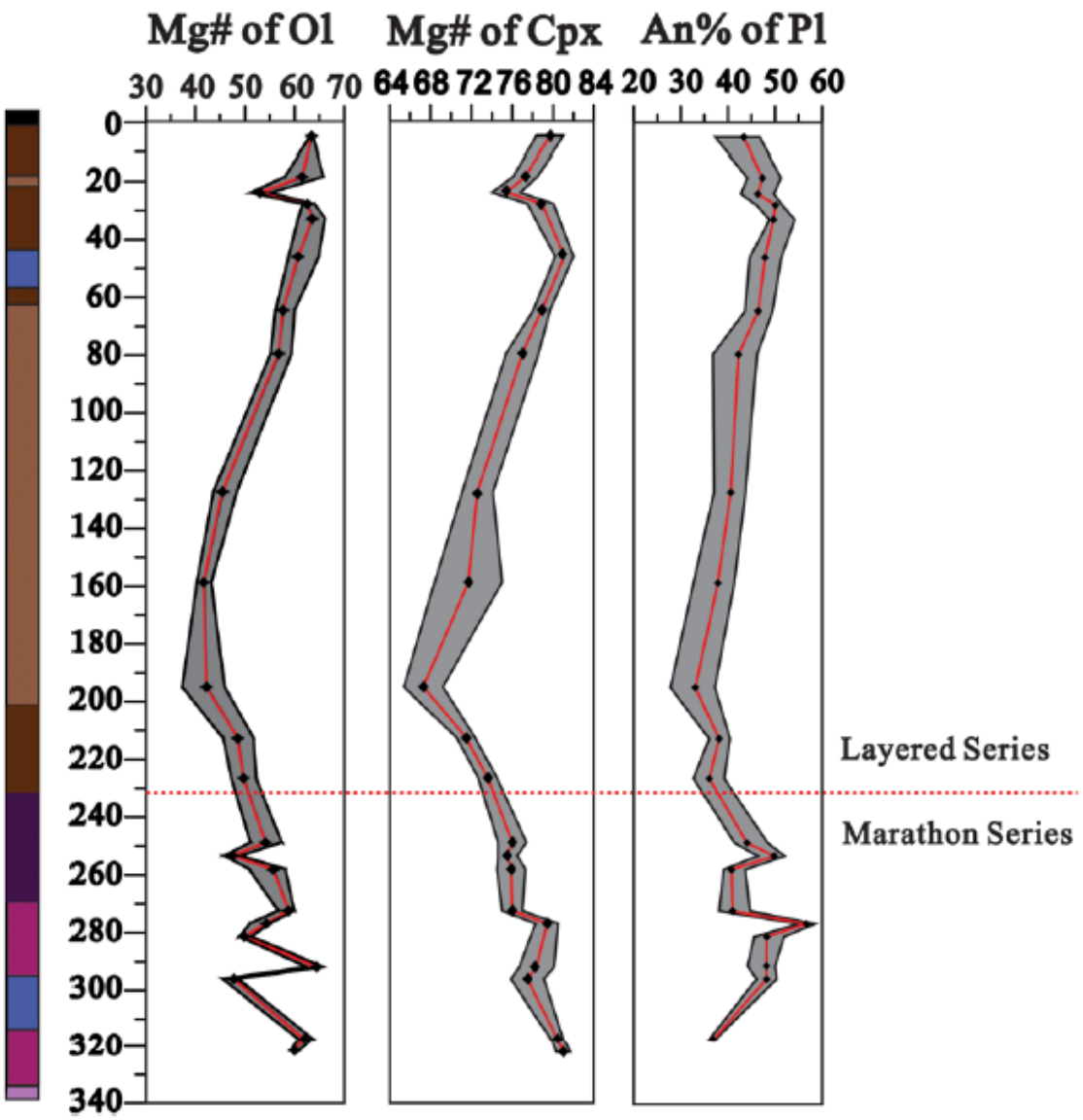

Figure 3-14. Down-hole variations in Mg#s of olivine and clinopyroxene, and An content of plagioclase. Average compositions are black points with minimum and maximum compositions represented by the grey envelope. Red dashed line represents the contact between the Layered Series and the Marathon Series. Legend for lithology as in in Figure 3-2.

3.6 Discussion

3.6.1 The application of pXRF and bSEM-EDS to Cu-Pd mineral exploration

As discussed above, applications of pXRF to mineral exploration has been demonstrated by many studies, whereas, to our knowledge, this is the first

application of bSEM-EDS to mineral exploration. In this section, we examine the combination of pXRF and bSEM-EDS to increase efficiency in mineral exploration.

The down-hole variations in Cu and S values from pXRF are compared to exploration assay data from drill hole FD-13-34 (Figure 3-15 and Table 3-6). There is a strong correlation between the two patterns, despite the different sampling intervals (assay data were determined on continuous 2 m sample intervals, whereas samples for this study were collected over 1 m intervals at 3 m spacing). These results show that pXRF is able to quantify Cu concentrations on powders down to at least 100 ppm. In addition, two zones of mineralization: a zone characterized by low Cu/S ratios at the top of the Layered Series and a zone characterized by high Cu/S ratios at the bottom of the Marathon Series (Fig. 3-15) are identified in drill hole FD-13-34 by both exploration assay and pXRF data. The Pd abundance in the upper zone with low Cu/S is at or below detection limits of ICP-MS analysis, whereas mineralization in the Marathon Series with high Cu/S is PGE enriched (unpublished Stillwater Canada data), suggesting high Cu/S ratios seem to be a proxy for PGE mineralization at this locality. Figure 3-16 further illustrates how the pXRF data can be plotted to identify two different Cu/S ratios corresponding to the two mineralized zones described above. Whereas pXRF is unable to detect PGE, bSEM-EDS can be used as a complimentary technique to verify Pd mineralization.

Table 3-6. Exploration assay data of Cu and S from Stillwater Canada Inc, which are analyzed by ICP-MS and Leco IR.

Depth/m	Lithology	Cu ppm (10)*	S % (0.01)*	Depth/m	Lithology	Cu ppm (10)*	S % (0.01)*
5.95	Oxide augite melatroctolite	962	0.4	249	Oxide melatroctolite	524	0.2
8	Oxide augite melatroctolite	286	0.2	251	Oxide melatroctolite	619	0.2
10	Oxide augite melatroctolite	537	0.3	253	Oxide melatroctolite	602	0.3
12	Oxide augite melatroctolite	1210	0.4	255	Oxide melatroctolite	651	0.2
14	Oxide augite melatroctolite	2860	0.9	257	Oxide melatroctolite	579	0.3
14	Oxide augite melatroctolite	2560	0.8	259	Oxide melatroctolite	779	0.3
16	Oxide augite melatroctolite	850	0.4	261	Oxide melatroctolite	983	0.3
18	Olivine gabbro	2680	1.0	263	Oxide melatroctolite	850	0.2
20	Oxide augite melatroctolite	2500	0.9	265	Oxide melatroctolite	2310	0.5
22	Olivine gabbro	375	0.2	267	Oxide melatroctolite	1380	0.3
24	Olivine gabbro	575	0.2	269	Oxide melatroctolite	999	0.2
26	Oxide augite melatroctolite	1085	0.3	271	Oxide melatroctolite	1745	0.2
28	Oxide augite melatroctolite	2790	0.9	273	Apatitic clinopyroxenite	5620	0.6
30	Oxide augite melatroctolite	3250	1.3	275	Apatitic clinopyroxenite	6440	0.6
32	Oxide augite melatroctolite	2910	0.9	277	Apatitic clinopyroxenite	4820	0.6
34	Oxide augite melatroctolite	3270	1.3	279	Apatitic clinopyroxenite	967	0.2
36	Oxide augite melatroctolite	2870	0.8	281	Apatitic clinopyroxenite	857	0.3
38	Oxide augite melatroctolite	654	0.3	283	Apatitic clinopyroxenite	555	0.2
40	Oxide augite melatroctolite	542	0.3	285	Apatitic clinopyroxenite	640	0.1
42	Oxide augite melatroctolite	846	0.4	287	Apatitic clinopyroxenite	1110	0.2
44	Oxide augite melatroctolite	1225	0.4	289	Apatitic clinopyroxenite	1160	0.2
46	Oxide augite melatroctolite	2450	1.0	291	Apatitic clinopyroxenite	3990	0.4
48	Olivine gabbro	3620	1.3	293	Apatitic clinopyroxenite	4250	0.5
50	Olivine gabbro	3360	1.5	295	Apatitic clinopyroxenite	2690	0.4
52	Olivine gabbro	2090	1.1	297	Apatitic clinopyroxenite	1240	0.3
54	Olivine gabbro	1305	0.7	299	Breccia	612	0.1
56	Olivine gabbro	3150	0.9	301	Breccia	1550	0.3
58	Olivine gabbro	3060	1.0	303	Breccia	3010	0.4
60	Olivine gabbro	3960	1.4	305	Breccia	3020	0.4
62	Oxide augite melatroctolite	4150	1.7	307	Breccia	788	0.1

64	Oxide augite melatroctolite	2100	1.0	309	Breccia	1080	0.1
66	Oxide augite melatroctolite	212	0.1	311	Breccia	1650	0.2
111	Olivine gabbro	113	0.3	313	Breccia	1500	0.2
113	Olivine gabbro	1335	1.2	315	Breccia	1080	0.2
115	Olivine gabbro	2480	1.8	317	Apatitic olivine clinopyroxenite	3170	0.4
117	Olivine gabbro	287	0.5	319	Apatitic olivine clinopyroxenite	2620	0.3
119	Olivine gabbro	64	0.2	321	Apatitic olivine clinopyroxenite	3570	0.5
233	Oxide augite melatroctolite	524	0.2	323	Apatitic olivine clinopyroxenite	3100	0.4
235	Oxide melatroctolite	616	0.4	325	Apatitic olivine clinopyroxenite	5280	0.6
237	Oxide melatroctolite	582	0.6	327	Apatitic wehrlite	3670	0.5
239	Oxide melatroctolite	666	0.5	329	Apatitic wehrlite	6260	0.8
241	Oxide melatroctolite	832	0.4	331	Apatitic olivine clinopyroxenite	4380	0.6
243	Oxide melatroctolite	683	0.4	333	Apatitic olivine clinopyroxenite	3180	0.5
245	Oxide melatroctolite	834	0.5	335	Two duck lake gabbro	2110	0.4
247	Oxide melatroctolite	587	0.4				

*2σ precision values are given in brackets

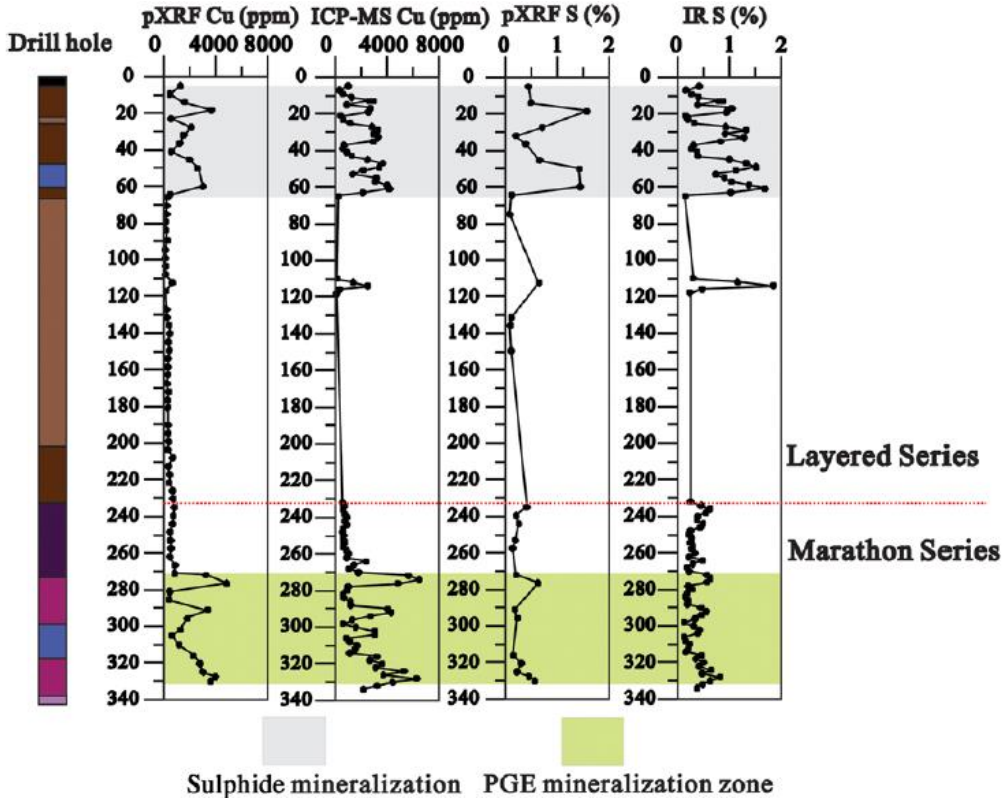

Figure 3-15. Down-hole comparisons between pXRF and ICP-MS/IR Cu and S results; two different mineralized zones are shaded in different colours. Legend for lithology as in Figure 3-2.

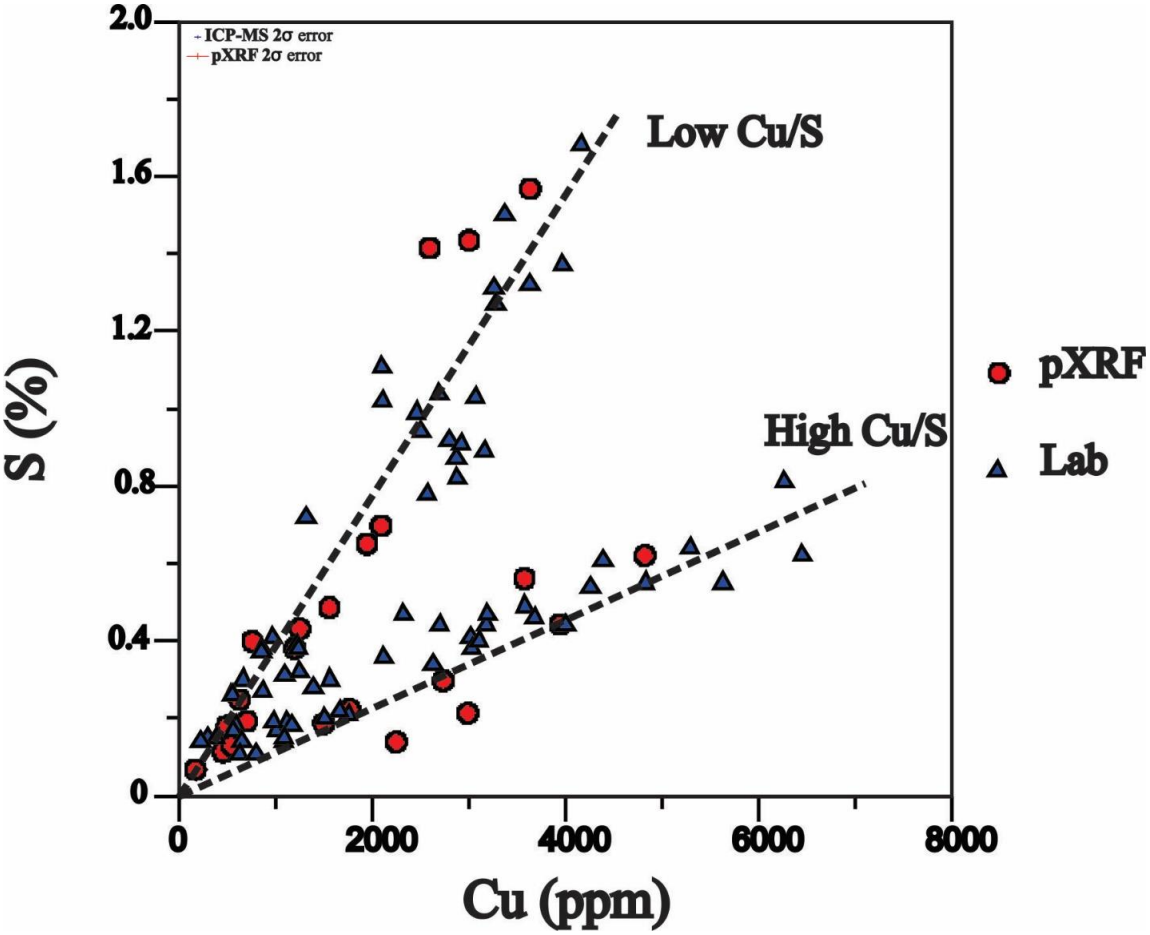

Figure 3-16. Two similar Cu/S trends shown by both pXRF and laboratory-based whole-rock data. 2σ error was determined through replicate analyses.

Several platinum group minerals (PGM) in Marathon Series gabbros within the high Cu/S ratio zone were identified using bSEM-EDS (Figs. 3-17 and 3-18) through scanning the thin sections and thin section blocks. Time needed for identification of PGM in either thin section or thin section block varies, but normally less than 30 minutes were spent on identifying PGM in each PGM-hosted sample. The PGM in Figure 3-17 are from carbon-coated polished thin sections, but the Ag-Au alloy shown in Figure 3-18 is from an unpolished block. This demonstrates that the bSEM-EDS can be used to identify mineralization in saw-cut drill core in the field, without having to wait for assays. In another example, down-hole variations in whole-rock MgO or $Mg\#_{WR}$ from pXRF (Figs. 3-4 and 3-11) are difficult to interpret

without knowledge of mineral chemistry. However, bSEM-EDS analyses show a "saw-tooth" pattern for Mg# of olivine between depths of 270 and 290 m (within the high Cu/S zone) (Figs. 3-8 and 3-14). Similar patterns have been interpreted by Good et al. (2015) as magma recharge conduits that are favorable for PGE mineralization. Thus, the combination of pXRF and bSEM can be used in the field to identify possible recharge zones. The last example is the replacement of early plagioclase by later more-calcic plagioclase, An50 by An60 by bSEM-EDS analysis (Fig. 3-19). This texture is notable because chalcopyrite is intergrown with the later plagioclase (Figs. 3-3E and 3F) and precious metals are associated with the chalcopyrite (Fig. 3-19). Similar textures were described in the Marathon Main zone by Good and Crocket (1994), thus another application of bSEM-EDS is to identify favourable textures in the field.

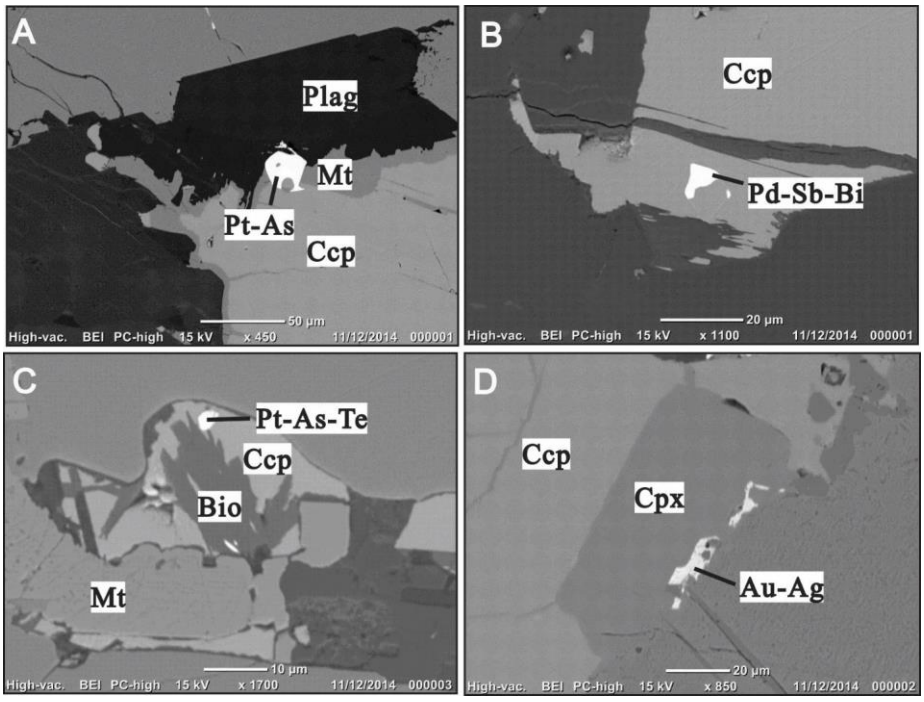

Figure 3-17. bSEM-BSE images showing PGM grains in the apatitic clinopyroxenite unit in the Marathon Series. (A) 272.1 m, Pt-As alloy at the contact between Plag and Ccp rimmed by hydrothermal magnetite; (B) 272.1 m, Pd-Sb-Bi alloy inclusions in Ccp; (C) 276.5 m, Pt-As-Te inclusion in Ccp; (D) 272.1 m, Au-Ag stringers at the contact between Mag and Cpx, in the vicinity of the Ccp.

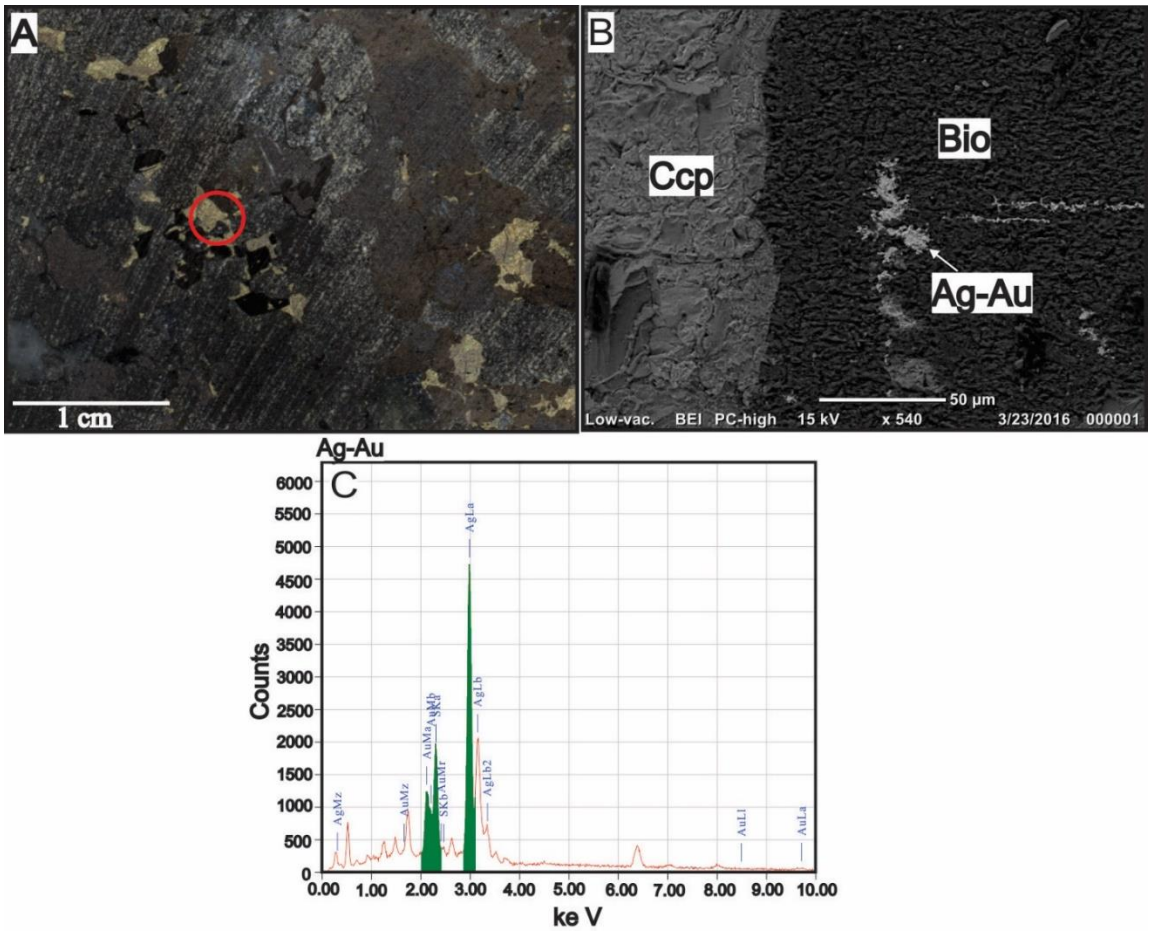

Figure 3-18. Location of Ag-Au alloy in an unpolished thin section block using the bSEM-EDS. (A) Sawed block from drill core with chalcopyrite mineralization; (B) bSEM-BSE image showing the Ag-Au alloy enclosed in Bio, adjacent to Ccp; (C) EDS spectrum of above Ag-Au alloy. The red circle gives the location of the sulfide that hosts the Ag-Au alloy. Note that Pd and Pt assay values for this sample (556 ppb Pd and 190 ppb Pt) are quite low. Several Pt and Pd alloys were found elsewhere, but BSE images of them are of poor quality. Abbreviations: Ccp- Chalcopyrite, Bio- Biotite.

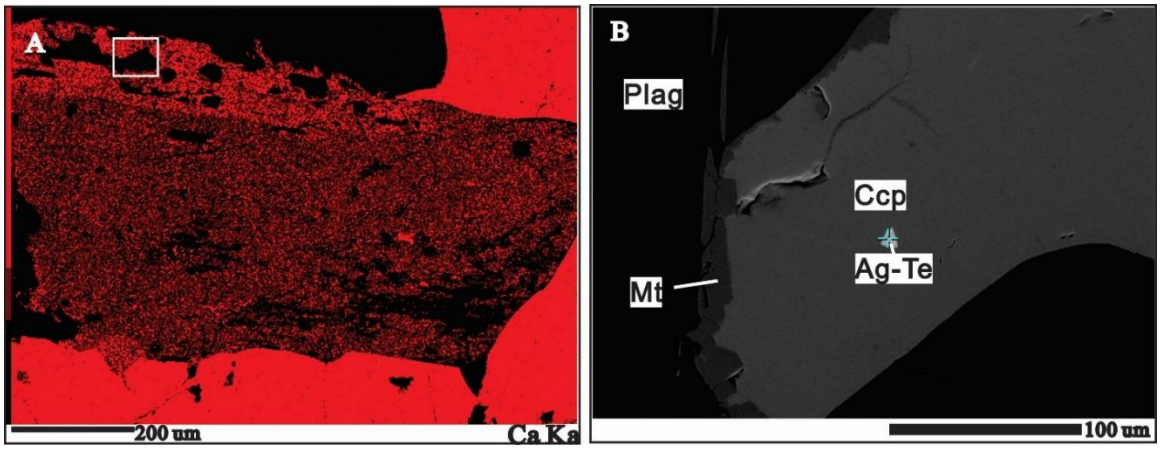

Figure 3-19. Two stages of plagioclase identified using bSEM-EDS. (A) CaKα X-ray map showing the replacement of early less-calcic plagioclase by late, more-calcic plagioclase; (B) BSE image showing a Ag-Te mineral inclusion hosted by one of the chalcopyrite grains (indicated using the while box in Figure 3-19A) occurring intergrown with the late plagioclase.

3.6.2 The application of pXRF and bSEM-EDS to mapping igneous stratigraphy

This study shows that the combination of pXRF and bSEM-EDS can be used in the field to map igneous stratigraphy in a manner similar to laboratory-based studies that combine whole-rock lithogeochemistry and mineral chemistry (Li et al., 2000; Egorova and Latypov, 2013). The interpretation of results from only one method is more difficult. In this study the Layered Series gabbros including the oxide augite melatroctolite (barren) and the Marathon Series gabbros including the oxide melatroctolite (potentially mineralized) can be distinguished from variations in the major-element and trace-element abundances, e.g., Layered Series rocks contain lower CaO, P_2O_5 and V/Ti ratio and higher Ba and Zr contents than Marathon Series rocks. We have also shown that Zr, determined by pXRF can serve as a proxy for other high field strength elements and the down-hole variations of these highly incompatible element abundances is useful to help differentiate between the PGE-barren Layered Series and the PGE-enriched Marathon Series (normal differentiation for the Marathon Series gabbros versus reverse differentiation for the Layered Series gabbros). Shaw (1997) described normal and reverse trends for mineral compositions in the Layered Series. In this study we have shown that these

trends can also be recognized using bSEM-EDS, in particular for the Mg#s of olivine and clinopyroxene, and An% of plagioclase. It is the combination of whole-rock lithogeochemical and mineral chemical data that allow for a more robust interpretation of the igneous stratigraphy. Unravelling the mechanisms that caused the reverse and normal trends for the Layered Series and the Marathon Series, respectively, is beyond the scope of this paper. The significance of this work is that variations and trends in the various igneous rocks in the Coldwell Alkaline Complex have been characterized using a combination of field portable techniques. This methodology can be used to guide sampling in an iterative fashion in the field, which increases the efficiency of both mineral exploration and academic research.

3.7 Conclusions

The reliability of results from the field portable pXRF and bSEM-EDS are demonstrated in the current study. Both portable instruments are able to provide analyses comparable to their lab-based counterparts. In addition, pXRF is capable of estimating Cu grade down to ca. 100 ppm and reliably identifies different Cu/S values that can assist in Cu-Pd mineral exploration because, for mineralization in the Coldwell Alkaline Complex, high Cu/S ratios serve as a proxy for potential PGE mineralization. The technique of bSEM-EDS can also be used to identify PGM grains directly in the unpolished blocks. The ability to rapidly identify PGE mineralization in the field can improve the decision-making process in exploration. This study was also successful in differentiating between petrographically similar gabbros that belong to two different magmatic series using pXRF and bSEM-EDS: the Marathon Series, which hosts PGE mineralization, and the Layered Series, which is barren of PGE mineralization. Overall, the combination of pXRF and bSEM-EDS can greatly improve sampling and hypothesis testing in field-based research.

3.8 Acknowledgements

We gratefully acknowledge NSERC, Stillwater Canada Inc. and the China Scholarship for funding this project. John McBride, Katrina McLean and Ryan Ruthart of Stillwater Canada are particularly thanked for their help with field work. Additional support for pXRF analyses was provided by Elemental Controls Ltd. and for bSEM analyses by JEOL. The manuscript was improved by constructive reviews by S. Piercey and G. Hall.

3.9 References

Arne D.C., Mackie R.A. and Jones S.A. 2014. The use of property-scale portable X-ray fluorescence data in gold exploration: advantages and limitations. *Geochemistry: Exploration, Environment, Analysis*, **14**, 233-244.

Barnes S.J. 2004. Platinum-group element distribution in the Main Zone and Upper Zone of the Bushveld Complex, South Africa. *Chemical Geology*, **208** (1-4), 293-317.

Egorova E and Latypov R. 2013. Mafic-ultramafic Sills: New insights from M- and S-shaped Mineral and whole-rock compositional profiles. *Journal of Petrology*, **10**, 2155-2191.

Fisher L., Gazley M.F., Baensch A., Barnes S.J., Cleverly J., and Duclaux, G. 2014. Resolution of geochemical and lithostratigraphic complexity: a workflow for application of portable X-ray fluorescence to mineral exploration. *Geochemistry: Exploration, Environment, Analysis*, **14**, 149-159.

Gazely M.F., Tutt C.M., Brisbout L.I., Fisher L.A., and Duclaux, G. 2014. Application of portable X-ray fluorescence analysis to characterize dolerite dykes at the Plutonic Gold Mine, Western Australia. *Geochemistry: Exploration, Environment, Analysis*, **14**, 223-231.

Good D.J., Epstein R, McLean K, Linnen R.L., and Samson I. 2015. Evolution of the Main Zone and the Marathon Cu-PGE Sulfide Deposit, Midcontinent Rift, Canada: Spatial Relationships in a Magma Conduit Setting. *Economic Geology*, **110**, 983-1008.

Good D.J. 1993. Genesis of copper-precious metal sulfide deposits in the Port Coldwell alkali complex, Ontario: Ontario Geological Survey Open File Report 5839, 231p.

Good D.J. and Crocket J.H. 1994. Genesis of the Marathon Cu-Platinum-Group Element Deposit, Port Coldwell Alkalic Complex: A Midcontinent Rife-related Magmatic Sulfide Deposit. *Economic Geology*, **89**, 131-149.

Haffert L. and Craw D. 2009. Field quantification and characterisation of extreme arsenic concentrations at a historic mine processing site, Waiuta, New Zealand. *New Zealand Journal of Geology and Geophysics*, **52**, 261-272.

Hall G, Bonham-Carter G.F. and Buchar A. 2014. Evaluation of portable X-ray fluorescence (pXRF) in exploration and mining; Phase 1, Control reference materials. *Geochemistry: Exploration, Environment, Analysis* **14**, 99-123.

Hall G., Buchar A., and Bonham-Carter G. 2012. Quality Control Assessment of Portable XRF Analysers: Development of Standard Operating Procedures, Performance on Variable Media and Recommended Uses. CAMIRO Project 10E01, Phase 1, http://www.appliedgeochemists.org.

Heaman L.M. and Machado N. 1992. Timing and origin of midcontinent rift alkaline magmatism, North America: evidence from the Coldwell Alkaline Complex. *Contributions to Mineralogy and Petrology*, **110**, 289-303

Li C., Lightfoot, P.C. and Naldrett A.J. 2000. Contrasting petrological and geochemical relationships in the Voisey's Bay and Mushuan intrusions, Labrado, Canada: Implications for ore genesis. *Economic Geology*, **95**, 771-799.

Makinen E., Korhonen M., Viskari E.-L., Haapa maki S., Jarvinen M., and Lu L. 2006. Comparison of XRF and FAAS methods in analysing CCA contaminated soils. *Water, Air and Soil Pollution*, **171**, 95-110.

Morris P.A. 2009. Field portable X-ray fluorescence analysis and its application in GSWA. Geological Survey of Western Australia, Perth, WA, Australia, **23**.

Mitchell R.H. and Platt R.G. 1982. Mineralogy and petrology of nepheline syenites from the Coldwell Alkaline Complex, Ontario, Journal of Petrology, **23**, 186-214.

Mungall J.E. and Naldrett A.J. 2008. Ore deposits of the platinum of the platinum-group elements. *Elements*, **4**, 253-258.

Nicola F., Peter G., Nancy V., and Lisa K. 2011. Non-destructive analysis using PXRF: methodology and application to archaeological ceramics. *X-RAY Spectrum*, **40**, 389-398.

Piercey S.J. and Devine M.C. 2014. Analysis of powdered reference materials and known samples with a benchtop, field portable X-ray fluorescence (pXRF) spectrometer: evaluation of performance and potential applications for exploration lithogeochemistry. *Geochemistry: Exploration, Environment, Analysis*, **14**, 139- 148.

Potts P.J., Webb P.C., Williams-Thorpe O., and Kilworth R. 1995. Analysis of silicate rocks using field-portable X-ray fluorescence instrumentation incorporating a mercury (II) iodide detector: A preliminary assessment of analytical performance. *The Analyst*, **120**, 1273-1278.

Ross P.S., Bourke A., and Fresia B. 2014. Improving lithological discrimination in exploration drill-cores using portable X-ray fluorescence measurements: (2) applications to the Zn-Cu Matagami mining camp, Canada. Geochemistry: *Exploration, Environment, Analysis*, **14**, 187-196.

Shaw C and Penczak R. 1996. Barium- and titanium-rich biotite and phlogopite from the western and eastern gabbro, Coldwell Alkaline Complex, northwestern Ontario. *Canadian. Mineralogist*. **34**, 967–975

Shaw C. 1997. The petrology of the layered gabbro intrusion, eastern gabbro, Coldwell alkaline complex, Northwestern Ontario, Canada: evidence from multiple phases of intrusion in a ring dike. *Lithos*, **40**, 243-259.

Simand, G.J., Fajber R. and Paradis S. 2014. Portable X-ray fluorescence in the assessment of rare earth element-enriched sedimentary phosphate deposits. *Geochemistry: Exploration, Environment, Analysis*, **14**, 161-169.

Walker E.C., Sutcliff R.H., Shaw C.S.J., Shore G.T., and Penczak R.S. 1993. Precambrian geology of the Coldwell Alkaline Complex, Ontario Geological Survey, Open File Report 5868, 23pp.

Wilkinson S.J. 1983. Geology and sulphide mineralization of the marginal phases of the Coldwell Alkaline Complex, northwestern Ontario: Unpublished M.Sc. thesis, Carleton University, Canada, 129 pp.

Chapter 4

Applications of the combined portable XRF-benchtop SEM methodology to exploration at the igneous complex scale: A case study of Cu-Pd exploration at the Coldwell Alkaline Complex"

Yonghua Cao[1], Robert Linnen[1], David Good[1], Iain Samson[2]

1. Western University, London, ON, Canada

2. The University of Windsor, Windsor, ON, Canada

4.1 Introduction

Geochemical analysis of drill core is an essential component of mineral exploration. Conventional lab-based geochemical analyses have high accuracy and precision, but the time needed to obtain results means that decisions cannot be made in the field, in a short time frame. Recent advances in technologies have resulted in a number of field portable analytical techniques that are designed to collect data with minimum time delay and at low cost, which facilitates rapid decision making in the field. Thus, the mineral exploration industry is increasingly using field-portable instruments in modern mineral exploration programs. Portable X-ray fluorescence (pXRF) and benchtop scanning electron microscopy equipped with energy dispersive spectroscopy (bSEM-EDS) are two analytical instruments that can collect rapid lithogeochemical and mineral chemical data in the field.

On-site pXRF lithogeochemical data have been used in mineral exploration applications for some years. For example, Houlihan et al. (2003) presented three cases studies at different Ni, Cu, and Cu-Au mines in Australia, wherein pXRF was evaluated for its ability to be used on-site for ore grade control, and Fisher et al.

(2014) developed a workflow for the collection of pXRF data in an exploration or mining setting. A thorough review of applications of pXRF to mineral exploration is provided by Hall et al. (2011). In contrast to pXRF, applications of bSEM-EDS are still new to mineral exploration. The bSEM-EDS can easily sit on a table in a field setting and can analyze field samples such as rock samples and saw cut blocks without polishing and carbon-coating, which enables the collection of images and EDS mineral chemical analyses at the sub-micron scale as descripted in chapter 2. Therefore, the bSEM-EDS has great potential for mineral exploration in a manner that is analogous to pXRF. Integrating lithogeochemical and mineral chemical analyses will result in a more comprehensive understanding of geology and mineralogy. The purpose of the current study is to evaluate whether pXRF and bSEM-EDS can be combined as a robust tool to increase the efficiency of both mineral exploration and academic research.

In Chapter 3, we used samples from a single drill hole from the Four Dams area of the Coldwell Alkaline Complex to evaluate the quality of mineral and whole-rock chemical data obtained using bSEM-EDS and pXRF, respectively. Mineral analyses included Mg# data of olivine and clinopyroxene (molar Mg/ (Mg+Fe)*100), and the anorthite content of plagioclase (molar Ca/ (Ca+Na)*100). It was demonstrated that both portable instruments were able to provide analyses comparable to their lab-based counterparts, acquired from electron microprobe and ICP-AES/MS/IR. Similar data quality from pXRF was also reported previously by Hall et al. (2014), Piercey and Devine (2014), and Ross et al. (2014). But the work in chapter 2 was the first study to apply bSEM-EDS to mineral exploration research.

The proof of concept study in Chapter 3 is expanded in the current work. The Eastern Gabbro of the Coldwell Alkaline Complex was selected as a case study of combining pXRF and bSEM-EDS for Cu-Pd exploration at a regional scale. Data from around the intrusion are used to evaluate whether field portable techniques can

be used to produce lithogeochemical and mineral chemical sections that can be applied to mineral exploration.

4.2 Geological setting

The Proterozoic Coldwell Alkaline Complex is a sub-circular intrusion that has a diameter of approximately 25 km and a surface area of 580 km^2 and is the largest alkaline intrusive complex in North America (Walker et al., 1993; Shaw, 1997). It intruded the Archean Shreiber-Hemlo greenstone belt along the northern edge of the Midcontinent rift at 1108-1094 Ma, which marked the beginning of the early stage of magmatism related to the Midcontinent system (Walker et al., 1993; Heaman et al., 2007; Good et al., 2015). Petrologic and field studies conducted by Puskas (1970), Mitchell and Platt (1978, 1982), Mitchell et al. (1993), and Shaw (1997) recognized three superimposed intrusive centers constituting this complex, from east to west, they are center I, center II, and center III (Fig. 4-1). Paleomagnetic work conducted by Ashley and Kerns (2012) suggests that Centers I and III are the same age but both are older than Center II. Center I forms the eastern margin of the Coldwell Alkaline Complex, and is composed by the Eastern Gabbro, the Western Gabbro, amphibole quartz syenite, iron-rich augite syenite, and mafic volcanic and subvolcanic rocks (Walker et al., 1993; Shaw, 1994; Good et al., 2015). Center II consists of alkali gabbro and syenite (Mitchell and Platt, 1978, 1982; Mulja, 1989). Center III is mainly composed of syenite and quartz syenite which are intrusive into most other phases of the complex and exhibit various degrees of crustal contamination (McLaughlin and Mitchell, 1989). It was proposed by Mitchell and Platt (1977, 1978) and Walker et al. (1993) that the emplacement of most rock units in the Coldwell Alkaline Complex was controlled by the faulting during cauldron subsidence at a subvolcanic depth.

According the previous studies of Shaw (1994, 1997), the Eastern Gabbro formed by multiple intrusions of basaltic magma with a subalkaline parentage into a partial ring dike structure that cut the Archean country rock. Good et al. (2015) identified

nine major lithologies that were further grouped into three major distinctive magmatic series. From oldest to youngest, they are the meta-basalt (equivalent to fine-grained gabbro in Good et al., 2015), the Layered Series, and the Marathon Series. The relative ages for these units were established from crosscutting relationships, particularly within the numerous units of igneous breccia (Good et al., 2015). The meta-basalt occurs along the base of the Eastern Gabbro and comprises picritic basalt that underwent pyroxene-hornfels grade metamorphism (Good et al., 2015). The Layered Series constitutes the bulk of the Eastern gabbro and is composed of massive to modally layered olivine gabbro, with a lesser amount of weakly layered oxide augite melatroctolite, and, less commonly, gabbroic anorthosite. The Marathon Series is the youngest unit and comprises numerous small intrusions composed predominantly of ophitic gabbro, apatitic clinopyroxenite, oxide melatroctolite, as well as small volumes of augite troctolite and wehrlite (Good et al., 2015).

A significant problem for mineral exploration in the Coldwell Alkaline Complex is that some phases of the Marathon Series and Layered Series can be difficult to distinguish in the field. However, most of the copper and all of the known PGE mineralization is hosted by the Marathon Series, particularly within an ophitic gabbro that is similar to the Two Duck Lake gabbro at the Marathon deposit, the largest Cu-Pd deposit of the Coldwell Alkaline Complex. By contrast, the meta-basalt and the Layered Series lack significant PGE mineralization. The latter locally hosts disseminated chalcopyrite and pyrrhotite mineralization, but is associated with albite-actinolite alteration, with only trace PGE (<0.005 ppm Pd plus Pt) (see Chapter 3). Therefore, being able to distinguish the entire suite of Marathon Series from other Eastern Gabbro rocks is critical for mineral exploration, particularly if it is possible to differentiate these units in the field.

In Chapter 3, we distinguished the Layered and Marathon Series using field portable techniques at one location, namely the Four Dams location (Fig. 4-1). The purpose

of this contribution is to evaluate whether the methods used in that study can be applied to the Coldwell Alkaline Complex as a whole. To accomplish this, two additional areas were selected: Area 41 and the WD zone (Fig. 4-1), and these are compared with the data from Four Dams. Area 41 is approximately 17 km northwest of the Marathon Cu-Pd deposit. The mineralization is hosted mainly by an ophitic, pegmatitic gabbro, with a small amount occurring within apatitic clinopyroxenite, this will be fully described in Chapter 6. The spatial distributions of different series of rock units at Area 41 are depicted in Figure 4-2. The Four Dams area is approximately 2.5 km north of the Marathon deposit. In contrast to Area 41, the Cu-Pd mineralization at Four Dams area is hosted mainly by an apatitic clinopyroxenite, and only a small amount of the ophitic gabbro unit outcrops in this area (see Chapter 3). The WD zone is located roughly 4 km south of the Marathon deposit. The Cu-Pd mineralization in the WD zone has a lower grade than that in Area 41 or Four Dams (unpublished Stillwater Canada Inc. exploration assay), and the mineralization is mainly hosted by an ophitic gabbro. These three mineralized areas were chosen, not only because they are spatially distributed through most of the length of the Eastern Gabbro, but also because they represent all recognized types of PGE mineralization in the Eastern Gabbro (cf. Good et al., 2015; Chapter 6).

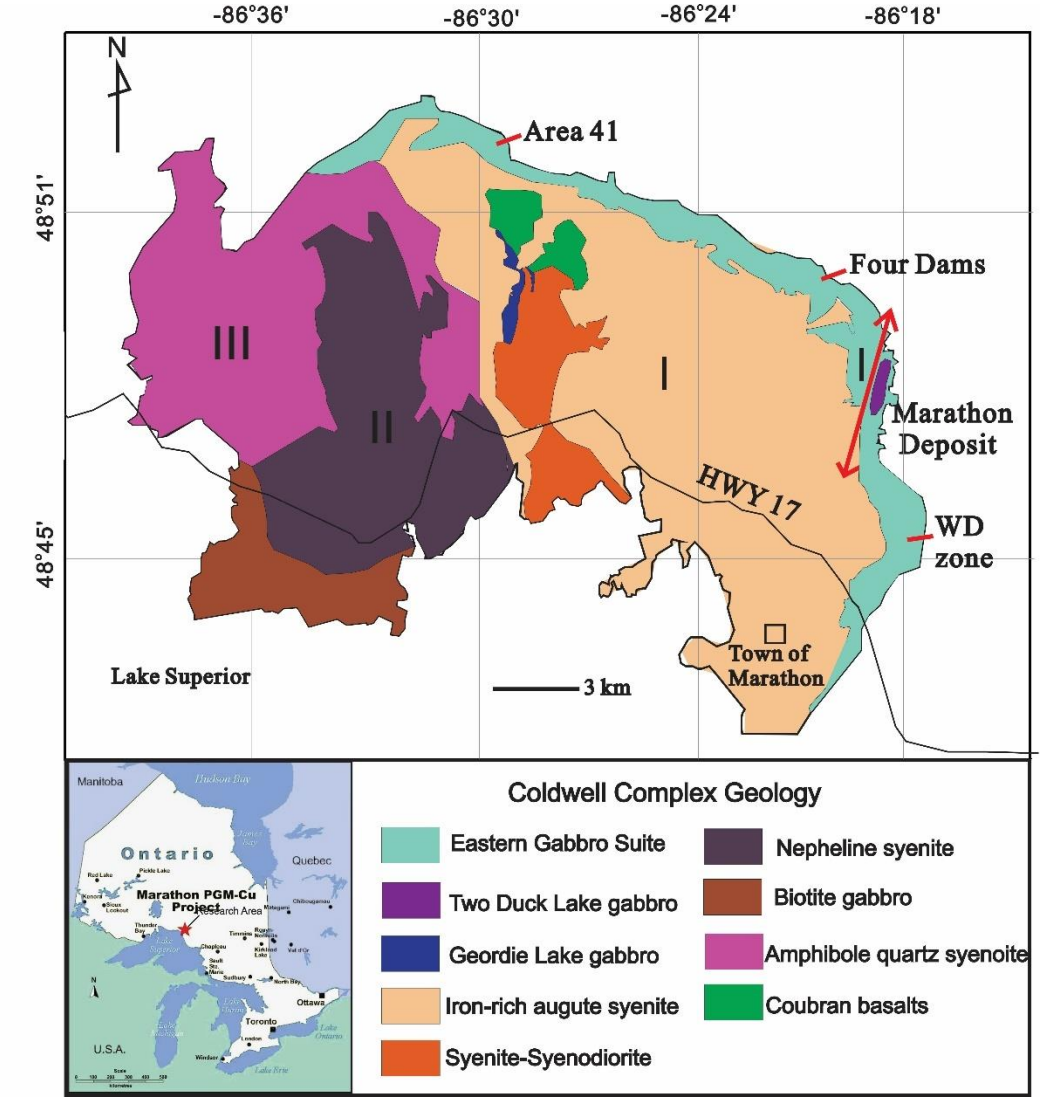

Figure 4-1. Geological map of the Coldwell alkaline complex, situated on the northern shore of Lake Superior. Locations of Area 41, Four Dams, and WD zone are represented as red dots (Simplified after Walker et al., 1993 and Good et al., 2015). The intrusive centers have been shown by Roman numerals (modified after Mulja and Mitchell, 1991). The location of the Marathon deposit is indicated using a double arrowed red line.

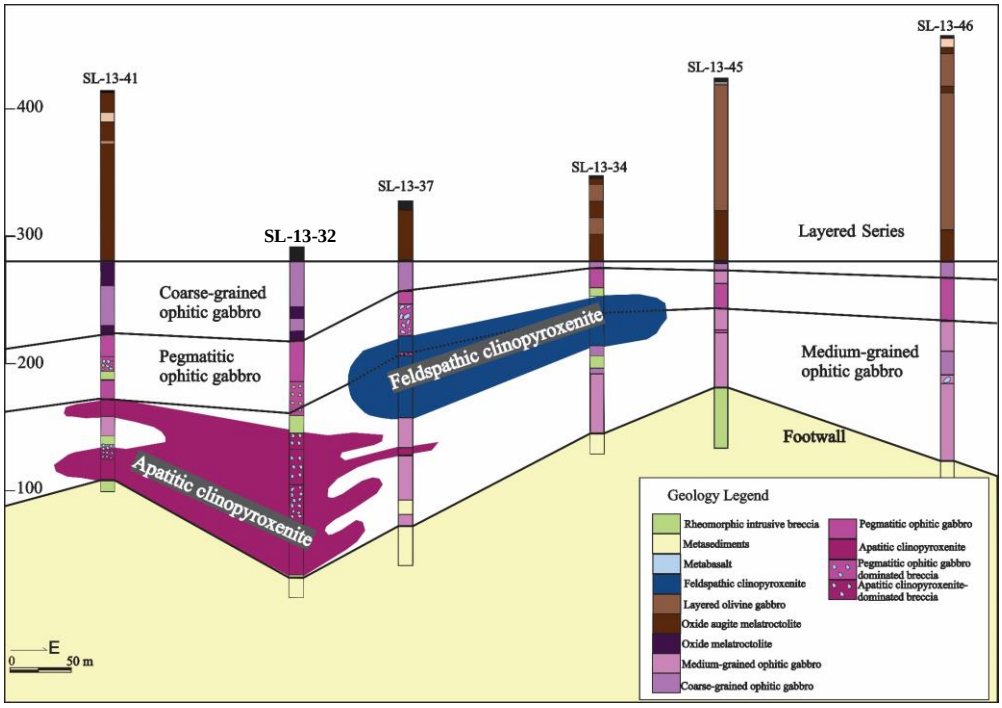

Figure 4-2. Igneous stratigraphy of Area 41 mineralization area. The columns represent the geological log of each of the drill holes, black lines indicate geological contacts.

4.3 Methods

4.3.1 Sample preparation

Powders and rock specimens were obtained from representative diamond drill holes at Area 41 (SL-13-32, SL-13-34, SL-13-37, SL-13-41), Four Dams (FD-13-34), and the WD zone (MW-07-06). All these drill holes intersect a sequence of the Layered Series and the Marathon Series rocks; their drilling parameters are tabulated in Table 4-1.

Table 4-1. Drilling parameters of sampled diamond drill holes (DDH).

Area	DDH Number	Azimuth	Collar	Total Depth (m)
Area 41	SL-13-32	20	-85	252
	SL-13-34	19.56	-80	201
	SL-13-37	20.42	-80	261
	SL-13-41	18.36	-80.05	291
Four Dams	FD-13-34	32.9	-69.6	375
WD zone	MW-07-06	89	-60	168

A total of 283 powdered samples were collected by grinding 1 m-long channels at regular intervals along the length of the drill core, approximately 2 mm wide and 1 cm deep, using a Thermo Scientific portable grinder. Sampling protocols have been described in Chapter 2. Sample locations for powdered samples are given in Figure 4-3. After grinding, powders were loaded into PREM-4331 XRF sample cups capped with 4-μm PREM-F2540 XRF sample cup film for pXRF analyses. A subset of representative powder samples was further pulverized and sent for lab-based analyses.

A total of 149 polished thin sections, representative of different series' gabbro units with different styles of mineralization (e.g., chalcopyrite-rich, and pyrrhotite-rich), were prepared for petrographic and mineral chemical studies. The interval between mineralogical samples was 5 to 20 meters; the locations of polished thin section samples are given in Figure 4-3. Note that although polished thin sections were used in this study, in Chapter 3 we demonstrated that analyses could also be obtained from cut blocks. A comparison of results from cut blocks (unpolished and polished) and polished thin sections is provided below, in section 4.3.2.2.

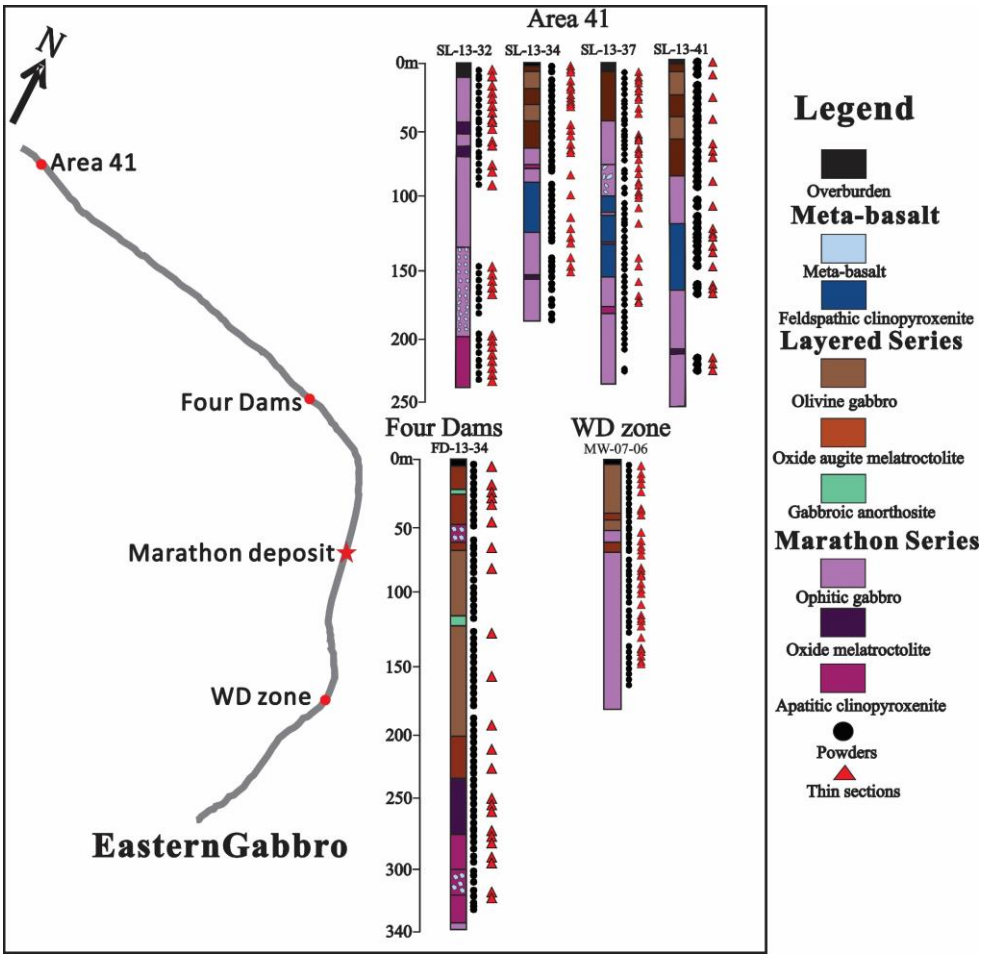

Figure 4-3. Sample locations for powders (circles) and thin sections (triangles) from six representative diamond drill holes: FD-13-34 at Four Dams (see Chapter 3), SL-13-32, SL-13-34, SL-13-37 and SL-13-41 at Area 41, and MW-07-06 at the WD zone. The columns represent the geological log of each of the drill holes. The outer contact of the Eastern Gabbro is represented by the thick grey line and different studied areas are outlined using three red dots. The location of the Marathon Cu-Pd deposit is also indicated by a red star.

4.3.2 Analytical equipment

4.3.2.1 Whole-rock analyses

A NitonXL3t+ GOLDD+ pXRF analyzer equipped with a SDD, and a high energy, 50Kv X-ray Ag anode tube was used to analyze powdered samples. Details of analytical strategies and QA/QC control are given in Chapter 3. The analytical error for pXRF analysis with 95% confidence (2σ) was determined through duplicate analyses conducted on the same sample. pXRF results with analytical errors for elements of interests (Cu, S, Zr, Ba, V, Ti) can be found in Appendix 5. Conventional lithogeochemical analyses were conducted on selected re-ground

samples by ALS Mineral Division in Vancouver. Major elements were analyzed by lithium borate fusion with inductively coupled plasma (ICP)-atomic emission spectroscopy (AES) on a minimum 2 g of pulp samples. Trace elements were analyzed by lithium borate fusion and ICP-mass spectroscopy (MS) on 2 g of pulp samples. Total S was determined using a Leco combustion furnace on 0.01 to 0.1 g of sample, in which the sample is heated to roughly 1350°C in an induction furnace. SO_2 is produced through a reaction with oxygen and is measured by an infra-red detector. Quality control was achieved using ALS geochemical quality-control procedures which involve analyses on a wide array of standards, blanks, and duplicates after each batch of samples. Conventional lithogeochemical results with 95% confidence (2σ standard deviation) are given in Table 4-2.

Table 4-2. Selected lab-based whole-rock Ba, Zr, Cu, S, V, Ti concentrations based on ICP-MS analyses, and ratios of V/Ti and Cu/S in this study. 95% confidence error for element is given in the bracket. Error for the ratio represents 95% confidence error calculated based on the equation $\sigma_{(A/B)}=A/B\times((\sigma_A/A)^2+(\sigma_B/B)^2)^{1/2}$

Drill hole	Depth	Elements (ppm)						Ratios			
		Ba (43.5)	Zr (10.4)	Cu (10.3)	S (60)	V (17.5)	Ti (180)	V/Ti	Error	Cu/S	Error
FD-13-34	5.0	392	53	1505	6900	559	40560	0.014	0.0004	0.218	0.0024
	9.5	786	60	580	2100	353	24240	0.015	0.0007	0.276	0.0093
	14.0	611	99	1935	8100	543	23460	0.023	0.0008	0.239	0.0022
	18.5	1710	42	5220	21400	221	9540	0.023	0.0019	0.244	0.0008
	23.0	1155	63	702	1800	427	17340	0.025	0.0010	0.390	0.0142
	27.5	248	64	2410	9000	1020	36120	0.028	0.0005	0.268	0.0021
	32.0	233	55	1740	5200	963	43200	0.022	0.0004	0.335	0.0043
	36.5	913	74	1490	6800	323	19500	0.017	0.0009	0.219	0.0025
	41.0	432	67	555	2700	513	26640	0.019	0.0007	0.206	0.0060
	45.5	307	66	2050	10100	686	44880	0.015	0.0004	0.203	0.0016
	60.0	866	37	4370	16600	169	11820	0.014	0.0015	0.263	0.0011
	64.5	985	52	686	2700	197	10380	0.019	0.0017	0.254	0.0068
	66.0	1200	56	241	1500	128	7140	0.018	0.0025	0.161	0.0094
	70.5	791	61	280	2100	257	15300	0.017	0.0012	0.133	0.0062
	75.0	906	65	263	2400	150	12480	0.012	0.0014	0.110	0.0051
	79.5	800	74	207	2300	189	14460	0.013	0.0012	0.090	0.0051
	84.0	570	71	176	2400	154	15720	0.010	0.0011	0.073	0.0047
	89.5	699	89	265	1800	141	18840	0.007	0.0009	0.147	0.0075
	94.5	723	84	164	2500	152	20400	0.007	0.0009	0.066	0.0044

99.0	508	64	103	2300	116	16680	0.007	0.0010	0.045	0.0046
103.5	488	73	117	1900	178	25620	0.007	0.0007	0.062	0.0058
108.0	630	69	180	2400	157	20100	0.008	0.0009	0.075	0.0047
112.5	394	50	770	9200	229	28260	0.008	0.0006	0.084	0.0012
117.0	796	55	188	3000	146	18540	0.008	0.0009	0.063	0.0037
127.0	680	64	231	2600	173	20280	0.009	0.0009	0.089	0.0045
131.5	763	63	346	2500	161	18660	0.009	0.0009	0.138	0.0053
136.0	828	63	532	2300	161	19260	0.008	0.0009	0.231	0.0075
140.5	656	66	621	2900	198	22560	0.009	0.0008	0.214	0.0057
145.0	704	62	418	2200	207	21300	0.010	0.0008	0.190	0.0070
149.5	532	62	505	2800	254	29580	0.009	0.0006	0.180	0.0053
154.0	901	85	420	2400	164	18600	0.009	0.0009	0.175	0.0061
158.5	859	79	344	2400	197	20460	0.010	0.0009	0.143	0.0056
163.0	824	86	329	2400	185	19740	0.009	0.0009	0.137	0.0055
167.5	929	92	241	2000	175	18000	0.010	0.0010	0.121	0.0063
172.0	914	93	264	2000	207	20460	0.010	0.0009	0.132	0.0065
176.5	946	96	312	2000	206	18900	0.011	0.0009	0.156	0.0070
181.0	995	107	350	2100	196	18180	0.011	0.0010	0.167	0.0068
190.0	1015	107	542	2100	183	16500	0.011	0.0011	0.258	0.0089
194.5	995	109	352	1800	199	17940	0.011	0.0010	0.196	0.0087
199.0	927	102	439	1900	224	19560	0.011	0.0009	0.231	0.0091
203.5	649	83	349	2100	239	22260	0.011	0.0008	0.166	0.0068
208.0	385	94	796	3100	448	33120	0.014	0.0005	0.257	0.0060
212.5	897	95	367	1700	285	21180	0.013	0.0008	0.216	0.0097
217.0	745	97	493	2300	320	24420	0.013	0.0007	0.214	0.0072
221.5	643	133	521	1700	309	25140	0.012	0.0007	0.306	0.0124
226.0	616	86	758	2200	383	29220	0.013	0.0006	0.345	0.0105
230.5	561	75	855	2500	522	36120	0.014	0.0005	0.342	0.0092
235.0	37	58	881	7300	708	49320	0.014	0.0004	0.121	0.0017
239.5	15.8	60	893	4400	691	46680	0.015	0.0004	0.203	0.0036
244.0	55.3	63	715	4800	716	38760	0.018	0.0005	0.149	0.0028
248.5	348	56	549	2100	474	27420	0.017	0.0006	0.261	0.0089
253.0	275	69	646	3200	554	27840	0.020	0.0006	0.202	0.0050
257.5	323	61	610	3100	680	32700	0.021	0.0005	0.197	0.0051
262.0	340	52	517	1400	670	23820	0.028	0.0008	0.369	0.0175
266.5	333	41	984	1900	765	21600	0.035	0.0009	0.518	0.0172
271.0	388	85	883	1300	1530	28560	0.054	0.0007	0.679	0.0323
272.0	327	42	3660	3200	1050	18060	0.058	0.0011	1.144	0.0217
276.5	128.5	46	6640	7600	874	11460	0.076	0.0019	0.874	0.0070
281.0	361	90	545	1500	621	19740	0.031	0.0009	0.363	0.0161
285.5	384	65	486	1000	447	9840	0.045	0.0020	0.486	0.0309

	291.0	150.5	29	4480	4700	163	2700	0.060	0.0076	0.953	0.0124
	295.5	342	94	1920	4700	314	7680	0.041	0.0025	0.409	0.0057
	302.0	151.5	41	1635	2100	341	7020	0.049	0.0028	0.779	0.0228
	305.0	465	31	880	500	344	4800	0.072	0.0045	1.760	0.2122
	310.0	203	44	1535	1500	463	7320	0.063	0.0028	1.023	0.0415
	316.0	115	47	3130	4200	396	6660	0.059	0.0031	0.745	0.0109
	320.5	109.5	38	3760	4600	367	5520	0.066	0.0038	0.655	0.0087
	325.0	80.7	29	3840	4600	157	2280	0.069	0.0094	0.835	0.0111
	327.5	139.5	36	6370	7600	118	2340	0.050	0.0084	0.838	0.0068
	330.0	250	37	5030	6600	178	3120	0.057	0.0065	0.762	0.0071
SL-13-32	17.0	1130	50	3340	15300	383	13440	0.028	0.0014	0.218	0.0011
	32.0	942	40	3980	8400	434	13500	0.032	0.0014	0.474	0.0036
	37.0	785	74	414	1400	468	14520	0.032	0.0013	0.296	0.0147
MW-07-06	3.9	10000	102	258	2000	121	15960	0.008	0.0011	0.129	0.0064
	11.9	7000	121	119	2000	176	24240	0.007	0.0007	0.060	0.0055
	19.9	4140	116	124	1800	194	19620	0.010	0.0009	0.069	0.0062
	23.9	3510	122	126	1900	201	17880	0.011	0.0010	0.066	0.0058
	38.0	2440	155	118	1200	278	23700	0.012	0.0007	0.098	0.0099
	80.6	1705	85	69	2000	83	12240	0.007	0.0014	0.035	0.0053
	91.5	1430	93	300	2600	116	23760	0.005	0.0007	0.115	0.0048
	95.5	835	84	742	5000	282	33180	0.008	0.0005	0.148	0.0027
	109.5	505	66	2310	4300	1110	30660	0.036	0.0006	0.537	0.0079
	113.5	314	46	653	1000	1030	21900	0.047	0.0009	0.653	0.0405
	117.5	272	66	1145	1800	1220	24240	0.050	0.0008	0.636	0.0220
	121.0	515	58	1225	1300	1000	19200	0.052	0.0010	0.942	0.0442
	135.5	239	42	696	700	1400	22860	0.061	0.0009	0.994	0.0865
	143.5	3.6	467	222	15600	344	32700	0.011	0.0005	0.014	0.0007
	147.5	284	35	2100	2200	899	17700	0.051	0.0011	0.955	0.0265

4.3.2.2 Mineral chemical analyses

Major constituents of olivine, clinopyroxene, and plagioclase were acquired on a JEOL JCM-6000 NeoScope SEM (bSEM) equipped with a JEOL JED-2300 energy-dispersive X-ray analyser at Western University. Analyses were conducted on all prepared carbon-coated polished thin sections using 15 keV accelerating voltage, a high beam current, a 19 mm working distance, a 30-40 μm beam size, and standardless ZAF corrections. The analytical precision of bSEM-EDS analyses has been determined in Chapter 3 by analyzing the same spot 10 times: results are ±0.51 for Mg# of olivine, ±1.0 for Mg# of clinopyroxene, and ±0.63 for anorthite content

of plagioclase (1σ standard deviation). The analytical precision (machine error), combing with the nature variation, constitute the sample variability determined through bSEM-EDS analyses on 3-5 grains of each mineral type in each sample (see Appendix 7). A subset of representative carbon-coated polished thin sections was chosen for electron microprobe analyses, conducted using a JEOL JXA-8530F field-emission probe at Western University. Major and minor constituents of olivine, plagioclase, clinopyroxene were measured. Operating conditions comprised an accelerating voltage of 15 keV and a beam current of 20 nA. The beam was focused to a 1 μm spot for analyzing olivine and clinopyroxene, and to a 5 μm spot for analyzing plagioclase. The peak counting time was 30 s for all elements and background counts were a total of 30 s. A variety of synthetic and natural standards were used to calibrate different elements during probe analyses (Table 4-3). The precision of electron microprobe analyses was determined in Chapter 3 to be ±0.07 for Mg# of olivine, ±0.30 for Mg# of clinopyroxene, and ±0.15 for plagioclase anorthite content (1σ standard deviation), determined by analysis of the same spot 10 times. These values (machine errors) are significantly lower than those for EDS analyses, and are also well below the sample variabilities which were determined through bSEM-EDS analyses conducted on 3-5 grains of each mineral type (Table 4-4).

Figure 4-4 compares bSEM-EDS analytical results and images for a sample prepared in three ways: unpolished cut thin section block, polished cut thin section block, and (carbon-coated) polished thin section. It shows that analytical results from both the unpolished block and polished block are close to those from the polished thin section, and that the polishing process for the block improved the results to some extent. BSE images and EDS mapping for all three sample preparations are similar in terms of identifying minerals and textures, although the rough surface is evident on the BSE image from the unpolished block.

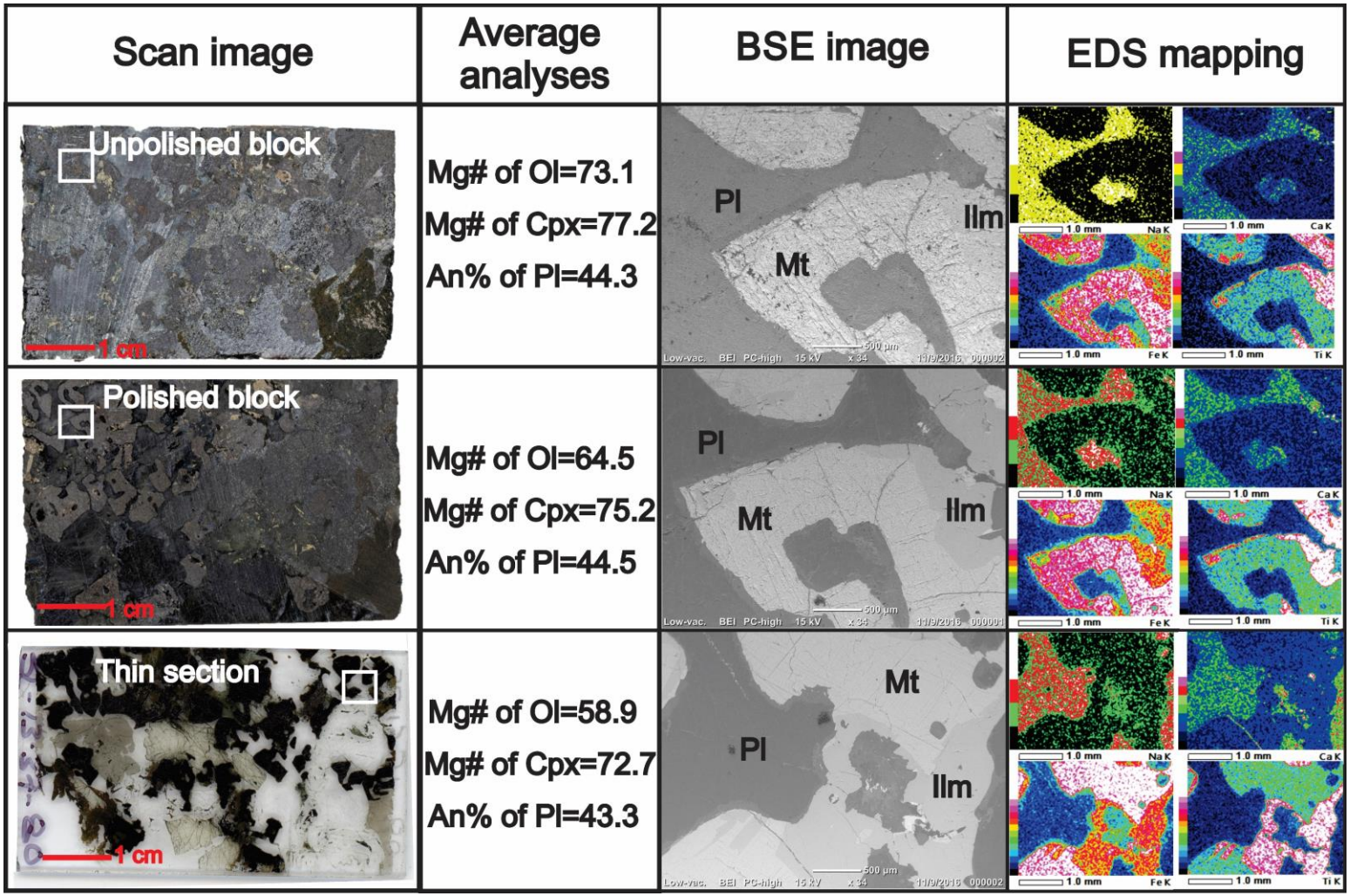

Figure 4-4. Comparison of EDS results, BSE images, and EDS mappings from a same sample (SL-13-37-80) in three different formats: unpolished cut thin section block, polished cut thin section block, and (carbon-coated) thin section. The white square denotes the location for BSE image. Abbreviations: Pl-plagioclase, Mt-magnetite, Ilm-ilmenite.

Table 4-3. Standards used for electron microprobe analyses of olivine, clinopyroxene, and plagioclase.

Olivine and Clinopyroxene		Plagioclase	
Element	Standard	Element	Standard
Si	Olivine	Si	Albite
Al	Cr-Augite	Al	Albite
Na	Albite-Amelia	Na	Albite
Mg	Olivine	Mg	Olivine
Ca	Anorthite	Ca	Anorthite
Ti	Rutile	P	Apatite
Sc	Scandium	Ba	Barite
Fe	Fayalite	K	Orthoclase
Mn	Rhodonite	Sr	Celestite
Ni	Nickel-Silicide	Ti	Rutile
Cr	Chromite	Fe	Fayalite

Table 4-4. Selected electron microprobe analyses in this study. SD refers to 1 σ standard deviation sample error determined on multiple analyses on 3-5 grains of each mineral type in each sample. N/A means the analysis is available.

Drill hole	Depth/m	Unit	Mg# of Ol	SD	Mg# of Cpx	SD	An% of Pl	SD
SL-13-34	3	Oxide augite melatroctolite	37.2	1.49	67.3	1.28	53.6	1.85
	5.1	Oxide augite melatroctolite	33.4	0.33	66.7	0.96	52.2	1.74
	7	Olivine gabbro	35.2	1.00	65.9	1.20	51.8	0.64
	13.3	Olivine gabbro	32.5	0.53	67.9	1.17	50.7	0.78
	17.4	Olivine gabbro	38.0	1.34	67.2	1.64	52.2	1.03
	19.4	Oxide augite melatroctolite	41.7	0.24	67.3	0.62	52.4	0.35
	25.7	Oxide augite melatroctolite	42.0	0.61	67.8	0.44	53.1	2.53
	28.1	Oxide augite melatroctolite	44.0	2.42	68.1	0.62	N/A	N/A
	30	Oxide augite melatroctolite	48.3	1.25	68.5	0.32	52.3	0.64
	32	Olivine gabbro	41.6	1.06	68.3	0.60	54.0	0.99
	45	Olivine gabbro	47.1	0.44	69.0	0.49	55.1	2.40
	49	Oxide augite melatroctolite	47.7	1.52	68.3	0.63	55.9	0.50
	53	Oxide augite melatroctolite	51.4	0.31	69.9	0.32	56.5	1.00
	58.9	Oxide augite melatroctolite	49.1	0.40	69.5	0.38	56.4	0.90
SL-13-41	3	Oxide augite melatroctolite	27.9	0.51	59.9	1.10	43.3	2.11
	7.5	Oxide augite melatroctolite	23.7	0.86	55.8	1.67	24.2	0.74

	12.1	Oxide augite melatroctolite	36.0	0.24	69.0	0.07	52.6	1.32
	45	Oxide augite melatroctolite	38.1	0.48	64.6	1.08	53.8	1.95
	63.2	Oxide augite melatroctolite	44.0	0.15	67.8	0.42	52.0	1.50
	68.9	Oxide augite melatroctolite	45.9	0.20	67.9	0.81	51.2	0.63
	73	Oxide augite melatroctolite	51.1	0.24	69.2	0.28	56.2	0.58
	91	Oxide augite melatroctolite	53.0	0.46	70.5	0.92	55.0	0.24
	109.1	Oxide augite melatroctolite	57.1	0.24	70.7	0.43	55.3	1.40
	5	Oxide augite melatroctolite	50.6	0.10	68.1	1.20	52.3	0.90
	18.6	Oxide augite melatroctolite	49.8	0.10	68.6	1.10	54.4	1.80
	24	Olivine gabbro	43.0	1.40	68.1	1.00	48.8	1.80
	27.9	Oxide augite melatroctolite	53.7	0.40	69.4	1.40	54.4	1.20
	33	Oxide augite melatroctolite	55.9	0.40	69.8	1.70	51.7	2.90
	46.1	Oxide augite melatroctolite	51.8	0.90	68.3	0.60	52.1	0.80
FD-13-34	64.6	Oxide augite melatroctolite	45.8	0.30	66.9	1.10	53.4	3.50
	79.6	Olivine gabbro	43.2	0.70	64.4	1.50	51.6	2.10
	127.3	Olivine gabbro	36.1	0.60	59.1	0.70	43.8	2.60
	158.6	Olivine gabbro	29.9	0.30	56.0	1.80	45.2	2.00
	194.8	Olivine gabbro	27.8	2.50	58.3	2.10	39.4	2.50
	212.5	Oxide augite melatroctolite	34.7	0.70	59.0	0.40	43.9	1.50
	226.3	Oxide augite melatroctolite	35.1	1.10	60.0	0.70	42.7	2.60

4.4 Lithology

Representative hand sample pictures for units as described below are shown in Figure 4-5. Note how similar appearances among these units, particularly to oxide augite melatroctolite and oxide melatroctolite.

4.4.1 Meta-basalt

The meta-basalt occurs along the base of the Eastern Gabbro and makes up approximately one quarter to a third of the total Eastern Gabbro package (Good et al., 2015, note that meta-basalt is equivalent to the fine-grained series described in this reference). This unit was intruded by the later Marathon Series intrusions such as an ophitic gabbro, and occurs locally as xenoliths within the Marathon Series rocks. Its composition varies from basalt to olivine basalt, and consists of equigranular, fine-grained subhedral clinopyroxene, olivine, and magnetite, with interstitial plagioclase. The meta-basalt is distinguished by its recrystallized

granoblastic texture (120° boundaries between crystals, Fig. 4-6A), reflecting the pyroxene hornfels-grade metamorphism, likely caused by heat from later intrusions.

4.4.2 Feldspathic clinopyroxenite

The feldspathic clinopyroxenite is exposed at Area 41, and is not observed at Four Dams or the WD zone. McBride (2013) suggested that the feldspathic clinopyroxenite is an older intrusion that is potentially related to the meta-basalt based on crosscutting relationships and mineral textures. The mineralogy of the feldspathic clinopyroxenite, in decreasing order of abundances, comprises medium- to coarse- grained clinopyroxene (60-80 modal%), olivine (5-15 modal%), plagioclase (5-10 modal%), magnetite (less than 5 modal%), and trace disseminated sulfide minerals that are dominated by pyrrhotite and chalcopyrite. Plagioclase occurs either as coarse-grained subhedral grains interstitial to cumulate olivine and clinopyroxene, or as rounded, fine-grained inclusions enclosed by clinopyroxene. Magnetite and sulfide minerals typically occur as inclusions within olivine and clinopyroxene. The feldspathic clinopyroxenite is moderately to extensively altered, as reflected by a network of chlorite stringers (Fig. 4-6B).

4.4.3 Layered Series

The Layered Series makes up most of the Eastern Gabbro, and has a consistent intergranular texture and mineralogy throughout. It is dominated by massive to modally layered olivine gabbro and weakly layered oxide augite melatroctolite, with lesser amounts of gabbroic anorthosite. As will be shown in Chapter 5, the olivine gabbro and the oxide augite melatroctolite represent compositional end-members of the same unit, with similar concentrations of high field strength elements (HFSE) and mineral chemistry.

4.4.3.1 Olivine gabbro

The olivine gabbro is medium- to coarse- grained (1-4 mm). Layering of this unit is defined by a gradational change in the abundance of plagioclase (Fig. 4-7A), or by the alternation of plagioclase-rich and clinopyroxene-rich sublayers. It consists of euhedral plagioclase (40-60 modal%), subhedral clinopyroxene (15-30 modal%),

subhedral olivine (10-15 modal%), less than 10 modal % apatite plus magnetite, and less than 5 modal % subhedral biotite and/or anhedral alkali feldspar. Locally, plagioclase grains occur as chadocrysts enclosed by olivine and clinopyroxene oikocrysts, and olivine is rimed by clinopyroxene, indicating a plagioclase-olivine-clinopyroxene crystallization sequence (from early to late). Minor phases such as apatite, magnetite, and biotite typically occur interstitial to olivine and plagioclase. Alkali feldspar (perthite) is only observed in olivine gabbro at Area 41 and the WD zone (Fig. 4-6C), whereas it is negligible in olivine gabbro at Four Dams.

4.4.3.2 Oxide augite melatroctolite

The oxide augite melatroctolite is medium grained and has textures that are similar to olivine gabbro. It displays weak modal layering and is distinguished from other units by a greater abundance (10 to 20 modal %) of disseminated magnetite. The mineralogy of this unit is similar in the different areas, in decreasing order of abundance, olivine (20-45 modal%), plagioclase (15-30 modal%), clinopyroxene (10-20 modal%), magnetite, and apatite (<10 modal%). Olivine and clinopyroxene are euhedral, and occur interstitial to subhedral to anhedral plagioclase clusters. Magnetite and apatite are generally enclosed by, or are less commonly interstitial to olivine and plagioclase.

4.4.3.3 Gabbroic anorthosite

The gabbroic anorthosite is older than the Layered Series gabbro because it typically occurs as meter-sized xenoliths throughout the Layered Series olivine gabbro (Good et al., 2015). This unit has a very distinctive mottled appearance and consists of approximately 80 modal % medium-grained, subhedral to anhedral plagioclase, very coarse-grained clinopyroxene (10 modal %) and olivine (5 modal %) oikocrysts, and 5 modal % medium- to coarse-grained, interstitial to poikilitic magnetite.

4.4.4 Marathon Series

4.4.4.1 Ophitic gabbro

The ophitic gabbro is medium-grained (<2 mm) to pegmatitic (>4 mm). It has a characteristic ophitic to subophitic texture that resembles the Two Duck Lake gabbro at the Marathon deposit (Fig. 4-7B). Minerals present are, in approximately decreasing order of abundance, subhedral plagioclase (40-70 modal%), subhedral clinopyroxene (15-30 modal%), euhedral to subhedral olivine (5-10 modal%), and less than 10 modal% magnetite and apatite. This unit constitutes the majority of the Marathon Series, and is the main host of Cu-Pd mineralization, at both Area 41 and the WD zone. However, at Four Dams, only a small amount of ophitic gabbro is present. At Area 41, the ophitic gabbro can be further subdivided into three subtypes based on differences in grain size (Fig. 4-2), namely medium-grained ophitic gabbro, coarse-grained ophitic gabbro, and pegmatitic gabbro, more details can be seen in Chapter 6. The medium-grained ophitic gabbro contains negligible olivine, and PGE mineralization is mainly hosted by the coarse-grained and pegmatitic ophitic gabbro. There is some local development of secondary minerals such as chlorite, amphibole, serpentine, and calcite particularly in the pegmatitic ophitic gabbro.

4.4.4.2 Apatitic (olivine) clinopyroxenite

The apatitic (olivine) clinopyroxenite is an apatite-rich rock which consists of up to 30 modal % apatite (Fig. 4-6D). Other minerals present are medium- to coarse-grained subhedral clinopyroxene (30-60 modal%) and olivine (10-20 modal%), subhedral plagioclase (5-10 modal%), and less than 10 modal% magnetite and biotite. At Four Dams, this unit is the main Marathon Series rock, and hosts the majority of Cu-Pd mineralization, in contrast to Area 41 and the WD zone. At Area 41 (and possibly the WD zone), the apatitic (olivine) clinopyroxenite constitutes a minor proportion of the Marathon Series and typically occurs as thin lenses within the ophitic gabbro. Moderate to strong chlorite and actinolite alteration is commonly observed in this unit.

4.4.4.3 Oxide melatroctolite

The oxide melatroctolite occurs as pods that typically are located within the main body of the ophitic gabbro at Area 41 and the WD zone. As described in Chapter 3, in the Four Dams area, this unit sits below the oxide augite melatroctolite, and constitutes an important Marker Horizon that indicates the transition from the PGE-barren Layered Series to the PGE-mineralized Marathon Series. Similar to the Layered Series oxide augite melatroctolite, the oxide melatroctolite also contains a greater abundance of subhedral magnetite (40-60 modal %). This unit also contains olivine, clinopyroxene, plagioclase (the total amount of the three minerals generally is less than 30 modal %), and from 2 to 30 modal % euhedral apatite.

4.4.5 Breccia

Breccias within the Marathon Series generally comprise either an ophitic gabbro matrix with angular xenoliths of meta-basalt or footwall rocks, or an apatite clinopyroxenite-dominated matrix with meta-basalt or footwall xenoliths. At Four Dams, breccia also cuts the Layered Series, and consists of meta-basalt rocks that were cut by multiple thin dikelets of the Marathon Series gabbro. Similar breccia rocks were observed by Good et al. (2015) at the Marathon deposit. It should be noted that these breccia rocks contain sulfide-bearing ophitic gabbro and apatitic clinopyroxenite, which are also important hosts to Cu-PGE mineralization, particularly at Area 41.

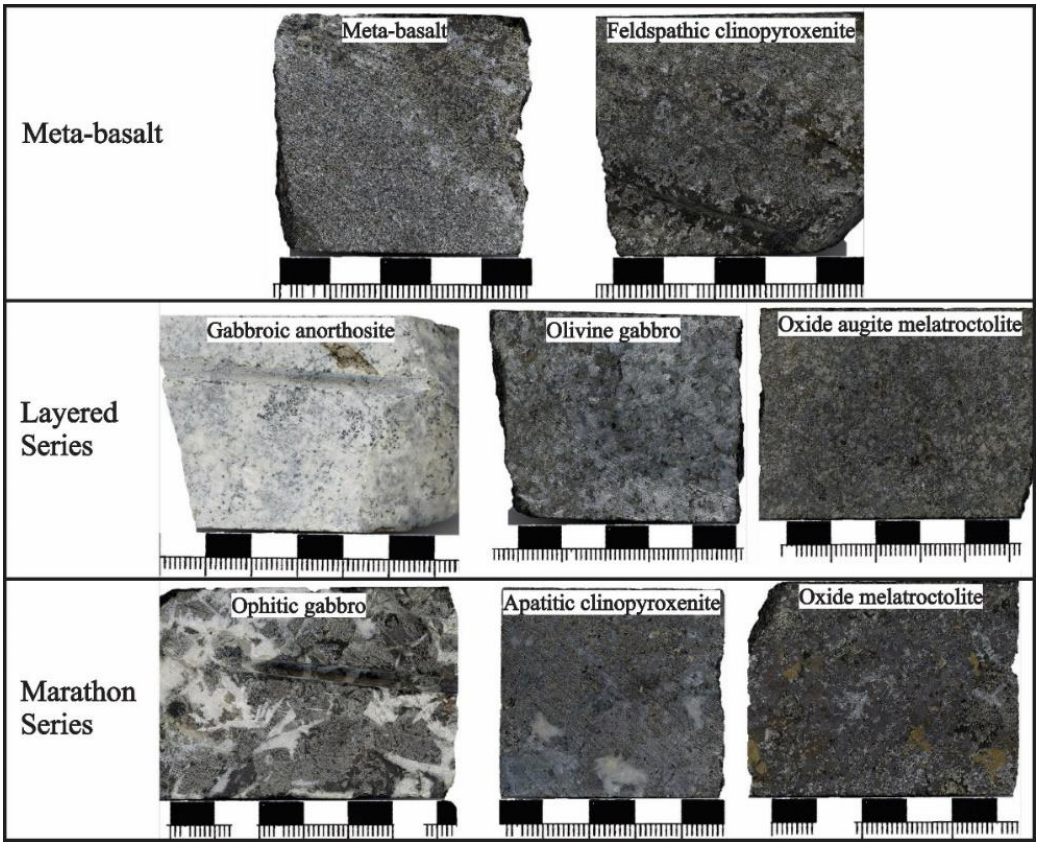

Figure 4-5. Representative hand sample pictures for different units at the Eastern Gabbro.

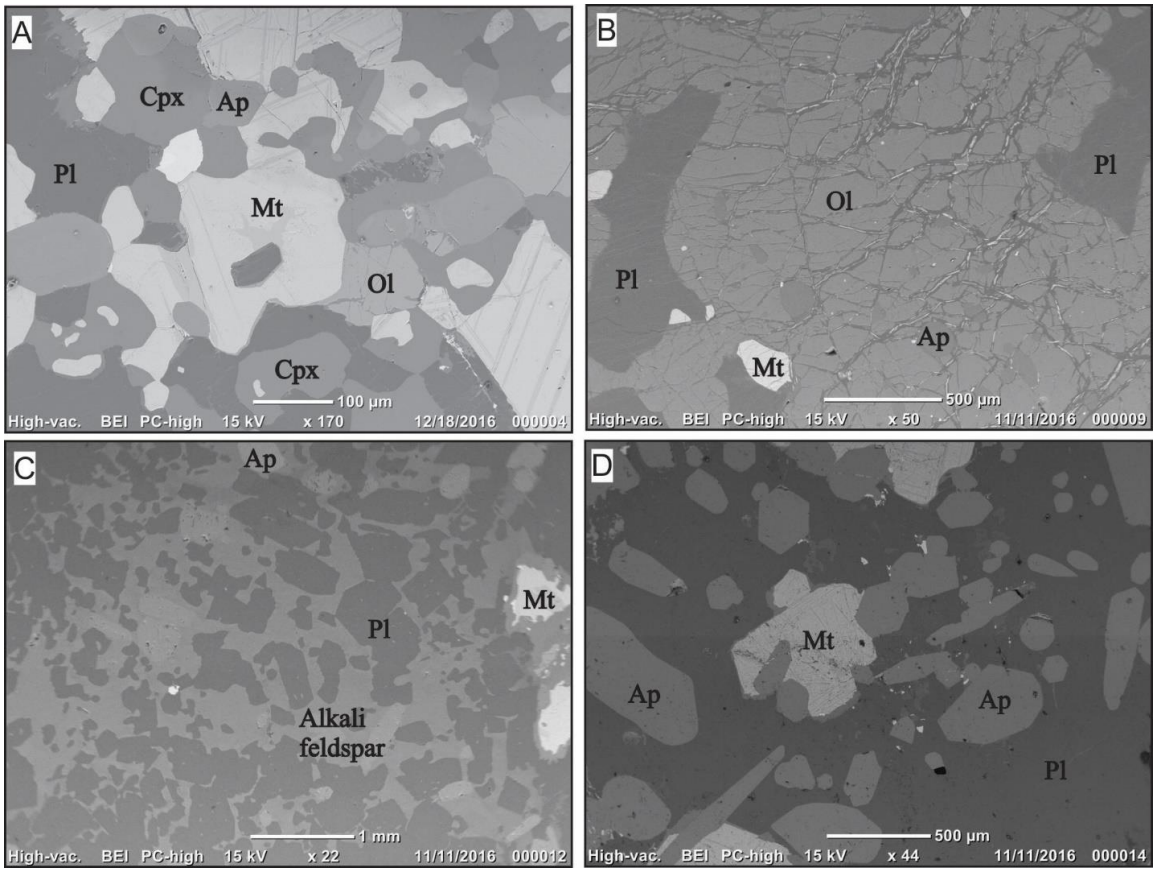

Figure 4-6. BSE images showing mineral compositions and textures for various units. (A) The recrystallized texture in the meta-basalt, note the nearly 120° angles of boundaries between different crystals; (B) The net-work chlorite stingers crosscutting the Ol crystal in feldspathic clinopyroxenite; (C) Alkali feldspar surrounds euhedral-subhedral Pl in the olivine gabbro at Area 41; (D) Many Ap inclusions in plagioclase, as observed in apatitic clinopyroxenite. Abbreviations: Ol-olivine, Cpx-clinopyroxene, Pl-plagioclase, Mt-magnetite, Ap-apatite.

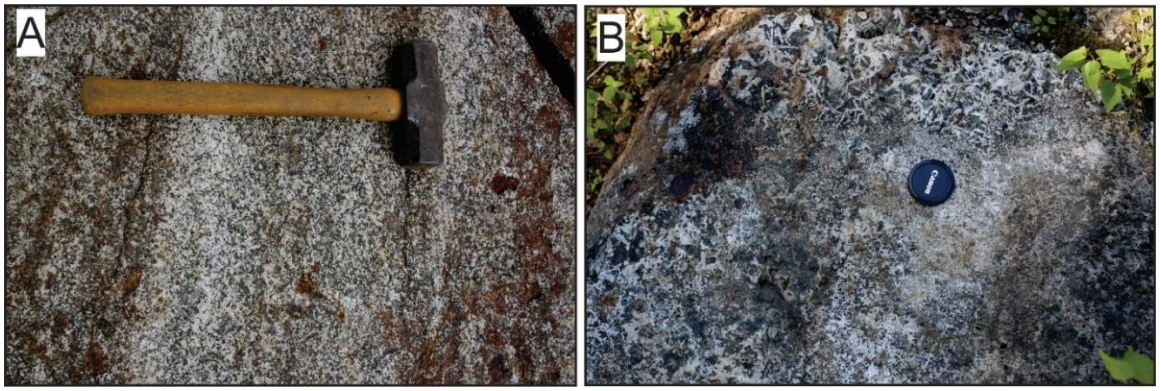

Figure 4-7. Outcrops for the Layered Series units and the Marathon Series ophitic gabbro. (A) The layering reflects a gradational change in the abundance of plagioclase; (B) The ophitic gabbro; note the typical ophitic texture for gabbro along the upper part of the photo and the finer grained xenolith beneath the lens cap.

4.5 Validation of results from portable techniques

Since the accuracy and precision of data collected by field portable analytical instruments are inevitably poorer than those of lab-based analyses, the quality of the data should be assessed prior to real-time measurements.

4.5.1 pXRF

pXRF analyses of Ba, Zr, Cu, S, V, Ti, Cu/S, and V/Ti are compared to their lab-based counterparts in Figure 4-8. Coefficients of determination (R^2) between pXRF and ICP-AES/ICP-MS/IR are above 0.8 for all elements and ratios, indicating excellent correlations for results between these two different methods. Therefore, when down-hole variations of these elements and ratios are of particular interest, pXRF analyses will generate comparable profiles to their lab-based counterparts. Moreover, the high accuracy of pXRF Zr, V, Ti, and V/Ti data are reflected by data distributions that fall close to the 1:1 line with lab-based data. By contrast, pXRF data accuracy for Ba, Cu, S, and Cu/S are poorer. However, since there are excellent correlations between pXRF and lab-based Ba, Cu, S, and Cu/S, recalibration can be applied to improve data accuracy, as shown in Chapter 3.

4.5.2 bSEM-EDS

On Figure 4-9, bSEM-EDS analyses of the Mg#s of olivine and clinopyroxene, and the anorthite content of plagioclase are compared to microprobe analyses, with both sets of analyses on the same grains. The correlation between data from the two methods are excellent for the Mg# of olivine (R^2=0.92) and the anorthite content of plagioclase (R^2=0.86), and reasonable for the Mg# of clinopyroxene (R^2=0.73), similar to the comparison made in Chapter 3. Therefore, down-hole variations in these parameters from bSEM-EDS analyses are comparable to their probe counterparts.

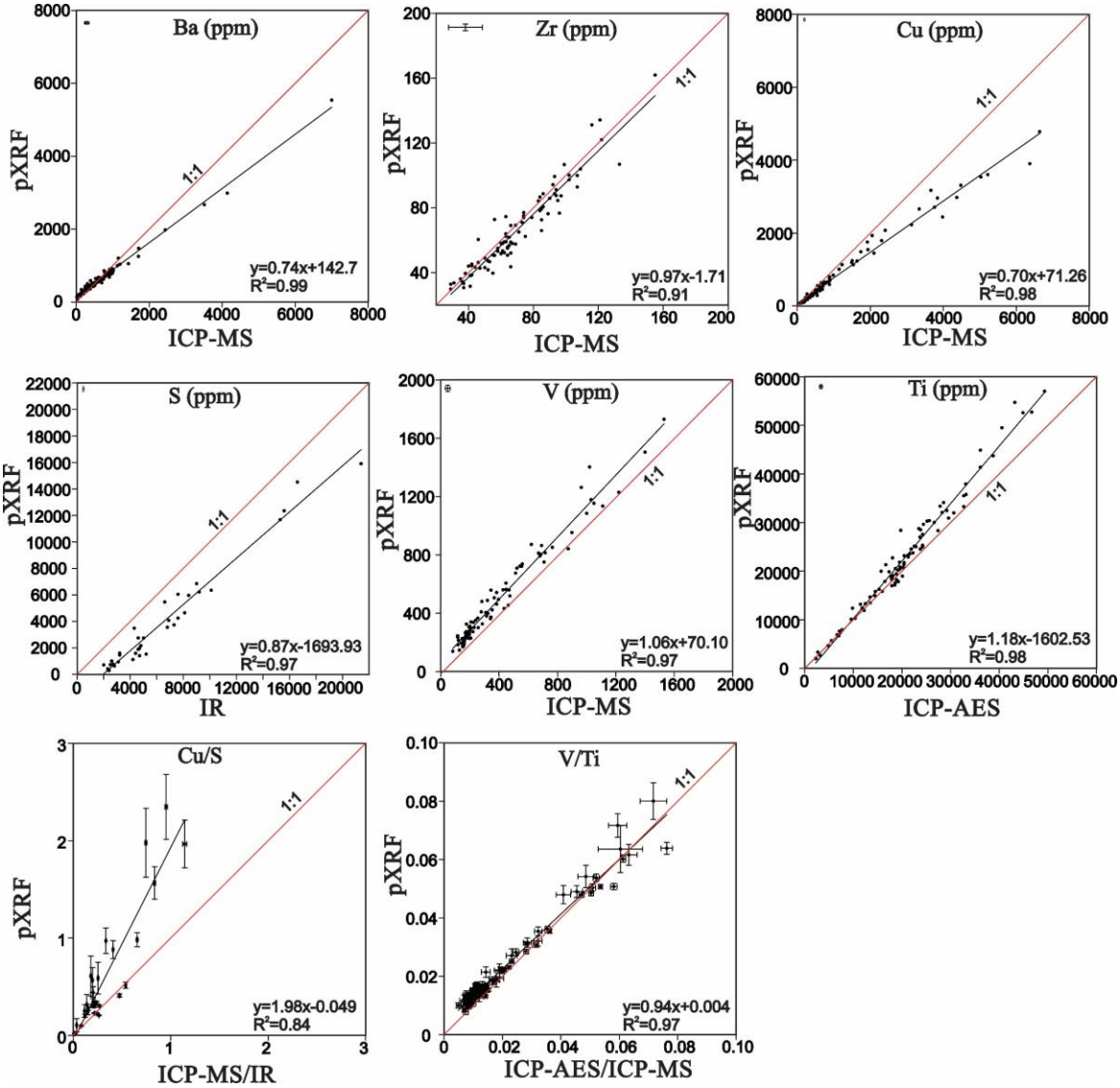

Figure 4-8. Comparisons between pXRF analyses and ICP-AES/ICP-MS/IR analyses. Error bar represents 95% confidence (2σ standard deviation) of analytical uncertainty determined by repetitive analyses.

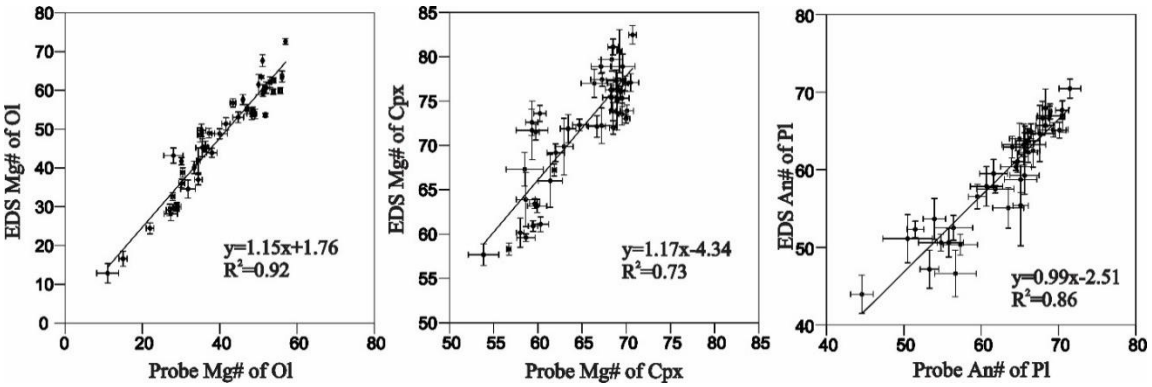

Figure 4-9. Binary diagrams correlating bSEM-EDS analyses with microprobe analyses. Error bars represents 1σ sample errors determined through EDS analyses conducted on 3 or 4 grains of each mineral type in each sample, and multiple spot analyses were conducted on each mineral grain. Average values are correlated in this figure.

4.6 Results

4.6.1 Whole-rock compositions

Concentrations of pXRF whole-rock Ba, Zr, and V/Ti ratios in Layered Series and Marathon Series units at the three locations are summarized in Figure 4-10. Generally, the Layered Series units contain higher Ba and Zr contents than the Marathon Series units. This is particularly evident by comparing various rock units from the same area. In addition, the Layered Series units from the WD zone and Area 41 contain higher Ba contents than those from Four Dams, and there is an increase in Zr contents for the Layered Series units from Area 41, through Four Dams, to the WD zone. V/Ti ratios for the Layered Series units from all three localities are lower than 0.025, whereas those for the Marathon Series units generally are above 0.03, up to around 0.09 for the apatitic clinopyroxenite at Four Dams.

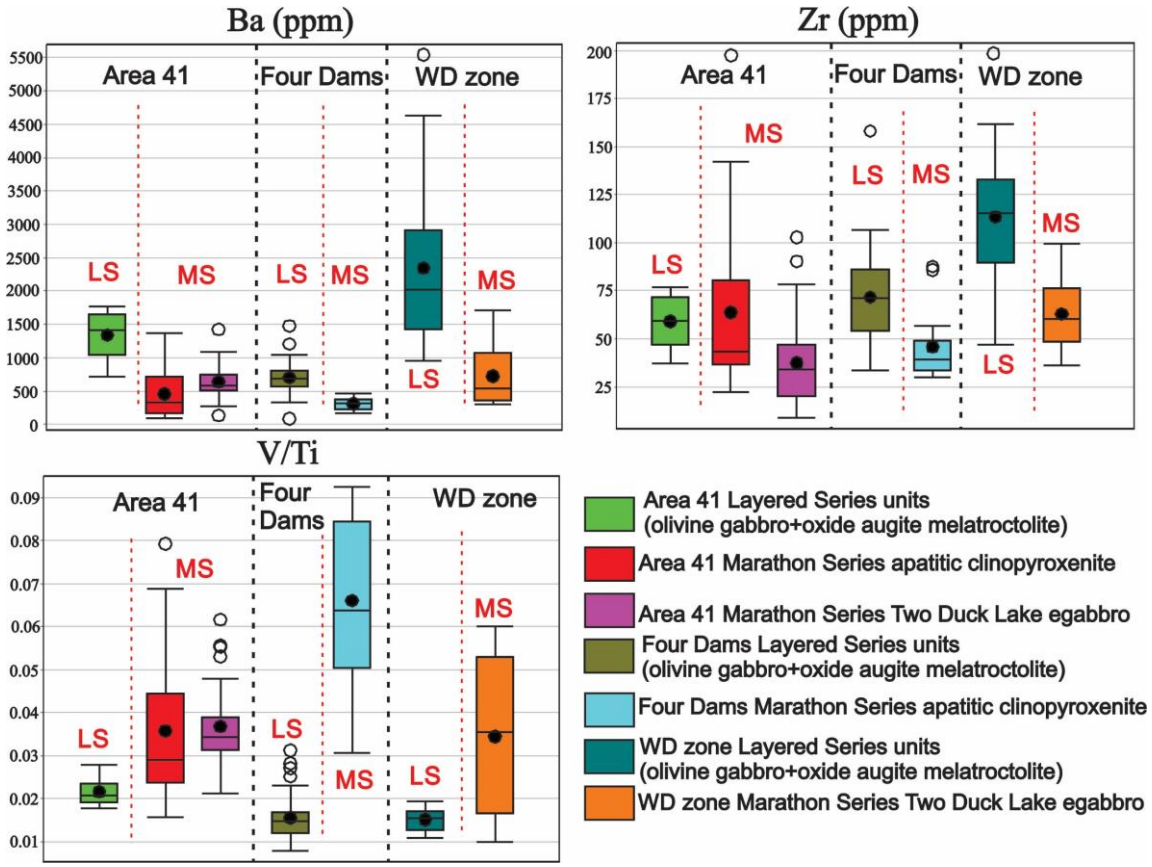

Figure 4-10. Box and whisker plots for selected trace elements in different rock units of different localities. Box and whisker plots are uniform in their use of the box: the bottom and top of the box are always the 25th and 75th percentile (the lower and upper quartiles, respectively), and the band near the middle of the box is always the 50th percentile (the median). The small black infilled circle is the average and the lines on the ends are the minimum and maximum values, black empty circles are outliers.

4.6.2 Mineral chemical compositions

The Mg#s of olivine and clinopyroxene, and the anorthite content of plagioclase determined by bSEM-EDS for Layered Series and Marathon Series units are summarized in Figure 4-11. Generally, the Marathon Series units have higher Mg#s of olivine and clinopyroxene, and anorthite content of plagioclase than the Layered Series rocks, particularly when comparing rock units of the same area. Interestingly, at Area 41 the apatitic clinopyroxenite has higher Mg# values but lower anorthite content of plagioclase than the Layered Series gabbro, this may indicate that the plagioclase was an entrapped phase in this unit, or reflect the great uptake of Ca by apatite and clinopyroxene. The Layered Series units and the Marathon Series ophitic

gabbro at the WD zone have lower Mg#s of olivine and clinopyroxene, and anorthite content of plagioclase, respectively, than the Area 41 and Four Dams Layered Series and Marathon Series units.

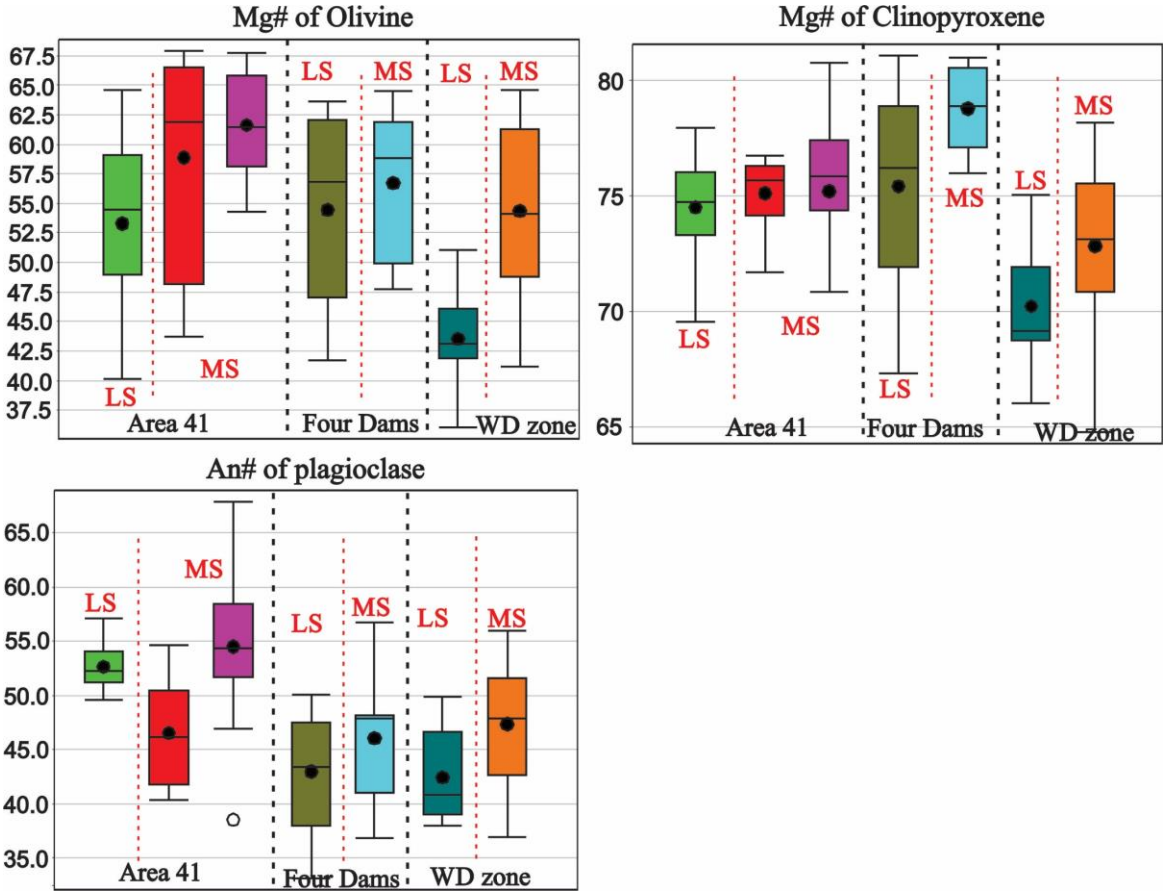

Figure 4-11. Box and whisker plots for mineral chemical compositions in different rock units of different localities, legends as in Figure 4-10.

4.6.3 Down-hole profiles

Down-hole geochemical profiles of Cu/S (pXRF-based and/or lab-based), pXRF Ba, pXRF V/Ti, pXRF Zr, and the bSEM-EDS Mg#s of olivine and clinopyroxene for three representative drill holes (SL-13-37, FD-13-34, MW-07-06) at Area 41, Four Dams, and WD zone are displayed in Figures 4-12, 4-13, and 4-14. Note that three PGE mineralized zones (defined by >100 ppb Pd plus Pt) are outlined in the three figures. Based on unpublished exploration assay data, the mineralized zone in SL-13-37 and FD-13-34 contain higher PGE grades than the that in MW-07-06 (430 ppm Pt and 630 ppm Pd on average for SL-13-37, 1690 ppb Pd and 800 ppb Pt on

average for FD-13-34, and 150 ppm Pt and 390 ppm Pd on average for MW-07-06). Seven significant characteristics of these down-hole profiles are:

1) the Layered Series units at Area 41 and the WD zone generally present down-hole decreases in Ba and Zr, and down-hole increases in V/Ti and the Mg#s of olivine and clinopyroxene;

2) the Layered Series at Four Dams does not show much variation in Ba and V/Ti with depth, but is characterized by a general down-hole increase in Zr and decrease in the Mg#s of olivine and clinopyroxene;

3) the Marathon Series, by contrast, lacks any consistent down-hole variations in these variables, and instead is characterized by fluctuations of these parameters in the ophitic gabbro at Area 41 and the WD zone;

4) the apatitic clinopyroxenite at Four Dams has a general down-hole decrease in Zr, and increase in V/Ti and the Mg#s of olivine and clinopyroxene, but all these variables also show zig-zag patterns;

5) it is apparent that the Layered Series units in the three areas have higher Ba and Zr, and lower V/Ti ratios than their Marathon Series counterparts;

6) Rock units within the PGE mineralized zones in the shown drill holes contain significantly higher Cu/S ratios than other rock units;

7) in SL-13-37, for the Marathon Series ophitic gabbro that contains PGE mineralization, the Mg#s of olivine and clinopyroxene are significantly more variable than the Layered Series units, as well as the rest of PGE-poor Marathon Series rocks. Note that other drill holes (see Appendix 5 & 7) exhibit similar characteristics as those illustrated above.

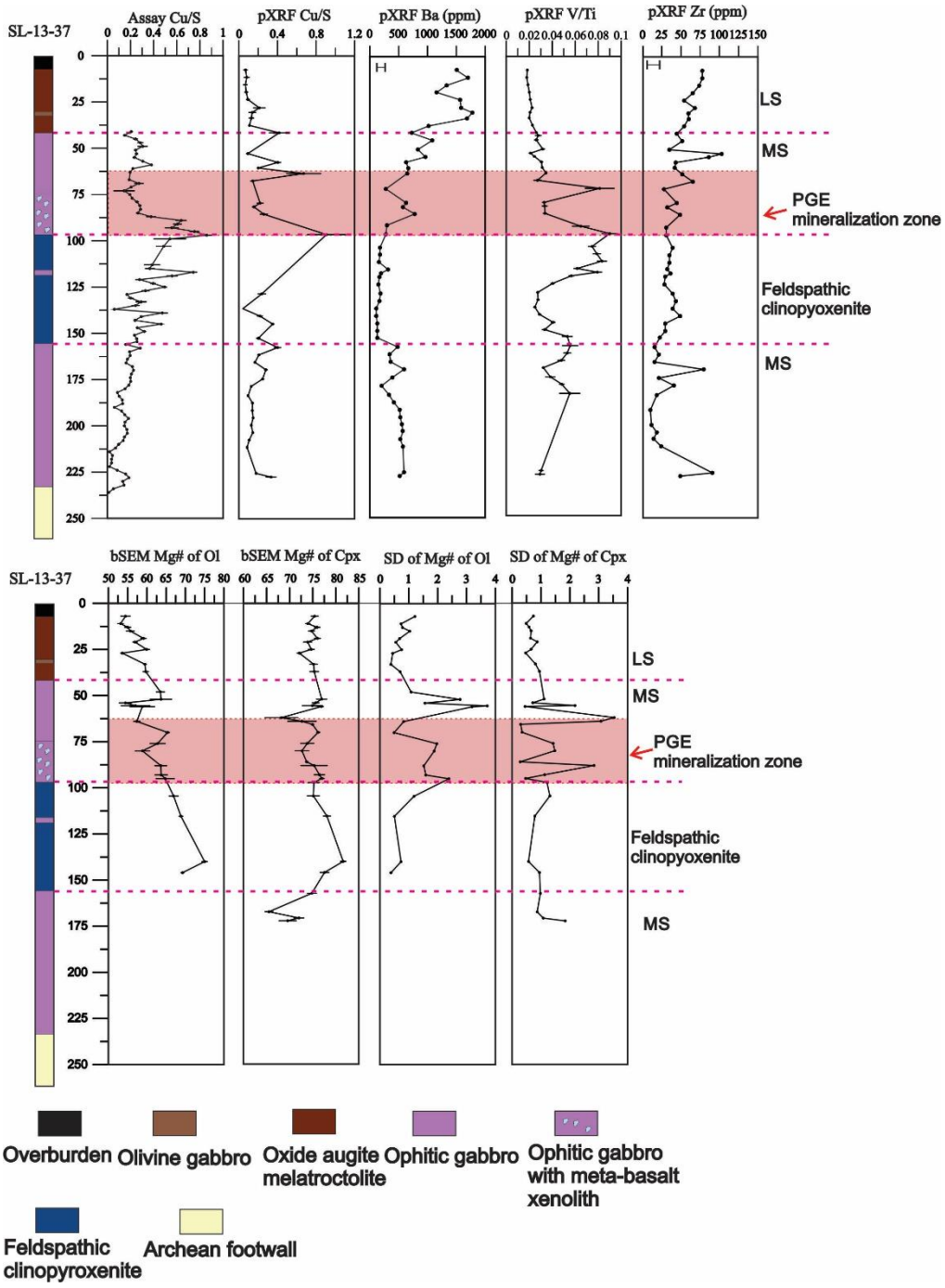

Figure 4-12. Geochemical profiles down the drill hole SL-13-37 at Area 41, the shaded area indicates the PGE mineralization zone. The error bar for pXRF analysis represents 2σ analytical uncertainty determined by multiple analyses on the same powder. The error bar for bSEM-EDS analysis represents 1σ sample variability determined by 3-5 analyses on 3-5 grains of each mineral type in each sample. SD means 1 sigma standard deviation.

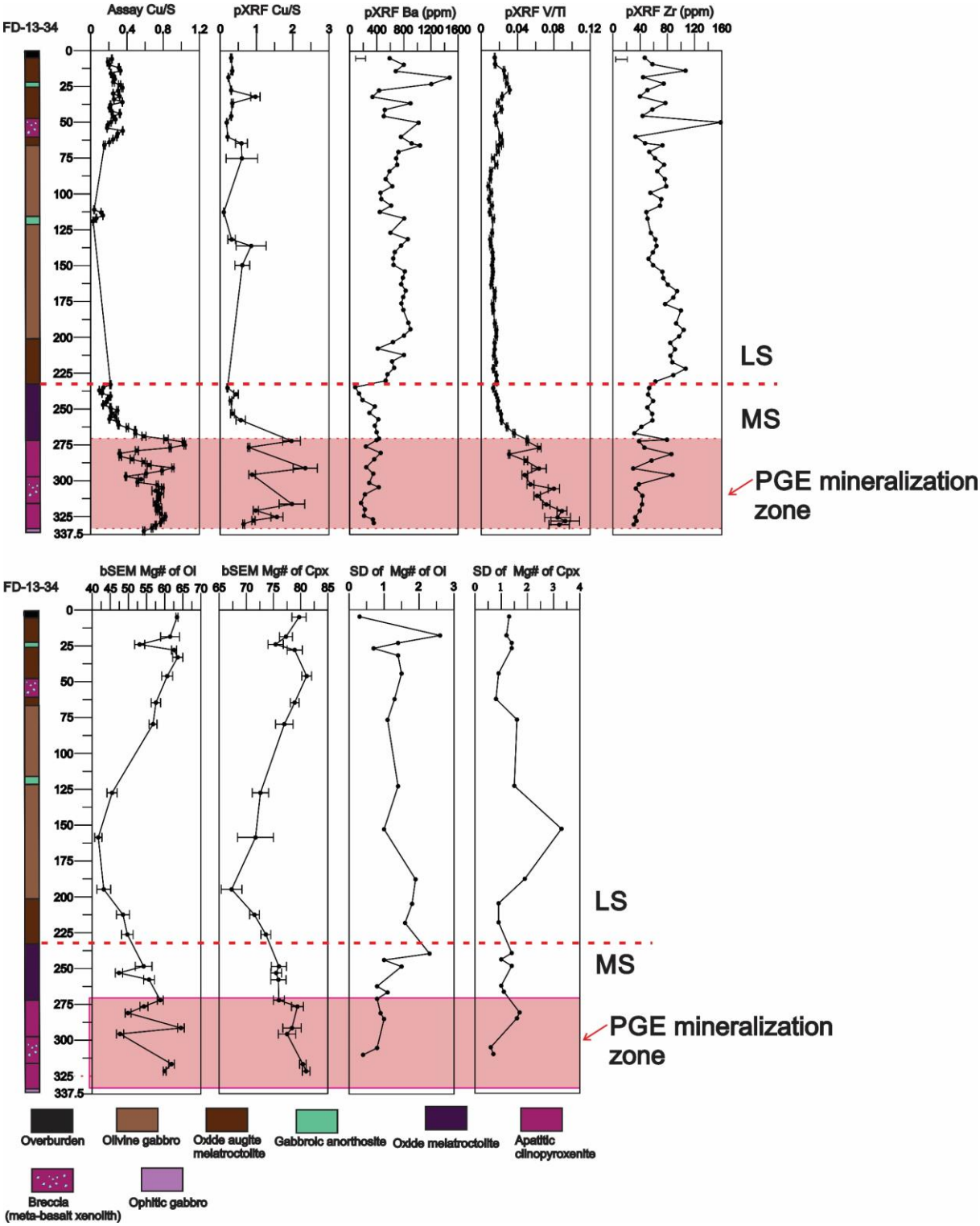

Figure 4-13. Geochemical profiles down the drill hole FD-13-34 at Four Dams, the shaded area indicates the PGE mineralization zone. The error bar for pXRF analysis represents 2σ analytical uncertainty determined by multiple analyses on the same powder. The error bar for bSEM-EDS analysis represents 1σ sample variability determined by 3-5 analyses on 3-5 grains of each mineral type in each sample. SD means 1 sigma standard deviation.

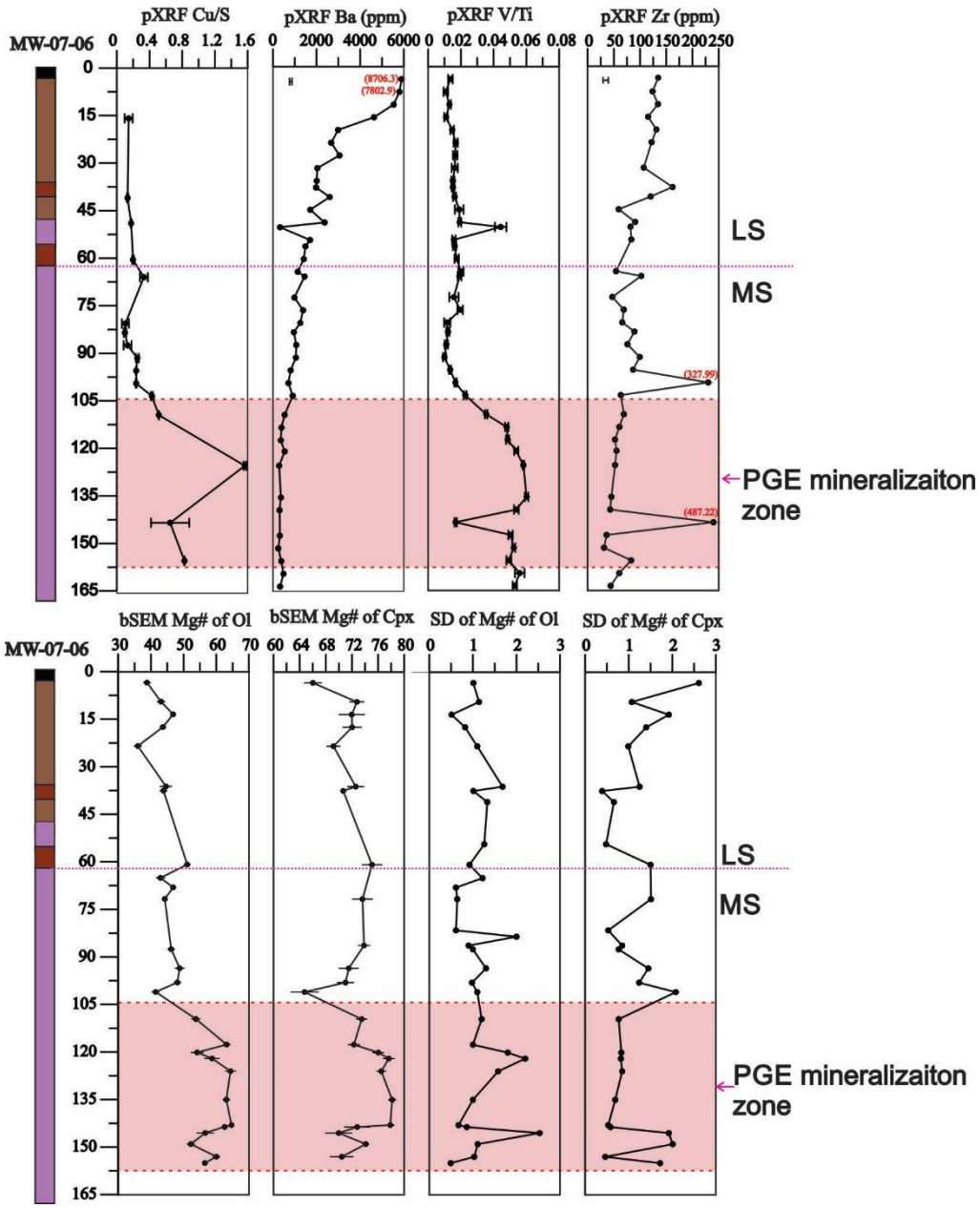

Figure 4-14. Geochemical profiles down the drill hole MW-07-06 at WD zone, the shaded area indicates the PGE mineralization zone, other legends as in Figure 4-12. The error bar for pXRF analysis represents 2σ analytical uncertainty determined by multiple analyses on the same powder. The error bar for bSEM-EDS analysis represents 1σ sample variability determined by 3-5 analyses on 3-5 grains of each mineral type in each sample. SD means 1 sigma standard deviation.

4.7 Discussion

4.7.1 Cu/S proxy

In Chapter 3, we identified two zones of sulfide mineralization located at the top and bottom of drill hole FD-13-34 using both exploration assay and pXRF data. The

upper zone (within the Layered Series and lacking PGE mineralization) is characterized by low Cu/S ratios, whereas the lower zone (within the Marathon Series and containing PGE mineralization) is characterized by high Cu/S ratios. It was thus suggested that high Cu/S ratios could serve as a proxy for PGE mineralization in the Four Dams area. In this study, within the PGE mineralized zones of Area 41, Four Dams, and the WD zone, Cu/S ratios are significantly elevated, indicating that high Cu/S seems to be a good proxy for PGE mineralization in all three areas. Both Cu and S can be acquired by pXRF, although the detection limit for S is normally high in most pXRF instruments; Hall et al. (2011) determined a S detection limit of around 300 ppm using five types of pXRF instrument. As long as Cu and S are detected by pXRF, their ratios are comparable to lab-based methods (Fig. 4-8). Therefore, although pXRF is unable to detect PGE due to the high detection limit relative to the PGE concentrations in most geological materials, it still can be used to vector towards potential PGE mineralization in the Eastern Gabbro by determining Cu/S ratios in the field.

Using the high Cu/S proxy as an exploration tool may also be applicable to other PGE-dominated deposits. Platinum-group elements, particularly Pd and Pt, tend to preferentially partition into the Cu-rich residual liquid after monosulfide solid solution (MSS) crystallization (Howell and McDonald, 2010). Provided that the magmatic sulfide liquids fractionated MSS, Pd and Pt would be concentrated in areas where Cu-rich sulfide minerals, such as chalcopyrite, cubanite, and bornite, are abundant, all of which have high Cu/S ratios. Barnes and Ripley (2016) also suggested that the Cu-rich ores are normally enriched in Pd and Pt. Notable examples include the PGE-enriched sulfide horizons at the Dunka Road Cu-Ni-PGE deposit at the Duluth Complex, which are typically composed of intergrown chalcopyrite, cubanite, and pentlandite, with less abundant pyrrhotite (Theriault et al., 1997), and the Platinova Reef in the Skaergaard Intrusion where magmatic sulfide minerals are present as a Cu-rich, Fe-poor assemblage (Nilsen, 2001).

4.7.2 Identification of possible magma recharge zones

Magma recharge is favorable for PGE mineralization because: 1) it implies the existence of a magma conduit setting, whereby PGE mineralization can be controlled by various fluid dynamic processes (Marsh, 2006); and, 2) the sulfide tenor can be gradually upgraded through a magma recharge process (Kerr and Leitch, 2005), thus increasing the potential for discovery of high-grade deposits. The work in Chapter 3 identified possible recharge zones within the PGE mineralized zone at Four Dams using the combination of pXRF and bSEM-EDS. The criteria used include the zig-zag down-hole variations in pXRF whole-rock MgO and the bSEM-EDS Mg# of olivine (reproduced in Figure 4-13), and the replacement of early plagioclase by later more calcic plagioclase. Figures 4-12 and 4-14 show that in the Marathon Series ophitic gabbro units in Area 41 and WD zone drill holes, particularly those within the PGE mineralized zone, the Mg#s of olivine and clinopyroxene fluctuates over short distances (Figs. 4-12 and 4-14), consistent with a magma recharge process that involves multiple intrusions. Furthermore, the more variable Mg#s of olivine and clinopyroxene for the ophitic gabbro units within the mineralized zone of SL-13-37 from Area 41 (Table 4-4, Fig. 4-12) imply a dynamic environment, which is consistent with a magma recharge environment. Note that brecciated rocks are observed in drill hole SL-13-37 (Fig. 4-12), which is a good indicative of recharge near magma conduits. By contrast, the PGE mineralized ophitic gabbro units in MW-07-06 from the WD zone exhibit a relatively small variation in the Mg#s of olivine and clinopyroxene, suggesting a less dynamic setting. Considering that the PGE mineralization in MW-07-06 has a lower grade than that in SL-13-37, differences in PGE grade may be related to differences in variations of Mg# values, i.e., greater variation corresponds to a higher PGE grade.

However, the apatitic clinopyroxenite in FD-13-34 from Four Dams, which contains a higher grade of PGE mineralization than the WD zone, also contains olivine and clinopyroxene that exhibit a small variation in their Mg# values. Therefore, the

greater variability of Mg# as a potential vector to higher PGE grades perhaps is only applicable to the ophitic gabbro that contains PGE mineralization, rather than the apatitic clinopyroxenite. Nevertheless, an initial impression of PGE mineralization can be gained through investigating the variability in mineral chemistry, particularly for the ophitic gabbro, by using bSEM-EDS prior to traditional assays, which can take weeks or more to complete.

Magma recharge zones may also be related to the replacement of early, less-calcic plagioclase by later more-calcic plagioclase (Fig. 4-15). This texture is observed in mineralized zones in SL-13-37, MW-07-06, as well as in FD-13-34 as described in Chapter 3. Similar textures were also observed by Good and Crocket (1994) and Shahabi Far (2016) in the Marathon deposit, where it was interpreted to reflect multiple intrusions. It is notable that the later plagioclase occurs intergrown with sulfide minerals that show close associations with PGM grains (Fig. 4-15). This was interpreted by Shahabi Far (2016) as the presence of sulfide liquid when late-stage hydrous melt/hydrous fluid replaced the early formed plagioclase. Therefore, using the bSEM-EDS to identify magma recharge zones is another exploration tool that seems well suited to the entire Eastern Gabbro, and may also be applicable to PGE deposits in other settings since magma conduits are a common factor favorable for PGE mineralization (Naldrett, 1999).

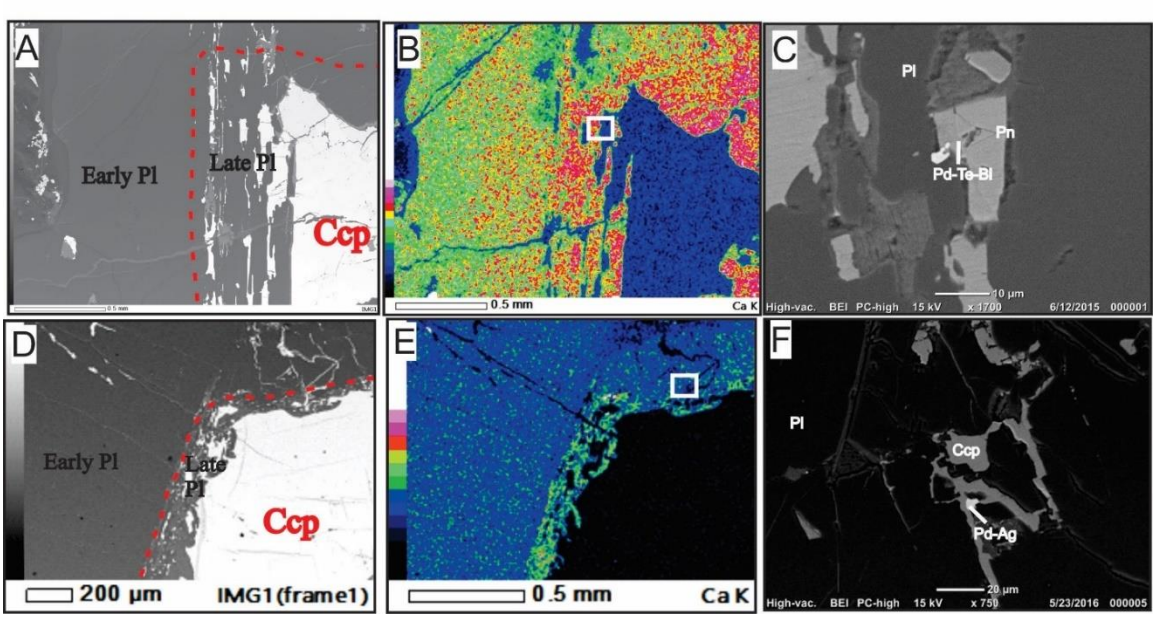

Figure 4-15. Possible magma recharge evidence as reflected by the replacement of earlier less calcic Pl by later more calcic Pl, the later plagioclase occurs intergrown with Ccp. PGM grains are observed in the intergrown Ccp. (A)-(C) are for the ophitic gabbro within the mineralization zone of SL-13-37, note that white particles on (A) and (B) are actually small grains of carbonates; (D)-(F) are for the ophitic gabbro within the mineralization zone of MW-07-06. The white unfilled boxes indicate locations where PGM grains were observed. Abbreviations: Ccp-chalcopyrite, Pn-pentlandite, Pl-plagioclase, Ol-olivine.

4.7.3 Discrimination of the Layered and Marathon Series

As mentioned above, successfully identifying the Marathon series units from the Layered Series units, particularly in the field, will help increase mineral exploration success. However, a challenge is that some Marathon Series rocks are petrographically similar to some Layered Series rocks (Fig. 4-4). Lab-based results of Good et al. (2015) show that the two series are geochemically distinctive, and can be discriminated in diagrams of Ce vs. Y and Nb vs. Zr. Zirconium is an element that can be measured by pXRF, but Ce, Y, and Nb in geological materials are normally below detection. This means that these two discrimination diagrams are not suited to the field-based approach. Additional discrimination diagrams using data from field-portable instruments therefore need to be developed.

Our pXRF results show that Ba and V/Ti in the Layered Series are significantly different from those in the Marathon Series. The Layered Series units have higher

Ba and lower V/Ti than the Marathon Series units. Shaw (1997) relate differences in Ba between these two series to the greater abundance of Ba-rich biotite and orthoclase in the Layered Series, consistent with the interpretation in Chapter 3. The lower V/Ti ratio of the Layered Series may indicate that it is more evolved than the Marathon Series, because down-hole V/Ti and mineral compositional profiles in the same holes in Layered Series (Figs. 4-12 and 4-14) suggest that V is more compatible than Ti in this magmatic system, i.e., V has a higher bulk partition coefficient than Ti due to the fractionation of clinopyroxene, magnetite, etc. Therefore, a discrimination diagram using Ba and V/Ti has application to discriminating between the Marathon and Layered Series throughout the Eastern Gabbro (Fig. 4-16). Since both Ba and V/Ti can be acquired by pXRF, this discrimination diagram can be tested directly in the field.

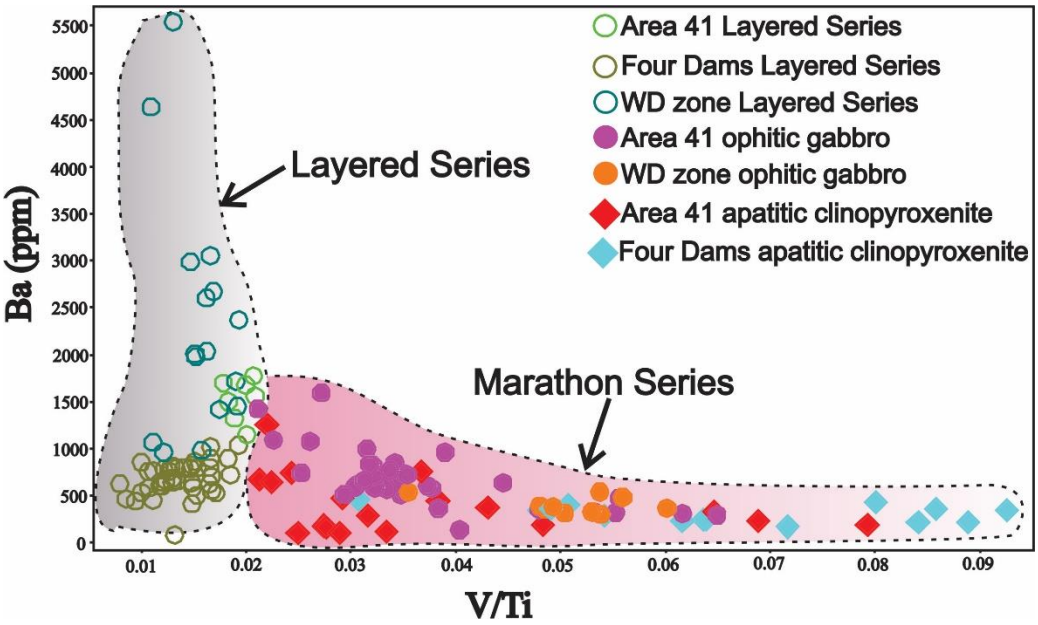

Figure 4-16. Discrimination diagram of Ba vs. V/Ti that separates the Marathon Series from the Layered Series.

4.7.4 Magma differentiation trends

Both pXRF and bSEM results show that the Layered Series units from Area 41 and the WD zone have consistent down-hole variations in Ba, Zr, V/Ti, and Mg#s of olivine and clinopyroxene (Figs. 4-12 and 4-14). These variations suggest a normal

differentiation trend for the Layered Series units at both areas. The Layered Series units at Four Dams also have consistent down-hole variations in these variables, but their variations reflect a reverse differentiation trend (Fig. 4-13). This is consistent with the observation of Shaw (1997), who also observed both normal and reverse differentiation for the Layered Series in the Bamoos and Highway traverses.

The Marathon Series ophitic gabbro units at Area 41 and the WD zone, by contrast, show fluctuations between normal and reverse differentiation. At Four Dams, although the Marathon Series apatitic clinopyroxenite shows an overall normal differentiation trend, variations in key variables (particularly V/Ti, Zr, Mg# of olivine) show zig-zag patterns (Fig. 4-13). Therefore, inspection of down-hole pXRF Ba, Zr, V/Ti, and bSEM-EDS Mg#s of olivine and clinopyroxene variations of drill cores will facilitate the identification of the Marathon Series from the Layered Series, that is, rock units with smooth down-hole variations in these variables more likely are Layered Series units, whereas rock units with fluctuating values in these variables more likely are Marathon Series units. This forms a useful exploration tool that can be used in the field at the Coldwell Alkaline Complex.

4.7.5 Mg-Fe partition between olivine and clinopyroxene

Figure 4-17 shows down-hole trends in the value of olivine-clinopyroxene Fe/Mg partitioning ($Kd_{Fe/Mg}^{Ol/Cpx} = (Fe/Mg)_{Ol}/(Fe/Mg)_{Cpx}$, in mole) measured by bSEM-EDS. The Layered Series at Area 41 and WD zone are characterized by a down-hole decrease in this value, whereas the Layered Series at Four Dams shows a down-hole increase in this value; these trends are similar to those determined by microprobe-based mineral chemical analyses, as will be shown in Chapter 5. In contrast, the Marathon Series in all three areas is characterized by small variations in olivine-clinopyroxene Fe/Mg partitioning; this is particularly true for the Marathon Series units within the PGE mineralized zones, where the value of olivine-clinopyroxene Mg/Fe partition is almost constant at a value around 1.8.

The Fe/Mg partitioning between olivine and clinopyroxene in natural basaltic and andesitic magmas was experimentally investigated by Loucks (1996). Provided that olivine and clinopyroxene are in chemical equilibrium, Loucks (1996) found that temperature was a major control on Fe/Mg partitioning between the two minerals. Shahabi Far (2016) estimated a crystallization temperature for the ophitic gabbro at the Marathon deposit of 1400 K, using a clinopyroxene-orthopyroxene geothermometer. At that temperature, the olivine-clinopyroxene Fe/Mg partition coefficient calculated using the equation of Loucks (1996) is around 1.8, close to the measured values for the ophitic gabbro and apatitic clinopyroxenite in this study. By contrast, the measured values for the Layered Series deviate from 1.8, and can increase or decrease with depth, but typically have values >1.8, ranging up to 4.0. The Marathon Series ophitic gabbro and apatitic clinopyroxenite thus apparently are closer to being in chemical equilibrium compared to the olivine and clinopyroxene in the Layered Series, or the two series formed at different temperatures. This feature also differentiates these two series of rocks. Thus, investigating olivine-clinopyroxene Fe/Mg partition value by using bSEM-EDS in the field potentially can be an exploration tool. Further, it seems that the values closer to chemical equilibrium at 1400 K (1.8) may serve as a vector to PGE mineralization at the Coldwell Alkaline Complex.

The different down-hole patterns and values in olivine-clinopyroxene Fe/Mg partitioning between the Layered Series and the Marathon Series mean that the two series have experienced different histories or conditions during their formation. There are several possible explanations. For example, the trapped liquid shift that results from the back-reaction of residual melt with cumulate minerals may result in disequilibrium between olivine and clinopyroxene (Latypov, 2015). In this case, the non-constant partitioning value for the Layered Series mean that it has undergone variable degrees of trapped liquid shift during its formation. The values for the Marathon Series units that are closer to equilibrium may suggest that the associated

magma has undergone longer re-equilibration between cumulates and residual melts. Another possible explanation is related to undercooling. The undercooling of magma will result in chemical disequilibrium between mineral phases (Latypov, 2015). In this case, the Layered Series seems to have undergone undercooling, whereas the Marathon Series has not. Further assessment of these hypotheses will be addressed in chapter 4 using lab-based analyses.

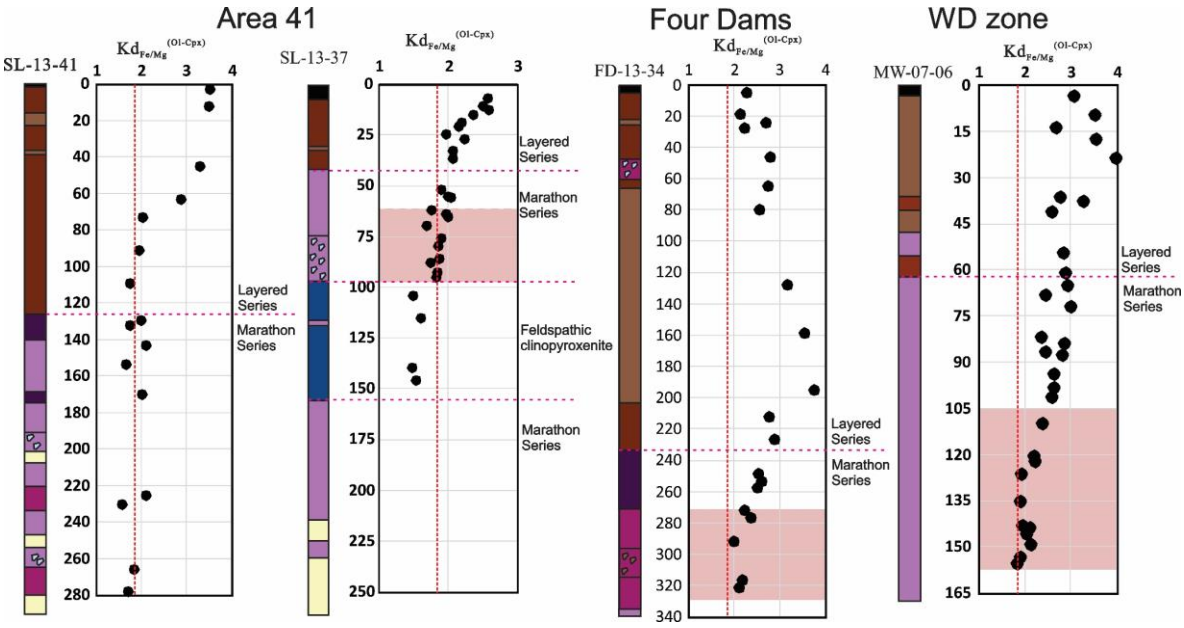

Figure 4-17. Down-hole variations in Fe-Mg exchange coefficient between olivine and clinopyroxene ($Kd_{Fe/Mg}^{Ol/Cpx}$= $(Fe/Mg)_{Ol}/(Fe/Mg)_{Cpx}$, in mole) for representative drill holes at Area 41, Four Dams, and WD zone. Red vertical dashed lines indicate the olivine-clinopyroxene equilibrium Mg-Fe exchange coefficient (1.8) at 1400 K. Pink boxes indicate the PGE mineralization zones. Legends for units as in Figure 4-2.

4.7.6 Geochemical stratigraphy

Understanding the spatial distribution of different series is of vital significance for mineral exploration in the Eastern Gabbro. In order to enhance exploration success, the establishment of a reliable igneous stratigraphy is needed, which normally requires high quality and quantity of drill core logging and petrographic analysis. The results presented above demonstrate that the combination of pXRF and bSEM-EDS is beneficial for differentiating rock units of the different series. Adopting this concept, a geochemical stratigraphy for Area 41 can be created from pXRF and

bSEM-EDS, and compared to the stratigraphy based on drill core logging (Fig. 4-18). The geochemical stratigraphy is distinctive and is generally in agreement with the igneous stratigraphy from core logging. For instance, the Layered Series generally contains higher K_2O, Ba, and Sr contents than the Marathon Series. The medium-grained ophitic gabbro contains lower P_2O_5, Fe_2O_3, higher Al_2O_3 and Sr contents than the coarse-grained and pegmatitic ophitic gabbro. The feldspathic clinopyroxenite and the apatitic clinopyroxenite are also clearly indicated by the geochemical stratigraphy, e.g., low Al_2O_3, P_2O_5, K_2O, Ba, Sr abundances and the highest Mg#s of olivine and clinopyroxene for the feldspathic clinopyroxenite, and high CaO and P_2O_5 abundances for the apatitic clinopyroxenite. Therefore, the combination of both portable techniques will provide a robust tool to aid in the interpretation of igneous units directly in the field. This is particularly important when the drill core was logged by several people with different interpretations of the petrographic characteristics of units, and when confirmation is needed to establish a reliable stratigraphy for mineral exploration.

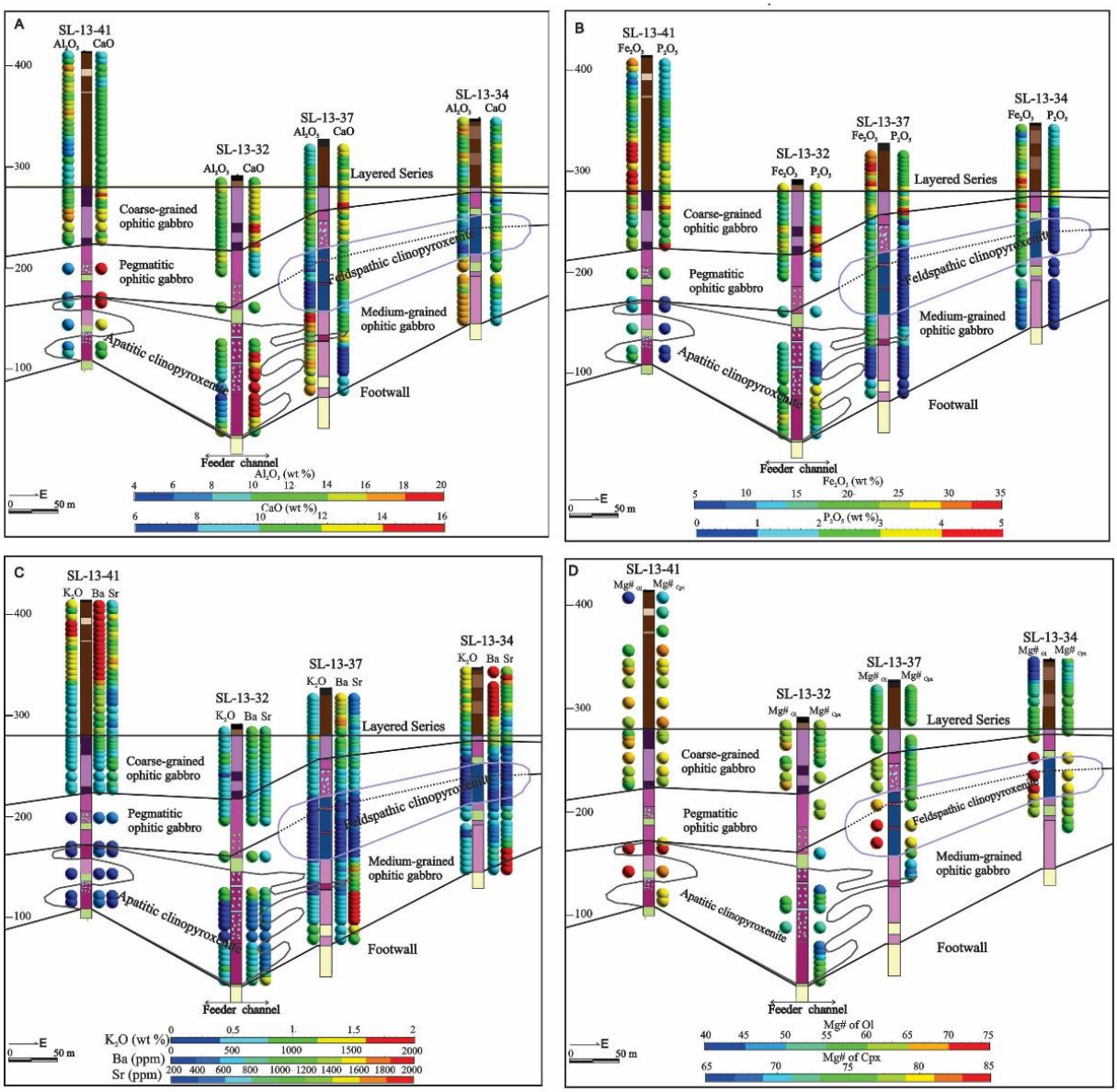

Figure 4-18. Geochemical stratigraphy at Area 41, created based on pXRF Al_2O_3, CaO, Fe_2O_3, P_2O_5, K_2O, Ba, and Sr, and the bSEM-EDS Mg#s of olivine and clinopyroxene. Legends of units as in Figure 4-2.

4.8 Conclusions

The combination of pXRF and bSEM-EDS has considerable promise as an exploration technique for the entire Eastern Gabbro of the Coldwell Alkaline Complex, and has potential to be applied to other PGE deposits in other settings such as the Skaergaard Intrusion:

(1) pXRF can be used in an indirect way to help exploration through acquiring Cu/S ratios, since high Cu/S ratio can serve as a proxy to PGE mineralization.

(2) Both pXRF and bSEM-EDS are able to help identify favorable, PGE mineralized magma recharge zones through investigation of down-hole profiles of whole-rock MgO, Mg#s of olivine and clinopyroxene, and sample variabilities of Mg#s of olivine and clinopyroxene, as well as the observation of favorable textures such as the replacement of earlier plagioclase by later more calcic plagioclase.

(3) The combination of pXRF and bSEM-EDS also provide a reliable tool to help distinguish the Marathon Series from the Layered Series through using whole-rock V/Ti vs. Ba, down-hole profiles of Mg#s of olivine and clinopyroxene.

(4) The Layered Series units have consistent down-hole variations in the partition coefficient of Fe/Mg between olivine and clinopyroxene. By contrast, the Marathon Series units, particularly for those within the PGE mineralized zone, have almost invariant olivine-clinopyroxene Mg/Fe partition coefficient, which is closer to the equilibrium value at 1400 K. Therefore, the Marathon Series can also be distinguished from the Layered Series by investigating olivine-clinopyroxene Fe/Mg partition coefficient using bSEM-EDS analysis.

(5) The geochemical stratigraphy created based on pXRF and bSEM-EDS analyses at Area 41 shows an agreement with the drill-log based counterpart, thus the combination of both techniques can assist igneous stratigraphy logging work in a field setting.

4.9 References

Ashley N., Kern E.V., Kulakov A.V., Smirnov J.F., Diehl K., and Chamberlain. 2012. Paleomagnetism of the Coldwell Alkaline Complex (Ontario, Canada): New Data and New Insights, Proceedings of the 58th Annual Meeting of the Institute on Lake Superior Geology, **1**, 53.

Barnes S.-J. and Ripley E.M. 2016. Highly Siderophile and Strongly Chalcophile Elements in Magmatic Ore Deposits. *Reviews in Mineralogy & Geochemistry*, **81**, 725-774.

Fisher L., Gazley M.F., Baensch A., Barnes S.J., Cleverly J., and Duclaux, G. 2014. Resolution of geochemical and lithostratigraphic complexity: a workflow for application of portable X-ray fluorescence to mineral exploration. *Geochemistry: Exploration, Environment, Analysis*, **14**, 149-159.

Good D.J. and Crocket J.H. 1994. Genesis of the Marathon Cu-platinum group element deposit, Port Coldwell alkalic complex, Ontario: A Midcontinent rift-related magmatic sulfide deposit. *Economic Geology*, **89**, 131-149

Good D.J., Epstein R., McLean K., Linnen, R.L., and Samson, I.M. 2015. Evolution of the Main Zone at the Marathon Cu-PGE Sulfide Deposit, Midcontinent Rift, Canada: Spatial Relationships in a Magma Conduit Setting. *Economic Geology*, **110**, 953-1008

Hall G., Buchar A., and Bonham-Carter, G. 2012. Quality Control Assessment of Portable XRF Analysers: Development of Standard Operating Procedures, Performance on Variable Media and Recommended Uses. CAMIRO Project 10E01, Phase 1.

Heaman L.M., Easton M., Hart T.R., Hollings P., Macdonald C.A., and Smyk M. 2007. Further refinement to the timing of Mesoproterozoic magmatism, Lake Nipigon region, Ontario. *Canadian Journal of Earth Sciences*, **44**, 1055-1086.

Houlahan T., Ramsay S., and Povey, D. 2003. Use of field portable X-ray fluorescence spectrum for grade control- a presentation of case studies. In: Proceedings of the 5th International Mining Conference, Bendigo, Australasian Institute of Mining and Metallurgy, 377-385.

Holwell, D.A. and McDonald, I. 2010. A Review of the Behaviour of Platinum Group Elements within Natural Magmatic Sulfide Ore Systems. *Platinum Metals Rev*iew, **54**, 26-36.

Kerr A., and Leitch A.M. 2005. Self-destructive sulfide segregation systems and the formation of high-grade magmatic ore deposits: *Economic Geology*, **100**, 311-332.

Latypov R. 2015. Basal Reversals in Mafic sills and Layered intrusions. In: Charlier B., Namur O., Latypov R., and Tegner C. (eds.), Layered Intrusions, Springer Published House, 749pp.

Loucks R.R. 1996. A precise olivine-augite Mg-Fe-exchange geothermometer. *Contributions to Mineralogy and Petrology*, **125**, 140-150.

Marsh B.D. 2006. Dynamics of magmatic systems. *Elements*, **2**, 287-292.

McBride J. 2013. Assessment Report for Diamond Drill Drilling on the Stillwater Canada Inc. Bermuda Property. Thunder Bay Division, Ontario, 39pp.

Mitchell R., Platt R., Lukosius-Sanders J., Artist-Downey M., and Moogk-Pickard, S. 1993. Petrology of syenites from center III of the Coldwell alkaline complex, northwestern Ontario, Canada. *Canadian Journal of Earth Sciences*, 30, 145-158.

Mitchell R.H. and Platt R.G. 1978. Mafic mineralogy of ferroaugite syenite from the Coldwell Alkaline Complex, Ontario, Canada. *Journal of Petrology*,19, 627-651.

Mitchell R. H. and Platt R. G. 1982. Mineralogy and petrology of nepheline syenites from the Coldwell Alkaline Complex, Ontario. *Journal of Petrology*, **23**, 186-214.

Mulja T. 1989. Petrology, Geochemistry, Sulphide and Platinum-Group Element Mineralization of the Geordie Lake Intrusion, Coldwell Alkaline Complex, Ontario. M.Sc. thesis, Lakehead University, Thunder Bay, Ontario.

Mulja T. and Mitchell R. 1991. The Geordie Lake Intrusion, Coldwell Alkaline Complex, Ontario; a palladium-and tellurium-rich disseminated sulfide occurrence derived from an evolved tholeiitic magma. *Economic Geology*, **86**, 1050-1069.

Naldrett A.J. 1999. World-class Ni-Cu-PGE deposits: key factors in their genesis. *Mineralium Deposita*, **34**, 227-240.

Puskas, F. 1970. The Port Coldwell alkalic complex: Institute of Lake Superior Geology Technical Sessions, Abstracts and Field Guides, 1970 Thunder Bay, Ontario, 85-89.

Nielsen, T. F. D. 2001. The palladium potential of the Skaergaard intrusion. GEUS Report, 39 pp.

Piercey S.J. and Devine M.C. 2014. Analysis of powdered reference materials and known samples with a benchtop, field portable X-ray fluorescence (pXRF) spectrometer: evaluation of performance and potential applications for exploration lithogeochemistry. *Geochemistry: Exploration, Environment, Analysis*, **14**, 139-148.

Ross P.S., Bourke A., and Fresia, B. 2014. Improving lithological discrimination in exploration drill-cores using portable X-ray fluorescence measurements: (2) applications to the Zn-Cu Matagami mining camp, Canada. *Geochemistry: Exploration, Environment, Analysis*, **14**, 187-196.

Shahabi Far M. 2016. The magmatic and volatile evolution of gabbros hosting the Marathon PGE-Cu deposit: evolution of a conduit system. Ph. D thesis, The university of Windsor, Windsor, ON.

Shaw C.S.J. 1994. Petrogenesis of the Eastern gabbro, Coldwell Alkaline Complex, Ontario: Ph.D. thesis, University of Western Ontario, London, ON.

Shaw C.S.J. 1997. The petrology of the layered gabbro intrusion, Eastern gabbro, Coldwell Alkaline Complex, Northwestern Ontario, Canada: Evidence for multiple phases of intrusion in a ring dyke. *Lithos*, **40**, 243-259.

Theriault R.D., Barnes S.-J., and Severso M.J. 1997. The influence of country-rock assimilation and silicate to sulphide ratio (R-factor) on the genesis of the Dunka Road Cu-Ni-PGE deposit, Duluth Complex, Minnesota. *Canadian Journal of Earth Sciences*, **34**, 375-389.

Walker E. C., Sutcliff R. H., Shaw C. S. J., Shore G. T., and Penczak R. S. 1993. Precambrian geology of the Coldwell Alkaline Complex. Ontario Geological Survey, Open File Report 5868, 23pp.

Chapter 5

Characteristics and Development of the Layered Series in the Eastern Gabbro, Coldwell Alkaline Complex, Ontario, Canada

Yonghua Cao[1], Robert Linnen[1], David Good[1], Iain Samson[2]

1. Western University, London, ON, Canada

2. The University of Windsor, Windsor, ON, Canada

5.1 Introduction

The Coldwell Alkaline Complex, located on the north shore of Lake Superior, is related to the Midcontinent Rift and consists dominantly of gabbros and syenites from three overlapping intrusions (Mitchell and Platt, 1977, 1982). Igneous units associated with this complex have received considerable attention because they potentially contain information on the formation of the Midcontinent rift and the nature of the sub-continental mantle (e.g., Heaman and Machado, 1992).

The Eastern Gabbro forms the oldest intrusive phase in the Coldwell Alkaline Complex. It has received many studies particularly after the discovery of significant Cu-Pd mineralization within a late gabbroic series known as the Two Duck Lake gabbro, *e.g.*, Wilkinson and Colvine (1978), Watkinson et al. (1983), Good and Crocket (1994), Dahl et al. (2001), and Good et al. (2015). The Layered Series gabbro constitutes the main part of the Eastern Gabbro and despite overlying the mineralized Marathon Series, it is interpreted to be older than the Marathon Series. However, owing to the lack of PGE mineralization it has received considerably less scientific scrutiny than the Marathon Series. To our knowledge, Shaw (1997) is the only study that focused on the Layered Series at the Eastern Gabbro. Thus, the

characteristics and the origin of this series are still poorly constrained. However, the origin of the Layered Series is critical for the interpretation of the early magmatic history of the Coldwell Alkaline Complex and for the identification of potential additional PGE resources. There are four main questions about the Layered Series that will be addressed in the current study:

(1) The Coldwell Cu-Pd deposits are hosted by gabbros of the Marathon Series, a group of small irregularly shaped rock suite that were proposed by Good et al. (2015) to have formed in a magma conduit setting. The Layered Series units are much larger and slightly older than the Marathon Series units, and they exhibit significantly different styles of intrusion and crystallization. However, it is unclear how the Layered Series formed and recognition of the role played by common magmatic processes such as Rayleigh fractional crystallization or recharge and tapping fractionation are an important first step to defining the magmatic setting.

(2) The Coubran basalts located in the center of the Coldwell Alkaline Complex was proposed by Cundari (2012) to be co-genetic with the Marathon Series. This basalt is highly evolved with high abundances of incompatible elements. However, the Layered Series units, as will be shown below, contain even higher concentrations of incompatible elements than the Coubran basalts. It is unclear what magma at the Coldwell Alkaline Complex can generate such highly evolved suite of gabbro units and whether it is related to the Coubran basalts. But by developing possible fractional crystallization scenarios to explain the Layered Series, it is possible to gain some insight as to what such an initial magma would have been.

(3) The Layered Series lacks PGE mineralization, in contrast to the Marathon Series. It is unclear whether the PGE-barren nature of the Layered Series is related to the source and is explained by a low degree of partial melting, or whether PGE were depleted during a sulfide melt saturation event.

(4) As first noted by Shaw (1997), the Layered Series commonly exhibits reverse evolution trends. Reverse compositional trends are common in silicate layers in layered intrusions, but their origins have been highly debated (*e.g.*, Gunn, 1966; Irvine, 1980; Lightfoot and Naldrett, 1984; Egorova and Latypov, 2012a, b). The exceptional pristine nature of the Layered Series provides a good opportunity to unravel these unusual compositional trends, which will help better understand mechanisms that occurred in the magma chamber and may also provide new insights into the origin of magma reversal trends in general.

This study presents the results of a comprehensive petrographic, mineral chemistry and geochemical study of the Layered Series rocks including the olivine gabbro and oxide augite melatroctolite units. Geochemical modeling work is used to constrain the magma sources, investigate their genetic relations, and evaluate the intrusion mechanisms for various Layered Series units. In particular, two types of magma reversals characterized by coupled/decoupled mineral and whole-rock compositional trends are studied. These can be explained using a fractionation-mixing model, which in turn can be used to propose the potential processes that took place in the magma chambers that generated the Layered Series.

5.2 Geological setting

The Midcontinent rift-related Coldwell Alkaline Complex is the largest alkaline intrusion in North America (Fig. 5-1). The complex is a sub-circular intrusion that has a diameter of approximately 25 km and a surface area of 580 km^2 (Walker et al., 1993). It intruded the low-grade metamorphic Archean Schreiber-White River greenstone belt of volcanic and sedimentary rocks at 1108 Ma, which marked the early stage of magmatism of the Midcontinent Rift system (Walker et al., 1993; Heaman et al., 2007). Previous petrological and field studies conducted by Mitchell & Platt (1978, 1982), Mitchell et al. (1993), and Shaw (1997) identified three superimposed intrusive centers for the Coldwell Alkaline Complex. From east to west, they are Center I, Center II, and Center III. Paleomagnetic work conducted by

Ashley et al. (2012) suggested that Centers I & III have identical ages, and that both are older than Center II. Center I includes the Eastern Gabbro, the Western Gabbro, amphibole quartz syenite, iron-rich augite syenite, and mafic volcanic and subvolcanic rocks (Walker et al., 1993). Center II consists of undersaturated alkaline rocks including alkaline gabbros and syenites (Mitchell and Platt, 1978, 1982; Laderoute, 1988). Center III is composed mainly of syenites and quartz syenites which intruded into most other phases of the complex and exhibit various degrees of crustal contamination (McLaughlin and Mitchell, 1989).

According to previous studies of Shaw (1994, 1997) the Eastern gabbro (Fig. 5-1) formed by multiple intrusions of subalkaline basaltic magma into a partial ring dike structure that cut the Archean country rock. Good et al. (2015) identified nine major lithologies that were further grouped into three major distinctive magmatic series based on new mapping of stripped areas and core logging. From oldest to youngest, they are the meta-basalt, the Layered Series, and the Marathon Series. The meta-basalt has undergone pyroxene hornfels grade metamorphism as a result of the heat from later magma intrusions (Good et al., 2015). The Layered Series constitutes the main part of the Eastern gabbro and is composed of massive to modally layered olivine gabbro with a lesser amount weakly layered oxide augite melatroctolite. Contacts between these units are typically gradational. In addition, the gabbroic anorthosite is believed to be part of the Layered Series based on geochemical evidence provided by Good et al. (2015). However, it is presumably an older Layered Series phase based on outcrop where gabbroic anorthosite xenoliths and blebs are wrapped by olivine gabbro and oxide augite melatroctolite layers (Good et al., 2015). The Marathon Series is younger and consists of the Two Duck Lake gabbro, small intrusions of apatitic clinopyroxenite and oxide melatroctolite, and a thin continuous layered sill composed of augite troctolite and wehrlite.

5.3 Sampling and analytical equipment

Powders and rock specimens were obtained from 5 diamond drill holes at Area 41 (SL-13-34, SL-13-36, and SL-13-41), Four Dams (FD-13-34), and WD zone (MW-07-06). Locations of these three areas are shown in Figure 5-1. All these drill holes intersect a significant portion of the Layered Series, their drilling parameters are tabulated in Table 5-1.

Table 5-1. Drilling parameters of selected drill holes.

Area	DDH	Azimuth/º	Collar/º	Total Depth/m	Interval of the Layered Series/m
Area 41	SL-13-34	19.56	-80	201	2.36-62.50
	SL-13-36	22.07	-44.59	228	9.4-34.25
	SL-13-41	18.36	-80.05	291	1.65-131.19
Four Dams	FD-13-34	32.9	-69.6	375	4.9-226.3
WD zone	MW-07-06	89	-60	168	3.4-49.39

Powdered samples of different layered series samples were collected down drill holes using a Thermo scientific portable grinder. The detailed sampling protocols have been described in Chapter 2. All powders were initially analyzed by using a portable X-ray fluorescence, in order to select a subset of representative powdered samples (n=87) for laboratory-based whole-rock analyses. Locations of the selected powdered samples are given in Figure 5-2. After further pulverization, the powders were sent to ALS Mineral Divisions in Vancouver and Thunder Bay for lithogeochemical analyses. Both labs analyzed major elements by inductively coupled plasma (ICP)-atomic emission spectroscopy (AES) on a minimum 2 g of pulp samples after lithium borate fusion. Trace elements were analyzed by ICP-mass spectroscopy (MS) on 2 g of sample after lithium borate fusion. Total S was determined using a Leco combustion furnace on a 0.01 to 0.1g of sample, which is heated to roughly 1350°C in an induction furnace. SO_2 is produced through a reaction with oxygen and is measured by an infra-red detector. Ferrous iron was determined by H_2SO_4-HF acid digestion and titration on 1 g of sample. Quality-

control was conducted based on ALS Chemex quality-control procedures which involve analyses on a wide array of standards, blanks, and duplicates after each batch of samples. The analytical error with 95% confidence (2σ) is estimated through replicate measurements on duplicates prepared for our routine laboratory-based analyses. Laboratory-based whole-rock analyses for different units of different localities are summarized in Table 5-2.

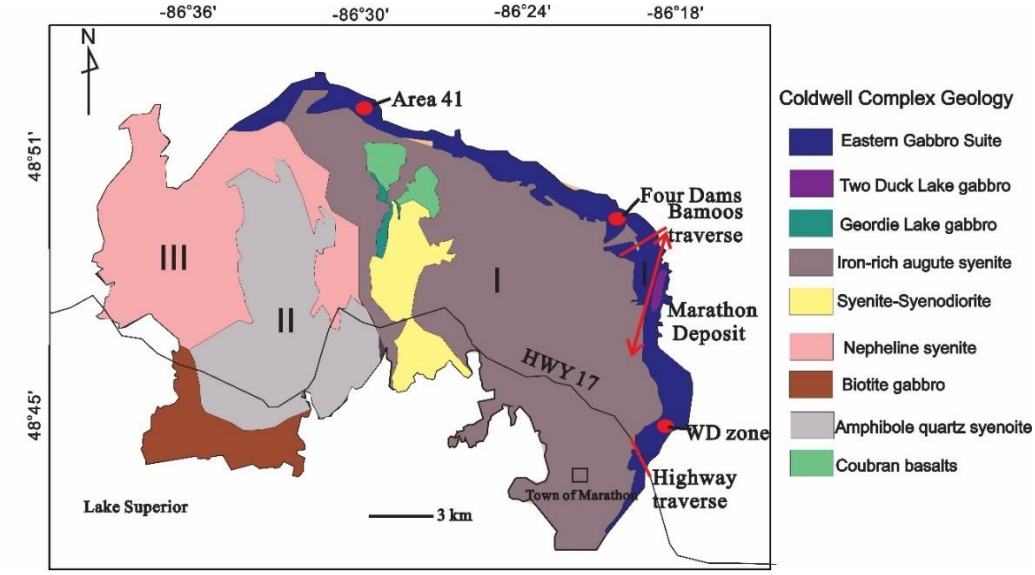

Figure 5-1. Geological map of the Coldwell Alkaline Complex, situated on the northern shore of Lake Superior. The intrusive centers have been shown by Roman numerals (modified after Mulja and Mitchell, 1991). Locations of Area 41, Four Dams, and WD zone are represented as three red dots, Bamoos and Highway traverses studied by Shaw (1997) are represented as two red lines, the Marathon deposit is indicated using a double-arrow line (Simplified after Walker et al., 1993 and Good et al., 2015).

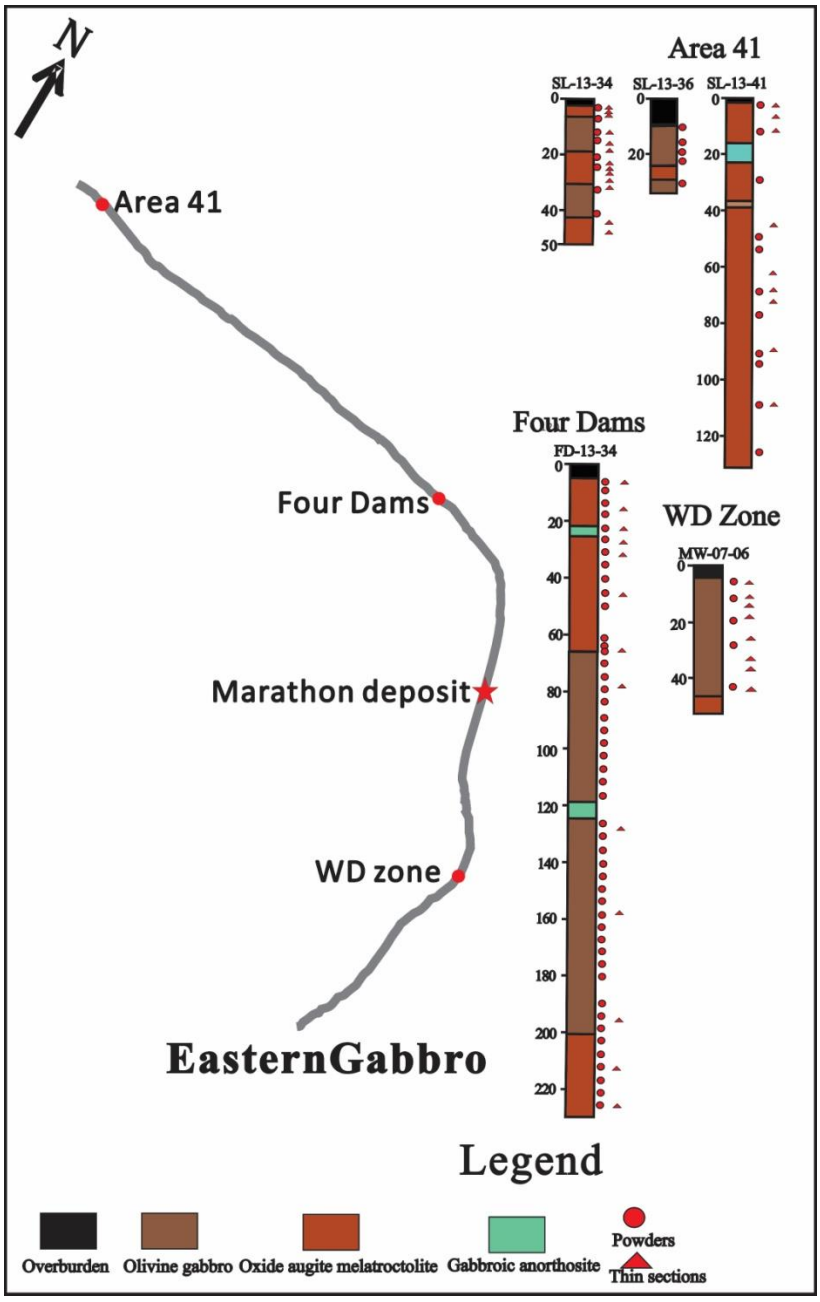

Figure 5-2. Sampling locations for powders (circles) and rock specimens (triangles) from 5 diamond drill holes: MW-07-06 at WD zone, FD-13-34 at Four Dams, and SL-13-34, SL-13-36 and SL-13-41 at Area 41. The columns represent the geological log of each of the drill holes. The outer contact of the Eastern Gabbro is represented by the thick grey line and study areas are represented by red dots. The location of the Marathon Cu-Pd deposit is indicated by a red star.

Table 5-2. Average major and trace element compositions. Number in parentheses represents number of samples analyzed for each unit; SD=1 σ standard derivation for sample set.

Rock units		Area 41					
		Olivine gabbro (11)			Oxide augite melatroctolite (12)		
		Avg	Range	SD	Avg	Range	SD
SiO_2	(wt %)	39.0	30.2-47.5	5.68	34.9	19.5-43.2	7.42
Al_2O_3		12.1	6.3-119.0	4.11	9.71	3.9-15.8	3.63
Fe_2O_3		21.2	9.8-32.1	7.17	26.6	14.1-46.2	9.31
FeO*		14.1	6.6-21.0	4.67	17.4	8.7-28.7	6.38
CaO		11.3	10.5-14.5	1.12	10.5	8.7-13.5	1.28
MgO		6.0	2.6-8.9	2.35	6.6	3.9-9.8	2.14
Na_2O		2.3	1.1-3.8	0.94	1.8	0.4-3.0	0.85
K_2O		1.0	0.4-1.5	0.35	1.0	0.2-1.6	0.51
TiO_2		3.5	1.7-2.8	1.21	4.6	2.2-8.2	1.79
MnO		0.3	0.1-0.4	0.07	0.4	0.2-0.4	0.07
P_2O_5		2.5	1.6-5.4	1.03	2.6	1.6-3.9	0.78
Total		99.1			98.6		
S		0.2	0.1-0.5	0.12	0.3	0.2-0.5	0.12
Ba	(ppm)	3225	1070-5307	1478.4	2820	431-5860	1858.3
Ce		191	158-229	27	179.3	124-229	30.7
Cr		51	10-150	56.5	26	10-80	24.5
Cs		1.1	0.5-4.0	1.01	1.5	0.2-3.3	0.91
Dy		7	5-8	1.1	7	5-8	1.0
Er		3	2-4	0.4	3	2-4	0.4
Eu		5	5-6	0.4	6	5-6	0.3
Ga		15	14-16	0.7	15	12-19	1.8
Gd		11	8-14	2.0	12	8-15	2.0
Hf		2	1-2	0.4	2	1-2	0.4
Ho		1	1-2	0.2	1	1-2	0.2
La		83	69-101	11.3	78	56-96	12.1
Lu		0.3	0.3-0.4	0.04	0.3	0.3-0.4	0.03
Nb		31	14-43	7.6	31	19-45	7.4

Nd		93	71-114	15.6	94	66-117	15.2
Pr		23	18-28	3.5	22	16-28	3.7
Rb		18	7-25	5.7	20	3-38	11.6
Sm		16	12-19	2.7	16	11-19	2.5
Sn		4	2-7	1.6	15	4-37	10.2
Sr		1144	568-1950	488.6	829	329-1625	382.9
Ta		1	1-2	0.3	1	1-2	0.3
Tb		1	1-2	0.2	1	1-2	0.2
Th		3	2-4	0.6	3	2-5	1.0
Tm		0.4	0.3-0.5	0.06	0.4	0.3-0.5	0.04
U		0.9	0.5-1.3	0.20	0.8	0.5-1.6	0.29
V		316	80-544	155.7	392	45-1090	313.3
Y		35	27-42	5.3	33	24-41	4.8
Yb		2.3	1.8-2.8	0.30	2.3	1.8-2.7	0.2
Zr		74	32-108	18.6	66	40-99	16.1
Cu		133	43-254	76.7	363	52-1485	430.7
Ni		33	3-152	41.1	51	7-186	59.1
Sc		36	17-51	11.7	36	23-51	7.1

Continue.

Rock units		Four Dams					
		Olivine gabbro (39)			Oxide augite melatroctolite (16)		
		Avg	Range	SD	Avg	Range	SD
SiO_2	(wt %)	40.7	33.6-46.5	2.73	31.2	20.1-39.7	6.26
Al_2O_3		12.8	8.8-19.6	2.26	7.4	3.2-15.6	3.40
Fe_2O_3		21.6	10.9-32.8	3.90	34.8	17.9-49.9	8.98
FeO*		15.0	7.3-23.7	3.10	24.4	10.5-33.5	6.16
CaO		10.1	8.0-11.5	0.69	8.9	5.0-10.5	1.58
MgO		5.1	3.1-8.0	1.08	8.1	4.6-11.9	2.21
Na_2O		2.6	1.5-3.8	0.52	1.4	0.4-2.7	0.74
K_2O		0.7	0.4-1.1	0.17	0.5	0.2-0.9	0.20

TiO_2		3.1	1.2-4.9	0.75	4.8	1.6-7.5	1.60
MnO		0.3	0.2-0.5	0.08	0.4	0.2-0.6	0.09
P_2O_5		1.8	1.3-3.0	0.36	2.7	1.8-3.2	0.42
Total		99.0			100.2		
S		0.3	0.2-1.7	0.26	0.6	0.2-2.1	0.51
Ba	(ppm)	805	394-1290	192.7	633	233-1710	358.2
Ce		156	104-239	32.4	190	142-257	32.7
Cr		9	5-30	9.2	42	20-80	24.4
Cs		0.5	0.0-0.9	0.21	0.4	0.1-0.8	0.2
Dy		7	5-9	1.2	8	6-11	1.3
Er		3	2-5	0.6	4	3-5	0.8
Eu		4	3-6	0.8	4	3-5	0.6
Ga		19	16-22	1.2	18	16-22	1.8
Gd		11	8-15	1.8	13	10-17	1.9
Hf		2	1-3	0.4	2	1-3	0.6
Ho		1	1-2	0.3	1	1-2	0.3
La		70	47-100	14	86	62-120	17.0
Lu		0.4	0.2-0.5	0.08	0.4	0.2-0.5	0.10
Nb		34	16-57	11.3	45	17-74	19.7
Nd		82	56-106	14.7	104	81-138	16.6
Pr		19	13-27	3.7	24	18-32	4.0
Rb		15	6-27	4.9	11	4-22	4.8
Sm		14	9-18	2.4	17	13-23	2.7
Sn		17	0-49	12.2	27	9-68	18.7
Sr		825	517-1230	169.0	478	193-1050	231.1
Ta		2	0-3	0.5	2	1-3	0.9
Tb		1	1-2	0.2	2	1-2	0.3
Th		3	2-5	0.6	3	2-4	0.6
Tm		0.4	0.3-0.6	0.08	0.5	0.3-0.6	0.10
U		0.8	0.4-1.4	0.18	0.8	0.5-1.5	0.26
V		178	101-427	55.1	480	221-1020	238

Y	31	19-45	6.1	37	25-51	7.5
Yb	2	1-3	0.5	3	2-4	0.7
Zr	75	37-112	18.6	78	42-133	22.7
Cu	409	60-4370	676.9	1352	349-5220	1228.7
Ni	24	4-223	42.9	108	8-419	104.3
Sc	28	11-35	5.4	28	16-36	6.2

Polished thin sections representative of each gabbro unit in the Layered Series were prepared from selected drill holes at an interval between 5 and 20 meters (n=36, Fig. 5-2). All polished thin sections were then carbon-coated and analyzed by a JEOL JXA-8530F field emission electron microprobe analyses at Western University. Major and minor constituents of olivine, clinopyroxene, plagioclase, alkali feldspar, and biotite were analyzed using an accelerating voltage of 15 keV and a beam current of 20 nA. The beam was focused to a 1 μm spot for analyzing olivine and clinopyroxene, and to a 5 μm spot for analyzing plagioclase, alkali feldspar, and biotite. The peak counting time was 30 s for all elements and background counts were a total of 30 s. A variety of synthetic and natural standards (Table 4-4 in Chapter 4) were used to calibrate different elements during probe analyses. The analytical precision for probe analyses has been determined in Chapter 3. Results are summarized in Table 5-3.

Table 5-3. Mg# of olivine, Mg# of clinopyroxene, and anorthite content of plagioclase data determined by probe for the Layered Series samples of different areas. SD values refer to 1 σ standard deviations of measurements on 3 to 5 grains. N/A means the analysis is not available.

Drill hole	Depth/m	Unit	Mg# of Ol	SD	Mg# of Cpx	SD	An% of Pl	SD
SL-13-34	3	Oxide augite melatroctolite	37.2	1.49	67.3	1.28	53.6	1.85
	5.1	Oxide augite melatroctolite	33.4	0.33	66.7	0.96	52.2	1.74
	7	Olivine gabbro	35.2	1.00	65.9	1.20	51.8	0.64
	13.3	Olivine gabbro	32.5	0.53	67.9	1.17	50.7	0.78
	17.4	Olivine gabbro	38.0	1.34	67.2	1.64	52.2	1.03
	19.4	Oxide augite melatroctolite	41.7	0.24	67.3	0.62	52.4	0.35
	25.7	Oxide augite melatroctolite	42.0	0.61	67.8	0.44	53.1	2.53
	28.1	Oxide augite melatroctolite	44.0	2.42	68.1	0.62	N/A	N/A
	30	Oxide augite melatroctolite	48.3	1.25	68.5	0.32	52.3	0.64
	32	Olivine gabbro	41.6	1.06	68.3	0.60	54.0	0.99
	45	Olivine gabbro	47.1	0.44	69.0	0.49	55.1	2.40
	49	Oxide augite melatroctolite	47.7	1.52	68.3	0.63	55.9	0.50
	53	Oxide augite melatroctolite	51.4	0.31	69.9	0.32	56.5	1.00
	58.9	Oxide augite melatroctolite	49.1	0.40	69.5	0.38	56.4	0.90
SL-13-41	3	Oxide augite melatroctolite	27.9	0.51	59.9	1.10	43.3	2.11
	7.5	Oxide augite melatroctolite	23.7	0.86	55.8	1.67	24.2	0.74
	12.1	Oxide augite melatroctolite	36.0	0.24	69.0	0.07	52.6	1.32
	45	Oxide augite melatroctolite	38.1	0.48	64.6	1.08	53.8	1.95
	63.2	Oxide augite melatroctolite	44.0	0.15	67.8	0.42	52.0	1.50
	68.9	Oxide augite melatroctolite	45.9	0.20	67.9	0.81	51.2	0.63
	73	Oxide augite melatroctolite	51.1	0.24	69.2	0.28	56.2	0.58
	91	Oxide augite melatroctolite	53.0	0.46	70.5	0.92	55.0	0.24
	109.1	Oxide augite melatroctolite	57.1	0.24	70.7	0.43	55.3	1.40
FD-13-34	5	Oxide augite melatroctolite	50.6	0.10	68.1	1.20	52.3	0.90
	18.6	Oxide augite melatroctolite	49.8	0.10	68.6	1.10	54.4	1.80
	24	Olivine gabbro	43.0	1.40	68.1	1.00	48.8	1.80
	27.9	Oxide augite melatroctolite	53.7	0.40	69.4	1.40	54.4	1.20
	33	Oxide augite melatroctolite	55.9	0.40	69.8	1.70	51.7	2.90
	46.1	Oxide augite melatroctolite	51.8	0.90	68.3	0.60	52.1	0.80
	64.6	Oxide augite melatroctolite	45.8	0.30	66.9	1.10	53.4	3.50
	79.6	Olivine gabbro	43.2	0.70	64.4	1.50	51.6	2.10
	127.3	Olivine gabbro	36.1	0.60	59.1	0.70	43.8	2.60
	158.6	Olivine gabbro	29.9	0.30	56.0	1.80	45.2	2.00
	194.8	Olivine gabbro	27.8	2.50	58.3	2.10	39.4	2.50
	212.5	Oxide augite melatroctolite	34.7	0.70	59.0	0.40	43.9	1.50
	226.3	Oxide augite melatroctolite	35.1	1.10	60.0	0.70	42.7	2.60

5.4 Petrography

5.4.1 Olivine gabbro

The olivine gabbro has an intergranular texture along the entire length of the Eastern Gabbro examined. It is medium grained (1-4 mm) and shows massive to rhythmic layering defined by gradational changes in the abundance of plagioclase, or alternations of clinopyroxene-rich and plagioclase-rich sublayers (Fig. 5-3A). Major mineral abundances were estimated using the combination of petrography and image analysis of thin sections (Photoshop), which vary subtly at different areas, and are composed of, in decreasing order of abundance, euhedral plagioclase (40-60 modal%), subhedral clinopyroxene (15-30 modal%), subhedral olivine (10-15 modal%). Plagioclase has bimodal size distribution. Generally, plagioclase is medium-grained and subhedral, but locally finer grained anhedral plagioclase occurs within olivine and clinopyroxene (Figs. 5-4A and B). Olivine locally is rimed by clinopyroxene (Fig. 5-4C), indicating its crystallization sequence is, from early to late, plagioclase, olivine, and clinopyroxene. Minor mineral phases in the olivine gabbro include less than 10 modal percent fine-grained apatite and magnetite, and less than 5 modal percent anhedral biotite. The apatite and magnetite typically are enclosed in, or less commonly interstitial to, olivine and plagioclase, and the biotite occurs either as an interstitial phase, or as a poikilitic phase enclosing plagioclase, olivine, and clinopyroxene (Fig. 5-4D). Plagioclase in the olivine gabbro shows weak to moderate sericite and albite alteration, and olivine and clinopyroxene have undergone weak alteration to chlorite or actinolite.

Less than 8 modal percent medium-grained subhedral alkali feldspar observed in the Layered Series gabbro from Area 41 and WD zone. By contrast, negligible alkali feldspar was observed in the Layered Series gabbro from Four Dams. The alkali feldspar is perthite which partially overprints and encloses euhedral or wormy-like plagioclase that formed the myrmekite texture (Figs. 5-4E, 5-5A and B).

5.4.2 Oxide augite melatroctolite

The oxide augite melatroctolite unit has a different mode of occurrence at Four Dams and Area 41. At Four Dams, this unit occurs at the top and bottom of the Layered Series, with the olivine gabbro in between, whereas at Area 41 oxide augite melatroctolite is interlayered with the olivine gabbro or locally is present as a separate massive layer. A small amount of oxide augite melatroctolite is observed in the Layered Series at WD zone.

The oxide augite melatroctolite is medium-grained and has textures similar to those of the olivine gabbro. It displays weak modal layering and is distinguished from other units by a great abundance (10 to 20 modal %) of disseminated magnetite. Mineral abundances of this unit are similar at different areas, which typically consist of, in decreasing order of abundance, olivine (20-45 modal%), plagioclase (15-30 modal%), clinopyroxene (10-20 modal%), magnetite, and apatite (<10 modal%). However, the oxide augite melatroctolite from Area 41 and WD zone also contains up to 8 modal percent alkali feldspar (perthite) whereas negligible alkali feldspar is observed in the oxide augite melatroctolite from Four Dams. Locally, the plagioclase presents deformed twinning (Fig. 5-4F), indicating the post-cumulus compaction during formation of this unit. At Four Dams, the upper oxide augite melatroctolite contains slightly higher abundances of olivine and magnetite than the lower oxide augite melatroctolite. Olivine and clinopyroxene are euhedral-subhedral, and occur interstitial to subhedral to anhedral plagioclase clusters. Magnetite and apatite are generally enclosed by, or are less commonly interstitial to olivine and plagioclase. The oxide augite melatroctolite contains disseminated sulfide minerals (2-3 modal %) that are dominantly fine-grained pyrrhotite with trace chalcopyrite.

5.4.3 Gabbroic anorthosite

Gabbroic anorthosite typically occurs throughout the Layered Series as meter-sized xenoliths (Fig. 5-3B), or as large units having strike lengths of several hundred

meters. It has a very distinctive mottled appearance and consists of approximately 75-90 modal percent medium grained, subhedral to anhedral plagioclase, very coarse grained (>4 mm) clinopyroxene (3 modal %) and olivine (2 modal %) oikocrysts, and 5 modal% medium to coarse grained, interstitial to poikilitic magnetite.

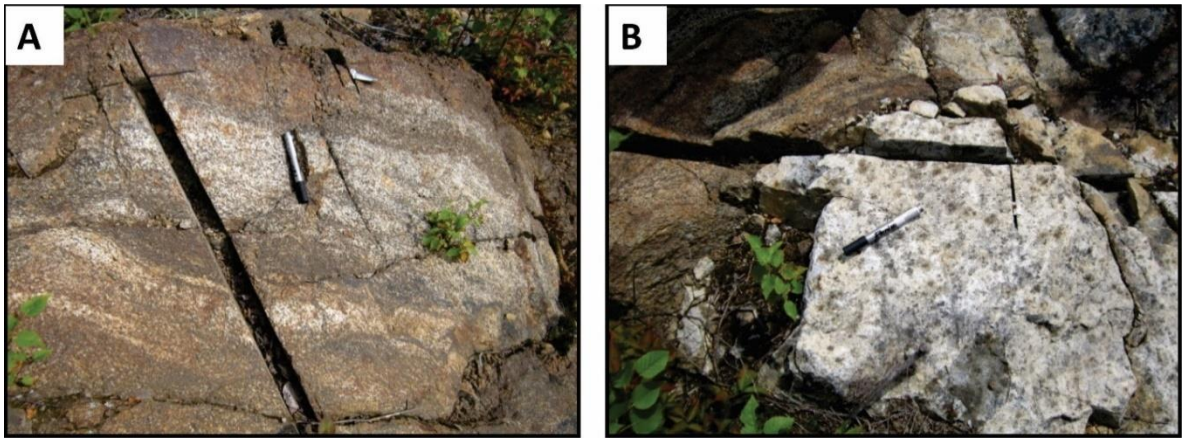

Figure 5-3. Field pictures of the Layered Series gabbro. (A) Outcrop showing the rhythmic layering of the olivine gabbro at Four Dams area, note the alternation of plagioclase-rich and clinopyroxene-rich sublayers; (B) Outcrop showing the rounded blocks of gabbroic anorthosite within the Layered Series, layering wraps around the xenoliths.

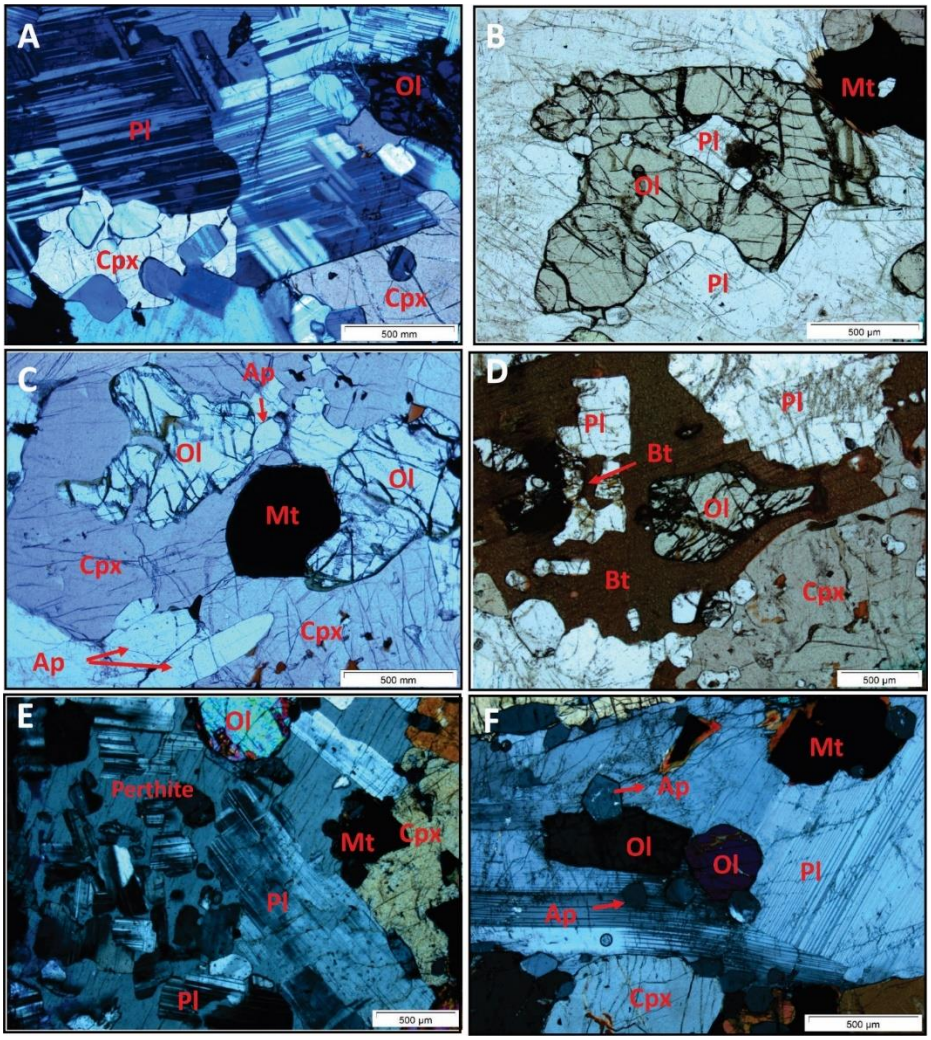

Figure 5-4. Photomicrographs showing textures and mineral compositions of different units. (A) FD-13-34-64.6 olivine gabbro, cross-polar transmitted light photomicrograph showing the Cpx partially encloses and bisects Pl chadocrysts; (B) SL-13-41-63.2 olivine gabbro, plane polarized light photomicrograph showing Ol encloses Pl chadocrysts, and Cpx is interstitial to Pl; (C) FD-13-34-46.1 olivine gabbro, plane polarized light photomicrograph showing Ol is rimed by Cpx; (D) SL-13-34-32 olivine gabbro, plane polarized light photomicrograph showing Ol and Pl are surrounded by Bt, note the locally resorption of Pl by Bt; (E) SL-13-34-5.1 olivine gabbro, cross-polar transmitted light photomicrograph showing perthite oikocrysts encloses many euhedral platy Pl grains; (F) FD-13-34-226.3 oxide augite melatroctolite, cross-polar transmitted light photomicrograph showing the deformed twinning of plagioclase. Abbreviations Ol: olivine, Cpx: clinopyroxene, Pl: plagioclase, Mt: Magnetite, Ap: apatite, Bt: biotite.

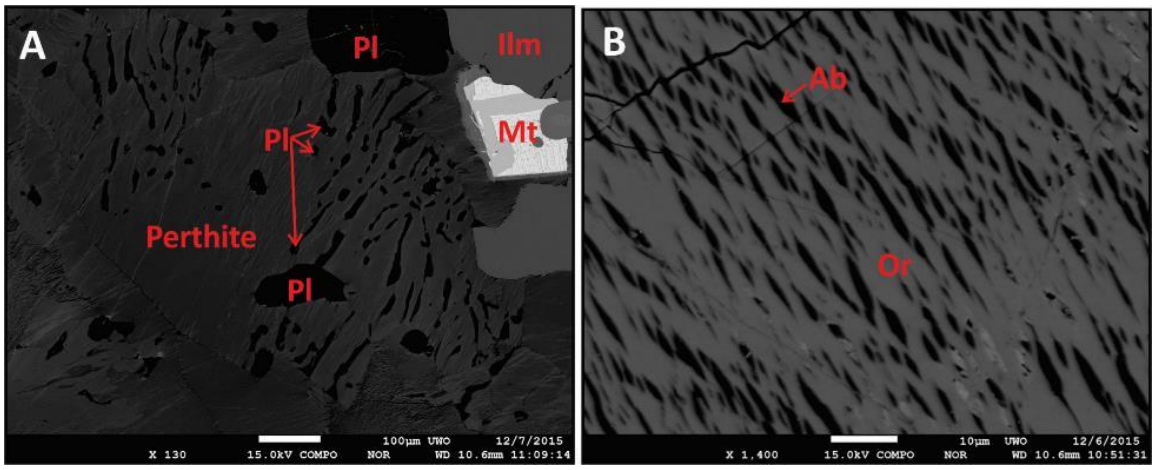

Figure 5-5. BSE images showing different alkali feldspar textures. (A) SL-13-41-3 oxide augite melatroctolite, the wormy shaped Pl grains within the perthite; (B) SL-13-34-13.3 olivine gabbro, the Ab exsolution in orthoclase host forming the typical perthite in the Layered Series rocks from Area 41. Abbreviations Ab: albite, Or: orthoclase, Pl: plagioclase, Mt: Magnetite, Ilm: ilmenite.

5.5 Down-hole profiles

5.5.1 Four Dams

Down-hole variations in Mg#s of olivine and clinopyroxene, anorthite content of plagioclase, whole-rock SiO_2, Fe_2O_3, P_2O_5, La, La/Sm, Al_2O_3, CaO, K_2O, Rb, Sr, Ba, Zr, and Gd/Yb for Layered Series units of drill hole FD-13-34 are displayed in Figure 5-6 and summarized in Table 5-3. Generally, from the upper oxide augite melatroctolite, through the olivine gabbro, to the lower oxide augite melatroctolite, three different trends are observed. The upper oxide augite melatroctolite unit has relatively constant mineral chemical compositions and whole-rock P_2O_5, La, and Zr concentrations. Concentrations of the remaining whole-rock major and trace elements in the upper oxide augite melatroctolite are highly variable and are generally lower than those in the underlying olivine gabbro except Fe_2O_3.

Throughout the thick unit of olivine gabbro, olivine, clinopyroxene and plagioclase trend towards more evolved compositions down-hole whereas whole-rock incompatible elements such as La and Zr generally increase with depth. In addition, P_2O_5 contents throughout the entire olivine gabbro are almost constant (1.5-2 wt.%). However, in detail there are step like variations in abundances of Rb, Sr, Ba and Zr that approximately correspond to variations in La/Sm and Gd/Yb that taken together

indicate the olivine gabbro can be subdivided into four sub units (I-IV). Table 5-4 summarizes mineral compositions and whole-rock La, Rb, Sr, Ba, Zr, La/Sm, and Gd/Yb for all the subdivided units identified at FD-13-34. These variations suggest that at least four pulses of magma were involved in generation of the current package of olivine gabbro rocks. In the lower oxide augite melatroctolite, the down-hole variations of major and trace elements are more consistent compared to the upper oxide augite melatroctolite unit. For instance, whole-rock Fe_2O_3, P_2O_5, and La increase with depth whereas the rest of whole-rock variables generally decrease with depth till to the base of the Layered Series. However, there are an inadequate number of rock samples from the lower oxide augite melatroctolite unit to fully interpret the mineral chemistry of this unit.

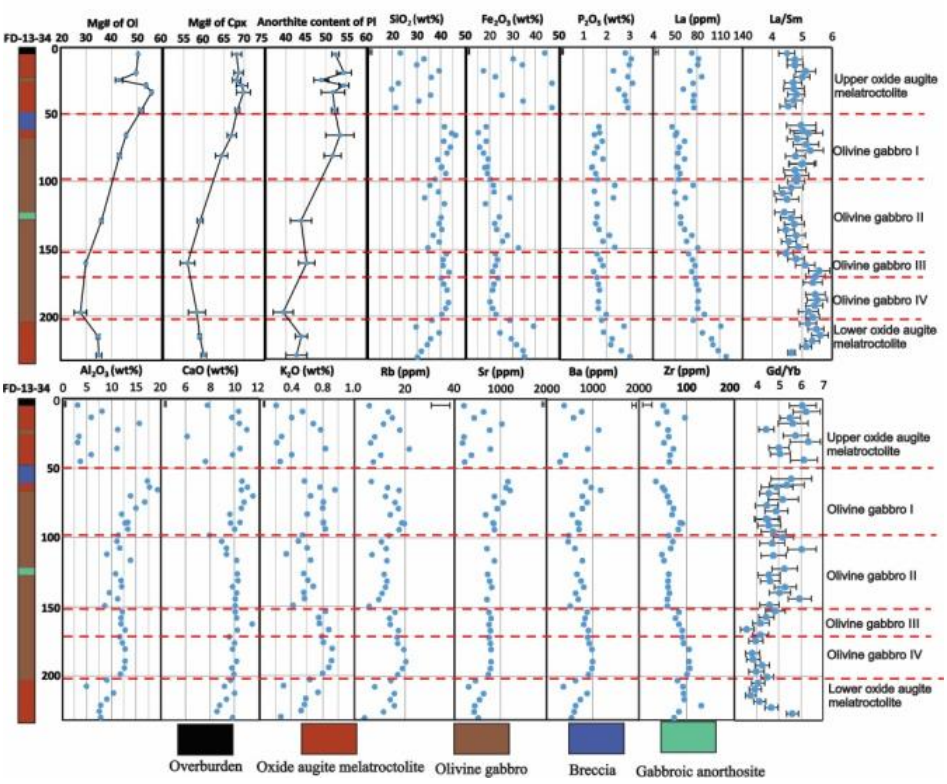

Figure 5-6. Down-hole mineral chemical and lithogeochemical profiles throughout the Layered Series gabbro units for drill hole FD-13-34 of Four Dams area. Note the coupled reverse differentiation trends for Mg#s of Ol and Cpx, anorthite content of Pl, and whole-rock La and Zr. The error bar for whole-rock analysis represents 2 σ analytical precision determined by multiple analyses on the same sample. The error bar for mineral chemical analysis represents 1 σ sample error determined by analyses on 3-4 spots of 3-5 grains of each type of mineral for each sample. Abbreviations: Ol-Olivine; Cpx-Clinopyroxene; Pl-Plagioclase.

Table 5-4. Summary of Mg#s of olivine and clinopyroxene, anorthite content of plagioclase, and whole-rock Rb, Sr, Ba, Zr, La/Sm, and Gd/Yb for sub-units identified in drill hole FD-13-34. Abbreviations: Ol-olivine, Cpx-clinopyroxene, Pl-plagioclase, OAM-oxide augite melatroctolite, OG- olivine gabbro.

Unit	Mg# of Ol	Mg# of Cpx	An content of Pl	Rb	Sr	Ba	Zr	La/Sm	Gd/Yb
Upper OAM	50-60	65-70	50-55	5-18	200-800	200-1000	40-80	4.5-5	5.0-6.4
OG I	40-50	62-68	50-53	12-20	700-1200	500-1000	50-90	4.8-5.3	4.5-5.6
OG II	30-40	56-62	45-50	6-13	550-800	450-800	60-70	4.3-4.8	4.6-6.0
OG III	30-32	55-57	~45	14-18	760-800	820-930	80-90	4.5-5.3	4.2-4.8
OG IV	~29	~58	~40	17-21	750-820	910-1000	90-105	5.4-5.6	3.6-4.3
Lower OAM	30-35	58-60	43-45	8-16	320-650	400-900	80-100	5.2-5.6	3.8-5.6

5.5.2 Area 41

Mineral chemical and whole-rock lithogeochemical profiles through the Layered Series in drill hole SL-13-34 at Area 41 are displayed in Figure 5-7. Near the top of the drill hole Mg#s of olivine and clinopyroxene, and anorthite content of plagioclase decrease slightly to around 10m, and then they increase with depth to the base of the Layered Series. It is notable that the consistent down-hole mineral chemical variations are not affected by the changes in rock types, *e.g.*, from the olivine gabbro to oxide augite melatroctolite. Combining this observation with the similarity of the REE distribution patterns for the olivine gabbro and oxide augite melatroctolite from Area 41, as will be shown later, it is reasonable to suggest that olivine gabbro and oxide augite melatroctolite are the same unit and that differences in mineral abundances (particularly magnetite) are a result of mechanical mineral sorting process.

Profiles of trace elements La, Zr, Gd, and Yb, and ratios of La/Sm and Gd/Yb fluctuate down hole, suggesting that multiple pulses of related intrusions formed the package of the Layered Series rocks. Generally, the down-hole variations of La and Zr are similar to mineral chemical profiles, which are in the opposite sense to the down-hole variation of Ba concentrations. The down-hole variation in whole-rock P_2O_5 is similar to La throughout the total package of the Layered Series, indicating

that La is mainly controlled by apatite. In addition, K_2O, Ba, Sr, and Rb have broadly similar down-hole profiles throughout the Layered Series.

The inspection of mineral compositions and whole-rock Zr, La/Sm, and Gd/Yb for olivine gabbro between 7 and 18 m down bore hole SL-13-34 closely resembles the olivine gabbro sub-unit III in bole hole FD-13-34, whereas the olivine gabbro from 21 to 45 m down bore hole SL-13-34 resembles the olivine gabbro sub-unit I in FD-13-34, respectively (see Table 5-4 for reference). However, it is noteworthy that the olivine gabbro at 7-18 and 21-45 m down the bore hole SL-13-34 also contains higher Ba, Sr, and Rb contents than the olivine gabbro sub-units III and I at FD-13-34, respectively.

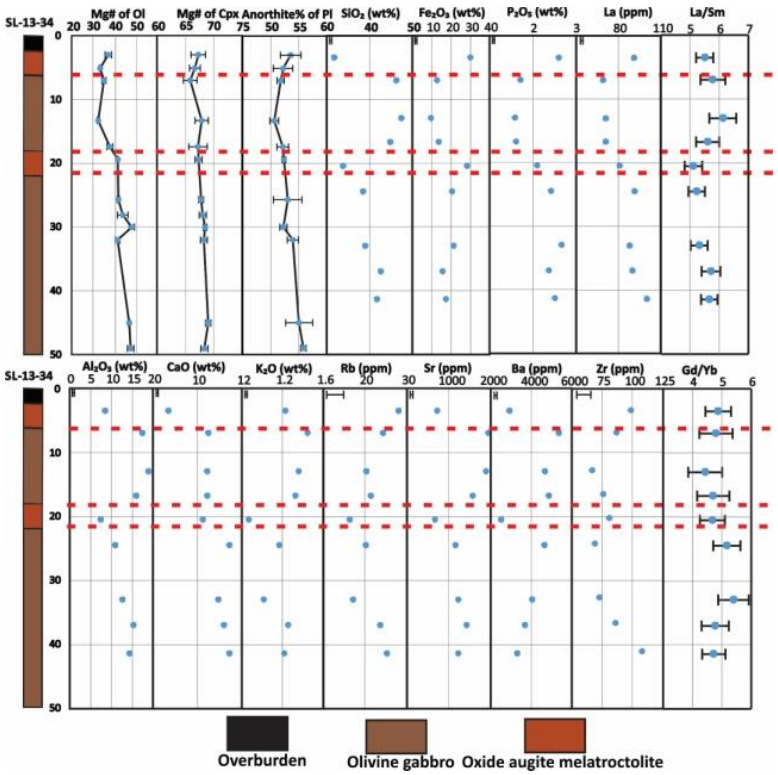

Figure 5-7. Down-hole mineral chemical and lithogeochemical profiles throughout the Layered Series units for drill hole SL-13-34 at Area 41. Note the similar trends between Mg#s of Ol and Cpx, anorthite content of Pl, and whole-rock La and Zr. The error bar for whole-rock analysis represents 2 σ analytical precision determined by multiple analyses on the same sample. The error bar for mineral chemical analysis represents 1 σ sample error determined by analyses on 3-4 spots of 3-5 grains of each type of mineral for each sample. Red dashed lines show the contact between olivine gabbro and oxide augite melatroctolite. Abbreviations: Ol-Olivine; Cpx-Clinopyroxene; Pl-Plagioclase.

5.5.3 WD zone

Down-hole profiles of mineral chemical and whole-rock compositions for drill hole MW-07-06 at WD zone are displayed in Figure 5-8. Down-hole variations in Mg#s of olivine and clinopyroxene, and anorthite content of plagioclase present an overall increasing trend with depth. La and Zr also present a general increasing trend with depth, in contrast to Ba which decreases with depth to the base of the sampled interval. These trends are similar to what is observed at Area 41 (SL-13-34). The trends for mineral compositions, Zr, La/Sm, and Gd/Yb resembles olivine gabbro subunit IV at Four Dams (FD-13-34), but, similar to Area 41, contain higher Rb, Sr, and Ba.

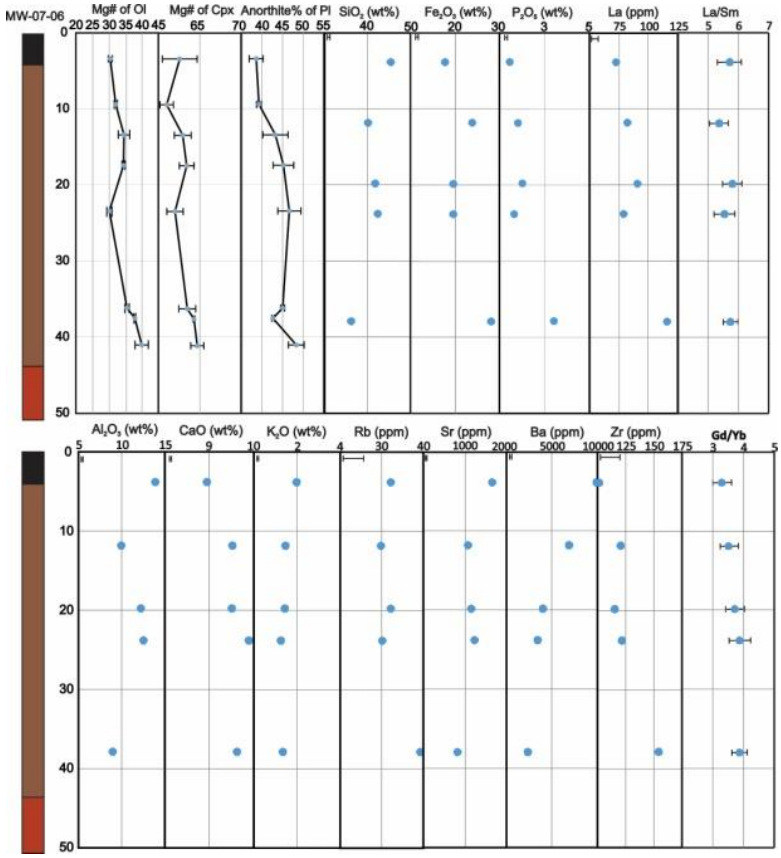

Figure 5-8. Down-hole mineral chemical and lithogeochemical profiles throughout the Layered Series gabbro units for drill hole MW-07-06 of WD zone area. The error bar for whole-rock analysis represents 2 σ analytical precision determined by multiple analyses on the same sample. The error bar for mineral chemical analysis represents 1 σ sample error determined by analyses on 3-4 spots of 3-5 grains of each type of mineral for each sample. Abbreviations: Ol-Olivine; Cpx-Clinopyroxene; Pl-Plagioclase, symbols as in Figure 5-7.

5.6 Mineral compositions

Mineral chemical compositions for the units at Area 41 and Four Dams are examined in this section. Note that due to the small amount of the gabbroic anorthosite in the Layered Series as well as the unavailable rock specimens for this unit, the gabbroic anorthosite is ignored in the following examination.

5.6.1 Summary of mineral chemical results

5.6.1.1 Olivine, clinopyroxene and plagioclase

Mg#s of olivine and clinopyroxene and anorthite content of plagioclase for olivine gabbro and oxide augite melatroctolite of the Layered Series are summarized in Figure 5-9. Note that olivine and clinopyroxene in our samples do not show obvious zoning, but plagioclase is normally zoned because of the relatively slow Na/Ca exchange at the crystal scale (Grove et al., 1984), compositional data from plagioclase cores are adopted here to represent mineral chemical compositions in each sample. Figure 5-9 shows that the olivine gabbro and oxide augite melatroctolite at Area 41 have similar values in Mg#s of olivine and clinopyroxene, and anorthite content of plagioclase, but overall the oxide augite melatroctolite seems to be more primitive than the olivine gabbro. At Four Dams, the oxide augite melatroctolite appears to be more primitive than its olivine gabbro counterpart. Generally, the Layered Series rocks at Area 41 are slightly more primitive than those at Four Dams area. It is also noteworthy that the Layered Series units at Four Dams have relatively wide ranges in both Mg#s of olivine and clinopyroxene. This is in contrast to the Layered Series units at Area 41 where values of Mg# of olivine are significantly more variable than those of Mg# of clinopyroxene.

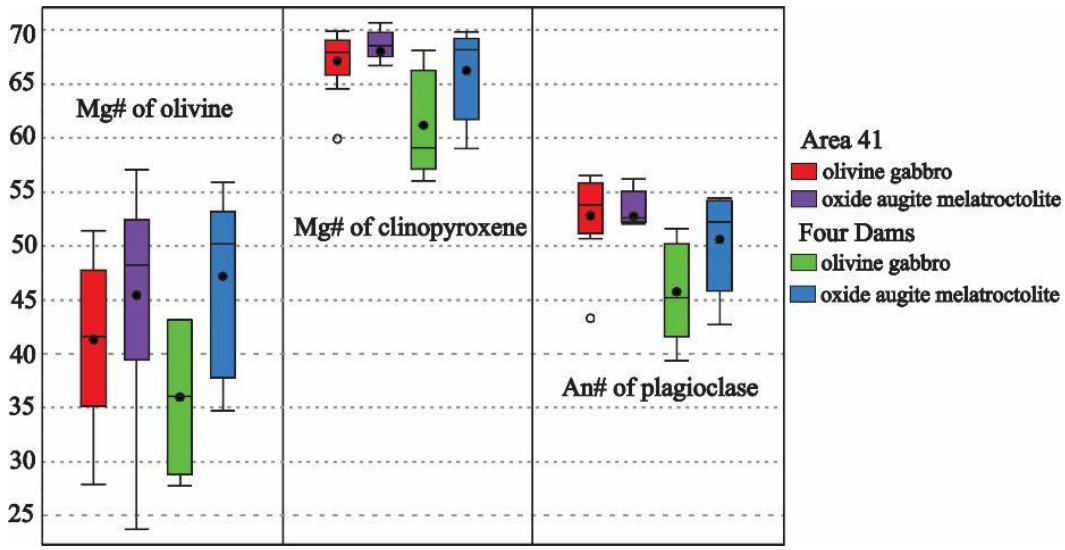

Figure 5-9. Box and whisker plots summarizing Mg# of olivine, Mg# of clinopyroxene, and anorthite content of plagioclase for the Layered units of different areas.

5.6.1.2 Biotite, orthoclase and plagioclase

Barium, Sr and K_2O contents of biotite, alkali feldspar (dominantly orthoclase), and plagioclase in the Layered Series units at Area 41 and Four Dams are tabulated in Table 5-5. Biotite and plagioclase in Area 41 units contain higher Ba and Sr contents, respectively, than at Four Dams, and alkali feldspar in Area 41 units contain significantly higher Ba (>60000 ppm) than both biotite and plagioclase. Note that mineral descriptions for olivine gabbro and oxide augite melatroctolite at each area are grouped together to facilitate the description. Figure 5-10 shows that there is a positive correlation between anorthite content and Ba concentrations in plagioclase for units at Area 41. By contrast, the units at Four Dams display an overall negative correlation between these two variables.

Table 5-5. Ba, Sr and K_2O concentrations in alkali feldspar, biotite and plagioclase of the Layered Series samples from different localities, results were determined electron microprobe analyses. SD refers to 1 σ sample variability determined by multiple analyses on 3-5 grains of each mineral type in each sample. N/A means thin sections are not available.

Mineral	Element		Area 41	Four Dams
Alkali feldspar	Ba (ppm)	Avg	66000	N/A
		SD	10000	N/A
	Sr (ppm)	Avg	3400	N/A
		SD	620	N/A
	K_2O (wt %)	Avg	7.9	N/A
		SD	1.33	N/A
Biotite	Ba (ppm)	Avg	13900	5900
		SD	6940	975
	Sr (ppm)	Avg	240	300
		SD	120	150
	K_2O (wt %)	Avg	8.7	8.8
		SD	0.40	0.15
Plagioclase	Ba (ppm)	Avg	3000	1600
		SD	730	540
	Sr (ppm)	Avg	2800	2100
		SD	390	270
	K_2O (wt %)	Avg	0.8	0.8
		SD	0.11	0.11

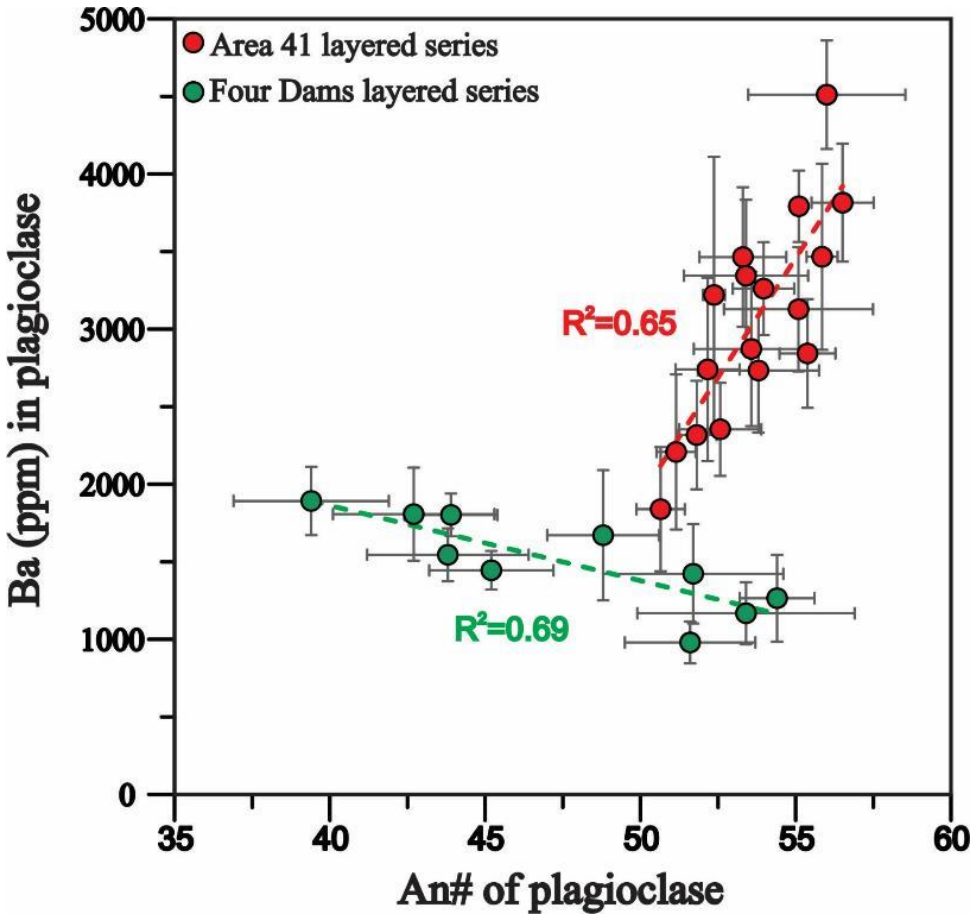

Figure 5-10. Relationships between anorthite content of plagioclase and Ba concentrations in plagioclase for the Layered Series units from Area 41 and Four Dams. Note that units at Four Dams and Area 41 has two different trends. R^2 refers to the coefficient of determination between anorthite content of plagioclase and Ba in plagioclase. The error bar represents 1 σ sample variability determined through multiple analyses on at least 3 plagioclase grains in each sample.

5.6.2 Fe/Mg exchange between olivine and clinopyroxene

Down-hole variations in Fe/Mg exchange partition coefficient ($Kd_{Fe/Mg}^{Ol/Cpx} = (Fe/Mg)_{Ol}/(Fe/Mg)_{Cpx}$, in mole) for the Layered Series intersected by SL-13-34 and FD-13-34 are summarized in Table 5-6 and shown in Figure 5-11. The red dashed lines in this diagram indicate the equilibrium $Kd_{Fe/Mg}^{Ol/Cpx}$ at 1100 °C (1.8) based on Loucks (1996b). Note that 1100 °C represents the forming temperature of the Layered Series units according to clinopyroxene-orthopyroxene geothermometer results from Shahabifar (pers. comm. 2016). Figure 5-11 shows that there is a general down-hole decrease in $Kd_{Fe/Mg}^{Ol/Cpx}$ for the Layered Series at Area 41, with values becoming increasingly closer to 1.8 with depth. By contrast, the Layered

Series at Four Dams presents a down-hole increasing trend in $Kd_{Fe/Mg}^{Ol/Cpx}$, with values becoming increasingly deflected away from 1.8 with depth.

Table 5-6. The summary of $Kd_{Fe/Mg}^{Ol/Cpx}$ for the Layered Series units intersected by drill hole SL-13-34 and FD-13-34.

Drill hole	Depth/m	Unit	(Fe/Mg)cpx	$(Fe/Mg)_{Ol}$	$Kd_{Fe/Mg}^{Ol/Cpx}$
SL-13-34	3.0	Oxide augite melatroctolite	0.49	1.69	3.47
	5.1	Oxide augite melatroctolite	0.50	1.99	3.99
	7.0	Olivine gabbro	0.52	1.84	3.55
	13.3	Olivine gabbro	0.47	2.08	4.39
	17.4	Olivine gabbro	0.49	1.63	3.35
	19.4	Oxide augite melatroctolite	0.49	1.40	2.88
	25.7	Oxide augite melatroctolite	0.48	1.38	2.91
	28.1	Oxide augite melatroctolite	0.47	1.27	2.71
	30.0	Oxide augite melatroctolite	0.46	1.07	2.33
	32.0	Olivine gabbro	0.46	1.40	3.02
	45.0	Olivine gabbro	0.45	1.12	2.51
	49.0	Oxide augite melatroctolite	0.46	1.10	2.36
FD-13-34	5.0	Oxide augite melatroctolite	0.47	0.98	2.08
	18.6	Oxide augite melatroctolite	0.46	1.01	2.20
	24.0	Olivine gabbro	0.47	1.33	2.83
	27.9	Oxide augite melatroctolite	0.44	0.86	1.96
	33.0	Oxide augite melatroctolite	0.43	0.79	1.82
	46.1	Oxide augite melatroctolite	0.46	0.93	2.00
	64.6	Oxide augite melatroctolite	0.49	1.18	2.39
	79.6	Olivine gabbro	0.55	1.31	2.38
	127.3	Olivine gabbro	0.69	1.77	2.56
	158.6	Olivine gabbro	0.79	2.34	2.98
	194.8	Olivine gabbro	0.72	2.60	3.63

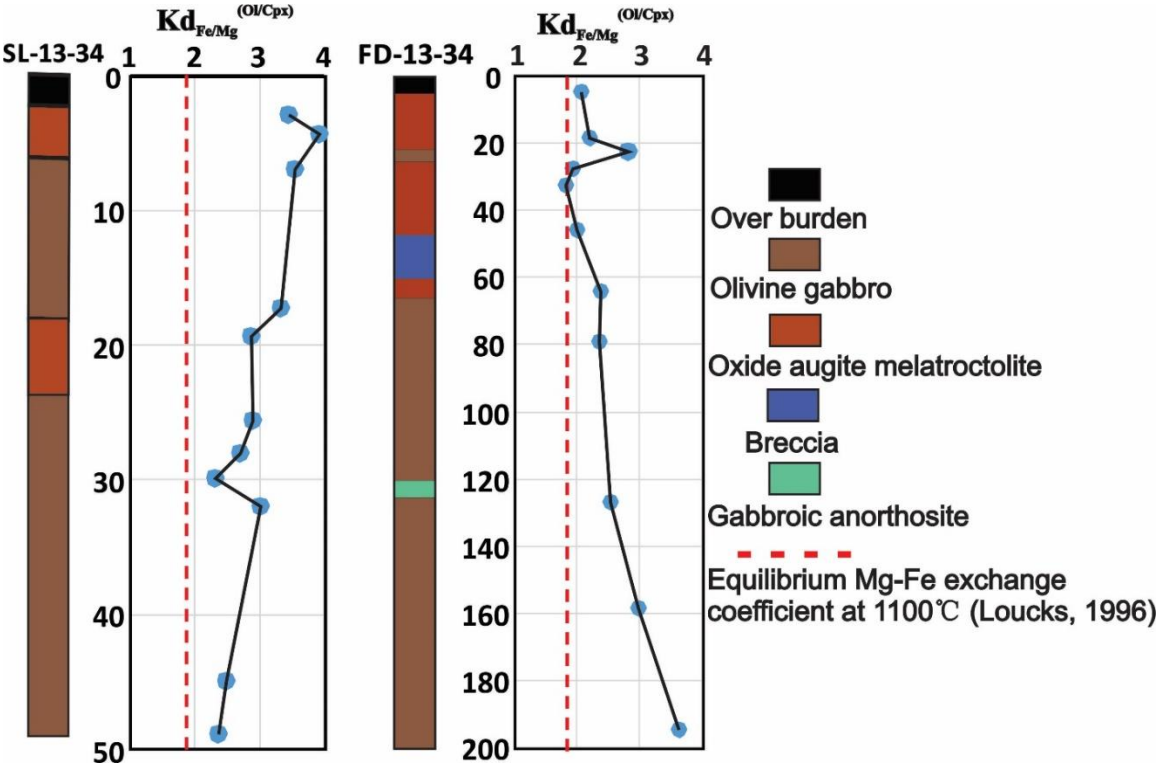

Figure 5-11. Down-hole variations in Mg-Fe exchange coefficient (Kd) between olivine and clinopyroxene for the Layered Series units intersected by SL-13-34 at Area 41 and FD-13-34 at Four Dams. Note the different down-hole trends for units at Four Dams and Area 41. The equilibrium coefficient (1.80) at 1100 ℃ based on Loucks (1996) is indicated using a red dashed line.

5.7 Geochemical characteristics

Shaw (1997) investigated down-hole mineral chemical profiles of the Layered Series at Bamoos and Highway traverses (locations are indicated in Figure 5-1), and found that the down-hole trends were not consistent and could not be correlated. In this study the Layered Series at Area 41 and WD zone exhibits different down-hole profiles compared to those at Four Dams, in agreement with Shaw (1997). The major differences between the two groups are the higher abundances of Ba, Sr, and Rb at Area 41 and WD zone. These differences are consistent with the mineral chemical observations described above and suggest that different processes must have taken place for development of the Layered Series at these locations. To further investigate igneous processes active in the Layered Series we examined additional geochemical features at Area 41 and Four Dams.

5.7.1 General element ratio diagram

A first step in comparing the Layered Series gabbro units at different areas is to verify the classification scheme that was used in the field and subsequent petrography. Good et al. (2015) found Pearce-General Element diagram of (Ca/Si-5/3P) (in mole) vs. Mg/Si (in mole) (Fig. 5-12) was useful in illustrating variations in olivine, clinopyroxene, and plagioclase in all rock types. Furthermore, this diagram can neglect the potential influence of sulfides, magnetite, apatite, and biotite because of normalizing molar proportions to Si and subtracting the proportion of Ca contributed by apatite, thus it is very useful in comparing different rock units. Note that plagioclase with different anorthite content are plotted along the vertical axis. In addition, Figure 5-12 includes average mineral chemical compositions of olivine, clinopyroxene, and plagioclase for the Layered Series gabbro from Area 41 and Four Dams as determined by electron microprobe analyses. This diagram successfully separates different layered series rocks. For example, the olivine gabbro at Area 41 and Four Dams plot close to the plagioclase with a composition of An_{50}, similar to average compositions of the plagioclase determined by electron microprobe analyses. Oxide augite melatroctolite samples display a nearly horizontal trend that is closer to the right hand side of the diagram and intersects clinopyroxene-olivine tie lines approximately at the midpoint, indicating this unit contains a variable amount of plagioclase and almost equal proportions of clinopyroxene and olivine. These observations are in good agreement with the petrography.

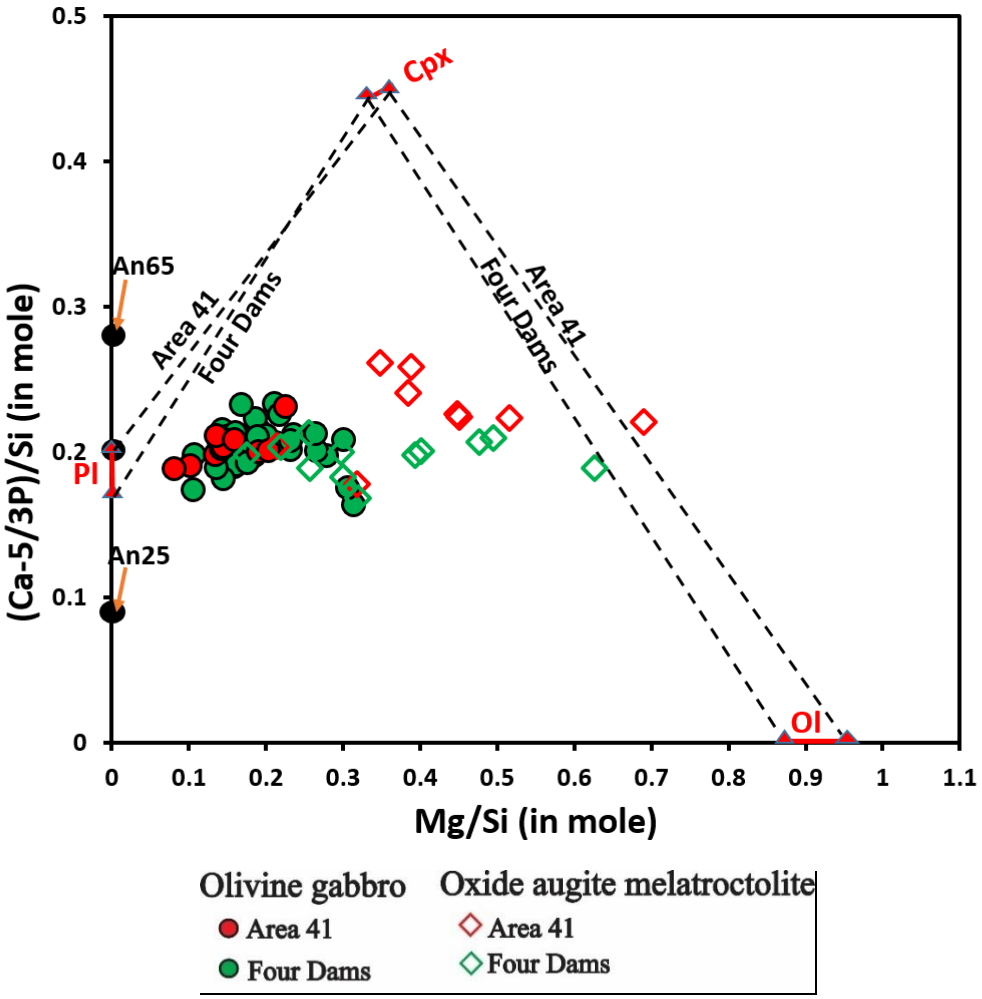

Figure 5-12. General element ratio diagram for major rock units of the Layered Series. Molar proportions of whole-rock data are plotted relative to major minerals. Grey dashed lines are clinopyroxene-olivine and clinopyroxene-plagioclase tie lines for the Layered Series gabbro at Area 41 and Four Dams. Average Mg# of olivine, Mg# of clinopyroxene, and anorthite content of plagioclase for the Layered Series gabbro at Area 41 and Four Dams are indicated using red triangles. Anorthite content of plagioclase plotted along the y-axis are values calculated based on plagioclase stoichiometry. Different sample groups are outlined with dashed circles in different colours. Average olivine and clinopyroxene compositions determined by probe analyses are indicated. Samples are corrected for Ca contained in apatite. The tringle indicates average probe analysis for the Layered Series gabbro.

5.7.2 Summary of whole-rock compositions

Concentrations of selected major and trace elements in various Layered Series units are shown in Figure 5-13. Variations in whole-rock major elements are mainly controlled by variations in major minerals. For example, the higher abundances of Fe_2O_3, TiO_2, P_2O_5, MgO, and the lower abundances of SiO_2, Al_2O_3, K_2O, Na_2O for

the oxide augite melatroctolite compared to the olivine gabbro indicate it has more magnetite, olivine and apatite, and less plagioclase than olivine gabbro and gabbroic anorthosite. These are all consistent with petrographic observations. The olivine gabbro at Area 41 contains higher K_2O contents than other units, reflecting the presence of alkali feldspar as observed by petrography.

The olivine gabbro and oxide augite melatroctolite from Area 41 contains pronounced higher Ba contents than those from Four Dams. Zr contents in the olivine gabbro and oxide augite melatroctolite from both areas are similar.

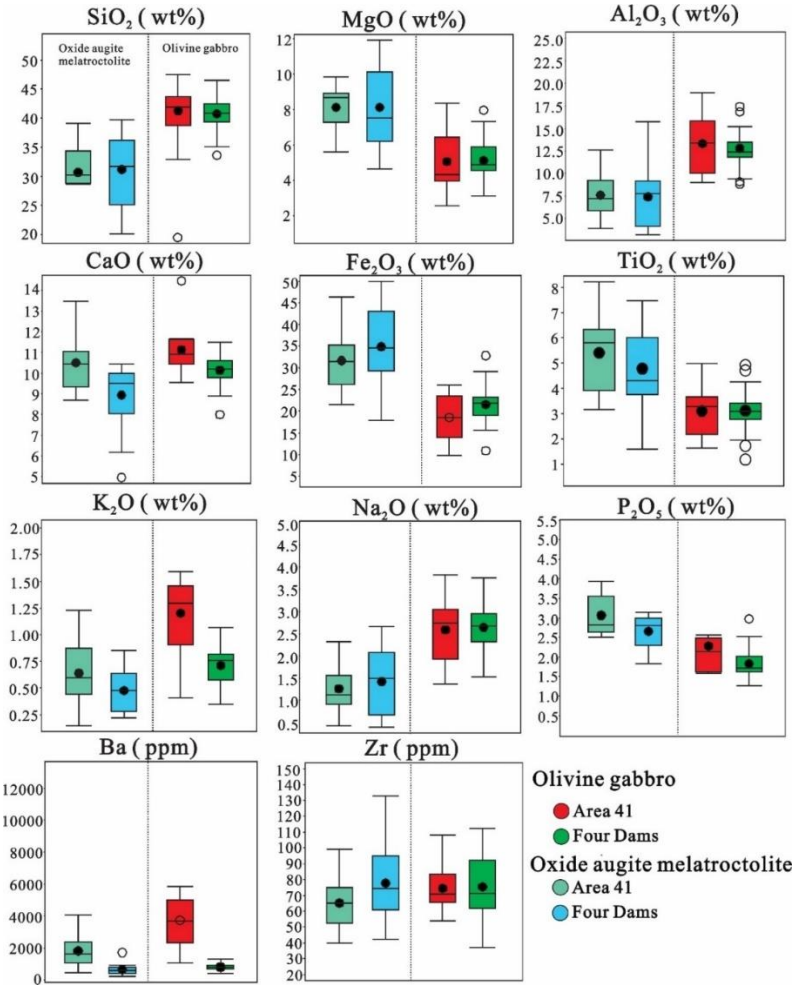

Figure **5-13**. Box and whisker plots for selected major and trace elements in different rock units of different localities. Box and whisker plots are uniform in their use of the box: the bottom and top of the box are always the 25th and 75th percentile (the lower and upper quartiles, respectively), and the band near the middle of the box is always the 50th percentile (the median). The small black infilled circle is the average and the lines on the ends are the minimum and maximum values, black empty circles are outliers.

5.7.3 Distribution of trace elements

5.7.3.1 Rare Earth Element (REE)

The Primitive mantle (Sun and McDonough, 1995) normalized average abundance of rare earth elements (REE) in the olivine gabbro and oxide augite melatroctolite from Area 41 and Four Dams, are compared to the average REE abundances for the Coubran basalts from Cundari (2012) in Figure 5-14. The Coubran basalts are located in the center of the Coldwell Alkaline Complex, and Cundari (2012) considered them to be co-genetic with PGE mineralization related the Marathon Series. Three important observations on the trace element data are: 1) REE patterns for average samples of the olivine gabbro and oxide augite melatroctolite are elevated and approximately parallel to the pattern for average samples of the Coubran basalts; 2) average samples of the oxide augite melatroctolite from Area 41 and Four Dams present very similar distribution patterns with their olivine gabbro counterparts, indicating both rock types may have crystallized from similar magmas; 3) at both areas, the REE for oxide augite melatroctolite is slightly higher than for olivine gabbro; and, 4) there is a pronounced inflection point at Nd for all of the trends.

Figure 5-15A shows there is a general positive relationship between Ce and P_2O_5 for all rock types, indicating apatite is likely the controlling phase of light REE. In addition, the olivine gabbro and oxide augite melatroctolite present an increasing P_2O_5 with increasing Ce/Yb trend (Fig. 5-15B), as expected given that the LREE are more compatible in apatite than Yb (Paster, 1974).

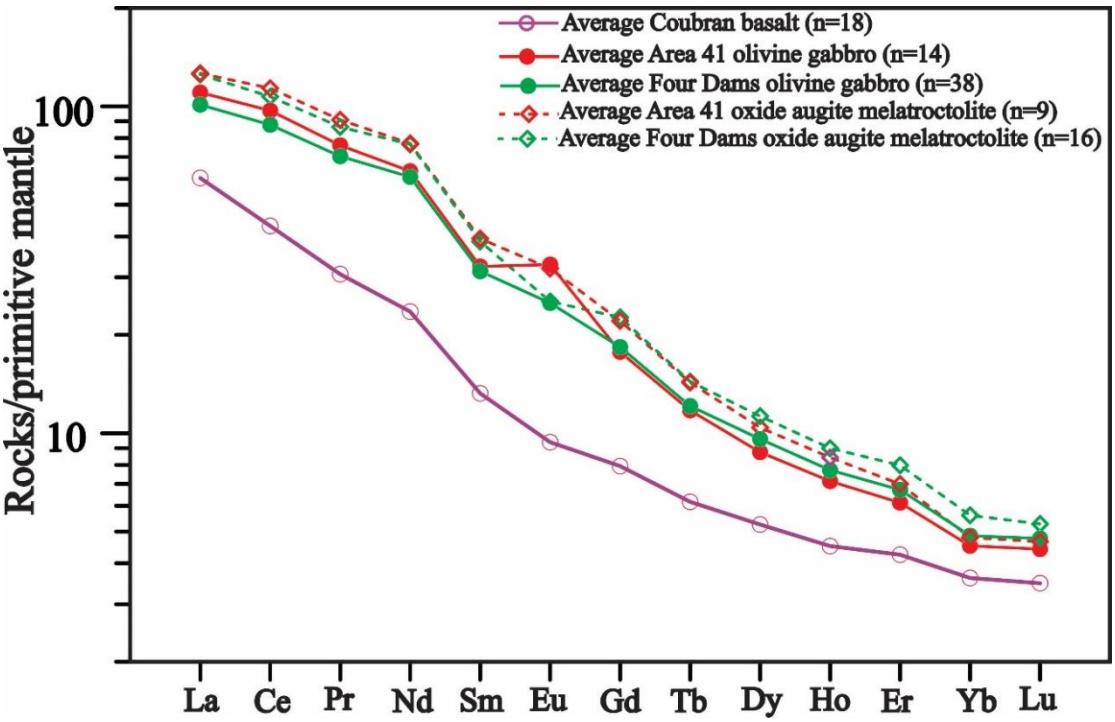

Figure 5-14. REE contents for the Layered Gabbro at different areas, and Coubran basalt normalized to the primitive mantle values of Sun and McDonough (1995). Data of samples from Area 41 and Four Dams are prepared in the current study, data of the Coubran basalt are from Cundari (2012).

5.7.3.2 Large Ion Lithophile Element (LILE)

The observed differences in behaviour of LILE at Area 41 and Four Dams are highlighted in Figures 5-15C to F. Samples from Area 41 show a negative correlation between Ba and La, whereas samples from Four Dams present a nearly horizontal trend between Ba and La (Fig. 5-15C). All these rock units show positive Rb vs. K_2O, and Ba vs. K_2O correlations (Figs. 5-15D and E), indicating Rb and Ba are mainly controlled by potassium-bearing phases, *e.g.*, biotite, orthoclase, plagioclase, etc. However, the trends for units at Area 41 on Ba vs. K_2O and Ba vs. Sr are much steeper than for data at Four Dams (Figs. 5-15E and F).

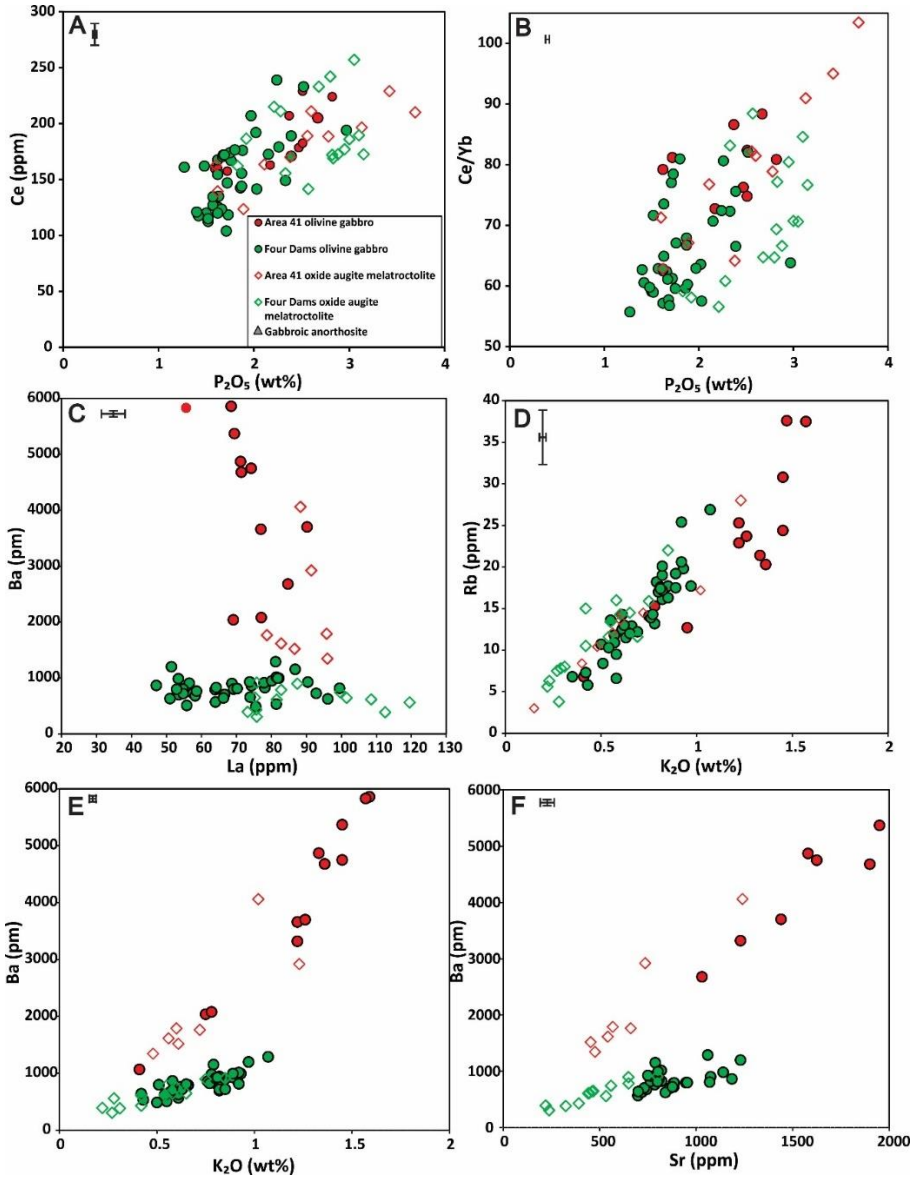

Figure 5-15. Binary diagrams correlating Ce vs. P_2O_5, Ce/Yb vs. P_2O_5, Ba vs. La, Rb vs. K_2O, Ba vs. K_2O, and Ba vs. Sr for various rock types. Error bar represents the 2 σ analytical precision for lithogeochemical analyses, determined through repetitive analyses on duplicates.

Diagrams of Ba vs. K_2O and Ba vs. Sr (Figs. 5-15 E and F) are converted into logarithmic scale plots in Figures 5-16 and 5-17 in order to further examine the different Ba and Sr behaviours at Area 41 and Four Dams. Conducting this conversion has two purposes. First, it allows the Layered Series units at different areas to be separated into two areas without any overlaps, thus facilitating the observations. Second, in logarithmic scale plot, lines with different ratios will be parallel to each other, thus facilitating the interpretations particularly after adding

mineral control lines. Average Ba/K_2O and Ba/Sr ratios for potassium-bearing minerals such as plagioclase, orthoclase, and biotite were determined by electron microprobe analyses. This allows us to add mineral control lines on both diagrams to interpret the mineral controls of whole-rock Ba and Sr in actual rocks. Both diagrams show that whole-rock Ba and Sr concentrations are controlled by a mixture of plagioclase, biotite, and/or orthoclase. For example, whole-rock Ba and Sr concentrations in Area 41 rocks can be explained by crystallization of plagioclase, orthoclase, and biotite with volume proportions of 90:6:4, whereas those in Four Dams rocks are controlled by plagioclase and biotite with volume proportions of 90:10. These relative proportions of potassium-bearing minerals are in agreement with average mineral compositions in the actual rocks.

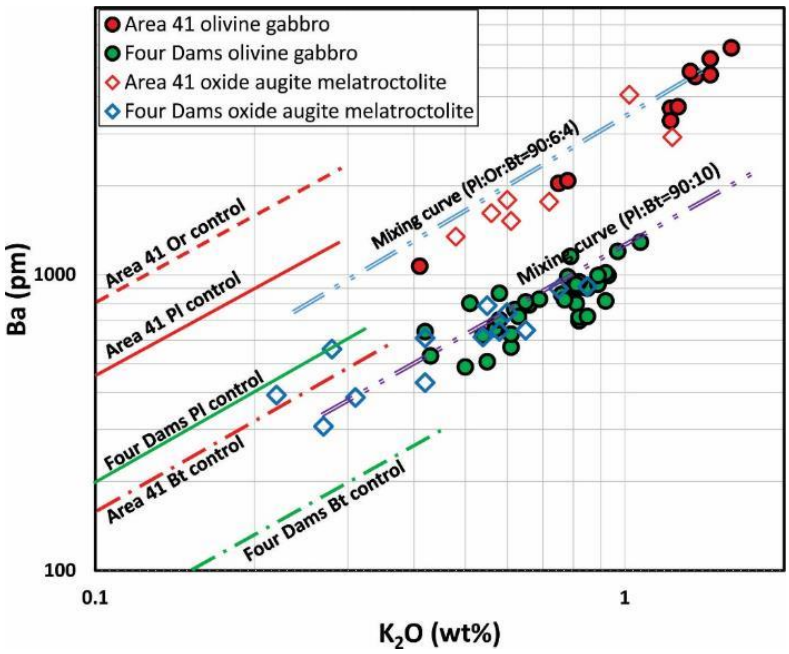

Figure 5-16. Logarithmic scale diagram correlating Ba with K_2O for the Layered Series units from Area 41 and Four Dams. Ba/K_2O ratios for different minerals determined by electron microprobe analyses are indicated using parallel vectors.

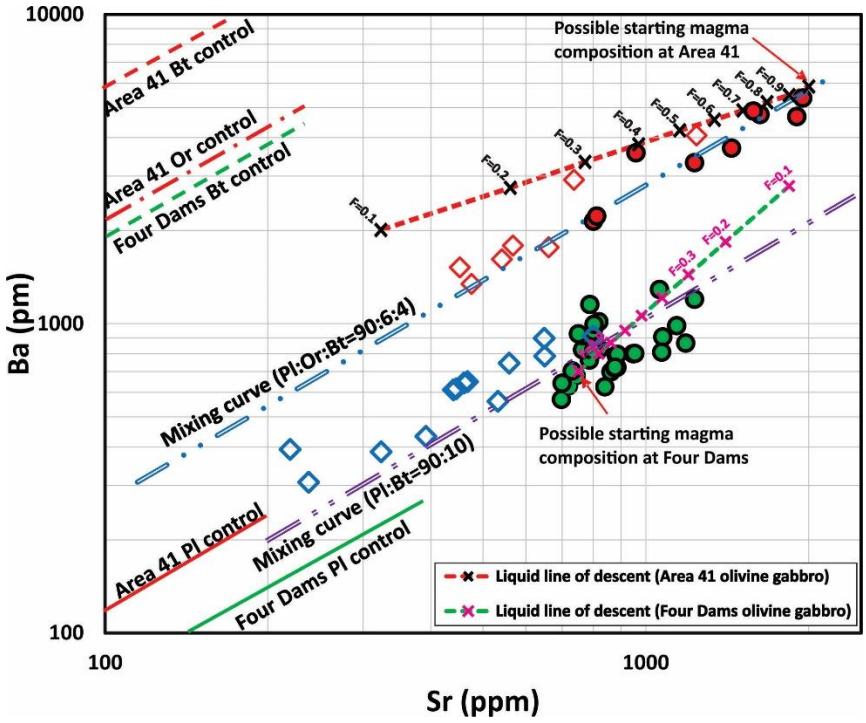

Figure 5-17. Logarithmic scale diagram correlating Ba versus Sr for the Layered Series units from Area 41 and Four Dams. Ba/Sr ratios for different minerals determined by electron microprobe analyses are indicated using parallel vectors. Liquid lines of descent for the Layered Series olivine gabbro from Area 41 and Four Dams are also indicated based on geochemical modeling results as will be shown in section 5.8.3. Other symbols as in Figure 5-16.

5.8 Geochemical modeling

In order to gain some insight into the parental magma of the Layered Series and evaluate whether it is co-genetic with the Coubran basalts, the Layered Series units are modeled by assuming Rayleigh fractional crystallization (RFC). Using RFC may be reasonable because the Layered Series units present consistent down-hole variations in both mineral chemical and whole-rock compositions. The equation for the RFC is:

$$C_L = C_o * F^{(D-1)}$$

where C_o is the initial concentration of the trace element, F is the fraction of melt remaining, C_L is the concentration of the trace element in the remaining melt, and D is the partition coefficient for the trace element into the mineral (Neuman et al., 1954).

The composition of instantaneous cumulate (Cc) crystallized from the residual melt is:

$$C_c = D * C_0 * F^{(D-1)}$$

When more than one mineral is fractionated, D here represents the bulk partition coefficient that is calculated using the following equation:

$$D = \sum X_\Phi D^\Phi$$

where X_Φ is the weight fraction of phase Φ and D^Φ is the distribution coefficient of the trace element into phase Φ.

After constraining the starting compositions (parental magma compositions for various units), this modeling allows us to estimate concentrations of trace elements in residual liquids and instantaneous cumulates at different F. In addition, at certain F, concentrations of trace elements in generated rocks with different proportions of interstitial liquids can be calculated using the following equation:

$$C_R = C_L * (1-\varphi) + C_c * \varphi$$

where C_R is the concentration of the trace element in the formed rock, φ is the weight proportion of cumulates in the rock.

As mentioned in section 5.5.2, the oxide augite melatroctolite is the same unit with the olivine gabbro, in order to simplify descriptions and avoid repetition, models shown here are for olivine gabbro at Four Dams and Area 41. High Field Strength Elements (HFSE) such as Nb, Zr, and La, and LILE such as Ba and Sr are selected for modelling because: 1) HFSE are often used to interpret petrogenesis of rock units because of their highly incompatible behaviour into most silicate phases; 2) Sr is a compatible element into plagioclase (the main constituent of the rock types), and Ba behaves similarly with Sr for the olivine gabbro according to the positive relationships between the two elements (Fig. 5-15F); and, 3) as mentioned above

the units at Area 41 and Four Dams have different Ba and Sr contents, modelling both elements may gain some insight on understanding these differences.

5.8.1 The selection of partition coefficients

The partition coefficients are critical data to establish suitable models and form the basis of all related arguments. However, the large available database of partition coefficients determined by studies over decades mean that selecting the most suitable partition coefficients is challenging. In order to constrain the usage of partition coefficients as best as possible, two strategies are applied. First, selecting partition coefficients determined in tholeiitic-alkaline basalt magma systems to minimize the effects of melt composition. Second, minimize the choice of authors because different authors may have determined the partition coefficients under different conditions including temperature, oxygen fugacity, etc. Doing this will largely reduce the biases introduced by these uncertainties. The selected partition coefficients that best satisfy the above two strategies are given in Table 5-7.

Table 5-7. Mineral/liquid partition coefficients selected in the current work. Ol-olivine, Cpx-clinopyroxene, Pl-plagioclase, Mt-magnetite, Ap-apatite, Bt-biotite.

	Ol	Reference	Cpx	Reference	Pl	Reference
Ba	0.03	Villemant et al. (1981)	0.04	Villemant et al. (1981)	0.58	Villemant et al. (1981)
Sr	0.02	Villemant et al. (1981)	0.16	Villemant et al. (1981)	3	Villemant et al. (1981)
Th	0.0300	Villemant et al. (1981)	0.04	Villemant et al. (1981)	0.1000	Villemant et al. (1981)
Nb	0.0020	Dun and Sen (1994)	0.0077	Zack and Brumm (1988)	0.03	Dun and Sen (1994)
La	0.0080	Fujimaki et al. (1984)	0.1047	Fujimaki et al. (1984)	0.0348	Fujimaki et al. (1984)
Zr	0.0047	Fujimaki et al. (1984)	0.1310	Fujimaki et al. (1984)	0.0094	Fujimaki et al. (1984)
	Mt	Reference	Ap	Reference	Bt	Reference
Ba	0.028	Okamoto (1979)	0.05	Paster et al. (1974)	10	Villemant et al. (1981)
Sr	0.11	Ewart and Griffin (1994)	1.1	Watson and Green (1981)	0.7	Villemant et al. (1981)
Th	0.1	Lemarchand et al. (1987)	0.4	Prowatke and Klemme (2006)		
Nb	0.05	Nieslon (1992)	N/A			
La	0.0029	Nieslon et al. (1992)	8.6	Paster et al. (1974)		
Zr	0.1200	Nieslon et al. (1992)	0.636	Fujimaki (1986)	2.5	Villemant et al. (1981)

5.8.2 HFSE

The weight proportions of the fractionated mineral phases used in modeling are 11% olivine, 28% clinopyroxene, 55% plagioclase, 2% magnetite, 4% apatite, using representative average mineral compositions of the olivine gabbro from Four Dams and Area 41. After the selection of best available partition coefficients (Table 5-7), the fitted La vs. Zr, and Th vs. Nb model curves for the olivine gabbro at Four Dams and Area 41 are displayed in Figures 5-18 A and B. Compositions of the Coubran basalts are indicated in these models for comparison. Note that Cundari (2012) subdivided the Coubran basalts into three groups (types A, B, and C), based on their incompatible element abundances and so each type is plotted for comparison.

The model curves in Figures 5-18 A and B represent a possible solution using a possible parental magma for the olivine gabbro at both areas. Note that no matter what the starting composition is, once bulk partition coefficients for modelled elements are determined, directions of these curves will not change. Possible melt starting composition that could resolve the observed rock compositions is tabulated in Table 5-8. This possibility requires a starting composition with considerably higher abundances of La, Zr, and Nb, and a lower abundance of Th than the three types of the Coubran basalts, suggesting that the Layered Series units cannot be produced directly from a Coubran basalt-like magma. Generally, La and Zr contents are similar to those in F=0.55 melt of the type B Coubran basalt (after fractionation of 65% olivine and 35% clinopyroxene). But Nb and Th in the possible parental magma cannot be related to the type B Coubran basalt by the mentioned fractional scheme.

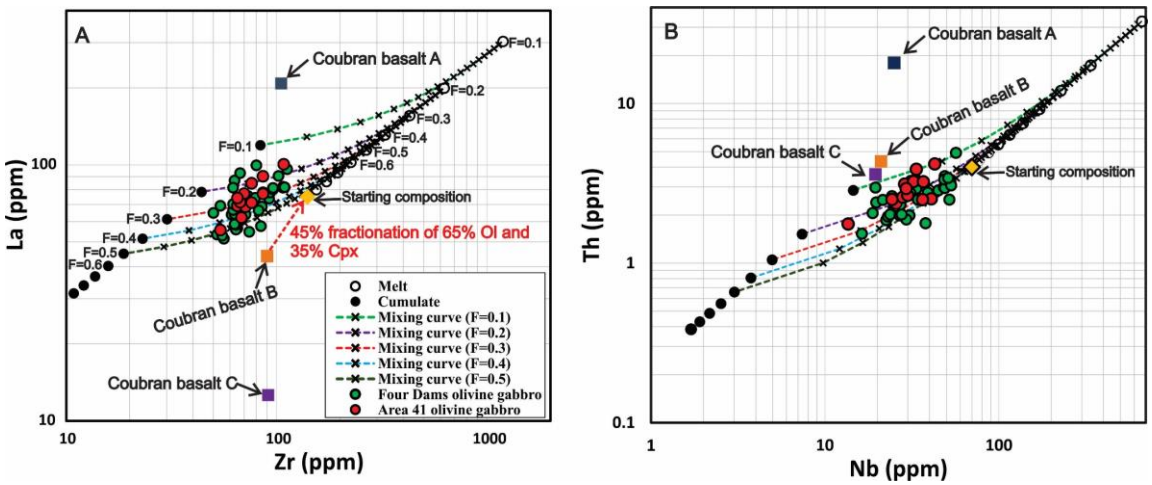

Figure 5-18. Geochemical model curves for La vs. Zr (A) and Th vs. Nb (B) for the olivine gabbro at Four Dams and Area 41. Black circles represent 100% instantaneous cumulates at different F, *e.g.*, the F=0.9 beside the black circle represents the cumulate composition at this degress of fractionation and the black circle beside the F=0.1 label represent cumulate at this degress of fractionation. Similarly, the open circles represent residual melt compositions at F varying from 0.9 (lowermost) to 0.1 (uppermost). The dashed curve that connects the cumulate and residual melt (both at the same F) indicate composition of the rock with different proportions of cumulate and interstitial melt formed at this F. The crosses on the curves denote 5% of cumulates, or 5% increments of interstitial melts, from left to right. Thus, data points of rocks fall on, or between, curve(s) can be explained by mixtures of cumulates and interstital melts at F of the starting liquid.

Table 5-8. Trace element composiitons of different liquids, units are all in ppm.

	Type B Coubran basalts	F=0.55 of type B Coubran basalts	Possible starting composition	
Ba	398	700	680 (Four Dams)	6000 (Area 41)
Sr	450	785	785 (Four Dams)	2000 (Area 41)
Th	4.3	7.7	4	
Nb	21	38	70	
La	46	82	82	
Zr	93	160	140	

5.8.3 LILE

Barium and Sr are used to model the olivine gabbro at Area 41 and Four Dams. Partition coefficients of Ba and Sr into plagioclase (D_{Ba}^{Pl}=0.60, D_{Sr}^{Pl}=3) used in this study are from Villemant et al. (1981), these values are close to those calculated by using equations of Blundy and Wood (1991) (shown below) assuming that the average anorthite content of plagioclase is 50 (Fig. 5-9 and Table 5-3) and the

temperature is 1400 degrees kelvin. Note that the temperature used here is based on orthopyroxene-clinopyroxene geothermometer results from Shahabifar Far (2016).

$$RT \ln D_{Sr}^{Pl} = 26{,}800 - 26{,}700 * X_{An}$$

$$RT \ln D_{Ba}^{Pl} = 10{,}200 - 38{,}200 * X_{An}$$

where R is ideal gas constant (8.314 $JK^{-1}mol^{-1}$), T is the absolute magma temperature (kelvin), X_{An} is the mole fraction An of plagioclase.

5.8.3.1 Low Ba Olivine gabbro (Four Dams)

The observed negative correlation between anorthite content of plagioclase and Ba concentrations in plagioclase for the units from Four Dams (Fig. 5-10) suggests that Ba is an incompatible element in this system. Since there is a positive correlation between whole-rock Ba and Sr for units at Four Dams (Fig. 5-15F), it is expected that Sr is also an incompatible element in this system. However, the assumed Sr partition coefficient into plagioclase (D_{Sr}^{Pl}=3.0) is too high to have Sr with a bulk partition coefficient less than 1. Alternatively, the appropriate Sr vs. Zr model that accommodates both the incompatible behavior of Sr and the fit for data points, is created based on D_{Sr}^{Pl}=1.3. The lower partition coefficient may be reasonable (see Bedard, 2001). It is uncertain why D_{Sr}^{Pl} is smaller in this case; perhaps it indicates the Layered Series magma at Four Dams has a higher temperature than that at Area 41 according to the Sr equation of Blundy and Wood (1991). Models of Ba vs. Zr and Sr vs. Zr for the olivine gabbro rocks at Four Dams are displayed in Figures 5-19A and B. Note that these two fitted models require the possible parental magma at Four Dams contain 680 ppm Ba and 785 ppm Sr, close to those in F=0.55 residual melt of the type B Coubran basalts (after fractionation of 65% olivine and 35% clinopyroxene, Table 5-8).

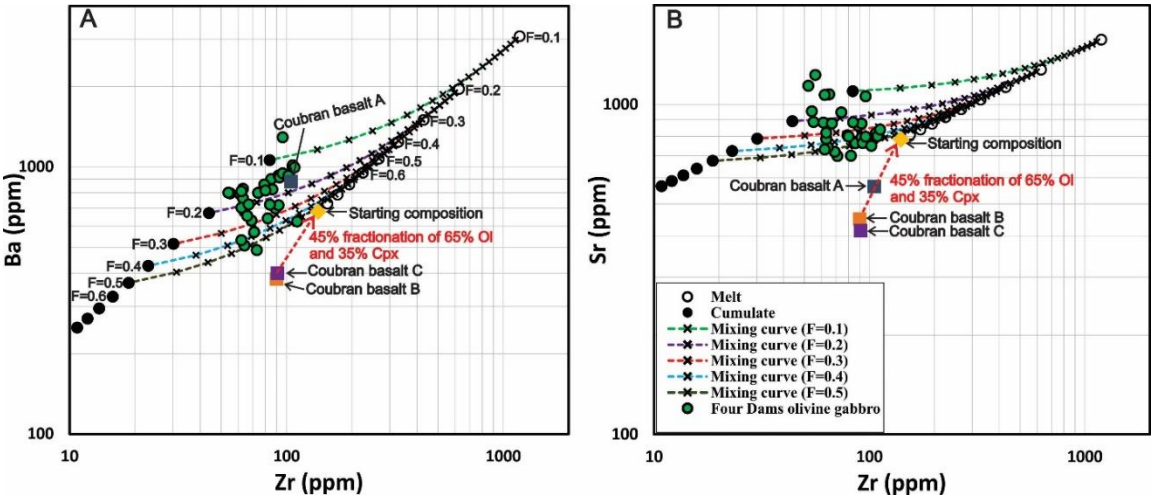

Figure 5-19. Geochemical model curves for Ba vs. Zr (A) and Sr vs. Zr (B) for the olivine gabbro at Four Dams. Black circles represent 100% instantaneous cumulates at different F, *e.g.*, the F=0.9 beside the black circle represents the cumulate composition at this degress of fractionation and the black circle beside the F=0.1 label represent cumulate atthis degress of fractionation. Similarly, the open circles represent residual melt compositions at F varying from 0.9 (lowermost) to 0.1 (uppermost). The dashed curve that connects the cumulate and residual melt (both at the same F) indicate composition of the rock with different proportions of cumulate and interstitial melt formed at this F. The crosses on the curves denote 5% of cumulates, or 5% increments of interstitial melts, from left to right. Thus, data points of rocks fall on, or between, curve(s) can be explained by mixtures of cumulates and interstital melts at F of the starting liquid.

5.8.3.2 High Ba Olivine gabbro (Area 41)

There is good evidence suggesting that Ba is a compatible element during formation of the olivine gabbro at Area 41, including : 1) whole-rock La and Ba in olivine gabbro are negatively correlated (Fig. 5-15C); 2) the down-hole Ba profile has an opposite trend with down-hole La and Zr profiles (Fig. 5-7); and, 3) anorthite content of plagioclase and Ba concentrations in plagioclase are positively correlated (Fig. 5-10), indicating the residual melt becomes increasingly depleted in Ba during fractionation. Therefore, in order for Ba to have a bulk partition coefficient>1, a Ba-rich phase such as orthoclase or biotite needs to be added to the fractionating phases. Note that adding several weight percent of either orthoclase or biotite onto the liquidus will have limited influence to the modeling scheme for HFSE as shown in section 5.8.2.

5.8.3.2.1 Orthoclase

According to petrography, 7 wt.% orthoclase is added onto the liquidus. Weight percent of other fractionating phases used when modeling HFSE is readjusted proportionally to make the total as 100%. To our knowledge, there are no Ba and Sr partition coefficients into orthoclase reported in any basaltic system. However, Table 5-5 shows that Ba and Sr contents in orthoclase for the Layered Series units at Area 41 are approximately 22 and 1.1 times, respectively, higher than those in plagioclase. Provided that orthoclase joined the plagioclase on liquidus, D_{Ba}^{Or} and D_{Sr}^{Or} can be reasonably deduced through multiplying D_{Ba}^{Pl} and D_{Sr}^{Pl} by factors of 22 and 1.1, respectively, which are around 13 and 3.3. Nevertheless, the lack of published Ba and Sr coefficients into orthoclase means that the Ba vs. Zr and Sr vs. Zr models (Figs. 5-20A and B) here are semi-quantitative. Note that fitted model curves in each case require that the possible parental magma contains around 6000 ppm Ba and 2000 ppm Sr (Table 5-8), respectively, to best explain the observed rock compositions. These values are significantly higher than Ba and Sr contents inferred for the Layered Series parental magma at Four Dams (680 ppm Ba, 785 ppm Sr, Fig. 5-19) and cannot be related to all three types of the Coubran basalts.

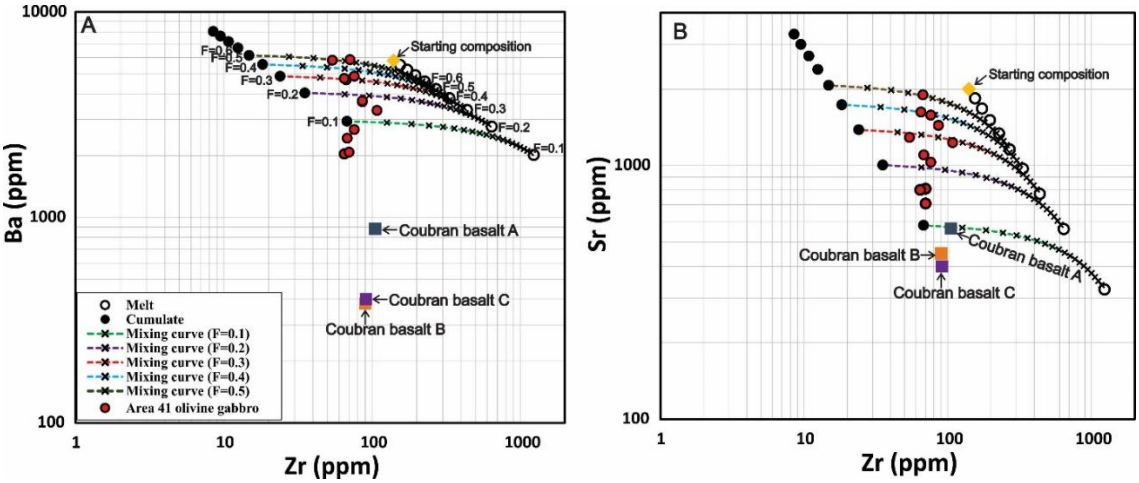

Figure 5-20. Geochemical model curves for Ba vs. Zr (A) and Sr vs. Zr (B) for the olivine gabbro rocks at Area 41 (assuming orthoclase is on liquidus). Black circles represent 100% instantaneous cumulates at different F, *e.g.*, the F=0.9 beside the black circle represents the cumulate composition at this degress of fractionation and the black circle beside the F=0.1 label represent cumulate atthis degress of fractionation. Similarly, the open circles represent residual melt compositions at F varying from 0.9 (lowermost) to 0.1 (uppermost). The dashed curve that connects the cumulate and residual melt (both at the same F) indicate composition of the rock with different proportions of cumulate and interstitial melt formed at this F. The crosses on the curves denote 5% of cumulates, or 5% increments of interstitial melts, from left to right. Thus, data points of rocks fall on, or between, curve(s) can be explained by mixtures of cumulates and interstital melts at F of the starting liquid.

5.8.3.2.2 Biotite

According to petrography, 5 wt.% biotite is added on liquidus in this case, and weight percent of other fractionating phases used in section 5.8.2 is readjusted proportionally to make the total as 100%. Note that Ba and Sr partition coefficients into biotite used in this case are 10 and 0.7, respectively, both values are from Villemant et al. (1981) determined in alkaline basalt system. Clearly, the Ba vs. Zr model (Fig. 5-21A) cannot explain the olivine gabbro samples at Area 41 and Ba also has a bulk partition coefficient <1. By contrast, Sr vs. Zr model (Fig. 5-21B) in this case is similar to that produced when assuming orthoclase is on liquidus, which works well for the olivine gabbro samples at Area 41. Note that Ba and Sr contents in the possible parental magma at Area 41 in this case are 5200 ppm and 2000 ppm, respectively, close to those in the Layered Series parental magma when assuming

orthoclase is on liquidus. The high Ba and Sr contents cannot be related to any type of the Coubran basalts.

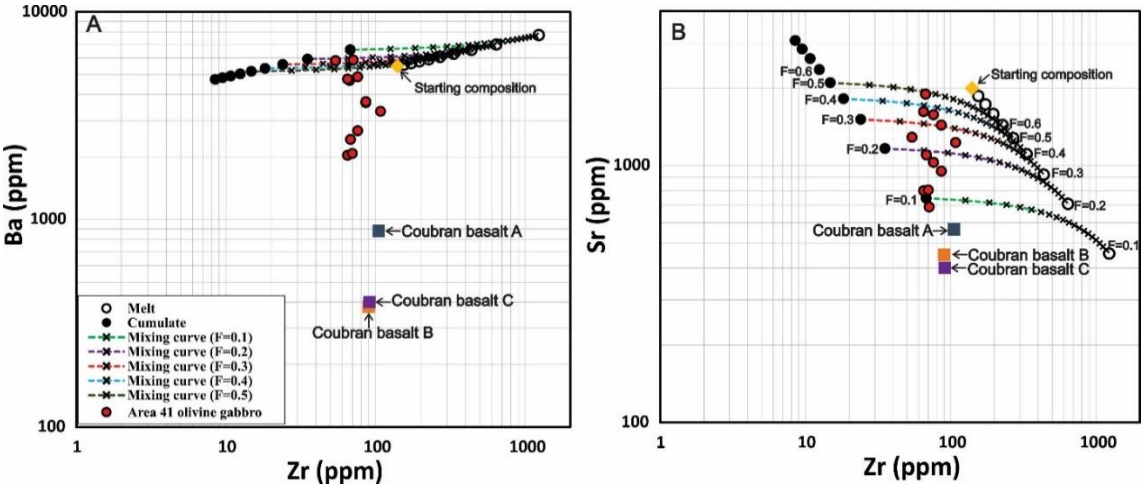

Figure 5-21. Geochemical model curvesfor Ba vs. Zr (A) and Sr vs. Zr (B) for the olivine gabbro rocks at Area 41 (assuming biotite is on liquidus). Black circles represent 100% instantaneous cumulates at different F, *e.g.*, the F=0.9 beside the black circle represents the cumulate composition at this degress of fractionation and the black circle beside the F=0.1 label represent cumulate atthis degress of fractionation. Similarly, the open circles represent residual melt compositions at F varying from 0.9 (lowermost) to 0.1 (uppermost). The dashed curve that connects the cumulate and residual melt (both at the same F) indicate composition of the rock with different proportions of cumulate and interstitial melt formed at this F. The crosses on the curves denote 5% of cumulates, or 5% increments of interstitial melts, from left to right. Thus, data points of rocks fall on, or between, curve(s) can be explained by mixtures of cumulates and interstital melts at F of the starting liquid.

5.9 Discussion

5.9.1 The parental magma of the Layered Series

Figure 5-14 shows that the average Layered Series units have almost parallel REE profiles with the average Coubran basalts, indicating a potential co-genetic relationship between the two rock groups. The inspection of the parental magma composition through geochemical modeling by assuming the Rayleigh fractionation scenarios indicates that the Layered Series parental magma at Area 41 and Four Dams has similar La, Zr with F=0.55 residual melt of the type B Coubran basalts (after fractionation of 65% olivine and 35% clinopyroxene). This also applies to Ba and Sr contents at Four Dams, but not at Area 41. Ba and Sr contents in the parental magma at Area 41 are too high to be related to any type of Coubran basalts, and

possible reasons for this will be addressed in the following section. Shahabifar Far (2016) investigated the Coubran basalts in the MELTS program and found that the olivine and clinopyroxene are the first crystallization phases. This is consistent with the fractionation scheme as mentioned above. Thus, based on these observations, it seems that a fractionated Coubran basalt-like magma with considerably higher La, Zr, Ba, and Sr could be considered as a parental magma for the Layered Series. However, as mentioned in section 5.8.2, Nb and Th do not work. Therefore, it is more reasonable to assume that the parental magma for the Layered Series can not be related to the Coubran basalts, but may share some characteristics with magma that is compositionally similar to the type B Coubran basalts.

5.9.2 Insights from the behavior of Ba and Sr

5.9.2.1 Ba and Sr differences between the starting liquids 1 and 2

The range and inter-element ratios for trace element abundances at Four Dams are very similar to those at Area 41, except for Ba and Sr. The possible parental magma at Area 41 has higher Ba and Sr contents than that at Four Dams. One possibility for their Ba and Sr differences may be real variations of these elements in the same magma, as for the Wolfcamp lake basalts, which exhibit highly variable Ba and Sr contents (216-1444 ppm Ba, 320-860 ppm Sr) with tightly constrained major constituents (48-52 wt.% SiO_2, 1.88-2.05 wt.% TiO_2, 13.85-15.21 wt.% Al_2O_3, etc.) (Good, pers. commun., 2016). However, the fitted Ba vs. Zr model (Fig. 5-20A) predicts that the Layered Series magma at Area 41 has around 6000 ppm Ba and 2000 ppm Sr. To our knowledge, such a high Ba content is rarely reported for any alkaline basalt. Therefore, rather than natural variation of the same basalt, something special must have occurred. To fully interpret this is difficult, here we propose two possibilities. First, this difference may be related to the different degrees of partial melting of Ba-hosting phases (e.g., amphibole) in the upper mantle. Second, this difference can also be related to metasomatism whereby extra Ba and Sr contents were introduced into the Layered Series parental magma at Area 41 through the involvement of fluids. The second hypothesis may be more reasonable because: 1)

Ba and Sr are fluid-mobile elements; and, 2) the Layered Series rocks from Area 41 also contain higher concentrations in other fluid-mobile elements such as Rb, K, Cs than the Layered Series rocks from Four Dams (see Appendix 6).

5.9.2.2 Controlling phases of whole-rock Ba and Sr

It is reasonably certain that whole-rock Ba and Sr are mainly controlled by potassium-bearing phases in light of the positive relationships between Ba vs. K_2O, and Ba vs. Sr (Figs. 5-15E and F). Figures 5-16 and 5-17 show that the different Ba vs. K_2O and Ba vs. Sr trends between the units at Area 41 and Four Dams can be explained by their different mixing controls of minerals. For example, at Area 41 Ba and Sr are controlled by plagioclase, orthoclase, and biotite with proportions of 90:6:4, whereas at Four Dams they are only controlled by plagioclase and biotite with proportions of 90:10. The possible fractionation of orthoclase or biotite at Area 41 perhaps results in the compatible behaviour of Ba, this will be fully discussed in the following section.

It is noteworthy that in Ba vs. Sr diagram (Fig. 5-17) the oxide augite melatroctolite samples at Four Dams are generally located above the mixing control line that goes through its olivine gabbro counterparts. The higher Ba/Sr for the oxide augite melatroctolite at Four Dams can be explained by: 1) at Four Dams the oxide augite melatroctolite contains a higher amount of interstitial liquid (*e.g.*, biotite); and, 2) the oxide augite melatroctolite has higher biotite: plagioclase ratio than olivine gabbro, thus its whole-rock Ba and Sr have a more control by biotite. The first possibility may be reasonable given that Ba seems to be more incompatible than Sr in the magma system at Four Dams (see Table 5-7). However, it can be ruled out considering that the similar ranges of Zr contents (80-100 ppm) between the olivine gabbro and oxide augite melatroctolite at Four Dams (Figs. 5-6 and 5-13) suggest that they contain a similar amount of interstitial melt. Alternatively, the second explanation is consistent with lithogeochemical results that at Four Dams the oxide

augite melatroctolite contains similar K_2O contents with, and significantly lower Al_2O_3 contents than, the olivine gabbro (Fig. 5-13).

5.9.2.3 Is orthoclase or biotite on liquidus?

As mentioned earlier, there is ample evidence suggesting that Ba is a compatible element in the Layered Series magma at Area 41. However, the equation of Blundy and Wood (1991) predicts that D_{Ba}^{Pl} is around 0.6. Thus, in order for Ba to be compatible (bulk partition coefficient>1), either orthoclase or biotite needs to be on liquidus. Orthoclase is favoured over biotite as a liquidus mineral for the following reasons: 1) biotite textures indicate that it typically crystallized very late, as an accessory mineral in the mafic magma system; 2) orthoclase appears to have crystallized earlier, as an interstitial phase; 3) orthoclase is more abundant than biotite in the units at Area 41; and, 4) orthoclase may formed simultaneously with, or slightly later than, the plagioclase based on petrographic observation that wormy-like plagioclase is within the perthite that formed the myrmekite texture (Fig. 5-5A). Furthermore, given that biotite is on liquidus, the Ba vs. Zr model (Fig. 5-21A) poorly fit all olivine gabbro samples from Area 41, the fitness can be even worse when considering that D_{Ba}^{Bt}=10 used in Figure 5-21A is likely overestimated because microprobe analyses of biotite and plagioclase in the Layered Series at Area 41 suggest D_{Ba}^{Bt} should be just 4.5 times of D_{Ba}^{Pl} (0.6) (Table 5-5). Alternatively, when considering orthoclase as a liquidus mineral, the fitted Ba vs. Zr and Sr vs. Zr models (Fig. 5-20) are produced based on D_{Ba}^{Or}=13 and D_{Sr}^{Or}=3.4, both are viable values deduced based on Ba and Sr contents in orthoclase and plagioclase (Table 5-5). The validity of Ba vs. Zr and Sr vs. Zr models when assuming orthoclase is on liquidus can be further tested using the following strategy: Figure 5-20 predicts that F=0.4 melt of the parental magma at Area 41 contains around 4000 ppm Ba and 970 ppm Sr, given that D_{Ba}^{Pl}=0.6 and D_{Sr}^{Pl}=3.0, 2400 ppm Ba and 2900 ppm Sr, respectively, in plagioclase are deduced, these are similar to Ba and Sr contents in plagioclase as determined by electron microprobe analyses (3000±390 ppm Ba, 2100±270 ppm Sr, Table 5-5).

However, although the Ba vs. Zr and Sr vs. Zr models by assuming orthoclase on liquidus seem to work from a geochemical perspective, it is still a challenge matter when considering the geological fact. Fractionating liquidus alkali feldspar more likely can occur in phonolites, minettes, and carbonatites which are of alkaline compositions (Zhang et al., 1993a; Deer et al., 2001; Azzone et al., 2009). Particularly, to our knowledge, no study ever reported orthoclase as a liquidus mineral in any basaltic magma system. Thus, in order to fully interpret this, it is necessary to investigate whether the Layered Series magma is still basaltic or not. The Coubran basalts contain around 50 wt.% SiO_2, it is reasonable to assume that the more evolved Layered Series parental magma contain > 50 wt.% SiO_2. The exact SiO_2 content in the parental magma is hard to quantify, but some insight can be gained from SiO_2 contents in the type B Coubran basalt (~50 wt.%). Geochemical modeling results show that the Layered Series parental magma likely has a similar composition with F=0.55 melt of the type B Coubran basalts (after fractionation of 65% olivine and 35% clinopyroxene). The F=0.55 melt of the type B Coubran basalts contains around 55 wt. % SiO_2 (partition coefficients used are: D_{Si}^{Ol}=0.77 (Beattie, 1994), D_{Si}^{Cpx}=1.11 (Vanwestrenen et al., 2000), and D_{Si}^{Pl}=0.9 (Bindeman and Davis, 2000)), this value may be close to SiO_2 content in the Layered Series parental magma. Apparently, a magma with 55 wt.% SiO_2 is nearly not basaltic (45-55 wt.% SiO_2 by the definition) and the later fractionated melts will tend to be andesitic or even syenitic. Under this condition, the orthoclase is possible to be on liquidus particularly in the later melts. If this is correct, it means that there might be a link between genesis of the Layered Series and the syenites during fractional crystallization of the basaltic magma at the Coldwell Alkaline Complex. This is a testable hypothesis and more work is needed to proof this, but at least we observed syenitic interstitial liquids in the Two Duck Lake gabbro at the Marathon deposit and also Mitchell et al. (1992) have ascribed the genesis of the syenites at the Coldwell Alkaline Complex to be the extensive fractional crystallization of mantle-derived basalt magma within the plutonic infrastructure of the complex.

5.9.3 Why is the Layered Series PGE barren?

As mentioned above, all known PGE mineralization at the Eastern Gabbro is solely related to the Marathon Series whereas the Layered Series lacks PGE mineralization (<0.005 ppm PGE). The Layered Series gabbro was proposed by Shaw (1997) to crystallize from an evolved, Fe-rich magma, its parental magma thus may be the result of a low degree partial melting of upper mantle (Mungall and Naldrett, 2008). Given this hypothesis, it is reasonable to assume that most of refractory sulfides that are main hosts to PGE elements were retained in the mantle, thus resulted in the poor PGE contents in the generated magma. However, as interpreted in section 5.9.1, the Layered Series magma, although is highly fractionated indeed, share some characteristics with magma that is compositionally similar with the type B Coubran basalts. The origin of the Coubran basalts is poorly constrained due to its very unusual geochemical composition, but there is geochemical evidence, *e.g.*, similar Ce/Y and Nb/Zr trends, suggesting that the Coubran basalts are co-genetic with the Marathon Series Two Duck Lake gabbro (Cundari, 2012). Thus, it is more reasonable to assume that the PGE-poor nature of the Layered Series magma is not related to the source. Alternatively, it is more likely related to processes during magma evolution.

Sulfide saturation prior to the generation of the Layered Series units is another hypothesis to explain the lack of PGE mineralization in the Layered Series. Due to high partition coefficients of PGE elements into sulfide minerals, this earlier sulfide saturation will inevitably drive the residual magma to become PGE depleted. Modeling variations of sulfur contents in residual liquids is a direct way to assess the potential sulfide saturation. Unfortunately, the sulfur contents of the Coubran basalts are not known, and thus sulfur saturation cannot be modelled. However, this process can be envisaged given that the Layered Series parental magma is more evolved than the Coubran basalts, but the former contains lower PGE (<0.005 ppm PGE) than the latter (0.01 ppm Pt and 0.01 ppm Pd). Furthermore, two Cu-rich

mineralization zones located at the top and bottom of bore hole FD-13-34 at Four Dams were described in Chapter 3. The top mineralization zone is within the Layered Series and lacks PGE mineralization (~2000 ppm Cu and <0.005 ppm PGE) whereas the bottom mineralization zone is within the Marathon Series and is relatively PGE-enriched (~2800 ppm Cu, 0.1 ppm Pt, and 0.18 ppm Pd). Note that the inspection of drill cores at Four Dams shows that the top Cu-rich and PGE-barren mineralization zone extents along strike for several hundred meters. The extremely high Cu/Pd for the top sulfide mineralization zone is a good indicative of PGE depletion as a result of earlier sulfide saturation. In addition, as will be explained below, the Layered Series magma may have undergone an undercooling process. The undercooling is favorable for inducing the separation of an immiscible sulfide melt through lowering down the sulfur solubility in the silicate magma (Li et al, 2001). Therefore, it is reasonable to assume that an earlier event of sulfide segregation occurred prior to the development of the Layered Series gabbro, which is responsible for the lacking PGE mineralization in the Layered Series. A similar example of sulfide segregation in the Midcontinent rift system is related to the Sonju Lake Intrusion (SLI) of the Duluth Complex, as proposed earlier by Miller (1999) and later confirmed by Li and Ripley (2005), the SLI intrusion reached sulfide saturation when magnetite joins plagioclase and clinopyroxene as a liquidus phase before ~60% fractional crystallization.

5.9.4 Evidence for multiple intrusions

5.9.4.1 Insights from the olivine-clinopyroxene Fe/Mg disequilibrium

Figure 5-15 shows that the olivine and clinopyroxene in the units at Area 41 and Four Dams have variable Fe/Mg exchange coefficients, similar to observations of Good (1992) for the Two Duck Lake gabbro at the Marathon deposit. The variable Fe/Mg exchange coefficient is not consistent with what is expected for this coefficient (constant) when olivine and clinopyroxene are in chemical equilibrium during magma fractionation at a certain temperature, reflecting something unusual happened that interfered the chemical equilibrium between the two phases. There

are also other evidence suggesting this disequilibrium, including: 1) the resorption of olivine by clinopyroxene (Fig. 5-4C); and, 2) the disparity between variation ranges of Mg#s of olivine and clinopyroxene particularly for the units at Area 41 (Fig. 5-9). Further, the units at Area 41 and Four Dams present different down-hole trends in olivine-clinopyroxene Fe/Mg exchange coefficients, suggesting that different processes occurred for the Layered Series magma at the two areas.

Good (1992) related the deflection of olivine-clinopyroxene Fe/Mg exchange at the base of the Two Duck Lake gabbro to the migration of partial melt and stratigraphically higher up in the intrusion to the collection of residual interstitial melt (granophyre). This, however, may not apply to the disequilibrium in this case because: 1) granophyric textures are never observed in the Layered Series units in this study; and, 2) tight ranges of whole-rock La and Zr (80-110 ppm La, 70-100 ppm Zr, Figs. 5-6 and 7) suggest that units contain similar amounts of interstitial melts. Two alternatives are proposed here. First, the olivine-clinopyroxene Fe/Mg disequilibrium can be a result of the mixing of olivine and clinopyroxene crystals from magma at different stages of evolution. This can occur in a dynamic magma chamber which was replenished by pulses of magma intrusions. Under this circumstance, early formed crystals were easily disturbed by the inflowing magmas, particularly when they were gravitationally unstable and underwent a slumping process. Second, Latypov (2015) suggested that the magma undercooling can result in the chemical disequilibrium between mineral phases. Loucks (1996a) also suggested that the cooling would result in short- range diffusive exchange and alter Mg#s of olivine and clinopyroxene to different extents, i.e., greater for olivine. If this is the case, then different Fe/Mg down-hole profiles between the units at Area 41 and Four Dams imply that they had undergone undercooling but in different manners at the two areas. Since the Fe/Mg exchange between olivine and clinopyroxene is inversely related to the magma temperature (Loucks, 1996a, b), the up-hole increase in the olivine-clinopyroxene exchange coefficient for the units at

Area 41 can be explained by an increase in the extent of magma undercooling. Conversely, the trend for the units at Four Dams can be attributed to a decrease in the degree of magma undercooling. It is, however, difficult to imagine that the two styles of magma undercooling can occur for a single magma intrusion en route. Instead, it is more likely associated with a magma conduit system where inflowing melts underwent different degrees of undercooling when passing through the conduit. Therefore, no matter under which scenario, the olivine-clinopyroxene Fe/Mg disequilibrium indicates a dynamic magma conduit system whereby the Layered Series formed by multiple intrusions. This is also consistent with the observed down-hole step-like/zig-zag variations in incompatible elements and ratios for the Layered Series at Area 41 and Four Dams (Figs. 5-6 and 7).

5.9.4.2 Insights from La/Sm and Gd/Yb

As mentioned in section 5.5.1, the olivine gabbro at Four Dams can be subdivided into four subgroups (olivine gabbro I-IV). Each sub unit has different values and down-hole variations of La/Sm and Gd/Yb. Since the REE are controlled to some extent by apatite, and partitioning of Sm and Gd into apatite is greater than for La and Yb, respectively (Paster et al., 1974), it is expected that La/Sm should increase whereas Gd/Yb should decrease with increasing apatite. However, this is not the case here because P_2O_5 in these sub units are nearly constant (Fig. 5-6), thus their systematic and clearly defined fluctuations of La/Sm and Gd/Yb must be a result of multiple intrusions with slightly different magma compositions, regardless of the amount of interstitial melt.

5.9.5 Magma reversal trends

The Mg#s of olivine and clinopyroxene, and the anorthite content of plagioclase grains in the Layered Series units at Area 41, decrease slightly with depth from beginning down to ~ 10m, generally become increasingly primitive downward (Fig. 5-7), suggesting a normal mineral compositional trend, except at the top of the hole. It is thus surprising that whole-rock incompatible elements such as La and Zr also generally increase with depth, and also there is a positive correlation between Mg#

of olivine and whole-rock La (Fig. 5-22). This is contradictory to what is expected for fractional crystallization, *i.e.*, the whole-rock La and Zr trends for the Layered Series at Area 41 are reversed. Therefore, the Layered Series at Area 41 is characterized by the normal fractionation in mineral chemistry and the reverse differentiation in whole-rock trace elements.

The Layered Series units from Four Dams show significantly different profiles with those from Area 41. Specifically, the upper oxide augite melatroctolite has nearly constant mineral chemical compositions and highly variable whole-rock compositions. The olivine gabbro can be subdivided into four subgroups. Each individual subgroup has a reverse trend in La, Zr (Fig. 5-6), and based on the general variation scheme of mineral chemistry, it also likely has a reverse mineral compositional trend that cannot be fully resolved by the current sampling density. The bottom oxide augite melatroctolite presents a reverse trend in whole-rock La. Since the oxide augite melatroctolite and the olivine gabbro essentially are the same unit, and here only the olivine gabbro package presents well developed magma reversal trends in both whole-rock and mineral chemical compositions, we thus focused on the olivine gabbro package to interpret the magma evolution at Four Dams.

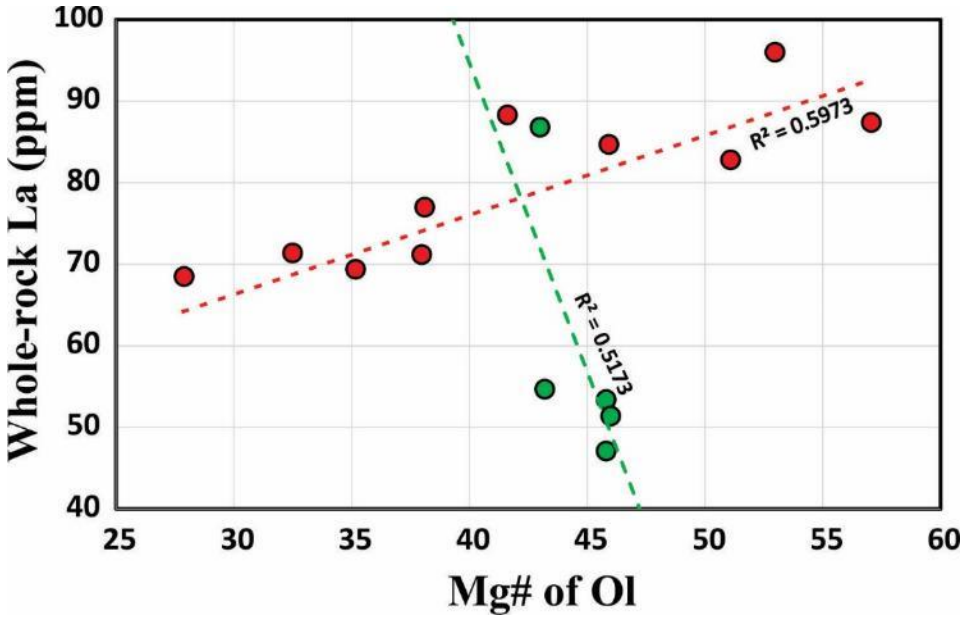

Figure 5-22. Relationship between Mg# of olivine and whole-rock La for olivine gabbro from Area 41 (red) and Four Dams (green). Note that the olivine gabbro at Four Dams does not necessarily have a negative trend and could also be considered as clusters. The important point is that the trend is clearly different than that for Area 41.

Shaw (1997) also observed both the normal and reverse mineral compositional trends in the Layered Series of Bamoos and Highway traverses (Figure 5-1) and suggested that its origin was uncertain, but might be related to either a trapped liquid effect, the assimilation of Archean footwall rocks, or the successive injections of more primitive magma. Reverse compositional trends are commonly observed in silicate layers in layered intrusions (Eales et al., 1990). Notable examples include the Insizwa complex of Transkei (Lightfoot and Naldrett, 1984), Duluth Complex of Minnesota (Miller and Ripley, 1996), and Fongen-Hyllingen intrusion of Norway (Egorova and Latypov, 2012b). Many different mechanisms have been proposed to explain compositional magma reversals, but none of them provide an entirely satisfactory explanation. Latypov (2015) comprehensively reviewed the current models for two types of reverse compositional profiles including coupled whole-rock and mineral compositional trends and decoupled whole-rock and mineral compositional trends, both of which are observed in this study, *e.g.*, the decoupled magma reversal at Area 41 and the coupled magma reversal at Four Dams.

A decoupled trend is where the whole-rock trend is reversed but the mineral compositional trend is normal. Latypov (2015) attribute this to an upward decrease in the amount of trapped melt in the rocks. As a result, rocks tend to contain decreasing abundances of incompatible elements upward, whereas their mineral compositional variations may still behave in a normal trend. However, this hypothesis cannot explain the decoupled magma reverse for the Layered Series units at Area 41 because all samples contain similar amounts of interstitial liquids based on their tight ranges of La and Zr abundances (Fig. 5-7). Thus, an alternative process must have resulted in the decoupled trends at this location. To investigate this, geochemical model of La vs. Zr for a subset of samples at Area 41 that have both whole-rock and mineral chemical analyses was created (Fig. 5-23). In addition, Mg# of olivine for these samples is indicated in this model for comparisons. It shows that the more primitive rocks trapped the more evolved liquids. This is not consistent with the classical fractional crystallization model, and may indicate that the interstitial liquid system was completely overturned. If this is correct, it means that the fractionated cumulate piles have trapped other stages of interstitial liquids and there is no chemical equilibrium established between the two. Perhaps the observed local resorption of plagioclase by biotite in Area 41 olivine gabbro (Fig. 5-4D) reflects this disequilibrium. The convection of interstitial liquids can be resulted by numerous factors including thermal convection (Turner, 1979), gas-driven (Ruprecht et al., 2008), or compaction (McBirney, 1995; Mathez et al., 1997). For example, McBirney (1995) attributed the enrichment of the Upper Border Series of the Skaergaard Intrusion to the rise of compaction-released liquids from the floor. Since the Layered Series units were developed by multiple intrusions (see section 5.9.4), the overall normal mineral compositional trend for units at Area 41 may indicate that the successively replenished magma became increasingly fractionated. Note that the down-hole olivine-clinopyroxene trend at Area 41, as explained in 5.9.4.2, indicates the Layered Series magma at Area 41 may have undergone a gradual increase in the degree of magma undercooling. If this is correct, the

inflowing magma would become increasingly fractionated after passing through the conduit (Latypov, 2015). Alternatively, the normal mineral chemical trend can also be produced when the rate of magma recharge is lower than the rate of magma crystallization. Under this circumstance, the generic evolution of the magma chamber was largely dependent on fractionation of the earlier pulses of magma.

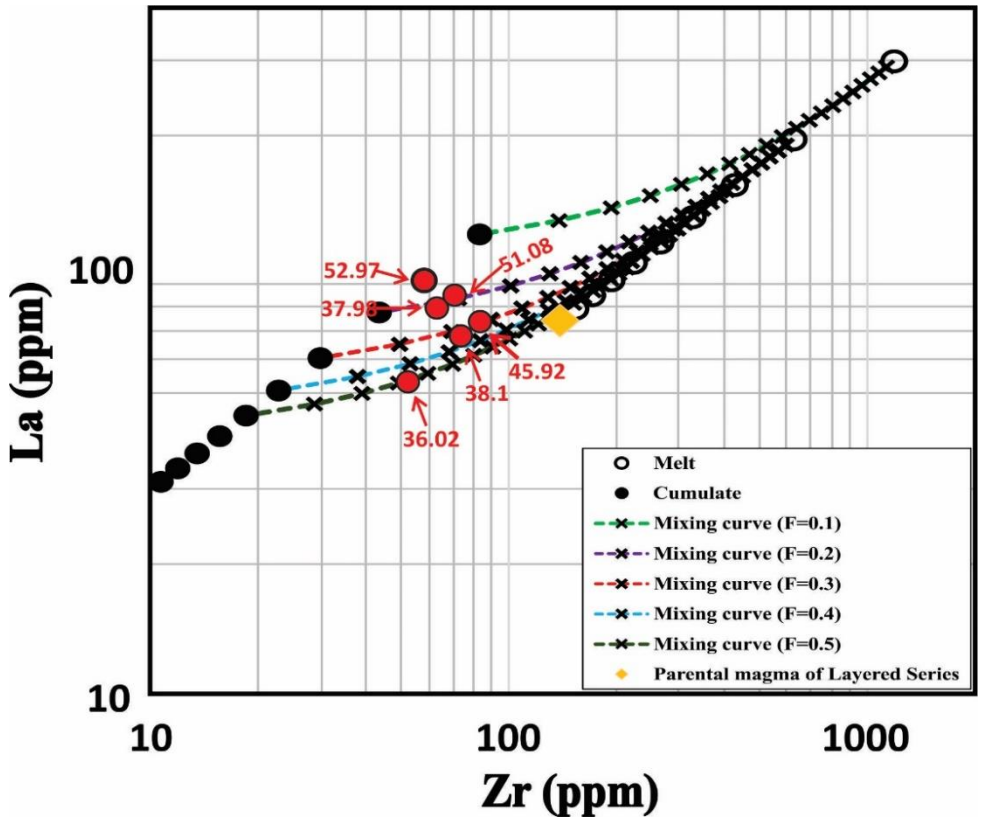

Figure 5-23. La vs. Zr model for a subset of the olivine gabbro (red infilled circles) from Area 41. Numbers beside each sample are Mg# of olivine. The observed Mg# do not match the predicted Mg# based on this model.

Since the units at Four Dams may have formed by multiple intrusions, one possible explanation to the coupled magma reversal (whole-rock compositions decrease upward and mineral chemical compositions increase upward) is related to successive injections of magma that is progressively more primitive. This is consistent with the scenario that the Layered Series magma at Four Dams underwent a gradual decrease in the degree of magma undercooling (see section 5.9.4.2) because: 1) decreasing the degree of undercooling will fractionate more primitive

minerals (Latypov, 2015); and, 2) this scenario implies that the conduit was increasingly heated, which can result in a gradual decrease in the degree of earlier fractional crystallization during magma flowing in the conduit. Note that the second reason also explains the whole-rock compositional reverse in this case. Another possible explanation to this coupled magma reversal is related to the rate of magma recharge and magma crystallization, i.e., the rate of magma recharge>the rate of magma crystallization. Under this circumstance, the preceding fractionated residual liquids will have progressively decreasing roles in dilution of later injected magma and the overall consequence is to make the chamber become increasingly condensed.

5.9.6 Evidence for crystal sorting

As first mentioned in section 5.5.2, the down-hole mineral chemical profiles and similar REE distribution patterns indicate that the olivine gabbro and oxide augite melatroctolite are the same unit. The differences in mineral abundances between the two units (particularly magnetite) are considered as a result of crystal sorting. This sorting process is supported by the experimental work of Forien et al. (2015) who demonstrated that during the slumping of semi-consolidated cumulates the smaller and dense magnetite tend to be separated from the larger and less dense plagioclase. In addition, there is other evidence suggesting a crystal sorting process occurred during the generation of the Layered Series. First, the observed chemical disequilibrium between olivine and clinopyroxene, as mentioned in section 5.9.4, can be explained by a crystal sorting process whereby olivine and clinopyroxene from different stages of crystallization were mixed up. Second, Figure 5-14 shows that the oxide augite melatroctolite contains slightly higher abundances of REE than olivine gabbro. This can be interpreted by: 1) oxide augite melatroctolite is more evolved than olivine gabbro; 2) oxide augite melatroctolite contains a higher proportion of interstitial melt; and, 3) oxide augite melatroctolite contains more apatite than olivine gabbro because REE is mainly controlled by apatite (Fig. 5-15A). The first two interpretations are easily ruled out because mineral chemical results (Fig. 5-9) shows that oxide augite melatroctolite has slightly higher Mg#s of

olivine and clinopyroxene than the olivine gabbro, and the similar ranges of Zr (Fig. 5-6) mean both units contain similar proportions of interstitial melts. Thus, this can only be explained by a high amount of apatite in the oxide augite melatroctolite. Realizing this is important because apatite is denser than plagioclase and will be sorted with clinopyroxene and olivine under the crystal sorting. Therefore, higher apatite and REE are consistent with mechanical sorting to form the oxide melatroctolite. In addition, this inference is more consistent with a model that has apatite as a cumulus phase, i.e., apatite does not crystalize in-situ.

5.9.7 Development of the Layered Series gabbro

It is possible to build a model to explain the observations as being the result of physical processes in a dynamic magma chamber. Based on characteristics of the Layered Series units and related interpretations, the development of the Layered Series gabbro is proposed to occur by multiple intrusions. Figure 5-24 illustrates the processes for formation of the Layered Series units, full details are given below.

Magma chambers at Four Dams and Area 41 were successively infilled by multiple pulses of the magma. The inflowing magma at Area 41 and Four Dams underwent some different processes. For example, at Area 41 the inflowing magma may either have progressively decreasing recharge rates, or have undergone a progressive increase in degrees of both magma undercooling and earlier fractional crystallization when it passed through the deep conduit. By contrast, at Four Dams the chamber was successively replenished by either progressively increasing amounts of magma, or by magma that underwent a gradual decrease in degrees of both magma undercooling and earlier fractional crystallization in the conduit. As interpreted in section 5.9.5, these provide explanations to the observed normal and reverse mineral compositional trends at Area 41 and Four Dams, respectively. When intruded magma cooled down from the walls of chambers at both areas, RFC governed the magma differentiation, which allowed crystals to be separated from the magma and the magma to evolve along the model curves. The crystallization

phases dominantly are plagioclase, olivine, and clinopyroxene, with minor amounts of apatite. Moreover, the compatible behavior for Ba for the Layered Series at Area 41 suggests that the magma at Area 41 also fractionated some orthoclase.

As the chamber was successively replenished and crystallization progressed, an increasing amount of crystalline materials were accumulated on the walls of the chamber. Gravity modeling (Mitchell et al., 1993) suggests that the eastern contact of the Eastern Gabbro is vertical to sub-vertical and generally shallows at depth. Our longitudinal sections (not shown) also indicate the contact of the Eastern Gabbro is nearly sub-vertical (>45°). Therefore, at some points crystal accumulations plus trapped liquids on the walls became gravitationally unstable and slumped down the chamber wall. This has also been proposed by Shaw (1997). The slumping of semi-consolidated cumulates allowed the creation of turbidity currents as well as the physical sorting of crystals by their densities and sizes. The consequences of this is the generation of two types of Layered Series units consisting of the olivine gabbro and oxide augite melatroctolite, as well as the development of scours, cross stratification and locally planar layering. After crystal slumping, the system was closed, the sorted crystal pile was compacted and the trapped liquids continued to cool and crystallized biotite and other interstitial minerals in situ. The final result is the formation of the Layered Series rocks as observed at the Eastern Gabbro.

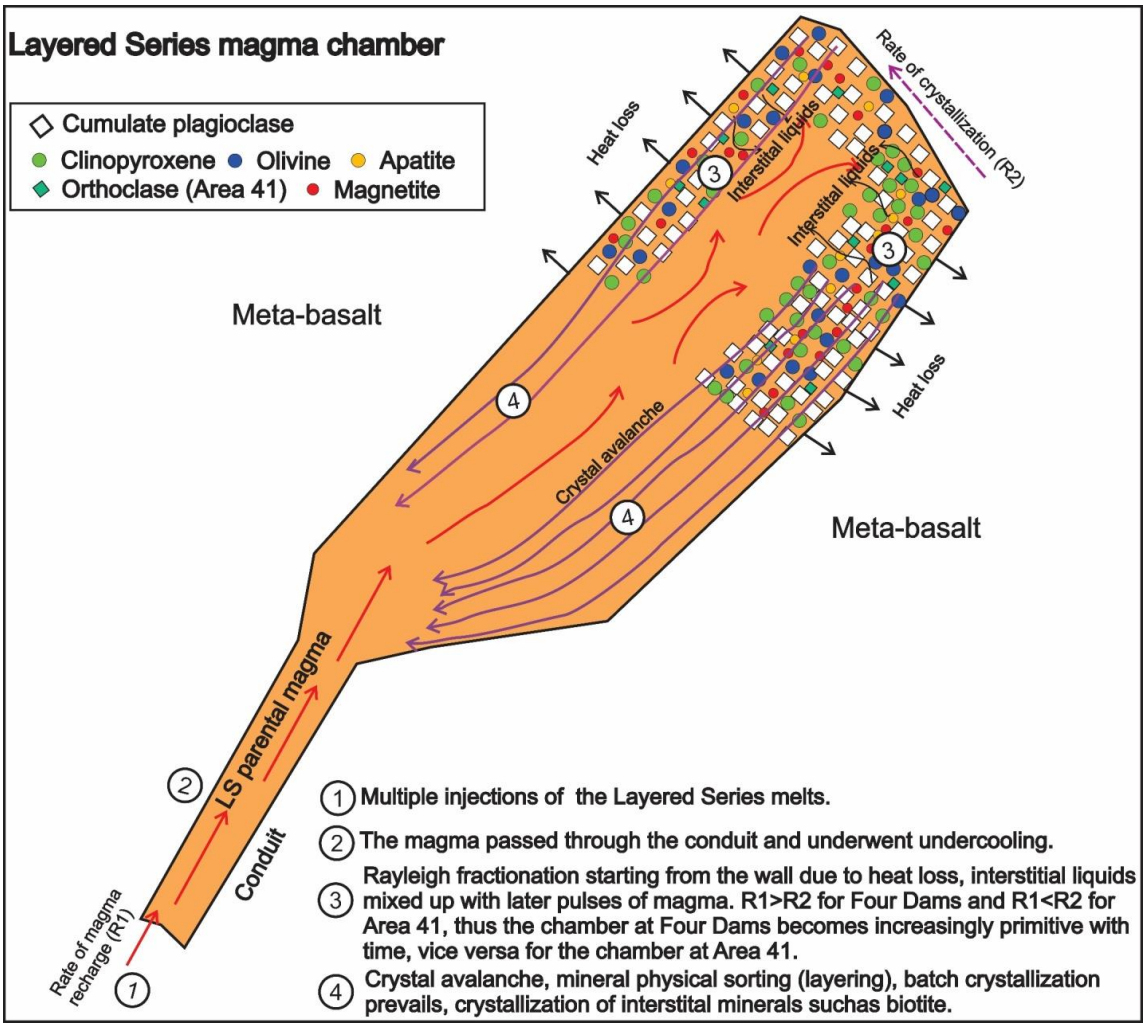

Figure 5-24. Schematic model showing the emplacement of the starting liquid for the Layered Series, the followed magma fractionation, crystal slumping, the development of the Layered Series rocks at Area 41 and Four Dams. See texts for full descriptions.

5.10 Conclusions

This contribution integrates petrography, whole-rock and mineral chemistry, geochemical modeling to comprehensively characterize the Layered Series at the Eastern Gabbro. Important conclusions are summarized as follows.

(1) The parental magma of the Layered Series units is not related to the Coubran basalts, but may share some characteristics with the type B Coubran basalt.

(2) The lack of PGE mineralization for the Layered Series is likely resulted by an early sulfide saturation.

(3) The Layered Series magma perhaps is no longer basaltic, and the late melt tends to be syenitic, which crystallized orthoclase on liquidus. This introduces a testable hypothesis regarding the potential connection between the genesis of the Layered Series and the syenites during fractionation of the basaltic magma.

(4) The geochemical magma reversal for the Layered Series at Area 41 is interpreted to be due to the convection of interstitial liquids. The coupled mineral and whole-rock compositional magma reversal for the Layered Series at Four Dams is interpreted to be related to multiple injections of magma that either has a progressively greater recharge rate, or underwent a gradual decrease in degrees of both magma undercooling and earlier fractional crystallization when the inflowing magma passed through the conduit.

(5) The Layered Series units formed by multiple intrusions within a conduit system. The crystallization of minerals was governed by Rayleigh fractional crystallization. The slumping of accumulated crystal piles on the walls of chambers generated the layering as well as the formation of olivine gabbro and oxide augite melatroctolite through a crystal physical sorting process.

5.11 References

Azzone R.G., Ruberti E., Enrich G.E.R., and Gomes C.B. 2009. Zr- and Ba-rich minerals from the Ponte Nova Alkaline mafic-ultramafic Massif, Southeastern Brazil: indication of an enriched mantle source. *The Canadian Mineralogist*, **47**, 1087-1103.

Beattie P. 1994. Systematics and energetics of trace-element partitioning between olivine and silicate melts: Implications for the nature of mineral/melt partitioning. *Chemical Geology*, **117**, 57-71.

Bedard J.H. 2001. Parental magmas of the Nain Plutonic Suite anorthosites and mafic cumulates: a trace element modelling approach. *Contributions to Mineralogy and Petrology*, **141**, 747-771.

Bennett N.R., Brenan J.M., and Koga K.T. 2014. The Solubility of platinum in silicate melt under reducing conditions: Results from experiments without metal inclusions. *Geochimical et Cosmochimical Acta*, **133**, 422-442.

Bindeman I. and Davis A. 2000. Trace element partitioning between plagioclase and melt: Investigation of dopant influence on partition behavior. *Geochimica et Cosmochimica Acta*, **64**, 2863-2878.

Blundy J.D. and Wood B.J. 1991. Crystal-chemical controls on the partitioning of Sr and Ba between plagioclase feldspar, silicate melts, and hydrothermal solutions. *Geochemica et Cosmochimica Acta*, **55**, 193-209.

Cundari R. 2012. Geology and geochemistry of Midcontinent Rift-related igneous rocks. Lakehead University M.Sc. thesis.

Dahl R., Watkinson D.H., and Taylor R.P. 2001. Geology of the Two Duck Lake intrusion and the Marathon Cu-PGE deposit, Coldwell Alkaline Complex, northern Ontario. *CIM Exploration and Mining Geology*, **10**, 51–65.

Deer W.A., Howie R.A., and Zussman, J. 2001. Rock-forming minerals. 4A. Framework silicates: Feldspars (2nd ed.). The Geological Society, London, U.K.

Dunn T. and Sen C. 1994. Mineral/Matrix Partition-Coefficients for OrthoPyroxene, Plagioclase, and Olivine in Basaltic to Andesitic Systems- a Combined Analytical and Experimental-Study. *Geochimica et Cosmochimica Acta*, **58(2)**, 717-733.

Eales, H. V., De Klerk, W. J. and Teigler, B. (1990). Evidence for magma mixing processes within the Critical and Lower Zones of the northwestern Bushveld Complex, South Africa. *Chemical Geology*, **88**, 261-278.

Egorova V. and Latypov R.M. 2012a. Processes operating during the initial stage of magma chamber evolution: Insights from marginal reversal of the Imandra layered intrusion, Russia. *Journal of petrology*, **53**, 3–26.

Egorova V. and Latypov R.M. 2012b. Prolonged magma emplacement as a mechanism for the origin of marginal reversal of the Fongen-Hyllingen layered intrusion, Norway. *Geological Magazine*, 53:1-18.

Forien M., Tremblay J., Barnes S.J., Burgisser A., and Page P. 2015. The role of viscous particle segregation in forming chromite layers from slumped crystal slurries: Insights from Analogue Experiments. *Journal of Petrology*, **56**, 2425-2444.

Fujimaki H., Tatsumoto M., and Aoki K.I. 1984. Partition coefficients of Hf, Zr, and REE between phenocrysts and groundmasses. *Journal of Geophysical Research*, **89**, 662-672.

Fujimaki H. 1986. Partition-Coefficients of Hf, Zr, and REE between Zircon, Apatite, and Liquid. *Contributions to Mineralogy and Petrology*, **94(1)**, 42-45.

Good D.J. and Crocket J.H. 1994. Genesis of the Marathon Cu-Platinum-Group Element Deposit, Port Coldwell Alkalic Complex: A Midcontinent Rife-related Magmatic Sulfide Deposit. *Economic Geology*, **89**, 131-149.

Good D. 1992. Genesis of the Marathon Cu-Platinum-Group Element Deposit, Port Coldwell Alkalic Complex, Ontario. Ph.D. thesis, McMaster University, 203 pp.

Good D.J., Epstein R., McLean K., Linnen R. L., and Samson I. 2015. Evolution of the Main Zone and the Marathon Cu-PGE Sulfide Deposit, Midcontinent Rift, Canada: Spatial Relationships in a Magma Conduit Setting. *Economic Geology*, **110**, 983-1008.

Grove T.L., Baker M.B., and Kinzler R.J. 1984. Coupled CaAl-NaSi diffusion in plagioclase feldspar: Experiments and application to cooling rate speedornetry. *Geochimica et Cosmochimica Acta*, **48**, 2113-2121.

Gunn B.M. 1996. Modal and element variation in Antarctic tholeiites. *Geochimica et Cosmochimica Acta*, **30**, 881-920.

Heaman L. M. and Machado N. 1992. Timing and origin of midcontinent rift alkaline magmatism, North America: evidence from the Coldwell Alkaline Complex. *Contributions to Mineralogy and Petrology*, **110**, 289-303

Heaman L.M., Easton M., Hart T.R., Hollings P., Macdonald C.A., and Smyk, M. 2007. Further refinement to the timing of Mesoproterozoic magmatism, Lake Nipigon region, Ontario. *Canadian Journal of Earth Sciences*, **44**, 1055-1086.

Irvine TN. (1980) Magmatic infiltration metasomatism, double diffusive fractional crystallization and adcumulus growth in the Muskox Intrusion and other layered intrusions. In: Hargraves RB (ed) Physics of magmatic processes. Princenton University press, Princenton, 325-383

Latypov R. 2015. Basal Reversals in Mafic sills and Layered intrusions. In: Layered Intrusions. Springer Publishing House.

Lemarchand F., Benoit V., and Calais, G. 1987. Trace element distribution coefficients in alkaline series. *Geochimica et Cosmochimica Acta*, **51**, 1071-1081.

Li C. and Ripley E.M. 2005. Empirical equations to predict the sulfur content of mafic magmas at sulfide saturation and applications to magmatic sulfide deposits. *Mineralium Deposita*, **40**, 218-230.

Lightfoot P.C. and Naldrett A.J. 1984. Chemical variation in the Insizwa complex, Transkei, and the nature of the parent magma. *The Canadian Mineralogist*, **22**, 111-123.

Loucks R.R. 1996a. Restoration of the elemental and stable-isotopic compositions of diffusionally altered minerals in slowly cooled rocks. *Contributions to Mineralogy and Petrology*, **123**, 346-358.

Loucks R.R. 1996b. A precise olivine-augite Mg-Fe-exchange geothermometer. *Contributions to Mineralogy and Petrology*, **125**, 140-150.

Mathez E.A., Hunter R.H., and Kinzler R. 1997. Petrologic evolution of partially molten cumulate: The Atok section of the Bushveld Complex. *Contributions to Mineralogy and Petrology*, **129**, 20-34.

McBirney A.R. 1995. Mechanisms of differentiation in the Skaergaard intrusion. *J Geol Soc London*, **152**, 421-435.

Miller J.D. and Ripley E.M. 1996. Layered intrusions of the Duluth Complex, Minnesota, USA. In: Cawthorn RG (eds.) Layered intrusions. Developments in petrology 15. Elsevier Science, B. V., 257–301

Miller J.D., Jr.1999. Geochemical evaluation of platinum group element (PGE) mineralization in the Sonju Lake Intrusion, Finland, Minnesota. Minnesota Geological Survey Information Circular, **44**, 32.

Miller J. and Nicholson S. 2013. Geology and mineral deposits of the 1.1Ga Midcontinent rift in the Lake Superior region-an overview: Cu-Ni-PGE Deposits of the Lake Superior Region. Precambrian Research Center Professional Workshop Series PRC WS-13-01.

Mungall J.E. and Naldrett A.J. 2008. Ore deposits of the Platinum-Group Elements. *Elements*, **4**, 253-258.

Naldrett A.J., Bray J.G., Gasparrini E.L., Podolsky T., and Rucklidge J.D. 1970. Cryptic variation and the petrology of the Sudbury nickel irruptive. *Economic Geology*, **65**, 122–155.

Neuman H., Mead J., and Vitaliano C.J. 1954. Trace element variations during fractional crystallization as calculated from the distribution law. *Geochimica et Cosmochimica Acta*, **6**, 90-101.

Nielsen R.L. 1992. BIGD: a FORTRAN program to calculate trace-element partition coefficients for natural mafic and intermediate composition magmas. *Computers and Geosciences*, **18**, 773-788.

Nielsen R.L., Gallahan W.E., and Newberger F. 1992. Experimentally determined mineral-melt partition coefficients for Sc, Y and REE for olivine, orthopyroxene, pigeonite, magnetite and ilmenite. *Contributions to Mineralogy and Petrology*, **110**, 488-499.

Okamoto, K. 1979. Geochemical study on magmatic differentiation of Asama Volcano, central Japan. *Journal of the Geological Society of Japan*, **85(8)**, 525-535.

Paster T.P., Schauwecker D.S., and Haskin L.A. 1974. The behavior of some trace elements during solidification of the Skaergaard layered series. *Geochimica et Cosmochimica Acta*, **38(10)**, 1549-1577.

Prowatke S. and Klemme S. 2006. Trace element partitioning between apatite and silicate melts. *Geochimica et Cosmochimica Acta*, **70**, 4513-4527.

Ruprecht P., Bergantz G.W., and Dufek J. 2008. Modeling of gas-driven magmatic overturn: Tracking of phenocryst dispersal and gathering during magma mixing. *Geochem. Geophys. Geosyst.*, **9**, 1-20.

Shaw C. (1997). The petrology of the layered gabbro intrusion, eastern gabbro, Coldwell alkaline complex, Northwestern Ontario, Canada: evidence from multiple phases of intrusion in a ring dike. *Lithos*, **40**, 243-259.

McDonough W.F. and Sun S.S. 1995. Composition of the Earth. *Chemical Geology*, **120**, 223-253.

Turner J.S. 1978. Double-diffusive intrusions into a density gradient. J. Geophys. Res. **83**, 2887-2901.

Wager L.R. and Brown G.M. 1968. Layered igneous rocks. Oliver and Boyd, Edinburgh, 588pp.

Vanwestrenen W., Blundy J., and Wood B. 2000. Effect of Fe^{2+} on garnet-melt trace element partitioning: experiments in FCMAS and quantification of crystal-chemical controls in natural systems. *Lithos*, **53**, 189-201.

Villemant B., Jaffrezic H., Joron J.L., and Treuil M. 1981. Distribution Coefficients of Major and Trace-Elements - Fractional Crystallization in the Alkali Basalt Series of Chaine-Des-Puys (Massif Central, France). *Geochimica et Cosmochimica Acta*, **45(11)**, 1997-2016.

Walker E.C., Sutcliff R.H., Shaw C.S.J., Shore G.T., and Penczak R.S. (1993). Precambrian geology of the Coldwell Alkaline Complex, Ontario Geological Survey, Open File Report 5868: 23pp.

Watkinson D.H., Whittaker P.J., and Jones P.L. 1983. Platinum group elements in the Eastern Gabbro, Coldwell Alkaline Complex, northwestern Ontario; in Geoscience Research Grant Program, Summary of Research 1982-1983, Ontario Geological Survey, Miscellaneous Paper, **96**, 183-191.

Wilkinson S. and Colvine A.C. 1978. Sulphide mineralization in the marginal phases of the Coldwell Alkaline Complex. *Ontario Geological Survey*, Misc. Paper, **82**, 210-215.

Zack T. and Brumm R. 1998. Ilmenite/liquid partition coefficients of 26 trace elements determined through ilmenite/clinopyroxene partitioning in garnet pyroxene. In: 7th International Kimberlite Conference. Gurney, J.J., Gurney, J.L., Pascoe, M.D. and Richardson, S.H. (eds.), Red Roof Design, Cape Town, 986-988.

Zhang M., Suddaby P., Thompson R.N., and Dungan, M.A. 1993a. The origins of contrasting zoning patterns in hyalophane from olivine leucitites, NE China. *Mineral magazine*, **57**, 565-573.

Chapter 6

Igneous stratigraphy and Cu-Pd mineralization at Area 41 within the Eastern Gabbro, Coldwell Alkaline Complex, Canada

Yonghua Cao[1], Robert Linnen[1], David Good[1], Iain Samson[2]

1. Western University, London, ON, Canada

2. The University of Windsor, Windsor, ON, Canada

6.1 Introduction

The Coldwell Alkaline Complex is an ideal site for studying PGE mineralization because: 1) it is host to several zones of PGE-enriched mineralization; 2) the geology of the Coldwell Alkaline Complex is well understood through decades of exploration and research; 3) a large database of over 40000 assays from over 750 drill holes is available for testing hypotheses and generating interpretations for this complex; and, 4) the igneous rocks of the complex are relatively unaltered and undeformed, offering a good opportunity to study the magmatic processes and associated mineralization. A general model for PGE exploration at the Coldwell Alkaline Complex is needed. A study of Area 41 and a comparison with the Marathon deposit to evaluate whether the different zones of mineralization are related will contribute to the development of this general model.

Area 41 is a zone of Cu-PGE mineralization, located approximately 18 km north-east of the Marathon Cu-Pd deposit, the largest deposit within the Coldwell Alkaline Complex. The Marathon deposit has been well characterized by studies of Good and Crocket (1994), Ruthart (2013), and Good et al. (2015). However, Area 41 has not received any studies since it was discovered in 2006. Generally, there are three questions that need to be tested in order to build a model for the origin of Cu-Pd

mineralization at Area 41 and investigate its relationship with the Marathon deposit. First, the Eastern Gabbro suite at the Marathon deposit involves three lithological and geochemically distinct series: the meta-basalt, the Layered Series, and the Marathon Series. The rock types of the Eastern Gabbro suite at Area 41 need to be established and compared to those at the Marathon deposit to evaluate whether the litho- and chemostratigraphy at Area 41 is similar to the Marathon deposit. Second, the Cu-Pd mineralization at the Marathon deposit is only hosted by the Marathon Series, it is unclear whether mineralization at Area 41 is also hosted solely by the Marathon Series. Third, the origin of PGE mineralization at the Marathon deposit has been attributed by Good et al. (2015) to be related to orthomagmatic processes in a conduit setting, it is unclear whether Area 41 is also a conduit system. Testing these three questions can help develop guidelines for continued mineral exploration at the Coldwell Alkaline Complex, particularly knowing whether Area 41 mineralization is conduit-related, which is favorable for high grade PGE deposits (Naldrett et al., 1995; Naldrett and Lightfoot, 1999).

In this study, drill core logging, petrography and lithogeochemistry are used to establish the igneous stratigraphy at Area 41. Stillwater Canada Inc. exploration assay data are used to identify platinum-group elements (PGE) mineralization horizons and investigate their relationships with the igneous stratigraphy. Platinum-group mineralogy (PGM) and the effects of any post-magmatic hydrothermal activity will be characterized. 3D modeling is then used to evaluate whether the depositional setting of the mineralization at Area 41 is similar to the Marathon deposit.

6.2 Sampling and analytical methods

Representative powdered samples and rock slabs were collected from 5 drill holes. These drill holes intersect a complete igneous sequence of the Eastern Gabbro Suite, including the meta-basalt, the Layered Series and the Marathon Series. Drilling parameters for these drill holes are listed in Table 6-1.

Table 6-1. Parameters of sampled drill holes at Area 41.

DDH Number	Azimuth	Collar	Total Depth/m
SL-13-32	19.61	-85.28	252
SL-13-34	19.56	-80	201
SL-13-36	22.07	-44.59	228
SL-13-37	20.42	-80	261
SL-13-41	18.36	-80.05	291

Powdered samples were collected by grinding 1 m long channels (approximately 2 mm wide and 1 cm deep) along the drill core using a Thermo Scientific portable grinder. Between every two samples there is a rough 4.5 m gap without grinding. All powdered samples were loaded into PREM-4331 XRF sample cups capped with 4-μm PREM-F2540 XRF sample cup films for pXRF whole-rock analysis first. The pXRF instrument used in this study is a Niton XL3t+ GOLDD+ pXRF analyzer that is equipped with a SDD, a high energy, and 50kV X-ray tube. Details of the analytical strategies and QA/QC control for pXRF analyses are given in Chapter 2, and the pXRF results are given in Table 6-2. A subset of representative powdered samples was selected after the inspection of pXRF results, which was then pulverized and sent to ALS Mineral Divisions in Thunder Bay for more accurate and precise lithogeochemical analysis. This analysis allows the evaluation of pXRF data quality, as well as the examination of rock forming mechanisms. Major elements were analyzed by lithium borate fusion with inductively coupled plasma (ICP)-atomic emission spectroscopy (AES) on a minimum 2 g of pulp samples. Trace elements were analyzed by lithium borate fusion and ICP-mass spectroscopy (MS) on 2 g of sample. Total S was analyzed using a Leco furnace on 1 g of sample. Ferrous Fe was analyzed by H_2SO_4-HF acid digestion and titration on 1 g of sample. Quality-control was conducted based on ALS Chemex quality-control procedures which involve analyses on a wide array of standards, blanks, and duplicates after each batch of samples. Average lab-based whole-rock major and trace element compositions for geologic units are summarized in Table 6-3. In addition, two

different data sets were also prepared, including Stillwater Canada Inc. exploration assays of Cu, S, Ni, Au, Pt, Pd down all included drill holes and 8 high precision S, Se, Pt, Pd, Au, Os, Ru, Ir, and Rh analyses down the PGE-enriched horizon in SL-13-36 (Table 6-4). The exploration assay data were determined on continuous 2 m sample intervals, and the other data set was collected from eight 2-m-thick, high-grade PGE intervals at drill hole SL-13-36. Both data sets were analyzed at ALS Thunder, Ontario, by fire assay and mass spectrometer finish (FAMS).

Polished thin sections representative of different gabbro units were prepared from selected drill holes at an interval between 5 and 20 meters. After petrographic examination, thin sections were carbon coated for mineral chemical analyses. Two sets of mineral chemical data were collected, including semi-quantitative and standardless analysis using benchtop scanning electron microscopy equipped with energy dispersive spectroscopy (bSEM-EDS) and standardized analysis using electron microprobe. The bSEM-EDS allows the acquisition of a large dataset that can be used for mapping igneous stratigraphy with low costs and high efficiency. The equipment used is a JEOL JCM-6000 Neoscope equipped with a JEOL JED-2300 energy dispersive X-ray analyzer at Western University. Analyses were conducted using 15 kV accelerating voltage, a high probe current, a 19 mm working distance, a 30-40 μm beam size, and standardless ZAF corrections. The analytical precision of bSEM-EDS analyses has been evaluated in Chapter 3, and bSEM-EDS results are given in Table 6-5. A subset of representative carbon-coated thin sections was chosen for electron microprobe analysis using a JEOL JXA-8530F field emission probe at Western University. The purpose of electron microprobe analysis is to validate of bSEM-EDS data quality, and acquire major and minor elemental compositions for minerals of interest (olivine, plagioclase, clinopyroxene, etc.). Analyses were conducted using a 15 kV, 20 nA beam. The beam was focused to a 1 μm spot for analyzing olivine and clinopyroxene, and to a 5 μm spot for analysing plagioclase. The peak counting time was 30 s for all elements and background

counts were a total of 30 s. A variety of synthetic and natural standards (Table 4-3 in Chapter 4) were used to calibrate different elements during probe analyses. The analytical precision for probe analyses has been evaluated in Chapter 3.

Table 6-2. pXRF analyses for mapped elements down two representative Area 41 drill holes. LOD means limit of detection.

Sample	Unit	Al_2O_3	$Fe_2O_3^T$	CaO	K_2O	P_2O_5	Ba	Zr	Sr
		wt. %	wt. %	wt. %	wt. %	wt. %	ppm	ppm	ppm
SL-13-32-5.5	Olivine gabbro	11.6	33.1	10.2	0.5	3.6	1049	37	724
SL-13-32-10	Olivine gabbro	13.4	24.8	11.8	0.5	2.7	1034	42	912
SL-13-32-12	Coarse-grained ophitic gabbro	16.6	15.7	12.2	0.7	2.1	1093	38	1228
SL-13-32-17	Coarse-grained ophitic gabbro	14.7	18.9	12.3	0.8	2.0	999	43	1033
SL-13-32-22	Coarse-grained ophitic gabbro	13.2	16.4	12.9	0.6	2.3	736	34	1005
SL-13-32-27	Coarse-grained ophitic gabbro	14.4	15.3	12.4	0.8	1.9	849	39	1042
SL-13-32-32	Coarse-grained ophitic gabbro	13.2	16.3	11.9	1.0	1.9	828	44	926
SL-13-32-37	Coarse-grained ophitic gabbro	14.4	16.1	12.1	0.7	2.2	725	74	1018
SL-13-32-42	Coarse-grained ophitic gabbro	12.8	22.9	11.8	0.5	2.5	708	51	823
SL-13-32-44	Oxide melatroctolite	9.5	30.8	14.7	0.3	5.8	559	39	698
SL-13-32-49	Oxide melatroctolite	10.8	22.2	14.3	0.4	3.9	446	44	743
SL-13-32-53	Coarse-grained ophitic gabbro	11.2	22.3	14.1	0.5	3.8	508	35	776
SL-13-32-58	Coarse-grained ophitic gabbro	10.4	25.7	13.3	0.4	3.2	582	46	716
SL-13-32-60.5	Oxide melatroctolite	10.7	28.7	12.9	0.6	4.9	604	47	700
SL-13-32-66.5	Oxide melatroctolite	10.3	23.0	15.8	0.4	5.9	592	29	819
SL-13-32-70	Pegmatitic ophitic gabbro	15.7	20.5	10.1	0.4	1.7	603	16	964
SL-13-32-75	Pegmatitic ophitic gabbro	14.5	14.8	9.9	0.6	0.6	636	18	957
SL-13-32-80	Pegmatitic ophitic gabbro	15.0	16.0	8.3	0.5	0.2	562	26	920
SL-13-32-85	Pegmatitic ophitic gabbro	12.3	23.2	9.0	0.8	2.5	743	44	716
SL-13-32-90	Pegmatitic ophitic gabbro	14.0	14.5	9.0	1.4	0.3	960	22	795
SL-13-32-150.5	Apatitic clinopyroxenite	10.3	18.9	12.7	1.0	2.5	1250	142	718
SL-13-32-155.5	Apatitic clinopyroxenite	15.5	12.7	10.5	1.3	1.3	1373	107	1096
SL-13-32-160.5	Apatitic clinopyroxenite	11.5	17.9	13.4	0.4	1.5	446	52	596
SL-13-32-165.5	Apatitic clinopyroxenite	8.6	15.6	15.5	0.3	1.5	232	43	471
SL-13-32-170	Apatitic clinopyroxenite	14.9	14.5	12.6	0.3	0.4	336	29	746
SL-13-32-175	Breccia (Marathon Series matrix)	8.5	19.4	15.3	0.3	0.9	351	59	415
SL-13-32-180	Breccia (Marathon Series matrix)	9.1	18.2	14.9	0.2	0.8	291	43	459
SL-13-32-185	Breccia (Marathon Series matrix)	9.2	17.3	14.9	0.4	2.9	417	42	616
SL-13-32-200	Apatitic clinopyroxenite	5.2	17.8	18.9	0.3	3.4	380	62	392
SL-13-32-204.5	Apatitic clinopyroxenite	5.0	19.4	17.4	0.5	4.2	476	71	439
SL-13-32-209	Apatitic clinopyroxenite	8.7	16.6	14.9	1.0	2.5	758	198	468
SL-13-32-214	Apatitic clinopyroxenite	5.8	27.2	16.1	0.2	3.1	288	60	364
SL-13-32-219.5	Apatitic clinopyroxenite	8.9	26.3	12.1	0.9	2.6	789	130	453

SL-13-32-224	Apatitic clinopyroxenite	9.7	21.0	14.2	0.9	2.5	675	90	679
SL-13-32-229.5	Apatitic clinopyroxenite	15.3	15.7	11.4	0.5	0.8	749	23	1262
SL-13-32-234	Apatitic clinopyroxenite	15.6	24.9	10.6	0.6	1.3	646	41	1579
SL-13-37-7.5	Oxide augite melatroctolite	8.2	31.1	11.8	0.8	2.4	1500	77	498
SL-13-37-11.5	Oxide augite melatroctolite	9.7	29.1	12.4	0.8	2.6	1698	77	634
SL-13-37-15.5	Oxide augite melatroctolite	8.9	32.5	11.8	0.8	3.0	1325	73	548
SL-13-37-19.5	Oxide augite melatroctolite	7.8	34.5	11.0	0.6	2.7	1149	64	403
SL-13-37-23.5	Oxide augite melatroctolite	8.5	38.5	10.8	0.5	3.2	1560	53	510
SL-13-37-28	Oxide augite melatroctolite	12.2	25.3	12.4	0.7	2.4	1574	68	818
SL-13-37-30.5	Olivine gabbro	14.5	23.9	12.2	0.7	2.5	1772	59	956
SL-13-37-33.5	Oxide augite melatroctolite	8.2	35.6	11.6	0.5	2.9	1677	60	464
SL-13-37-37.5	Oxide augite melatroctolite	10.0	32.0	11.8	0.6	2.9	1014	54	614
SL-13-37-41.5	Oxide augite melatroctolite	11.2	25.8	15.5	0.5	4.5	718	45	740
SL-13-37-43.1	Apatitic clinopyroxenite	10.7	13.6	5.8	2.1	0.4	<LOD	<LOD	503
SL-13-37-45.5	Coarse-grained ophitic gabbro	12.2	19.5	12.6	0.7	2.9	1077	51	875
SL-13-37-50.5	Coarse-grained ophitic gabbro	15.3	23.6	11.5	0.5	3.7	831	34	995
SL-13-37-52.7	Pegmatitic ophitic gabbro	13.8	17.8	13.8	0.8	2.0	1426	103	947
SL-13-37-54.5	Oxide melatroctolite	7.3	30.9	10.8	0.8	2.4	962	86	411
SL-13-37-57.5	Coarse-grained ophitic gabbro	11.6	22.9	14.5	0.4	3.8	621	43	862
SL-13-37-60.5	Coarse-grained ophitic gabbro	11.3	31.8	13.6	0.4	4.8	664	41	747
SL-13-37-63.5	Coarse-grained ophitic gabbro	11.8	25.1	14.9	0.4	3.3	641	50	727
SL-13-37-67.5	Pegmatitic ophitic gabbro	16.3	14.5	9.7	1.0	1.2	1595	65	984
SL-13-37-71.9	Pegmatitic ophitic gabbro	13.2	11.6	13.1	0.4	0.1	274	28	641
SL-13-37-79.5	Pegmatitic ophitic gabbro	11.9	20.4	14.3	0.5	3.0	622	43	885
SL-13-37-81.5	Pegmatitic ophitic gabbro	12.8	22.2	10.1	0.5	2.1	570	31	687
SL-13-37-85.5	Pegmatitic ophitic gabbro	13.7	18.8	12.7	0.5	2.1	768	47	877
SL-13-37-92.5	Pegmatitic ophitic gabbro	12.8	14.5	11.6	0.4	0.1	294	30	534
SL-13-37-96.5	Feldspathic clinopyroxenite	10.7	18.1	10.8	0.5	0.1	265	30	372
SL-13-37-103.5	Feldspathic clinopyroxenite	7.5	22.6	11.5	0.1	0.1	172	38	258
SL-13-37-107.5	Feldspathic clinopyroxenite	7.0	22.1	11.0	0.2	0.1	172	35	221
SL-13-37-111.5	Feldspathic clinopyroxenite	6.1	22.3	11.2	0.1	0.0	151	35	211
SL-13-37-115.5	Pegmatitic ophitic gabbro	9.7	19.4	10.5	0.3	0.1	310	32	363
SL-13-37-117.5	Apatitic clinopyroxenite	4.8	19.0	13.0	0.1	0.0	186	36	208
SL-13-37-119.5	Feldspathic clinopyroxenite	5.5	24.3	10.6	0.1	0.1	157	29	213
SL-13-37-123.6	Pegmatitic ophitic gabbro	11.7	16.0	13.7	0.2	0.1	137	28	585
SL-13-37-128.5	Apatitic clinopyroxenite	6.0	21.7	10.6	0.1	0.3	183	39	372
SL-13-37-132.5	Apatitic clinopyroxenite	5.9	21.1	10.8	0.0	0.3	159	42	392
SL-13-37-136.5	Apatitic clinopyroxenite	4.8	22.2	10.7	0.0	0.2	99	38	319
SL-13-37-140.5	Apatitic clinopyroxenite	5.1	21.1	11.1	0.0	0.3	101	48	301
SL-13-37-144.8	Apatitic clinopyroxenite	5.1	24.7	10.3	0.1	0.1	127	29	228
SL-13-37-148.8	Apatitic clinopyroxenite	6.0	19.3	9.7	0.1	0.1	125	29	322
SL-13-37-152.5	Apatitic clinopyroxenite	4.0	23.2	8.3	0.1	0.1	125	22	164
SL-13-37-157.5	Medium-grained ophitic gabbro	18.1	9.8	10.3	0.6	0.1	475	14	1255

SL-13-37-161.5	Medium-grained ophitic gabbro	20.5	14.4	10.8	0.4	0.1	333	20	1417
SL-13-37-165.5	Medium-grained ophitic gabbro	19.0	15.4	9.7	0.5	0.1	356	15	1840
SL-13-37-169.5	Coarse-grained ophitic gabbro	15.6	27.0	11.3	0.6	2.1	583	78	788
SL-13-37-174.5	Medium-grained ophitic gabbro	17.5	13.1	11.1	0.5	0.2	363	20	1725
SL-13-37-178.5	Apatitic clinopyroxenite	7.8	25.5	15.8	0.2	1.9	192	39	501
SL-13-37-183.5	Medium-grained ophitic gabbro	17.9	12.5	10.4	0.4	0.4	321	17	1695
SL-13-37-187.5	Medium-grained ophitic gabbro	15.8	7.0	7.7	0.4	0.3	411	<LOD	2325
SL-13-37-191.5	Medium-grained ophitic gabbro	15.6	6.0	7.4	0.5	0.4	518	9	2160
SL-13-37-195.5	Medium-grained ophitic gabbro	15.7	7.1	7.3	0.4	0.4	523	<LOD	2039
SL-13-37-199.5	Medium-grained ophitic gabbro	16.3	7.1	6.9	0.6	0.4	546	10	2126
SL-13-37-203.5	Medium-grained ophitic gabbro	16.5	7.1	6.8	0.6	0.3	564	18	2082
SL-13-37-207.5	Medium-grained ophitic gabbro	15.8	5.8	7.0	0.6	0.4	523	13	2153
SL-13-37-211.5	Medium-grained ophitic gabbro	15.1	4.2	6.5	0.7	0.3	567	23	2089
SL-13-37-225.5	Coarse-grained ophitic gabbro	16.3	22.7	10.2	1.1	1.2	587	90	912
SL-13-37-227.5	Medium-grained ophitic gabbro	17.1	11.3	9.5	0.6	0.6	515	49	1462

Table 6-3. Average major and trace element compositions for geological units determined in this study. Number in parentheses represents number of samples analyzed for each unit; SD= 1 σ standard deviation for sample set.

Rock Series		Meta-basalt		Layered Series				Marathon Series					
Unit		Feldspathic clinopyroxenite (6)		Olivine gabbro (11)		Oxide augite melatroctolite (12)		Ophitic gabbro (13)		Apatitic (olivine) clinopyroxenite (7)		Oxide melatroctolite (7)	
		Avg	SD	Avg	SD.	Avg	SD.	Avg	SD	Avg	SD.	Avg	SD
SiO_2	wt %	41.3	1.51	39.0	5.68	34.9	7.42	40.8	5.65	41.0	6.06	29.1	8.58
Al_2O_3		5.9	0.96	12.1	4.11	9.7	3.63	15.1	2.82	9.0	4.82	8.9	3.11
Fe_2O_3		19.5	1.96	21.2	7.17	26.6	9.31	16.8	4.94	20.6	8.84	27.5	8.31
FeO*		13.6	0.63	14.1	4.67	17.4	6.38	10.4	3.72	13.9	6.15	13.6	
CaO		10.9	0.94	11.3	1.12	10.5	1.28	12.1	1.55	11.1	3.81	13.9	1.33
MgO		17.7	1.34	6.0	2.35	6.6	2.14	5.3	1.31	12.1	4.94	6.9	0.67
Na_2O		0.7	0.13	2.3	0.94	1.8	0.85	2.7	0.97	1.3	0.82	1.4	0.61
K_2O		0.1	0.05	1.0	0.35	1.0	0.51	0.6	0.19	0.4	0.38	0.6	0.23
TiO_2		1.6	1.20	3.5	1.21	4.6	1.79	1.9	0.91	1.3	1.05	3.7	1.53
MnO		0.3	0.02	0.3	0.07	0.4	0.07	0.2	0.05	0.3	0.10	0.3	0.06
P_2O_5		0.1	0.10	2.5	1.03	2.6	0.78	2.6	1.67	0.9	1.05	5.9	2.47
Total		98.1		99.1		98.6		98.1		98.0		98.2	
S		0.1	0.04	0.2	0.12	0.3	0.12	0.7	0.57	0.7	0.47	0.9	0.62
Ba	ppm	78	43.6	3226	1478	2820	1858	840	402	400	310	880	388
Ce		19	4.1	191	27.1	180	30.7	123	59.8	59	57.4	258	79.5
Cr		1372	198.9	51	56.5	26	24.5	78	57	225	214.7	23	29.8
Cs		0.5	0.36	1.1	1.01	1.5	0.91	1.3	1.15	0.9	0.39	1.6	1.35
Dy		3	1.1	7	1.1	7	1.0	5	1.9	3	1.9	10	3.1
Er		1	0.4	3	0.4	3	0.4	2	0.7	2	0.9	4	1.3
Eu		1	0.5	5	0.4	6	0.3	3	1.3	2	1.0	6	1.7
Ga		10	2.9	15	0.7	15	1.8	16	2.3	11	4.0	17	2.2
Gd		4	1.4	12	2.0	12	2.0	8	3.7	5	3.3	18	6.3
Hf		1	0.4	2	0.4	2	0.4	1	0.3	1	0.6	1	0.4
Ho		0.5	0.18	1.3	0.20	1.2	0.18	0.9	0.33	0.6	0.36	1.8	0.56

La	7	1.2	83	11.3	78	12.1	54	24.6	25	25.4	112	33.8
Lu	0.2	0.02	0.4	0.04	0.3	0.03	0.2	0.06	0.2	0.10	0.4	0.11
Nb	4	1.4	31	7.6	31	7.4	15	4.8	10	12.4	23	5.5
Nd	15	5.0	93	15.6	94	15.2	63	31.1	32	27.3	142.	48.3
Pr	3	0.8	23	3.5	22	3.7	15	7.4	8	6.8	34	11.1
Rb	3	2.8	18	5.7	20	11.6	15	9.2	11	9.1	17	12.4
Sm	4	1.5	16	2.7	16	2.5	11	5.0	6	4.5	24	8.1
Sn	3	1.8	4	1.6	15	10.2	6	6.4	10	10.6	9	5.2
Sr	255	87.0	1144	488.6	829	382.9	1109	466.5	445	267.2	708	177.2
Ta	0.2	0.12	1.4	0.34	1.4	0.31	0.6	0.19	0.4	0.53	1.0	0.27
Tb	0.5	0.21	1.4	0.23	1.4	0.23	1.0	0.41	0.6	0.40	2.1	0.68
Th	0.3	0.15	2.9	0.62	2.8	0.99	1.6	0.77	1.0	1.04	2.9	0.78
Tm	0.2	0.04	0.4	0.06	0.4	0.04	0.3	0.08	0.2	0.12	0.5	0.15
U	0.1	0.04	0.9	0.20	0.8	0.29	0.5	0.22	0.3	0.29	0.9	0.25
V	400	105.1	320	155.7	390	313.3	432	221.3	425	229.5	725	340.0
Y	13	3.9	35	5.3	33	4.8	24	9.5	17	10.0	49	14.5
Yb	1	0.1	2	0.3	2	0.2	2	0.5	1	0.7	3	0.6
Zr	28	7.7	74	18.6	66	16.1	40	13.6	36	23.5	59	18.2
Cu	250	155.5	130	76.7	360	430.7	1547	1270.2	2024	1405.3	1680	630.8
Ni	670	232.8	33	41.1	51	59.1	130	62.4	276	90.1	135	64.9
Sc	40	5.9	36	11.7	36	7.1	21	7.3	36	18.5	22	5.8

Table 6-4. Analytical results of complete PGE, Au, S, and Se for a suite of PGE-enriched samples in SL-13-36. The unit is pegmatitic ophitic gabbro.

DDH	Avg. depth/m	S	Se	Pt	Pd	Cu	Au	Os	Ru	Ir	Rh
		%	ppm	ppm	ppm	ppm	ppm	ppm	ppm	ppm	ppm
SL-13-36	47	0.58	3.1	0.25	0.57	1265	0.011	<0.01	<0.05	0.002	0.032
	53	0.17	1.8	0.79	1.2	1260	0.22	<0.01	<0.05	0.003	0.039
	57	0.21	2.7	1.6	1.9	1815	0.32	<0.01	<0.05	0.006	0.1
	61	0.26	2.5	0.45	0.97	1830	0.38	<0.01	<0.05	0.003	0.035
	65	0.24	1.8	0.16	0.42	1445	0.05	<0.01	<0.05	0.001	0.012
	69	0.2	1.3	0.41	0.78	948	0.072	<0.01	<0.05	0.002	0.026
	73	0.27	1.8	0.3	0.79	1770	0.19	<0.01	<0.05	0.002	0.022
	79	0.54	4.7	0.3	0.66	3690	0.16	<0.01	<0.05	0.002	0.024

Table 6-5. bSEM-EDS analyses down two representative Area 41 drill holes. SD means 1 σ sample error. N/A means the analysis is not available; this happens when the sample does not contain any olivine and/or clinopyroxene.

DDH	Depth/m	Rock unit	Mg# of olivine				Mg# of clinopyroxene			
			Min	Max	Avg.	SD	Min.	Max.	Avg.	SD
SL-13-32	5.9	Olivine gabbro	61.5	65.0	62.8	0.90	75.6	79.1	77.0	1.00
	10.7	Olivine gabbro	61.5	64.1	62.8	0.90	76.6	79.5	77.9	0.80
	17.5	Coarse grained ophitic gabbro	57.5	61.3	59.9	1.60	73.3	76.6	74.5	0.80
	22.9	Coarse grained ophitic gabbro	64.0	69.0	65.8	1.40	73.9	78.1	75.4	1.10
	27.1	Coarse grained ophitic gabbro	61.5	70.2	66.0	2.60	73.6	81.4	77.6	2.60
	32.2	Coarse grained ophitic gabbro	N/A	N/A	N/A	N/A	76.1	80.5	78.5	1.20
	37	Coarse grained ophitic gabbro	54.9	62.4	58.2	2.30	70.8	75.7	74.3	1.30
	42.3	Coarse grained ophitic gabbro	59.0	61.9	60.8	0.90	72.3	77.0	74.8	1.30
	44	Oxide melatroctolie	65.3	69.1	67.5	1.20	N/A	N/A	N/A	N/A
	49.3	Oxide melatroctolie	59.0	62.1	60.8	0.70	73.3	78.4	76.2	1.30
	58.5	Coarse grained ophitic gabbro	66.5	68.7	67.6	0.60	78.4	83.6	80.8	1.50
	61.2	Oxide melatroctolie	64.5	70.6	68.2	2.00	N/A	N/A	N/A	N/A
	75.8	Pegmatitic ophitic gabbro	N/A	N/A	N/A	N/A	73.0	80.7	78.9	1.80
	80.5	Pegmatitic ophitic gabbro	62.8	69.8	66.2	2.00	75.2	80.7	77.9	1.90
	90.6	Pegmatitic ophitic gabbro	N/A	N/A	N/A	N/A	72.8	81.3	76.9	2.50
	150.5	Apatitic clinopyroxenite	N/A	N/A	N/A	N/A	63.4	66.7	65.0	1.00
	156.1	Apatitic clinopyroxenite	N/A	N/A	N/A	N/A	69.6	73.2	71.7	0.90
	161	Apatitic clinopyroxenite	60.4	65.2	61.7	1.20	73.6	77.0	75.6	1.00
	165.5	Apatitic clinopyroxenite	53.7	54.9	54.3	0.30	69.9	73.0	71.3	0.80
	170.6	Apatitic clinopyroxenite	61.3	63.2	62.1	0.40	72.2	76.6	74.8	1.30
	200.6	Apatitic clinopyroxenite	42.9	44.6	43.7	0.70	66.4	69.0	67.7	0.70
	204.5	Apatitic clinopyroxenite	N/A	N/A	N/A	N/A	67.0	70.2	68.6	1.10
	209.2	Apatitic clinopyroxenite	N/A	N/A	N/A	N/A	65.2	69.0	66.6	0.80

	214.5	Apatitic clinopyroxenite	N/A	N/A	N/A	N/A	72.6	76.1	73.9	1.00
	219.5	Apatitic clinopyroxenite	N/A	N/A	N/A	N/A	74.6	78.6	76.4	1.20
	224.6	Apatitic clinopyroxenite	N/A	N/A	N/A	N/A	73.6	78.4	75.8	1.70
	229.6	Apatitic clinopyroxenite	N/A	N/A	N/A	N/A	74.3	78.3	76.0	1.10
	234.4	Apatitic clinopyroxenite	N/A	N/A	N/A	N/A	75.5	78.1	76.7	0.90
SL-13-37	7	Oxide augite melatroctolite	52.8	56.5	54.4	1.20	73.6	76.6	75.4	0.70
	11	Oxide augite melatroctolite	52.0	54.1	53.1	0.70	73.2	74.8	73.9	0.50
	13	Oxide augite melatroctolite	53.6	56.9	55.0	0.80	74.6	76.4	76.0	0.70
	15	Oxide augite melatroctolite	54.8	58.9	55.7	1.00	73.2	75.7	74.7	0.70
	19	Oxide augite melatroctolite	57.9	60.4	59.1	0.70	75.2	77.1	76.0	0.60
	21	Oxide augite melatroctolite	55.8	58.2	56.9	0.60	73.4	76.6	73.9	0.90
	25	Oxide augite melatroctolite	58.8	61.4	59.9	0.80	72.7	74.8	74.7	0.70
	27	Oxide augite melatroctolite	52.9	54.7	53.6	0.40	71.8	73.0	72.1	0.50
	33	Oxide augite melatroctolite	59.2	60.5	59.5	0.40	73.6	76.4	75.2	0.80
	37	Oxide augite melatroctolite	58.7	60.8	59.7	0.70	73.6	77.1	75.0	1.00
	48	Coarse grained ophitic gabbro	61.9	65.5	63.5	1.10	N/A	N/A	N/A	N/A
	52	Coarse grained ophitic gabbro	59.5	66.0	63.7	2.80	74.1	78.2	76.9	1.10
	54	Coarse grained ophitic gabbro	52.3	56.6	54.4	1.60	74.3	75.7	75.6	0.70
	55.5	Coarse grained ophitic gabbro	52.5	61.7	57.0	3.70	72.3	77.0	74.9	2.20
	56	Coarse grained ophitic gabbro	53.9	61.9	58.8	3.20	76.2	77.5	76.9	0.50
	62	Pegmatitic ophitic gabbro	N/A	N/A	N/A	N/A	63.8	71.8	68.2	3.50
	64	Pegmatitic ophitic gabbro	55.1	58.9	57.4	0.80	65.0	76.4	72.7	2.30
	76	Pegmatitic ophitic gabbro	61.8	66.8	62.8	1.40	71.8	75.7	73.8	1.40
	80	Pegmatitic ophitic gabbro	56.8	60.8	58.9	1.90	70.5	74.8	72.7	1.50
	88	Pegmatitic ophitic gabbro	62.2	67.5	63.6	1.50	66.4	76.4	75.3	3.80
	93	Pegmatitic ophitic gabbro	62.0	65.3	63.7	1.60	75.5	78.2	76.5	1.10
	95	Feldspathic clinopyroxenite	64.5	67.5	64.8	1.30	76.4	78.0	77.0	0.50
	97.2	Feldspathic clinopyroxenite	N/A	N/A	N/A	N/A	73.6	76.8	75.3	1.20
	104.5	Feldspathic clinopyroxenite	65.4	69.3	67.0	1.20	72.0	77.3	75.2	1.30
	115.4	Feldspathic clinopyroxenite	68.2	69.9	68.8	0.50	76.6	79.3	78.1	0.80
	140	Feldspathic clinopyroxenite	74.1	76.7	75.0	0.70	80.7	82.6	81.6	0.60
	146	Feldspathic clinopyroxenite	68.8	70.0	69.3	0.40	76.0	79.1	77.6	1.00
	157.3	Medium grained ophitic gabbro	N/A	N/A	N/A	N/A	72.6	76.3	74.8	1.00
	167.3	Coarse grained ophitic gabbro	N/A	N/A	N/A	N/A	64.6	66.7	65.5	0.90
	170.7	Medium grained ophitic gabbro	N/A	N/A	N/A	N/A	70.1	73.2	72.0	1.10
	172.2	Medium grained ophitic gabbro	N/A	N/A	N/A	N/A	67.0	72.7	69.6	1.80
	176	Medium grained ophitic gabbro	N/A	N/A	N/A	N/A	77.6	82.1	80.2	1.20
	182	Medium grained ophitic gabbro	N/A	N/A	N/A	N/A	76.6	81.7	79.7	1.20
	227	Medium grained ophitic gabbro	N/A	N/A	N/A	N/A	73.1	78.8	76.0	1.80

Table 6-6. A subset of samples chosen for electron microprobe analyses

DDH	Depth/m	Units	Mg# of olivine	SD	Mg# of clinopyroxene	SD
SL-13-34	3.0	Oxide augite melatroctolite	37.2	1.50	67.3	1.30
	5.1	Oxide augite melatroctolite	33.4	0.30	66.7	1.00
	17.4	Olivine gabbro	38.0	1.30	67.2	1.60
	30.0	Oxide augite melatroctolite	48.3	1.30	68.5	0.30
	32.0	Olivine gabbro	41.6	1.10	68.3	0.60
	45.0	Oxide augite melatroctolite	47.1	0.40	69.0	0.50
	53.0	Oxide augite melatroctolite	51.4	0.30	69.9	0.30
	58.9	Oxide augite melatroctolite	49.1	0.40	69.5	0.40
SL-13-37	7.0	Oxide augite melatroctolite	48.5	0.60	68.5	0.40
	19.0	Oxide augite melatroctolite	51.2	0.20	69.4	0.40
	25.0	Oxide augite melatroctolite	55.7	0.60	70.1	0.80
	27.0	Oxide augite melatroctolite	51.8	0.20	70.0	0.40
	37.0	Oxide augite melatroctolite	53.8	0.50	69.6	0.80
SL-13-41	3.0	Oxide augite melatroctolite	27.9	0.50	59.9	1.10
	12.1	Oxide augite melatroctolite	36.0	0.20	69.0	0.10
	73.0	Oxide augite melatroctolite	51.1	0.20	69.2	0.30
	91.0	Oxide augite melatroctolite	53.0	0.50	70.5	0.90
	109.1	Oxide augite melatroctolite	57.1	0.20	70.7	0.40

6.3 Regional geology

The Proterozoic Coldwell Alkaline Complex is a sub-circular intrusion that has a diameter of approximately 25 km and a surface area of 580 km^2 and is the largest alkaline intrusive complex in North America (Walker et al., 1993; Shaw, 1997). It intruded the Archean Shreiber-Hemlo greenstone belt along the northern edge of the Midcontinent rift at 1108-1094 Ma, which marked the beginning of the main stage of magmatism related to the Midcontinent system (Walker et al., 1993; Heaman et al., 2007; Good et al., 2015). Petrologic and field studies conducted by Puskas (1970), Mitchell and Platt (1978, 1982), Mitchell et al. (1993), and Shaw (1997) recognized three superimposed intrusive centers constituting this complex, from east to west, they are center I, center II, and center III (Fig. 6-1). Paleomagnetic work conducted by Ashley and Kerns (2012) suggests that Centers I and III are the same age but both are older than Center II. Center I forms the eastern margin of the Coldwell Alkaline Complex, and is composed by the Eastern Gabbro, the Western

Gabbro, amphibole quartz syenite, iron-rich augite syenite, and mafic volcanic and subvolcanic rocks (Walker et al., 1993; Shaw, 1994; Good et al., 2015). Center II consists of alkali gabbro and syenite (Mitchell and Platt, 1978, 1982; Mulja, 1989). Center III is mainly composed of syenite and quartz syenite which are intrusive into most other phases of the complex and exhibit various degrees of crustal contamination (McLaughlin and Mitchell, 1989). It was proposed by Mitchell and Platt (1977, 1978) and Walker et al. (1993) that the emplacement of most rock units in the Coldwell Alkaline Complex was controlled by the faulting during cauldron subsidence at a subvolcanic depth.

6.4 Geology of Area 41

The Area 41 occurrence is situated near Sally Lake at the north east margin of the Eastern Gabbro (Fig. 6-1). The mineralization zone strikes east-southeast, dips at 45-50 degrees south and extends for over 1.2 km along strike. The geology of Area 41 is complex due to the intrusive crosscutting relationships, the complicated nature of the basal contact with the partially melted Archean rocks, and also the presence of some block faults. Geology and igneous stratigraphy of this property are depicted in Figures 6-2 and 6-3.

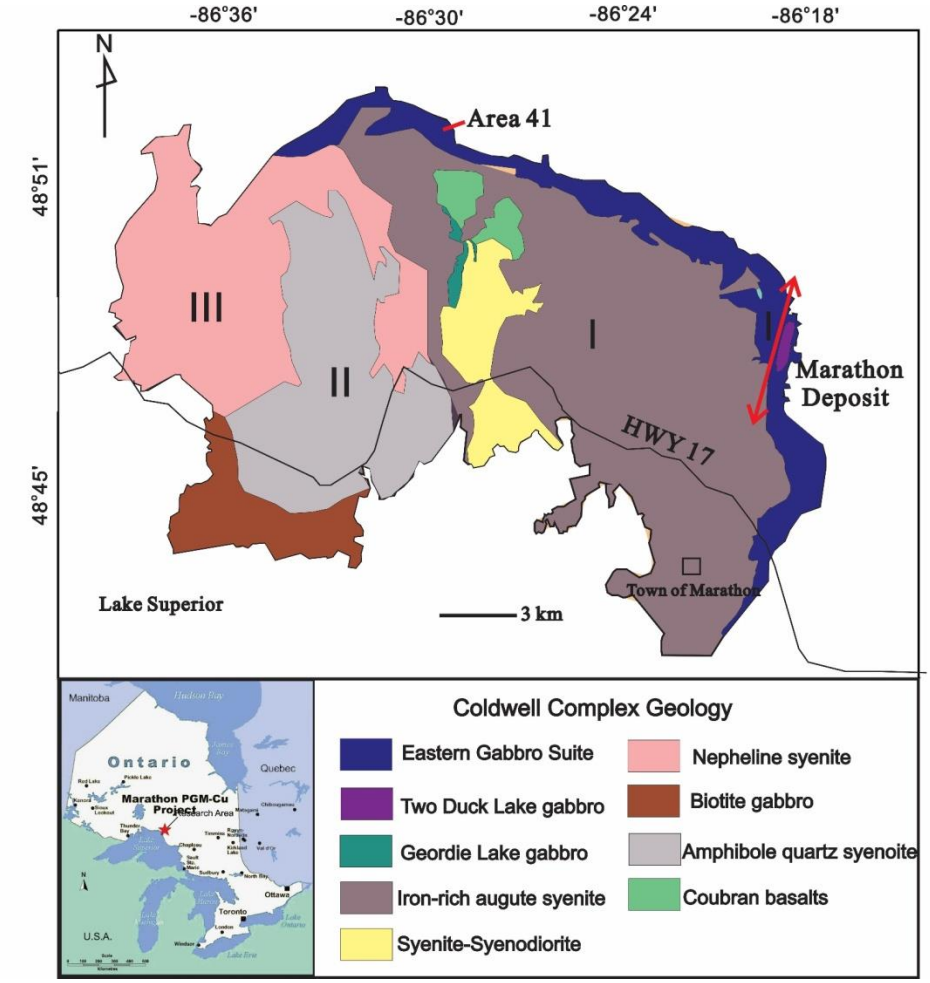

Figure 6-1. Geological map of the Coldwell alkaline complex, situated on the northern shore of Lake Superior (modified after Walker et al., 1993)., the location of Area 41 is represented as the red dot. The intrusive centers have been shown by Roman numerals (modified after Mulja and Mitchell, 1991).

6.4.1 Footwall contact

The footwall of Area 41 typically sits stratigraphically below ophitic gabbro of the Marathon Series with a variable or undetermined dip and thickness. Its mineral composition varies significantly but generally include three different rock types, from east to west: Archean granitoid rocks, metasediments, and rheomorphic intrusive breccia (Fig. 6-2). All three types of footwall rocks have undergone pyroxene hornfels metamorphism to local partial melting resulted by the heat from intrusions of the Eastern Gabbro (Currie, 1980). The ophitic gabbro crosscuts the footwall and has an igneous contact. The contact between granitoid footwall and the

ophitic gabbro strikes nearly NW-SE for a distance of around 1 km (Fig. 6-2). The rheomorphic intrusive breccia and/or gabbro contact at Area 41 is complicated because some blocks of rheomorphic intrusive breccia occur at the footwall underlain by the Archean granitoid rocks whereas others occur as xenoliths within the Marathon Series and (Fig. 6-3). An outcrop of rheomorphic intrusive breccia is shown in Figure 6-4A.

6.4.2 Meta-basalt

The meta-basalt at Area 41 makes up approximately 20 % of the total Eastern Gabbro package, similar to the proportion of the meta-basalt at the Marathon deposit as estimated by Good et al. (2015). At Area 41, the meta-basalt is exposed north-west of the mineralization at the surface and stratigraphically occurs close to the base of the Eastern Gabbro (Fig. 6-3). Locally the meta-basalt is intruded by numerous thin dykes of ophitic gabbro (Fig. 6-4B), which obscures its textures and features. The mineral composition of meta-basalt varies from basalt to olivine basalt, and consists of equigranular fine grained subhedral clinopyroxene, olivine, magnetite with interstitial plagioclase. Layering of this unit is weak and can be detected at the meter scale by gradational change in grain size, and locally by thin magnetite-rich horizons. A common texture for the meta-basalt unit is 120° angles of boundaries between crystals (granoblastic texture, Fig. 6-5A), which is interpreted by Good et al. (2015) as a result of pyroxene hornfels metamorphism. In addition, the formation of 1-2 cm sized zoned amoeboid shaped blebs with either a clinopyroxene or olivine core and a thin plagioclase rim is commonly observed within this unit particularly for that close to intrusions of the ophitic gabbro. This texture is interpreted to have formed either by migration of material from the ophitic gabbro magma along a very fine 3d network or by pyroxene hornfels metamorphism related to intrusion of the ophitic gabbro.

6.4.3 Feldspathic clinopyroxenite

Crosscutting relationships suggest that the feldspathic clinopyroxenite is an older rock type that is potentially related to the meta-basalt (McBride, 2013). This rock

type is present either at the footwall/ophitic gabbro contact, meta- basalt/ophitic gabbro contact, or as amoeboid blebs within the ophitic gabbro (Figs. 6-3A, 6-3B, and 6-4C). The longitudinal section (Fig. 6-3A) shows that the feldspathic clinopyroxenite occurs as a large xeolith (~60 m thick and ~300 m long) within later ophitic gabbro intrusion, and also is stratigraphically underlain by a PGE mineralization zone which, as will be described later, is characterized by high PGE grades and low Cu/Pd. Thus, this rock type is an important stratigraphic marker above mineralization at this property. The mineralogy of the feldspathic clinopyroxenite, in decreasing order of abundances, comprises medium- to coarse-grained clinopyroxene (60-80 modal%), olivine (5-15 modal%), plagioclase (5-10 modal%), magnetite (less than 5 modal%), and trace disseminated sulfide minerals that are dominated by pyrrhotite and chalcopyrite. Both olivine and clinopyroxene are extensively fractured and replaced by secondary serpentine and chlorite (Fig. 6-5B). Plagioclase occurs either as coarse-grained subhedral phase interstitial to olivine and clinopyroxene cumulates, or as rounded fine-grained inclusions enclosed by clinopyroxene. Magnetite and sulfide minerals are typically within olivine and clinopyroxene as inclusions.

6.4.4 Layered Series

The Layered Series constitutes the main part of the Eastern Gabbro and is compositionally and texturally similar along the Eastern Gabbro (Good et al., 2015), this also applies to Area 41. It mainly consists of massive to modally layered olivine gabbro and weakly layered oxide augite melatroctolite, with a lesser amount of gabbroic anorthosite. The olivine gabbro and oxide augite melatroctolite are shown to be the same unit in Chapter 5. The Layered Series locally contains disseminated copper-sulfide mineralization, but the mineralization is typically related to albite-actinolite alteration and lacks PGE mineralization (Good et al., 2015; see Chapter 3). At Area 41, as elsewhere along the Eastern Gabbro, the Layered Series occurs stratigraphically above the Marathon Series (Figs. 6-3A and B).

6.4.4.1 Gabbroic anorthosite

The gabbroic anorthosite typically occurs as meter-sized xenoliths throughout the olivine gabbro at Area 41 and thus is older. However, this unit is believed to be genetically related to the Layered Series based on its similar inter-element ratios of incompatible elements with the Layered Series gabbro (Good et al., 2015). The gabbroic anorthosite has a very distinctive mottled appearance and consists of approximately 80 modal percent medium- grained, subhedral to anhedral plagioclase, very coarse- grained clinopyroxene (10 modal %) and olivine (5 modal %) oikocrysts, and 5 percent medium- to coarse- grained, interstitial to poikilitic magnetite.

6.4.4.2 Olivine gabbro

The olivine gabbro is medium to coarse grained (1-4mm) and shows massive to modal layering defined by a gradational increase in the abundance of plagioclase, or by alternating plagioclase-rich and clinopyroxene-rich layers (Fig. 6-4D). It consists of euhedral plagioclase (40-60 modal%), subhedral clinopyroxene (15-30 modal%), subhedral olivine (10-15 modal%), less than 10 modal% apatite and magnetite, less than 8 modal percent of subhedral alkaline feldspar, and less 5 modal% subhedral to anhedral biotite. Plagioclase locally occurs as chadocryst enclosed by olivine and clinopyroxene oikocrysts, and olivine is rimed by clinopyroxene, indicating that the crystallization sequence is plagioclase, followed by olivine, then clinopyroxene. Apatite and magnetite normally are enclosed in, or interstitial to, olivine and plagioclase. Biotite occurs either as an interstitial phase, or as a poikilitic phase enclosing plagioclase, olivine, and clinopyroxene. Alkali feldspar in the olivine gabbro is perthite which partially encloses euhedral plagioclase grains (Fig. 6-5C).

6.4.4.3 Oxide augite melatroctolite

The oxide augite melatroctolite is texturally similar and gradational to the olivine gabbro at Area 41. It presents weak modal layering and is distinguished by a high abundance (10 to 20 modal %) of disseminated magnetite (Fig. 6-4D). The mineral

composition of this unit comprises, in approximately decreasing order of abundances, olivine (20-45 modal%), plagioclase (15-30 modal%), clinopyroxene (10-20 modal%), magnetite, and apatite (<10 modal%). Olivine and clinopyroxene are euhedral-subhedral, and occur between subhedral to anhedral plagioclase clusters. Magnetite and apatite are normally enclosed by, or less commonly interstitial to olivine and plagioclase.

6.4.5 Marathon Series

At surface at Area 41, the Marathon Series occurs as a band between the footwall and the Layered Series (Fig. 6-2). The Marathon Series is stratigraphically below the Layered Series (Figs. 6-3A and B). Ophitic gabbro is the dominant lithology of the Marathon Series, with lesser amounts of apatitic (olivine) clinopyroxenite and oxide melatroctolite. Based on the crosscutting relationships, e.g., the Marathon Series crosscuts both the meta-basalt and the Layered Series at Area 41, indicating the Marathon Series is the youngest series, although it stratigraphically is below the Layered Series (Fig. 6-3).

6.4.5.1 Ophitic gabbro

The ophitic gabbro resembles the Two Duck Lake gabbro at the Marathon deposit (Good et al., 2015), which is the main host to Cu-PGE mineralization at that deposit. It has a distinctive ophitic to subophitic texture (Fig. 6-4E), and consists of, in approximately decreasing order of abundance, subhedral plagioclase (40-70 modal%), subhedral clinopyroxene (15-30 modal%), euhedral to subhedral olivine (5-10 modal%), and less than 10 modal% magnetite and apatite. Based on textural relationships between various minerals (e.g., the overgrowth of olivine by clinopyroxene, the inclusion of apatite in the olivine, etc.), the crystallization sequence of this unit, from early to late, is plagioclase (apatite)-olivine-clinopyroxene-magnetite. Locally, the ophitic gabbro grades into the leucogabbro that contains a greater amount of plagioclase.

Based on variations in grain size, the ophitic gabbro can be subdivided into three subgroups: pegmatitic (>2 cm), coarse-grained (0.5-2cm), and medium-grained ophitic gabbro (<0.5 cm). The coarse-grained ophitic gabbro typically sits stratigraphically above the pegmatitic ophitic gabbro, and the latter is underlain by the medium-grained ophitic gabbro (Figs. 6-3A and B). Locally, the pegmatitic ophitic gabbro also occurs as pods within coarse-grained ophitic gabbro or as rims of Eastern Gabbro xenoliths. In contrast to coarse-grained and pegmatitic ophitic gabbro, olivine is rare in the medium-grained ophitic gabbro.

An important texture observed particularly in the pegmatitic ophitic gabbro is the replacement of earlier plagioclase by later plagioclase, and the later plagioclase is intergrown with chalcopyrite. EDS mapping (Fig. 6-6) and spot analyses show that the later plagioclase is more calcic than the earlier plagioclase. Similar textures were also observed by Good and Crocket (1994) and Shahabifar Far (2016) in the Two Duck Lake gabbro at the Marathon deposit, at the Four Dams in Chapter 3, and at the WD zone in Chapter 4. At Area 41, minerals in the ophitic gabbro are generally unaltered. However, there is some local development of secondary minerals such as chlorite, amphibole, serpentine, and calcite, particularly in the coarse- grained and pegmatitic ophitic gabbro (Fig. 6-5D). In addition, in pegmatitic ophitic gabbro, the magmatic apatite and biotite are locally replaced by the secondary apatite and biotite (Figs. 6-5E, 6-7, and 6-8), which are chlorine-rich relative to the primary phases (Figs. 6-7 and 6-8).

6.4.5.2 Apatitic (olivine) clinopyroxenite

The apatitic clinopyroxenite occurs as irregular-shaped pods stratigraphically below the ophitic gabbro, or is heterogeneously mixed with the ophitic gabbro (Figs. 6-3A, 6-3B, and 6-4F). Locally, it occurs as thin dikelets crosscutting the ophitic gabbro (Fig. 6-3A), indicating it perhaps is relatively younger than the ophitic gabbro. Outcrops of this unit are extremely rare as it is preferentially eroded. This unit hosts some PGE mineralization, but is less well mineralized than the ophitic gabbro. It

mainly consists of, in approximately decreasing order of abundance, medium- to coarse-grained subhedral clinopyroxene (30-60 modal%), olivine (10-20 modal%), euhedral apatite (5-15 modal%), plagioclase (5-10 modal%), and les than 10 modal% magnetite and biotite (Fig. 6-5F). Moderate to strong chlorite and actinolite alteration is commonly observed in this unit.

6.4.5.3 Oxide melatroctolite

The oxide melatroctolite pods typically are located within the main body of ophitic gabbro (particularly within the coarse-grained ophitic gabbro) (Figs. 6-3A and B). This unit contains a high abundance of subhedral magnetite (40-60 modal %), similar to the oxide augite melatroctolite in the Layered Series. This unit also contains olivine, clinopyroxene, plagioclase (the total amount of the three minerals generally is less than 30 modal %), and from 2 to 30 modal % euhedral apatite.

6.4.6 Breccia units

Three types of breccia units with different compositions of matrix and xenoliths were recognized. Type A consists of an ophitic gabbro matrix and angular xenoliths of meta-basalt rocks or footwall materials, which is similar to type A and B breccia units defined by Good et al. (2015) at the Marathon deposit. Type B is composed of an apatite clinopyroxenite-dominated matrix with meta-basalt or footwall xenoliths. Type C consists of meta-basalt rocks that were cut by multiple thin dikelets of the Marathon Series ophitic gabbro and/or apatitic clinopyroxenite, similar to type C breccia defined by Good et al. (2015) at the Marathon deposit. Note that these breccia rocks contain sulfide-bearing ophitic gabbro and apatitic clinopyroxenite, which are also important hosts to Cu-PGE mineralization at Area 41.

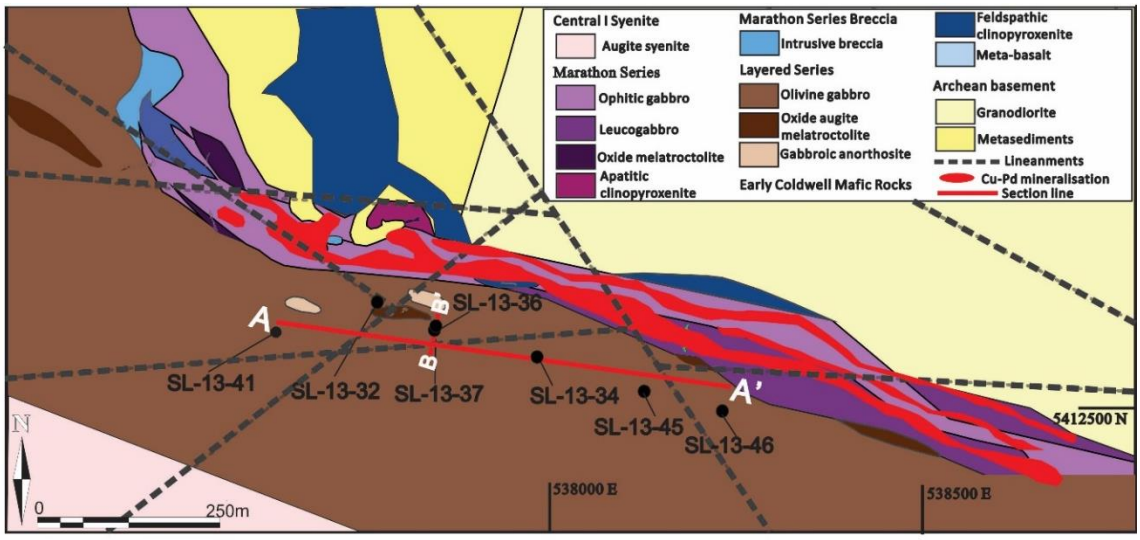

Figure 6-2. The surface geology at Area 41 (after McBride, 2013).

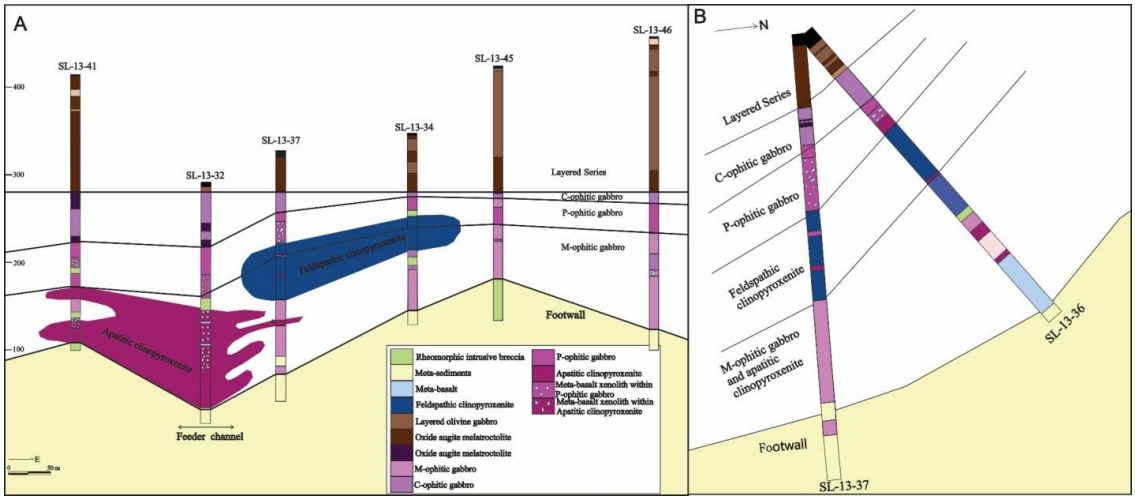

Figure 6-3. Stratigraphic relationships between different rock units. (A) A-A' longitudinal section as indicated in Figure 6-2 showing spatial distributions of different units; (B) B-B' cross section as indicated in Figure 6-2 showing geological boundaries of gabbro series. Prefix: P-pegmatitic, C-coarse-grained, M-medium-grained.

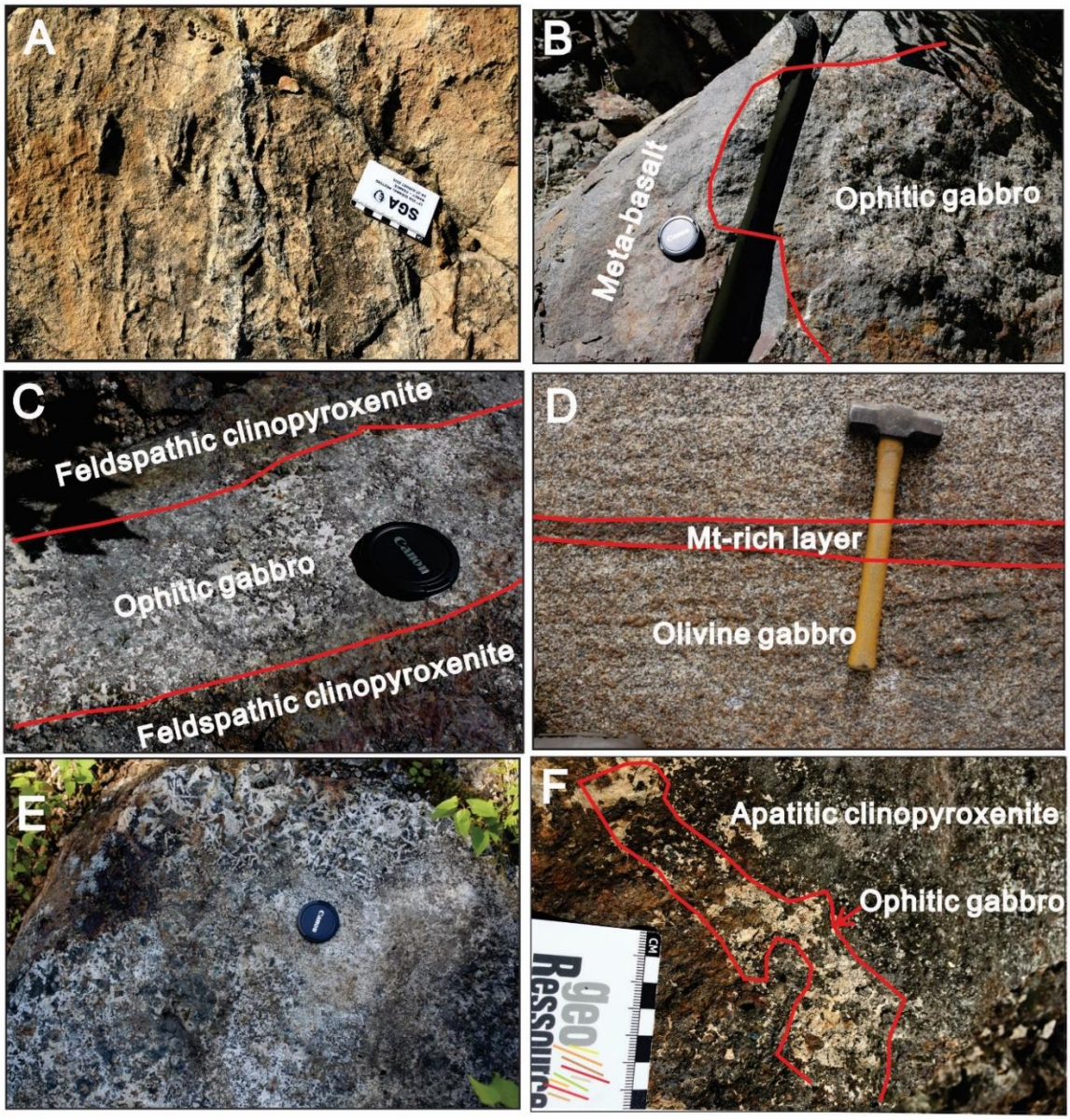

Figure 6-4. Field pictures of various rock units and textures. (A) Outcrop of rheomorphic intrusive breccia; (B) The meta-basalt is intruded by ophitic gabbro; (C) The feldspathic clinopyroxenite is crosscut by the ophitic gabbro; (D) The layering defined by the alternation of clinopyroxene and olivine- rich and plagioclase-rich sublayers of the layered series olivine gabbro, locally the olivine gabbro graded into the magnetite-rich oxide augite melatroctolite; (E) The typical ophitic texture of the ophitic gabbro; (F) The outcrop of apatitic clinopyroxenite, the non-weathered surface shows this unit is invariably mixed with the ophitic gabbro material.

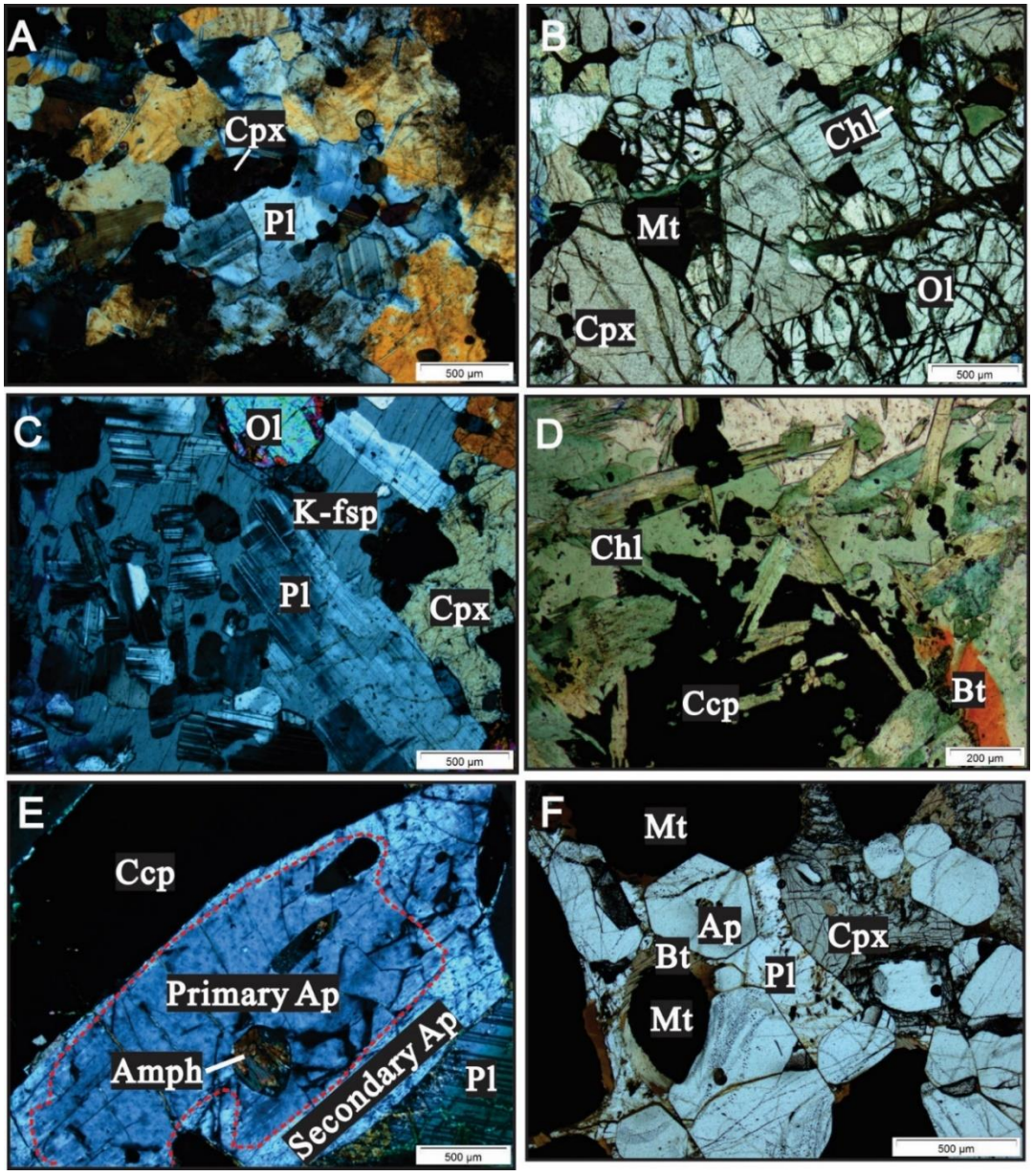

Figure 6-5. Photomicrographs showing textures and alterations of different units. (A) Cross-polarized transmitted light photomicrograph showing the hornfels grade metamorphism of the meta-basalt unit, note the nearly 120° angles of boundaries between Pl crystals, the yellow mineral is the sericitic altered Pl; (B) Plane-polarized transmitted light photomicrograph showing the random Chl veinlets cutting Ol and Cpx in the feldspathic clinopyroxenite; (C) Cross-polarized transmitted light photomicrograph showing the poikilitic texture reflected by euhedral Pl chadocrysts enclosed by k-fsp oikocrysts, the sample is the olivine gabbro; (E) Cross-polarized transmitted light photomicrograph showing the Chl aggregates in the pegmatitic ophitic gabbro (D) Cross-polarized transmitted light photomicrograph showing the secondary Ap rims the primary magmatic Ap in the pegmatitic ophitic gabbro; (F) Plane-polarized transmitted light photomicrograph showing euhedral Ap cumulates with interstitial Pl in the apatitic clinopyroxenite. Abbreviations: Amph=amphibole, Ap=apatite, Bt=biotite, Ccp=chalcopyrite, Chl=chlorite, Cpx=clinopyroxene, K-fsp=K feldspar, Mt=magnetite, Ol=olivine, Pl=plagioclase.

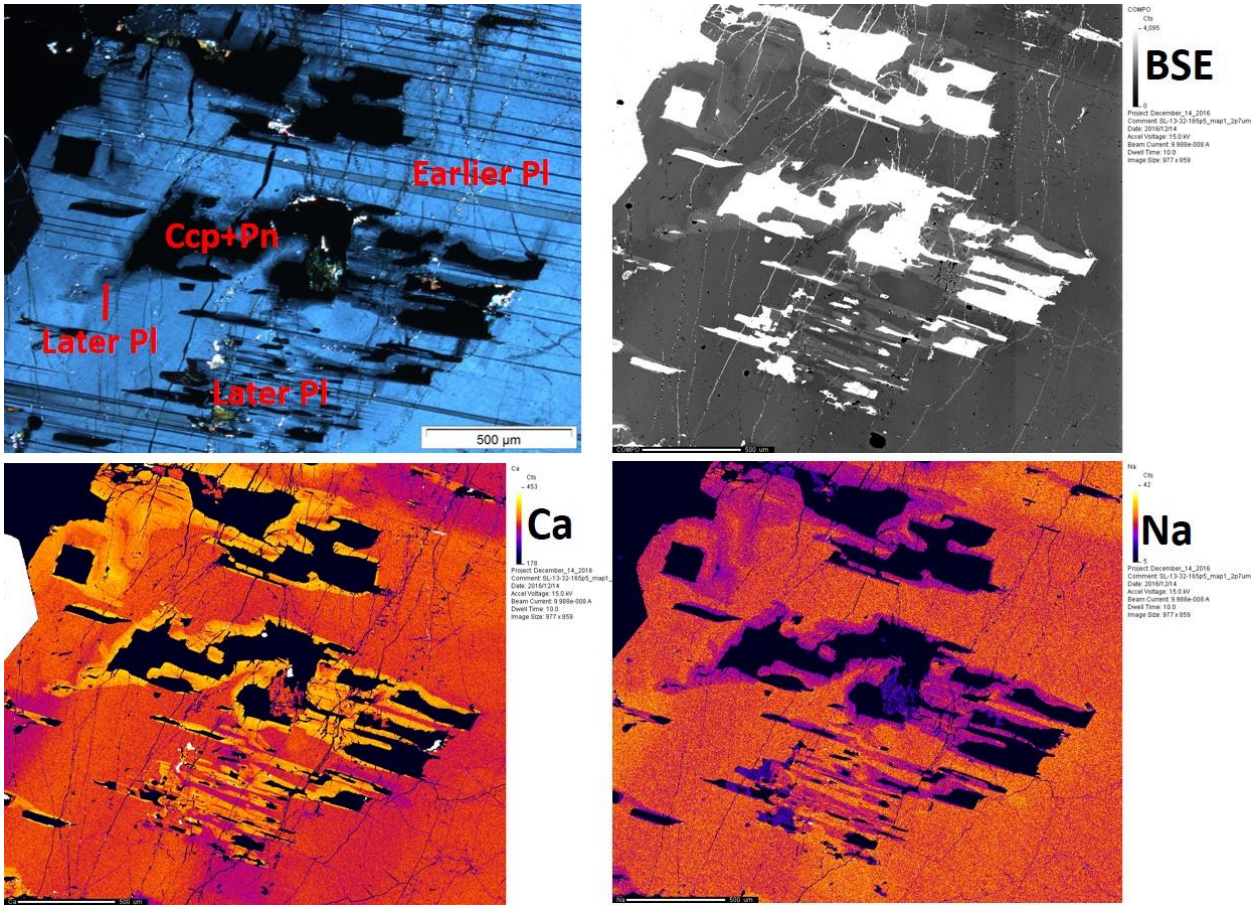

Figure 6-6. Textures showing earlier plagioclase was replaced by later more calcic plagioclase that occurs intergrown with chalcopyrite (and pentlandite). Note that there is some carbonate alteration on the plagioclase (see the white mineral on Ca mapping).

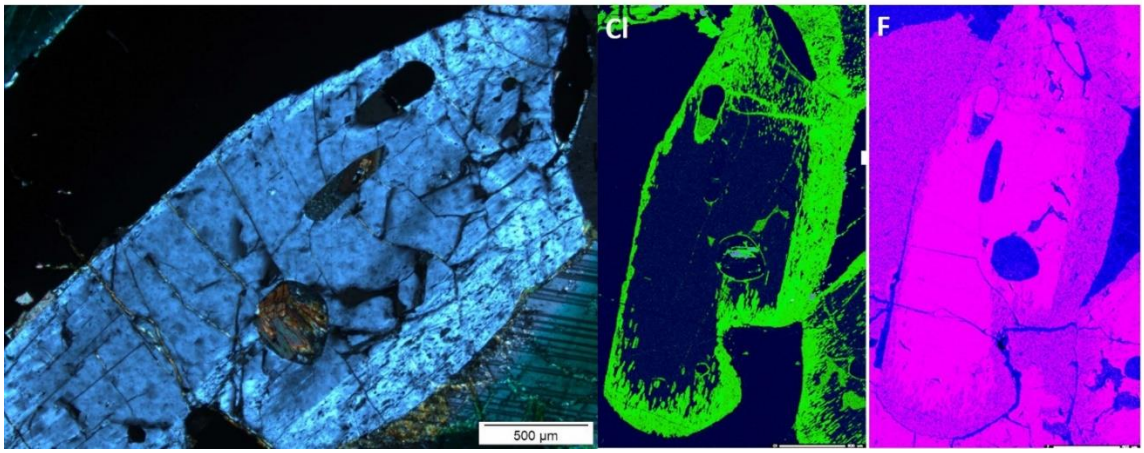

Figure 6-7. Wavelength dispersive spectroscopy (WDS) Cl and F mapping showing secondary apatite replaces the magmatic apatite in pegmatitic ophitic gabbro, the magmatic apatite is rich in F, whereas the secondary apatite is rich in chlorine.

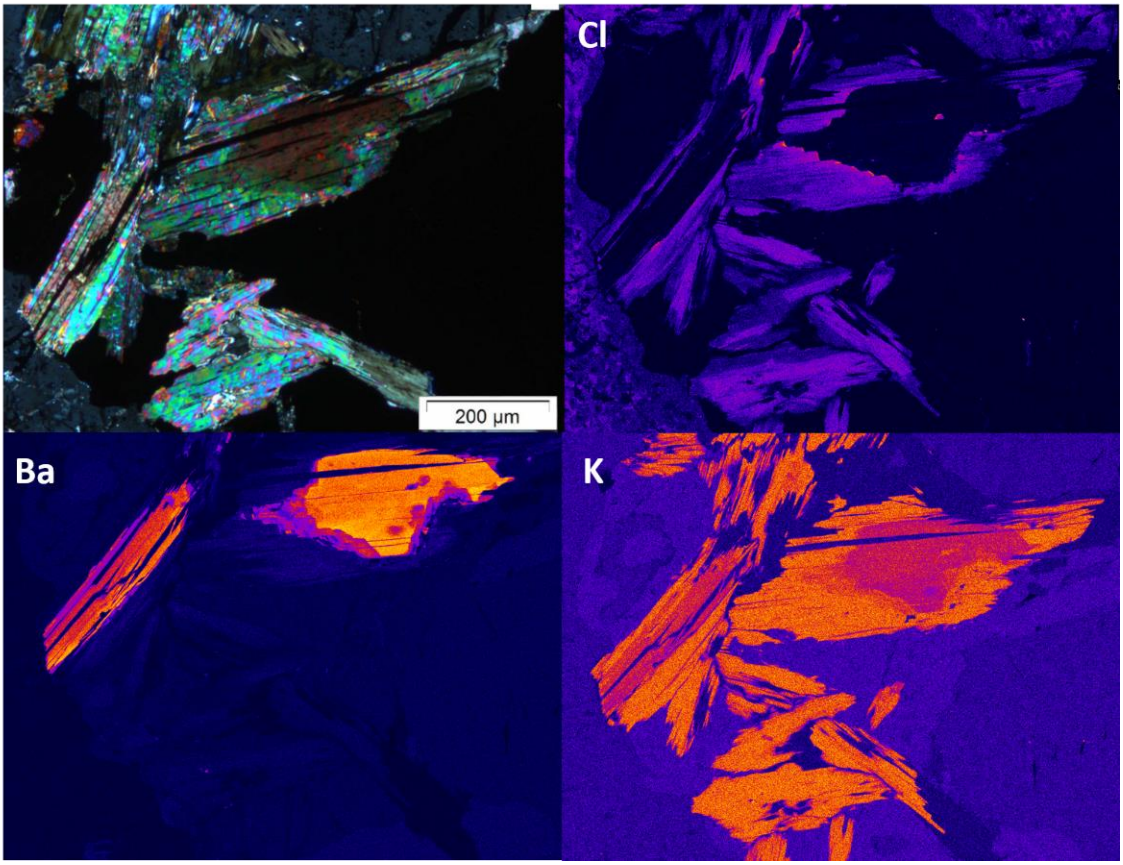

Figure 6-8. WDS Cl, Ba, and K mapping showing secondary biotite replaces the magmatic biotite in pegmatitic ophitic gabbro, the magmatic biotite is rich in Ba and K, whereas the secondary biotite is rich in chlorine.

All three series' units at Area 41 share similar petrographic characteristics with the same series' units at the Marathon deposit as described by Good et al. (2015), and also similar to those at Four Dams as described in Chapter 3. Note that Four Dams area is about 15 km south of Area 41.

6.5 Geochemical Characteristics of the Layered and Marathon Series at Area 41

Results of Good et al. (2015) and the work in Chapter 3 show that the units of the Eastern Gabbro assemblage at the Marathon deposit and Four Dams are geochemically distinctive. Adopting this concept, the classification of units recognized by drill core logging and petrography at Area 41 is evaluated using lithogeochemistry in order to establish the reliable stratigraphy and investigate its relationship with PGE mineralization. This is particularly important when considering that some rock units in the Eastern Gabbro assemblage are hosts to

significant Cu-Pd mineralization but are petrographically similar to other barren gabbroic units. For example, as will be shown in section 6.6.1, at Area 41 the Marathon Series hosts all known PGE mineralization whereas the Layered Series and meta-basalt lack PGE mineralization, therefore successfully recognizing these series' units is key to mineral exploration. The meta-basalt makes up a small portion of the Eastern Gabbro and shows unique pyroxene hornfels metamorphic texture, and thus is easily identified. The Layered Series constitutes the bulk of the Eastern Gabbro and is petrographically similar to the Marathon Series units. An important objective of this study is to create a tool for exploration at Area 41 through geochemical discrimination of the Marathon Series gabbro from the Layered Series gabbro.

6.5.1 Discrimination using lab-based results

Rock units are characterized by the primitive mantle-normalized abundances of Ce, Y, Nb, and Zr. The purpose for normalizing these elements is to keep consistent with the results from Good et al. (2015) for the units at the Marathon deposit, thus facilitating the comparison. These trace elements are chosen because: 1) they are all incompatible elements in mafic rocks, and as such, their ratios, can serve as indices to degrees of either partial melting and/or crustal contamination; and, 2) cerium and Y are the most and second most abundant REE in the data set and so will minimize the impact of analytical uncertainty in the interpretation. The average normalized Ce/Y and Nb/Zr values for various gabbro units are summarized in Table 6-7.

The meta-basalt, Layered Series, and Marathon Series are geochemically different. For example, the average normalized Ce/Y and Nb/Zr for the feldspathic clinopyroxenite are 3.95 (1σ=0.77) and 2.42 (1σ=0.42), lower than those for the olivine gabbro (average Ce/Y=14.23 (1σ=0.77), average Nb/Zr=6.79 (1σ=0.55)), and the Marathon Series ophitic gabbro (average normalized Ce/Y=11.91 (1σ=2.53), average Nb/Zr=5.69 (1σ=0.85)). These values are broadly similar to those determined by Good et al. (2015) for the same series' units at the Marathon deposit

except for the ophitic gabbro. At the Marathon deposit, the average normalized Ce/Y and Nb/Zr for the Two Duck Lake gabbro are 6.58 (1σ=1.0) and 3.63 (1σ=1.13), lower than those determined in the current work. Primitive mantle-normalized Ce vs. Y and Nb vs. Zr diagrams (Figs. 6-9 and 6-10) are created to better illustrate differences for different series units. Excluding the apatitic clinopyroxenite, which shows somewhat randomly distributed data points possibly because of the influence of apatite cumulates, the feldspathic clinopyroxenite, the Layered Series, and the Marathon Series are divided almost into three fields as separated by ratio lines of 6.2 and 15. Therefore, it seems that primitive mantle-normalized Ce/Y and Nb/Zr are useful to distinguish the Marathon Series rocks from the Layered Series and the meta-basalt at the Eastern Gabbro. Differences in Ce/Y and Nb/Zr for these igneous series are not likely to have resulted by fractional crystallization of a single batch of magma (they are incompatible), but rather reflect their different magma sources or degrees of contamination.

Table 6-7. Summary of primitive Mantle-Normalized Ce/Y and Nb/Zr for various gabbro units within the Eastern Gabbro at Area 41. Notes: Primitive mantle values for Ce, Y, Zr, and Nb of 1.675, 4.3, 10.5, and 0.658 ppm, respectively from McDonough and Sun (1995).

Series	Unit	No. of samples	Normalized Ce/Y			Normalized Nb/Zr		
			Avg	SD	Range	Avg	SD	Range
Meta basalt	Feldspathic clinopyroxenite	6	3.9	0.77	12.7-13.8	2.4	0.42	2.1-3.2
Layered	Olivine gabbro	11	14.2	0.68	13.4-15.5	6.8	0.55	6.1-7.8
	Oxide augite melatroctolite	12	13.9	0.64	13.1-14.8	7.8	1.21	6.3-10.2
	Ophitic gabbro	13	11.9	2.33	7.0-14.4	5.7	0.85	4.5-7.6
Marathon	Apatitic clinopyroxenite	7	6.1	2.68	4.0-10.0	2.4	1.23	1.4-8.0
	Oxide melatroctolite	7	13.4	0.41	12.7-13.8	6.3	0.86	5.1-7.1
	Coubran basalt*	18	8.9	3.63	5.0-17.7	3.5	0.33	2.8-4.2

*Data are from Cundari (2012).

The work in Chapter 3 successfully applied Ba and V/Ti to distinguish the Marathon Series units from the Layered Series units at Four Dams area. These two parameters are adopted here to differentiate igneous series at Area 41. Lab-based Ba and V/Ti are used here, but it is also possible to use pXRF Ba and V/Ti because all these elements can be acquired by pXRF (see Chapters 3 and 4). Figure 6-11 shows that

the Layered Series gabbro contains Ba contents (*ca.* 1000- *ca.* 6000 ppm) significantly higher than the Marathon Series rocks (<1000 ppm) and the feldspathic clinopyroxenite (<100 ppm). By contrast, V/Ti ratios for the Layered Series units (below *ca.* 0.02) are lower than those for the Marathon Series units (*ca.* 0.02- *ca.*0.07) and the feldspathic clinopyroxenite (*ca.* 0.02- *ca.* 0.05). Therefore, in addition to Ce/Y and Nb/Zr, whole-rock Ba and V/Ti are also useful parameters to distinguish the Marathon Series from other igneous series.

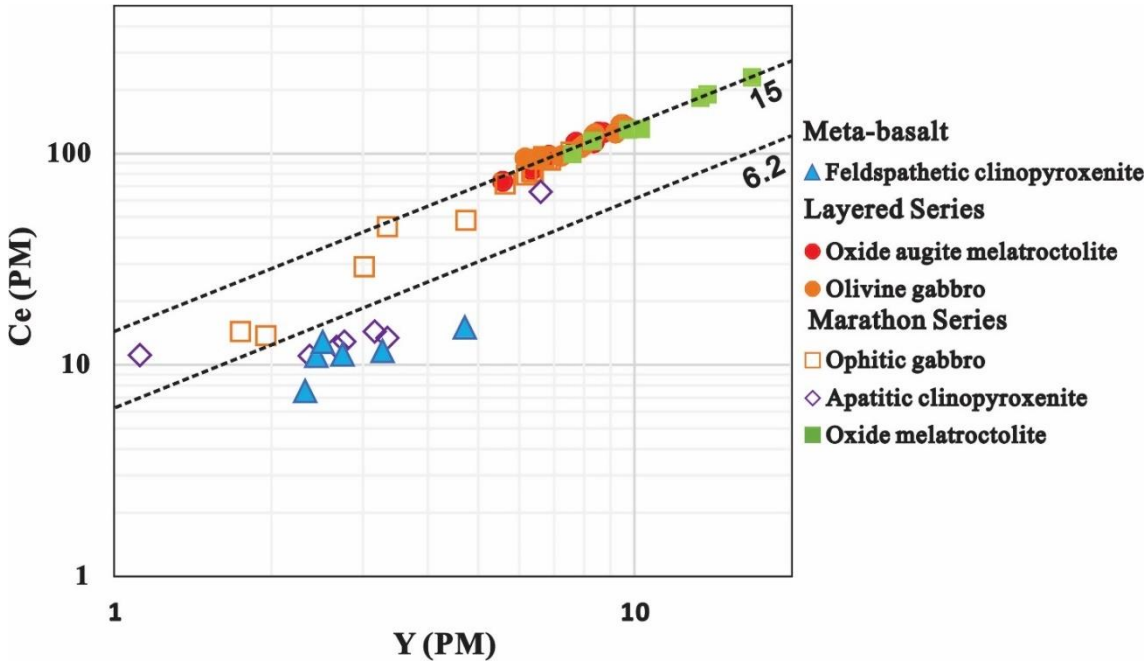

Figure 6-9. Comparison of primitive mantle-normalized Ce vs. Y for various units of the Eastern Gabbro at Area 41. Primitive values for Ce (1.675 ppm) and Y (4.3 ppm) are from McDonough and Sun (1995). PM=primitive mantle.

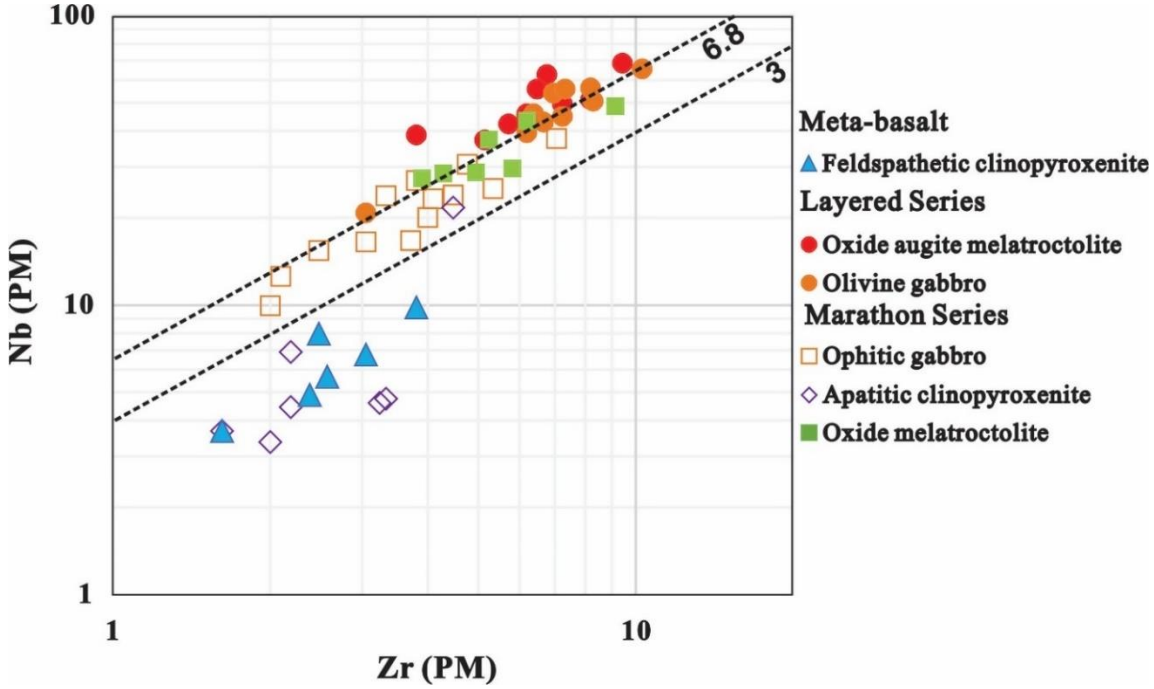

Figure 6-10. Comparison of primitive mantle-normalized Nb vs. Zr for various units of the Eastern Gabbro at Area 41. Primitive values for Nb (0.658 ppm) and Zr (10.5 ppm) are from McDonough and Sun (1995). PM=primitive mantle.

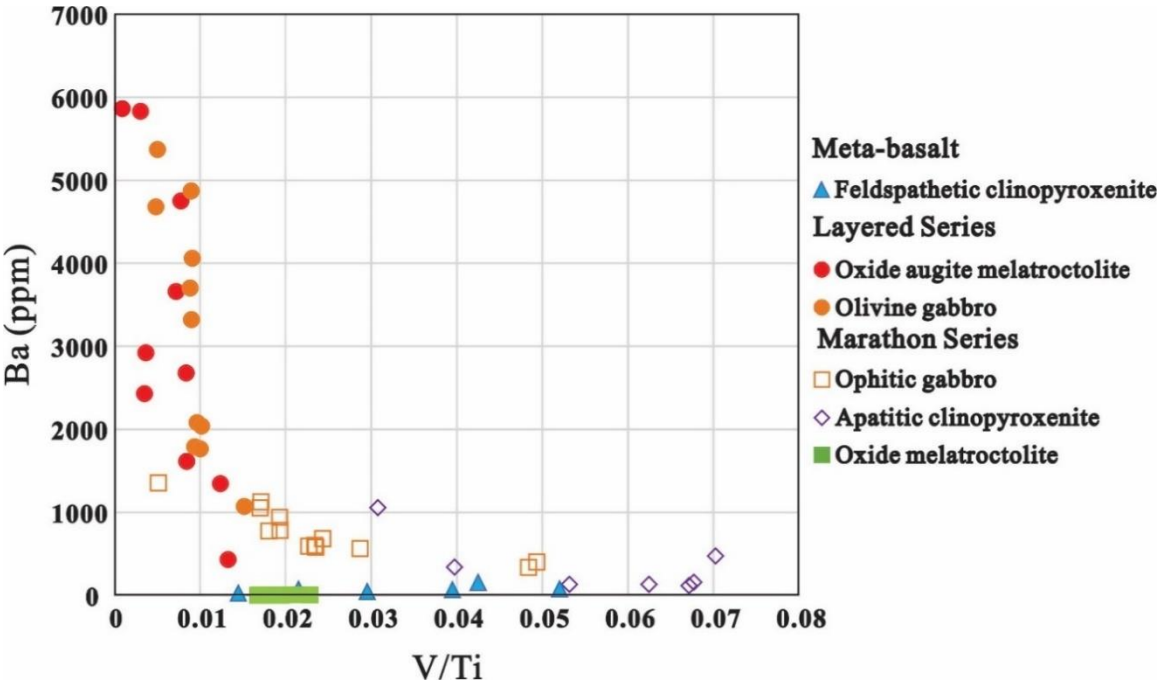

Figure 6-11. Whole-rock Ba vs. V/Ti for various rocks of the Eastern Gabbro at Area 41.

6.5.2 Discrimination using field portable instruments-based results

The evaluation of results from field portable techniques to distinguish the units is significant because: 1) the results can be acquired directly in the field without any time delay, thus improving the decision-making process; and, 2) it allows the acquisition of a large data set at a relatively low cost, thus can be used to create the high dense chemostratigraphy, which can then be compared to the stratigraphy from core logging. pXRF Al_2O_3, CaO, Fe_2O_3, P_2O_5, K_2O, Ba, Sr, Zr, and bSEM-EDS Mg#s of olivine and clinopyroxene are used in this section to distinguish different series units at Area 41 and establish the geochemical stratigraphy. Data accuracy and precision acquired from both portable techniques have been established in Chapters 3 and 4.

6.5.2.1 Down-hole profiles

In Chapter 3, we found that the Layered Series and the Marathon Series at Four Dams can be distinguished by investigating down-hole variations in whole-rock Zr and Mg#s of olivine and clinopyroxene, i.e., the Layered Series presents smooth trends in these parameters whereas the Marathon Series does not. Note that all these parameters are useful proxies to denote magma differentiation trends. In this section, we investigate whether this method still works at Area 41. Geochemical profiles of bSEM-EDS Mg#s of olivine and clinopyroxene, and pXRF whole-rock Zr down two representative drill holes (SL-13-37 and SL-13-32) are displayed in Figures 6-12 and 6-13.

Two significant observations from the down-hole profiles are made. First, the Mg#s of olivine and clinopyroxene of the Layered Series increase down hole, and whole-rock Zr contents of the Layered Series decrease down hole, which is a normal evolution trend. The Marathon Series units including the ophitic gabbro and apatitic clinopyroxenite, by contrast, have erratic variations in these parameters over short distances. The feldspathic clinopyroxenite also displays an overall normal evolution trend, but it appears to be more primitive than the Layered Series and the Marathon

Series. Second, the Mg#s of olivine and clinopyroxene for coarse-grained and pegmatitic ophitic gabbro samples have 1σ standard deviation= ~1-~3 (Table 6-5), which are more variable than the medium-grained ophitic gabbro (SD= ~1-~1.8, Table 6-5), the Layered Series (SD= ~0.5-~1, Table 6-5), and the feldspathic clinopyroxenite (SD= ~0.4-~1.3 Table 6-5). These differences are highlighted in Figures 6-12 and 6-13 (see error bars in both figures).

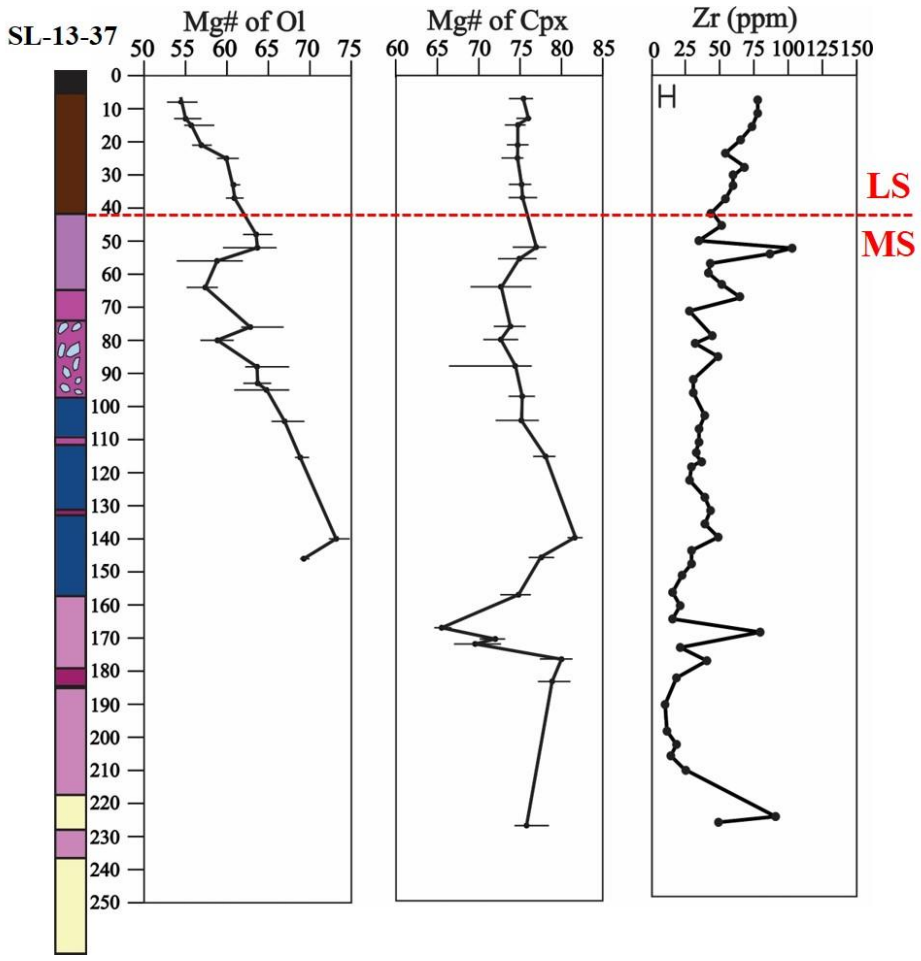

Figure 6-12. Down-hole variations in Mg# of olivine, Mg# of clinopyroxene, and whole-rock Zr for drill hole SL-13-37. Two ends of the error bar represent the minimum and maximum of the mineral chemical data, see text for full explanations. Note that the Cu/Pd ratios are in log-scale and ratios>20000 are not shown. LS: The Layered Series, MS: The Marathon Series. Lithology legend is same as Figure 6-3.

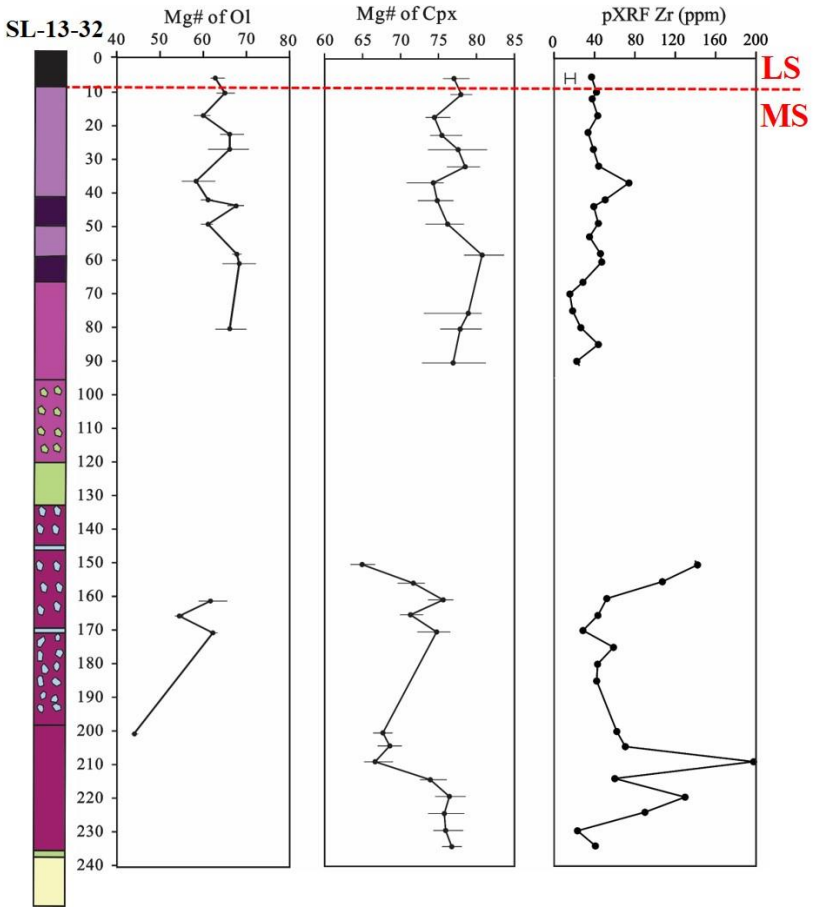

Figure 6-13. Down-hole variations in Mg# of olivine, Mg# of clinopyroxene, and Zr contents for drill hole SL-13-32. LS: The Layered Series, MS: The Marathon Series. Lithology legend is the same as Figure 6-3.

6.5.2.2 Chemical stratigraphy

In order to establish the reliable stratigraphy, particularly when the drill cores were logged by several people, a geochemical stratigraphy created based on pXRF and bSEM-EDS analyses are compared to the stratigraphy. Down-hole mapping of pXRF whole-rock Al_2O_3, CaO, Fe_2O_3, P_2O_5, K_2O, Sr, and Ba, and bSEM-EDS Mg#s of olivine and clinopyroxene are correlated with the igneous stratigraphy in Figure 6-14. The chemostratigraphy is basically consistent with the stratigraphy. For instance, it shows that the Layered Series generally contains higher K_2O, Ba, and Sr contents than the Marathon Series. The medium-grained ophitic gabbro contains lower P_2O_5, Fe_2O_3, higher Al_2O_3 and Sr contents than the coarse-grained and pegmatitic ophitic gabbro. The feldspathic clinopyroxenite and the apatitic

clinopyroxenite are also clearly indicated in the geochemical stratigraphy by their low Al_2O_3, P_2O_5, K_2O, Ba, Sr abundances for the feldspathic clinopyroxenite, the high Mg#s of olivine and clinopyroxene for the feldspathic clinopyroxenite, and high CaO and P_2O_5 abundances for the apatitic clinopyroxenite.

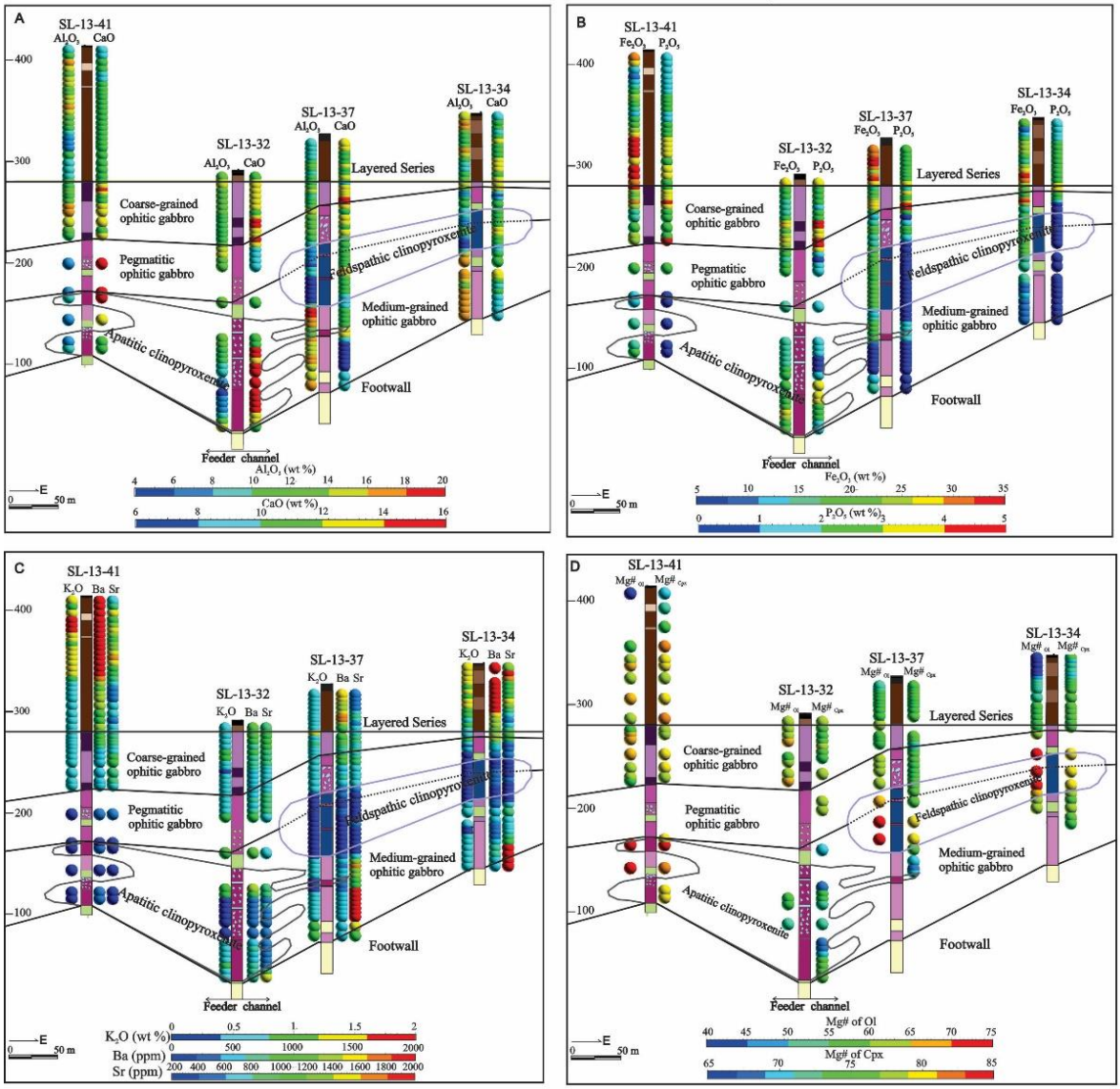

Figure 6-14. Chemical stratigraphy created based on pXRF and bSEM-EDS analyses. Legends for lithology as in Figure 6-3.

6.6 Characterization of mineralization

6.6.1 The relationship between mineralization and stratigraphy

The distribution of Cu-PGE mineralization at surface is shown in Figure 6-2. The mineralization is mainly hosted by, and has a similar strike with, the ophitic gabbro

of the Marathon Series. To further examine the relationship between the mineralization and stratigraphy and determine the types of mineralization, down-hole variations in Cu/Pd (calculated using exploration assay provided by Stillwater Canada Inc.) relative to igneous stratigraphy are shown in Figure 6-15 because, this ratio can be used to evaluate whether the mineralization is PGE rich or Cu rich. In addition, boundaries of mineralization that were defined by Stillwater Canada Inc. were added in this figure.

Generally, three types of mineralization characterized by different Cu/Pd are recognized. Type 1 mineralization is Cu-rich and PGE-poor, with Cu/Pd >16000. It is mainly hosted by the coarse-grained ophitic gabbro, with lesser amounts hosted by the medium-grained ophitic gabbro. Type 2 is PGE mineralization with Cu/Pd varying from 2000 to 10000. It is mainly hosted by the apatitic clinopyroxenite, with lesser amounts hosted by the pegmatitic ophitic gabbro. Type 3 mineralization is characterized by high PGE grades and low Cu contents, with Cu/Pd <2000. This mineralization type is predominantly hosted by the pegmatitic ophitic gabbro.

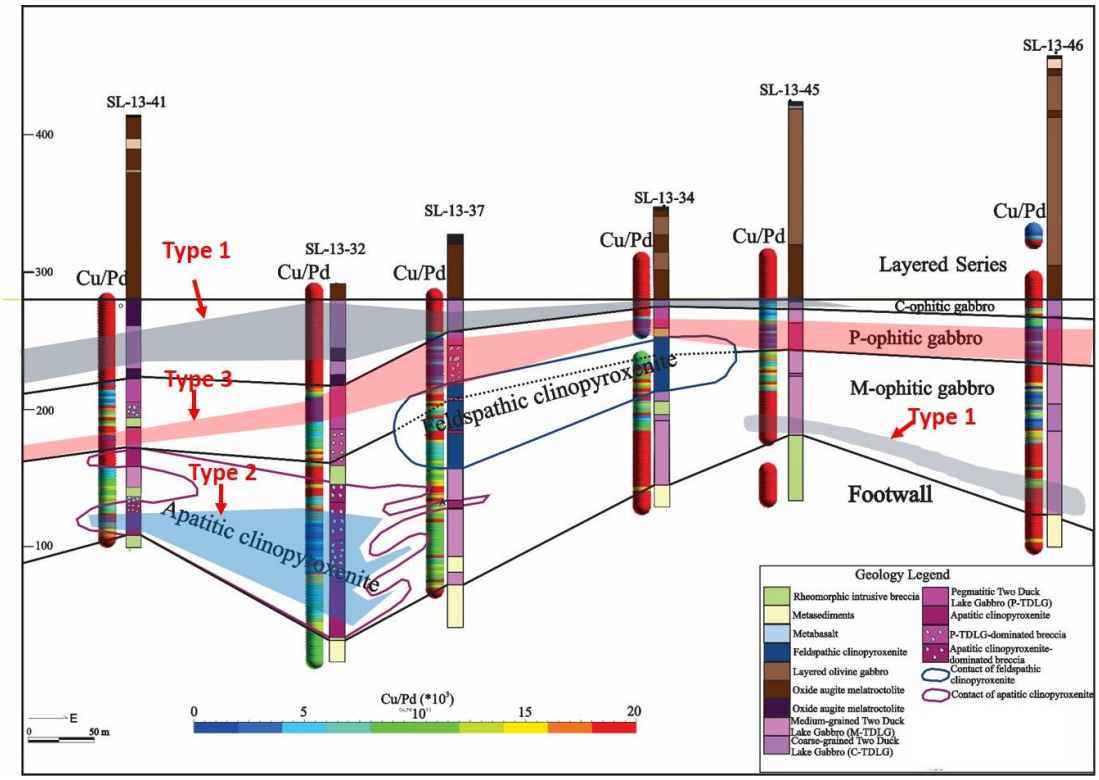

Figure 6-15. Longitudinal section showing stratigraphic distributions of Cu/Pd and different types of mineralization. The column represents drill holes, and bubbles at both sides of the column represent geochemical values. Different types of sulfide mineralization (see text for full details) are outlined using coloured transparent shaded columns. Prefix: P-pegmatitic, C-coarse-grained, M-medium-grained.

6.6.2 Sulfide minerals and textures

In this section, sulfide minerals within the pegmatitic, coarse-grained, and medium-grained ophitic gabbro, as well as those within the apatitic clinopyroxenite are described with emphasis on their mineralogy and textures. The bulk of sulfide mineralization in these units is disseminated that generally comprises less than 5 modal percent of the rock and are dominantly interstitial to the silicate minerals. However, sulfide mineralogy appears to be different in these units, particularly the relative proportions of pyrrhotite and chalcopyrite.

6.6.2.1 Medium-grained ophitic gabbro

In medium-grained ophitic gabbro, sulfide minerals generally consist of pyrrhotite, chalcopyrite, with minor amounts of cubanite and pentlandite. The relative proportion of pyrrhotite is higher than that of the chalcopyrite, and in rare cases the

pyrrhotite appears to be the dominant sulfide phase (Fig. 6-16A). In addition, chalcopyrite normally replaces pyrrhotite, and both are very rarely associated with hydrous silicate minerals (Fig. 6-17A). Samson et al. (2008) also observed the replacement of pyrrhotite by chalcopyrite in mineralized samples at the Marathon deposit.

6.6.2.2 Coarse-grained ophitic gabbro

The coarse-grained ophitic gabbro also contains pyrrhotite and chalcopyrite as the main sulfide minerals. However, compared to the medium-grained ophitic gabbro, it has a higher relative proportion of chalcopyrite (Fig. 6-16B). In addition, minor pentlandite is rimed by chalcopyrite (Fig. 6-17B). Sulfide minerals in this unit normally are interstitial to silicate minerals, locally the chalcopyrite and pyrrhotite are closely related to secondary magnetite aggregates (Fig. 6-17C). The secondary magnetite is free of ilmenite exsolution and does not show a visible Ti peak in the X-ray spectrum when analyzed by bSEM-EDS.

6.6.2.3 Pegmatitic ophitic gabbro

The modal percent of sulfide minerals in the pegmatitic ophitic gabbro varies significantly from 10% (Fig. 6-16C) to less than 0.5% (Fig. 6-16D). Sulfide minerals consist predominantly of chalcopyrite and pyrrhotite, with minor amounts of pentlandite, cubanite, galena, pyrite, and trace bornite. The relative proportion of chalcopyrite in this unit is higher than that in the coarse- grained ophitic gabbro. This is particularly true for the pegmatitic ophitic gabbro with trace sulfide minerals (<0.5 modal %) where the relative proportion of chalcopyrite can increase up to nearly 100% (Fig. 6-16D). Sulfide minerals normally occur either interstitial to primary silicate minerals, or show close associations with secondary minerals such as amphibole, chlorite, and secondary magnetite (Fig. 6-19D). Some chalcopyrite is intergrown with plagioclase (Figs. 6-17E and F), which replaces the earlier less calcic plagioclase (Fig. 6-6). In the case when the pegmatitic ophitic gabbro contains trace sulfide minerals, chalcopyrite grains occur interstitial to primary olivine grains (Figs. 6-17G and H). It is noteworthy that these chalcopyrite grains commonly

enclose, or show close spatial relations, to PGM minerals, and locally are rimed by pyrrhotite, pentlandite, secondary magnetite, and/or partially are overlapped by chlorite (Fig. 6-17H).

6.6.2.4 Apatitic clinopyroxenite

Sulfide mineral assemblage and relative proportions of chalcopyrite and pyrrhotite in the apatitic clinopyroxenite are generally similar to those in the pegmatitic ophitic gabbro (Fig. 6-16E). However, a higher amount of pyrite is observed in this unit. Pyrite grains are euhedral to subhedral, and locally occur as aggregates within calcite that are surrounded by chalcopyrite and pyrrhotite (Fig. 6-17I). Some pyrrhotite grains host many sphalerite inclusions and are replaced by chalcopyrite at their rims (Fig. 6-17J). Figures 6-17K and L show that locally sulfide minerals in this unit are rimed by secondary magnetite, which are all enclosed by hydrothermal chlorite.

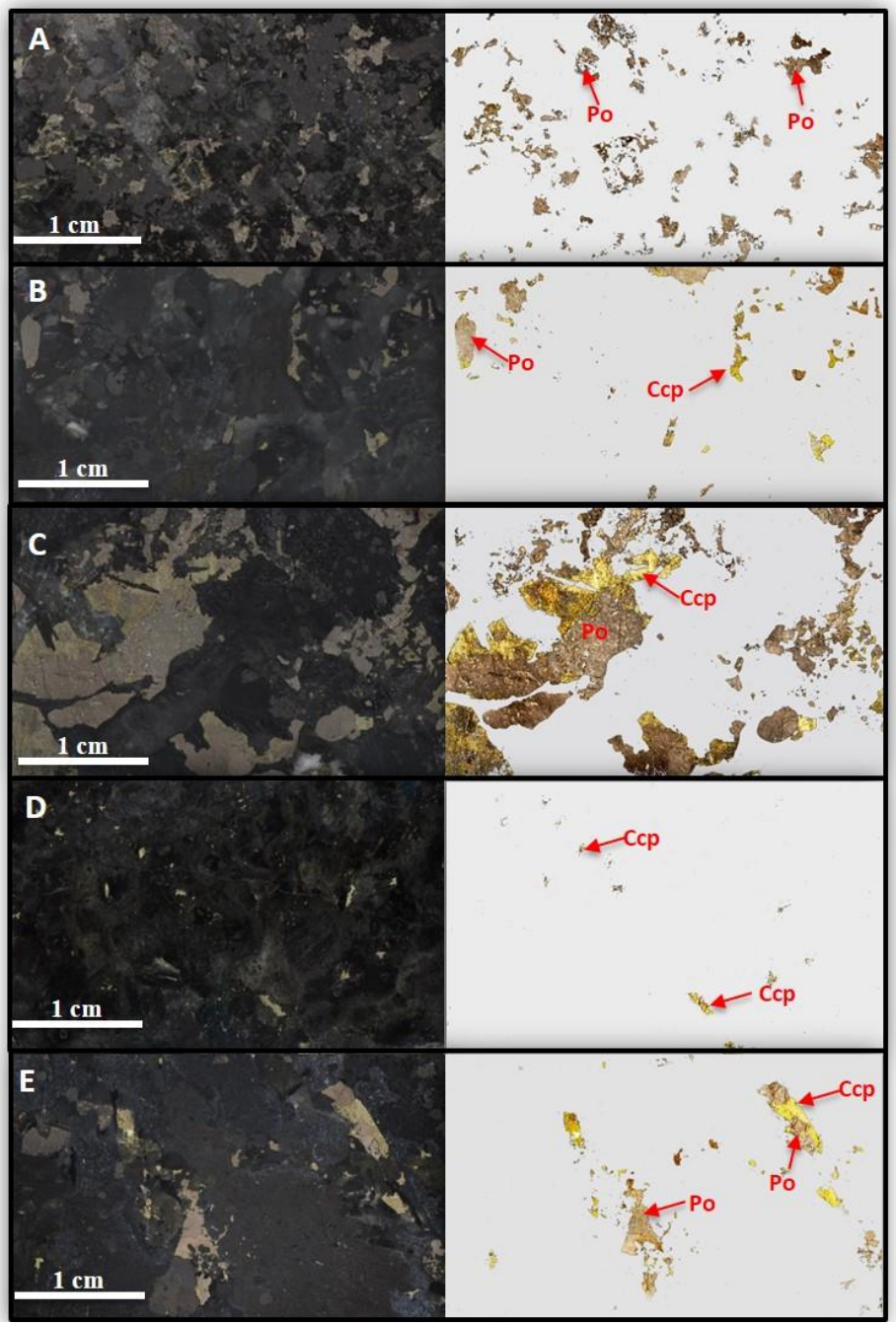

Figure 6-16. Polished thin section scans and corrected photos with sulfide mineralization highlighted and silicate phases plus magnetite ignored. (A) SL-13-36-152.8, medium-grained ophitic gabbro, Po is the dominant sulfide mineral; (B) SL-13-27-80.4, coarse grained ophitic gabbro which shows an elevated proportion of Ccp that occurs intergrown with Po; (C) SL-13-37-65.7, pegmatitic ophitic gabbro with a high proportion (>10 modal %) of sulfide mineralization, note that Ccp replaces Po; (D) SL-13-36-62, pegmatitic ophitic gabbro with trace sulfide mineralization (<0.5 modal %), Ccp is the only visible sulfide mineral; (E) SL-13-32-214.5, disseminated sulfide mineralization including Ccp and Po in apatitic clinopyroxenite. Abbreviations: Ccp=chalcopyrite, Po=pyrrhotite.

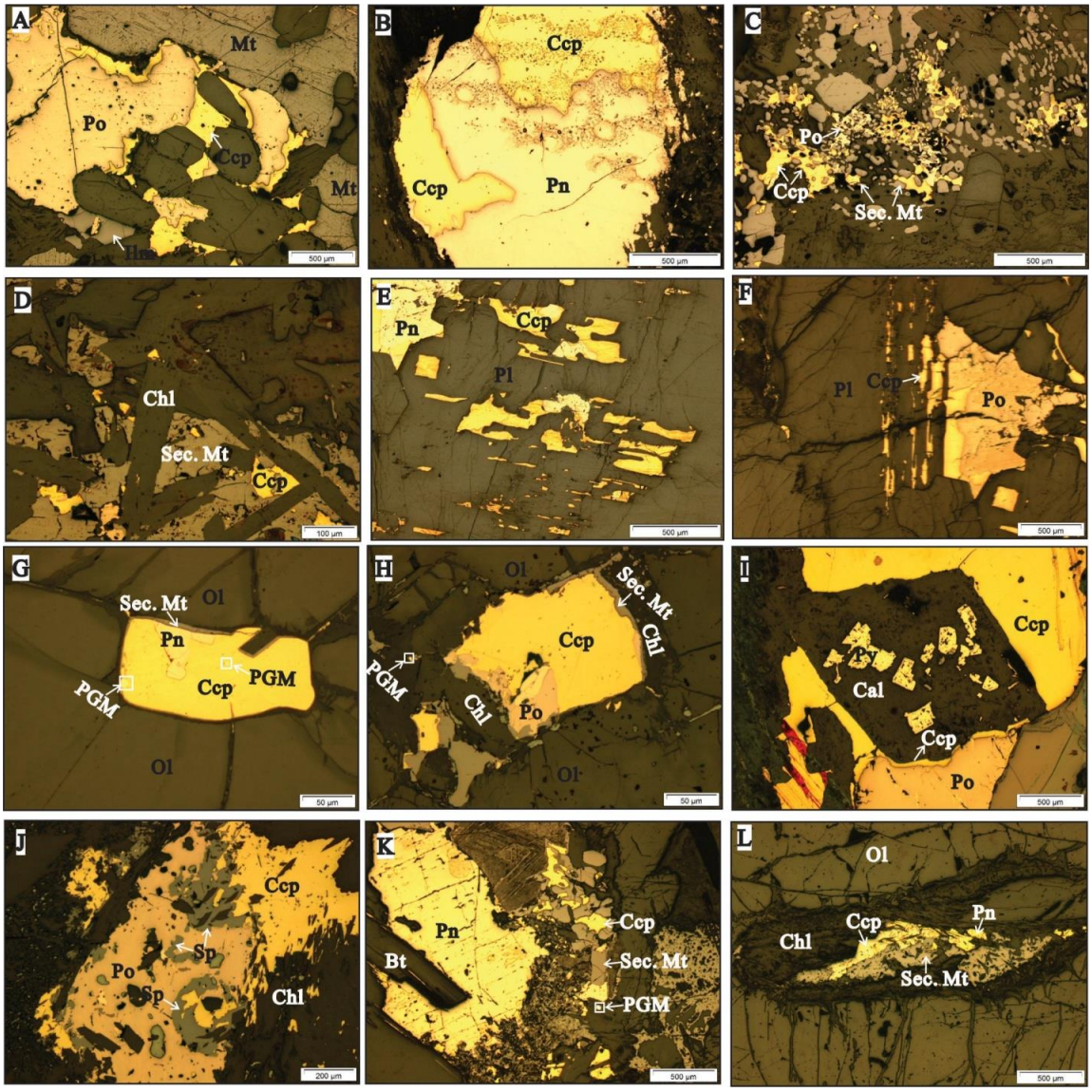

Figure 6-17. Reflected light photomicrography showing the assemblage and textures of sulfide minerals. (A) SL-13-36-156.8 medium-grained ophitic gabbro, Ccp replaces Po, both are interstitial to plagioclase, olivine, and clinopyroxene; (B) SL-13-32-37 coarse-grained ophitic gabbro, Pn is replaced by Ccp at the rim; (C) SL-13-27-80.4 coarse-grained ophitic gabbro, tiny grained Ccp and Po occur rimed or surrounded by secondary Mt; (D) SL-13-37-70 pegmatitic ophitic gabbro, Ccp grains are replaced by secondary Mt, all are surrounded by chlorite clusters; (E)-(F) SL-13-32-165.5 pegmatitic ophitic gabbro, Ccp and Pn (and Po) occur intergrown with Pl; (G)-(H) SL-13-37-80.05 pegmatitic TDLG, the separate Ccp grain interstitial to olivine aggregates, the Ccp is rimed by secondary Mt and hosts some PGM grains; (I) SL-13-32-204.5 apatitic clinopyroxenite, Py aggregates surrounded by Ccp and Po; (J) SL-13-36-76 apatitic clinopyroxenite, Po contains many Sp inclusions and have Ccp rims; (K) SL-13-34-75 apatitic olivine clinopyroxenite, Pn and Ccp are surrounded by hydrothermal minerals, note the Ccp is partially replaced by secondary Mt and there is a PGM grain related to the Ccp; (L) SL-13-34-75 apatitic clinopyroxenite, Ccp and Pn are replaced by secondary Mt, all are enclosed by hydrothermal Chl. Abbreviations: Cal-calcite,

Ccp=chalcopyrite, Chl-chlorite, Mt=magnetite, Pn=pentlandite, Po=pyrrhotite, Py=pyrite, Sp=sphalerite.

6.6.3 Platinum-group minerals (PGM) mineralogy

A detailed characterization of PGM and gold minerals for Area 41 occurrence was conducted by Cabri (2014). In that study, samples were screened, split, assayed size by size, and followed by high-grade heavy mineral concentrates using hydroseparation. Mineral separates (238 grains) were then mounted on monolayer polished sections (6 polished sections) and analyzed by SEM-EDS. Cabri (2014) concluded that the PGM mineralogical compositions vary significantly, but can be basically subdivided into two groups: Pd-PGM and Pt-PGM. By mass%, the plumbian PGM (e.g., zvyagintsevite) and sperrylite are the dominant Pd-PGM and Pt-PGM, respectively.

In this study, we conducted a separate characterization of PGM mineralogy using bSEM-EDS. Instead of using mineral separates, thin sections and thin section blocks were scanned by bSEM for the search of potential PGM minerals, their compositions are then analyzed by the equipped EDS analyzer. Compared to the method of Cabri (2014), sample preparation in this study is simpler and less time consuming. The proportions of PGM are less quantitative but PGM-related textures such as their hosts and relations to surrounding silicates can be used to establish the paragenesis of PGE mineralization, thus the results are complementary to those of Cabri (2014).

A total of 81 PGM grains were found (Table 6-8, Fig. 6-18). Of them, 68.75% (55 grains) are Pd-PGM, 21.25% (17 grains) are Pt-PGM, 10% (8 grains) are electrum and telluride minerals including Au-Ag and Ag-Te alloys. Sperrylite is the dominant Pt-PGM, similar to results of Cabri (2014). In addition, the most common Pd-PGM is kotulskite which is also the most frequent Pd-PGM found by Cabri (2014). Thus, results of the current work are comparable to those of Cabri (2014), and the bSEM-EDS is capable of providing reliable results on PGM characterization.

Representative thin sections with PGE grades, Cu/Pd ratios, degrees of alteration, and PGM assemblages are tabulated in Table 6-9. Backscattered images of representative PGM minerals are displayed in Figure 6-19. Kotulskite is the most common PGM and is present in both fresh and extensively altered samples. Skaergaardite, tetraferroplatinum, plumbopalladinite grains were commonly observed in fresh samples. By contrast, As-, Sb-, and Te-bearing PGM such as sperrylite, arsenopalladinite, menshikovite, hollingworthite, mertierite-II, stillwaterite, and telluride were only found in samples with minor, moderate and extensive alteration. Backscattered images show that the kotulskite occurs typically as inclusions or at margins of base metal sulfide minerals such as chalcopyrite, pyrrhotite, pyrite, and pentlandite (Figs. 6-19A and B). Rarely, kotulskite is intergrown with stillwaterite and mertierite-II that form the PGM aggregates (Figs. 6-19C and D). Skaergaardite, isoferroplatinum, and tetraferroplatinum are typically occur within or at the margins of chalcopyrite grains (Figs. 6-19E-H). Some PGM grains, particularly As-bearing PGM are enclosed by secondary minerals such as chlorite, amphibole, and actinolite (Figs. 6-19I-K). However, magmatic sulfide grains are also observed in the very proximity of these PGM grains. Telluride minerals and electrum are observed within chalcopyrite grains (Fig. 6-19L).

Table 6-8. Mineralogy of Platinum Group Minerals

PGM	Formula	No.	Description
Sperrylite	$PtAs_2$	13	Commonly hosted by secondary minerals in the vicinity of sulfides, some occur at the contact of Pl grains or intergrown with Ccp
Tetraferroplatinum	PtFe	3	Commonly occur intergrown with Ccp, or as inclusions in Ccp
Isoferroplatinum	$(Pt, Pd)_3Fe$	1	Intergrown with Ccp
Kotulskite	Pd(Te,Bi)	34	Mostly occur as inclusions or at margins of Ccp, Po, and Pn, rarely is enclosed by Py, Hbl, and Pl
Arsenopalladinite	$Pd_8(As, Sb, Te, Bi)_3$	6	Mostly show close relations to secondary minerals such as Act and Amph, rarely within Pl and Ccp.
Menshikovite	$Pd_3As_3Ni_2$	5	Commonly at the contact between Ccp and Pl, or secondary minerals

Hollingworthite	(Rh, Pt, Pd)AsS	3	Commonly at the contact between sulfides and biotite (secondary?), or within allanite.
Mertierite-II	$Pd_8(Sb)_3$	3	Intergrown with kotulskite
Sobolevskite	PdBi	2	Hosted by Ccp
Stillwaterite	Pd_8As_3	1	Intergrown with kotulskite
Plumbopalladinite	Pd_3Pb_2	1	Within Pl
Skaergaardite	PdCu	1	Intergrown with Ccp
Telluride	Ag_2Te	3	Within Pl and Ccp
Electrum	Au-Ag	5	Intergrown with Ccp

Mineral abbreviations: Amph=amphibole, Ccp=chalcopyrite, Hbl=hornblende, Pl-plagioclase, Pn=pentlandite, Po=pyrrhotite, Py=pyrite, Sp=sphalerite.

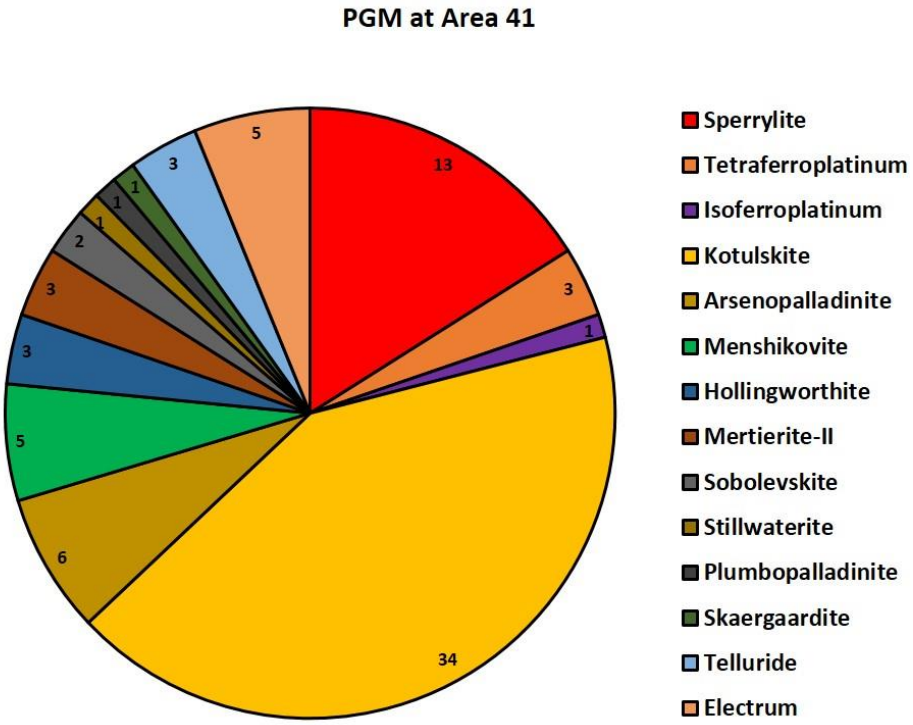

Figure 6-18. The pie diagram showing proportions of different PGM minerals observed in the current study, number for each type PGM is indicated.

Table 6-9. PGE assay, Cu/Pd, degree of alteration, and the observed PGM assemblages for representative thin sections.

DDH	Depth/m	Rock unit	Pt (ppb)	Pd (ppb)	Cu/Pd	Alteration	Observed PGM assemblage
SL-13-32	80.5	Pegmatitic ophitic gabbro	1755	5270	30.55	Fresh	Skaergaardite, Tetraferroplatinum, Plumbopalladinite
	90.55	Pegmatitic ophitic gabbro	1205	1715	950.44	Moderate	Sperrylite, Kotulskite, Arsenopalladinite, Hollingworthite
	165.5	Apatitic clinopyroxenite	340	536	3619.40	Minor	Telluride, Kotulskite, Sperrylite
	204.5	Apatitic clinopyroxenite	172	345	6637.68	Moderate	Sperrylite, Kotulskite
	214.5	Apatitic clinopyroxenite	147	358	8547.49	Moderate	Kotulskite, Electrum
	219	Apatitic clinopyroxenite	124	308	5860.39	Fresh	Kotulskite
	234.4	Apatitic clinopyroxenite	139	228	9780.70	Minor	Kotulskite
SL-13-36	53.5	Pegmatitic ophitic gabbro	938	1345	593.31	Fresh	Plumbopalladinite, Kotulskite
	57.3	Pegmatitic ophitic gabbro	1450	2030	894.09	Moderate	Tetraferroplatinum, Menshikovite, Sperrylite, Arsenopalladinite, Mertierite-II, Isoferroplatinum, Kotulskite, Electrum
	62	Pegmatitic ophitic gabbro	865	1220	1254.10	Minor	Kotulskite, Mertierite-II, Electrum
	63	Pegmatitic ophitic gabbro	647	963	3624.09	Moderate	Kotulskite, Sperrylite
	74	Apatitic clinopyroxenite	447	873	3482.25	Extensive	Sperrylite
	76	Apatitic clinopyroxenite	167	248	12459.68	Extensive	Telluride
SL-13-37	65.7	Pegmatitic ophitic gabbro	495	163	11748.47	Moderate	Rh-rich Hollingworthite
	70	Pegmatitic ophitic gabbro	2180	2990	206.02	Minor	Sperrylite, Kotulskite
SL-13-34	75	Apatitic clinopyroxenite	514	283	7632.51	Minor	Sperrylite

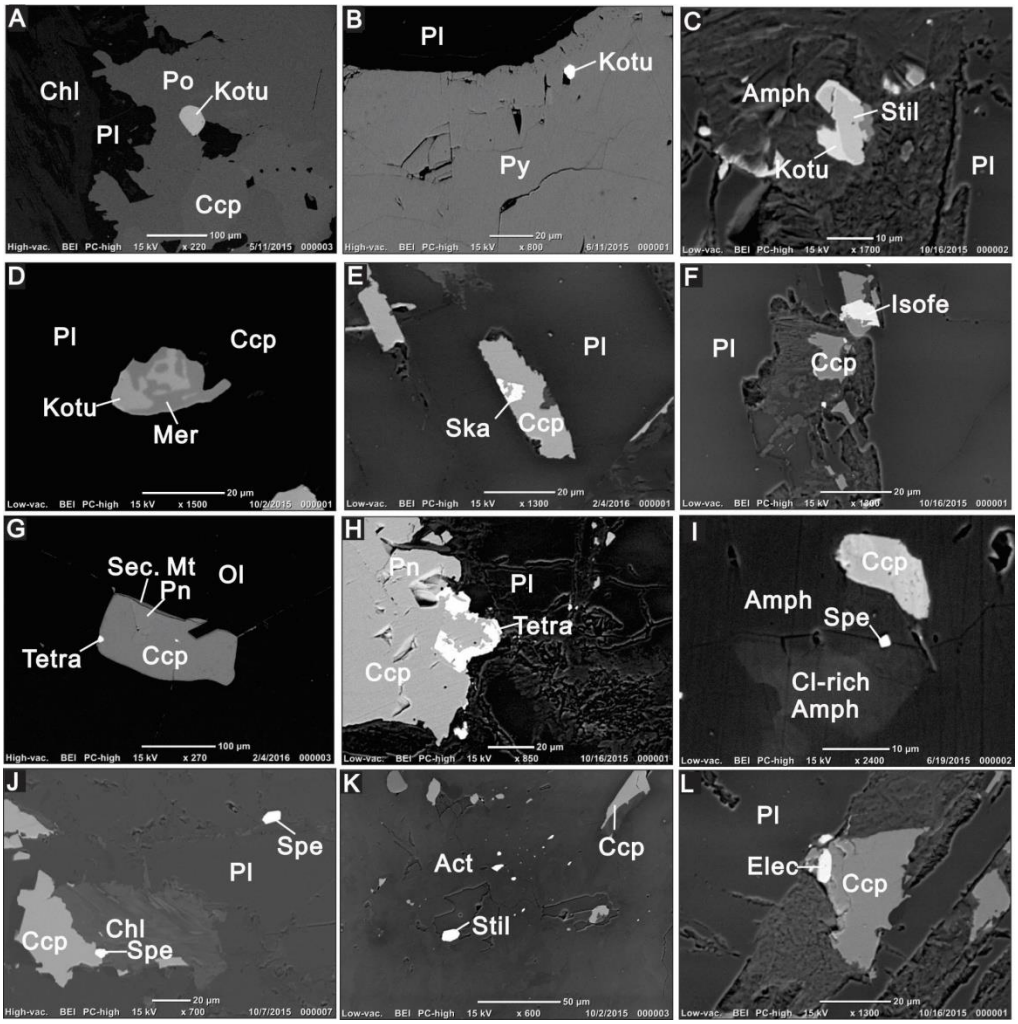

Figure 6-19. Backscatter images of PGM minerals. (A) SL-13-32-214.5 apatitic clinopyroxenite, Kotu inclusion in Po, Po is intergrown with Ccp; (B) SL-13-32-204.5 apatitic clinopyroxenite, Kotu inclusion in Py; (C)-(D) SL-13-36-57.3 pegmatitic ophitic gabbro, composite PGM grains; (E) SL-13-37-80.05 pegmatitic ophitic gabbro, Ska inclusions in Ccp, all are within the fresh Pl; (F) SL-13-37-80.05 pegmatitic ophitic gabbro, Isofe occurs intergrown with Ccp, hosted by an unidentified silicate mineral; (G) SL-13-37-80.05 pegmatitic ophitic gabbro, Tetra inclusions in Ccp, Ccp is interstitial to fresh Ol cumulates and is rimed by hydrothermal Mt; (H) SL-13-37-80.05 pegmatitic ophitic gabbro, Tetra occurs intergrown with Ccp at the margin; (I) SL-13-32-90.05 pegmatitic ophitic gabbro, Spe and Ccp hosted by Amph, a patchy Cl-rich Amph is also observed; (J) SL-13-37-70 pegmatitic ophitic gabbro, Spe is spatially related to Chl; (K) SL-13-36-62 pegmatitic ophitic gabbro, Stil inclusions in Act aggregates; (L) SL-13-36-57.3 pegmatitic ophitic gabbro, Elec grains in Ccp. Abbreviations: Act=actinolite, Amph=amphibole, Ccp=chalcopyrite, Chl=chlorite, Elec=electrum, Holl=Hollingworthite, Isofe=isoferroplatinum, Kotu=kotulskite, Mt=magnetite, Mer=Mertierite-II, Ol=olivine, Pl=plagioclase, Pn=pentlandite, Po=pyrrhotite, Py=pyrite, Ska=skaergaardite, Spe=sperrylite, Stil=Stillwaterite, Tetra=tetraferroplatinum.

6.6.4 Inter-element relationships

Developing an understanding of the inter-relationships for Cu, Pd, Pt, Ir, Rh, S, and Se is key to unravel the dominant processes responsible for sulfide deposition at Area 41. Cu, S, Pd, and Pt used in this section mostly are Stillwater Inc. exploration assays, Rh, Ir, Se and additional Cu and S results are from analyses on a small subset of PGE well mineralized pegmatitic ophitic gabbro samples. Note that only Marathon Series samples that contain >0.01 ppm Pd and Pt are considered in this section. Most coarse-grained ophitic gabbro is PGE-poor (Cu/Pd>10000 and <0.01 ppm Pt+Pd) with PGE grades orders of magnitude lower than other rock types, thus this filter only allows a small subset of this unit to be included.

Whole-rock Cu/S is largely dependent on proportions of chalcopyrite, pyrrhotite, and bornite, thus it can be used to predict proportions of sulfide minerals. Figure 6-20A shows that all samples fall along a positive trend within the field between 100% chalcopyrite and 95% pyrrhotite. Specifically, the medium-grained ophitic gabbro contains a higher abundance of sulfur than other units and plots close to the 5% chalcopyrite-95% pyrrhotite line, indicating that the dominant sulfide mineral of this unit is pyrrhotite. Compared to the medium-grained ophitic gabbro, the coarse-grained ophitic gabbro has a slightly higher proportion of chalcopyrite. The pegmatitic ophitic gabbro and the apatitic clinopyroxenite samples plot close to the 50% chalcopyrite-50% pyrrhotite line, some of pegmatitic ophitic gabbro samples even almost fall along the 100% chalcopyrite line. These suggest that the pegmatitic ophitic gabbro and apatitic clinopyroxenite contain higher proportions of chalcopyrite than the medium-grained and the coarse-grained ophitic gabbro. All these observations agree with petrographic descriptions in section 6.6.2.

Three important observations on Pd vs. S and Pt vs. S diagrams (Figs. 6-20B and C) are: 1) there is a positive relationship between Pd (and Pt) and S for the medium-grained ophitic gabbro, but not for the other units; 2) several pegmatitic ophitic gabbro samples are very enriched in Pd and Pt (Pd>3000 ppb, Pt>1000 ppb Pt, type

3 mineralization), but contain trace amounts of sulfide minerals as reflected by their low S contents (<0.1 wt.%); and, 3) the similarity between Pd vs. S and Pt vs. S diagrams indicate the coherent behaviour of Pd and Pt, Pd/Pt ratios for all rock units are within 1-4 (Fig. 6-20D). However, Figure 6-20E displays a general increasing Pd/Pt with increasing Pt trend and so the behavior is nonlinear and can best be fit by a power expression.

Figure 6-20F shows that the medium-grained ophitic gabbro generally falls along the line of Cu/Pd =10000. By contrast, the coarse-grained and pegmatitic ophitic gabbro, as well as the apatitic clinopyroxenite show poor correlations between Cu and Pd. Cu/Pd values for the apatitic clinopyroxenite are generally within 1000-10000 (the mantle range), whereas those for the pegmatitic ophitic gabbro vary significantly from <500 to >10000.

Figures 6-20G-I show that there are good correlations between Pd and Ir, Pd and Rh, and Ir and Rh for selected PGE-enriched pegmatitic ophitic gabbro samples. In addition, this suite of samples has S/Se ratios vary between 800 and 2000 with an average of *ca.* 1200 (Fig. 6-20J), which are below the mantle range and similar to S/Se of the PGE mineralized samples at W-horizon of the Marathon deposit as measured by Ruthart (2013). Figures 6-20 K and L show that this suite of pegmatitic ophitic gabbro samples has a negative relationship between PGE (Pd+Pt) grade and S/Se, and has a poor relationship between Pd/Ir and S/Se, with Pd/Ir nearly constant at around 400. Figure 6-21 shows that S/Se ratios for this suite of samples present a zig-zag down-hole variations, which is in a roughly opposite sense with the down-hole profile of Pt+Pd. Both are significant different with the profile of the degree of alteration which seems generally increase with depth (Fig. 6-21).

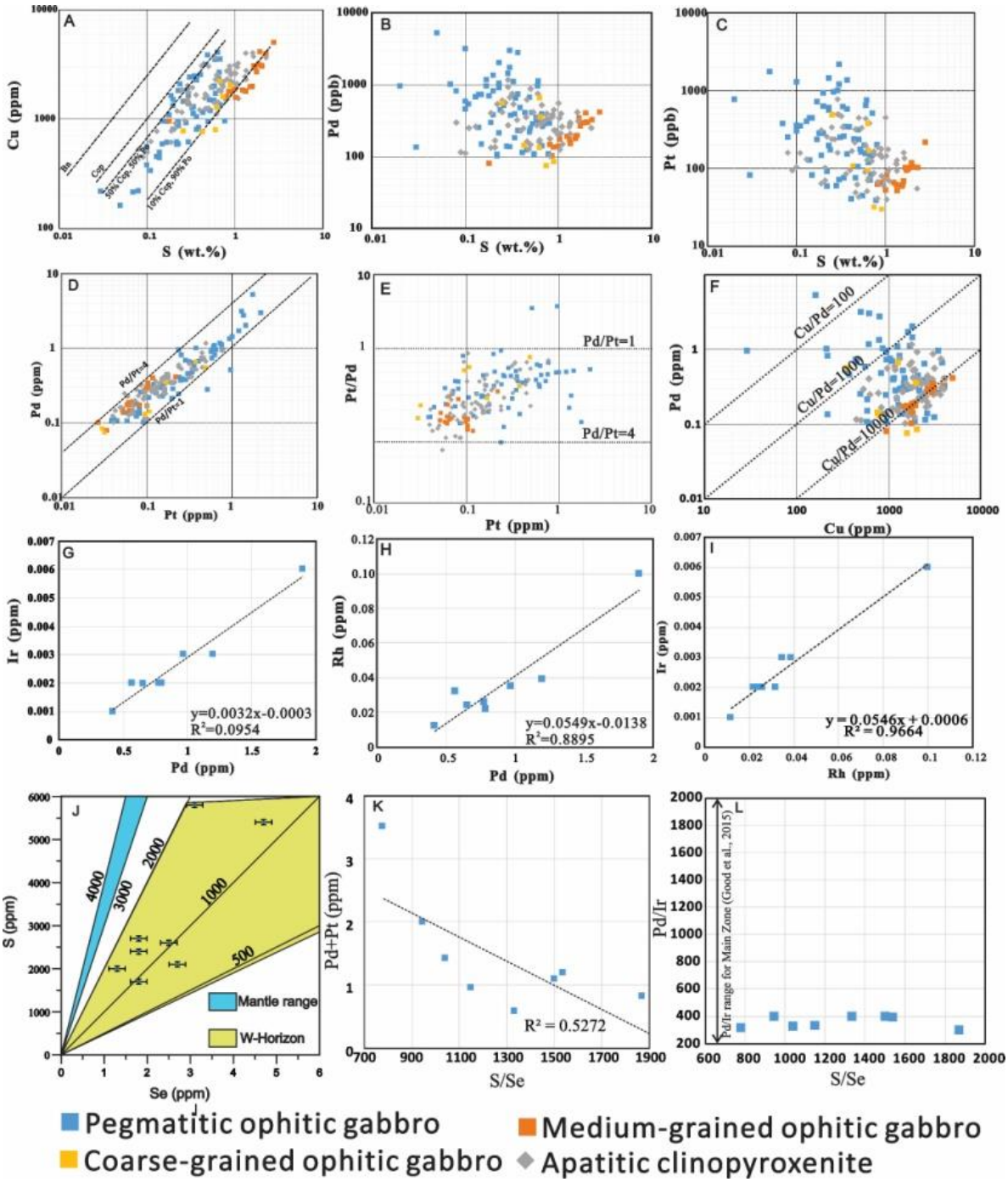

Figure 6-20. Inter-element relationships between PGE elements, S, and Se for sulfide mineralized samples at Area 41. (A) Cu vs. S, dashed lines indicate different proportions of chalcopyrite and pyrrhotite; (B) Pd vs. S; (C) Pt vs. S; (D) Pd vs. Pt; (E) Pt/Pd vs. Pt; (F) Pd vs. Cu, dashed lines indicate different Cu/Pd ratios; (G) Pd vs. Ir; (H) Pd vs. Rh; (I) Rh vs. Ir; (J) S vs. Se, the error bar represents 2 σ analytical precision determined by multiple analyses on the same sample; (K) (Pd+Pt) vs. S/Se; (L) Pd/Ir vs. S/Se.

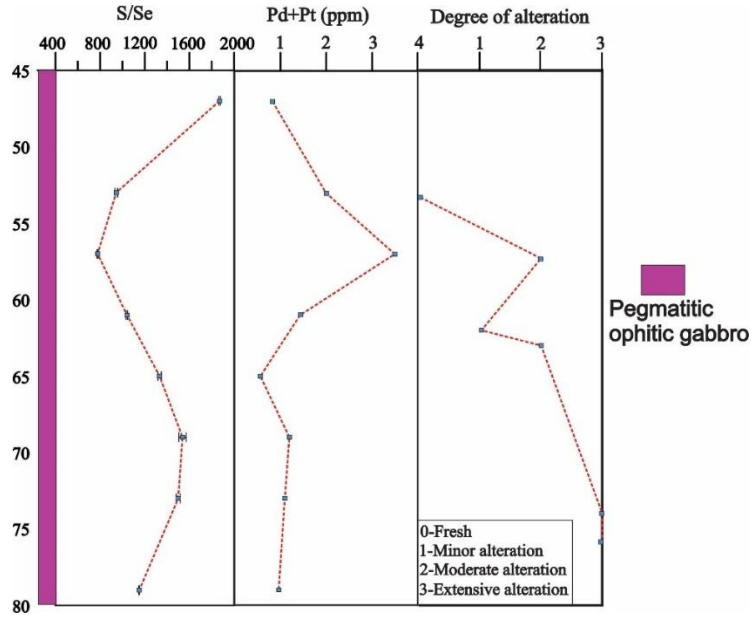

Figure 6-21. Down-hole variation in S/Se, Pt+Pd, and the degree of alteration for PGE well mineralized pegmatitic ophitic gabbro in SL-13-36.

6.7 Discussion

Based on examination of crosscutting and other field relationships, the following sequence of events is proposed to explain the Eastern Gabbro Suite at Area 41.

1. The meta-basalt and feldspathic clinopyroxenite are the earliest igneous events. The latter was initially emplaced as thick sills along Archean unconformity and later intruded preferentially into the Archean meta-sediments
2. Intrusion of the Layered Series as thick sills into the early formed meta-basalt. Copper sulfide mineralization occurs within the Layered Series rocks, but it is typically associated with actinolite and albite alteration and lacks PGE mineralization, similar to the Layered Series at the Marathon deposit (Good et al., 2015) and at Four Dams (see Chapter 3).
3. Intrusion of the ophitic gabbro by multiple pulses of a plagioclase-rich crystal mush that intruded through the meta-basalt and is confined by the footwall. The crystal mush intrusion crystallized three subtypes of ophitic gabbro with

different grain sizes: the medium- grained, the coarse- grained, and the pegmatitic ophitic gabbro.

4. The apatitic clinopyroxenite and oxide melatroctolite intruded along the margin of the feldspathic clinopyroxenite. The oxide melatroctolite typically cuts the coarse-grained ophitic gabbro whereas the apatitic clinopyroxenite cuts the medium- grained ophitic gabbro, and also less commonly footwall.

6.7.1 Sulfur loss

Mantle S/Se values are around 3100 to 3300, *e.g.*, 3333 (McDonough and Sun, 1995), 3300 (Hattori et al., 2002), and 3150 (Lorand et al., 2003). S/Se ratios greater than mantle values are interpreted to be the result of the contamination of the magma by sulfur-rich country rocks, whereas those lower than mantle values can indicate S loss during post-crystallization (Queffurus and Barnes, 2015). Figure 6-20J shows that S/Se ratios of PGE-enriched pegmatitic ophitic gabbro are typically within 500-2000 (1200 in average), below the mantle value, which is consistent with the S loss.

Two processes have been proposed to account for S loss: hydrothermal remobilization (Queffurus and Barnes, 2015) and partial dissolution of the sulfide by a process of 'multistage-dissolution-upgrading' (Kerr and Leitch, 2005). The involvement of hydrothermal fluids might be a reasonable interpretation in this case because: 1) sulfide minerals that are rimed by secondary magnetite commonly are surrounded by secondary minerals such as chlorite (Figs. 6-17D and L); and, 2) sulfur has a higher mobility in oxidized hydrous fluids below 300 ℃ (Queffurus and Barnes, 2015). However, Figure 6-20L shows that the PGE-enriched pegmatitic ophitic gabbro has almost constant Pd/Ir with variable S/Se, this is more consistent with a magmatic process considering the different mobilities of Pd and Ir in hydrothermal fluids (Keays et al., 1982). In addition, the poor correlation between S/Se and the degree of alteration is expected based on their different down-hole profiles (Fig. 6-21). Furthermore, the wave-like down-hole variations of S/Se

throughout around 40 m thick PGE-enriched pegmatitic ophitic gabbro (Fig. 6-21) is hard to explain by the involvement of fluids.

Instead, this pattern more likely reflects multiple injections of magma considering the variable Mg# values exhibited by the ophitic gabbro (Figs. 6-12 and 6-13), which can be linked to another mechanism named sulfide dissolution by a process of 'multistage-dissolution-upgrading'. The partial dissolution of sulfide may occur when multiple pulses of sulfur undersaturated magmas interact with a sulfide liquid. This process has been modeled by Kerr and Leitch (2005), and the result of this is the upgrading the metal tenors of chalcophile elements that have high partition coefficients into sulfide minerals, such as PGE and Se. Conversely, elements with low partition coefficients such as Fe and S will be preferentially resorbed by the magma. Therefore, the highest tenor sulfides will exhibit the lowest S/Se ratio (Ihlenfeld and Keays, 2011). This is consistent with the broad negative relationship exhibited between S/Se ratios and PGE grades for the PGE-enriched units (Fig. 6-20K).

6.7.2 Possible origins of sulfide mineralization

6.7.2.1 The role of hydrothermal fluids

Some PGE mineralized ophitic gabbro and apatitic clinopyroxenite are moderately to extensively altered by chlorite and actinolite. In addition, some PGM grains are observed within hydrothermal minerals such as chlorite and actinolite (Figs. 6-19I-K). Furthermore, in the PGE-enriched pegmatitic ophitic gabbro we observed the replacement of primary apatite and biotite by later chlorine-rich secondary apatite and biotite (Figs. 6-7 and 6-8), indicating the involvement of chlorine-rich hydrothermal fluids during generation of this unit. These fluids are capable of remobilizing PGE elements (Mathez, 1989; Marshall et al., 1999). These lines of evidence suggest that hydrothermal fluids were potentially important for PGE mineralization at Area 41.

If the hydrothermal mobilization was responsible for the concentration of Cu and PGE, then a positive correlation between the degree of alteration and PGE grades is expected. However, the detailed petrographic work show that some samples with extensive alteration actually contain lower PGE grades than those with negligible-minor alteration (Table 6-9). Furthermore, if PGE elements were concentrated by hydrothermal fluids, the mobilities of PPGE (Pt, Pd, and Rh) are different from IPGE (Ir, Os, Ru) in chlorine-rich fluids. This will result in scatter in correlations between the two groups of PGE elements (Keays et al., 1982; Holwell et al., 2014). However, ratios of Pd /Ir, and Ir / Rh in PGE-enriched samples are almost constant (Figs. 6-20G-I). Therefore, the role of hydrothermal fluids on concentrating PGE is negligible.

Alternatively, hydrothermal fluids may affect PGE mineralization through modification of PGM mineralogy. This role has been attributed by many studies to account for the mineralogical and chemical variations of the PGM in some PGE deposits, *e.g.*, the Merensky reef in the Bushveld Complex (Li et al. 2004), the J-M reef in the Stillwater Complex (Meurer et al., 1999), and Ferguson Lake deposit in Nunavut of Canada (Campos-Alvarez et al. 2012). Typically, the PGM modified by hydrothermal fluids will tend to be enriched in As, Sb, or Te, all are highly mobile elements in hydrothermal fluids. Our results show that As-, Sb-, and Te-bearing PGM such as sperrylite, arsenopalladinite, menshikovite, hollingworthite, mertierite-II, stillwaterite, and telluride are only observed in altered samples (Table 6-9) and are in association with to secondary minerals such as chlorite and actinolite, but also occurs in close proximity to sulfides (Figs. 6-19I-K). Therefore, it is likely that hydrothermal fluids were responsible for the release of PGE from sulfides, but without much transportation prior to the precipitation of PGM with modified mineralogy.

6.7.2.2 Magmatic processes

Most PGM grains are spatially related to sulfide minerals such as chalcopyrite and pyrrhotite (Figs. 6-19A, B, E, and H). In addition, element pairs Pd-Pt, Pd-Ir, Pd-Rh, and Rh-Ir (Figs. 6-20D, G, I, and J) are positively correlated, and there is a negative relationship between S/Se and PGE grades exhibited by the PGE-enriched pegmatitic ophitic gabbro (Fig. 6-20K). Cu- and Pd-enriched subzones also occur in the footwall troughs (Fig. 6-15), which is strong evidence for accumulation of sulfides in flow dynamic traps (Naldrett, 1997; Rice and Moore, 2001; Good et al., 2015). All these are evidence for a magmatic control on PGE mineralization, whereby Cu and PGE were concentrated in sulfide droplets within a magma column.

Three types of mineralization are recognized at Area 41, they are Cu-rich and PGE-poor mineralization (type 1), PGE mineralization (type 2), and Pd (and Pt)-enriched and Cu-poor mineralization (type 3) (Fig. 6-15). The following section evaluates the processes that may have given rise to the different mineralization styles.

6.7.2.2.1 Type 1 Cu-rich and PGE-poor mineralization

Type 1 mineralization is mainly hosted by the coarse-grained ophitic gabbro. It has a low PGE tenor with PGE (Pt+Pd) grade<0.01 ppm and Cu/Pd>16000. This can be the result of two possible mechanisms. First, given that sulfide saturation occurred in this system, the high Cu/Pd corresponds to a small R-factor (where R is fraction of silicate melt/fraction of sulfide liquid), e.g., <100 estimated based on the Cu/Pd vs. Pd diagram from Theriault et al. (1997). In this case, the interaction between silicate melt and sulfide liquid is minor, which suggests a magma system that is not dynamic.

However, Figures 6-12 and 6-13 show that Mg#s of olivine and clinopyroxene and whole-rock Zr of the coarse-grained ophitic gabbro fluctuate. In addition, the sample variabilities of Mg# values are greater in the coarse-grained ophitic gabbro than in the Layered Series and the feldspathic clinopyroxenite. These indicate the coarse-grained ophitic gabbro likely formed by multiple recharge events, i.e., from a

dynamic magma system. Alternatively, the poor PGE tenor of this type of mineralization could have resulted from an early sulfide saturation event. Due to high partition coefficients of PGE elements into sulfides, this earlier sulfide saturation will inevitably drive the residual magma to become PGE depleted. This interpretation may be reasonable considering that the coarse-grained ophitic gabbro sits stratigraphically above the pegmatitic ophitic gabbro which hosts the PGE-enriched type 3 mineralization (Fig. 6-15).

6.7.2.2.2 Type 2 PGE mineralization

Type 2 PGE mineralization is mainly hosted by the apatitic clinopyroxenite. The high abundance (up to 50 modal %) of apatite in this rock is significant given that apatite is typically an associate or minor phase in gabbroic rocks. Since apatite is denser (~3.19 g/cm^3, www.webmineral.com) than plagioclase (~2.68 g/cm^3, www.webmineral.com), a likely interpretation for formation of this cumulate rock is the mechanical settling of apatite during magma ascent particularly if the magma was slowed when conduits are more restricted. This mechanism was also proposed by Tollari et al. (2008) to explain the presence of nelsonite in the Sept-Iles intrusive suite, Quebec, and by Good et al. (2015) to explain the apatite-rich intrusions at the Marathon deposit.

From a mass balance perspective, the volume of magma required to produce this unit would have been much greater than the volume of the current cumulate rock. This unit has mantle range of Cu/Pd (1000-10000), reflecting small variations in R-factor, e.g., vary between 1500-10000 based on the Cu/Pd vs. Pd diagram from Theriault et al. (1997). Therefore, the apatitic clinopyroxenite might have formed by one single pulse of magma, and thus the associated type 2 PGE mineralization may be related to a mechanism whereby PGE mineralization is controlled by the accumulation of sulfides from magma in a relatively simple closed system. In this scenario, PGE tenor of sulfide minerals is governed by partition coefficients of Cu and Pd between silicate melt and sulfide liquid, and also by the R-factor, without

any further upgrading. The small variations in R-factor for this type mineralization suggest a turbulent setting for the single magma intrusion, through which, the segregated sulfide droplets were suspended and disproportionally interacted with silicate melts prior to the settlement.

5.7.2.2.3 Type 3 PGE-enriched mineralization

Type 3 mineralization is mainly hosted by the pegmatitic ophitic gabbro. This unit has fluctuating down-hole variations in Mg#s of olivine and clinopyroxene and whole-rock Zr, as well as more variable Mg# values compared to other units (Figs. 6-12 and 6-13). Both are evidence suggesting that it formed in a dynamic system that involves multiple intrusions. This is consistent with the observed replacement of earlier plagioclase by later more calcic plagioclase in the pegmatitic ophitic gabbro (Fig. 6-6). Similar textures were interpreted by Good and Crocket (1994) and Shahabifar Far (2016) as indicative of magma recharge in a conduit system.

Cu/Pd ratios for this mineralization typically vary from < 100 to 1000, which corresponds to extremely high R-factors (>10^5) based on the Cu/Pd vs. Pd diagram from Theriault et al. (1997). The mechanism to attain such high R-factors is likely related to a conduit-type dynamic magma system where Pd plus Pt tenors of sulfide minerals were progressively increased though a process of multistage dissolution upgrading, which is supported by the low S/Se ratio. This process generally involves: 1) the segregation of sulfide liquids likely due to the lowering of temperature, 2) enrichment of sulfide droplets with PGE during turbulent interaction between sulfide melt and magma within the conduit system, 3) upgrading of sulfide metal tenor when sulfide droplets were suspended and interacted with later pulses of sulfide undersaturated magma, which resulted in the dissolution of sulfide and increase of PGE tenor in the sulfide droplet, and, 4) settling of PGE-enriched sulfide liquid in a staging chamber.

6.7.3 Evidence for the feeder channel

The topography of Area 41 has deeply eroded lineaments striking in different directions (Fig. 6-2). Lineaments are commonly observed at the topography of the Coldwell Alkaline Complex. Mitchell and Platt (1982) and Walker et al. (1993) related formation of lineaments to at least two stages of faulting resulted by either the Cauldron subsidence during the formation of the Coldwell Alkaline Complex, or late block faulting at the end of formation of the Complex. This proposed fault history was consistent with observations of Good et al. (2015) at the Marathon deposit, and also agrees with observations at Area 41 that magma intruded along the earlier faulting event.

A 3D geological model (Fig. 6-22) was constructed using GOCAD^{R} to investigate the possible locations of magma feeder channels. It shows that there is a north south keel-shaped trough located below the drill hole SL-13-32 (and SL-13-31). Figure 6-2 shows that two major surface lineaments crosscut approximately at the collar of SL-13-32 (and SL-13-31), indicating a faulting setting around this trough. This trough is also filled with the thickest zone of the Marathon Series rocks (Fig. 6-3A), indicating the Marathon Series magma may initially emplace at the location of this trough. Furthermore, the occurrence of the apatitic clinopyroxenite is accumulated in, or in proximity to, this trough (Fig. 6-3A). Owing to the high density of apatite, it is reasonable to assume that the high concentration of apatite settled from the magma in the conduit during ascent. Good et al. (2015) also found that there was a close spatial relationship between the location of feeder channels and the prevalence of apatite and magnetite cumulate rocks at the Marathon deposit. Taken together, this evidence suggests the trough in the footwall is a feeder channel.

To further investigate the intrusive and spatial relationships near the trough, Figure 6-22 shows variations in thickness of the Marathon Series package, and the relative proportions of pegmatitic ophitic gabbro, breccia units, mineralized zones, apatitic clinopyroxenite, and oxide melatroctolite along a longitudinal section. Note that this

longitudinal section involves 21 representative drill holes at Area 41. The progressive decrease in these parameters away from drill hole SL-13-32 (and SL-13-31) is consistent with a scenario where magma intrusions emplaced through the feeder channel in proximity to SL-13-32, and then flowed away as sills in different directions. In addition to the feeder channel close to SL-13-32, the spatial variations suggest a feeder channel is located at the east end of this longitudinal section (Fig. 6-22). Note that drill hole SL-13-32 contains the type 3 mineralization which is interpreted to be likely related to be a conduit-type deposition (see section 6.7.2.2), the confirmation of a feeder zone close to this drill hole thus establish the relationship between the PGE mineralization and the conduit system.

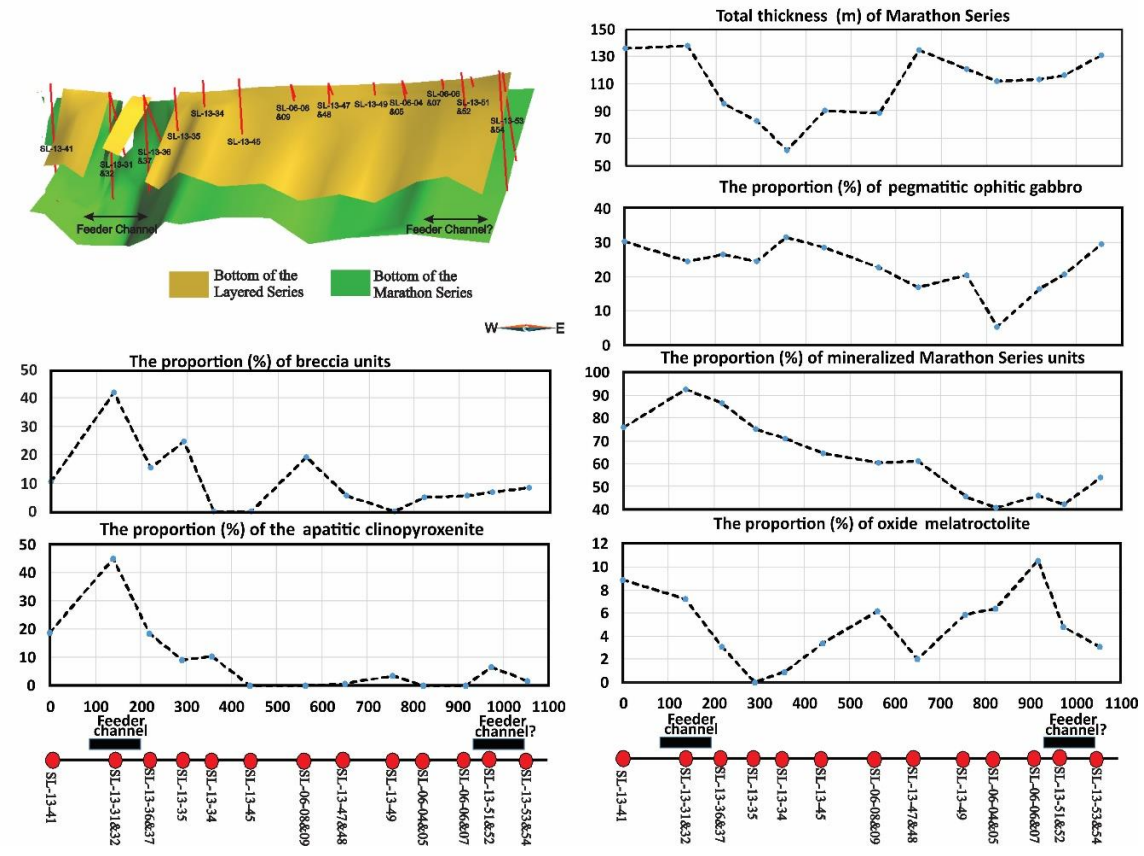

Figure 6-22. Spatial variations of the thickness of the Marathon Series rocks, the proportion of pegmatitic ophitic gabbro, the proportion of the breccia units, the proportion of mineralized Marathon Series units, the proportion of the apatitic clinopyroxenite, and the proportion of the oxide melatroctolite. The 3D model illustrates the stratigraphy of Area 41, and red lines on the cartoon represent drill holes. Drill holes are indicated using red infilled circles on the longitudinal line, potential feeder channels are indicated using the black rectangles.

6.7.4 Comparisons to the Marathon deposit and implications to mineral exploration

The Marathon deposit is the largest and best explored deposit within the Coldwell Alkaline Complex. Its PGE mineralization was defined as a contact-type by Barrie et al. (2002). However, based on well documented field, petrographic, and geochemical evidence, Ruthart (2013) and Good et al. (2015) proposed a conduit model to interpret its PGE mineralization. Four zones of PGE mineralization recognized at the Marathon deposit: Main zone, Footwall zone, Hanging-wall zone, and an extremely PGE enriched zone named W-Horizon. The Main zone and W-Horizon are of particular economic interest. The Main zone has Cu/Pd ratios typically within 1000-10000 (mantle range). It was interpreted by Good et al. (2015) to form by a closed system R-factor model within the conduit system, which is similar to the type 2 PGE mineralization at Area 41. The only difference between the two is their host units, i.e., the Two Duck Lake gabbro at the Marathon deposit whereas the apatitic clinopyroxenite at Area 41. The W-Horizon is characterized by an extreme enrichment in Pd plus Pt relative to Cu (Cu/Pd<1000), and S/Se (800 in average) (Ruthart, 2013; Good et al. 2015). Ruthart (2013) proposed that the W-Horizon formed by a 'multistage dissolution upgrading' process in a very dynamic system. The geochemical characteristics and the proposed deposition model for W-Horizon are similar with those for type 3 mineralization at Area 41.

The roughly 18-km Eastern Gabbro suite between the Marathon deposit and the Area 41 lacks mappable, continuous stratigraphic horizons, but both areas display similar types of PGE mineralization hosted by generally similar lithologies. The importance of conduit settings for PGE mineralization at both the Marathon deposit and Area 41 is that other conduits and associated PGE mineralization may occur elsewhere in the Eastern Gabbro. Recognition of this is significant because the conduit model predicts that mineralization can occur at any Marathon Series stratigraphic horizon in the Eastern Gabbro, and may contain disseminated to massive sulfides that have variable Cu/Pd and metal tenors. Furthermore, of

particular interest is that the conduit-related model also predicts the possibility for extreme PGE concentrations as a result of upgrading by a 'multistage dissolution upgrading' process, as already demonstrated by the W-Horizon at the Marathon deposit and type 3 PGE mineralization at Area 41.

6.8 Conclusions

This contribution integrates petrography, whole-rock and mineral chemistry, and 3D modeling to comprehensively characterize the igneous stratigraphy and Cu-Pd mineralization at Area 41. Important conclusions are:

(1) The units of the Eastern Gabbro assemblage are composed of three series: meta-basalt, the Layered Series, and the Marathon Series, the same as those observed at the Marathon deposit.

(2) Cu-Pd mineralization at Area 41 is hosted by the Marathon Series, particularly a pegmatitic ophitic gabbro. Lab-based and field portable instruments-based results show that at Area 41 the Marathon Series is geochemically distinctive with the meta-basalt and Layered Series, which forms a significant component for mineral exploration.

(3) Thee types of sulfide mineralization are identified at Area 41. Type 1 is the Cu-rich and PGE-poor mineralization mainly hosted by the coarse-grained ophitic gabbro, which likely formed by an early sulfide saturation event. Type 2 is the PGE mineralization mainly hosted by the apatitic clinopyroxenite, which is interpreted to form by a closed R system. Type 3 is the PGE-enriched mineralization, which is proposed to form by a 'multi-stage dissolution upgrading' process in a conduit system. The 3D modeling confirms the presence of magma feeder channel at Area 41.

(4) Overall, mineralization at Area 41 is similar with that at the Marathon Cu-Pd deposit, both are related to a conduit-type deposition, suggesting that mineralization in all probability elsewhere in the Coldwell Alkaline Complex is conduit-related.

Recognizing this will increase the potential for discovery high grade deposits in the Coldwell Alkaline Complex.

6.9 References

Anderson J.C.Ø. 2006. Postmagmatic sulphur loss in Skaergaard Intrusion: Implications for the formation of the Platinova Reef. *Lithos*, **92**, 198-221.

Ashley N., Kern E.V., Kulakov A.V., Smirnov J.F., Diehl K., and Chamberlain. 2012. Paleomagnetism of the Coldwell Alkaline Complex (Ontario, Canada): New Data and New Insights, Proceedings of the 58th Annual Meeting of the Institute on Lake Superior Geology, **1**, 53.

Barrie C.T., MacTavish A.D., Walford P.C., Chataway R., and Middaugh, R. 2002. Contact-type and magnetitite reef-type Pd-Cu mineralization in ferroan olivine gabbros of the Coldwell Alkaline Complex, Ontario. In: Cabri, L.J. (Ed.), Can. Inst. Min. Metall. Petrol., Spec. the Geology, Geochemistry, Mineralogy and Mineral Beneficiation of Platinum-group Elements, **54**, 321-338.

Cabri L.J. 2014. Mineralogical characterization of three composite samples from the Coldwell Alkaline Complex for Stillwater Canada Inc. Report to Stillwater Canada Inc., 46pp.

Campos-Alvarez N.O., Samson I.M., and Fryer B.J. The roles of magmatic and hydrothermal processes in PGE mineralization, Ferguson Lake deposit, Nunavut, Canada. Mineralium Deposita, **47**, 441-465.

Cundari R. 2012. Geology and geochemistry of Midcontinent Rift-related igneous rocks. Lakehead University M.Sc. thesis.

Currie K. 1980. A contribution to the petrology of the Coldwell alkaline complex, northwestern Ontario, in Geological survey of Canada Bulletin, 287pp.

Good D.J. and Crocket J.H. 1994. Genesis of the Marathon Cu-Platinum-Group Element Deposit, Port Coldwell Alkalic Complex: A Midcontinent Rife-related Magmatic Sulfide Deposit. Economic Geology, **89**, 131-149.

Good D.J., Epstein R., McLean K., Linnen R. L., and Samson I. 2015. Evolution of the Main Zone and the Marathon Cu-PGE Sulfide Deposit, Midcontinent Rift, Canada: Spatial Relationships in a Magma Conduit Setting. *Economic Geology*, **110**, 983-1008.

Hattori K.H., Arai S., and Clarke D.B. 2002. Selenium, tellurium, arsenic and antimony contents of primary mantle sulfides. *Canadian Mineralogist*, **40**, 637-650.

Holwell D., Keays R., Firth E., and Findlay J. 2014. Geochemistry and mineralogy of platinum group element mineralization in the River Valley Intrusion, Ontario, Canada: A model for early-stage sulfur saturation and multistage emplacement and the implication for "Contact-Type" Ni-Cu-PGE sulfide mineralization. *Economic Geology*, **109**, 689-712.

Ihlenfeld C. and Keays R.R. 2011. Crustal contamination and PGE mineralization in the Platreef, Bushveld Complex, South Africa: evidence for multiple contamination events and transport of magmatic sulfides. *Mineralium Deposita*, **46**, 813-832.

Keays R.R., Nickel E.H., Groves D.I., and McGoldrick P.J. 1982. Iridium and palladium as discriminants of volcanic exhalative, hydrothermal, and magmatic nickel sulfide mineralization. *Economic Geology*, **77**, 1535-1547.

Kerr A. and Leitch A.M. 2005. Self-destructive sulfide segregation systems and the formation of high-grade magmatic ore deposits. *Economic Geology*, **100**, 311-332.

Li C., Ripley E.M., Merino E., and Maier W.D. 2004. Replacement of base metal sulfides by actinolite, epidote, calcite, and magnetite in the UG2 and Merensky Reef of the Bushveld Complex, South Africa. *Economic Geology*, **99**, 0173-0184.

Lorand J.P., Alard O., Luguet A., Keays R.R. 2003. Sulfur and selenium systematics of the subcontinental lithospheric mantle: inferences from the Massif Central xenolith suite (France). *Geochim. Cosmochim. Acta*, **67**, 4137-4151.

Marshall D.D., Watkinson D.H., Farrow C.E.G., Molnar F., and Fouillac A.-M. 1999. Multiple fluid generations in the Sudbury Igneous Complex: fluid inclusion, Ar, O, H, Rb and Sr evidence. *Chemical Geology*, **154**, 1-19.

Mathez E.A. 1989. Vapor associated with mafic magma and controls on its composition. In: Whitney J.A. (eds.), Ore Deposition Associated with Magmas, *Reviews in Economic Geology*, **4**, 21-44.

McBride J. 2013. Assessment Report for Diamond Drill Drilling on the Stillwater Canada Inc. Bermuda Property. Thunder Bay Division, Ontario, 39pp.

McDonough W.F. and Sun S.S. 1995. Composition of the Earth. *Chemical Geology*, **120**, 223-253.

Meurer W.P., Willmore C.C., and Boudreau A.E. 1999. Metal redistribution during fluid exsolution and migration in the Middle Banded series of the Stillwater Complex, Montana. *Lithos*, **47**, 143-156.

Mitchell R.H. and Platt R.G. 1978. Mafic mineralogy of ferroaugite syenite from the Coldwell Alkaline Complex, Ontario, Canada. *Journal of Petrology*,19, 627-651.

Mulja, T. and Mitchell R. 1991. The Geordie Lake Intrusion, Coldwell Alkaline Complex, Ontario: a palladium-and tellurium-rich disseminated sulfide occurrence derived from an evolved tholeiitic magma. *Economic Geology*, **86**, 1050-1069.

Naldrett A.J. 1997. Key factors in the genesis of Noril'sk, Sudbury, Jinchuan, Voisey's Bay and other world-class Ni-Cu-PGE deposits: Implications for exploration. *Australian Journal of Earth Sciences*, **44**, 283-315.

Naldrett A.J. and Lightfoot P.C. 1999. Ni-Cu-PGE deposits of Noril'sk region, Siberia: Their formation in conduits for flood basalt volcanism: St John's. Geological Association of Canada, **104**, 195-249.

Naldrett A.J., Federenko V.A., Lightfoot P.C., Kunilov V.E., Gorbachev N.S., Doherty W., and Johan J. 1995. Ni-Cu-PGE deposits of the Noril'sk region Siberia: Their formation in conduits for flood basalt volcanism. *Transactions of the Institution of Mining and Metallurgy*, **104**, 18-36.

Queffurus M. and Barnes S.-J. A review of sulfur to selenium ratios in magmatic nickel-copper and platinum-group element deposits. *Ore Geology Reviews*, **69**, 301-324.

Rice A. and Moor J. 2001. Physical modeling of the formation of komatiite-hosted Ni deposits and a review of the thermal erosion paradigm. *Canadian Mineralogist*, **39**, 491-503.

Ruthart R. 2013. Characterization of high-PGE, low-sulphur mineralization at the Marathon PGE-Cu deposit, Ontario: M.Sc. thesis, Waterloo, ON, University of Waterloo, 145 pp.

Samson I.M., Fryer B.J., and Gagnon J.E. 2008. The Marathon Cu-PGE deposit, Ontario: Insights from sulphide chemistry and textures, in Goldschmidt conference, 820.

Shahabi Far M. 2016. The magmatic and volatile evolution of gabbros hosting the Marathon PGE-Cu deposit: evolution of a conduit system. Ph.D. thesis, The university of Windsor, Windsor, ON.

Thériault R.D., Barnes S.J., and Severson M.J. 1997. The Influence of Country-Rock Assimilation and Silicate to Sulfide Ratios (R-Factor) On the Genesis of the Dunka Road Cu-Ni-Platinum-Group Element Deposit, Duluth Complex, Minnesota. *Canadian Journal of Earth Sciences*, **34**, 375-389.

Tollari N., Barnes S.-J., Cox A., and Nabil H. 2008. Trace element concentrations in apatites from the Sept-Îles intrusive suite, Canada-implications for the genesis of nelsonites. *Chemical Geology*, **252**, 180-190.

Walker E.C., Sutcliff R.H., Shaw C.S.J., Shore G.T., and Penczak R. S. 1993. Precambrian geology of the Coldwell Alkaline Complex, Ontario Geological Survey, Open File Report 5868: 23pp.

Chapter 7
Discussions and Conclusions

7.1 Discussions

Petrography, lithogeochemistry (pXRF- and lab-based), geochemical modeling, 3D modeling, and mineral chemistry (bSEM-EDS- and electron microprobe-based) were applied as main means in this thesis to address the three main problems as set up in Chapter 1. The overall objective of this project was to: 1) develop a field-suitable exploration tool to help mineral exploration at the whole Coldwell Alkaline Complex, 2) examine the genesis of the Layered Series and its relevance to PGE mineralization, and, 3) develop a general exploration model applicable for the whole Coldwell Alkaline Complex. The successful accomplishment of the goal in this thesis will provide at least three implications for mineral exploration, as well as the understanding of geology and associated Cu-PGE mineralization, in the Coldwell Alkaline Complex and elsewhere.

7.1.1 Implications of mineral exploration

This thesis demonstrated that the pXRF and bSEM-EDS results can be applied to explore for Cu-Pd along the entire Eastern Gabbro package in the Coldwell Alkaline Complex by measuring aspects that are consistent with the deposit model, such as: 1) high Cu/S ratios as a vector to mineralization; 2) identification of platinum group minerals in favorable magma recharge zones; and, 3) inter element ratios that help to distinguish the Marathon Series from the Layered Series.

Since Platinum-group elements, particularly Pd and Pt, tend to preferentially partition into the Cu-rich residual liquid after MSS crystallization (Howell and McDonald, 2010). Provided that the magmatic sulfide liquids fractionated MSS, Pd and Pt would be concentrated in areas where Cu-rich sulfide minerals, such as chalcopyrite, cubanite, and bornite, are abundant, all of which have high Cu/S ratios. Barnes and Ripley (2016) also suggested that the Cu-rich ores are normally enriched

in Pd and Pt. Examples of PGE mineralization concentrated in high Cu-rich ores include the PGE-enriched sulfide horizons at the Dunka Road Cu-Ni-PGE deposit at the Duluth Complex, which are typically composed of intergrown chalcopyrite, cubanite, and pentlandite, with less abundant pyrrhotite (Theriault et al., 1997), and the Platinova Reef in the Skaergaard Intrusion where magmatic sulfide minerals are present as a Cu-rich, Fe-poor assemblage (Nilsen, 2001). It is thus reasonable to suggest that high Cu/S proxy as an exploration tool may also be applicable to other PGE-dominated deposits. This indicates that pXRF can be used to explore for Cu-PGE at other settings.

In addition, magma recharge is considered favorable for PGE mineralization because: it implies the existence of a magma conduit setting, whereby PGE mineralization can be controlled by various fluid dynamic processes (Marsh, 2006), and, 2) the sulfide tenor can be gradually upgraded through a magma recharge process (Kerr and Leitch, 2005), thus increasing the potential for discovery of high-grade deposits. Therefore, using the combination of pXRF and bSEM-EDS to envisage magma conduits as an exploration tool may also be applicable to PGE deposits in other settings.

At least, but not least, geochemically mapping the igneous stratigraphy is key to mineral exploration at elsewhere, not only limited to PGE-related deposits, but also may apply to other types of deposits. This is particularly true when mineralization is only hosted by certain stratigraphic horizons that are geochemically distinctive with other horizons. For example, the Tamarack magmatic sulfide deposit consists of two intrusive units such as fine-grained olivine and coarse-grained olivine intrusions, but the latter is a preferable host to mineralization (Taranovic et al., 2016). The thesis has demonstrated the considerable promise of using pXRF and bSEM-EDS to map the igneous stratigraphy at the Coldwell Alkaline Complex, both techniques can be combined to map the igneous stratigraphy at other complex settings to serve mineral exploration.

7.1.2 Implications for petrogenesis of the layered gabbro

Portable XRF and bSEM-EDS results show that the Layered Series at Four Dams and Area 41 has different fractionation trends, indicating different processes occurred for the Layered Series at different locations of the Eastern Gabbro. This aroused an academic interest regarding the development of the Layered Series, which were further examined by applying lab-based results in this thesis. This means that the combination of pXRF and bSEM-EDS also can be combined to improve hypothesis testing regarding the petrogenesis of intrusions from elsewhere.

It has long been assumed that the layered rocks represent an upward-aggrading piles of crystals deposited on the floor of a vast, long-lived magma chamber (Wagner, 1929; Cameron, 1980; Kruger, 2005). However, over the past decade a new concept that challenges this long recognized model has been growing, which suggests that the ultramafic layers formed by out-of-sequence injection of thin sills into order mafic layers (Mitchell and Scoon, 2007, 2012; Mungall et al., 2016). Mungall et al. (2016) examined the Rustenburg Layered Suite of the enormous Bushveld Igneous Complex using U-Pb geochronology and suggested that it formed within a stack of discrete sheet-like intrusions emplaced and solidified as separate bodies beneath older layers. The current study suggests that the Layered Series at the Coldwell Alkaline Complex formed by multiple intrusions within a conduit system, which provides a good example to the new school of recognition regarding the development of large layered intrusions. In addition, this thesis also has discussed possible reasons for the lack of PGE mineralization of the Layered Series that formed in magma conduits. Since magma conduits are favorable for PGE mineralization (Naldrett, 1999), the study of the Layered Series thus is a notable example showing that magma conduits do not necessarily form the PGE mineralization, other factors such as the source of magma intrusions and mechanisms during magma emplacement (e.g., early sulfide saturation) should also be considered.

7.1.3 Implications for PGE mineralization

The magma conduit model has grown in favor since it was proposed for gabbro-hosted deposits in the Norilsk region, Siberia, by Naldrett et al. (1995) and Naldrett and Lightfoot (1999), to account for the enrichment of PGE relative to Cu and Ni in disseminated sulfide minerals. Acceptance of the dynamic conduit model for formation of PGE-related deposits by far was almost universal, notable examples include Jinchuan (Naldrett, 1999), Eagle Intrusion (Ding et al., 2012), River Valley Intrusion (Howell et al., 2014). In this thesis, a general conduit model also has been proposed to explain the PGE mineralization at the whole Coldwell Alkaline Complex. It is therefore a good example showing the applicability of the conduit model in terms of explaining PGE mineralization in a complex setting.

In addition, PGE mineralization discussed in this study is hosted by the Coldwell Alkaline Complex consisting of gabbroic to syenitic units, this is in contrast to most PGE deposits that are hosted by mafic-ultramafic complexes. Since many PGE-related deposits hosted within mafic-ultramafic complexes have been proposed to be related to magma conduits, the formation of PGE mineralization in the alkaline complex thus is similar with that in mafic-ultramafic intrusions.

7.2 Conclusions

Corresponding to the three main questions as mentioned in Chapter 1, the main conclusions for this thesis are summarized as follows.

(1) pXRF and bSEM-EDS can be combined as an exploration tool to help mineral exploration at the entire Coldwell Alkaline Complex and may also be applicable to PGE-related deposits in other settings.

(2) The Layered Series developed by multiple intrusions in a dynamic system. However, it is not co-genetic with the Marathon Series and perhaps has undergone an early sulfide saturation event, which resulted in its PGE-barren nature.

(3) Cu-Pd mineralization in Area 41 can be explained by a conduit-model, which is similar to mineralization in the Marathon deposit. This indicates that other potential

PGE mineralized zones in the Coldwell Alkaline Complex perhaps are also conduit-related.

7.3 References

Barnes S.-J. and Ripley E.M. 2016. Highly Siderophile and Strongly Chalcophile Elements in Magmatic Ore Deposits. *Reviews in Mineralogy and Geochemistry*, **81**, 725-774.

Cameron, E. N. 1980. Evolution of the Lower Critical Zone, Central Sector, Eastern Bushveld Complex, and its chromite deposits. *Economic Geology*, **75**, 845-871.

Ding X., Ripley E.M., and Li C. 2012. PGE geochemistry of the Eagle Ni-Cu-(PGE) deposit, Upper Michigan: constraints on ore genesis in a dynamic magma conduit. *Mineralium Deposita*, **47**, 89-104.

Holwell D., Keays R., Firth E., and Findlay J. 2014. Geochemistry and mineralogy of platinum group element mineralization in the River Valley Intrusion, Ontario, Canada: A model for early-stage sulfur saturation and multistage emplacement and the implication for "Contact-Type" Ni-Cu-PGE sulfide mineralization. *Economic Geology*, **109**, 689-712.

Holwell D.A. and McDonald, I. 2010. A Review of the Behaviour of Platinum Group Elements within Natural Magmatic Sulfide Ore Systems. *Platinum Metals Review*, **54**, 26-36.

Kerr A. and Leitch A.M. 2005. Self-destructive sulfide segregation systems and the formation of high-grade magmatic ore deposits: *Economic Geology*, **100**, 311-332.

Kruger F. J. 2005. Filling the Bushveld Complex magma chamber: lateral expansion, roof and floor interaction, magmatic unconformities, and the formation of giant chromitite, PGE and Ti-V-magnetite deposits. *Mineralium Deposita*, **40**, 451-472.

Marsh B.D. 2006. Dynamics of magmatic systems. *Elements*, **2**, 287-292.

Mitchell A. A. and Scoon R. N. 2007.The Merensky Reef at Winnaarshoek, Eastern Bushveld Complex: a primary magmatic hypothesis based on a wide reef facies. *Economic Geology*, **102**, 971-1109.

Mitchell A. A. and Scoon R. N. 2012. The Platreef of the Bushveld Complex, South Africa: a new hypothesis of multiple, non-sequential magma replenishment based on observations at the Akanani Project, northwest of Mokopane. *South Africa Journal of Geology*, **115**, 535-550.

Mungall J.E., Kamo S.L., and McQuade S. 2016. U-Pb geochronology documents out-of-sequence emplacement of ultramafic layers in the Bushveld Igneous Complex of South Africa. *Nature Communications*, **7**, 1-13.

Naldrett A.J. 1999. World-class Ni-Cu-PGE deposits: key factors in their genesis. *Mineralium Deposita*, **34**, 227-240.

Naldrett A.J. and Lightfoot, P.C. 1999, Ni-Cu-PGE deposits of Noril'sk region, Siberia: Their formation in conduits for flood basalt volcanism: St John's, Geological Association of Canada, **104**, 195-249.

Naldrett A.J., Federenko V.A., Lightfoot P.C., Kunilov V.E., Gorbachev N.S., Doherty W., and Johan J. 1995. Ni-Cu-PGE deposits of the Noril'sk region Siberia: Their formation in conduits for flood basalt volcanism. *Transactions of the Institution of Mining and Metallurgy*, **104**, 18-36.

Nielsen, T. F. D. 2001. The palladium potential of the Skaergaard intrusion. GEUS Report, 39 pp.

Taranovic V., Ripley E.M., Li C., and Rossell D. 2016. Chalcophile element (Ni, Cu, PGE, and Au) variations in the Tamarack magmatic sulfide deposit in the Midcontinent Rift System: implications for dynamic ore-forming processes. *Mineralium Deposita*, **7**, 937-951.

Thériault R.D., Barnes S.J., and Severson M.J. 1997. The Influence of Country-Rock Assimilation and Silicate to Sulfide Ratios (R Factor) On the Genesis of the Dunka Road Cu-Ni-Platinum-Group Element Deposit, Duluth Complex, Minnesota. *Canadian Journal of Earth Sciences*, **34**, 375-389.

Wagner P. A. 1929. The Platinum Mines and Deposits of Southern Africa (Oliver and Boyd).

CONTRIBUTIONS TO ORIGINAL KNOWLEDGE

1) This is the first study that combines pXRF and bSEM-EDS as an exploration tool in a complex geological setting. This method was then tested for the complex as a whole.

2) This is the first study that examined the parental magma of Layered Series within the Eastern Gabbro and investigated its relationship with the Coubran basalts using geochemical modeling.

3) This is one of a small number of investigations that examined origins of both the decoupled and coupled magma reverse evolutions for the Layered Series intrusions, and related them to magmatic processes occurred in the magma chamber.

4) This is the first study of Area 41 PGE mineralization. The recognition of a conduit system at Area 41 is encouraging for the exploration of other conduits in the Coldwell Alkaline Complex.

5) To our knowledge, this study is one of a small number of investigations that have studied the origin of PGE mineralization hosted by a gabbro-alkaline complex.

RECOMMENDATIONS FOR FUTURE WORK

This study has characterized the Layered Series in great detail, but there are still some problems remain unresolved. First, the Layered Series parental magma can not be directly related to the Coubran basalts, but it has similar compositions with F=0.55 residual melt of the Coubran basalts. It is not certain if there is another basalt candidate within the Coldwell Complex that can be related to the parental magma

of the Layered Series units. Further, it is expected that if such a basalt candidate is present, it may have a relationship with the Coubran basalts, but the origin of the Coubran basalts is still poorly constrained.

Another special rock type (the Malpas Lake Intrusion) which has almost the same petrographical characteristics with the Layered Series unit is distinguished by its unique geochemical characteristics. Results show that the Malpas Lake Intrusion is even more evolved than the Layered Series units and seems to have some relationships with the syenites, but the syenites are the youngest rock unit in the Coldwell Complex. However, during the course of this thesis, it still has not been well characterized particularly with respect to the origin. Future work on this Intrusion is suggested.

A conduit system is interpreted to be close to drill hole SL-13-32 at Area 41. The inspection of thin sections shows that the Marathon Series units at this drill hole were more extensively altered than units intersected by other drill holes at Area 41. Particularly, chlorine-rich apatite and biotite were observed in the ophitic gabbro rocks in SL-13-32. It can therefore be hypothesised that the conduit system might have facilitated the flow of chlorine-rich fluids, which modified the PGE mineralization. If this is correct, there should be consistent spatial variations in the degree of alteration as well as the chances for observations of As- and Te- rich PGM away from the conduit. It would be worthwhile to investigate this possibility using more detailed petrography. In addition, electron microprobe analyses show that the chlorine-rich biotite contains higher than 1 wt.% chlorine (it can be treated as a major element), it is unclear whether this biotite crystallized from magmatic fluids from the Coldwell Alkaline Complex or from other fluids of an unknown nature.

Appendices

Appendix 1: Copyright permission for Chapter 2 **"**The application of portable XRF and benchtop SEM-EDS to Cu-Pd exploration in the Coldwell Alkaline Complex, Ontario, Canada".

From: Jessica Pollitt
Sent: October 27, 2016 11:31 AM
To: Yonghua Cao
Subject: RE: GEEA paper

Dear Yonghua,

Yes, thanks for asking – that is fine.

Here is the wording from our website:

Authors may re-use their own material without permission subject to the exceptions listed below. They may include the whole article in a PhD or other thesis provided that it will not be published, and that the original source is fully acknowledged in the standard form. If the thesis is to be included in the institution's electronic repository or other online host, authors must use their own finally accepted version, not the typeset PDF (unless it is Gold Open Access). Authors may not re-publish their whole article, or a substantial part of it, without permission. Such permission will be granted only in exceptional circumstances.

Good luck in your viva!

With best wishes,
Jessica

Appendix 2: List of all powdered samples that have done portable XRF and/or ICP-AES/MS/IR analyses.

Area	DDH	Coordination			Depth	Unit	Portable XRF	ICP-AES/MS/IR
		Northing	Easting	Elevation				
Four Dams	FD-13-34	5408836	548073	375.7	5.0	Oxide augite melatroctolite	X	X
					9.5	Oxide augite melatroctolite	X	X
					14.0	Oxide augite melatroctolite	X	X
					18.5	Oxide augite melatroctolite	X	X
					23.0	olivine gabbro	X	X
					27.5	Oxide augite melatroctolite	X	X
					32.0	Oxide augite melatroctolite	X	X
					36.5	Oxide augite melatroctolite	X	X
					41.0	Oxide augite melatroctolite	X	X
					45.5	Oxide augite melatroctolite	X	X
					50.0	Apatitic clinopyroxenite	X	X
					60.0	Oxide augite melatroctolite	X	X
					64.5	Oxide augite melatroctolite	X	X
					66.0	Oxide augite melatroctolite	X	X
					70.5	olivine gabbro	X	X
					75.0	olivine gabbro	X	X
					79.5	olivine gabbro	X	X
					84.0	olivine gabbro	X	X
					89.5	olivine gabbro	X	X
					94.5	olivine gabbro	X	X
					99.0	olivine gabbro	X	X
					103.5	olivine gabbro	X	X
					108.0	olivine gabbro	X	X
					112.5	olivine gabbro	X	X
					117.0	olivine gabbro	X	X
					127.0	olivine gabbro	X	X

131.5	olivine gabbro	X	X
136.0	olivine gabbro	X	X
140.5	olivine gabbro	X	X
145.0	olivine gabbro	X	X
149.5	olivine gabbro	X	X
154.0	olivine gabbro	X	X
158.5	olivine gabbro	X	X
163.0	olivine gabbro	X	X
167.5	olivine gabbro	X	X
172.0	olivine gabbro	X	X
176.5	olivine gabbro	X	X
181.0	olivine gabbro	X	X
190.0	olivine gabbro	X	X
194.5	olivine gabbro	X	X
199.0	olivine gabbro	X	X
203.5	Oxide augite melatroctolite	X	X
208.0	Oxide augite melatroctolite	X	X
212.5	Oxide augite melatroctolite	X	X
217.0	Oxide augite melatroctolite	X	X
221.5	Oxide augite melatroctolite	X	X
226.0	Oxide augite melatroctolite	X	X
230.5	Oxide augite melatroctolite	X	X
235.0	Oxide melatroctolite	X	X
239.5	Oxide melatroctolite	X	X
244.0	Oxide melatroctolite	X	X
248.5	Oxide melatroctolite	X	X
253.0	Oxide melatroctolite	X	X
257.5	Oxide melatroctolite	X	X
262.0	Oxide melatroctolite	X	X
266.5	Oxide melatroctolite	X	X

				271.0	Oxide melatroctolite	X	X
				272.0	Apatitic clinopyroxenite	X	X
				276.5	Apatitic clinopyroxenite	X	X
				281.0	Apatitic clinopyroxenite	X	X
				285.5	Apatitic clinopyroxenite	X	X
				291.0	Apatitic clinopyroxenite	X	X
				295.5	Apatitic clinopyroxenite	X	X
				302.0	Apatitic clinopyroxenite	X	X
				305.0	Apatitic clinopyroxenite	X	X
				310.0	Apatitic clinopyroxenite	X	X
				316.0	(olivine) apatitic clinopyroxenite	X	X
				320.5	(olivine) apatitic clinopyroxenite	X	X
				325.0	(olivine) apatitic clinopyroxenite	X	X
				327.5	(olivine) apatitic clinopyroxenite	X	X
				330.0	(olivine) apatitic clinopyroxenite	X	X
FD-13-41	5409252	547787	380.7	2.5	Oxide augite melatroctolite	X	
				7	Oxide augite melatroctolite	X	
				11.5	Oxide augite melatroctolite	X	
				16	olivine gabbro	X	
				20.5	Oxide augite melatroctolite	X	
				25	olivine gabbro	X	
				29.5	olivine gabbro	X	
				34	olivine gabbro	X	
				38.5	olivine gabbro	X	
				43	olivine gabbro	X	
				47.5	olivine gabbro	X	
				52	olivine gabbro	X	
				56.5	olivine gabbro	X	
				61	olivine gabbro	X	
				65.5	olivine gabbro	X	

					67	Oxide augite melatroctolite	X
					71.5	Oxide augite melatroctolite	X
					76	Oxide augite melatroctolite	X
					80.5	Oxide augite melatroctolite	X
					89.5	Oxide augite melatroctolite	X
					94	Oxide augite melatroctolite	X
					99.5	Oxide augite melatroctolite	X
					104	Oxide augite melatroctolite	X
					108.5	Oxide augite melatroctolite	X
					113	Oxide augite melatroctolite	X
					117.5	Oxide augite melatroctolite	X
Area 41	SL-13-27	5412632	537606	372.1	4	Olivine gabbro	X
					8.5	Olivine gabbro	X
					17	Ophitic gabbro	X
					25	Ophitic gabbro	X
					30	Ophitic gabbro	X
					35	Ophitic gabbro	X
					37.3	Oxide melatroctolite	X
					41.5	Oxide melatroctolite	X
					46	Oxide melatroctolite	X
					50.5	Oxide melatroctolite	X
					55	Oxide melatroctolite	X
					66	Ophitic gabbro	X
					70	Ophitic gabbro	X
					80	Ophitic gabbro	X
					85	Ophitic gabbro	X
					90	Ophitic gabbro	X
					95	Ophitic gabbro	X
					100	Ophitic gabbro	X
					105	Ophitic gabbro	X

				174.5	Oxide melatroctolite	X	
				179	Oxide melatroctolite	X	
				183.5	Oxide melatroctolite	X	
				231	Apatitic clinopyroxenite	X	
				235.5	Apatitic clinopyroxenite	X	
				5.5	Olivine gabbro	X	
				10	Olivine gabbro	X	
				12	Ophitic gabbro	X	
				17	Ophitic gabbro	X	X
				22	Ophitic gabbro	X	
				27	Ophitic gabbro	X	
				32	Ophitic gabbro	X	X
				37	Ophitic gabbro	X	X
				42	Ophitic gabbro	X	
				44	Oxide melatroctolite	X	
				49	Oxide melatroctolite	X	
				53	Ophitic gabbro	X	
SL-13-32	5412610	537774	363.9	58	Ophitic gabbro	X	
				60.5	Oxide melatroctolite	X	
				66.5	Oxide melatroctolite	X	
				70	Ophitic gabbro	X	
				75	Ophitic gabbro	X	
				80	Ophitic gabbro	X	
				85	Ophitic gabbro	X	
				90	Ophitic gabbro	X	
				150.5	Apatitic clinopyroxenite	X	
				155.5	Apatitic clinopyroxenite	X	
				160.5	Apatitic clinopyroxenite	X	
				165.5	Apatitic clinopyroxenite	X	
				170	Apatitic clinopyroxenite	X	

				175	Breccia	X	
				180	Breccia	X	
				185	Breccia	X	
				200	Apatitic clinopyroxenite	X	
				204.5	Apatitic clinopyroxenite	X	
				209	Apatitic clinopyroxenite	X	
				214	Apatitic clinopyroxenite	X	
				219.5	Apatitic clinopyroxenite	X	
				224	Apatitic clinopyroxenite	X	
				229.5	Apatitic clinopyroxenite	X	
				234	Apatitic clinopyroxenite	X	
SL-13-34	5412536	537993	392	3.5	Oxide augite melatroctolite	X	X
				7	Olivine gabbro	X	X
				13	Olivine gabbro	X	X
				17	Olivine gabbro	X	X
				20.5	Pl-rich Oxide augite melatroctolite	X	X
				24.5	Pl-rich Oxide augite melatroctolite	X	X
				28.5	Oxide augite melatroctolite	X	
				33	Olivine gabbro	X	X
				37	Olivine gabbro	X	X
				41.4	Olivine gabbro	X	X
				45.7	Oxide augite melatroctolite	X	
				50.1	Oxide augite melatroctolite	X	
				54.1	Oxide augite melatroctolite	X	
				58.9	Oxide augite melatroctolite	X	
				63.5	Ophitic gabbro	X	X
				67.5	Ophitic gabbro	X	X
				71.5	Ophitic gabbro	X	
				75	Apatitic (olivine) clinopyroxenite	X	X
				76.5	Apatitic (olivine) clinopyroxenite	X	X

				78.5	Ophitic gabbro	X	
				88	Feldspathic clinopyroxenite	X	X
				92	Feldspathic clinopyroxenite	X	
				96	Feldspathic clinopyroxenite	X	X
				99.5	Feldspathic clinopyroxenite	X	
				103.5	Feldspathic clinopyroxenite	X	
				107.8	Ophitic gabbro	X	
				111.8	Feldspathic clinopyroxenite	X	X
				115.8	Feldspathic clinopyroxenite	X	
				119.5	Feldspathic clinopyroxenite	X	X
				123.5	Feldspathic clinopyroxenite	X	
				126.5	Ophitic gabbro	X	
				128.8	Ophitic gabbro	X	
				141	Ophitic gabbro	X	
				143.5	Ophitic gabbro	X	
				146.5	Ophitic gabbro	X	X
				147.3	Apatitic clinopyroxenite	X	X
				150.5	Ophitic gabbro	X	X
				154.5	Ophitic gabbro	X	
				159.5	Ophitic gabbro	X	X
				163.5	Ophitic gabbro	X	
				171	Ophitic gabbro	X	X
				175	Ophitic gabbro	X	
				181.4	Ophitic gabbro	X	X
				185.4	Ophitic gabbro	X	
				10.5	Olivine gabbro	X	X
				14	Oxide augite melatroctolite	X	
SL-13-36	5412573	537854	354.9	15.5	Olivine gabbro	X	X
				19.5	Olivine gabbro	X	X
				23.5	Olivine gabbro	X	X

26.5	Oxide augite melatroctolite	X	
30.5	Olivine gabbro	X	X
36.5	Ophitic gabbro	X	
39.5	Ophitic gabbro	X	X
51.5	Ophitic gabbro	X	
54.5	Ophitic gabbro	X	
58.5	Ophitic gabbro	X	
63	Ophitic gabbro	X	
67.5	Ophitic gabbro	X	
71.5	Apatitic clinopyroxenite	X	X
76.5	Apatitic clinopyroxenite	X	X
80.5	Feldspathic clinopyroxenite	X	
83.2	Feldspathic clinopyroxenite	X	
86.5	Feldspathic clinopyroxenite	X	X
90.5	Feldspathic clinopyroxenite	X	
94.5	Feldspathic clinopyroxenite	X	
99.5	Feldspathic clinopyroxenite	X	
103.5	Feldspathic clinopyroxenite	X	X
107.5	Feldspathic clinopyroxenite	X	
114.5	Feldspathic clinopyroxenite	X	
117.5	Apatitic clinopyroxenite	X	
119.5	Breccia	X	
123.5	Olivine gabbro	X	
127.5	Apatitic clinopyroxenite	X	
131.6	Oxide augite melatroctolite	X	
134.5	Breccia	X	
138.5	Breccia	X	
143.5	Oxide melatroctolite	X	
146.5	Ophitic gabbro	X	
149.5	Ophitic gabbro	X	

				153.5	Ophitic gabbro	X	
				157.5	Apatitic clinopyroxenite	X	X
				161.5	Apatitic clinopyroxenite	X	
				179	Ophitic gabbro	X	
				183.5	Meta-basalt	X	
				187.5	Meta-basalt	X	
				195.5	Meta-basalt	X	
				199.5	Meta-basalt	X	
				203.5	Meta-basalt	X	
				207.5	Meta-basalt	X	
				211.5	Meta-basalt	X	
				215.5	Meta-basalt	X	
SL-13-37	5412576	537855	356.5	7.5	Oxide augite melatroctolite	X	
				11.5	Oxide augite melatroctolite	X	
				15.5	Oxide augite melatroctolite	X	
				19.5	Oxide augite melatroctolite	X	
				23.5	Oxide augite melatroctolite	X	
				28	Oxide augite melatroctolite	X	
				30.5	Olivine gabbro	X	
				33.5	Oxide augite melatroctolite	X	
				37.5	Oxide augite melatroctolite	X	
				41.5	Oxide augite melatroctolite	X	
				43.1	Apatitic clinopyroxenite	X	
				45.5	Ophitic gabbro	X	
				50.5	Ophitic gabbro	X	
				52.7	Ophitic gabbro	X	
				54.5	Oxide melatroctolite	X	
				57.5	Ophitic gabbro	X	
				60.5	Ophitic gabbro	X	
				63.5	Ophitic gabbro	X	

67.5	Ophitic gabbro	X
71.9	Ophitic gabbro	X
79.5	Ophitic gabbro	X
81.5	Ophitic gabbro	X
85.5	Ophitic gabbro	X
92.5	Ophitic gabbro	X
96.5	Feldspathic clinopyroxenite	X
103.5	Feldspathic clinopyroxenite	X
107.5	Feldspathic clinopyroxenite	X
111.5	Feldspathic clinopyroxenite	X
115.5	Ophitic gabbro	X
117.5	Apatitic clinopyroxenite	X
119.5	Feldspathic clinopyroxenite	X
123.6	Ophitic gabbro	X
128.5	Apatitic clinopyroxenite	X
132.5	Apatitic clinopyroxenite	X
136.5	Apatitic clinopyroxenite	X
140.5	Apatitic clinopyroxenite	X
144.8	Apatitic clinopyroxenite	X
148.8	Apatitic clinopyroxenite	X
152.5	Apatitic clinopyroxenite	X
157.5	Ophitic gabbro	X
161.5	Ophitic gabbro	X
165.5	Ophitic gabbro	X
169.5	Ophitic gabbro	X
174.5	Ophitic gabbro	X
178.5	Apatitic clinopyroxenite	X
183.5	Ophitic gabbro	X
187.5	Ophitic gabbro	X
191.5	Ophitic gabbro	X

				195.5	Ophitic gabbro	X	
				199.5	Ophitic gabbro	X	
				203.5	Ophitic gabbro	X	
				207.5	Ophitic gabbro	X	
				211.5	Ophitic gabbro	X	
				225.5	Ophitic gabbro	X	
				227.5	Ophitic gabbro	X	
SL-13-41	5412570	537636	383.8	3.0	Oxide augite melatroctolite	X	X
				7.5	Oxide augite melatroctolite	X	
				12.0	Oxide augite melatroctolite	X	X
				20.0	Oxide augite melatroctolite	X	
				24.5	Oxide augite melatroctolite	X	
				29.0	Oxide augite melatroctolite	X	
				33.5	Oxide augite melatroctolite	X	X
				38.0	Oxide augite melatroctolite	X	
				42.5	Oxide augite melatroctolite	X	
				45.0	Oxide augite melatroctolite	X	
				49.5	Oxide augite melatroctolite	X	X
				54.0	Oxide augite melatroctolite	X	X
				58.5	Oxide augite melatroctolite	X	
				63.0	Oxide augite melatroctolite	X	
				68.5	Oxide augite melatroctolite	X	X
				73.0	Oxide augite melatroctolite	X	
				77.5	Oxide augite melatroctolite	X	X
				82.0	Oxide augite melatroctolite	X	
				86.5	Oxide augite melatroctolite	X	
				91.0	Oxide augite melatroctolite	X	X
				94.5	Oxide augite melatroctolite	X	X
				104.5	Oxide augite melatroctolite	X	
				109.0	Oxide augite melatroctolite	X	X

					116.5	Oxide augite melatroctolite	X	
					121.0	Oxide augite melatroctolite	X	
					125.0	Oxide melatroctolite?	X	
					129.5	Oxide melatroctolite?	X	X
					132.0	Oxide melatroctolite	X	X
					135.0	Oxide melatroctolite	X	
					138.0	Oxide melatroctolite	X	
					143.0	Ophitic gabbro	X	X
					148.0	Ophitic gabbro	X	X
					153.0	Ophitic gabbro	X	X
					167.0	Ophitic gabbro	X	X
					169.0	Oxide melatroctolite	X	
					173.5	Oxide melatroctolite	X	
					221.0	Apatitic clinopyroxenite	X	
					225.5	Apatitic clinopyroxenite	X	
					230.0	Apatitic clinopyroxenite	X	X
					265.5	Apatitic clinopyroxenite	X	X
					270.0	Apatitic clinopyroxenite	X	X
					277.0	Apatitic clinopyroxenite	X	X
WD zone	MW-07-06	5400647	550172	295.42	3.9	Olivine gabbro	X	X
					7.9	Olivine gabbro	X	
					11.9	Olivine gabbro	X	X
					15.9	Olivine gabbro	X	
					19.9	Olivine gabbro	X	X
					23.9	Olivine gabbro	X	X
					27.9	Olivine gabbro	X	
					31.9	Gabbroic anorthosite	X	
					35.9	Oxide augite melatroctolite	X	
					38	Oxide augite melatroctolite	X	X
					41	Oxide augite melatroctolite	X	

45	Gabbroic anorthosite	X	
49	Oxide augite melatroctolite	X	
50.5	Meta-basalt	X	
54.5	Ophitic gabbro	X	
56.5	Breccia	X	
60.5	Oxide augite melatroctolite	X	
64.5	Ophitic gabbro	X	
66	Olivine gabbro	X	
72.6	Olivine gabbro	X	
76.6	Ophitic gabbro	X	
80.6	Ophitic gabbro	X	X
83.5	Oxide augite melatroctolite	X	
87.5	Oxide augite melatroctolite	X	
91.5	Ophitic gabbro	X	X
95.5	Ophitic gabbro	X	X
99.5	Ophitic gabbro	X	
103.5	Ophitic gabbro	X	
109.5	Ophitic gabbro	X	X
113.5	Ophitic gabbro	X	X
117.5	Ophitic gabbro	X	X
121	Ophitic gabbro	X	X
125.5	Oxide augite melatroctolite	X	
135.5	Ophitic gabbro	X	X
139.5	Ophitic gabbro	X	
143.5	Ophitic gabbro	X	X
147.5	Ophitic gabbro	X	X
151.5	Oxide augite melatroctolite	X	
155.5	Ophitic gabbro	X	
159.5	Ophitic gabbro	X	
163.5	Ophitic gabbro	X	

MW-07-08	5401050	550325	12	Meta-basalt	X	
			16	Meta-basalt	X	
			21.5	Meta-basalt	X	
			24.5	Meta-basalt	X	
			31	Malpas lake Intrusion	X	X
			34.7	Malpas lake Intrusion	X	
			39.5	Malpas lake Intrusion	X	X
			43.5	Malpas lake Intrusion	X	
			48.5	Malpas lake Intrusion	X	X
			52.5	Malpas lake Intrusion	X	X
			57.5	Malpas lake Intrusion	X	
			61.5	Malpas lake Intrusion	X	
			65.5	Malpas lake Intrusion	X	
			69.5	Malpas lake Intrusion	X	X
			73.5	Malpas lake Intrusion	X	
			85.5	Malpas lake Intrusion	X	
			92.5	Malpas lake Intrusion	X	X
			99.5	Malpas lake Intrusion	X	
			103.5	Malpas lake Intrusion	X	X
			107.5	Malpas lake Intrusion	X	
			111.5	Malpas lake Intrusion	X	X
			116	Malpas lake Intrusion	X	
			120	Malpas lake Intrusion	X	X
			124.7	Malpas lake Intrusion	X	
			128.5	Malpas lake Intrusion	X	X
			132.5	Malpas lake Intrusion	X	
			139.5	Malpas lake Intrusion	X	
			143	Malpas lake Intrusion	X	
			147	Malpas lake Intrusion	X	X

Appendix 3. Summary of thin sections that have done bSEM-EDS analyses or probe analyses.

Area	DDH	Depth	Unit	bSEM-EDS	Probe
Four Dams	FD-13-34	5	Oxide augite melatroctolite	X	X
		18.6	Oxide augite melatroctolite	X	X
		24	Olivine gabbro	X	X
		27.9	Oxide augite melatroctolite	X	X
		33	Oxide augite melatroctolite	X	X
		46.1	Oxide augite melatroctolite	X	X
		64.6	Oxide augite melatroctolite	X	X
		79.6	Olivine gabbro	X	X
		127.25	Olivine gabbro	X	X
		158.6	Olivine gabbro	X	X
		194.8	Olivine gabbro	X	X
		212.5	Oxide augite melatroctolite	X	X
		226.3	Oxide augite melatroctolite	X	X
		248.5	Oxide melatroctolite	X	X
		253.1	Oxide melatroctolite	X	X
		257.8	Oxide melatroctolite	X	X
		272.1	Apatitic clinopyroxenite	X	X
		276.5	Apatitic clinopyroxenite	X	X
		281.05	Apatitic clinopyroxenite	X	X
		291.5	Apatitic clinopyroxenite	X	X
		295.7	Apatitic clinopyroxenite	X	X
		316.7	Apatitic olivine clinopyroxenite	X	X
		321.1	Apatitic olivine clinopyroxenite	X	X
Area 41	SL-13-27	4.8	Olivine gabbro	X	X
		9	Olivine gabbro	X	X
		17.7	Ophitic gabbro	X	X
		36	Ophitic gabbro	X	X

	42.5	Oxide melatroctolite	X	X
	46.1	Oxide melatroctolite	X	X
	51	Oxide melatroctolite	X	X
	54.4	Oxide melatroctolite	X	X
	66	Ophitic gabbro	X	X
	80.4	Ophitic gabbro	X	X
	85.5	Ophitic gabbro	X	X
	90.05	Ophitic gabbro	X	X
	95.2	Ophitic gabbro	X	X
	105.3	Oxide melatroctolite	X	X
	174.7	Oxide melatroctolite	X	X
	183.6	Oxide melatroctolite	X	X
	231.1	Apatitic clinopyroxenite	X	X
	235.5	Apatitic clinopyroxenite	X	X
SL-13-32	5.95	Olivine gabbro	X	
	10.7	Olivine gabbro	X	
	17.5	Ophitic gabbro	X	
	22.9	Ophitic gabbro	X	
	27.1	Ophitic gabbro	X	
	32.2	Ophitic gabbro	X	
	37	Ophitic gabbro	X	
	42.3	Ophitic gabbro	X	
	44	Oxide melatroctolite	X	
	49.3	Oxide melatroctolite	X	
	58.5	Ophitic gabbro	X	
	61.2	Oxide melatroctolite	X	
	75.8	Ophitic gabbro	X	
	80.5	Ophitic gabbro	X	
	90.55	Ophitic gabbro	X	
	150.5	Apatitic clinopyroxenite	X	

	156.1	Apatitic clinopyroxenite	X	
	161	Apatitic clinopyroxenite	X	
	165.5	Ophitic gabbro	X	
	170.55	Apatitic clinopyroxenite	X	
	200.6	Apatitic clinopyroxenite	X	
	204.5	Apatitic clinopyroxenite	X	
	209.2	Apatitic clinopyroxenite	X	
	214.5	Apatitic clinopyroxenite	X	
	219.5	Apatitic clinopyroxenite	X	
	224.6	Apatitic clinopyroxenite	X	
	229.6	Apatitic clinopyroxenite	X	
	234.4	Apatitic clinopyroxenite	X	
SL-13-34	3.0	Oxide augite melatroctolite	X	X
	5.1	Oxide augite melatroctolite	X	X
	7.0	Olivine gabbro	X	X
	13.3	Olivine gabbro	X	X
	17.4	Olivine gabbro	X	X
	19.4	Oxide augite melatroctolite	X	X
	23.4	Oxide augite melatroctolite	X	
	25.7	Oxide augite melatroctolite	X	X
	28.1	Oxide augite melatroctolite	X	X
	30.0	Oxide augite melatroctolite	X	X
	32.0	olivine gabbro	X	X
	45.0	Oxide augite melatroctolite	X	X
	49.0	Oxide augite melatroctolite	X	X
	53.0	Oxide augite melatroctolite	X	X
	59.0	Oxide augite melatroctolite	X	X
	63.0	Ophitic gabbro	X	
	65.0	Ophitic gabbro	X	
	75.0	Apatitic clinopyroxenite	X	

	77.2	Ophitic gabbro	X	
	81.0	Ophitic gabbro	X	
	95.5	Feldspathic clinopyroxenite	X	
	111.6	Feldspathic clinopyroxenite	X	
	119.5	Feldspathic clinopyroxenite	X	
	126.0	Ophitic gabbro	X	
	130.2	Ophitic gabbro	X	
	140.5	Ophitic gabbro	X	
	146.9	Ophitic gabbro	X	
	150.9	Ophitic gabbro	X	
SL-13-36	10	Olivine gabbro	X	
	11.1	Olivine gabbro	X	
	16.6	Olivine gabbro	X	X
	20.7	Olivine gabbro	X	X
	22.7	Olivine gabbro	X	
	24.85	Oxide augite melatroctolite	X	
	35.2	Ophitic gabbro	X	
	39.3	Ophitic gabbro	X	
	53.5	Ophitic gabbro	X	
	57.3	Ophitic gabbro	X	
	62	Ophitic gabbro	X	
	63	Ophitic gabbro	X	
	67.8	Ophitic gabbro	X	
	72	Apatitic clinopyroxenite	X	
	74	Apatitic clinopyroxenite	X	
	76	Apatitic clinopyroxenite	X	
	79.9	Feldspathic clinopyroxenite	X	
	96	Feldspathic clinopyroxenite	X	
	113.9	Feldspathic clinopyroxenite	X	
	125.8	Ophitic gabbro	X	

	130	Ophitic gabbro	X	
	134.5	Ophitic gabbro	X	
	143	Ophitic gabbro	X	
	143.7	Ophitic gabbro	X	
	148.7	Ophitic gabbro	X	
	152.8	Ophitic gabbro	X	
	156.8	Ophitic gabbro	X	
	158.8	Apatitic clinopyroxenite	X	
	161.8	Apatitic clinopyroxenite	X	
	177	Apatitic clinopyroxenite	X	
SL-13-37	7.0	Oxide augite melatroctolite	X	X
	11.0	Oxide augite melatroctolite	X	
	13.0	Oxide augite melatroctolite	X	
	15.0	Oxide augite melatroctolite	X	
	19.0	Oxide augite melatroctolite	X	X
	21.0	Oxide augite melatroctolite	X	
	25.0	Oxide augite melatroctolite	X	X
	27.0	Oxide augite melatroctolite	X	X
	33.0	Oxide augite melatroctolite	X	
	37.0	Oxide augite melatroctolite	X	X
	48.0	Ophitic gabbro	X	
	52.0	Ophitic gabbro	X	
	54.0	Ophitic gabbro	X	
	55.5	Ophitic gabbro	X	
	56.0	Ophitic gabbro	X	
	62.0	Ophitic gabbro	X	
	64.0	Ophitic gabbro	X	
	65.7	Ophitic gabbro	X	
	70.0	Ophitic gabbro	X	
	76.0	Ophitic gabbro	X	

	80.0	Ophitic gabbro	X	
	86.0	Ophitic gabbro	X	
	88.0	Ophitic gabbro	X	
	93.0	Ophitic gabbro	X	
	95.0	Ophitic gabbro	X	
	97.2	Ophitic gabbro	X	
	104.5	Feldspathic clinopyroxenite	X	
	115.4	Feldspathic clinopyroxenite	X	
	140.0	Feldspathic clinopyroxenite	X	
	146.0	Feldspathic clinopyroxenite	X	
	157.3	Ophitic gabbro	X	
	167.3	Ophitic gabbro	X	
	170.7	Ophitic gabbro	X	
	172.2	Ophitic gabbro	X	
SL-13-41	3.0	Oxide augite melatroctolite	X	X
	12.1	Oxide augite melatroctolite	X	X
	29.0	Oxide augite melatroctolite	X	
	45.0	Oxide augite melatroctolite	X	X
	63.2	Oxide augite melatroctolite	X	X
	68.7	Oxide augite melatroctolite	X	X
	73.0	Oxide augite melatroctolite	X	X
	91.0	Oxide augite melatroctolite	X	X
	109.1	Oxide augite melatroctolite	X	X
	125.8	Oxide melatroctolite	X	
	129.5	Oxide melatroctolite	X	
	132.2	Oxide melatroctolite	X	
	138.6	Oxide melatroctolite	X	
	143.5	Ophitic gabbro	X	
	153.9	Ophitic gabbro	X	
	167.4	Ophitic gabbro	X	

		170.0	Oxide melatroctolite	X	
		173.6	Oxide melatroctolite	X	
		221.4	Apatitic clinopyroxenite	X	
		225.6	Apatitic clinopyroxenite	X	
		230.7	Apatitic clinopyroxenite	X	
		266.0	Apatitic clinopyroxenite	X	
		270.5	Apatitic clinopyroxenite	X	
		278.0	Apatitic clinopyroxenite	X	
WD zone	MW-07-06	3.4	Olivine gabbro	X	X
		9.4	Olivine gabbro	X	X
		13.4	Olivine gabbro	X	X
		17.4	Olivine gabbro	X	X
		23.4	Olivine gabbro	X	X
		36.2	Olivine gabbro	X	X
		37.5	Oxide augite melatroctolite	X	X
		41.0	Oxide augite melatroctolite	X	X
		54.3	ophitic gabbro	X	
		60.8	Oxide augite melatroctolite	X	
		65.0	Ophitic gabbro	X	
		68.0	Ophitic gabbro	X	
		71.7	Ophitic gabbro	X	
		81.5	Ophitic gabbro	X	
		83.5	Oxide augite melatroctolite	X	
		86.3	Oxide augite melatroctolite	X	
		87.5	Oxide augite melatroctolite	X	
		93.5	Ophitic gabbro	X	
		98.0	Ophitic gabbro	X	
		101.0	Ophitic gabbro	X	
		109.6	Ophitic gabbro	X	
		117.6	Ophitic gabbro	X	

	120.1	Ophitic gabbro	X	
	122.0	Ophitic gabbro	X	
	126.0	Ophitic gabbro	X	
	135.0	Ophitic gabbro	X	
	143.0	Ophitic gabbro	X	
	143.6	Ophitic gabbro	X	
	145.5	Ophitic gabbro	X	
	149.0	Ophitic gabbro	X	
	153.0	Ophitic gabbro	X	
	155.0	Ophitic gabbro	X	
MW-07-08	11.5	Meta-basalt	X	
	17.5	Meta-basalt	X	
	23	Meta-basalt	X	
	25	Meta-basalt	X	
	31	Malpas Lake Intrusion	X	X
	40.7	Malpas Lake Intrusion	X	X
	48.6	Malpas Lake Intrusion	X	X
	56.3	Malpas Lake Intrusion	X	
	71.5	Malpas Lake Intrusion	X	X
	85.1	Malpas Lake Intrusion	X	X
	93.7	Malpas Lake Intrusion	X	X
	101	Malpas Lake Intrusion	X	X
	111.3	Malpas Lake Intrusion	X	X
	119.14	Malpas Lake Intrusion	X	
	127.2	Malpas Lake Intrusion	X	X
	145	Malpas Lake Intrusion	X	

Appendix 4. pXRF whole-rock analyses. Unit for major oxides (except MnO) is weight percent, unit for others is ppm. Major oxides were determined using the mining mode, and trace elements were determined using the soil mode. Numbers given below oxides (and elements) are 95% confidence analytical precision determined by repetitive analyses. Symbols for rocks: 2a-meta-basalt, 2i-feldspathic clinopyroxenite, 2b-olivine gabbro, 2f-oxide augite melatroctolite, 3a-medium-grained ophitic gabbro, 3b-coarse-grained ophitic gabbro, 3d-pegmatitic ophitic gabbro, 3g-oxide melatroctolite, 3h-apatitic clinopyroxenite, 3i-apatitic olivine clinopyroxenite, MLI-malpas lake intrusion. Samples begin with FD, SL, and MS were sampled at drill holes at Four Dams, Area 41 and WD zone, respectively.

Sample	Rock name	SiO_2	Al_2O_3	MgO	$Fe_2O_3^T$	CaO	K_2O	P_2O_5	TiO_2	MnO	Cu	S	Ni	V	Cr	Ba	Zr	Sr
		0.6	**0.5**	**0.72**	**0.3**	**0.09**	**0.02**	**0.07**	**0.04**	**79**	**44**	**223**	**16**	**22**	**8**	**22**	**2**	**35**
FD-13-34-5	2f	27	5	12.1	43	10.1	0.2	3.0	8.3	6479	1245	4081	340	738		590	47	286
FD-13-34-9.5	2f	34	11	8.6	30	11.6	0.6	2.9	4.6	4500	454		180	422		798	58	719
FD-13-34-14	2f	32	8	9.0	35	11.7	0.5	3.0	4.8	5239	1547	4653	185	723		681	107	532
FD-13-34-18.5	2f	41	16	6.0	17	11.7	0.8	2.0	1.7	2146	3604	15907	267	274		1475	44	1146
FD-13-34-23	2b	39	13	7.7	23	12.4	0.9	2.8	3.3	3038	545		179	561		1206	75	862
FD-13-34-27.5	2f	24	5	13.8	47	7.8	0.3	3.3	7.5	7424	2076	6852	381	1403		434	51	293
FD-13-34-32	2f	24	5	11.6	48	6.9	0.3	3.0	9.1	7397	1489	1533	351	1263		337	40	271
FD-13-34-36.5	2f	37	14	7.1	24	12.2	1.0	3.0	3.6	3208	1193	3560	207	399	61	898	77	888
FD-13-34-41	2f	33	9	10.1	34	11.8	0.5	3.2	5.0	5206	559		245	675		519	58	507
FD-13-34-45.5	2f	25	6	10.0	45	10.0	0.3	3.5	8.8	6559	1933	6358	333	804		503	44	312
FD-13-34-50	3h	37	9	8.5	35	8.4	1.4	2.3	4.2	5058	2570	14271	254	421	73	1017	158	346
FD-13-34-60	2f	42	19	5.9	17	11.6	0.6	1.5	2.1	2238	2978	14518	177	266		757	33	1280
FD-13-34-64.5	2f	46	19	4.8	15	11.9	0.8	1.5	1.7	2150	455	775	45	227		914	47	1239
FD-13-34-66	2f	47	18	4.8	10	11.7	1.0	1.5	1.3	1646	194		51	147		1038	73	1323
FD-13-34-70.5	2b	43	16	5.2	18	12.9	0.7	1.9	2.7	2502	179		80	301		720	53	956
FD-13-34-75	2b	46	18	5.4	14	12.2	1.0	1.7	2.2	1989	176	294	31	173		687	62	1152
FD-13-34-79.5	2b	45	17	6.7	17	12.0	0.9	1.6	2.5	2367	134		32	249		702	75	1038
FD-13-34-84	2b	40	13	5.9	19	11.6	0.7	2.0	3.3	2500	146		64	214		588	65	771
FD-13-34-89.5	2b	44	16	5.3	18	11.2	1.0	1.6	3.2	2513	244		82	195		532	76	968
FD-13-34-94.5	2b	45	16	5.5	18	11.6	1.0	1.7	3.6	2404	97		43	170		629	78	1015
FD-13-34-99	2b	40	13	6.1	19	10.0	0.8	1.9	3.6	2448	86		84	236		455	55	648
FD-13-34-103.5	2b	35	11	6.6	23	9.9	0.5	2.2	5.1	3361	107		73	259		468	71	604
FD-13-34-108	2b	42	14	6.0	22	10.7	0.7	1.7	3.2	3044	109		52	224		612	69	792

FD-13-34-112.5	2b	37	12	7.0	30	11.1	0.4	2.3	5.3	4533	622	6226	109	302		445	49	617
FD-13-34-117	2b	44	15	5.3	18	11.7	0.7	1.6	2.9	2510	133		53	226		804	51	977
FD-13-34-127	2b	42	14	5.0	23	12.3	0.7	2.1	3.5	3762	174		53	247		602	56	841
FD-13-34-131.5	2b	44	15	5.5	22	11.7	0.8	1.8	3.4	3337	233	741	76	206		858	62	883
FD-13-34-136	2b	44	16	5.1	21	11.5	0.8	2.0	3.0	3242	365	427	93	190		759	64	1006
FD-13-34-140.5	2b	40	13	5.2	27	12.0	0.7	2.5	4.2	4576	419		114	310		667	59	726
FD-13-34-145	2b	41	14	5.3	25	11.6	0.6	2.1	3.8	4046	299		120	297		643	52	846
FD-13-34-149.5	2b	38	13	5.0	30	11.7	0.5	2.5	5.2	5158	389	637	168	366		649	59	716
FD-13-34-154	2b	46	15	4.8	20	11.6	1.0	1.8	2.9	3327	283		78	226		814	73	904
FD-13-34-158.5	2b	43	15	5.3	22	11.8	0.8	2.1	3.6	3577	279		102	264		785	74	877
FD-13-34-163	2b	43	15	5.1	21	12.1	0.8	2.1	3.5	3483	253		89	232		761	81	911
FD-13-34-167.5	2b	45	15	5.4	20	11.3	1.0	1.6	3.1	3345	206		106	274		827	94	908
FD-13-34-172	2b	43	14	4.8	23	11.3	0.9	1.9	3.9	3852	328		94	340		790	89	869
FD-13-34-176.5	2b	45	15	5.3	20	11.7	1.0	1.9	3.0	3339	261		85	230		763	77	929
FD-13-34-181	2b	45	15	5.2	21	11.4	1.0	2.0	3.2	3361	271		78	253		792	100	934
FD-13-34-190	2b	45	15	4.8	21	11.6	1.0	1.8	3.0	3397	289		96	271		866	93	900
FD-13-34-194.5	2b	46	15	5.1	21	11.4	1.0	1.8	2.8	3375	277		76	283		897	104	912
FD-13-34-199	2b	42	15	6.0	22	11.3	0.9	2.0	3.4	3624	327		126	338		803	97	926
FD-13-34-203.5	2f	39	12	5.8	28	10.2	0.8	2.2	4.0	4820	279		112	352		639	84	663
FD-13-34-208	2f	32	8	5.8	38	10.4	0.4	3.2	6.3	7070	655		192	563		415	91	408
FD-13-34-212.5	2f	42	13	6.5	24	10.6	0.9	2.2	3.9	3860	309		110	327		802	85	786
FD-13-34-217	2f	37	12	6.8	29	9.9	0.6	2.4	4.9	4998	419		174	488		626	87	651
FD-13-34-221.5	2f	37	11	7.3	32	9.7	0.6	2.5	5.0	5865	362		183	405		656	107	601
FD-13-34-226	2f	35	10	6.3	34	9.7	0.6	2.9	5.4	6060	631		151	542		558	89	587
FD-13-34-230.5	2f	33	11	5.4	34	11.0	0.3	3.3	6.9	5458	665		202	709		531	62	678
FD-13-34-235	3g	21	3	8.7	45	14.0	0.1	6.0	9.5	7516	759	3742	247	751	64	83	53	251
FD-13-34-239.5	3g	23	2	8.7	41	16.8	0.0	6.5	8.8	6457	700	1597	180	865		139	52	240
FD-13-34-244	3g	27	2	9.6	39	15.4	0.0	5.3	7.3	6569	626	2179	251	815		190	59	223
FD-13-34-248.5	3g	35	13	5.6	28	13.1	0.3	3.8	4.7	4196	446		148	519		372	51	816
FD-13-34-253	3g	32	9	7.9	32	12.8	0.3	3.9	5.6	5184	498	1467	178	722		292	58	544
FD-13-34-257.5	3g	33	10	7.8	33	13.0	0.3	4.3	5.9	5263	542	953	159	793		423	58	691

FD-13-34-262	3g	33	10	6.0	32	12.4	0.3	4.7	4.8	5541	443		205	813		372	42	650
FD-13-34-266.5	3g	30	11	7.2	30	15.5	0.2	7.0	3.9	5054	847		210	852		399	32	818
FD-13-34-271	3g	24	7	9.7	35	15.1	0.4	7.8	5.7	4680	800		284	1730	110	433	79	510
FD-13-34-272	3h	34	11	8.9	35	7.6	0.3	2.3	3.8	5237	3173	1614	360	1154	101	398	39	601
FD-13-34-276.5	3h	40	6	9.7	25	14.5	0.2	2.1	2.2	3549	4781	6051	301	842	300	240	46	268
FD-13-34-281	3h	33	7	8.1	33	11.8	0.5	3.2	4.7	5732	438		252	872	95	458	86	415
FD-13-34-285.5	3h	42	14	5.6	21	11.9	0.4	1.8	2.1	3030	364		160	607	70	363	57	671
FD-13-34-291	3h	39	5	13.0	34	5.5	0.2	0.7	0.6	5961	3312	1411	433	211		245	30	182
FD-13-34-295.5	3h	38	3	8.9	26	14.4	0.7	3.2	1.3	4307	1753	1989	233	381	95	349	88	199
FD-13-34-302	3h	35	3	9.1	30	13.2	0.1	4.2	1.1	5188	1235		268	363	69	289	38	261
FD-13-34-305	3h	49	13	5.7	13	11.8	0.4	0.2	0.8	2156	592		122	374	179	429	34	693
FD-13-34-310	3h	40	4	9.7	28	12.1	0.3	2.2	1.2	4571	1132		266	455	89	226	43	221
FD-13-34-316	3i	35	2	11.7	32	12.8	0.1	4.6	1.2	5047	2231	1127	301	495	96	168	43	183
FD-13-34-320.5	3i	37	2	11.0	28	13.0	0.2	3.3	0.9	4538	2710	2757	300	506	104	224	40	153
FD-13-34-325	3i	33	2	11.5	30	13.7	0.2	5.7	0.4	4998	2960	1890	320	177	85	213	33	214
FD-13-34-327.5	3i	29	1	11.4	31	15.9	0.3	8.1	0.3	5066	3904	4255	393	184	102	343	35	261
FD-13-34-330	3i	30	3	11.0	29	14.7	0.4	6.9	0.4	4900	3539	5470	381	232	75	356	31	275
FD-13-41-2.5	2f	46	15	9.7	21	9.9	0.7	1.6	3.6	3098	192		97	165		1006	61	936
FD-13-41-7	2f	32	6	11.4	45	8.8	0.1	2.5	8.0	8970	403		201	539		328	35	317
FD-13-41-11.5	2f	33	7	12.1	42	8.8	0.2	2.1	7.2	7739	374		208	465		403	41	329
FD-13-41-16	2b	44	15	9.6	27	9.8	0.6	2.1	4.3	4262	428	771	110	270		932	46	938
FD-13-41-20.5	2f	39	12	10.5	33	10.2	0.4	2.3	4.7	5853	429		149	305		529	50	644
FD-13-41-25	2b	48	14	9.6	17	9.3	1.0	1.4	2.6	2629	186		78	199		1141	70	1072
FD-13-41-29.5	2b	38	10	10.2	34	10.3	0.4	2.4	5.9	5691	405		149	347		629	63	583
FD-13-41-34	2b	47	14	11.3	18	9.6	0.8	1.4	2.7	2720	167		83	195		1219	81	1014
FD-13-41-38.5	2b	44	14	12.0	27	9.7	0.8	1.6	4.3	4083	227		139	322		902	95	847
FD-13-41-43	2b	30	6	12.4	46	8.3	0.2	2.6	7.5	8858	2116	7474	234	573		397	48	312
FD-13-41-47.5	2b	48	14	9.6	20	9.9	0.9	2.3	2.8	3466	252		98	231		520	1286	1033
FD-13-41-52	2b	50	14	9.6	17	9.0	1.2	1.3	2.5	2762	169		81	184		544	269	1046
FD-13-41-56.5	2b	35	9	11.9	39	10.1	0.3	2.8	6.7	6568	431		178	441		554	67	459
FD-13-41-61	2b	42	13	10.4	29	10.5	0.5	2.3	4.6	4502	566		141	407		784	63	763

FD-13-41-65.5	2b	44	15	11.4	23	10.9	0.4	2.0	3.5	3542	331		88	320		760	55	1046
FD-13-41-67	2f	34	10	10.5	35	10.9	0.2	2.8	6.1	5588	1085	3879	182	462		500	47	651
FD-13-41-71.5	2f	40	13	9.9	27	12.0	0.6	2.9	4.3	3929	2563	8386	148	273		865	79	779
FD-13-41-76	2f	41	13	10.8	26	11.6	0.4	2.7	4.0	4099	394		139	363		576	48	897
FD-13-41-80.5	2f	41	12	10.6	28	11.4	0.4	2.6	4.4	4233	378		120	454		571	58	806
FD-13-41-89.5	2f	41	14	11.1	25	12.7	0.3	3.2	4.3	3682	283		87	440		459	60	856
FD-13-41-94	2f	41	12	11.3	26	12.7	0.4	3.1	4.3	3958	406	709	110	492		502	53	774
FD-13-41-99.5	2f	38	12	9.6	25	12.9	0.5	4.2	4.1	3652	504		119	584		576	49	881
FD-13-41-104	2f	37	12	11.6	29	12.5	0.6	3.9	5.3	4229	484		162	763		565	64	706
FD-13-41-108.5	2f	40	13	10.8	28	12.5	0.5	3.6	4.2	4251	583		137	646		522	57	718
FD-13-41-113	2f	39	12	10.6	26	12.6	0.4	3.5	4.0	3716	558		139	781		584	52	738
FD-13-41-117.5	2f	39	12	12.2	27	13.7	0.4	4.3	4.1	3618	813		140	920		416	48	739
SL-13-27-4	2b	37	12	11.1	26	12.2	0.8	2.7	5.8	3146	167	2595	111	538		1934	85	908
SL-13-27-8.5	2b	39	14	9.9	22	12.3	0.9	2.3	2.8	2519	1519	15073	188	319		1439	68	976
SL-13-27-17	3b	41	15	9.6	18	11.4	1.3	2.9	2.1	2494	564	4801	140	233		1911	82	1087
SL-13-27-25	3b	42	15	9.5	17	14.3	0.7	2.4	2.4	2217	926	3360	120	331		1068	45	1051
SL-13-27-30	3a	42	16	9.6	16	13.2	0.7	2.4	2.4	2131	175		103	386		1065	48	1196
SL-13-27-35	3a	37	13	10.9	24	13.0	0.5	2.7	2.9	2697	2088	11992	226	559		874	37	895
SL-13-27-37.3	3g	40	15	10.5	19	12.7	0.9	2.8	2.1	2450	960	6541	155	322		1257	50	1073
SL-13-27-41.5	3g	36	13	7.9	24	13.5	0.8	3.6	3.3	2840	1556	11871	211	555		1224	55	990
SL-13-27-46	3g	25	8	13.0	35	14.4	1.0	6.9	5.4	4458	1683	11853	267	974		951	50	627
SL-13-27-50.5	3g	17	5	13.9	40	16.8	0.3	9.2	7.1	4334	1249	6290	312	1340		673	39	570
SL-13-27-55	3g	23	8	12.9	35	15.1	0.4	7.8	5.1	4323	1481	8185	198	971		831	37	773
SL-13-27-66	3d	40	14	10.8	20	11.9	0.9	2.9	2.1	2601	2060	7666	181	415		1198	95	948
SL-13-27-70	3d	38	14	11.2	23	12.4	0.7	2.8	3.2	2845	1100	7955	149	558		1234	46	1023
SL-13-27-80	3b	36	12	11.7	24	12.7	0.6	2.6	4.1	2981	564	1269	163	510		1517	38	955
SL-13-27-85	3b	44	15	10.4	19	12.4	0.7	2.3	2.5	3047	202		81	219		1341	70	1209
SL-13-27-90	3b	51	12	9.7	17	9.5	2.0	2.2	2.2	2429	498	3116	105	350		878	151	755
SL-13-27-95	3b	37	12	11.7	22	13.6	0.5	3.0	3.2	2732	1604	6328	164	547		825	36	878
SL-13-27-100	3b	55	9	8.9	14	9.0	2.5	2.1	2.1	2669	384	3983	87	156	91	383	234	313
SL-13-27-105	3b	33	14	10.2	26	13.0	0.5	4.4	4.0	3113	2511	7446	217	712		836	28	960

SL-13-27-174.5	3g	11	5	7.6	60	9.4	0.2	3.9	18.6	6201	1026	10674	446	2450	167	328	22	220
SL-13-27-179	3g	14	5	7.6	57	10.3	0.3	3.9	15.9	6039	1075	25353	369	1474	191	411	18	224
SL-13-27-183.5	3g	19	6	9.7	50	10.3	0.7	2.5	14.4	6180	1033	20262	352	1579	294	619	47	201
SL-13-27-231	3h	42	6	13.8	20	13.9	0.2	1.0	1.0	3253	799	5133	149	520	250	390	46	285
SL-13-27-235.5	3h	46	6	11.1	14	14.9	0.2	0.2	0.5	2547	634	4574	102	461	311	224	34	257
SL-13-32-5.5	2b	30	12	10.9	33	10.2	0.5	3.6	5.3	4314	2691	7029	307	885	330	1049	37	724
SL-13-32-10	2b	36	13	12.2	25	11.8	0.5	2.6	3.2	3425	1824	5926	246	448		1034	42	912
SL-13-32-12	3c	45	17	9.2	16	12.2	0.7	2.1	1.6	2142	1442	5811	151	214		1093	38	1228
SL-13-32-17	3b	42	15	8.7	19	12.3	0.8	2.0	2.4	2444	2662	11680	206	463		999	43	1033
SL-13-32-22	3b	42	13	9.6	16	12.9	0.6	2.3	2.2	2138	1355	3081	150	463		736	34	1005
SL-13-32-27	3b	42	14	9.4	15	12.4	0.8	1.9	2.0	2188	938	3397	115	403		849	39	1042
SL-13-32-32	3b	41	13	10.7	16	11.9	1.0	1.9	2.2	2388	2443	5970	158	433		828	44	926
SL-13-32-37	3b	44	14	10.5	16	12.1	0.7	2.2	2.6	2018	333		98	560		725	74	1018
SL-13-32-42	3b	40	13	11.4	23	11.8	0.5	2.5	2.8	2913	1064	1689	141	549		708	51	823
SL-13-32-44	3g	30	9	12.1	31	14.7	0.3	5.8	5.3	3435	2798	7246	209	1006		559	39	698
SL-13-32-49	3g	36	11	12.5	22	14.3	0.4	3.9	3.5	2674	1782	2587	105	702		446	44	743
SL-13-32-53	3b	37	11	12.0	22	14.1	0.5	3.8	3.5	2776	876		120	720		508	35	776
SL-13-32-58	3b	37	10	11.3	26	13.3	0.4	3.2	4.9	2922	581		116	1104		582	46	716
SL-13-32-60.5	3g	33	11	12.8	29	12.9	0.6	4.9	4.7	3513	663		145	947		604	47	700
SL-13-32-66.5	3g	32	10	10.6	23	15.8	0.4	5.9	3.3	2896	643	411	114	741		592	29	819
SL-13-32-70	3d	42	16	10.7	20	10.0	0.4	1.7	2.0	2669	923	2299	105	441		603	16	964
SL-13-32-75	3d	45	14	11.3	15	9.9	0.6	0.6	0.7	2335	261		112	184	68	636	18	957
SL-13-32-80	3d	45	15	10.6	16	8.3	0.5	0.2	0.5	2390	119		157	96		562	26	920
SL-13-32-85	3d	39	12	12.0	23	9.0	0.8	2.5	2.5	3189	1092	1811	141	381	71	743	44	716
SL-13-32-90	3d	45	14	12.8	14	9.0	1.4	0.3	0.9	2643	685		166	203		960	22	795
SL-13-32-150.5	3h	41	10	8.9	19	12.7	1.0	2.5	3.0	2845	484		103	398		1250	142	718
SL-13-32-155.5	3h	49	15	8.6	13	10.5	1.3	1.3	1.9	2137	391	69	81	203		1373	107	1096
SL-13-32-160.5	3h	44	11	10.5	18	13.4	0.4	1.5	2.3	2551	573		146	539	116	446	52	596
SL-13-32-165.5	3h	45	9	13.1	16	15.5	0.3	1.5	1.1	2495	1226	1188	186	466	85	232	43	471
SL-13-32-170	3h	47	15	9.4	15	12.6	0.3	0.4	1.6	2090	470		127	626	166	336	29	746
SL-13-32-175	4a	45	8	12.6	19	15.2	0.3	0.9	2.7	2737	1442	1075	158	799	136	351	59	415

SL-13-32-180	4a	46	9	11.9	18	14.9	0.2	0.8	1.9	2707	869	1203	143	676	61	291	43	459
SL-13-32-185	4a	42	9	11.0	17	14.9	0.4	2.9	2.0	2503	1033	3110	148	338	106	417	42	616
SL-13-32-200	3h	41	5	12.6	18	18.9	0.3	3.4	1.7	3029	1795	6129	181	426	93	380	62	392
SL-13-32-204.5	3h	38	5	12.0	19	17.4	0.5	4.2	2.5	3079	1358	5037	176	440	95	476	71	439
SL-13-32-209	3h	43	9	10.8	17	14.9	1.0	2.5	2.3	2917	1359	4334	165	512	95	758	198	468
SL-13-32-214	3h	34	6	12.3	27	16.1	0.2	3.1	5.7	3922	2035	8198	241	1087	96	288	60	364
SL-13-32-219.5	3h	40	9	10.6	26	12.1	0.9	2.6	5.0	3690	1777	7805	180	476	106	789	130	453
SL-13-32-224	3h	41	10	10.9	21	14.2	0.9	2.5	3.4	2911	1603	4434	164	434	92	675	90	679
SL-13-32-229.5	3h	45	15	9.7	16	11.4	0.5	0.7	1.4	2053	2396	11294	218	207		749	23	1262
SL-13-32-234	3h	43	16	11.4	25	10.6	0.6	1.3	2.9	2484	1490	5523	180	396		646	41	1579
SL-13-41-3	2f	42	11	10.5	23	9.9	1.8	1.7	5.1	4156	96		148		76	5439	74	832
SL-13-41-7.5	2f	36	8	11.4	38	7.9	0.9	1.3	7.0	7746	82		238			1962	66	411
SL-13-41-12	2f	44	14	10.1	17	10.5	1.5	1.5	3.1	2932	155	1978	102	83		4627	44	1429
SL-13-41-20	2f	48	19	9.6	6	10.5	1.2	0.5	1.5	1483	136		62	121		3022	73	1476
SL-13-41-24.5	2f	49	10	9.9	14	10.3	2.0	1.8	1.6	2881	126	996	116	113		1896	161	705
SL-13-41-29	2f	51	16	9.6	11	7.2	2.7	1.1	1.8	2149	142		137			8519	77	1820
SL-13-41-33.5	2f	45	15	10.3	18	11.1	1.0	1.7	3.6	3019	112	952	111	115		2270	59	1216
SL-13-41-38	2f	44	15	10.6	19	10.6	1.5	1.8	3.4	3078	131		162	232		4357	71	1250
SL-13-41-42.5	2f	37	11	12.9	27	10.8	1.0	2.4	5.7	3859	119		121	520		3067	101	927
SL-13-41-45	2f	44	15	9.8	17	11.7	1.1	2.0	3.2	2460	104		121	160		3860	66	1498
SL-13-41-49.5	2f	43	14	11.1	19	11.8	1.5	2.4	3.6	2763	117	1386	138	308		3992	94	1191
SL-13-41-54	2f	43	15	10.7	14	10.7	1.5	1.8	2.3	2088	105	916	88	135		3490	54	1751
SL-13-41-58.5	2f	45	17	10.5	12	10.4	1.3	1.6	2.0	1953	139		97	97		3725	60	1792
SL-13-41-63	2f	41	14	13.7	22	10.8	1.3	2.4	3.6	3120	289	2900	122	327		2295	98	1150
SL-13-41-68.5	2f	40	13	10.3	19	11.2	1.4	2.4	3.8	3017	151	1231	117	299		2408	78	1186
SL-13-41-73	2f	36	11	13.2	28	12.4	1.0	3.1	5.6	3509	292	4133	142	611		1965	66	867
SL-13-41-77.5	2f	35	10	11.5	30	11.1	0.9	2.9	5.6	3910	202	2175	152	411		1617	50	750
SL-13-41-82	2f	29	6	13.8	36	11.7	0.3	3.4	7.0	4764	330	3093	158	578		850	50	454
SL-13-41-86.5	2f	34	9	13.0	31	11.8	0.8	3.2	5.3	4060	319		166	634		1421	66	588
SL-13-41-91	2f	31	7	12.8	35	11.2	0.6	3.4	6.6	4525	409		175	784		1257	52	507
SL-13-41-94.5	2f	31	8	13.9	31	11.1	0.6	2.9	5.4	4182	283	1094	166	661		1300	45	500

SL-13-41-104.5	2f	38	13	11.5	24	12.5	0.7	2.7	3.6	3186	370	1401	118	408		1337	50	962
SL-13-41-109	2f	22	6	15.4	46	10.5	0.2	3.9	10.5	5658	856	1526	284	1335		614	30	368
SL-13-41-116.5	2f	37	11	12.8	25	11.7	0.9	2.7	4.0	3314	379		147	509	93	1377	48	805
SL-13-41-121	2f	30	9	13.8	37	10.5	0.5	2.8	7.9	4437	672	1288	204	993	85	1081	42	563
SL-13-41-125	3g	34	12	11.7	29	11.4	0.6	3.2	4.6	3639	975	1914	218	690	71	884	56	818
SL-13-41-129.5	3g	36	12	13.3	22	14.3	0.4	3.7	3.1	2707	1083	3422	170	456		759	41	860
SL-13-41-132	3g	38	13	13.4	20	13.7	0.6	3.7	2.4	2640	869	2458	170	374	60	958	90	1000
SL-13-41-135	3g	34	14	12.4	27	12.3	0.5	3.9	3.9	3095	1009	3284	171	704	243	686	34	898
SL-13-41-138	3g	30	7	16.5	34	10.4	0.5	4.1	3.5	4349	1849	9985	275	657	205	525	75	475
SL-13-41-143	3b	42	17	12.1	17	13.3	0.5	2.4	1.8	2028	2045	14957	158	359		505	30	1008
SL-13-41-148	3b	44	16	11.3	15	13.1	0.6	2.3	1.6	2085	1063	5459	116	336		580	39	1001
SL-13-41-153	3b	43	16	11.8	16	13.5	0.4	2.6	2.2	2180	245		90	445		559	32	999
SL-13-41-167	3b	39	14	10.5	22	12.3	0.5	2.8	2.8	2732	1917	5204	158	642		547	31	890
SL-13-41-169	3g	36	12	12.8	25	11.6	0.6	3.0	3.0	3221	2940	9576	138	626		543	43	751
SL-13-41-173.5	3g	33	12	13.5	24	15.6	0.4	5.5	2.7	2862	2081	7163	155	565		565	29	785
SL-13-41-221	3h	46	4	14.8	14	16.8	0.1	0.0	0.6	2318	1750	2825	211	434	200	113	38	145
SL-13-41-225.5	3h	45	9	14.3	14	14.3	0.2	0.1	0.4	2249	1265	3622	187	303	135	207	29	374
SL-13-41-230	3h	46	9	12.6	12	15.5	0.2	0.1	0.5	2110	1413	4939	219	331	115	220	33	406
SL-13-41-265.5	3h	42	5	16.5	20	10.7	0.2	0.1	0.5	2925	874	2981	191	312	85	118	30	156
SL-13-41-270	3h	45	10	14.1	13	12.4	0.5	0.1	0.4	2083	822	3715	170	228	57	468	24	473
SL-13-41-277	3h	41	6	15.7	23	9.7	0.1	0.1	0.6	3488	834	2951	236	398	168	253	21	274
SL-13-34-3.5	2f	34	12	8.2	31	9.5	1.5	2.5	6.6	4347	73	2805	113	440		2461	118	759
SL-13-34-7	2b	48	18	4.2	12	10.5	1.6	1.4	2.0	1973	63		72	165		3886	92	1983
SL-13-34-13	2b	48	18	3.6	9	10.6	1.5	1.5	1.5	1578	74		57	112		3086	88	1968
SL-13-34-17	2b	48	17	4.4	13	10.9	1.6	1.7	1.8	1887	86		76	208	33	3479	75	1616
SL-13-34-20.5	2f	30	8	6.9	27	8.9	0.8	1.8	3.5	4145	92		117	564		2150	100	778
SL-13-34-24.5	2f	42	14	6.2	20	12.3	1.4	2.3	3.6	2961	77	973	92	318	42	3594	83	1231
SL-13-34-28.5	2f	34	10	9.1	29	12.5	1.1	3.3	5.3	3973	101	2567	134	529	37	2585	90	802
SL-13-34-33	2b	41	16	5.4	21	11.1	1.2	2.2	3.0	3112	119	1700	118	361	40	3109	83	1306
SL-13-34-37	2b	45	17	4.5	15	11.4	1.5	2.0	2.3	2211	71		76	291	35	2514	98	1504
SL-13-34-41.4	2b	43	15	5.9	17	11.8	1.3	2.1	2.7	2550	159	1483	79	334		2278	111	1188

SL-13-34-45.7	2f	35	9	10.0	30	12.6	0.9	2.7	5.1	4267	170	2454	137	751	35	1387	88	573
SL-13-34-50.1	2f	37	10	7.9	27	13.3	0.8	2.5	4.4	3515	191	1970	118	554	54	1587	89	705
SL-13-34-54.1	2f	28	8	11.5	38	11.1	0.7	3.2	5.6	4711	1292	22314	268	738	82	1104	64	476
SL-13-34-58.9	2f	40	13	6.8	22	12.2	1.0	2.1	3.1	2841	164	1086	116	451	94	1530	72	964
SL-13-34-63.5	3b	33	13	9.5	28	14.1	0.4	4.1	4.2	3366	911	7581	171	659	99	833	46	794
SL-13-34-67.5	3d	39	16	4.3	15	12.0	0.8	2.7	1.5	2097	1028	7739	138	254	78	1653	38	1469
SL-13-34-71.5	3d	38	12	6.2	22	12.3	1.2	3.0	3.6	3004	959	9434	140	472	91	994	113	739
SL-13-34-75	3i	29	4	18.2	40	4.7	0.3	1.4	2.6	6025	1025	2751	311	732	298	448	18	209
SL-13-34-76.5	3i	32	8	15.8	32	6.2	0.5	1.6	2.4	4655	1187	3636	268	564	280	746	62	433
SL-13-34-78.5	3d	45	15	8.9	15	11.5	0.4	0.1	0.4	2188	294		167	196	261	411	27	647
SL-13-34-88	2i	43	7	13.7	17	12.1	0.1	0.1	0.4	2616	83		325	257	904	194	29	231
SL-13-34-92	2i	42	9	13.2	18	11.2	0.1	0.1	0.5	2602	364		376	283	1323	181	27	308
SL-13-34-96	2i	42	8	13.5	19	11.2	0.2	0.1	0.7	2707	342		387	375	1290	209	33	262
SL-13-34-99.5	2i	42	7	13.9	20	11.3	0.1	0.1	0.7	2835	208		552	352	1355	203	36	217
SL-13-34-103.5	2i	42	8	13.2	22	10.9	0.1	0.1	0.9	3103	131		494	457	1242	243	31	220
SL-13-34-107.8	3d	48	14	8.1	14	13.7	0.5	0.2	1.2	2083	294		115	465	106	352	42	608
SL-13-34-111.8	2i	42	7	15.5	21	11.5	0.1	0.1	0.9	2924	266		529	429	1295	160	34	178
SL-13-34-115.8	2i	42	6	15.3	20	11.5	0.1	0.0	0.8	2913	1064	994	570	413	1398	166	32	190
SL-13-34-119.5	2i	39	4	17.2	22	8.8	0.1		1.1	2799	132		808	438	1379	112	22	175
SL-13-34-123.5	2i	33	3	15.2	22	7.5	0.1		0.6	2969	444		800	374	1201	139	34	146
SL-13-34-126.5	3d	41	13	10.1	22	11.0	0.6	0.3	2.7	2761	123		201	991	211	445	43	512
SL-13-34-128.8	3d	47	18	5.6	7	12.3	0.6	0.1	0.3	1435	1685	1224	185	159	52	293	19	939
SL-13-34-141	3d	42	16	8.1	21	10.9	0.6	1.1	2.9	2447	589	1275	157	821	208	729	140	673
SL-13-34-143.5	3d									2203	1007	2071	124	596	136	426	33	744
SL-13-34-146.5	3a	47	19	6.2	11	12.0	0.5	0.1	1.0	1491	501		114	538	127	273	24	849
SL-13-34-147.3	3h	44	14	7.3	18	15.3	0.4	1.5	2.2	2145	1491	1707	154	872	166	298	50	598
SL-13-34-150.5	3a	46	19	5.2	14	12.5	0.3	0.1	1.7	1818	996		134	705	146	285	37	723
SL-13-34-154.5	3a	32	11	4.5	7	8.2	0.3	0.1	0.7	1575	464		94	495	80	281	24	846
SL-13-34-159.5	3a	46	16	5.2	13	11.7	0.6	0.7	1.4	1684	705	967	96	484	99	476	37	1139
SL-13-34-163.5	3a	50	19	6.0	13	10.5	0.6	0.7	1.1	1822	389		40	314	81	410	35	1205
SL-13-34-171	3a	54	17	4.9	7	7.7	0.8	0.5	0.3	1630	264	901	29	43		809	44	2472

SL-13-34-175	3a	54	17	5.3	10	8.8	0.8	0.6	0.4	1692	785	4261	45	40	40	619	32	2480
SL-13-34-181.4	3a	50	17	5.4	11	9.6	0.6	0.3	0.7	1640	301			186	38	563	27	1818
SL-13-34-185.4	3a	54	17	6.1	8	7.9	0.7	0.5	0.4	1460	177			96	27	463	29	2123
SL-13-36-10.5	2b	34	9	10.4	31	12.1	0.7	2.8	5.6	3913	206	2329	103	780	63	1518	71	601
SL-13-36-14	2f	30	8	11.1	36	11.1	0.6	3.1	5.9	4759	191	2088	170	833	66	1240	71	474
SL-13-36-15.5	2b	40	13	8.5	24	12.2	0.8	2.1	3.5	3171	185	1508	81	511	101	1673	69	883
SL-13-36-19.5	2b	38	12	8.8	27	11.9	0.8	2.3	4.1	3643	215	2007	113	552	135	1690	65	726
SL-13-36-23.5	2b	39	12	8.8	25	11.8	0.8	1.9	3.7	3252	179	1065	105	569	144	1835	62	792
SL-13-36-26.5	2f	36	9	10.3	28	12.1	0.8	2.6	4.2	3589	173	1690	118	651	127	1525	67	497
SL-13-36-30.5	2e	37	13	9.4	22	14.7	0.4	3.9	2.8	2730	265		180	530	54	969	32	884
SL-13-36-36.5	3b	42	20	7.6	19	11.3	0.8	2.2	1.7	2216	1228	8562	148	370	55	1050	36	1272
SL-13-36-39.5	3b	39	15	8.7	18	12.7	0.6	3.2	1.3	2180	2017	6522	178	319	184	915	23	1027
SL-13-36-51.5	3d	44	14	9.8	17	11.3	0.6	0.7	0.9	2499	344		148	282	138	515	34	714
SL-13-36-54.5	3d	40	17	10.5	25	9.5	0.6	1.3	2.4	2913	2108	4064	227	488	140	524	33	757
SL-13-36-58.5	3d	44	11	10.4	17	12.9	0.5	0.1	1.0	2435	661		196	366	237	388	30	501
SL-13-36-63	3d	46	13	8.0	12	12.4	0.4	0.2	0.5	1994	1518	2972	223	208	184	348	42	639
SL-13-36-67.5	3d	44	12	7.8	13	14.1	0.5	0.1	0.9	2048	317		127	294	175	359	42	553
SL-13-36-71.5	3h	44	16	7.9	11	9.6	1.2	0.1	0.2	1776	403	970	137	90	89	953	23	873
SL-13-36-76.5	3h	45	6	12.2	16	14.6	0.2	0.1	0.7	2431	1718	1877	356	418	684	192	39	170
SL-13-36-80.5	2i	41	7	13.2	22	11.5	0.1	0.1	1.4	2821	448		583	618	1061	177	36	221
SL-13-36-83.2	2i	42	13	9.2	23	10.3	0.7	0.3	2.0	2614	458	1923	169	818	134	654	35	590
SL-13-36-86.5	2i	40	6	13.8	21	10.8	0.1	0.1	2.1	2514	176		601	614	1139	165	38	248
SL-13-36-90.5	2i	41	6	14.8	21	11.4	0.0	0.3	3.1	2522	181		592	612	1146	110	47	334
SL-13-36-94.5	2i	40	6	14.4	21	10.4	0.1	0.2	3.0	2537	233		620	640	1111	133	39	364
SL-13-36-99.5	2i	40	6	14.3	21	10.5	0.0	0.3	3.1	2573	215		609	651	1104	161	43	381
SL-13-36-103.5	2i	40	7	14.2	21	11.1	0.0	0.3	3.2	2511	197		580	635	1089	89	45	429
SL-13-36-107.5	2i	40	5	14.0	21	11.3	0.1	0.3	2.7	2644	840	3576	574	577	1090	145	48	350
SL-13-36-114.5	2i	39	6	13.4	21	10.7	0.0	0.4	3.0	2559	273		635	614	1117	114	47	396
SL-13-36-117.5	3h	38	4	12.8	22	11.1	0.1	0.1	2.2	2840	617	2528	558	570	1212	143	43	201
SL-13-36-119.5	2d	40	5	15.4	14	12.8	0.0	0.4	1.4	2135	143		662	369	1508	79	66	362
SL-13-36-123.5	2k	41	5	13.3	22	10.5	0.1	0.1	1.2	3055	872	3695	509	452	1300	178	31	239

SL-13-36-127.5	3h	39	4	15.3	23	8.7	0.1	0.2	1.6	2830	1085	3326	825	418	1232	89	55	195
SL-13-36-131.6	2f	50	12	5.2	35	5.3	2.1	0.8	3.8	4485	482	9415	237	766	129	200	354	341
SL-13-36-134.5	2d	64	12	4.1	7	5.4	2.2	0.6	0.4	1424	379	1994	96	113	49		795	766
SL-13-36-138.5	2d	54	10	5.5	23	7.5	1.9	0.5	2.0	4456	191		128	277	240		1917	269
SL-13-36-143.5	3g	41	16	6.2	27	10.7	0.8	1.5	2.8	2698	919	2744	181	651	60	539	50	1096
SL-13-36-146.5	3b	47	12	6.1	24	10.0	1.7	1.6	2.1	2805	1133	8168	269	479	99	491	240	569
SL-13-36-149.5	3a	53	16	4.1	10	7.9	0.8	0.4	0.3	1468	2251	13446	265	66	46	672	16	2359
SL-13-36-153.5	3a	51	16	4.6	12	8.2	0.9	0.4	0.3	1659	2416	16192	330	66	42	643	68	2163
SL-13-36-157.5	3h	42	14	6.5	24	11.6	0.7	1.6	2.4	2762	1909	12724	302	584	107	508	88	872
SL-13-36-161.5	3h	40	11	8.2	26	12.9	0.7	2.0	3.1	3051	1807	5443	216	854	111	426	96	583
SL-13-36-179	3a	42	6	9.1	21	15.4	0.5	2.1	1.6	3240	1138	3550	150	582	154	478	61	508
SL-13-36-183.5	2a	45	14	5.1	23	10.4	0.4	0.9	2.0	3200	132		81	694	71	703	39	746
SL-13-36-187.5	2a	45	14	6.5	20	10.6	0.6	1.1	1.8	3073	220		80	586	70	831	47	795
SL-13-36-195.5	2a	45	14	4.7	23	11.0	0.5	1.1	2.0	3262	301		86	682	54	675	58	775
SL-13-36-199.5	2a	47	14	5.1	19	9.9	0.8	1.0	1.8	3020	291		78	592	79	910	60	799
SL-13-36-203.5	2a	47	14	5.2	20	10.1	0.9	1.0	1.8	2987	231		67	596	59	790	57	792
SL-13-36-207.5	2a	49	15	6.1	16	10.1	0.9	0.6	1.4	2448	147		50	541	53	553	88	757
SL-13-36-211.5	2a	48	14	5.8	20	9.8	1.0	0.9	1.7	2905	159		68	570	61	792	86	740
SL-13-36-215.5	2a	47	14	6.4	21	9.8	0.9	1.0	1.9	3196	181		74	608	76	873	72	758
SL-13-37-7.5	2f	33	8	10.3	31	11.8	0.8	2.4	5.4	3984	162	2380	136	692	42	1500	77	498
SL-13-37-11.5	2f	35	10	9.9	29	12.4	0.8	2.6	5.0	3803	146	1800	131	639	42	1698	77	634
SL-13-37-15.5	2f	33	9	10.4	33	11.8	0.7	3.0	5.3	4274	162	2435	168	704	61	1325	73	548
SL-13-37-19.5	2f	32	8	11.3	35	11.0	0.6	2.7	5.4	4629	224	2952	167	793	55	1149	64	403
SL-13-37-23.5	2f	28	8	9.8	39	10.8	0.5	3.2	6.9	4681	278	2969	217	1054	43	1560	53	510
SL-13-37-28	2f	38	12	7.5	25	12.4	0.7	2.4	4.0	3240	215	1016	88	617	84	1574	68	818
SL-13-37-30.5	2b	39	14	7.7	24	12.2	0.7	2.5	3.6	3125	200	1449	122	527	75	1772	59	956
SL-13-37-33.5	2f	31	8	11.4	36	11.6	0.5	2.9	6.2	4577	287	2215	199	891	55	1677	60	464
SL-13-37-37.5	2f	33	10	10.6	32	11.8	0.6	2.9	4.4	3903	775	7083	148	712	67	1014	54	614
SL-13-37-41.5	2f	33	11	9.1	26	15.5	0.5	4.5	3.8	3014	386	925	193	670	49	718	45	740
SL-13-37-43.1	3h	59	11	4.8	14	5.8	2.1	0.4	1.2	2878	148		107	259	232			503
SL-13-37-45.5	3b	38	12	9.0	19	12.6	0.7	2.9	2.1	2518	302		128	395		1077	51	875

SL-13-37-50.5	3b	37	15	9.5	24	11.5	0.5	3.7	2.1	3257	176		129	465	43	831	34	995
SL-13-37-52.7	3d	43	14	7.1	18	13.8	0.8	2.0	2.4	2680	305	3285	94	350	41	1426	103	947
SL-13-37-54.5	3g	35	7	9.3	31	10.8	0.8	2.4	4.1	4210	240		168	742	68	962	86	411
SL-13-37-57.5	3b	34	12	9.4	23	14.5	0.4	3.8	3.0	2742	1268	3141	152	638	31	621	43	862
SL-13-37-60.5	3b	29	11	8.9	32	13.6	0.4	4.8	3.8	3484	1880	9416	124	841		664	41	747
SL-13-37-63.5	3b	35	12	8.4	25	14.9	0.4	3.3	4.0	2789	538	802	103	939	48	641	50	727
SL-13-37-67.5	3d	43	16	5.9	14	9.7	1.0	1.2	1.0	2099	364	2544	78	193	44	1595	65	984
SL-13-37-71.9	3d	44	13	9.3	12	13.1	0.3	0.1	0.4	1918	49		131	191	305	274	28	641
SL-13-37-79.5	3d	39	12	8.8	20	14.3	0.5	3.0	2.3	2498	444	2020	148	515	131	622	43	885
SL-13-37-81.5	3d	37	13	10.3	22	10.1	0.5	2.1	1.5	2847	555	3572	210	361	109	570	31	687
SL-13-37-85.5	3d	40	14	7.7	19	12.7	0.5	2.0	2.3	2383	457	1762	134	553	83	768	47	877
SL-13-37-92.5	3d	44	13	9.7	15	11.6	0.4	0.1	0.6	2126	390		162	238	211	294	30	534
SL-13-37-96.5	2i	42	11	10.7	18	10.8	0.5	0.1	0.7	2717	863	950	346	412	885	265	30	372
SL-13-37-103.5	2i	41	7	13.9	23	11.5	0.1	0.1	1.3	3033	505		430	664	1098	172	38	258
SL-13-37-107.5	2i	41	7	12.7	22	11.0	0.1	0.1	1.2	3056	382		601	703	1091	172	35	221
SL-13-37-111.5	2i	40	6	13.3	22	11.2	0.1	0.0	1.1	2974	1353	1356	660	624	966	151	35	211
SL-13-37-115.5	3d	41	10	11.8	19	10.5	0.2	0.1	1.4	2592	649		384	606	819	310	32	363
SL-13-37-117.5	3h	42	5	13.0	19	13.0	0.1	0.0	1.2	2609	681		312	610	653	186	36	208
SL-13-37-119.5	2i	39	5	15.4	24	10.6	0.1	0.1	1.7	3220	595		436	711	1260	157	29	213
SL-13-37-123.6	3d	41	12	9.7	16	13.7	0.2	0.1	2.5	2007	1406	2541	277	698	259	137	28	585
SL-13-37-128.5	3h	39	6	14.2	22	10.6	0.1	0.3	3.0	2682	397	1670	412	609	1079	183	39	372
SL-13-37-132.5	3h	39	6	13.8	21	10.8	0.0	0.3	3.2	2558	134		435	651	1083	159	42	392
SL-13-37-136.5	3h	38	5	14.0	22	10.7	0.0	0.2	3.0	2582	333	8190	564	564	1171	99	38	319
SL-13-37-140.5	3h	39	5	15.6	21	11.1	0.0	0.3	2.8	2567	515	2371	457	606	1236	101	48	301
SL-13-37-144.8	3h	38	5	15.5	25	10.3	0.1	0.1	2.0	3157	2226	6356	499	585	1229	127	29	228
SL-13-37-148.8	3h	41	6	16.9	19	9.7	0.1	0.1	1.5	2538	489		582	375	1147	125	29	322
SL-13-37-152.5	3h	40	4	19.1	23	8.3	0.1	0.1	0.8	3377	654	3240	602	314	1160	125	22	164
SL-13-37-157.5	3a	48	18	5.9	10	10.3	0.6	0.1	0.6	1455	1112	2775	148	213	51	475	14	1255
SL-13-37-161.5	3a	49	21	6.5	14	10.7	0.4	0.1	1.2	1578	1102	5331	177	441	57	333	20	1417
SL-13-37-165.5	3a	48	19	4.7	15	9.7	0.5	0.1	1.2	1588	1404	8434	182	413	53	356	15	1840
SL-13-37-169.5	3b	40	16	8.5	27	11.3	0.6	2.1	3.2	3470	1412	5043	161	735	43	583	78	788

SL-13-37-174.5	3a	49	17	6.4	13	11.1	0.5	0.2	0.9	1684	1379	5609	159	224	54	363	20	1725
SL-13-37-178.5	3h	41	8	13.0	26	15.8	0.2	1.9	1.9	2902	1335	10463	288	606	155	192	39	501
SL-13-37-183.5	3a	51	18	6.7	13	10.4	0.4	0.4	0.5	1555	1187	12463	299	161	62	321	17	1695
SL-13-37-187.5	3a	56	16	5.8	7	7.7	0.4	0.3	0.1	1296	1167	8281	208		18	411		2325
SL-13-37-191.5	3a	57	16	5.6	6	7.4	0.5	0.4	0.1	1223	1177	8461	191			518	9	2160
SL-13-37-195.5	3a	56	16	5.8	7	7.3	0.4	0.4	0.1	1232	1862	12619	282			523		2039
SL-13-37-199.5	3a	56	16	4.6	7	6.9	0.6	0.3	0.1	1266	2075	16217	274			546	10	2126
SL-13-37-203.5	3a	57	16	5.2	7	6.8	0.6	0.3	0.1	1314	2245	15594	256			564	18	2082
SL-13-37-207.5	3a	57	16	5.5	6	7.0	0.6	0.4	0.1	1252	1294	12140	170			523	13	2153
SL-13-37-211.5	3a	58	15	5.4	4	6.4	0.7	0.3	0.1	1170	508	6021	91			567	23	2089
SL-13-37-225.5	3b	46	16	7.4	23	10.2	1.1	1.2	1.9	2336	2359	13224	308	394	67	587	90	912
SL-13-37-227.5	3a	51	17	6.1	11	9.5	0.6	0.6	0.9	1764	533	1599	56	170	63	515	49	1462
MW-07-06-3.9	2e	48	15	6.8	17	9.2	1.9	1.4	2.4	2795	208		116	215	97	8706	100	1746
MW-07-06-7.9	2e	45	15	5.8	17	9.5	1.9	1.6	2.5	2801	151		107	177	82	7803	124	1792
MW-07-06-11.9	2e	43	13	7.7	24	10.2	1.5	1.9	3.7	3654	114		125	326	79	5540	134	1160
MW-07-06-15.9	2e	44	14	7.2	22	10.5	1.4	1.8	3.1	3319	91	629	101	234	62	4636	115	1374
MW-07-06-19.9	2e	45	14	7.3	18	10.1	1.5	1.9	3.0	2705	119		69	306	45	2989	131	1242
MW-07-06-23.9	2e	45	15	7.5	19	10.2	1.3	1.7	2.6	2834	123		71	309	31	2672	122	1313
MW-07-06-27.9	2e	44	14	6.7	19	10.6	1.5	1.9	2.5	3015	108		74	288	43	3052	150	1261
MW-07-06-31.9	2g	48	18	5.5	13	10.3	1.1	1.2	1.7	1944	103			192		2037	107	1397
MW-07-06-35.9	2f	42	12	6.7	23	9.8	2.0	1.9	3.4	3286	171		94	360	50	2008	199	774
MW-07-06-38	2f	38	12	9.2	28	9.3	1.5	2.6	3.7	4466	113		105	410	33	1980	162	884
MW-07-06-41	2f	39	12	9.5	26	10.7	1.2	2.6	3.5	3893	206	1568	108	401	44	2604	120	811
MW-07-06-45	2g	49	19	5.2	9	9.9	0.9	1.0	1.2	1580	67			163		1716	59	1671
MW-07-06-49	2f	38	12	9.7	28	10.1	1.0	2.4	3.6	4521	299	1706	133	495	42	2369	91	876
MW-07-06-50.5	2a	51	15	7.4	13	10.2	0.7	0.2	1.1	1960	85		52	306	193	329	82	312
MW-07-06-54.5	3b	41	14	9.4	25	10.0	1.1	2.4	2.8	3877	165		103	327	45	1702	83	1054
MW-07-06-56.5	2d	41	12	9.3	28	7.1	1.8	1.6	3.1	4681	187		120	382	43	1490	209	659
MW-07-06-60.5	2f	45	15	6.4	20	11.2	1.3	2.4	2.6	3045	261	1320	89	305	45	1417	328	1051
MW-07-06-64.5	3b	46	16	5.9	15	10.8	0.9	1.1	2.0	2144	124		58	278		1138	54	1046
MW-07-06-66	2e	42	15	9.6	22	12.1	1.0	2.4	3.0	3180	208	627	82	394		1452	102	945

MW-07-06-72.6	2e	48	19	5.5	12	9.0	0.9	0.6	1.2	1700	68		32	127		983	47	1296
MW-07-06-76.6	3b	45	18	7.5	16	10.0	1.0	2.0	2.0	2169	120		36	276		1384	69	1260
MW-07-06-80.6	3b	45	15	7.2	15	10.2	1.2	1.4	1.6	1987	76	725	44	139		1254	66	1251
MW-07-06-83.5	2f	38	11	9.0	28	9.6	1.0	2.0	3.2	4193	121	1224	95	291		960	89	682
MW-07-06-87.5	2f	40	13	7.1	22	10.5	0.9	2.0	3.2	3036	84	641	55	260		1069	76	946
MW-07-06-91.5	3b	41	13	5.9	22	10.8	1.1	2.1	3.4	3026	255	1017	64	245		1053	99	955
MW-07-06-95.5	3b	36	11	7.3	30	11.0	0.8	2.7	5.1	4050	651	2751	64	481		812	87	654
MW-07-06-99.5	3b	40	12	7.0	26	11.3	1.0	3.2	4.9	3558	437	1846	85	567	48	712	328	701
MW-07-06-103.5	3b	33	11	4.9	28	13.6	0.6	5.3	4.2	4080	567	1324	127	669	61	908	63	767
MW-07-06-109.5	3b	31	9	7.7	32	13.8	0.6	5.2	4.6	4067	1794	3488	162	1135	81	539	69	501
MW-07-06-113.5	3b	27	11	8.8	34	13.9	0.4	6.8	3.6	4554	638		204	1179	134	390	61	580
MW-07-06-117.5	3b	26	10	10.0	31	16.9	0.5	8.2	3.7	3820	1009		230	1229	129	362	52	574
MW-07-06-121	3b	42	17	10.0	27	7.2	0.9	0.4	2.7	3352	1135		202	1085	595	541	55	621
MW-07-06-125.5	2f	28	13	13.4	48	5.4	0.4	0.5	6.7	5482	3188	2035	475	3173	1215	284	52	286
MW-07-06-135.5	3b	38	14	10.3	30	10.1	0.4	1.2	3.4	3541	625		260	1505	365	368	45	500
MW-07-06-139.5	3b	40	13	8.7	25	10.7	0.5	0.8	2.4	2981	436		174	941	430	303	43	556
MW-07-06-143.5	3b	34	4	20.3	20	14.5	0.0	0.8	4.9	2870	230	12353	339	559	866		487	156
MW-07-06-147.5	3b	39	15	10.6	27	9.3	0.4	0.9	2.5	3466	1450		230	954	459	318	36	578
MW-07-06-151.5	2f	33	11	13.4	39	6.6	0.3	1.2	3.4	5496	1589		427	1412	729	245	31	346
MW-07-06-155.5	3b	41	12	9.3	25	10.2	0.5	1.2	2.3	3288	4498	5431	276	835	435	382	83	517
MW-07-06-159.5	3b	42	13	8.6	17	12.7	0.8	2.7	1.3	2483	375		150	500	97	485	60	682
MW-07-06-163.5	3b	41	13	9.4	25	10.3	0.4	0.5	2.7	3144	435		269	1030	964	328	44	532
MW-07-08-12	2a	50	13	5.1	19	7.2	2.4	1.0	2.4	3740	97		76	135	70	2523	41	1100
MW-07-08-16	2a	50	13	6.1	19	7.5	1.7	1.1	2.3	3618	369	752	85	173	68	2042	38	1122
MW-07-08-21.5	2a	48	13	6.5	21	8.2	1.4	1.4	2.6	3733	309	872	77	251	73	1780	47	1150
MW-07-08-24.5	2a	46	12	6.0	23	8.4	1.2	1.6	2.8	4159	145		77	281	75	1665	49	1065
MW-07-08-31	MLI	53	15	4.9	15	6.7	2.0	0.9	1.6	2628	1076	1858	53	175	36	1625	72	1217
MW-07-08-34.7	MLI	55	15	3.6	12	6.3	2.4	0.7	1.5	2359	147			120	44	1684	96	1233
MW-07-08-39.5	MLI	56	16	4.6	13	6.3	2.1	0.9	1.4	2371	826	1446	56	128	48	1683	72	1265
MW-07-08-43.5	MLI	53	15	6.1	16	7.0	2.0	0.9	1.9	2980	737		65	156	50	1648	62	1059
MW-07-08-48.5	MLI	55	16	3.8	14	6.8	2.5	0.8	1.6	2601	347		67	174	56	2082	96	1000

MW-07-08-52.5	MLI	54	18	4.0	12	6.8	1.8	0.9	1.2	1897	3281	6193	122	164	27	1474	81	1481
MW-07-08-57.5	MLI	52	17	5.1	15	8.2	1.4	1.0	1.6	2520	1147	2620	81	264	30	1014	141	1244
MW-07-08-61.5	MLI	52	17	4.3	14	8.6	1.3	1.1	1.4	2380	719	1335	48	257	34	1086	90	1378
MW-07-08-65.5	MLI	51	16	5.2	15	8.4	1.4	1.0	1.4	2603	2632	6010	102	289	57	937	145	1187
MW-07-08-69.5	MLI	53	17	5.0	14	8.3	1.5	1.1	1.5	2519	584	818	63	248	28	1110	133	1308
MW-07-08-73.5	MLI	53	17	5.1	14	8.2	1.5	1.0	1.5	2545	315		60	257	37	1143	126	1228
MW-07-08-85.5	MLI	54	14	5.0	15	7.2	2.2	0.9	1.4	2871	122		66	197	73	1535	132	889
MW-07-08-92.5	MLI	55	16	4.7	14	7.1	2.3	1.0	1.3	2695	128		64	252	75	1421	136	915
MW-07-08-99.5	MLI	55	15	4.7	14	7.2	2.2	1.1	1.4	2636	73		55	270	49	1279	98	966
MW-07-08-103.5	MLI	58	15	4.9	13	5.9	2.9	0.7	1.2	2489	229		39	194	75	1142	186	707
MW-07-08-107.5	MLI	56	15	4.4	13	6.9	2.5	0.9	1.2	2512	193		47	218	70	1199	169	903
MW-07-08-111.5	MLI	56	16	4.6	13	6.8	2.4	1.0	1.3	2428	81			245	54	1099	190	961
MW-07-08-116	MLI	55	15	5.5	14	7.0	2.3	0.9	1.3	2740	89		55	238	66	1198	167	884
MW-07-08-120	MLI	55	16	5.0	14	7.1	2.2	1.0	1.3	2521	75		53	259	54	1251	144	1020
MW-07-08-124.7	MLI	56	16	4.8	13	7.1	2.4	1.0	1.3	2427	82		49	252	65	1052	169	981
MW-07-08-128.5	MLI	52	14	4.5	14	7.2	2.3	1.0	1.5	2609	160		74	298	68	1077	234	952
MW-07-08-132.5	MLI	52	14	5.3	15	7.2	2.2	1.1	1.4	2720	750		69	260	63	1239	154	1007
MW-07-08-139.5	MLI	55	15	5.1	14	7.0	2.2	1.0	1.4	2581	72		56	274	62	1071	201	1034
MW-07-08-143	MLI	53	14	5.2	14	7.0	2.2	0.9	1.3	2506	66		63	266	63	1245	202	999
MW-07-08-147	MLI	54	15	4.2	13	6.7	2.4	0.9	1.2	2379	79		55	239	60	1243	168	1009

Appendix 5. Laboratory-based whole-rock analyses. Unit for major oxides, S, and C is weight%, unit for trace elements is ppm. Major elements were determined by ICP-AES, trace elements were determined by ICP-MS, both after lithium borate fusion on a minimum 2 g of pulp samples. Total S was determined using a Leco combustion furnace on 0.01-0.1 g of sample, ferrous Fe was determined by H2SO4-HF acid digestion and titration on 1 g of sample. Symbols for rocks: 2i-feldspathic clinopyroxenite, 2b-olivine gabbro, 2f-oxide augite melatroctolite, 3b-ophitic gabbro, 3g-oxide melatroctolite, 3h-apatitic clinopyroxenite, 3i-apatitic olivine clinopyroxenite, MLI-malpas lake intrusion. Samples begin with FD, SL, and MS were sampled at drill holes at Four Dams, Area 41 and WD zone, respectively.

Sample	FD-13-34-5	FD-13-34-9.5	FD-13-34-14	FD-13-34-18.5	FD-13-34-23	FD-13-34-27.5	FD-13-34-32	FD-13-34-36.5	FD-13-34-36.5
Unit	2f	2f	2f	2f	2b	2f	2f	2f	2f
SiO_2	23.5	33.5	30.3	39.7	36.5	22.7	20.1	36.2	36.2
Al_2O_3	3.22	8.24	6.06	15.75	11.4	3.49	3.23	11.2	10.95
Fe_2O_{3*}	44.3	30.6	34.6	17.85	22.8	47.3	49.9	25.6	25.6
FeO	30.4	21.4	23.7	10.45	15.2	32.4	33.5	16.95	
CaO	7.85	10.35	9.79	10.4	11	6.16	4.96	10.45	10.45
MgO	10.65	8.96	9.64	4.64	7.3	11.45	11.9	7.16	7.1
Na_2O	0.41	1.37	1.1	2.66	2.06	0.45	0.4	2.1	2.1
K_2O	0.22	0.55	0.42	0.69	0.79	0.29	0.23	0.85	0.88
Cr_2O_3	<0.01	0.01	0.01	<0.01	<0.01	<0.01	<0.01	0.01	0.01
TiO_2	6.76	4.04	3.91	1.59	2.89	6.02	7.2	3.25	3.34
MnO	0.47	0.39	0.4	0.18	0.28	0.5	0.48	0.29	0.31
P_2O_5	2.83	3.1	3	2.33	2.97	3.15	2.57	2.82	2.86
SrO	0.03	0.07	0.05	0.12	0.09	0.03	0.02	0.09	0.09
BaO	0.04	0.09	0.07	0.2	0.13	0.03	0.03	0.1	0.11
LOI	-2.04	-1.27	-1.28	2.14	-0.18	-1.89	-2.52	-0.5	-0.34
Total	98.24	100	98.07	98.25	98.03	99.68	98.5	99.62	99.66
C	0.05	0.1	0.03	0.08	0.03	0.03	0.04	0.01	0.03
S	0.69	0.21	0.81	2.14	0.18	0.9	0.52	0.68	0.69
Ba	392	786	611	1710	1155	248	233	913	906
Ce	169	189.5	186	155.5	194	172.5	141.5	172	168.5
Cr	20	40	50	20	30	30	20	80	90
Cs	0.27	0.54	0.68	0.71	0.92	0.47	0.3	0.8	0.66
Dy	7.24	8.26	8.52	6.65	8.73	7.48	6.12	7.67	6.73
Er	3.07	3.49	3.96	3.1	3.73	3.05	2.75	3.22	3.1
Eu	3.85	4.46	4.25	4.39	4.19	3.59	3.09	4.28	4.16
Ga	15.6	16.2	16.6	17.3	19.1	17.9	21.6	18.7	15.8

Gd	13.35	14.05	14.55	10.6	13.55	13	10.2	12.45	11.1
Hf	1.4	1.4	2.7	1.1	1.7	1.6	1.3	1.9	1.8
Ho	1.21	1.34	1.55	1.19	1.59	1.24	1.01	1.34	1.26
La	73.2	82.8	81.5	71.1	86.8	74.9	61.7	75.8	76.4
Lu	0.28	0.36	0.35	0.29	0.4	0.32	0.23	0.33	0.32
Nb	27.4	27.3	37.5	16.7	31.1	36.5	29.9	27.2	26.8
Nd	97.5	104.5	103.5	82.3	106	96.8	80.8	95.7	91
Pr	22	24.3	23.3	19.15	24.3	22	18.2	21.8	22.9
Rb	5.6	13.4	15	11.6	18.2	7.8	6.3	22	22.4
Sm	16.3	17.4	17.1	13.9	17.35	15.95	13.05	15.75	14.6
Sn	51	26	21	27	22	16	13	15	16
Sr	220	650	441	1050	788	227	193	799	720
Ta	1.3	1.3	1.8	0.8	1.5	1.8	1.5	1.3	1.4
Tb	1.34	1.5	1.56	1.26	1.59	1.35	1.16	1.39	1.37
Th	1.95	2.59	4.01	1.97	3.28	2.6	1.8	3.41	3.66
Tl	0.04	0.05	0.06	0.12	0.07	0.07	0.05	0.07	<0.5
Tm	0.41	0.44	0.48	0.34	0.45	0.43	0.26	0.4	0.36
U	0.61	0.76	1.45	0.59	0.83	0.65	0.54	0.94	0.96
V	559	353	543	221	427	1020	963	323	348
W	4	3	2	1	1	1	1	1	1
Y	31.9	35.7	37.5	28	36.7	31.3	25.2	32.6	31.6
Yb	2.19	2.24	2.63	1.87	3.04	2.25	1.6	2.48	2.09
Zr	53	60	99	42	63	64	55	74	86
As	0.2	0.3	0.6	0.4	0.8	18	0.3	0.5	<0.1
Bi	0.28	0.1	0.45	0.65	0.07	0.43	0.36	0.25	0.33
Sb	<0.05	<0.05	<0.05	0.05	<0.05	0.15	<0.05	<0.05	0.06
Se	2.7	1.9	3.7	8.5	1.7	4	2.4	3.4	3.4
Te	0.02	0.01	0.03	0.09	0.02	0.04	0.04	0.03	0.04
Ag	<0.5	<0.5	<0.5	1.3	<0.5	<0.5	<0.5	<0.5	<0.5
Cd	2.1	1.3	1.9	1.1	1.1	1.9	1.9	0.9	1.1
Co	157	110	135	104	86	190	183	97	91
Cu	1505	580	1935	5220	702	2410	1740	1490	1440
Li	10	10	<10	10	10	10	<10	10	10
Mo	1	1	1	1	1	2	1	1	1
Ni	145	141	136	419	136	190	137	127	119
Pb	12	8	12	15	2	7	8	10	11

Sc	36	29	35	16	27	17	19	25	25
Zn	288	207	227	109	153	318	299	158	150

* Total Fe, as also for the follows.

Sample	FD-13-34-41	FD-13-34-45.5	FD-13-34-45.5	FD-13-34-50	FD-13-34-60	FD-13-34-64.5	FD-13-34-66	FD-13-34-70.5	FD-13-34-75
Unit	2f	2f	2f	3h	2f	2f	2f	2b	2b
SiO_2	31.1	21.4	21.6	33.7	41.8	44.9	46.5	41.6	44.2
Al_2O_3	6.04	3.77	3.86	6.63	17.45	17.9	19.55	14.05	16.85
Fe_2O_3	34.7	46.1	47.4	34.2	18.9	15.6	10.9	19.05	15.95
FeO	23.9		31	23.9	12.15	10.3	7.33	12.55	10.6
CaO	9.86	7.61	7.68	7.6	10.65	11.1	10.6	11.5	10.8
MgO	10.25	8.97	9.01	8.74	3.97	4.43	3.32	5.85	4.56
Na_2O	1.08	0.52	0.53	1.52	3.02	3.17	3.55	2.56	3.16
K_2O	0.42	0.27	0.27	1.32	0.58	0.78	0.97	0.66	0.82
Cr_2O_3	0.01	0.01	0.01	0.01	<0.01	<0.01	<0.01	<0.01	<0.01
TiO_2	4.44	7.5	7.48	3.73	1.97	1.73	1.19	2.55	2.08
MnO	0.43	0.48	0.47	0.42	0.2	0.21	0.15	0.24	0.2
P_2O_5	2.88	3.03	2.95	1.91	1.71	1.73	1.52	1.86	1.63
SrO	0.05	0.03	0.03	0.03	0.14	0.14	0.14	0.1	0.12
BaO	0.05	0.04	0.04	0.15	0.1	0.12	0.14	0.09	0.1
LOI	-1.69	-1.05	-1.12	0.07	0.19	0.17	0.59	-0.18	-0.2
Total	99.62	98.68	100.21	100.03	100.68	101.98	99.12	99.93	100.27
C	0.03	0.04	0.04	0.11	0.03	0.08	0.03	0.03	0.04
S	0.27	0.99	1.01	1.67	1.66	0.27	0.15	0.21	0.24
Ba	432	336	307	1270	866	985	1200	791	906
Ce	172.5	176	177	199	104	118.5	112.5	142.5	125
Cr	80	70	60	70	20	<10	<10	<10	<10
Cs	0.48	0.33	0.36	1.06	0.32	0.61	0.74	0.61	0.65
Dy	8.05	7.24	7.93	9.24	4.61	5.42	4.8	6.72	5.53
Er	3.48	3.09	3.55	4.25	2.11	2.28	2.15	3.17	2.3
Eu	3.97	4.06	3.83	3.64	3.23	3.37	3.42	3.6	3.22
Ga	16.9	18.8	21.2	17.8	18.8	19.4	19.6	19.7	20.5
Gd	13.15	12.15	13.55	13.85	7.54	8.11	7.74	10.95	8.87
Hf	1.8	1.4	1.6	4	0.9	1.3	1.4	1.6	1.6

Ho	1.4	1.29	1.35	1.66	0.83	0.82	0.8	1.18	1
La	75.7	78.1	75.8	89.8	47.1	53.4	51.4	63.9	56.5
Lu	0.34	0.32	0.33	0.56	0.19	0.23	0.23	0.29	0.23
Nb	27.9	32.8	33	73.4	16.3	19.7	19.5	25.2	24.3
Nd	96.4	96.2	99.6	102.5	55.6	63.6	58.3	78.7	63.9
Pr	21.9	24.2	22.4	24.3	13.15	14.5	13.9	17.65	15.25
Rb	10.5	8.1	7.5	43.9	6.6	13.2	17.7	12.4	16.1
Sm	16	16	16.75	17.1	9.47	10.6	9.86	13.2	11
Sn	14	10	9	24	26	12	14	16	39
Sr	392	235	238	283	1185	1140	1230	882	1075
Ta	1.4	1.8	1.7	3	0.7	1	0.9	1.1	1.1
Tb	1.49	1.45	1.6	1.68	0.84	0.92	0.87	1.28	1.04
Th	2.7	2.3	2.79	5.45	1.53	2.4	2.98	2.27	2.63
Tl	0.04	<0.5	0.06	0.11	0.06	0.04	0.04	0.03	0.04
Tm	0.46	0.39	0.4	0.55	0.25	0.27	0.27	0.35	0.34
U	0.69	0.65	0.63	1.69	0.44	0.73	0.76	0.65	0.79
V	513	723	686	304	169	197	128	257	150
W	1	<1	1	1	2	1	1	1	2
Y	33.2	33	33.3	40.2	19.2	22	20.8	28.4	24
Yb	2.59	2.15	2.2	3.8	1.35	1.51	1.57	2.39	1.7
Zr	67	66	66	168	37	52	56	61	65
As	0.3	0.1	0.3	0.6	0.3	0.2	0.4	0.2	0.2
Bi	0.09	0.36	0.36	0.39	0.49	0.13	0.05	0.05	0.03
Sb	<0.05	0.05	<0.05	<0.05	<0.05	<0.05	<0.05	<0.05	<0.05
Se	1.8	4.6	3.3	6.4	7	1.6	1.2	1.3	1.2
Te	0.01	0.05	0.04	0.15	0.07	0.01	<0.01	<0.01	<0.01
Ag	<0.5	0.6	<0.5	0.9	1.2	<0.5	<0.5	<0.5	<0.5
Cd	1.6	2.2	2.4	2.3	1.2	0.7	0.5	0.9	0.8
Co	121	151	159	131	87	52	37	67	57
Cu	555	2070	2050	3480	4370	686	241	280	263
Li	<10	10	<10	30	<10	<10	10	10	<10
Mo	1	1	2	4	<1	<1	<1	1	1
Ni	138	148	143	163	223	41	17	8	18
Pb	7	15	9	12	10	2	<2	<2	3
Sc	33	29	30	27	16	17	11	30	21
Zn	220	306	313	273	119	111	86	142	112

Sample	FD-13-34-79.5	FD-13-34-84	FD-13-34-89.5	FD-13-34-90	FD-13-34-94.5	FD-13-34-99	FD-13-34-103.5	FD-13-34-108	FD-13-34-112.5
Unit	2b	2b	2b	2b	2b	2b	2b	2b	2b
SiO_2	42.9	39.2	40.7	40.4	42.3	38.1	35.7	39.4	33.6
Al_2O_3	15.05	12.2	13.4	12.9	13.45	11.55	11.2	11.8	9.11
Fe_2O_3	17.85	19.8	19.55	18.25	19.35	20.6	22	22.2	29.1
FeO	12.1	12.95	12.8	12.65	12.2	13.55	14.9	15.7	19.15
CaO	10.6	9.67	10.45	9.7	10.05	8	8.99	9.4	9.37
MgO	5.32	7.28	5.89	5.15	4.93	7.95	7.26	6.07	5.93
Na_2O	2.88	1.97	2.65	2.47	2.6	1.68	1.68	2.32	1.52
K_2O	0.81	0.61	0.82	0.82	0.85	0.55	0.5	0.61	0.35
Cr_2O_3	<0.01	<0.01	<0.01	<0.01	<0.01	<0.01	<0.01	<0.01	<0.01
TiO_2	2.41	2.62	3.14	2.93	3.4	2.78	4.27	3.35	4.71
MnO	0.23	0.23	0.25	0.23	0.23	0.23	0.33	0.31	0.41
P_2O_5	1.5	1.87	1.42	1.4	1.57	1.66	2.39	1.52	2.33
SrO	0.11	0.08	0.1	0.1	0.1	0.06	0.07	0.08	0.06
BaO	0.09	0.07	0.08	0.08	0.08	0.06	0.06	0.07	0.04
LOI	-0.27	2.74	0.62	0.56	1	5.32	3.79	1.11	1.94
Total	99.48	98.34	99.07	94.99	99.91	98.54	98.24	98.24	98.47
C	0.02	0.14	0.12	0.09	0.05	0.16	0.06	0.08	0.03
S	0.23	0.24	0.18	0.16	0.25	0.23	0.19	0.24	0.92
Ba	800	570	699	719	723	508	488	630	394
Ce	120	144	117.5	121	127	123.5	171	115	149
Cr	<10	<10	<10	<10	<10	<10	<10	<10	<10
Cs	0.61	0.75	0.78	0.75	0.72	0.67	0.68	0.66	0.42
Dy	5.96	7.04	5.78	5.72	5.9	6.14	7.74	5.29	7.3
Er	2.46	3.02	2.39	2.71	2.85	2.88	3.46	2.47	3.16
Eu	3.24	3.33	3.2	3.27	3.5	3.32	3.92	3.45	4.1
Ga	19.4	19.1	19.5	18.6	19.4	18.1	17.9	19.1	15.7
Gd	9.07	10.4	8.64	8.75	9.25	9.45	13.4	9.21	12.5
Hf	1.8	1.8	2.1	2	1.9	1.5	1.8	1.7	1.4
Ho	0.94	1.23	0.96	1	1.08	1.05	1.43	0.88	1.29
La	54.7	64	53.5	54.8	57.6	55.8	75.5	51	64.8

Lu	0.27	0.31	0.32	0.32	0.27	0.29	0.35	0.28	0.31
Nb	31.4	28.5	32.1	33	32.5	25.9	33	27.2	22.5
Nd	64	77.1	63.4	63.9	69.1	67.6	92.6	64	84.6
Pr	14.9	18.05	14.7	15.1	15.85	15.6	21.3	14.8	18.9
Rb	17.6	14.3	19	20.1	17.7	13.6	10.7	12.5	6.8
Sm	10.4	13.4	10.65	11	12.1	11.55	15.7	11	14.9
Sn	21	21	31	32	14	7	3	13	7
Sr	947	698	862	876	884	530	538	719	517
Ta	1.5	1.4	1.5	1.7	1.6	1.2	1.5	1.3	1.1
Tb	1.06	1.25	1	1.08	1.1	1.07	1.47	1.02	1.44
Th	2.93	2.58	3.11	3.3	2.91	2.28	2.71	2.33	1.86
Tl	0.04	0.04	0.05	0.05	0.05	0.05	0.03	0.04	0.04
Tm	0.36	0.38	0.3	0.32	0.36	0.31	0.38	0.32	0.37
U	0.82	0.76	0.92	1.06	0.82	0.71	0.75	0.64	0.72
V	189	154	141	135	152	116	178	157	229
W	1	1	2	2	1	1	1	1	1
Y	23.9	29.7	24.1	24.5	26.4	26.3	35.4	24.4	32.4
Yb	2.03	2.12	1.94	1.93	2.02	1.98	2.57	1.95	2.06
Zr	74	71	89	92	84	64	73	69	50
As	0.4	0.3	0.4	0.4	0.3	0.4	0.3	0.3	0.4
Bi	0.02	0.02	0.04	0.04	0.02	0.01	0.02	0.02	0.11
Sb	<0.05	<0.05	<0.05	<0.05	<0.05	<0.05	<0.05	<0.05	<0.05
Se	1.1	1.4	1	1.2	1.2	1.4	1.4	1.4	3.4
Te	<0.01	<0.01	<0.01	<0.01	<0.01	<0.01	<0.01	<0.01	0.01
Ag	<0.5	<0.5	<0.5	<0.5	<0.5	<0.5	<0.5	<0.5	<0.5
Cd	0.6	0.5	<0.5	0.5	<0.5	0.5	<0.5	<0.5	<0.5
Co	68	64	64	68	67	55	70	62	95
Cu	207	176	265	318	164	103	117	180	770
Li	10	20	10	10	10	20	20	10	10
Mo	<1	1	1	<1	2	<1	1	2	1
Ni	8	12	14	9	13	8	6	11	26
Pb	<2	<2	<2	5	3	14	<2	4	5
Sc	26	28	29	29	30	24	31	32	34
Zn	136	111	349	189	143	218	133	135	210

Sample	FD-13-34-117	FD-13-34-127	FD-13-34-131.5	FD-13-34-136	FD-13-34-140.5	FD-13-34-145	FD-13-34-149.5	FD-13-34-154	FD-13-34-158.5
Unit	2b	2b	2b	2b	2b	2b	2b	2b	2b
SiO_2	41.7	40.5	39.6	40.6	37.3	39.7	35.1	42.5	41.3
Al_2O_3	13.95	11	12.1	12.25	9.66	11.35	8.82	12.4	12.05
Fe_2O_3	18.65	24.7	22.6	23.5	27.9	25.9	32.8	23	23.7
FeO	12.65	17.8	15.8	17.2	21	18.4	23.7	16.85	16.95
CaO	10.2	10.25	10.3	9.88	10.2	10.1	10.1	10.1	10.2
MgO	3.88	5.15	4.9	4.87	5.86	5.61	6.17	4.73	4.69
Na_2O	2.89	2.29	2.52	2.67	2.05	2.32	1.8	2.73	2.67
K_2O	0.66	0.57	0.62	0.69	0.57	0.58	0.43	0.85	0.76
Cr_2O_3	<0.01	<0.01	<0.01	<0.01	<0.01	<0.01	<0.01	<0.01	<0.01
TiO_2	3.09	3.38	3.11	3.21	3.76	3.55	4.93	3.1	3.41
MnO	0.26	0.37	0.34	0.36	0.43	0.4	0.48	0.36	0.37
P_2O_5	1.62	1.63	1.57	1.72	2.15	1.87	2.39	1.62	1.76
SrO	0.1	0.09	0.09	0.1	0.08	0.09	0.07	0.09	0.09
BaO	0.09	0.08	0.09	0.1	0.08	0.08	0.06	0.11	0.1
LOI	1.12	-0.31	0.18	-0.84	-1.2	-0.33	-1.53	-0.79	-0.84
Total	98.21	99.7	98.02	99.11	98.84	101.22	101.62	100.8	100.26
C	0.13	0.11	0.06	0.1	0.01	0.02	0.02	0.02	0.05
S	0.3	0.26	0.25	0.23	0.29	0.22	0.28	0.24	0.24
Ba	796	680	763	828	656	704	532	901	859
Ce	120	135	134.5	147	172.5	155.5	189	154.5	167
Cr	<10	<10	<10	<10	<10	<10	<10	<10	<10
Cs	0.78	0.57	0.61	0.54	0.41	0.46	0.26	0.58	0.54
Dy	5.85	6.8	6.59	6.71	8.08	7.78	8.93	7.66	8.09
Er	2.71	2.71	2.88	3.19	3.7	3.31	3.85	3.47	3.57
Eu	4.01	4.22	3.87	4.14	4.39	4.15	4.4	4.36	4.56
Ga	20.2	18.5	20.7	19.6	18.8	19.6	19.8	20.8	21.6
Gd	9.19	11	9.8	11.1	12.95	11.8	14.9	11.3	12.1
Hf	1.4	1.5	1.7	1.8	1.8	1.8	1.8	2.2	2.1
Ho	1.08	1.17	1.12	1.18	1.36	1.39	1.55	1.32	1.34
La	52.9	58.2	58.6	64.2	73.9	66.6	81.4	68.7	74.3
Lu	0.25	0.31	0.32	0.36	0.42	0.35	0.41	0.39	0.4
Nb	18.8	23	23.7	30.6	26.9	29.4	37.9	33.5	34.2

Nd	67.4	77.9	73.2	82.5	97.8	85.1	104.5	84.5	90.7
Pr	15.35	17.7	17.2	18.75	22.2	19.6	24	19.45	21.1
Rb	12.9	11.8	13	12.2	10.9	9.5	5.8	16.3	13.9
Sm	11.75	13.2	12.65	13.55	16.55	13.9	17.85	14.1	16.65
Sn	17	25	15	38	49	22	20	31	15
Sr	886	743	786	821	609	731	552	770	807
Ta	0.9	1.1	1.2	1.6	1.4	1.5	2	1.6	1.8
Tb	1.11	1.28	1.21	1.3	1.53	1.42	1.67	1.37	1.42
Th	2.06	1.96	2.02	1.99	1.99	1.88	1.78	2.93	2.5
Tl	0.04	0.03	0.03	0.03	0.03	0.03	0.02	0.04	0.03
Tm	0.32	0.37	0.33	0.37	0.42	0.39	0.46	0.36	0.43
U	0.62	0.6	0.61	0.58	0.67	0.54	0.48	0.9	0.68
V	146	173	161	161	198	207	254	164	197
W	1	1	1	1	2	1	1	1	1
Y	25.7	28.6	27.9	29.4	35.1	31.4	37.3	31.6	33.9
Yb	1.92	2.08	2.14	2.4	2.44	2.33	2.5	2.46	2.49
Zr	55	64	63	63	66	62	62	85	79
As	0.3	0.2	0.3	0.3	0.2	0.2	0.2	0.4	0.5
Bi	0.02	0.03	0.06	0.11	0.19	0.13	0.17	0.14	0.12
Sb	<0.05	<0.05	<0.05	<0.05	<0.05	<0.05	<0.05	<0.05	<0.05
Se	1.3	1.3	1.4	1.5	2.1	1.6	1.8	1.5	1.7
Te	<0.01	<0.01	<0.01	0.01	<0.01	0.01	0.01	<0.01	<0.01
Ag	<0.5	<0.5	<0.5	<0.5	<0.5	<0.5	<0.5	<0.5	<0.5
Cd	<0.5	<0.5	<0.5	<0.5	0.8	<0.5	0.9	0.6	0.6
Co	55	67	59	61	74	62	83	55	59
Cu	188	231	346	532	621	418	505	420	344
Li	20	10	10	10	10	10	10	20	20
Mo	<1	<1	<1	1	1	3	3	2	4
Ni	9	11	12	30	19	20	8	16	13
Pb	2	<2	2	5	2	<2	<2	8	2
Sc	28	35	31	31	35	31	33	31	31
Zn	161	204	180	203	231	213	266	202	207

Sample	FD-13-34-163	FD-13-34-167.5	FD-13-34-172	FD-13-34-176.5	FD-13-34-181	FD-13-34-190	FD-13-34-194.5	FD-13-34-199	FD-13-34-203.5
Unit	2b	2b	2b	2b	2b	2b	2b	2b	2f
SiO_2	41.3	43.8	40.5	41.6	42.8	43.3	42.4	40.8	36.6
Al_2O_3	12	12.85	11.8	12.3	12.85	12.95	12.7	11.95	9.11
Fe_2O_3	23	21.7	24.1	22.3	21.9	20.6	21.8	23.1	29.1
FeO	16.1	15.1	17.5	16.05	16.1	15.3	15.85	16.85	21.4
CaO	11.45	10.25	9.59	10.05	9.89	10.2	9.8	10	9.68
MgO	4.63	4.64	4.98	4.73	4.53	4.54	4.56	4.78	6.25
Na_2O	2.64	2.86	2.64	2.75	2.94	2.97	2.92	2.74	2.04
K_2O	0.77	0.89	0.8	0.82	0.93	0.92	0.89	0.81	0.65
Cr_2O_3	<0.01	<0.01	<0.01	<0.01	<0.01	<0.01	<0.01	<0.01	<0.01
TiO_2	3.29	3	3.41	3.15	3.03	2.75	2.99	3.26	3.71
MnO	0.37	0.34	0.37	0.34	0.34	0.32	0.34	0.35	0.46
P_2O_5	1.88	1.48	1.62	1.67	1.75	1.68	1.69	2.02	1.83
SrO	0.09	0.09	0.09	0.09	0.1	0.1	0.1	0.09	0.07
BaO	0.1	0.11	0.1	0.11	0.11	0.12	0.11	0.11	0.08
LOI	0.28	-0.31	-0.86	-0.62	-0.79	-0.69	-0.83	-0.88	-1.18
Total	101.8	101.7	99.14	99.29	100.38	99.76	99.47	99.13	98.4
C	0.37	0.04	0.02	0.02	0.04	0.05	0.04	0.04	0.04
S	0.24	0.2	0.2	0.2	0.21	0.21	0.18	0.19	0.21
Ba	824	929	914	946	995	1015	995	927	649
Ce	176	162	167.5	170.5	174	172	172	192	162
Cr	<10	<10	<10	<10	<10	<10	<10	<10	<10
Cs	0.5	0.56	0.62	0.74	0.65	0.65	0.46	0.2	0.4
Dy	8.39	7.79	7.39	7.99	7.43	7.71	7.65	8.79	7.37
Er	4.05	3.46	3.72	3.69	3.77	3.61	3.65	4.62	3.43
Eu	4.73	4.4	4.46	4.47	4.77	4.51	4.66	4.73	3.68
Ga	20	20.5	18.4	18.4	17.9	18.6	18.5	19.1	15.6
Gd	13	11.4	10.5	11.7	11.6	11.4	11.7	12.9	10.95
Hf	2.2	2.3	2.4	2.3	2.6	2.6	2.6	2.4	2.2
Ho	1.38	1.44	1.42	1.42	1.59	1.51	1.5	1.59	1.33
La	78.1	73.8	77.9	80.1	82.1	81.4	81.8	90.4	75.3
Lu	0.41	0.45	0.43	0.38	0.41	0.4	0.42	0.42	0.4
Nb	40.8	44.9	48.2	48.9	48.8	48.5	52.6	53.2	49.8

Nd	94.5	84.9	88.3	89.7	91.7	88.7	91.4	102	84.6
Pr	22	19.9	21	21.2	21.5	21.2	21.3	23.9	20
Rb	14.3	17.5	17	17.2	19.8	20.6	19.2	17.4	14.5
Sm	16.3	14.45	14	14.7	15.3	14.95	14.85	16.7	14.45
Sn	10	9	11	13	17	31	24	28	9
Sr	764	795	765	799	807	819	802	750	468
Ta	2.1	2.2	2.1	2.1	2.1	2.1	2.3	2.4	2.2
Tb	1.46	1.35	1.32	1.44	1.44	1.34	1.5	1.61	1.41
Th	2.67	2.86	3	2.96	3.51	3.35	3.24	3.07	2.27
Tl	0.04	0.04	0.04	0.04	0.04	0.04	0.04	0.03	0.04
Tm	0.47	0.45	0.46	0.5	0.48	0.45	0.49	0.53	0.44
U	0.71	0.83	0.94	0.83	1.25	0.95	0.97	0.87	0.68
V	185	175	207	206	196	183	199	224	239
W	1	1	1	1	1	1	1	1	1
Y	34.9	33.2	34.6	35.4	36.3	36.2	35.8	39.5	34.4
Yb	2.92	2.71	2.93	2.79	2.92	2.98	3.03	3.02	2.74
Zr	86	92	93	96	107	107	109	102	83
As	0.4	0.5	0.4	0.5	0.4	0.5	0.5	0.5	0.4
Bi	0.1	0.06	0.08	0.11	0.1	0.09	0.09	0.1	0.08
Sb	<0.05	<0.05	<0.05	<0.05	<0.05	<0.05	<0.05	<0.05	<0.05
Se	1.5	1.3	1.5	1.4	1.4	1.3	1.4	1.6	1.5
Te	<0.01	0.01	0.01	<0.01	<0.01	<0.01	0.01	<0.01	<0.01
Ag	<0.5	<0.5	<0.5	<0.5	<0.5	<0.5	<0.5	<0.5	<0.5
Cd	<0.5	<0.5	0.5	0.5	0.7	<0.5	<0.5	<0.5	1
Co	59	54	61	56	53	55	53	58	79
Cu	329	241	264	312	350	542	352	439	349
Li	20	10	10	10	10	10	10	10	10
Mo	2	2	3	2	3	2	2	2	3
Ni	4	9	8	9	11	14	11	23	11
Pb	<2	<2	<2	9	2	5	2	7	2
Sc	32	31	29	30	28	31	28	29	32
Zn	204	190	203	192	193	188	192	200	255

Sample	FD-13-34-208	FD-13-34-212.5	FD-13-34-217	FD-13-34-217	FD-13-34-221.5	FD-13-34-226	FD-13-34-226	FD-13-34-230.5	FD-13-34-235
Unit	2f	2f	2f	2f	2f	2f	2f	2f	3g
SiO_2	30.1	39.6	36	36.4	34.7	32.3	32.3	30.6	18.2
Al_2O_3	5.09	10.55	9.22	9.24	7.94	7.53	7.66	7.89	1.98
Fe_2O_3	39.3	24.8	29.8	30.5	32	34.9	34.7	35.3	47.2
FeO	29.4	18.1	22		24.1		25.8	25.4	
CaO	9.23	10.05	9.35	9.56	8.81	8.77	8.6	9.87	12.35
MgO	7.9	5.78	6.15	6.02	6.92	6.71	6.87	6.13	7.05
Na_2O	1.07	2.43	2.09	2.13	1.76	1.64	1.6	1.61	0.16
K_2O	0.31	0.75	0.6	0.65	0.58	0.57	0.54	0.28	0.07
Cr_2O_3	<0.01	<0.01	<0.01	<0.01	<0.01	<0.01	<0.01	<0.01	<0.01
TiO_2	5.52	3.53	4.07	4.28	4.19	5.03	4.87	6.02	8.41
MnO	0.57	0.37	0.44	0.47	0.48	0.52	0.49	0.44	0.56
P_2O_5	2.8	1.92	2.28	2.31	2.21	2.68	2.68	3.05	5.98
SrO	0.04	0.08	0.07	0.07	0.06	0.06	0.06	0.07	0.02
BaO	0.04	0.1	0.08	0.09	0.07	0.07	0.07	0.06	0.01
LOI	-2.46	-1.09	-1.24	-1.25	-1.63	-1.47	-1.41	-1.88	-1.66
Total	99.51	98.87	98.91	100.47	98.09	99.31	99.03	99.44	100.33
C	0.02	0.03	0.03	0.05	0.07	0.06	0.08	0.08	0.06
S	0.31	0.17	0.23	0.2	0.17	0.2	0.22	0.25	0.71
Ba	385	897	745	761	643	648	616	561	42.3
Ce	242	186.5	211	235	215	259	233	257	396
Cr	20	<10	<10	10	<10	10	<10	<10	10
Cs	0.39	0.48	0.08	0.5	0.53	0.38	0.09	0.08	0.43
Dy	10.15	8.27	9.13	9.47	9.32	10	9.85	11	15.8
Er	5.02	4.07	4.53	4.66	4.74	4.84	4.87	4.98	6.86
Eu	4.62	4.79	4.6	4.89	4.5	5.02	4.61	5.47	7.34
Ga	16.1	18.4	18.8	19.2	17.3	18.9	18.8	19.7	19.8
Gd	16.8	13.1	13.7	14.35	14.25	15.25	14.95	17.05	26.6
Hf	2.5	2.5	2.5	2.8	3.1	2.3	2.1	1.9	1.5
Ho	2.01	1.53	1.67	1.75	1.7	1.83	1.73	2.01	2.84
La	112.5	87.4	99.6	104.5	101.5	115.5	108.5	119.5	169
Lu	0.52	0.47	0.48	0.56	0.54	0.55	0.49	0.52	0.69
Nb	70.1	55.4	63.8	66.3	74.1	72.5	68.2	72.7	50.4
Nd	133.5	99.4	111	116	111	126.5	122.5	138	214

Pr	30.5	23.5	25.8	29.7	25.9	32.7	28.9	32.3	52.9
Rb	8	15.9	14.3	14.1	16	12.6	11.6	3.8	5.6
Sm	21	16.8	18.2	18.65	18.1	20.6	20.3	23.3	35.1
Sn	16	17	30	30	38	65	68	63	14
Sr	324	649	559	589	461	480	446	533	205
Ta	3.2	2.5	3	3.5	3.3	3.5	3.1	3.4	2.9
Tb	1.98	1.61	1.61	1.83	1.65	1.85	1.85	2.13	3.15
Th	2.37	2.73	2.94	3.39	2.95	2.78	2.68	1.8	2.88
Tl	0.03	0.04	0.04	<0.5	0.04	<0.5	0.03	<0.02	<0.5
Tm	0.61	0.53	0.56	0.6	0.58	0.6	0.59	0.61	0.86
U	0.73	0.77	0.91	1.07	1.31	0.72	0.82	0.53	0.78
V	448	285	320	353	309	427	383	522	727
W	1	1	1	1	1	3	3	2	1
Y	49.3	39.9	43.2	44.9	44.6	47.2	45.2	51	72.5
Yb	3.74	3.21	3.47	3.53	3.8	3.49	3.6	3.64	4.58
Zr	94	95	97	114	133	102	86	75	65
As	0.3	0.3	0.7	<0.1	0.4	<0.1	0.5	0.4	0.1
Bi	0.23	0.09	0.11	0.15	0.12	0.17	0.16	0.17	0.19
Sb	<0.05	<0.05	<0.05	0.05	<0.05	<0.05	<0.05	<0.05	0.05
Se	2.2	1.4	1.9	2.8	1.8	3.3	1.9	2	2.2
Te	0.01	0.01	<0.01	0.01	<0.01	0.02	0.01	<0.01	0.03
Ag	<0.5	<0.5	<0.5	<0.5	<0.5	<0.5	<0.5	<0.5	<0.5
Cd	1.1	0.5	1	1	0.7	1.2	0.8	1.1	1.7
Co	112	69	80	73	88	88	96	96	115
Cu	796	367	493	466	521	774	758	855	826
Li	10	10	10	10	10	10	10	10	10
Mo	3	2	3	3	4	3	5	3	3
Ni	11	8	15	20	26	35	50	33	17
Pb	10	2	2	5	6	11	4	<2	6
Sc	33	33	28	27	29	24	26	28	30
Zn	340	210	260	252	279	287	295	304	327

Sample	FD-13-34-235	FD-13-34-239.5	FD-13-34-244	FD-13-34-244	FD-13-34-248.5	FD-13-34-248.5	FD-13-34-253	FD-13-34-257.5	FD-13-34-257.5
Unit	3g	3g	3g	3g	3g	3g	3g	3g	3g
SiO_2	17.9	20.1	23.9	24.2	32.1	32.3	30.5	29.1	29.4
Al_2O_3	1.92	1.67	2	2	9.38	9.53	6.97	7.34	7.43
Fe_2O_3	47	43	40.1	40	28.3	28.8	31.7	33.1	33.6
FeO	28.4	24.8	25.4			19	21.5	21.7	
CaO	12	14.5	13.45	13.9	12.45	12.4	12.05	11.9	12.2
MgO	7.09	6.96	8.01	7.92	5.72	5.93	6.93	6.11	5.98
Na_2O	0.16	0.13	0.23	0.24	1.52	1.49	1	1.23	1.28
K_2O	0.04	<0.01	0.04	0.05	0.26	0.25	0.26	0.22	0.25
Cr_2O_3	<0.01	<0.01	<0.01	<0.01	<0.01	<0.01	<0.01	<0.01	<0.01
TiO_2	8.22	7.78	6.46	6.53	4.49	4.57	4.64	5.45	5.6
MnO	0.53	0.49	0.51	0.54	0.4	0.38	0.45	0.44	0.48
P_2O_5	5.98	6.07	5.1	5.13	3.78	3.86	4.12	4.38	4.41
SrO	0.02	0.02	0.02	0.02	0.08	0.08	0.06	0.07	0.07
BaO	<0.01	<0.01	0.01	0.01	0.04	0.04	0.03	0.04	0.04
LOI	-1.75	-1.46	-1.25	-1.19	-0.25	-0.06	0.13	-0.7	-0.82
Total	99.11	99.26	98.58	99.35	98.27	99.57	98.84	98.68	99.92
C	0.05	0.02	0.02	0.03	0.05	0.02	0.03	0.02	0.02
S	0.73	0.44	0.48	0.5	0.18	0.21	0.32	0.31	0.28
Ba	37	15.8	55.3	55.2	359	348	275	323	326
Ce	357	382	314	311	258	237	254	266	278
Cr	10	<10	10	10	10	<10	<10	<10	10
Cs	0.35	0.06	0.07	0.09	0.24	0.18	0.09	0.2	0.2
Dy	15.85	17.35	14.75	13.3	10.65	10.35	10.95	11.65	11.2
Er	6.32	7.49	6.47	5.8	4.56	4.86	4.78	5.41	4.93
Eu	6.56	6.93	6.03	5.73	5.59	5.17	5.43	5.47	5.59
Ga	19.7	19.7	17.1	15.5	18.8	18.7	16.2	19.1	18.4
Gd	25.1	28	23.7	21.4	16.25	17.5	18.05	18.95	17.65
Hf	1.7	1.7	1.8	1.6	1.5	1.6	1.9	1.7	1.5
Ho	2.72	2.96	2.67	2.45	1.88	1.93	2.01	2.08	2.01
La	158	170	138.5	133	111.5	106.5	115.5	119.5	120.5
Lu	0.59	0.64	0.61	0.62	0.5	0.45	0.47	0.46	0.52
Nb	48.1	47	42.9	41.5	38.1	38.7	41.7	48.9	48.6

Nd	202	215	178.5	172.5	136.5	130.5	142	146	146
Pr	46.4	49.7	40.9	42.5	33.9	30.4	32.8	34.3	36.6
Rb	5.4	0.5	1.2	1.3	5.4	5.3	7.5	4.9	4.4
Sm	34	36.3	30.1	29	22.3	22.6	23.4	24.4	24.2
Sn	13	21	19	20	19	19	30	11	13
Sr	192.5	189	178.5	172	694	714	469	538	557
Ta	2.5	2.4	2.1	2.3	2.1	1.7	2	2.4	2.7
Tb	3.04	3.21	2.71	2.62	2.06	1.96	2.21	2.25	2.19
Th	2.48	2.33	2.1	2.24	2.15	1.9	2.42	2.11	2.3
Tl	0.04	<0.02	<0.02	<0.5	<0.5	0.02	0.04	<0.02	<0.5
Tm	0.74	0.87	0.78	0.75	0.6	0.58	0.63	0.56	0.61
U	0.71	0.58	0.62	0.77	0.55	0.54	0.74	0.64	0.59
V	708	691	716	686	494	474	554	680	711
W	1	1	1	1	1	1	1	1	<1
Y	69.5	78.5	66.3	61.5	48.5	48.8	52.2	54	51.9
Yb	4.46	4.77	4.12	4.14	3.31	3.3	3.46	3.46	3.52
Zr	58	60	63	62	57	56	69	61	63
As	2.8	0.4	0.8	<0.1	<0.1	0.3	0.9	0.2	<0.1
Bi	0.14	0.17	0.2	0.21	0.15	0.17	0.15	0.17	0.19
Sb	<0.05	<0.05	<0.05	0.35	<0.05	<0.05	<0.05	<0.05	<0.05
Se	3.4	3.1	2.9	2.1	1.6	2	2.3	2.3	1.9
Te	0.01	0.01	0.01	0.03	0.02	0.01	0.01	0.01	0.03
Ag	<0.5	0.6	<0.5	<0.5	<0.5	<0.5	<0.5	<0.5	<0.5
Cd	1.7	1.7	1	1.8	1	<0.5	1	1.4	1.2
Co	128	115	111	99	71	77	88	87	80
Cu	881	893	715	716	513	549	646	610	591
Li	<10	<10	<10	10	10	10	<10	<10	10
Mo	3	3	2	3	2	2	2	3	3
Ni	17	21	19	16	15	23	29	26	25
Pb	4	<2	<2	4	7	<2	6	<2	5
Sc	33	45	43	41	28	29	31	28	27
Zn	352	344	306	298	230	233	247	270	265

Sample	FD-13-34-262	FD-13-34-266.5	FD-13-34-266.5	FD-13-34-271	FD-13-34-272	FD-13-34-276.5	FD-13-34-281	FD-13-34-285.5	FD-13-34-291
Unit	3g	3g	3g	3g	3h	3h	3h	3h	3h
SiO_2	30.3	28.5	27.8	21	31	37.4	32	40.9	37.1
Al_2O_3	7.64	7.87	7.68	5.13	8.05	4.86	5.88	12.3	3.8
Fe_2O_3	31.9	31.1	29.9	34.7	34.7	23.9	30.9	19.35	32.3
FeO	22.3		22	22.7	23.6	16.6	21	13.4	24.7
CaO	11.65	14.4	14.15	14.4	7.14	14.35	12	12	5.03
MgO	6.73	6.34	5.88	8.09	10.85	10.65	8.15	7.39	17.55
Na_2O	1.33	1.4	1.28	0.8	1.26	0.64	0.96	2.1	0.54
K_2O	0.25	0.19	0.2	0.42	0.3	0.22	0.53	0.37	0.25
Cr_2O_3	<0.01	<0.01	<0.01	0.02	0.02	0.04	0.01	0.01	0.01
TiO_2	3.97	3.8	3.6	4.76	3.01	1.91	3.29	1.64	0.45
MnO	0.47	0.44	0.4	0.35	0.39	0.31	0.46	0.28	0.49
P_2O_5	4.86	7.25	6.6	9.24	2.89	2.35	4.22	2.26	0.68
SrO	0.07	0.08	0.08	0.05	0.06	0.03	0.05	0.08	0.02
BaO	0.04	0.04	0.04	0.04	0.04	0.01	0.04	0.04	0.02
LOI	-0.96	-1.55	-1.57	-0.8	-1.27	0.22	-0.14	0.68	-0.85
Total	98.25	99.86	96.04	98.2	98.44	96.89	98.35	99.4	97.39
C	0.03	0.02	0.02	0.02	0.04	0.08	0.06	0.15	0.2
S	0.14	0.19	0.19	0.13	0.32	0.76	0.15	0.1	0.47
Ba	340	343	333	388	327	128.5	361	384	150.5
Ce	273	424	406	392	127.5	105	258	109.5	42.9
Cr	10	30	20	120	140	300	60	80	50
Cs	0.34	0.07	0.19	0.54	0.27	0.22	0.66	0.22	0.29
Dy	11.2	16.4	16.8	16.4	5.47	5.92	11.7	5.91	2.37
Er	5.23	6.99	7.31	7.53	2.68	2.9	5.7	2.72	1.18
Eu	5.63	7.95	8.1	8.04	3.01	2.81	5.17	3.03	0.92
Ga	17.6	17.5	18.5	20.1	16.9	12.1	16.1	16.6	4.9
Gd	18.85	26.4	28	27.5	8.93	9.06	18.05	8.34	3.27
Hf	1.4	1	1	2.2	1	1.5	2.3	1.6	0.7
Ho	1.97	2.99	3.03	3	1	1.09	2.11	0.92	0.41
La	125.5	190	187.5	180.5	59	45.8	118.5	50.4	20.3
Lu	0.48	0.67	0.62	0.67	0.26	0.31	0.55	0.28	0.16
Nb	35.8	35.2	35.9	51.2	27.9	10.7	47.1	19.8	7.4

Nd	149	221	221	217	70.4	63.3	140.5	61.6	23.5
Pr	34.2	55.3	50.7	50.1	15.85	14.15	32.9	14.15	5.45
Rb	6	2.4	2.2	9.6	6.7	3.7	20.1	7.9	6.7
Sm	24.5	34.5	36.3	36.8	11	11.4	23.3	10.35	4.13
Sn	9	9	9	13	8	10	7	8	4
Sr	542	666	668	389	457	220	365	646	172.5
Ta	1.7	1.9	1.7	2.3	1.2	0.4	2	0.8	0.2
Tb	2.06	3.17	3.31	3.2	1.03	1.13	2.19	1.07	0.44
Th	2.18	2.81	2.39	3.99	1.34	1.1	3.73	1.56	0.91
Tl	0.02	<0.5	<0.02	0.04	0.06	0.04	0.08	0.04	0.06
Tm	0.55	0.9	0.86	0.87	0.3	0.36	0.66	0.34	0.16
U	0.58	0.69	0.71	1.14	0.36	0.28	1.02	0.47	0.27
V	670	750	765	1530	1050	874	621	447	163
W	1	<1	1	1	<1	2	1	<1	1
Y	53.6	75.8	76.4	80	25.7	28.8	55.4	25.9	11.1
Yb	3.15	4.7	4.78	5.01	1.73	2.09	3.87	1.84	1.01
Zr	52	42	41	85	42	46	90	65	29
As	0.5	<0.1	0.5	1.5	1	6.4	1.1	0.5	14.5
Bi	0.13	0.13	0.14	0.08	1.06	0.34	0.08	0.05	1.39
Sb	<0.05	<0.05	<0.05	0.06	0.42	0.18	<0.05	<0.05	0.18
Se	2	2	3.2	3	2.8	6	2.1	1	3.8
Te	0.01	0.03	0.02	0.06	0.28	0.52	0.02	0.03	0.52
Ag	<0.5	<0.5	<0.5	<0.5	1.4	2.8	<0.5	<0.5	2
Cd	0.7	1	0.8	0.8	1.1	1.1	1	0.8	1.2
Co	87	90	94	115	144	106	91	74	176
Cu	517	1010	984	883	3660	6640	545	486	4480
Li	<10	10	10	10	<10	<10	10	10	10
Mo	2	2	2	1	<1	<1	3	<1	1
Ni	30	57	70	169	273	313	89	94	340
Pb	<2	14	3	<2	8	6	<2	3	10
Sc	21	16	16	16	9	51	31	28	20
Zn	249	256	251	228	240	143	252	147	207

Sample	FD-13-34-295.5	FD-13-34-316	FD-13-34-320.5	FD-13-34-325	FD-13-34-327.5	FD-13-34-302	FD-13-34-305	FD-13-34-310	FD-13-34-330
Unit	3h	3i	3i	3i	3i	3h	3h	3h	3i
SiO_2	36	31.6	35.9	32.2	26	34.3	46.7	37.4	30.2
Al_2O_3	3.63	2.13	2.6	1.68	1.67	2.9	13.45	4.07	3.06
Fe_2O_3	25	30.5	28.3	30.8	28.5	29.4	13.25	27.2	27.1
FeO	19.1	20.9	20.5	22.6	21.5	22.5	10.3	19.75	20.4
CaO	14.3	12.8	12.7	13.35	16.2	13.1	12.05	11.95	15.5
MgO	9.63	14.4	14.9	15.9	13.5	13.65	7.87	13.45	13.35
Na_2O	0.48	0.35	0.37	0.22	0.17	0.41	2.46	0.6	0.54
K_2O	0.77	0.18	0.17	0.13	0.26	0.13	0.42	0.28	0.4
Cr_2O_3	0.01	0.01	0.02	0.01	0.01	0.01	0.03	0.02	0.01
TiO_2	1.28	1.11	0.92	0.38	0.39	1.17	0.8	1.22	0.52
MnO	0.42	0.47	0.45	0.49	0.46	0.49	0.23	0.45	0.44
P_2O_5	3.99	5.09	3.84	6.95	10.8	4.56	0.17	2.49	8.07
SrO	0.02	0.02	0.01	0.02	0.03	0.03	0.08	0.03	0.03
BaO	0.04	0.01	0.01	0.01	0.02	0.02	0.05	0.02	0.03
LOI	1.27	-0.14	-0.13	-0.61	0.13	-0.68	1.54	0.46	-0.23
Total	96.84	98.53	100.06	101.53	98.14	99.49	99.1	99.64	99.02
C	0.13	0.17	0.15	0.07	0.14	0.04	0.12	0.15	0.22
S	0.47	0.42	0.46	0.46	0.76	0.21	0.05	0.15	0.66
Ba	342	115	109.5	80.7	139.5	151.5	465	203	250
Ce	298	229	165	257	408	235	29.8	145	317
Cr	70	90	130	50	40	70	190	120	50
Cs	0.91	0.2	0.3	0.15	0.25	0.2	0.83	0.43	0.4
Dy	13.5	10.55	8.36	12.05	18.3	10.65	2.51	6.95	13.75
Er	6.56	5.2	3.97	5.36	8.25	4.99	1.19	3.33	6.44
Eu	5.43	4.59	3.49	4.97	7.71	4.59	1.83	3.48	6.86
Ga	10.5	7.4	6.8	5.1	5.3	7.6	15.5	8.5	5.8
Gd	21.2	17.6	13.75	21.2	29.8	16.95	3.01	10.2	23.3
Hf	2.5	1.3	1.2	0.6	0.8	1.3	1	1.2	0.8
Ho	2.49	1.91	1.47	2.17	3.44	1.91	0.45	1.23	2.47
La	136.5	106.5	74.1	115.5	184	107.5	13.2	64	138
Lu	0.69	0.48	0.39	0.49	0.69	0.52	0.17	0.41	0.6
Nb	24.3	15.2	8.8	7.1	12	15.2	6.2	11.7	11.9
Nd	160	128.5	94.1	149.5	232	130.5	18.2	76.4	172.5

Pr	37.3	30.1	21.8	33.3	52.6	29.9	4.08	18.35	40.7
Rb	23.5	5.5	6	4.7	9.5	4	6.4	7.4	10.8
Sm	27.4	22	16.5	26.4	39	22.3	3.86	14.55	29.9
Sn	5	6	12	6	2	40	27	16	2
Sr	173	165.5	143	157	224	216	607	211	255
Ta	1	0.6	0.3	0.2	0.4	0.5	0.1	0.6	0.5
Tb	2.6	2.06	1.63	2.39	3.61	1.98	0.4	1.21	2.57
Th	4.16	2.52	1.92	2.23	3.99	1.88	0.4	1.2	3.12
Tl	0.14	0.05	0.07	0.03	0.07	0.02	0.04	0.1	0.07
Tm	0.75	0.61	0.46	0.65	0.93	0.6	0.16	0.46	0.77
U	1.13	0.81	0.54	0.7	1.13	0.49	0.13	0.33	0.79
V	314	396	367	157	118	341	344	463	178
W	1	1	<1	<1	<1	1	1	1	<1
Y	62.9	51.1	40.6	58.3	86.8	50.4	11.5	34.8	68.7
Yb	4.69	3.52	2.87	3.75	5.22	3.43	1.12	2.78	4.44
Zr	94	47	38	29	36	41	31	44	37
As	1.2	4.9	2.3	0.5	4	0.3	3	3.1	3.8
Bi	0.35	0.37	0.35	0.23	0.69	0.13	0.23	0.19	0.44
Sb	<0.05	0.06	0.06	<0.05	0.08	<0.05	0.06	0.06	0.11
Se	4.3	3.9	4	4.6	7.5	2.4	0.8	1.9	6.5
Te	0.13	0.19	0.29	0.2	0.32	0.1	0.06	0.08	0.28
Ag	0.6	1.2	1.7	1.5	2.5	0.5	<0.5	<0.5	1.9
Cd	0.8	0.9	1.1	1.3	1	0.9	<0.5	0.7	1.2
Co	92	139	134	151	138	125	58	121	121
Cu	1920	3130	3760	3840	6370	1635	880	1535	5030
Li	10	<10	<10	10	10	10	10	10	10
Mo	1	<1	3	<1	<1	1	<1	1	1
Ni	147	262	292	325	392	182	120	200	346
Pb	6	3	12	5	13	9	<2	7	20
Sc	44	32	43	25	15	38	44	43	21
Zn	182	193	173	189	171	215	92	191	159

Sample	SL-13-27-37.3	SL-13-27-46	SL-13-27-50.5	SL-13-27-41.5	SL-13-32-49	SL-13-32-66.5	SL-13-41-94.5	SL-13-41-129.5	SL-13-41-138
Unit	3g	3g	3g	3g	3g	3g	2f	3g	3g
SiO_2	38.5	20.7	14.85	33.3	31.2	28.5	28.9	34	28.6
Al_2O_3	12.6	5.72	3.83	10.65	9.39	9.33	7.21	9.9	6.25
Fe_2O_3	19.9	38.3	40.2	25.9	23.5	23.6	31.5	23.7	34.4
FeO									
CaO	12.75	13.2	15.8	12.5	14.15	15.65	10.15	13.45	9.45
MgO	6.95	6.58	6.96	6.14	6.6	6.51	8.67	7.88	11.95
Na_2O	2.18	0.74	0.47	1.82	1.38	1.44	0.93	1.48	0.86
K_2O	0.75	0.78	0.25	0.8	0.32	0.4	0.61	0.4	0.53
Cr_2O_3	<0.01	<0.01	<0.01	<0.01	<0.01	<0.01	<0.01	<0.01	0.1
TiO_2	2.08	5.43	6.18	3.23	3.62	3.2	5.09	3.16	3.34
MnO	0.24	0.42	0.33	0.26	0.26	0.26	0.38	0.27	0.39
P_2O_5	3.24	7.53	10.15	4.05	5.09	7.2	3.13	3.93	4.68
SrO	0.11	0.06	0.05	0.1	0.08	0.08	0.05	0.09	0.05
BaO	0.16	0.09	0.06	0.15	0.05	0.06	0.17	0.09	0.06
LOI	0.17	0.32	-0.73	0.47	2.59	1.85	2.62	0.18	-0.03
Total	99.63	99.87	98.4	99.37	98.23	98.08	99.41	98.53	100.63
C	0.06	0.11	0.1	0.15	0.21	0.53	0.37	0.11	0.07
S	0.96	1.76	0.94	1.73	0.5	0.29	0.41	0.42	1.12
Ba	1400	858	541	1310	444	543	1520	808	584
Ce	166.5	319	384	217	219	307	196.5	168	194
Cr	10	10	10	10	10	20	40	20	680
Cs	1.4	4.6	1.37	1.3	0.77	0.98	2	0.8	1.37
Dy	6.96	12.25	15.45	8.76	9.34	12.55	8.29	7.3	7.95
Er	3.13	5.23	6.64	3.65	4.14	5.05	3.27	3.17	3.33
Eu	4.27	7.37	9.07	5.44	5.37	7.18	5.36	4.83	4.73
Ga	15.9	19.3	20.1	17.3	16.9	16.9	16.5	16.3	15.2
Gd	11.7	23	28.7	14.2	15.85	21.9	13.6	12.85	13.4
Hf	1.2	1.9	1.1	1.4	1.1	0.7	1	1.1	1.1
Ho	1.23	2.19	2.71	1.52	1.68	2.24	1.41	1.32	1.31
La	74.9	140	164.5	97.4	94.5	133	86.6	73.5	86.1
Lu	0.3	0.5	0.58	0.38	0.37	0.43	0.32	0.32	0.35
Nb	19.4	31.8	24.4	28.3	18.8	17.9	24.8	18.9	23.4

Nd	89.1	173.5	223	117	124.5	171.5	108	95.5	105.5
Pr	21.2	41.5	51.6	27.8	29.1	39.8	25.7	22.5	25.6
Rb	20.1	42.5	7.9	21.1	7.6	10.6	14.3	8.4	16.4
Sm	15.35	29.8	37.7	20.3	21.5	29.4	19.2	16.15	18.05
Sn	7	8	11	10	4	4	7	18	9
Sr	889	494	485	801	644	721	453	722	433
Ta	0.9	1.4	1.2	1.3	0.9	0.8	1.1	0.8	1
Tb	1.32	2.47	3.25	1.72	1.8	2.49	1.53	1.46	1.53
Th	2.25	3.91	3.9	3.29	2.5	2.8	2.35	1.78	2.64
Tl	<0.5	<0.5	<0.5	<0.5	<0.5	<0.5	<0.5	<0.5	<0.5
Tm	0.37	0.65	0.74	0.41	0.52	0.61	0.41	0.38	0.41
U	0.68	1.25	1.14	0.82	0.68	0.8	0.69	0.52	0.72
V	363	1030	1300	540	706	732	641	522	629
W	1	1	1	1	<1	<1	1	<1	1
Y	32.7	59.6	72.6	42	44.3	57.7	37.3	34.9	36.8
Yb	2.12	3.39	3.77	2.48	2.68	3.09	2.16	2.18	2.35
Zr	61	96	55	65	52	41	55	50	57
As	<0.1	<0.1	<0.1	<0.1	<0.1	<0.1	<0.1	<0.1	<0.1
Bi	0.27	0.19	0.52	0.46	0.36	0.15	0.07	0.23	0.38
Sb	0.05	0.09	0.06	0.06	<0.05	<0.05	0.07	<0.05	0.07
Se	3.8	5	3	5.4	2.7	1.6	1.7	1.9	3.8
Te	0.05	0.08	0.05	0.07	0.04	0.03	0.04	0.05	0.07
Ag	<0.5	<0.5	<0.5	<0.5	0.5	<0.5	<0.5	<0.5	<0.5
Cd	0.7	1.4	1.3	1	0.7	<0.5	1.2	0.8	1.6
Co	86	154	135	111	73	82	95	86	154
Cu	1230	2270	1460	2180	2530	921	340	1485	2070
Li	20	30	10	10	20	20	30	10	10
Mo	1	2	1	1	1	1	1	<1	1
Ni	139	213	144	189	75	26	61	186	238
Pb	6	12	17	9	5	5	8	5	11
Sc	25	16	17	27	29	16	34	36	16
Zn	134	402	270	173	137	156	275	141	205

Sample	FD-13-41-71.5	FD-13-41-94	SL-13-41-3	SL-13-41-12	SL-13-41-33.5	SL-13-41-49.5	SL-13-41-54	SL-13-41-68.5	SL-13-41-77.5
Unit	2f	2f	2f	2f	2f	2f	2f	2f	2f
SiO_2	36.2	35.1	39.8	41.9	43.2	39.5	43.1	39.1	29.1
Al_2O_3	9.55	9.35	9	13.5	13.25	11.1	15.75	12.6	6.32
Fe_2O_3	28.6	29.3	24.6	18.1	18.9	21.2	14.05	19.65	34.2
FeO			17.7	12.3	13.25	13.7	8.69	12.4	22.7
CaO	11.95	11.85	9.53	10.45	10.65	11.65	11.15	10.7	9.8
MgO	5.45	5.36	5.05	4.04	3.88	5.93	4.2	5.3	8.68
Na_2O	1.84	1.9	2	2.6	2.98	2.11	2.91	2.38	1.08
K_2O	0.64	0.33	1.59	1.57	0.95	1.22	1.45	1.47	0.56
Cr_2O_3	<0.01	<0.01	<0.01	<0.01	<0.01	<0.01	<0.01	<0.01	<0.01
TiO_2	3.69	4.31	4.98	3.25	3.31	3.56	2.2	3.33	6.03
MnO	0.41	0.45	0.44	0.32	0.34	0.29	0.2	0.33	0.39
P_2O_5	3.18	3.33	1.6	1.89	1.62	2.38	2.11	2.56	2.78
SrO	0.08	0.08	0.09	0.16	0.14	0.13	0.2	0.13	0.07
BaO	0.1	0.06	0.68	0.66	0.28	0.46	0.51	0.32	0.18
LOI	0.13	0.03	-0.56	1.25	0.07	0.12	1.9	1.6	-0.54
Total	101.82	101.45	98.8	99.69	99.57	99.65	99.73	99.47	98.65
C	0.03	0.02	0.08	0.34	0.13	0.06	0.18	0.13	0.12
S	1.1	0.17	0.16	0.27	0.2	0.24	0.15	0.27	0.52
Ba	866	553	5860	5830	2430	3660	4750	2680	1615
Ce	253	263	162.5	123.5	139.5	170	163.5	189	188.5
Cr	10	10	<10	<10	<10	10	10	10	10
Cs	0.55	0.31	1.15	3.29	1.25	1.82	2.16	2.45	0.74
Dy	10.75	11.45	6.13	4.81	5.91	7.03	6.25	6.84	7.46
Er	5	4.92	2.94	2.21	2.54	2.96	2.81	3.2	3.37
Eu	5.61	5.94	6.02	5.95	5.74	5.66	5.87	5.56	5.31
Ga	17.5	19.8	12.4	13.5	15.5	12.9	15.7	14.5	15.4
Gd	17.1	17.4	10.05	8.37	9.18	11.45	9.96	11.05	12.55
Hf	1.8	1.5	1.8	1.2	1.5	1.8	1.3	1.8	1.6
Ho	1.95	2.06	1.14	0.86	1.01	1.23	1.13	1.22	1.27
La	111.5	115.5	68.5	55.6	62.2	77	74.2	84.7	82.8
Lu	0.53	0.51	0.35	0.27	0.32	0.36	0.35	0.3	0.33
Nb	37.2	49.1	40.9	24.3	36.4	33.5	28.7	32.3	29.9
Nd	136	138.5	80.9	66.1	74.1	88.5	84	98.2	102.5

Pr	33	33.6	19.65	15.6	17.7	21.4	20.1	23.5	23.7
Rb	21.5	6.1	21.7	37.5	12.7	22.9	30.8	37.6	12.1
Sm	23.5	24.4	13.65	11.25	12.75	15.35	14	15.9	16.75
Sn	16	12	9	20	15	11	9	5	15
Sr	664	621	691	1290	1100	952	1625	1030	542
Ta	1.6	2.2	1.7	1.1	1.8	1.5	1.3	1.4	1.5
Tb	2.11	2.24	1.19	0.94	1.13	1.28	1.11	1.26	1.38
Th	3.39	2.03	2.53	2.51	2.5	3.88	3.13	3.25	2.4
Tl	<0.5	<0.5	0.06	0.15	0.07	0.07	0.07	0.19	0.06
Tm	0.63	0.6	0.37	0.31	0.35	0.42	0.36	0.41	0.44
U	0.94	0.6	0.77	0.74	0.6	1.08	0.87	0.89	0.72
V	264	516	45	99	117	257	171	279	510
W	1	<1	1	1	1	1	1	1	1
Y	51.7	53.4	31.1	24	27.3	32.8	29.5	33.2	36
Yb	3.64	3.65	2.28	1.84	2.22	2.65	2.13	2.3	2.39
Zr	81	70	71	54	68	86	65	76	65
As	<0.1	<0.1	1.6	1.1	0.4	0.4	0.6	2.6	0.4
Bi	1.24	0.17	0.05	0.04	0.04	0.03	0.03	0.09	0.06
Sb	<0.05	<0.05	<0.05	<0.05	<0.05	<0.05	<0.05	<0.05	<0.05
Se	4.3	1.4	1.2	1	1.4	1.2	1.3	1.6	2.1
Te	0.08	0.02	0.01	<0.01	<0.01	<0.01	<0.01	0.01	0.01
Ag	1.2	<0.5	<0.5	<0.5	<0.5	<0.5	<0.5	<0.5	<0.5
Cd	1.8	1.2	1.2	<0.5	0.5	0.5	<0.5	<0.5	1.2
Co	79	64	32	33	33	63	44	59	111
Cu	3390	530	81	214	143	114	116	148	235
Li	<10	10	10	40	10	10	20	40	10
Mo	2	2	2	2	2	1	1	1	<1
Ni	18	12	9	13	9	16	15	31	40
Pb	16	3	33	10	14	12	10	17	12
Sc	35	30	51	33	33	40	23	28	38
Zn	211	242	210	165	160	148	117	253	209

Sample	SL-13-41-91	SL-13-41-109	SL-13-41-132	SL-13-41-143	SL-13-41-148	SL-13-41-153	SL-13-41-167	SL-13-41-230	SL-13-41-265.5
Unit	2f	2f	3g	3b	3b	3b	3b	3b	3b
SiO_2	28.6	19.45	36.7	38.3	39.5	39.5	34.7	47	42.4
Al_2O_3	5.43	3.91	11.15	14.15	13.95	14.3	11.25	9.43	5.82
Fe_2O_3	36.4	46.2	20.8	18.95	17.4	16.45	22	12.45	19.2
FeO	23.6	28.7	13.55	12.15	11.4	10.05	14.7	10.1	11.8
CaO	10.45	8.86	13.5	12.9	13	13.35	12.2	15.5	10.7
MgO	9.82	8.94	8.24	5.6	5.78	5.93	7.21	10.85	14.3
Na_2O	0.89	0.42	1.78	2.28	2.38	2.39	1.9	1.38	0.61
K_2O	0.48	0.15	0.53	0.47	0.53	0.43	0.46	0.18	0.22
Cr_2O_3	<0.01	0.01	0.01	<0.01	<0.01	<0.01	<0.01	0.02	0.02
TiO_2	5.91	8.21	2.37	1.83	1.89	2.06	2.58	0.52	0.42
MnO	0.41	0.43	0.26	0.18	0.19	0.19	0.24	0.21	0.28
P_2O_5	3.42	3.69	4.15	3.05	3.23	3.31	3.36	0.06	0.06
SrO	0.05	0.04	0.11	0.11	0.1	0.11	0.09	0.05	0.02
BaO	0.15	0.05	0.12	0.07	0.08	0.07	0.06	0.02	0.01
LOI	-1.21	-2.05	0.47	1.12	0.59	0.42	-0.11	0.9	5.41
Total	100.8	98.31	100.19	99.01	98.62	98.51	95.94	98.57	99.47
C	0.06	0.07	0.08	0.11	0.12	0.12	0.14	0.47	0.13
S	0.29	0.46	0.34	1.87	0.76	0.1	0.62	0.51	0.53
Ba	1345	431	1050	604	685	594	581	159	118.5
Ce	229	210	192	120	156	137	170	24.1	20.4
Cr	30	80	90	20	10	<10	<10	150	120
Cs	0.47	0.19	0.73	0.86	0.79	0.47	0.36	0.13	0.8
Dy	8.15	7.73	7.29	4.86	5.9	5.46	6.46	2.65	2.35
Er	3.62	3.1	3.22	2.09	2.55	2.43	2.73	1.47	1.11
Eu	5.64	5.39	4.98	3.26	3.67	3.56	4.03	1.24	0.98
Ga	15.6	19.3	13.4	14.2	14.8	15.2	14.9	9.3	7.9
Gd	14.55	13.65	12.7	8.89	10	9.83	11.65	3.54	2.84
Hf	1.6	1.2	1.3	1	1	0.9	1.2	1.2	0.8
Ho	1.52	1.34	1.27	0.87	1.1	0.98	1.19	0.56	0.45
La	96	87.4	80.8	52.7	65.6	59.4	71.5	8.9	8.4
Lu	0.34	0.3	0.29	0.19	0.26	0.23	0.29	0.19	0.17
Nb	27.6	25.3	18.6	10.9	15.6	10.8	15.2	3	2.2

Nd	116.5	109	99	65.3	78.5	74.1	87.6	16.6	13.9
Pr	28.2	26.1	23.6	15.4	18.85	17.5	21.2	3.6	3.01
Rb	10.4	3	11.4	8.6	10.3	7.3	9.2	2.7	6.1
Sm	19.35	17.9	16.75	11.2	12.75	12.45	14.4	3.83	3.15
Sn	31	37	19	7	12	4	27	33	17
Sr	476	329	925	940	942	944	810	397	164
Ta	1.3	1.3	0.7	0.4	0.6	0.4	0.7	0.1	<0.1
Tb	1.71	1.6	1.51	1.02	1.23	1.11	1.36	0.51	0.41
Th	2.49	1.49	1.93	1.54	1.92	1.47	2.32	0.36	0.23
Tl	0.03	0.02	0.05	0.08	0.07	0.03	0.04	0.02	0.35
Tm	0.45	0.37	0.38	0.26	0.34	0.3	0.34	0.19	0.17
U	0.78	0.5	0.6	0.44	0.58	0.41	0.65	0.11	0.08
V	732	1090	402	428	460	468	607	352	282
W	1	1	1	<1	1	<1	1	1	2
Y	40.9	37.5	35.8	24.3	29.7	27.5	32.5	13.6	11.5
Yb	2.41	2.03	2.13	1.46	1.88	1.62	1.92	1.29	1.05
Zr	60	40	45	39	35	32	43	34	21
As	0.3	0.3	0.4	0.3	0.4	0.5	0.2	0.1	11
Bi	0.1	0.18	0.14	0.54	0.27	0.05	0.28	0.3	0.41
Sb	<0.05	<0.05	<0.05	<0.05	<0.05	<0.05	<0.05	<0.05	0.05
Se	1.8	2.5	2.6	7.6	3.8	1.5	4	2.2	1.8
Te	0.02	0.02	0.03	0.07	0.04	0.01	0.05	0.13	0.1
Ag	<0.5	<0.5	<0.5	0.7	<0.5	<0.5	<0.5	0.8	0.6
Cd	1.6	2.4	1.1	1.6	0.7	0.8	1	0.9	1.5
Co	120	154	81	103	75	58	89	81	127
Cu	482	941	1190	2870	1260	330	2810	2250	1220
Li	10	10	10	10	10	10	10	10	10
Mo	1	<1	<1	<1	<1	<1	<1	<1	<1
Ni	78	148	162	179	115	61	131	328	257
Pb	12	15	10	13	15	7	7	7	4
Sc	43	35	27	23	23	24	26	61	46
Zn	226	283	142	115	108	112	149	72	117

Sample	SL-13-41-270	SL-13-41-277	SL-13-34-3.5	SL-13-34-7	SL-13-34-13	SL-13-34-16.75	SL-13-34-20.5	SL-13-34-24.5	SL-13-34-33
Unit	3b	3b	2f	2b	2b	2b	2b	2b	2b
SiO_2	47	42	31.8	46.4	47.5	45	33.9	38.6	39.1
Al_2O_3	10.85	6.26	8.53	17.4	18.95	16.05	7.51	10.95	12.65
Fe_2O_3	12.65	21.9	30.2	12.7	9.78	13.75	28.5	20.5	21.6
FeO	8.55	16.85	21.1	8.46	6.55	9.42	20	14.35	15.2
CaO	13.1	9.49	8.69	10.5	10.45	10.45	10.25	11.45	10.95
MgO	10.6	15.85	6.75	3.12	2.57	4	8.26	5.4	5.59
Na_2O	1.53	0.85	1.64	3.47	3.82	3.22	1.41	2.14	2.31
K_2O	0.46	0.14	1.23	1.45	1.36	1.33	0.87	1.17	1.02
Cr_2O_3	0.01	0.02	<0.01	<0.01	<0.01	<0.01	<0.01	<0.01	<0.01
TiO_2	0.41	0.53	6.63	2.16	1.65	2.18	4.84	3.9	3.37
MnO	0.21	0.33	0.4	0.21	0.14	0.19	0.39	0.31	0.31
P_2O_5	0.05	0.08	2.6	1.72	1.59	1.62	2.1	2.43	2.67
SrO	0.05	0.03	0.09	0.22	0.22	0.18	0.08	0.14	0.15
BaO	0.05	0.02	0.33	0.6	0.53	0.53	0.28	0.51	0.46
LOI	2.76	1.56	-0.43	0.3	0.56	-0.1	-1.12	1.65	-0.73
Total	99.73	99.06	98.46	100.25	99.12	98.4	97.27	99.15	99.45
C	0.16	0.18	0.15	0.11	0.1	0.05	0.09	0.13	0.08
S	0.61	0.46	0.36	0.17	0.12	0.11	0.19	0.28	0.35
Ba	477	136	2920	5370	4680	4870	2530	4660	4060
Ce	21.6	18.5	211	157.5	159.5	160	192	213	205
Cr	80	180	<10	<10	<10	<10	<10	10	20
Cs	0.85	0.61	1.88	1.14	1.16	1.13	0.47	1.54	0.62
Dy	2.48	1.91	7.33	5.34	5.4	5.77	7.27	7.99	7.22
Er	1.1	1.03	3.37	2.63	2.67	2.77	3.33	3.58	3.24
Eu	1.25	0.89	5.35	5.27	5.17	5.38	4.67	5.99	5.48
Ga	10.6	7.4	14.9	15.5	15.6	15.7	13	14.5	14.8
Gd	2.85	2.43	12.6	9.3	8.06	9.49	12.1	12.95	12.5
Hf	0.9	0.7	2.3	2	1.6	1.8	2.1	1.7	1.8
Ho	0.47	0.38	1.32	1.01	0.96	1.09	1.31	1.45	1.31
La	8.7	6.9	91.4	69.4	71.4	71.2	81	91.8	88.3
Lu	0.18	0.16	0.39	0.3	0.29	0.29	0.39	0.43	0.36
Nb	2.9	2.4	44.8	33.1	29.9	29.3	37.7	31.2	35.2
Nd	14.6	12.5	100.5	72.8	71.2	77.2	94.4	105	101

Pr	3.13	2.76	25.2	18.4	18.4	19.2	23.3	26.1	24.6
Rb	10.6	3.3	28	24.4	20.3	21.4	16.4	20.2	17.2
Sm	3.36	2.85	16.6	12	11.65	12.7	15.85	17.55	16.6
Sn	19	13	4	5	7	4	4	7	6
Sr	461	259	736	1950	1900	1580	685	1175	1240
Ta	0.1	0.1	1.9	1.4	1.3	1.3	1.7	1.3	1.5
Tb	0.42	0.32	1.55	1.08	1.03	1.22	1.46	1.57	1.46
Th	0.4	0.2	5.2	3.32	2.66	2.94	3.2	2.78	2.8
Tl	0.1	0.07	0.1	0.05	0.03	0.04	0.04	0.07	0.03
Tm	0.19	0.15	0.41	0.33	0.32	0.36	0.44	0.46	0.42
U	0.12	0.07	1.56	1.01	0.83	0.95	0.91	0.82	0.84
V	288	331	243	109	80	196	408	226	307
W	1	1	1	1	1	1	1	1	1
Y	11.9	10.2	36.7	27.3	26.5	28.4	36.2	39.2	36
Yb	1.11	0.94	2.59	1.94	1.82	2.02	2.59	2.51	2.32
Zr	23	17	99	87	67	76	81	69	73
As	7.5	0.2	1.1	0.4	0.5	0.4	0.5	0.4	0.3
Bi	0.21	0.19	0.05	0.02	0.02	0.02	0.02	0.04	0.04
Sb	0.05	<0.05	0.05	<0.05	<0.05	<0.05	<0.05	<0.05	<0.05
Se	1.7	1.6	2.1	1.2	1.3	1.4	1.9	2	2.2
Te	0.09	0.11	<0.01	<0.01	0.01	<0.01	<0.01	<0.01	<0.01
Ag	0.5	0.7	<0.5	<0.5	<0.5	<0.5	<0.5	<0.5	<0.5
Cd	0.8	1.4	1.6	<0.5	0.5	0.5	1.7	1.3	1.2
Co	79	137	81	31	25	42	91	54	67
Cu	1200	1160	52	43	65	60	72	64	121
Li	20	10	10	10	10	10	10	10	10
Mo	<1	<1	1	<1	<1	<1	<1	<1	<1
Ni	231	268	7	6	3	17	13	10	22
Pb	19	11	10	3	7	<2	2	7	<2
Sc	47	38	34	23	17	28	47	41	29
Zn	76	140	271	101	83	199	200	214	164

Sample	SL-13-34-37	SL-13-34-41.4	SL-13-34-63.5	SL-13-34-67.5	SL-13-34-75	SL-13-34-76.5	SL-13-34-88	SL-13-34-96	SL-13-34-111.8
Unit	2b	2b	3b	3b	3i	3i	2i	2i	2i
SiO_2	42.8	41.9	30.7	38	29.4	32.9	43.3	42.3	42.1
Al_2O_3	15.3	14.35	8.29	16.55	2.98	6.44	6.35	7.29	5.28
Fe_2O_3	15.8	17.4	29.3	16.2	38.6	31	16.45	17.8	19.95
FeO	9.8	12.15	19.65	10.95	26.9	21.2	13.2	13.1	14.8
CaO	11.2	11.45	13.5	12.55	4.21	6.66	11.9	11.15	11.25
MgO	4.05	4.44	7.69	3.66	19.4	16.7	17.9	16.45	18.15
Na_2O	2.88	2.97	1.25	2.72	0.33	0.9	0.68	0.85	0.61
K_2O	1.26	1.22	0.35	0.74	0.24	0.44	0.09	0.17	0.08
Cr_2O_3	<0.01	<0.01	0.01	0.01	0.05	0.04	0.14	0.2	0.21
TiO_2	2.53	3.01	4.44	1.77	2.87	2.28	0.5	0.76	0.98
MnO	0.23	0.3	0.31	0.2	0.47	0.4	0.26	0.27	0.29
P_2O_5	2.37	2.51	4.72	4.35	1.48	2.15	0.05	0.06	0.05
SrO	0.17	0.14	0.08	0.17	0.02	0.05	0.03	0.03	0.02
BaO	0.41	0.36	0.1	0.21	0.04	0.09	0.01	0.02	0.01
LOI	0.33	0.91	-0.7	1.3	-0.84	0.82	0.35	1.33	0.19
Total	99.33	100.96	100.04	98.43	99.25	100.87	98.01	98.68	99.17
C	0.11	0.12	0.08	0.13	0.18	0.21	0.14	0.17	0.09
S	0.15	0.25	1.14	1.22	0.58	0.64	0.01	0.09	0.04
Ba	3700	3320	870	1900	323	752	82.1	156.5	71
Ce	207	229	213	202	64.8	102.5	18.5	21.5	18.8
Cr	<10	10	90	80	350	280	1020	1470	1470
Cs	1.05	4.04	0.45	2.89	1.11	1.46	0.29	1.22	0.54
Dy	7.18	7.98	7.9	6.47	2.52	4.12	2.07	2.2	2.41
Er	3.16	3.68	3.3	2.67	1.13	1.87	1.1	1.14	1.17
Eu	5.29	5.77	5.48	5.42	1.54	2.55	0.87	0.96	0.97
Ga	15.6	16.4	14.5	15.2	9.7	11	7.5	9	8.7
Gd	11.4	13.1	13.95	11.9	4.28	6.67	2.71	2.72	3.31
Hf	2	2.4	1.1	0.8	0.6	1.2	1.1	1	1.1
Ho	1.32	1.48	1.41	1.17	0.44	0.73	0.4	0.4	0.46
La	90.2	100.5	88	87.4	28.4	44.8	6.8	8.3	6.9
Lu	0.36	0.42	0.32	0.27	0.13	0.2	0.15	0.14	0.16
Nb	36.8	42.8	18	17.6	10	15.8	3.2	5.2	3.7

Nd	97.8	108	112	100.5	34.5	53.6	12.8	13.8	13.7
Pr	24.4	27.2	26.5	24.5	8.15	12.95	2.69	3.1	2.85
Rb	23.7	25.3	7.3	20.6	7.4	11.9	2.5	8.2	2.1
Sm	15.75	17.75	18.7	16	6.07	8.87	2.9	3.13	3.38
Sn	4	4	2	4	3	2	6	3	2
Sr	1440	1230	761	1470	210	472	233	275	171.5
Ta	1.6	1.9	0.8	0.7	0.4	0.7	0.1	0.2	0.1
Tb	1.47	1.61	1.62	1.36	0.53	0.81	0.37	0.42	0.43
Th	3.24	4.19	1.82	1.9	0.8	2.32	0.38	0.55	0.34
Tl	0.05	0.11	0.05	0.23	0.07	0.07	<0.02	0.09	0.02
Tm	0.43	0.5	0.39	0.35	0.13	0.25	0.15	0.16	0.16
U	1	1.28	0.58	0.57	0.23	0.77	0.13	0.14	0.11
V	224	271	589	202	619	448	260	323	387
W	<1	1	<1	1	<1	1	1	1	<1
Y	36.1	40.5	39.2	34	12.8	20.5	10.5	10.8	11.8
Yb	2.39	2.78	2.21	1.9	0.81	1.34	0.92	0.98	0.97
Zr	86	108	38	33	20	49	25	26	27
As	0.8	8.5	0.3	2.3	0.3	0.4	0.6	2	<0.1
Bi	0.04	0.05	0.29	0.1	0.27	0.16	0.01	0.03	0.03
Sb	<0.05	0.05	<0.05	<0.05	0.06	<0.05	<0.05	0.05	<0.05
Se	2	2.3	4.3	5.1	2.4	2.9	<0.2	0.5	<0.2
Te	<0.01	0.01	0.05	0.06	0.07	0.04	<0.01	0.09	0.01
Ag	<0.5	<0.5	<0.5	<0.5	0.6	0.5	<0.5	<0.5	<0.5
Cd	0.5	1	1.6	0.9	1.2	0.9	0.5	0.7	0.7
Co	40	51	107	75	184	148	107	107	121
Cu	62	186	1160	1490	1460	1520	59	506	323
Li	10	40	10	30	10	20	<10	10	<10
Mo	1	<1	<1	<1	<1	<1	<1	1	<1
Ni	15	23	150	143	255	230	388	468	682
Pb	<2	11	12	12	9	14	2	3	<2
Sc	26	30	34	8	15	16	48	43	44
Zn	131	301	177	219	236	204	101	123	120

Sample	SL-13-34-119.5	SL-13-34-146.5	SL-13-34-147.3	SL-13-34-150.5	SL-13-34-159.5	SL-13-34-171	SL-13-34-181.4	SL-13-36-10.5	SL-13-36-15.5
Unit	2i	3b	3h	3b	3b	3b	3b	2b	2b
SiO_2	40.4	46.5	39.6	43.7	44.8	52.7	48.8	30.2	36.9
Al_2O_3	4.45	18.8	10.7	17.45	16.35	18.6	18.45	6.29	9.64
Fe_2O_3	20.5	11.95	19.05	15.05	13.45	7.77	12	32.1	25.1
FeO	13.3	7.28	11.15	7.97	7.86	3.84	6.36	21	16.35
CaO	9.14	11.85	15	12.1	11.7	7.56	9.69	11	11.65
MgO	20.1	4.97	6.4	4.3	3.95	3.56	3.72	7.81	7.9
Na_2O	0.55	2.81	1.8	2.66	3.26	5.25	4.25	1.12	1.73
K_2O	0.07	0.52	0.37	0.33	0.62	0.84	0.66	0.6	0.78
Cr_2O_3	0.22	0.02	0.02	0.02	0.01	0.01	0.01	<0.01	0.01
TiO_2	1.27	1.2	2.34	1.97	1.6	0.35	0.91	5.8	3.97
MnO	0.26	0.12	0.21	0.14	0.15	0.16	0.14	0.37	0.32
P_2O_5	0.04	0.11	2.1	0.11	0.99	0.52	0.27	2.82	2.47
SrO	0.02	0.1	0.06	0.09	0.12	0.28	0.21	0.06	0.1
BaO	0.01	0.05	0.04	0.04	0.07	0.15	0.09	0.18	0.23
LOI	3.18	1.1	0.48	0.28	1.21	1.26	1.27	-0.32	-0.41
Total	100.21	100.1	98.17	98.24	98.28	99.01	100.47	98.03	100.39
C	0.09	0.23	0.32	0.16	0.32	0.15	0.27	0.1	0.09
S	0.07	0.16	0.98	0.03	0.28	0.27	0.14	0.45	0.32
Ba	49.4	402	342	339	565	1355	777	1790	2080
Ce	12.6	24.1	110.5	23	81	75.4	48.8	224	178.5
Cr	1600	140	150	130	90	80	70	20	80
Cs	0.36	1.76	1.21	0.99	1.07	0.85	0.74	0.68	0.55
Dy	2.02	1.55	5.47	1.76	3.81	2.75	2.53	8.53	7.01
Er	0.98	0.79	2.57	0.8	1.9	1.34	1.39	3.87	3.24
Eu	0.84	1.24	2.79	1.25	2.47	2.38	1.98	5.84	5.06
Ga	8.8	17.3	15.7	18.6	18.6	20.6	21	16.1	14.3
Gd	2.78	1.91	8.83	2.2	5.85	4.02	3.4	14.35	11.15
Hf	0.9	0.8	1.5	0.8	1.3	1.3	1.2	1.9	1.8
Ho	0.37	0.3	1.03	0.33	0.74	0.53	0.51	1.62	1.33
La	4.7	11.3	47.3	10.5	36.3	38.2	24.2	95.8	77.1
Lu	0.11	0.11	0.29	0.11	0.23	0.17	0.19	0.4	0.34
Nb	2.4	6.5	14.2	8.2	15.7	16.5	13.1	36.4	28

Nd	10.2	12.5	60.6	13	41.5	33.4	23.7	114	89.2
Pr	2.03	2.96	14.4	3.01	10.2	8.69	5.92	27.5	22
Rb	1.7	25.9	16	4.6	18.9	15.9	9.7	13.6	15.3
Sm	2.7	2.5	11.1	2.64	7.51	5.46	4.39	19.05	15.3
Sn	2	2	2	3	2	5	3	4	2
Sr	187.5	869	567	786	1055	2500	1755	568	804
Ta	0.1	0.3	0.6	0.4	0.6	0.6	0.5	1.6	1.2
Tb	0.4	0.28	1.09	0.3	0.76	0.54	0.5	1.74	1.44
Th	0.19	0.39	1.41	0.24	1.17	1.7	0.95	2.95	2.59
Tl	0.05	0.1	0.13	<0.02	0.06	0.05	0.03	0.04	0.04
Tm	0.13	0.12	0.34	0.12	0.26	0.2	0.19	0.48	0.4
U	0.07	0.12	0.4	0.08	0.35	0.51	0.28	0.85	0.78
V	375	592	930	953	459	18	164	544	384
W	<1	1	1	<1	1	1	<1	1	1
Y	10	7.5	28.4	8.4	20.4	14.4	13	41.5	34
Yb	0.88	0.7	2.06	0.69	1.47	1.22	1.17	2.77	2.34
Zr	17	21	47	22	47	56	42	77	70
As	<0.1	2.1	1.3	0.9	0.4	0.2	0.7	0.4	0.3
Bi	0.02	0.09	0.55	0.17	0.05	0.07	0.07	0.06	0.05
Sb	<0.05	<0.05	<0.05	<0.05	<0.05	<0.05	<0.05	<0.05	<0.05
Se	0.2	0.9	6.1	0.4	1.8	0.6	0.7	2.4	2
Te	0.02	0.11	0.48	0.08	0.03	<0.01	0.02	0.01	0.01
Ag	<0.5	<0.5	3.2	<0.5	<0.5	<0.5	<0.5	<0.5	<0.5
Cd	0.6	<0.5	1.1	<0.5	<0.5	<0.5	<0.5	0.9	0.8
Co	118	42	65	45	45	18	26	105	80
Cu	135	655	5460	349	957	323	404	185	183
Li	<10	10	10	10	10	10	<10	10	10
Mo	<1	<1	<1	<1	<1	<1	<1	<1	1
Ni	1050	153	248	128	112	52	48	38	46
Pb	2	<2	4	<2	4	5	2	4	5
Sc	32	21	44	27	24	7	15	51	46
Zn	149	82	143	95	100	78	90	213	159

Sample	SL-13-36-19.5	SL-13-36-23.5	SL-13-36-30.5	SL-13-36-39.5	SL-13-36-71.5	SL-13-36-76.5	SL-13-36-86.5	SL-13-36-103.5	SL-13-36-157.5
Unit	2b	2b	2b	2b	3h	3h	2i	2i	3h
SiO_2	34.7	37.6	32.9	36.4	47	44.3	40	39.5	38.5
Al_2O_3	8.17	9.58	10.15	14.4	20.1	5.7	6.05	5.92	11.8
Fe_2O_3	28.7	26	23.2	18.15	10.25	16.55	21.2	21.2	24.1
FeO	19.25	16.95	13.65	10.6	7.01	11.35	13.45	13.75	14.05
CaO	11.1	11.6	14.45	12.45	9.9	15.65	10.9	11.3	11.05
MgO	8.89	8.36	8.04	6.92	6.61	15	17.25	16.6	4.95
Na_2O	1.47	1.72	1.36	1.91	2.65	0.65	0.71	0.87	2.62
K_2O	0.72	0.75	0.41	0.68	1.42	0.21	0.08	0.02	0.68
Cr_2O_3	0.02	0.02	<0.01	0.03	0.01	0.1	0.18	0.18	0.01
TiO_2	4.47	4.06	3.32	1.51	0.26	0.76	2.38	3.65	2.47
MnO	0.35	0.32	0.27	0.18	0.15	0.26	0.23	0.24	0.25
P_2O_5	2.51	2.17	5.36	4.5	0.07	0.06	0.05	0.3	2.45
SrO	0.08	0.09	0.1	0.12	0.11	0.02	0.03	0.05	0.1
BaO	0.19	0.22	0.12	0.12	0.12	0.02	0.01	<0.01	0.06
LOI	-1.09	-0.55	0.35	2.48	3.2	2.13	1.78	1.1	1.26
Total	100.28	101.94	100.03	99.85	101.85	101.41	100.85	100.93	100.3
C	0.09	0.12	0.08	0.2	0.4	0.53	0.1	0.05	0.24
S	0.38	0.25	0.16	0.75	0.23	0.38	0.1	0.11	1.91
Ba	1765	2040	1070	1055	1060	133.5	78.8	28.4	530
Ce	182.5	163	209	161.5	18.6	22.5	19.5	25.2	187
Cr	110	150	10	190	100	780	1330	1340	60
Cs	0.49	0.58	0.76	0.98	1.25	0.56	0.4	0.26	0.95
Dy	7.03	6.56	8.06	5.84	0.98	2.9	3.12	4.93	7.52
Er	3.19	2.94	3.44	2.42	0.51	1.43	1.37	1.98	3.74
Eu	5.06	4.69	5.75	4.09	1.05	1.13	1.35	2.22	4
Ga	14.3	14.7	14.7	13.3	14.7	8.2	12.1	15.1	19.7
Gd	11.75	10.45	13.7	10.35	1.23	3.42	4.01	6.28	11.55
Hf	1.8	1.9	0.9	0.7	0.8	1.2	1.5	2	2.5
Ho	1.33	1.2	1.4	1.08	0.19	0.54	0.59	0.85	1.43
La	78.7	69.1	89.1	70.1	9.7	8	6.6	6.8	82
Lu	0.34	0.31	0.32	0.25	0.07	0.21	0.14	0.18	0.44
Nb	28.7	25.7	13.6	10.1	4.5	3.1	4.4	6.4	42.2
Nd	91.4	80.3	112	84.1	8.7	16.5	16.1	24.7	90.1

Pr	22.3	19.6	26.4	20.1	2.22	3.53	3.16	4.53	22.4
Rb	14.5	14.1	6.8	11.1	33.4	6	1.4	0.6	16.5
Sm	15.85	13.85	19.2	14.1	1.52	3.84	4.15	6.83	15.5
Sn	2	5	2	2	2	2	1	2	4
Sr	661	799	845	982	919	167	246	414	837
Ta	1.2	1.1	0.6	0.4	0.1	0.1	0.2	0.4	1.7
Tb	1.46	1.34	1.66	1.26	0.18	0.53	0.59	0.92	1.49
Th	2.46	2.38	1.76	1.59	0.55	0.3	0.18	<0.05	3.25
Tl	0.04	0.03	0.05	0.1	0.08	0.04	<0.02	<0.02	0.13
Tm	0.39	0.37	0.42	0.3	0.07	0.2	0.18	0.24	0.48
U	0.76	0.72	0.47	0.46	0.14	0.08	0.05	<0.05	0.84
V	448	413	504	257	80	404	512	528	514
W	<1	<1	<1	<1	<1	1	<1	<1	2
Y	34.4	31.2	39.6	28.8	4.8	14.4	14.1	20.3	38.5
Yb	2.44	2.24	2.27	1.63	0.52	1.33	1.1	1.25	2.88
Zr	66	65	32	26	23	35	32	40	95
As	0.3	0.4	0.4	0.5	0.5	0.3	<0.1	<0.1	0.5
Bi	0.07	0.06	0.07	0.29	0.11	0.19	0.04	0.02	0.31
Sb	<0.05	<0.05	<0.05	<0.05	0.05	<0.05	<0.05	<0.05	<0.05
Se	1.9	1.6	2.3	4.4	0.7	2.8	0.3	0.4	6.3
Te	0.01	0.01	0.03	0.11	0.06	0.29	0.01	0.02	0.14
Ag	<0.5	<0.5	<0.5	0.9	<0.5	1.3	<0.5	<0.5	1.1
Cd	0.8	0.8	0.5	0.5	<0.5	0.5	0.8	0.7	1
Co	97	84	80	84	49	90	108	102	92
Cu	232	201	254	2860	557	3010	238	237	2410
Li	10	10	10	10	10	10	10	<10	10
Mo	<1	1	1	<1	<1	<1	<1	<1	<1
Ni	50	40	152	158	115	416	747	682	414
Pb	3	4	9	8	<2	6	6	<2	13
Sc	46	49	32	13	11	60	38	36	25
Zn	182	170	165	134	66	99	146	143	172

Sample	SL-13-32-17	SL-13-32-32	SL-13-32-37	MW-07-06-3.9	MW-07-06-11.9	MW-07-06-19.9	MW-07-06-23.9	MW-07-06-38	MW-07-06-80.6
Unit	3b	3b	3b	2b	2b	2b	2b	2f	3b
SiO_2	38.9	38.7	40.8	45.7	40.3	42	42.6	36.4	44.4
Al_2O_3	14.6	14.5	14.95	13.95	9.98	12.25	12.55	8.99	15.9
Fe_2O_3	19.65	17.35	16.85	17.95	24	19.8	19.85	28.4	14.75
FeO	12.2	10.8	9.7	13.25	17.9	13.8	14.5	20.4	10.15
CaO	13.05	12.5	12.85	8.95	9.53	9.51	9.89	9.63	10.25
MgO	5.68	5.59	5.17	4.62	6.42	5.32	5	7.2	4.23
Na_2O	2.37	2.3	2.68	3.04	2.24	2.88	2.92	1.92	3.77
K_2O	0.77	1.02	0.68	2.02	1.5	1.46	1.26	1.36	1.31
Cr_2O_3	<0.01	<0.01	<0.01	<0.01	<0.01	<0.01	<0.01	<0.01	<0.01
TiO_2	2.24	2.25	2.42	2.66	4.04	3.27	2.98	3.95	2.04
MnO	0.22	0.24	0.19	0.28	0.35	0.28	0.29	0.42	0.19
P_2O_5	3.27	3.21	3.4	1.47	1.83	2.02	1.68	3.43	2.02
SrO	0.12	0.11	0.11	0.2	0.13	0.14	0.14	0.1	0.15
BaO	0.13	0.1	0.09	1.33	0.79	0.45	0.37	0.27	0.19
LOI	0.57	1.7	0.28	-0.28	-0.82	0.04	-0.47	-1.04	2.43
Total	101.57	99.57	100.47	101.89	100.29	99.42	99.06	101.03	101.63
C	0.1	0.27	0.12	0.04	0.04	0.04	0.03	0.04	0.4
S	1.53	0.84	0.14	0.2	0.2	0.18	0.19	0.12	0.2
Ba	1130	942	785	>10000	7000	4140	3510	2440	1705
Ce	138	132.5	157	161.5	185	201	178	259	146.5
Cr	20	<10	10	<10	<10	<10	<10	<10	<10
Cs	2.09	4.65	0.76	0.79	0.76	0.97	1	1.27	5.8
Dy	5.31	5.38	5.97	6.21	7.23	7.83	6.84	9.3	5.49
Er	2.52	2.29	2.6	3.14	3.59	3.61	3.33	4.43	2.63
Eu	3.83	3.59	3.87	4.94	5.1	5.54	4.7	5.03	3.8
Ga	15.5	16	16.5	15.3	15	16.8	16.8	15.5	16.8
Gd	8.94	9.18	9.74	9.35	10.4	11.35	10.4	14.4	8.68
Hf	1.3	1.1	1.9	2.4	2.9	2.8	2.9	3.3	2
Ho	1.03	0.97	1.1	1.18	1.35	1.41	1.3	1.74	1.03
La	61.2	59	69.1	73.3	82.6	91.1	79.5	116.5	65.6
Lu	0.26	0.25	0.3	0.42	0.45	0.43	0.43	0.55	0.32
Nb	20	17.6	24.6	48.9	57.2	52.8	51	68.3	32.9
Nd	72.8	70.5	78.4	74.5	86	93.1	85.2	121.5	69.1

Pr	17.4	16.75	18.85	19.1	21.9	23.3	21	30.6	17.3
Rb	19.4	40.2	15.4	32.3	29.9	32.3	30.3	39.4	71.5
Sm	12.3	12.25	13.1	12.85	15.4	15.7	14.35	20.3	11.6
Sn	5	6	6	33	12	10	9	8	5
Sr	996	894	935	1665	1080	1170	1240	837	1240
Ta	0.8	0.7	1	2	2.4	2.2	2.1	2.9	1.4
Tb	1.07	1.06	1.2	1.15	1.45	1.49	1.34	1.82	1.1
Th	2.1	1.92	3.4	3.95	4.19	4.72	4.69	6.14	3.33
Tl	0.11	0.22	0.04	0.05	0.06	0.07	0.07	0.1	0.4
Tm	0.3	0.29	0.34	0.41	0.48	0.48	0.45	0.6	0.35
U	0.67	0.58	0.96	1.11	1.25	1.4	1.33	1.86	1.05
V	383	434	468	121	176	194	201	278	83
W	1	1	1	1	1	1	1	12	7
Y	27.3	26.7	29.3	31.5	36.8	37.6	34.1	47.3	27.6
Yb	1.74	1.82	2.01	2.83	2.94	3.04	2.68	3.71	2.1
Zr	50	40	74	102	121	116	122	155	85
As	3.8	1.4	0.3	0.4	0.5	0.6	0.4	0.8	14.9
Bi	0.25	0.17	0.07	0.27	0.06	0.14	0.11	0.11	0.03
Sb	<0.05	<0.05	<0.05	<0.05	<0.05	<0.05	<0.05	<0.05	0.06
Se	6.6	5.1	1.6	1.5	1.6	1.7	1.5	2.3	1.6
Te	0.13	0.16	0.02	0.01	<0.01	<0.01	0.01	0.01	0.01
Ag	0.6	0.5	<0.5	<0.5	<0.5	<0.5	<0.5	<0.5	<0.5
Cd	0.8	0.7	<0.5	0.5	<0.5	<0.5	0.6	0.6	<0.5
Co	93	80	53	46	63	53	52	75	48
Cu	3340	3980	414	258	119	124	126	118	69
Li	20	40	20	10	10	10	10	10	10
Mo	<1	<1	<1	1	1	1	1	1	4
Ni	275	194	46	18	3	4	5	9	2
Pb	4	5	3	8	4	5	7	6	6
Sc	25	23	24	33	43	35	34	27	21
Zn	225	310	119	142	175	147	159	208	98

Sample	MW-07-06-91.5	MW-07-06-95.5	MW-07-06-109.5	MW-07-06-113.5	MW-07-06-117.5	MW-07-06-121	MW-07-06-135.5	MW-07-06-143.5	MW-07-06-147.5
Unit	3b	3b	3b	3b	3b	3b	3b	3b	3b
SiO_2	38.8	32	26.9	24.5	22.8	37.6	33.6	33	36.6
Al_2O_3	11.7	8.06	6.32	6.52	5.71	11.85	8.88	4.31	10.35
Fe_2O_3	22.9	30.5	32.7	32.4	32.3	28.9	31.8	20.8	28
FeO	15.4	20.6	20.6	23.2	20.8	19.2	20.8	15.2	19.35
CaO	10.9	10.45	13.5	13.4	16.3	6.45	9.28	14.1	9.16
MgO	5.36	6.42	5.81	8.83	7.53	8.45	10.05	20.4	10.1
Na_2O	2.68	1.65	1.36	1.16	1	2.23	1.39	0.06	1.69
K_2O	1	0.68	0.51	0.29	0.33	0.86	0.27	<0.01	0.27
Cr_2O_3	<0.01	<0.01	0.01	0.02	0.01	0.1	0.07	0.14	0.08
TiO_2	3.96	5.53	5.11	3.65	4.04	3.2	3.81	5.45	2.95
MnO	0.31	0.39	0.36	0.38	0.35	0.32	0.33	0.29	0.32
P_2O_5	2.88	3.4	6.81	9.09	9.63	0.48	1.63	0.89	1.4
SrO	0.11	0.07	0.05	0.07	0.06	0.07	0.05	0.02	0.07
BaO	0.15	0.09	0.06	0.04	0.03	0.06	0.03	<0.01	0.03
LOI	-0.33	-0.54	-0.84	-2.09	-1.59	-1.27	-1.47	0.39	-1.31
Total	100.42	98.7	98.66	98.26	98.5	99.3	99.72	99.85	99.71
C	0.1	0.03	0.05	0.02	0.04	0.02	0.06	0.05	0.03
S	0.26	0.5	0.43	0.1	0.18	0.13	0.07	1.56	0.22
Ba	1430	835	505	314	272	515	239	3.6	284
Ce	198	212	380	378	439	48.8	81	298	71.9
Cr	<10	10	40	110	90	750	490	1020	570
Cs	2.69	1.34	0.72	0.17	0.37	0.57	0.33	0.02	0.08
Dy	7.42	8.09	14.4	13.75	16.8	2.25	3.85	7.75	3.43
Er	3.53	3.88	6.67	6	7.25	1.23	1.88	2.33	1.7
Eu	4.68	4.61	6.98	7.03	8.32	1.52	1.96	6.46	1.98
Ga	16.9	16.6	20.1	16.2	17.5	18.9	17.9	22.6	16.3
Gd	11.9	13.2	22.8	22.8	28.4	2.95	5.74	15.35	5.07
Hf	2.3	2	1.9	1.3	1.6	1.6	1.3	10.4	1
Ho	1.41	1.48	2.68	2.56	3.07	0.45	0.72	1.14	0.63
La	87.5	91	172.5	172.5	197.5	23.6	35.9	127.5	31.8
Lu	0.42	0.44	0.69	0.61	0.75	0.21	0.22	0.16	0.21
Nb	41.8	39.8	67.5	37	34.1	42.1	23	288	17.9

Nd	97.1	106.5	186	190	225	22.6	42.4	138.5	37.9
Pr	23.9	25.9	46.1	46.3	54.5	5.8	10.3	34.9	9.14
Rb	37	19.3	13.9	5.4	9	22.5	4.8	0.2	3.3
Sm	16.65	18.25	31.3	31.7	37.7	3.93	8.07	24.1	6.78
Sn	7	8	6	6	9	9	12	13	7
Sr	911	626	440	528	498	534	425	148.5	530
Ta	1.8	1.7	3.4	1.7	1.6	1.8	1	14.9	0.8
Tb	1.49	1.66	2.87	2.85	3.43	0.42	0.72	1.8	0.67
Th	3.86	3.08	5.47	3.26	4.09	2.08	0.97	21.8	0.83
Tl	0.16	0.11	0.11	0.02	0.03	0.03	0.02	<0.02	<0.02
Tm	0.45	0.49	0.81	0.77	0.86	0.17	0.23	0.24	0.2
U	1.14	0.94	2	0.94	1.12	0.86	0.3	7.15	0.25
V	116	282	1110	1030	1220	1000	1400	344	899
W	2	5	1	<1	1	1	<1	2	<1
Y	38.3	41.2	73.7	71.5	84.3	12.1	19.3	25.9	17.2
Yb	2.84	2.91	4.93	4.41	5.14	1.23	1.51	1.2	1.29
Zr	93	84	66	46	66	58	42	467	35
As	0.4	1	0.4	0.3	0.5	0.4	0.2	22.3	0.2
Bi	0.11	0.19	0.25	0.07	0.1	0.17	0.06	0.08	0.15
Sb	<0.05	<0.05	<0.05	<0.05	<0.05	0.05	<0.05	0.14	<0.05
Se	2.2	2.6	4.4	3.7	5.1	1.2	1.2	2.7	1.8
Te	0.01	0.01	0.1	0.04	0.07	0.1	0.05	0.22	0.17
Ag	<0.5	<0.5	0.6	<0.5	<0.5	<0.5	<0.5	<0.5	1.2
Cd	0.6	0.8	0.8	0.7	<0.5	<0.5	0.8	<0.5	<0.5
Co	58	87	86	115	109	101	122	72	107
Cu	300	742	2310	653	1145	1225	696	222	2100
Li	10	10	10	10	10	30	20	<10	10
Mo	2	1	2	1	2	1	1	1	<1
Ni	3	7	82	136	164	228	249	414	275
Pb	8	15	9	5	10	<2	4	2	<2
Sc	29	34	25	9	16	14	19	26	19
Zn	170	223	245	226	224	198	209	395	186

Sample	MW-07-08-31	MW-07-08-39.5	MW-07-08-48.5	MW-07-08-52.5	MW-07-08-69.5	MW-07-08-92.5	MW-07-08-103.5	MW-07-08-111.5	MW-07-08-120	MW-07-08-128.5	MW-07-08-147
Unit	MLI	MLI	MLI	MLI	MLI	MLI	MLI	MLI	MLI	MLI	MLI
SiO_2	49.4	51.4	50.4	50.4	49.1	51.3	54.4	52.3	51.6	51.4	52.8
Al_2O_3	14.25	15.25	14.35	17.5	15.2	13.6	14.05	14.3	14.15	13.6	14.65
Fe_2O_3	15.25	13.65	14.9	11.9	14.8	14.65	13.55	13.55	14.25	15.3	13.35
FeO	10.35	9.12	9.71	8.09	10.65	10.9	9.7	10.05	10.85	11	9.81
CaO	6.8	6.3	6.67	6.59	8.19	7.11	6	6.88	7.14	7.38	6.8
MgO	3.18	2.68	2.39	1.98	3.54	3.42	2.67	3.32	3.63	3.84	3.35
Na_2O	4.48	5	4.47	5.27	4.39	4.22	4.71	4.5	4.32	4.11	4.47
K_2O	2.01	2.15	2.48	1.78	1.47	2.3	2.96	2.35	2.2	2.28	2.37
Cr_2O_3	<0.01	<0.01	<0.01	<0.01	<0.01	<0.01	<0.01	<0.01	<0.01	<0.01	<0.01
TiO_2	1.81	1.66	1.88	1.3	1.7	1.43	1.32	1.41	1.45	1.7	1.33
MnO	0.28	0.27	0.28	0.18	0.27	0.32	0.29	0.28	0.3	0.31	0.27
P_2O_5	1.06	0.89	0.84	1.03	1.26	0.96	0.71	0.94	1	1.07	0.97
SrO	0.14	0.15	0.12	0.17	0.15	0.1	0.08	0.11	0.11	0.11	0.11
BaO	0.25	0.27	0.34	0.23	0.18	0.23	0.21	0.19	0.2	0.17	0.2
LOI	0.46	0.29	0.37	0.57	0.04	-0.22	-0.16	-0.24	-0.28	-0.25	-0.34
Total	99.37	99.96	99.49	98.9	100.29	99.42	100.79	99.89	100.07	101.02	100.33
C	0.06	0.04	0.06	0.04	0.04	0.04	0.03	0.03	0.03	0.04	0.04
S	0.48	0.39	0.21	0.94	0.33	0.09	0.12	0.05	0.06	0.09	0.06
Ba	2350	2570	3090	2160	1725	2090	1920	1710	1875	1565	1895
Ce	213	191.5	191.5	183	209	237	236	221	214	240	226
Cr	<10	<10	<10	<10	10	10	10	10	10	10	10
Cs	1.39	1.41	1.54	3.07	1.93	1.71	1.64	1.2	1.19	0.9	1.23
Dy	6.04	5.44	6.49	4.45	6.06	7.01	7.92	6.59	6.06	7.18	6.45
Er	2.69	2.42	2.96	1.91	2.85	3.38	4.14	3.23	2.96	3.38	3
Eu	5.49	5.83	6.15	4.92	4.93	4.53	4.52	4.24	4.41	4.11	4.63
Ga	18	18.3	18	18.8	18.6	17.7	19.7	18.5	18	18.6	19.1
Gd	9.78	9.15	10.15	7.41	10.05	11.65	12.25	11	10.65	12.1	11.25
Hf	1.8	1.8	2.7	2	2.6	2.8	5.4	3.6	2.8	5.6	3.9
Ho	1.07	0.93	1.23	0.81	1.14	1.25	1.46	1.2	1.09	1.33	1.17
La	99.2	88.3	87.6	87.4	95.6	110.5	108.5	102.5	98.9	110.5	106
Lu	0.35	0.31	0.43	0.24	0.39	0.47	0.61	0.45	0.43	0.49	0.44

Nb	55.1	50	70.1	47.1	59.3	77.5	106.5	76.8	72.4	87.1	76.7
Nd	94.3	86.3	91.8	77.3	93.3	102.5	102.5	95.4	92.8	106.5	96.4
Pr	24.5	22.2	22.9	20.4	24.3	27.4	27.4	25.4	24.6	28.3	25.6
Rb	23.4	23.1	29	23.9	22.6	28.8	56.6	27.7	29	33.2	38
Sm	15.55	14.4	14.9	11.9	15.65	16.5	17	15.3	15.05	17.25	15.45
Sn	2	3	4	4	6	5	4	2	3	3	6
Sr	1175	1230	970	1445	1270	838	664	882	919	863	949
Ta	2.1	2	2.9	1.8	2.4	3.2	4.1	3.2	2.9	3.4	3.1
Tb	1.27	1.15	1.33	0.89	1.26	1.49	1.59	1.39	1.33	1.51	1.41
Th	1.84	1.72	2.37	3.76	4.21	5.4	9.12	4.17	2.52	3.68	4.01
Tl	0.11	0.06	0.04	0.08	0.05	0.07	0.07	0.04	0.03	0.03	0.03
Tm	0.34	0.32	0.44	0.25	0.39	0.49	0.61	0.46	0.43	0.48	0.45
U	0.42	0.45	0.68	0.97	1.27	1.32	2.23	1.35	0.69	1.07	1.07
V	104	81	86	133	228	195	153	196	211	226	202
W	1	1	3	1	1	1	1	1	1	1	1
Y	28.1	24.8	30.7	21.1	30.4	33	38.7	31.4	29.4	33.6	30
Yb	2.28	2.06	2.67	1.63	2.61	2.98	3.88	2.95	2.67	2.99	2.67
Zr	67	69	109	91	104	128	245	175	126	341	196
As	0.8	0.2	0.2	1.4	0.5	0.4	1.2	0.3	0.2	0.1	0.3
Bi	0.09	0.09	0.07	0.84	0.07	0.02	0.09	0.01	0.01	0.03	0.01
Sb	0.05	<0.05	<0.05	0.1	<0.05	<0.05	<0.05	<0.05	<0.05	<0.05	<0.05
Se	1.7	1.3	1.5	2.4	1.4	1.3	1.4	1.1	0.8	1.1	1.2
Te	0.04	0.04	0.01	0.16	0.03	0.01	0.02	0.01	<0.01	0.01	0.01
Ag	0.8	0.7	<0.5	2.4	<0.5	<0.5	<0.5	<0.5	<0.5	<0.5	<0.5
Cd	<0.5	0.5	<0.5	0.5	<0.5	<0.5	<0.5	<0.5	<0.5	<0.5	<0.5
Co	38	30	23	37	36	32	26	30	35	34	31
Cu	1375	1155	443	4630	835	155	278	68	60	152	74
Li	20	20	20	20	20	20	20	20	20	20	20
Mo	1	2	2	1	1	2	7	2	2	3	2
Ni	49	40	20	152	33	16	18	11	12	19	13
Pb	5	8	7	17	7	6	11	7	8	7	6
Sc	20	18	19	11	20	19	16	18	19	20	17
Zn	163	159	174	115	156	185	195	165	170	175	163

Appendix 6. Mineral chemical results determined by bSEM-EDS. SD is the 1 sigma standard deviation of sample error determined by multiple analyses on 3-5 grains for each mineral type in each sample.

Drill hole	Depth/m	Rock name	Mg# of Ol		Mg# of Cpx		An# of Pl	
			AVG	SD	AVG	SD	AVG	SD
FD-13-34	5.00	Oxide augite melatroctolite	63.40	0.30	79.70	1.30	43.40	4.50
	18.60	Oxide augite melatroctolite	61.50	2.60	77.30	1.20	47.30	2.50
	24.00	Olivine gabbro	53.10	1.40	75.40	1.40	46.30	2.20
	27.90	Oxide augite melatroctolite	62.60	0.70	78.90	1.40	50.10	1.60
	33.00	Oxide augite melatroctolite	63.60	1.40			49.60	2.30
	46.10	Oxide augite melatroctolite	60.70	1.50	81.10	0.90	47.80	1.60
	64.60	Oxide augite melatroctolite	57.60	1.30	78.90	0.80	46.40	1.60
	79.60	Olivine gabbro	56.80	1.10	77.00	1.60	42.30	2.60
	127.50	Olivine gabbro	45.50	1.40	72.60	1.50	40.60	2.00
	158.60	Olivine gabbro	41.70	1.00	71.70	3.30	37.80	2.60
	194.80	Olivine gabbro	43.20	1.90	67.30	1.90	33.10	3.40
	212.50	Oxide augite melatroctolite	48.50	1.80	71.50	0.90	38.10	1.70
	226.30	Oxide augite melatroctolite	49.70	1.60	73.60	0.90	36.00	2.10
	248.50	Oxide melatroctolite	54.20	2.30	76.00	1.40	44.00	2.30
	253.10	Oxide melatroctolite	47.40	1.00	75.50	1.00	49.80	2.10
	257.80	Oxide melatroctolite	55.70	1.50	75.90	1.40	40.80	1.40
	272.10	Apatitic clinopyroxenite	58.80	0.80	76.00	1.00	41.00	2.10
	276.50	Apatitic clinopyroxenite	54.30	1.10	79.40	1.10	56.70	1.10
	281.10	Apatitic clinopyroxenite	49.90	0.80			48.20	2.40
	291.50	Apatitic clinopyroxenite	64.50	0.90	78.40	1.70	48.10	1.60
	295.70	Apatitic clinopyroxenite	47.70	1.00	77.50	1.60	48.20	1.30
	316.70	Apatitic olivine clinopyroxenite	61.90	0.80	80.40	0.60	36.80	0.40
	321.60	Apatitic olivine clinopyroxenite	60.00	0.40	81.00	0.70	43.40	4.50
SL-13-27	4.80	Olivine gabbro	49.19	0.47	71.12	0.73	52.51	2.75
	9.00	Olivine gabbro	64.60	0.80	78.24	4.59	57.26	3.01
	17.70	Medium-grained ophitic gabbro			71.01	0.88	60.87	2.06
	36.00	Coarse-grained ophitic gabbro	64.72	0.54	78.84	0.75	50.58	2.51
	42.50	Oxide melatroctolite	56.55	1.00	73.94	0.51	53.70	2.88
	46.10	Oxide melatroctolite	59.65	0.88	77.77	1.25	50.69	2.28
	51.00	Oxide melatroctolite	63.89	0.83	78.77	0.63	50.55	2.56
	54.40	Oxide melatroctolite	65.61	1.13			48.36	2.94
	66.00	Pegmatitic ophitic gabbro	55.75	0.51			54.27	2.13
	80.40	Coarse-grained ophitic gabbro	51.69	0.64	75.79	0.94	53.35	1.39
	85.50	Coarse-grained ophitic gabbro			73.81	1.91	49.58	2.13
	90.05	Coarse-grained ophitic gabbro	54.39	0.98	73.48	0.65	53.63	2.17
	95.20	Coarse-grained ophitic gabbro	60.54	0.75	76.06	0.71	50.91	1.66
	105.30	Oxide melatroctolite	61.83	1.03	74.99	1.24	52.02	3.37

	174.70	Oxide melatroctolite			77.17	1.46		
	183.60	Oxide melatroctolite			76.06	1.57	43.62	1.60
	231.10	Apatitic clinopyroxenite	59.25	2.43	78.14	2.47	30.71	1.74
	235.50	Apatitic clinopyroxenite			73.03	0.94	52.59	1.07
	5.95	Olivine gabbro	61.54	0.85	74.79	0.99	57.11	2.09
	10.70	Olivine gabbro	61.54	2.69	76.58	0.78	54.83	2.99
	17.50	Ophitic gabbro	57.50	1.58	69.37	0.82	55.94	2.16
	22.90	Ophitic gabbro	63.96	1.44	69.83	1.12	54.44	2.28
	27.10	Ophitic gabbro	60.91	2.58	72.65	2.55	52.61	1.24
	32.20	Ophitic gabbro			72.27	1.22	47.93	1.96
	37.00	Ophitic gabbro	54.90	2.34	70.83	1.25	54.03	2.05
	42.30	Ophitic gabbro	59.00	0.86	72.27	1.33	51.78	1.88
	44.00	Oxide melatroctolite	65.31	1.18			48.24	1.85
	49.30	Oxide melatroctolite	59.00	0.71	73.28	1.31	53.00	1.10
	58.50	Ophitic gabbro	66.49	0.64	78.38	1.46	46.97	1.37
	61.20	Oxide melatroctolite	64.50	2.15			44.91	2.08
	75.80	Ophitic gabbro			73.04	1.75	57.20	2.30
SL-13-32	80.50	Ophitic gabbro	62.81	1.98	75.22	1.88	54.24	1.96
	90.55	Ophitic gabbro			72.81	2.54	48.08	1.30
	150.50	Apatitic clinopyroxenite			62.50	1.00	40.73	0.57
	156.10	Apatitic clinopyroxenite			67.23	0.89	49.42	1.51
	161.00	Apatitic clinopyroxenite	58.67	1.22	73.64	0.96	48.56	1.34
	165.50	Ophitic gabbro	53.66	0.34	61.90	0.83	60.10	2.20
	170.55	Apatitic clinopyroxenite	61.34	0.40	71.93	1.29	54.69	1.28
	200.60	Apatitic clinopyroxenite	42.86	70.00	64.17	0.71	51.55	0.90
	204.50	Apatitic clinopyroxenite			66.96	1.10		
	209.20	Apatitic clinopyroxenite			63.25	0.79		
	214.50	Apatitic clinopyroxenite			70.27	0.97		
	219.50	Apatitic clinopyroxenite			73.40	1.41	42.83	2.07
	224.60	Apatitic clinopyroxenite			72.73	1.74	44.59	2.49
	229.60	Apatitic clinopyroxenite			74.31	1.08	40.38	1.46
	234.40	Apatitic clinopyroxenite			75.45	0.88		
	3.00	Oxide augite melatroctolite	48.94	1.24	77.43	0.77	53.04	3.57
	5.10	Oxide augite melatroctolite	40.10	1.60	72.13	1.22	51.88	1.16
	7.00	Olivine gabbro	41.51	1.10	69.86	2.46	51.29	0.63
	13.30	Olivine gabbro	41.82	2.80	73.31	1.14	53.88	6.50
	17.40	Olivine gabbro	43.90	1.20	72.22	2.00	52.05	1.20
SL-13-34	19.40	Oxide augite melatroctolite	45.92	0.68	69.57	0.83	54.79	2.27
	23.40	Oxide augite melatroctolite	48.16	1.52	72.51	0.98	51.10	1.85
	25.70	Oxide augite melatroctolite	52.95	1.23	75.30	2.47	52.20	1.15
	28.10	Oxide augite melatroctolite	49.78	1.47	74.25	0.76	49.86	0.98
	30.00	Oxide augite melatroctolite	53.97	1.52	73.84	1.00	52.11	1.15
	32.00	olivine gabbro	51.38	1.57	76.28	0.70	48.74	2.24

	45.00	Oxide augite melatroctolite	55.15	1.24	76.39	1.19	52.22	1.22
	49.00	Oxide augite melatroctolite	56.20	0.75	75.68	0.62	53.18	2.10
	53.00	Oxide augite melatroctolite	60.29	1.15	76.98	0.84	51.86	1.24
	59.00	Oxide augite melatroctolite	53.91	1.25	73.54	1.24	54.95	2.36
	63.00	Ophitic gabbro	57.82	0.83	76.11	1.48	58.14	1.77
	65.00	Ophitic gabbro	60.49	0.44	76.77	1.11	56.80	3.89
	75.00	Apatitic clinopyroxenite	66.09	1.94				
	77.20	Ophitic gabbro	67.96	1.45			46.15	1.12
	81.00	Ophitic gabbro	67.74	1.18	78.11	0.61	66.43	2.66
	95.50	Feldspathic clinopyroxenite	74.31	1.40	82.33	0.96	66.33	2.97
	111.60	Feldspathic clinopyroxenite	73.92	0.51	81.11	0.81	66.47	3.77
	119.50	Feldspathic clinopyroxenite	75.27	1.27	82.52	1.52	56.59	1.86
	126.00	Ophitic gabbro	62.07	0.47	75.87	1.44	50.83	1.21
	130.20	Ophitic gabbro	59.84	0.77	77.26	0.48	52.24	1.76
	140.50	Ophitic gabbro	62.99	0.87	78.06	1.65	55.03	2.47
	146.90	Ophitic gabbro			75.08	0.96	53.64	0.97
	150.90	Ophitic gabbro			72.44	0.72	57.56	2.49
	10.00	Olivine gabbro	56.03	1.12	74.75	1.19	41.77	2.12
	11.10	Olivine gabbro	58.46	0.43	76.35	1.42	45.69	1.51
	16.60	Olivine gabbro	55.79	0.42	75.72	0.67	51.88	2.49
	20.70	Olivine gabbro	55.99	1.57	76.23	1.02	45.30	3.65
	22.70	Olivine gabbro	59.09	0.62	76.06	0.67		
	24.85	Oxide augite melatroctolite			78.14	0.88		
	35.20	Ophitic gabbro	64.56	0.28			54.88	1.58
	39.30	Ophitic gabbro	65.56	1.20	78.08	0.83	55.01	1.13
	53.50	Ophitic gabbro	68.65	0.55	78.48	0.51	63.67	2.61
	57.30	Ophitic gabbro			77.50	0.80		
	62.00	Ophitic gabbro			78.06	0.35		
	63.00	Ophitic gabbro			78.27	0.87	56.35	2.56
SL-13-36	67.80	Ophitic gabbro	63.76	0.71	78.50	0.50		
	72.00	Apatitic clinopyroxenite	65.65	0.38	77.13	0.83	54.12	2.41
	74.00	Apatitic clinopyroxenite			75.73	1.38		
	76.00	Apatitic clinopyroxenite	67.84	1.13	77.71	6.02		
	79.90	Feldspathic clinopyroxenite	70.51	0.27	79.76	0.55	59.34	1.81
	96.00	Feldspathic clinopyroxenite	73.50	0.68	81.24	1.12	51.65	2.84
	113.90	Feldspathic clinopyroxenite	76.57	0.72	83.10	0.64		
	125.80	Ophitic gabbro			72.09	1.79	47.18	1.69
	130.00	Ophitic gabbro			71.81	3.81		
	134.50	Ophitic gabbro			75.60	1.54		
	143.00	Ophitic gabbro			75.70	1.37		
	143.70	Ophitic gabbro			75.66	0.95		
	148.70	Ophitic gabbro			74.80	0.89	37.68	1.68
	152.80	Ophitic gabbro			82.35	1.78	31.83	1.36

	156.80	Ophitic gabbro			72.89	1.58	41.97	1.81
	158.80	Apatitic clinopyroxenite			76.87	0.80		
	161.80	Apatitic clinopyroxenite			75.90	1.34	42.88	0.61
	177.00	Apatitic clinopyroxenite			79.02	0.87	40.10	0.41
	7.00	Oxide augite melatroctolite	54.43	1.21	75.42	0.74	49.59	2.16
	11.00	Oxide augite melatroctolite	53.14	0.73	73.93	0.49	55.26	2.28
	13.00	Oxide augite melatroctolite	55.00	0.78	75.97	0.59	52.45	1.31
	15.00	Oxide augite melatroctolite	55.68	1.03	74.74	0.66	53.56	0.96
	19.00	Oxide augite melatroctolite	59.11	0.68	76.03	0.64	50.55	2.20
	21.00	Oxide augite melatroctolite	56.90	0.55	73.90	0.87	50.91	0.82
	25.00	Oxide augite melatroctolite	59.92	0.75	74.69	0.66	52.56	1.58
	27.00	Oxide augite melatroctolite	53.60	0.44	72.09	0.47	54.55	2.23
	33.00	Oxide augite melatroctolite	59.47	0.38	75.19	0.81	50.94	1.52
	37.00	Oxide augite melatroctolite	59.69	0.70	75.33	0.95	52.35	1.77
	48.00	Ophitic gabbro	63.51	1.08			60.35	3.64
	52.00	Ophitic gabbro	63.66	2.78	76.94	1.11	58.57	1.74
	54.00	Ophitic gabbro	54.41	1.56	75.64	0.72	52.78	2.38
	55.50	Ophitic gabbro	57.04	3.72	74.91	2.18	38.54	1.28
	56.00	Ophitic gabbro	58.79	3.19	76.85	0.45	58.76	1.37
	62.00	Ophitic gabbro			68.21	3.54		
SL-13-37	64.00	Ophitic gabbro	57.38	0.82	72.67	3.08	60.33	1.62
	65.70	Ophitic gabbro			74.95	0.30	51.70	1.46
	70.00	Ophitic gabbro	65.36	0.49	76.19	0.35	67.92	4.15
	76.00	Ophitic gabbro	62.78	1.97	73.83	1.42	64.66	2.83
	80.00	Ophitic gabbro	58.85	1.88	72.67	1.48	43.28	1.66
	86.00	Ophitic gabbro			73.70	0.28	54.13	1.65
	88.00	Ophitic gabbro	63.62	1.52	75.31	2.84	68.68	2.58
	93.00	Ophitic gabbro	63.71	1.59	76.45	1.13	65.57	1.00
	95.00	Ophitic gabbro	64.76	2.39	77.02	0.47	71.62	2.00
	97.20	Ophitic gabbro			75.26	1.21	68.03	3.54
	104.50	Feldspathic clinopyroxenite	66.95	1.18	75.15	1.31	69.69	1.66
	115.40	Feldspathic clinopyroxenite	68.84	0.50	78.08	0.79	63.80	1.93
	140.00	Feldspathic clinopyroxenite	75.01	0.73	81.61	0.57	56.28	2.04
	146.00	Feldspathic clinopyroxenite	69.25	0.38	77.57	0.95	56.25	1.69
	157.30	Ophitic gabbro			74.81	0.98	54.45	1.76
	167.30	Ophitic gabbro			65.52	0.87	47.40	1.55
	170.70	Ophitic gabbro			72.00	1.08	52.68	1.65
	172.20	Ophitic gabbro			69.56	1.84		
	3.00	Oxide augite melatroctolite	32.62	1.01	63.16	0.75	29.34	1.85
	12.10	Oxide augite melatroctolite	44.72	0.73	77.94	3.21	45.27	2.37
SL-13-41	29.00	Oxide augite melatroctolite			67.87	2.63	30.85	1.21
	45.00	Oxide augite melatroctolite	53.53	1.34	79.43	1.17	44.38	1.65
	63.20	Oxide augite melatroctolite	62.32	1.48	82.98	0.75	48.08	2.43

	68.70	Oxide augite melatroctolite	65.89	1.23	77.72	1.46	40.95	1.24
	73.00	Oxide augite melatroctolite	67.65	1.53	80.64	3.30	43.93	2.12
	91.00	Oxide augite melatroctolite	62.14	1.34	76.41	0.99	47.06	3.40
	109.10	Oxide augite melatroctolite	72.61	0.74	82.46	0.60	44.18	2.15
	125.80	Oxide melatroctolite	54.94	0.55	81.17	1.61	57.27	2.66
	129.50	Oxide melatroctolite	59.74	0.53	74.81	1.04	59.82	2.75
	132.20	Oxide melatroctolite	72.35	1.18	82.22	0.87	53.30	1.27
	138.60	Oxide melatroctolite	63.81	1.94			50.38	2.56
	143.45	Ophitic gabbro	67.26	4.21	79.81	3.60	48.35	1.71
	153.90	Ophitic gabbro	65.08	2.22	79.58	2.98	53.26	1.79
	167.40	Ophitic gabbro	64.22	3.77	80.62	1.49	51.92	2.75
	170.00	Oxide melatroctolite	59.69	1.21	75.00	2.33	53.24	1.81
	173.60	Oxide melatroctolite	60.26	1.11			52.13	2.20
	221.40	Apatitic clinopyroxenite			75.42	2.98	64.64	3.50
	225.60	Apatitic clinopyroxenite	71.86	4.21	82.91	1.57	53.20	2.39
	230.70	Apatitic clinopyroxenite	76.62	0.88	83.91	2.91	51.45	2.81
	266.00	Apatitic clinopyroxenite	67.06	0.67	79.07	1.08		
	270.50	Apatitic clinopyroxenite			82.27	0.54	49.40	1.67
	278.00	Apatitic clinopyroxenite	67.83	0.58	78.47	0.86	52.51	1.05
	3.40	Olivine gabbro	38.80	1.20	66.01	2.61	37.95	1.78
	9.40	Olivine gabbro	43.10	1.14	72.76	1.07	39.50	2.20
	13.40	Olivine gabbro	45.20	2.30	68.92	1.92	40.87	1.70
	17.40	Olivine gabbro	41.90	3.20	71.88	1.40	42.18	2.75
	23.40	Olivine gabbro	36.00	1.10	69.17	0.99	39.75	1.12
	36.15	Olivine gabbro	44.60	1.84	72.58	1.25	46.85	2.55
	37.50	Oxide augite melatroctolite	42.30	2.63	70.67	0.39	38.54	1.34
	41.00	Oxide augite melatroctolite	48.80	1.33	72.27	0.66	46.72	1.66
	54.30	ophitic gabbro	49.70	1.53	73.72	0.48	43.24	1.04
	60.80	Oxide augite melatroctolite	51.10	0.92	75.07	1.52	49.88	2.16
	65.00	Ophitic gabbro	42.93	1.22	68.77	0.89		
MW-07-06	68.00	Ophitic gabbro	46.79	0.61	68.26	1.77		
	71.65	Ophitic gabbro	46.06	3.83	71.90	1.52		
	81.50	Ophitic gabbro	54.10	0.61	73.61	0.53	42.69	2.14
	83.50	Oxide augite melatroctolite	41.15	2.00	66.78	0.91		
	86.30	Oxide augite melatroctolite	53.50	0.90	73.85	0.85	41.58	0.96
	87.50	Oxide augite melatroctolite	46.20	1.00	70.77	0.77	43.43	1.83
	93.50	Ophitic gabbro	48.80	1.30	71.52	1.45	40.80	1.23
	98.00	Ophitic gabbro	48.10	0.98	71.02	1.24	41.39	0.72
	101.00	Ophitic gabbro	41.46	1.10	64.76	2.08		
	109.55	Ophitic gabbro	53.76	1.20	73.49	0.77	48.37	1.35
	117.60	Ophitic gabbro	63.16	1.00			47.89	1.32
	120.10	Ophitic gabbro	54.14	1.80	72.30	0.83	36.92	1.42
	122.00	Ophitic gabbro	58.70	2.20	76.03	0.82	50.96	1.70

	126.00	Ophitic gabbro	64.34	1.58	77.64	0.85	51.63	1.38
	135.00	Ophitic gabbro	63.08	1.00	76.49	0.69	51.98	1.63
	143.00	Ophitic gabbro	64.64	0.67	78.16	0.53	51.77	1.22
	143.60	Ophitic gabbro	62.53	0.86	77.87	0.58	47.41	1.70
	145.50	Ophitic gabbro	56.60	2.53	72.81	1.92	51.43	1.25
	149.00	Ophitic gabbro	52.20	1.11	69.97	2.00	55.95	2.12
	153.00	Ophitic gabbro	60.02	1.03	74.12	0.46	51.59	1.82
	155.00	Ophitic gabbro	56.50	0.49	70.44	1.72	54.04	1.34
	11.50	Meta-basalt	28.26	1.58	56.68	2.29		
	17.50	Meta-basalt	35.23	2.07	61.35	2.91		
	23.00	Meta-basalt	36.41	0.79	62.35	3.89		
	25.00	Meta-basalt	39.01	0.53	66.70	0.92	28.17	2.21
	31.00	Malpas Lake Intrusion	29.16	1.51	60.16	1.65		
	40.70	Malpas Lake Intrusion	29.96	1.11	58.30	0.69	31.91	2.23
	48.60	Malpas Lake Intrusion	24.43	1.41	57.67	1.22		
MW-07-08	56.30	Malpas Lake Intrusion	28.85	1.86	62.98	4.17		
	71.50	Malpas Lake Intrusion	36.98	1.32	67.22	0.69	29.39	1.69
	85.10	Malpas Lake Intrusion	16.59	1.94	61.13	0.83	38.89	2.12
	93.70	Malpas Lake Intrusion	12.86	2.52	63.89	3.05	38.27	0.98
	101.00	Malpas Lake Intrusion	29.93	0.73	60.90	0.90	57.44	1.44
	111.30	Malpas Lake Intrusion	28.15	1.72	58.55	0.43	54.01	1.14
	119.14	Malpas Lake Intrusion	32.85	3.18	63.08	1.77		
	127.20	Malpas Lake Intrusion	34.56	2.35	63.43	0.56		
	145.00	Malpas Lake Intrusion	33.66	1.91	60.64	2.47	30.20	2.32

Appendix 7. Mineral chemical data of olivine determined by electron microprobe. Sample names can be referred to appendix 3.

Sample No.	FD-13-34-5	FD-13-34-5	FD-13-34-5	FD-13-34-5	FD-13-34-5	FD-13-34-18.6	FD-13-34-18.6	FD-13-34-24	FD-13-34-24	FD-13-34-24	FD-13-34-24	FD-13-34-24
Spot No.	1	2	3	4	5	1	2	1	2	3	4	5
SiO_2	35.089	35.114	35.192	35.066	35.046	34.998	34.936	34.418	33.949	34.194	34.117	34.009
Al_2O_3	-0.002	0.002	0.009	0.008	0.002	-0.001	-0.003	0.020	-0.012	0.005	-0.005	0.008
Na_2O												
MgO	23.383	23.535	23.573	23.227	23.538	23.189	23.311	21.488	20.052	20.654	19.981	19.580
FeO	40.780	40.841	40.960	40.872	40.964	41.618	41.964	43.171	45.350	44.549	45.217	45.797
MnO	0.810	0.794	0.844	0.819	0.862	0.917	0.869	0.967	0.995	0.974	1.103	1.100
Cr_2O_3	0.006	0.033	0.026	0.023	-0.004	0.003	0.012	-0.003	0.011	-0.010	0.003	0.027
CoO	0.080	0.066	0.070	0.080	0.084	0.067	0.101	0.094	0.106	0.092	0.062	0.110
CaO	0.123	0.130	0.157	0.115	0.128	0.171	0.167	0.142	0.098	0.121	0.155	0.151
NiO	0.010	-0.017	0.009	-0.003	0.019	0.024	0.024	0.021	0.042	0.019	0.025	0.031
TiO_2	0.031	0.044	0.027	0.018	0.047	0.034	0.041	0.034	0.017	0.046	0.034	0.037
Sc_2O_3												
Total	100.310	100.542	100.867	100.225	100.686	101.020	101.422	100.352	100.608	100.644	100.692	100.850
Si	1.001	1.000	0.999	1.002	0.997	0.996	0.992	0.996	0.992	0.994	0.995	0.994
Al	0.000	0.000	0.000	0.000	0.000	0.000	0.000	0.001	0.000	0.000	0.000	0.000
Na	0.000	0.000	0.000	0.000	0.000	0.000	0.000	0.000	0.000	0.000	0.000	0.000
Mg	1.001	1.005	1.004	0.996	1.005	0.990	0.993	0.933	0.879	0.901	0.874	0.858
Fe	0.970	0.969	0.969	0.973	0.971	0.987	0.993	1.041	1.105	1.079	1.099	1.115
Mn	0.020	0.019	0.020	0.020	0.021	0.022	0.021	0.024	0.025	0.024	0.027	0.027
Cr	0.000	0.001	0.001	0.001	0.000	0.000	0.000	0.000	0.000	0.000	0.000	0.001
Co	0.002	0.002	0.002	0.002	0.002	0.002	0.002	0.002	0.002	0.002	0.001	0.003
Ca	0.004	0.004	0.005	0.004	0.004	0.005	0.005	0.004	0.003	0.004	0.005	0.005
Ni	0.000	0.000	0.000	0.000	0.000	0.001	0.001	0.000	0.001	0.000	0.001	0.001
Ti	0.001	0.001	0.001	0.000	0.001	0.001	0.001	0.001	0.000	0.001	0.001	0.001
Sc	0.000	0.000	0.000	0.000	0.000	0.000	0.000	0.000	0.000	0.000	0.000	0.000
O	4.000	4.000	4.000	4.000	4.000	4.000	4.000	4.000	4.000	4.000	4.000	4.000
Fo	**50.790**	**50.915**	**50.882**	**50.566**	**50.843**	**50.073**	**49.997**	**47.256**	**44.317**	**45.490**	**44.302**	**43.489**
Fa	**49.210**	**49.085**	**49.118**	**49.434**	**49.157**	**49.927**	**50.003**	**52.744**	**55.683**	**54.510**	**55.698**	**56.511**

Sample No.	FD-13-34-24	FD-13-34-27.9	FD-13-34-27.9	FD-13-34-27.9	FD-13-34-27.9	FD-13-34-27.9	FD-13-34-27.9	FD-13-34-27.9	FD-13-34-27.9	FD-13-34-27.9	FD-13-34-27.9
Spot No.	6	1	2	3	4	5	6	7	8	9	10
SiO_2	34.147	35.362	35.462	35.325	35.605	35.380	35.382	35.279	35.610	35.522	35.378
Al_2O_3	-0.016	0.002	-0.004	0.003	0.019	-0.003	0.004	-0.014	-0.002	-0.006	0.006
Na_2O											

MgO	19.807	25.483	25.411	24.889	25.177	25.196	25.372	25.258	25.502	25.673	25.391
FeO	45.592	38.802	38.940	39.685	39.166	39.288	38.701	38.737	38.618	38.642	38.335
MnO	1.042	0.758	0.753	0.816	0.796	0.795	0.792	0.832	0.752	0.748	0.845
Cr_2O_3	-0.031	0.015	-0.013	-0.003	0.008	-0.006	-0.021	0.001	-0.025	0.011	0.001
CoO	0.078	0.099	0.109	0.095	0.072	0.072	0.088	0.073	0.056	0.080	0.086
CaO	0.147	0.147	0.142	0.126	0.170	0.171	0.136	0.187	0.141	0.163	0.159
NiO	0.027	0.041	0.020	-0.002	0.031	0.010	0.020	0.014	0.021	0.021	0.034
TiO_2	0.037	0.017	0.024	0.022	0.029	0.041	0.022	0.035	0.026	0.032	0.028
Sc_2O_3											
Total	100.830	100.726	100.844	100.956	101.073	100.944	100.496	100.402	100.699	100.886	100.263
Si	0.996	0.994	0.996	0.995	0.998	0.995	0.997	0.996	1.000	0.996	0.998
Al	-0.001	0.000	0.000	0.000	0.001	0.000	0.000	0.000	0.000	0.000	0.000
Na	0.000	0.000	0.000	0.000	0.000	0.000	0.000	0.000	0.000	0.000	0.000
Mg	0.867	1.075	1.071	1.052	1.059	1.063	1.072	1.069	1.074	1.080	1.074
Fe	1.108	0.909	0.912	0.932	0.915	0.921	0.909	0.911	0.903	0.903	0.901
Mn	0.026	0.018	0.018	0.019	0.019	0.019	0.019	0.020	0.018	0.018	0.020
Cr	-0.001	0.000	0.000	0.000	0.000	0.000	0.000	0.000	-0.001	0.000	0.000
Co	0.002	0.002	0.002	0.002	0.002	0.002	0.002	0.002	0.001	0.002	0.002
Ca	0.005	0.004	0.004	0.004	0.005	0.005	0.004	0.006	0.004	0.005	0.005
Ni	0.001	0.001	0.000	0.000	0.001	0.000	0.000	0.000	0.000	0.000	0.001
Ti	0.001	0.000	0.001	0.000	0.001	0.001	0.000	0.001	0.001	0.001	0.001
Sc	0.000	0.000	0.000	0.000	0.000	0.000	0.000	0.000	0.000	0.000	0.000
O	4.000	4.000	4.000	4.000	4.000	4.000	4.000	4.000	4.000	4.000	4.000
Fo	**43.883**	**54.173**	**54.015**	**53.027**	**53.641**	**53.583**	**54.130**	**53.995**	**54.310**	**54.460**	**54.384**
Fa	**56.117**	**45.827**	**45.985**	**46.973**	**46.359**	**46.417**	**45.870**	**46.005**	**45.690**	**45.540**	**45.616**

Sample No.	FD-13-34-27.9	FD-13-34-33	FD-13-34-33	FD-13-34-33	FD-13-34-33	FD-13-34-33	FD-13-34-33	FD-13-34-46.1	FD-13-34-46.1	FD-13-34-46.1	FD-13-34-46.1
Spot No.	11	1	2	3	4	5	6	1	2	3	4
SiO_2	35.318	35.744	35.621	35.724	35.853	35.734	35.472	35.158	34.746	35.022	35.238
Al_2O_3	-0.003	-0.002	0.005	0.011	0.006	0.010	0.007	-0.004	0.001	-0.019	-0.002
Na_2O											
MgO	25.223	26.525	26.383	26.773	26.733	26.749	26.273	24.236	24.160	23.988	24.255
FeO	39.091	37.641	37.756	36.899	37.263	37.165	37.763	39.802	40.086	39.914	39.799
MnO	0.771	0.731	0.778	0.650	0.762	0.642	0.639	0.841	0.855	0.746	0.744
Cr_2O_3	0.015	-0.037	-0.030	-0.004	0.021	-0.011	-0.028	-0.008	-0.018	-0.028	0.010
CoO	0.100	0.077	0.088	0.062	0.058	0.067	0.072	0.058	0.078	0.093	0.072
CaO	0.102	0.166	0.155	0.134	0.200	0.111	0.160	0.181	0.200	0.168	0.150
NiO	0.009	0.001	0.005	-0.002	-0.001	0.003	0.013	0.009	0.016	0.034	0.012
TiO_2	0.017	0.034	0.036	0.030	0.019	0.034	0.024	0.033	0.032	0.022	0.031

Sc_2O_3											
Total	100.643	100.880	100.797	100.277	100.914	100.504	100.395	100.306	100.156	99.940	100.309
Si	0.995	0.996	0.995	0.998	0.997	0.997	0.995	0.999	0.991	0.999	1.000
Al	0.000	0.000	0.000	0.000	0.000	0.000	0.000	0.000	0.000	-0.001	0.000
Na	0.000	0.000	0.000	0.000	0.000	0.000	0.000	0.000	0.000	0.000	0.000
Mg	1.066	1.109	1.105	1.122	1.115	1.120	1.105	1.033	1.034	1.027	1.033
Fe	0.918	0.874	0.879	0.859	0.864	0.864	0.883	0.942	0.953	0.949	0.941
Mn	0.018	0.017	0.018	0.015	0.018	0.015	0.015	0.020	0.021	0.018	0.018
Cr	0.000	-0.001	-0.001	0.000	0.000	0.000	-0.001	0.000	0.000	-0.001	0.000
Co	0.002	0.002	0.002	0.001	0.001	0.001	0.002	0.001	0.002	0.002	0.002
Ca	0.003	0.005	0.005	0.004	0.006	0.003	0.005	0.006	0.006	0.005	0.005
Ni	0.000	0.000	0.000	0.000	0.000	0.000	0.000	0.000	0.000	0.001	0.000
Ti	0.000	0.001	0.001	0.001	0.000	0.001	0.001	0.001	0.001	0.000	0.001
Sc	0.000	0.000	0.000	0.000	0.000	0.000	0.000	0.000	0.000	0.000	0.000
O	4.000	4.000	4.000	4.000	4.000	4.000	4.000	4.000	4.000	4.000	4.000
Fo	**53.734**	**55.917**	**55.709**	**56.636**	**56.358**	**56.437**	**55.601**	**52.291**	**52.035**	**51.964**	**52.313**
Fa	**46.266**	**44.083**	**44.291**	**43.364**	**43.642**	**43.563**	**44.399**	**47.709**	**47.965**	**48.036**	**47.687**

Sample No.	FD-13-34-46.1	FD-13-34-46.1	FD-13-34-46.1	FD-13-34-46.1	FD-13-34-46.1	FD-13-34-46.1	FD-13-34-64.6	FD-13-34-64.6	FD-13-34-64.6	FD-13-34-64.6	FD-13-34-64.6
Spot No.	5	6	7	8	9	10	1	2	3	4	5
SiO_2	34.990	34.923	34.709	35.361	35.383	35.067	34.202	34.012	34.317	34.000	34.352
Al_2O_3	0.015	0.010	0.010	0.011	0.010	0.017	-0.004	0.008	-0.005	-0.012	0.010
Na_2O											
MgO	24.260	23.464	23.346	24.822	24.725	23.545	20.882	20.752	20.987	20.832	20.960
FeO	39.804	40.643	40.641	38.979	39.253	40.628	43.761	44.468	44.117	43.908	43.804
MnO	0.830	0.835	0.847	0.841	0.813	0.778	0.953	1.003	0.975	0.967	0.987
Cr_2O_3	-0.027	-0.004	-0.038	0.003	0.015	-0.018	-0.015	0.010	-0.021	0.006	0.028
CoO	0.056	0.067	0.084	0.064	0.066	0.088	0.053	0.120	0.079	0.098	0.091
CaO	0.150	0.138	0.139	0.158	0.154	0.136	0.134	0.121	0.139	0.121	0.112
NiO	0.003	0.001	0.009	-0.001	0.006	0.027	0.032	0.004	0.010	0.008	-0.002
TiO_2	0.040	0.026	0.029	0.034	0.043	0.031	0.014	0.025	0.029	0.029	0.028
Sc_2O_3											
Total	100.121	100.103	99.776	100.272	100.468	100.299	100.012	100.523	100.627	99.957	100.370
Si	0.996	0.999	0.997	1.000	1.000	1.000	0.997	0.991	0.995	0.993	0.997
Al	0.001	0.000	0.000	0.000	0.000	0.001	0.000	0.000	0.000	0.000	0.000
Na	0.000	0.000	0.000	0.000	0.000	0.000	0.000	0.000	0.000	0.000	0.000
Mg	1.036	1.007	1.006	1.053	1.048	1.007	0.913	0.907	0.913	0.913	0.913
Fe	0.944	0.969	0.973	0.919	0.924	0.966	1.063	1.079	1.066	1.069	1.060
Mn	0.020	0.020	0.021	0.020	0.019	0.019	0.023	0.025	0.024	0.024	0.024

Cr	-0.001	0.000	-0.001	0.000	0.000	0.000	0.000	0.000	0.000	0.000	0.001
Co	0.001	0.002	0.002	0.001	0.001	0.002	0.001	0.003	0.002	0.002	0.002
Ca	0.005	0.004	0.004	0.005	0.005	0.004	0.004	0.004	0.004	0.004	0.003
Ni	0.000	0.000	0.000	0.000	0.000	0.001	0.001	0.000	0.000	0.000	0.000
Ti	0.001	0.001	0.001	0.001	0.001	0.001	0.000	0.001	0.001	0.001	0.001
Sc	0.000	0.000	0.000	0.000	0.000	0.000	0.000	0.000	0.000	0.000	0.000
O	4.000	4.000	4.000	4.000	4.000	4.000	4.000	4.000	4.000	4.000	4.000
Fo	**52.315**	**50.961**	**50.836**	**53.407**	**53.135**	**51.056**	**46.206**	**45.652**	**46.129**	**46.063**	**46.274**
Fa	**47.685**	**49.039**	**49.164**	**46.593**	**46.865**	**48.944**	**53.794**	**54.348**	**53.871**	**53.937**	**53.726**

Sample No.	FD-13-34-64.6	FD-13-34-79.6	FD-13-34-79.6	FD-13-34-79.6	FD-13-34-79.6	FD-13-34-79.6	FD-13-34-79.6	FD-13-34-127.25	FD-13-34-127.25	FD-13-34-127.25	FD-13-34-127.25
Spot No.	6	1	2	3	4	5	6	1	2	3	4
SiO_2	34.288	34.161	34.087	33.884	34.014	33.946	33.988	32.935	33.116	32.590	33.355
Al_2O_3	0.006	0.001	0.021	-0.003	0.011	-0.010	-0.007	-0.002	0.023	0.007	-0.015
Na_2O											
MgO	20.709	19.853	19.495	19.582	19.915	19.077	18.997	15.690	15.631	15.281	16.115
FeO	44.324	45.366	45.802	45.515	44.991	46.158	46.288	49.280	50.183	49.871	50.023
MnO	1.007	0.918	0.967	0.942	0.946	1.012	1.007	1.134	1.181	1.163	1.160
Cr_2O_3	0.006	0.034	0.010	-0.007	-0.014	0.005	-0.018	-0.008	-0.030	-0.016	0.011
CoO	0.098	0.081	0.105	0.083	0.077	0.088	0.090	0.077	0.085	0.062	0.111
CaO	0.118	0.135	0.132	0.155	0.137	0.103	0.100	0.233	0.223	0.200	0.230
NiO	0.027	-0.024	0.005	-0.016	-0.006	0.008	0.028	0.012	0.012	0.015	-0.002
TiO_2	0.027	0.016	0.043	0.028	0.021	0.031	0.026	0.031	0.050	0.030	0.041
Sc_2O_3											
Total	100.610	100.541	100.667	100.163	100.092	100.418	100.499	99.382	100.474	99.203	101.029
Si	0.996	0.998	0.997	0.996	0.997	0.998	0.999	1.000	0.997	0.995	0.996
Al	0.000	0.000	0.001	0.000	0.000	0.000	0.000	0.000	0.001	0.000	-0.001
Na	0.000	0.000	0.000	0.000	0.000	0.000	0.000	0.000	0.000	0.000	0.000
Mg	0.902	0.870	0.855	0.863	0.876	0.841	0.837	0.714	0.706	0.700	0.722
Fe	1.073	1.104	1.116	1.115	1.099	1.131	1.134	1.246	1.259	1.269	1.245
Mn	0.025	0.023	0.024	0.023	0.023	0.025	0.025	0.029	0.030	0.030	0.029
Cr	0.000	0.001	0.000	0.000	0.000	0.000	0.000	0.000	-0.001	0.000	0.000
Co	0.002	0.002	0.002	0.002	0.002	0.002	0.002	0.002	0.002	0.002	0.003
Ca	0.004	0.004	0.004	0.005	0.004	0.003	0.003	0.008	0.007	0.007	0.007
Ni	0.001	-0.001	0.000	0.000	0.000	0.000	0.001	0.000	0.000	0.000	0.000
Ti	0.001	0.000	0.001	0.001	0.000	0.001	0.001	0.001	0.001	0.001	0.001
Sc	0.000	0.000	0.000	0.000	0.000	0.000	0.000	0.000	0.000	0.000	0.000
O	4.000	4.000	4.000	4.000	4.000	4.000	4.000	4.000	4.000	4.000	4.000

Fo	**45.682**	**44.063**	**43.380**	**43.643**	**44.344**	**42.658**	**42.487**	**36.431**	**35.925**	**35.548**	**36.704**
Fa	**54.318**	**55.937**	**56.620**	**56.357**	**55.656**	**57.342**	**57.513**	**63.569**	**64.075**	**64.452**	**63.296**

Sample No.	FD-13-34-127.25	FD-13-34-158.6	FD-13-34-158.6	FD-13-34-158.6	FD-13-34-158.6	FD-13-34-194.8	FD-13-34-194.8	FD-13-34-194.8	FD-13-34-194.8	FD-13-34-194.8	FD-13-34-194.8
Spot No.	5	1	2	3	4	1	2	3	4	5	6
SiO_2	33.066	32.183	32.102	32.089	32.173	32.184	32.310	32.345	32.200	32.224	31.592
Al_2O_3	0.010	0.002	-0.003	0.000	-0.024	0.007	-0.018	0.000	0.028	-0.011	0.009
Na_2O											
MgO	16.062	12.891	12.763	13.010	12.642	13.011	12.935	12.856	12.532	12.601	11.106
FeO	49.471	53.437	53.849	53.439	53.404	53.500	53.347	53.214	53.921	53.537	55.262
MnO	1.124	1.328	1.240	1.350	1.220	1.204	1.274	1.272	1.350	1.306	1.297
Cr_2O_3	0.037	0.004	0.003	-0.009	-0.004	0.015	0.017	-0.032	-0.027	-0.032	-0.033
CoO	0.092	0.110	0.080	0.090	0.087	0.108	0.102	0.095	0.092	0.091	0.095
CaO	0.225	0.203	0.177	0.232	0.225	0.210	0.217	0.215	0.156	0.161	0.144
NiO	-0.006	0.020	-0.009	0.005	-0.007	0.010	0.001	-0.008	-0.022	-0.007	-0.012
TiO_2	0.042	0.059	0.048	0.022	0.056	0.045	0.015	0.033	0.034	0.023	0.033
Sc_2O_3											
Total	100.123	100.237	100.250	100.228	99.772	100.294	100.200	99.990	100.264	99.893	99.493
Si	0.996	0.992	0.991	0.990	0.996	0.991	0.995	0.997	0.994	0.997	0.993
Al	0.000	0.000	0.000	0.000	-0.001	0.000	-0.001	0.000	0.001	0.000	0.000
Na	0.000	0.000	0.000	0.000	0.000	0.000	0.000	0.000	0.000	0.000	0.000
Mg	0.725	0.596	0.591	0.602	0.587	0.601	0.598	0.595	0.580	0.585	0.524
Fe	1.241	1.373	1.385	1.373	1.378	1.373	1.369	1.368	1.387	1.380	1.448
Mn	0.029	0.035	0.032	0.035	0.032	0.031	0.033	0.033	0.035	0.034	0.034
Cr	0.001	0.000	0.000	0.000	0.000	0.000	0.000	-0.001	-0.001	-0.001	-0.001
Co	0.002	0.003	0.002	0.002	0.002	0.003	0.003	0.002	0.002	0.002	0.002
Ca	0.007	0.007	0.006	0.008	0.007	0.007	0.007	0.007	0.005	0.005	0.005
Ni	0.000	0.000	0.000	0.000	0.000	0.000	0.000	0.000	-0.001	0.000	0.000
Ti	0.001	0.001	0.001	0.001	0.001	0.001	0.000	0.001	0.001	0.001	0.001
Sc	0.000	0.000	0.000	0.000	0.000	0.000	0.000	0.000	0.000	0.000	0.000
O	4.000	4.000	4.000	4.000	4.000	4.000	4.000	4.000	4.000	4.000	4.000
Fo	**36.885**	**30.276**	**29.905**	**30.470**	**29.879**	**30.447**	**30.384**	**30.307**	**29.495**	**29.759**	**26.565**
Fa	**63.115**	**69.724**	**70.095**	**69.530**	**70.121**	**69.553**	**69.616**	**69.693**	**70.505**	**70.241**	**73.435**

Sample No.	FD-13-34-194.8	FD-13-34-194.8	FD-13-34-194.8	FD-13-34-212.5	FD-13-34-212.5	FD-13-34-212.5	FD-13-34-212.5	FD-13-34-212.5	FD-13-34-212.5	FD-13-34-212.5	FD-13-34-212.5
Spot No.	7	8	9	1	2	3	4	5	6	7	8

SiO_2	31.754	31.545	31.626	32.847	32.720	32.739	32.833	32.881	32.946	32.718	32.349
Al_2O_3	0.005	0.006	-0.009	0.005	-0.006	-0.003	0.015	-0.012	-0.009	-0.014	0.012
Na_2O											
MgO	10.794	10.706	9.917	14.771	14.737	14.964	15.165	14.986	15.163	14.679	15.035
FeO	55.829	55.984	56.673	51.714	51.211	51.111	50.972	51.243	50.900	51.339	48.768
MnO	1.395	1.382	1.349	1.124	1.136	1.107	1.166	1.129	1.207	1.167	1.159
Cr_2O_3	0.021	-0.013	-0.009	0.008	0.020	-0.009	-0.062	0.009	-0.026	0.003	-0.009
CoO	0.108	0.105	0.108	0.093	0.102	0.087	0.076	0.091	0.119	0.083	0.096
CaO	0.170	0.167	0.138	0.171	0.200	0.185	0.200	0.172	0.207	0.233	0.168
NiO	-0.019	-0.011	-0.023	-0.016	0.010	0.008	0.015	-0.005	-0.012	-0.013	-0.002
TiO_2	0.050	0.051	0.041	0.038	0.037	0.044	0.047	0.038	0.034	0.116	0.042
Sc_2O_3											
Total	100.107	99.922	99.811	100.755	100.167	100.233	100.427	100.532	100.529	100.311	97.618
Si	0.994	0.991	0.998	0.994	0.995	0.994	0.994	0.995	0.995	0.994	1.002
Al	0.000	0.000	0.000	0.000	0.000	0.000	0.001	0.000	0.000	-0.001	0.000
Na	0.000	0.000	0.000	0.000	0.000	0.000	0.000	0.000	0.000	0.000	0.000
Mg	0.507	0.505	0.469	0.670	0.672	0.681	0.688	0.680	0.687	0.669	0.698
Fe	1.457	1.466	1.490	1.304	1.298	1.293	1.285	1.292	1.282	1.300	1.258
Mn	0.037	0.037	0.036	0.029	0.029	0.028	0.030	0.029	0.031	0.030	0.030
Cr	0.001	0.000	0.000	0.000	0.000	0.000	-0.001	0.000	-0.001	0.000	0.000
Co	0.003	0.003	0.003	0.002	0.002	0.002	0.002	0.002	0.003	0.002	0.002
Ca	0.006	0.006	0.005	0.006	0.007	0.006	0.006	0.006	0.007	0.008	0.006
Ni	0.000	0.000	-0.001	0.000	0.000	0.000	0.000	0.000	0.000	0.000	0.000
Ti	0.001	0.001	0.001	0.001	0.001	0.001	0.001	0.001	0.001	0.003	0.001
Sc	0.000	0.000	0.000	0.000	0.000	0.000	0.000	0.000	0.000	0.000	0.000
O	4.000	4.000	4.000	4.000	4.000	4.000	4.000	4.000	4.000	4.000	4.000
Fo	**25.817**	**25.607**	**23.953**	**33.956**	**34.123**	**34.512**	**34.876**	**34.487**	**34.905**	**33.979**	**35.689**
Fa	**74.183**	**74.393**	**76.047**	**66.044**	**65.877**	**65.488**	**65.124**	**65.513**	**65.095**	**66.021**	**64.311**

Sample No.	FD-13-34-212.5	FD-13-34-212.5	FD-13-34-212.5	FD-13-34-212.5	FD-13-34-212.5	FD-13-34-212.5	FD-13-34-226.3	FD-13-34-226.3	FD-13-34-226.3	FD-13-34-226.3	FD-13-34-226.3
Spot No.	9	10	11	12	13	14	1	2	3	4	5
SiO_2	32.319	32.370	29.834	32.786	31.927	31.891	32.676	32.667	32.584	32.779	32.775
Al_2O_3	0.013	0.005	0.028	-0.009	-0.006	-0.007	-0.007	-0.009	0.000	-0.001	0.001
Na_2O											
MgO	15.040	15.018	13.532	15.202	14.573	14.444	14.736	14.828	14.287	15.261	15.187
FeO	48.598	49.011	42.837	50.882	48.406	48.195	50.996	50.743	51.332	50.015	49.767
MnO	1.127	1.038	0.995	1.200	1.157	1.135	1.158	1.127	1.096	1.189	1.223
Cr_2O_3	-0.005	-0.008	-0.018	-0.019	0.011	0.001	-0.018	-0.005	-0.022	-0.016	-0.038

CoO	0.085	0.109	0.081	0.100	0.100	0.090	0.094	0.111	0.100	0.100	0.121
CaO	0.147	0.116	0.125	0.203	0.207	0.189	0.204	0.202	0.152	0.180	0.183
NiO	0.020	-0.006	-0.021	-0.009	0.010	0.006	0.010	-0.005	-0.020	-0.005	-0.017
TiO_2	0.040	0.039	0.031	0.028	0.040	0.022	0.044	0.029	0.033	0.035	0.051
Sc_2O_3											
Total	97.384	97.692	87.424	100.364	96.425	95.966	99.893	99.688	99.542	99.537	99.253
Si	1.002	1.002	1.022	0.993	1.002	1.005	0.996	0.996	0.998	0.998	1.000
Al	0.000	0.000	0.001	0.000	0.000	0.000	0.000	0.000	0.000	0.000	0.000
Na	0.000	0.000	0.000	0.000	0.000	0.000	0.000	0.000	0.000	0.000	0.000
Mg	0.700	0.697	0.695	0.691	0.686	0.683	0.674	0.678	0.657	0.697	0.695
Fe	1.256	1.264	1.223	1.284	1.266	1.266	1.295	1.290	1.311	1.268	1.265
Mn	0.030	0.027	0.029	0.031	0.031	0.030	0.030	0.029	0.028	0.031	0.032
Cr	0.000	0.000	0.000	0.000	0.000	0.000	0.000	0.000	-0.001	0.000	-0.001
Co	0.002	0.003	0.002	0.002	0.003	0.002	0.002	0.003	0.002	0.002	0.003
Ca	0.005	0.004	0.005	0.007	0.007	0.006	0.007	0.007	0.005	0.006	0.006
Ni	0.000	0.000	-0.001	0.000	0.000	0.000	0.000	0.000	0.000	0.000	0.000
Ti	0.001	0.001	0.001	0.001	0.001	0.001	0.001	0.001	0.001	0.001	0.001
Sc	0.000	0.000	0.000	0.000	0.000	0.000	0.000	0.000	0.000	0.000	0.000
O	4.000	4.000	4.000	4.000	4.000	4.000	4.000	4.000	4.000	4.000	4.000
Fo	**35.776**	**35.549**	**36.249**	**34.971**	**35.145**	**35.042**	**34.216**	**34.469**	**33.377**	**35.452**	**35.454**
Fa	**64.224**	**64.451**	**63.751**	**65.029**	**64.855**	**64.958**	**65.784**	**65.531**	**66.623**	**64.548**	**64.546**

Sample No.	FD-13-34-226.3	FD-13-34-226.3	FD-13-34-226.3	FD-13-34-226.3	FD-13-34-253.1	FD-13-34-253.1	FD-13-34-253.1	FD-13-34-253.1	FD-13-34-253.1	FD-13-34-253.1	FD-13-34-253.1
Spot No.	6	7	8	9	1	2	3	4	5	6	7
SiO_2	32.817	33.059	32.967	32.980	33.271	33.401	33.416	33.342	33.224	33.127	33.124
Al_2O_3	-0.005	-0.021	-0.024	0.011	-0.005	0.012	0.008	-0.006	-0.01	-0.019	-0.001
Na_2O											
MgO	15.462	15.848	15.805	15.747	17.32	16.924	17.063	16.566	16.462	16.164	16.206
FeO	50.055	49.627	49.986	49.894	48.422	48.471	48.945	49.007	49.421	49.829	49.769
MnO	1.285	1.198	1.141	1.065	1.128	1.126	1.115	1.151	1.186	1.137	1.147
Cr_2O_3	-0.003	-0.004	0.012	-0.019	-0.024	0	0.028	0.003	0.014	0.016	-0.015
CoO	0.085	0.113	0.077	0.096	0.085	0.072	0.101	0.12	0.092	0.091	0.099
CaO	0.180	0.173	0.203	0.205	0.146	0.158	0.154	0.131	0.227	0.222	0.182
NiO	-0.025	-0.011	0.012	-0.002	0.008	-0.006	-0.023	0.01	-0.007	0.008	-0.011
TiO_2	0.041	0.025	0.038	0.035	0.04	0.045	0.04	0.044	0.022	0.041	0.024
Sc_2O_3											
Total	99.892	100.007	100.217	100.012	100.391	100.203	100.847	100.368	100.631	100.616	100.524
Si	0.995	0.998	0.995	0.996	0.993	0.998	0.994	0.998	0.994	0.994	0.994

Al	0.000	-0.001	-0.001	0.000	0.000	0.000	0.000	0.000	0.000	-0.001	0.000
Na	0.000	0.000	0.000	0.000	0.000	0.000	0.000	0.000	0.000	0.000	0.000
Mg	0.703	0.718	0.715	0.714	0.775	0.759	0.761	0.744	0.739	0.727	0.730
Fe	1.265	1.248	1.257	1.256	1.204	1.207	1.213	1.222	1.232	1.246	1.245
Mn	0.033	0.031	0.029	0.027	0.028	0.028	0.028	0.029	0.030	0.029	0.029
Cr	0.000	0.000	0.000	0.000	-0.001	0.000	0.001	0.000	0.000	0.000	0.000
Co	0.002	0.003	0.002	0.002	0.002	0.002	0.002	0.003	0.002	0.002	0.002
Ca	0.006	0.006	0.007	0.007	0.005	0.005	0.005	0.004	0.007	0.007	0.006
Ni	-0.001	0.000	0.000	0.000	0.000	0.000	-0.001	0.000	0.000	0.000	0.000
Ti	0.001	0.001	0.001	0.001	0.001	0.001	0.001	0.001	0.000	0.001	0.001
Sc	0.000	0.000	0.000	0.000	0.000	0.000	0.000	0.000	0.000	0.000	0.000
O	4.000	4.000	4.000	4.000	4.000	4.000	4.000	4.000	4.000	4.000	4.000
Fo	**35.733**	**36.501**	**36.271**	**36.228**	**39.167**	**38.593**	**38.556**	**37.829**	**37.483**	**36.865**	**36.953**
Fa	**64.267**	**63.499**	**63.729**	**63.772**	**60.833**	**61.407**	**61.444**	**62.171**	**62.517**	**63.135**	**63.047**

Sample No.	FD-13-34-253.1	FD-13-34-253.1	FD-13-34-253.1	FD-13-34-253.1	FD-13-34-253.1	FD-13-34-253.1	FD-13-34-253.1	FD-13-34-253.1	FD-13-34-257.8	FD-13-34-257.8	FD-13-34-257.8
Spot No.	8	9	10	11	12	13	14	15	1	2	3
SiO_2	33.144	33.271	33.259	33.175	33.154	33.032	33.2	33.335	33.463	33.233	33.579
Al_2O_3	0.009	-0.016	-0.008	-0.014	-0.001	-0.012	0.002	0.015	-0.021	-0.004	0.004
Na_2O											
MgO	16.03	16.341	16.618	16.352	15.935	16.415	16.172	16.34	16.517	16.537	16.65
FeO	49.765	49.143	49.119	49.722	50.081	49.517	49.649	49.404	48.648	49.173	49.336
MnO	1.129	1.063	1.12	1.151	1.156	1.151	1.128	1.204	1.096	1.177	1.145
Cr_2O_3	0.012	-0.023	-0.039	-0.012	0.008	-0.018	0.003	0.022	-0.027	0.012	-0.019
CoO	0.085	0.09	0.114	0.102	0.094	0.114	0.11	0.084	0.102	0.096	0.076
CaO	0.211	0.207	0.222	0.237	0.203	0.227	0.216	0.233	0.173	0.221	0.218
NiO	-0.004	0.002	0.003	-0.008	-0.006	0.014	-0.005	-0.016	-0.002	0.024	-0.019
TiO_2	0.037	0.015	0.031	0.023	0.033	0.029	0.029	0.032	0.012	0.02	0.034
Sc_2O_3											
Total	100.418	100.093	100.439	100.728	100.657	100.469	100.504	100.653	99.961	100.489	101.004
Si	0.996	0.999	0.995	0.993	0.995	0.991	0.996	0.997	1.004	0.995	0.998
Al	0.000	-0.001	0.000	0.000	0.000	0.000	0.000	0.001	-0.001	0.000	0.000
Na	0.000	0.000	0.000	0.000	0.000	0.000	0.000	0.000	0.000	0.000	0.000
Mg	0.722	0.736	0.746	0.734	0.717	0.739	0.728	0.733	0.743	0.743	0.743
Fe	1.246	1.230	1.225	1.240	1.253	1.239	1.241	1.231	1.216	1.227	1.222
Mn	0.029	0.027	0.028	0.029	0.029	0.029	0.029	0.030	0.028	0.030	0.029
Cr	0.000	-0.001	-0.001	0.000	0.000	0.000	0.000	0.001	-0.001	0.000	0.000
Co	0.002	0.002	0.003	0.002	0.002	0.003	0.003	0.002	0.002	0.002	0.002

Ca	0.007	0.007	0.007	0.008	0.007	0.007	0.007	0.007	0.006	0.007	0.007
Ni	0.000	0.000	0.000	0.000	0.000	0.000	0.000	0.000	0.000	0.001	0.000
Ti	0.001	0.000	0.001	0.001	0.001	0.001	0.001	0.001	0.000	0.000	0.001
Sc	0.000	0.000	0.000	0.000	0.000	0.000	0.000	0.000	0.000	0.000	0.000
O	4.000	4.000	4.000	4.000	4.000	4.000	4.000	4.000	4.000	4.000	4.000
Fo	**36.701**	**37.443**	**37.849**	**37.184**	**36.416**	**37.371**	**36.961**	**37.317**	**37.932**	**37.708**	**37.790**
Fa	**63.299**	**62.557**	**62.151**	**62.816**	**63.584**	**62.629**	**63.039**	**62.683**	**62.068**	**62.292**	**62.210**

Sample No.	FD-13-34-257.8	FD-13-34-257.8	FD-13-34-257.8	FD-13-34-257.8	FD-13-34-257.8	FD-13-34-257.8	FD-13-34-272.1	FD-13-34-272.1	FD-13-34-272.1	FD-13-34-272.1	FD-13-34-272.1
Spot No.	4	5	6	7	8	9	1	2	3	4	5
SiO_2	33.393	33.383	33.245	33.34	33.228	33.381	34.549	34.644	34.704	34.557	34.64
Al_2O_3	-0.025	0.013	-0.01	-0.021	0.002	-0.013	-0.002	0.001	-0.018	0.003	-0.003
Na_2O											
MgO	16.858	16.362	16.091	16.617	16.651	16.595	21.885	21.937	22.036	21.99	21.959
FeO	48.521	49.115	49.49	48.656	48.477	48.625	42.55	42.232	42.224	42.357	42.252
MnO	1.065	1.124	1.168	1.169	1.188	1.142	0.819	0.752	0.759	0.777	0.735
Cr_2O_3	-0.004	-0.016	0.023	-0.003	-0.001	0.034	-0.01	0.007	-0.003	-0.032	-0.001
CoO	0.087	0.099	0.091	0.084	0.061	0.09	0.111	0.072	0.063	0.112	0.082
CaO	0.152	0.14	0.113	0.183	0.237	0.235	0.219	0.209	0.2	0.217	0.224
NiO	0.007	0	-0.014	0.006	0.005	0	0.045	0.049	0.016	0.047	0.053
TiO_2	0.018	0.039	0.032	0.013	0.03	0.036	0.032	0.024	0.02	0.03	0.027
Sc_2O_3											
Total	100.072	100.259	100.229	100.044	99.878	100.125	100.198	99.927	100.001	100.058	99.968
Si	1.000	1.000	0.999	1.000	0.998	1.000	0.998	1.001	1.002	0.999	1.001
Al	-0.001	0.000	0.000	-0.001	0.000	0.000	0.000	0.000	-0.001	0.000	0.000
Na	0.000	0.000	0.000	0.000	0.000	0.000	0.000	0.000	0.000	0.000	0.000
Mg	0.757	0.735	0.725	0.747	0.750	0.746	0.948	0.951	0.954	0.953	0.952
Fe	1.210	1.227	1.239	1.216	1.213	1.214	1.024	1.017	1.016	1.020	1.017
Mn	0.027	0.028	0.030	0.030	0.030	0.029	0.020	0.018	0.019	0.019	0.018
Cr	0.000	0.000	0.001	0.000	0.000	0.001	0.000	0.000	0.000	-0.001	0.000
Co	0.002	0.002	0.002	0.002	0.001	0.002	0.003	0.002	0.001	0.003	0.002
Ca	0.005	0.004	0.004	0.006	0.008	0.008	0.007	0.006	0.006	0.007	0.007
Ni	0.000	0.000	0.000	0.000	0.000	0.000	0.001	0.001	0.000	0.001	0.001
Ti	0.000	0.001	0.001	0.000	0.001	0.001	0.001	0.001	0.000	0.001	0.001
Sc	0.000	0.000	0.000	0.000	0.000	0.000	0.000	0.000	0.000	0.000	0.000
O	4.000	4.000	4.000	4.000	4.000	4.000	4.000	4.000	4.000	4.000	4.000
Fo	**38.476**	**37.486**	**36.918**	**38.070**	**38.206**	**38.054**	**48.074**	**48.320**	**48.437**	**48.307**	**48.333**
Fa	**61.524**	**62.514**	**63.082**	**61.930**	**61.794**	**61.946**	**51.926**	**51.680**	**51.563**	**51.693**	**51.667**

Sample No.	FD-13-34-272.1	FD-13-34-272.1	FD-13-34-272.1	FD-13-34-272.1	FD-13-34-272.1	FD-13-34-276.5	FD-13-34-276.5	FD-13-34-276.5	FD-13-34-276.5	FD-13-34-276.5	FD-13-34-276.5
Spot No.	6	7	8	9	10	1	2	3	4	5	6
SiO_2	34.47	34.359	34.671	34.795	34.792	34.315	34.414	34.595	34.366	34.494	34.524
Al_2O_3	-0.015	0.004	0.006	0.001	-0.006	0.002	-0.013	0.002	-0.022	0	-0.002
Na_2O											
MgO	21.697	21.359	22.583	22.454	22.688	21.58	21.693	21.596	21.785	21.874	21.634
FeO	42.701	42.95	41.289	41.584	41.559	42.488	43.042	42.835	42.687	42.685	42.585
MnO	0.797	0.75	0.672	0.793	0.703	0.794	0.83	0.835	0.773	0.81	0.747
Cr_2O_3	-0.004	0.001	-0.008	0.019	0.036	0.022	0.018	-0.017	0.023	0.015	-0.044
CoO	0.081	0.112	0.083	0.092	0.08	0.086	0.077	0.078	0.071	0.094	0.093
CaO	0.182	0.162	0.206	0.199	0.094	0.217	0.231	0.204	0.219	0.211	0.199
NiO	0.02	0.041	0.024	0.029	0.028	0.021	0.03	0.028	0.03	0.024	0.03
TiO_2	0.009	0.02	0.038	0.041	0.034	0.03	0.026	0.03	0.028	0.037	0.019
Sc_2O_3											
Total	99.938	99.758	99.564	100.007	100.008	99.555	100.348	100.186	99.96	100.244	99.785
Si	0.999	0.999	1.001	1.001	1.000	0.998	0.995	1.000	0.996	0.997	1.001
Al	-0.001	0.000	0.000	0.000	0.000	0.000	0.000	0.000	-0.001	0.000	0.000
Na	0.000	0.000	0.000	0.000	0.000	0.000	0.000	0.000	0.000	0.000	0.000
Mg	0.943	0.932	0.978	0.969	0.979	0.942	0.941	0.937	0.947	0.948	0.941
Fe	1.031	1.041	0.993	0.997	0.996	1.030	1.037	1.032	1.031	1.028	1.029
Mn	0.020	0.018	0.016	0.019	0.017	0.020	0.020	0.020	0.019	0.020	0.018
Cr	0.000	0.000	0.000	0.000	0.001	0.001	0.000	0.000	0.001	0.000	-0.001
Co	0.002	0.003	0.002	0.002	0.002	0.002	0.002	0.002	0.002	0.002	0.002
Ca	0.006	0.005	0.006	0.006	0.003	0.007	0.007	0.006	0.007	0.007	0.006
Ni	0.000	0.001	0.001	0.001	0.001	0.000	0.001	0.001	0.001	0.001	0.001
Ti	0.000	0.000	0.001	0.001	0.001	0.001	0.001	0.001	0.001	0.001	0.000
Sc	0.000	0.000	0.000	0.000	0.000	0.000	0.000	0.000	0.000	0.000	0.000
O	4.000	4.000	4.000	4.000	4.000	4.000	4.000	4.000	4.000	4.000	4.000
Fo	**47.770**	**47.233**	**49.610**	**49.289**	**49.563**	**47.760**	**47.567**	**47.575**	**47.879**	**47.982**	**47.765**
Fa	**52.230**	**52.767**	**50.390**	**50.711**	**50.437**	**52.240**	**52.433**	**52.425**	**52.121**	**52.018**	**52.235**

Sample No.	FD-13-34-276.5	FD-13-34-276.5	FD-13-34-281.05	FD-13-34-281.05	FD-13-34-281.05	FD-13-34-281.05	FD-13-34-281.05	FD-13-34-281.05	FD-13-34-281.05	FD-13-34-281.05	FD-13-34-281.05
Spot No.	7	8	1	2	3	4	5	6	7	8	9
SiO_2	34.594	34.581	33.587	33.218	33.427	33.588	33.571	33.389	33.638	33.27	33.374
Al_2O_3	0.003	0.004	-0.02	-0.011	0.018	-0.003	0.012	-0.006	0.005	-0.03	-0.016

Na_2O											
MgO	21.656	21.676	17.031	16.827	16.997	17.1	16.728	16.769	16.93	16.857	16.863
FeO	42.727	43.233	48.331	48.124	48.247	47.918	48.303	48.389	48.359	48.099	48.19
MnO	0.77	0.73	1.171	1.181	1.215	1.129	1.159	1.218	1.117	1.137	1.218
Cr_2O_3	-0.011	-0.029	-0.004	-0.007	0.016	0.004	-0.004	-0.009	-0.005	0.003	0.032
CoO	0.093	0.132	0.082	0.078	0.112	0.099	0.1	0.107	0.103	0.085	0.082
CaO	0.204	0.215	0.245	0.22	0.242	0.258	0.196	0.268	0.209	0.265	0.136
NiO	0.053	0.03	0.03	0	0.022	0.016	0.022	0.011	-0.001	0.024	0.019
TiO_2	0.022	0.039	0.022	0.02	0.024	0.021	0.018	0.022	0.019	0.022	0.025
Sc_2O_3											
Total	100.111	100.611	100.475	99.65	100.32	100.13	100.105	100.158	100.374	99.732	99.923
Si	1.001	0.997	1.000	0.998	0.998	1.002	1.003	0.999	1.002	0.999	1.000
Al	0.000	0.000	-0.001	0.000	0.001	0.000	0.000	0.000	0.000	-0.001	-0.001
Na	0.000	0.000	0.000	0.000	0.000	0.000	0.000	0.000	0.000	0.000	0.000
Mg	0.940	0.938	0.761	0.759	0.761	0.765	0.750	0.753	0.757	0.759	0.758
Fe	1.030	1.039	1.199	1.205	1.200	1.191	1.203	1.207	1.201	1.203	1.203
Mn	0.019	0.018	0.029	0.030	0.031	0.028	0.029	0.031	0.028	0.029	0.031
Cr	0.000	-0.001	0.000	0.000	0.000	0.000	0.000	0.000	0.000	0.000	0.001
Co	0.002	0.003	0.002	0.002	0.003	0.002	0.002	0.003	0.002	0.002	0.002
Ca	0.006	0.007	0.008	0.007	0.008	0.008	0.006	0.009	0.007	0.009	0.004
Ni	0.001	0.001	0.001	0.000	0.001	0.000	0.001	0.000	0.000	0.001	0.000
Ti	0.000	0.001	0.000	0.000	0.001	0.000	0.000	0.000	0.000	0.000	0.001
Sc	0.000	0.000	0.000	0.000	0.000	0.000	0.000	0.000	0.000	0.000	0.000
O	4.000	4.000	4.000	4.000	4.000	4.000	4.000	4.000	4.000	4.000	4.000
Fo	**47.708**	**47.437**	**38.811**	**38.627**	**38.805**	**39.112**	**38.400**	**38.415**	**38.656**	**38.682**	**38.645**
Fa	**52.292**	**52.563**	**61.189**	**61.373**	**61.195**	**60.888**	**61.600**	**61.585**	**61.344**	**61.318**	**61.355**

Sample No.	FD-13-34-281.05	FD-13-34-291.5	FD-13-34-291.5	FD-13-34-291.5	FD-13-34-291.5	FD-13-34-291.5	FD-13-34-291.5	FD-13-34-295.7	FD-13-34-295.7	FD-13-34-316.7	FD-13-34-316.7
Spot No.	10	1	2	3	4	5	6	1	2	1	2
SiO_2	33.5	35.29	35.258	35.132	35.138	35.302	35.142	33.405	33.433	34.64	34.617
Al_2O_3	0	0.004	-0.023	-0.004	-0.004	-0.007	-0.01	0.003	-0.008	-0.017	-0.001
Na_2O											
MgO	16.919	24.136	24.203	24.36	24.211	24.3	24.171	16.597	16.472	22.588	22.564
FeO	48.512	39.98	39.856	39.66	40.187	39.813	40.259	48.996	49.858	42.113	42.267
MnO	1.258	0.749	0.707	0.686	0.657	0.719	0.687	1.142	1.136	0.826	0.802
Cr_2O_3	0.014	0.019	0.006	0.011	-0.021	-0.039	-0.019	-0.019	0.005	0.029	-0.011
CoO	0.095	0.05	0.091	0.089	0.091	0.068	0.087	0.069	0.064	0.067	0.08
CaO	0.133	0.17	0.176	0.125	0.187	0.213	0.207	0.238	0.201	0.177	0.19

NiO	0.004	0.018	0.053	0.039	0.025	0.048	0.01	0.001	0.027	0.043	0.03
TiO_2	0.027	0.026	0.023	0.032	0.035	0.025	0.031	0.018	0.028	0.023	0.023
Sc_2O_3											
Total	100.462	100.442	100.35	100.13	100.506	100.442	100.565	100.45	101.216	100.489	100.561
Si	0.999	1.001	1.001	0.999	0.997	1.000	0.997	0.998	0.995	0.995	0.994
Al	0.000	0.000	-0.001	0.000	0.000	0.000	0.000	0.000	0.000	-0.001	0.000
Na	0.000	0.000	0.000	0.000	0.000	0.000	0.000	0.000	0.000	0.000	0.000
Mg	0.757	1.027	1.030	1.039	1.031	1.033	1.029	0.744	0.735	0.973	0.972
Fe	1.205	0.945	0.943	0.939	0.950	0.940	0.952	1.220	1.237	1.008	1.011
Mn	0.032	0.018	0.017	0.016	0.016	0.017	0.016	0.029	0.029	0.020	0.019
Cr	0.000	0.000	0.000	0.000	0.000	-0.001	0.000	0.000	0.000	0.001	0.000
Co	0.002	0.001	0.002	0.002	0.002	0.002	0.002	0.002	0.002	0.002	0.002
Ca	0.004	0.005	0.005	0.004	0.006	0.006	0.006	0.008	0.006	0.005	0.006
Ni	0.000	0.000	0.001	0.001	0.001	0.001	0.000	0.000	0.001	0.001	0.001
Ti	0.001	0.001	0.000	0.001	0.001	0.001	0.001	0.000	0.001	0.000	0.000
Sc	0.000	0.000	0.000	0.000	0.000	0.000	0.000	0.000	0.000	0.000	0.000
O	4.000	4.000	4.000	4.000	4.000	4.000	4.000	4.000	4.000	4.000	4.000
Fo	**38.566**	**52.077**	**52.223**	**52.508**	**52.025**	**52.350**	**51.939**	**37.878**	**37.292**	**49.121**	**49.004**
Fa	**61.434**	**47.923**	**47.777**	**47.492**	**47.975**	**47.650**	**48.061**	**62.122**	**62.708**	**50.879**	**50.996**

Sample No.	FD-13-34-316.7	FD-13-34-316.7	FD-13-34-321.1	FD-13-34-321.1	FD-13-34-321.1	FD-13-34-321.1	FD-13-34-321.1	FD-13-34-321.1	FD-13-34-321.1	FD-13-34-321.1	FD-13-34-321.1
Spot No.	3	4	1	2	3	4	5	6	7	8	9
SiO_2	34.577	34.522	34.92	34.813	34.825	34.953	35.021	35.075	34.466	34.961	34.808
Al_2O_3	-0.008	-0.007	-0.004	-0.018	-0.014	0.006	-0.01	-0.019	-0.008	-0.019	-0.015
Na_2O											
MgO	22.524	22.587	23.34	23.149	23.226	23.256	23.247	23.303	23.219	23.267	23.267
FeO	42.296	41.912	41.414	41.313	41.284	40.883	41.302	41.693	38.726	41.224	41.458
MnO	0.807	0.743	0.731	0.797	0.83	0.788	0.754	0.751	0.77	0.76	0.769
Cr_2O_3	-0.003	-0.046	-0.011	-0.004	0.025	0.01	-0.01	0.005	0	0.008	-0.022
CoO	0.096	0.063	0.064	0.084	0.084	0.102	0.1	0.083	0.09	0.106	0.089
CaO	0.183	0.153	0.155	0.156	0.17	0.16	0.167	0.162	0.171	0.174	0.046
NiO	0.005	0.018	0.037	0.024	0.044	0.031	0.041	0.006	0.035	0.033	0.032
TiO_2	0.027	0.027	0.024	0.025	0.019	0.032	0.011	0.032	0.026	0.023	0.028
Sc_2O_3											
Total	100.504	99.972	100.67	100.339	100.493	100.221	100.623	101.091	97.495	100.537	100.46
Si	0.994	0.996	0.996	0.997	0.996	1.000	0.999	0.997	1.006	0.998	0.996
Al	0.000	0.000	0.000	-0.001	0.000	0.000	0.000	-0.001	0.000	-0.001	-0.001
Na	0.000	0.000	0.000	0.000	0.000	0.000	0.000	0.000	0.000	0.000	0.000

Mg	0.971	0.977	0.999	0.994	0.996	0.998	0.995	0.993	1.017	0.996	0.998
Fe	1.013	1.007	0.984	0.986	0.984	0.974	0.982	0.987	0.942	0.981	0.988
Mn	0.020	0.018	0.018	0.019	0.020	0.019	0.018	0.018	0.019	0.018	0.019
Cr	0.000	-0.001	0.000	0.000	0.001	0.000	0.000	0.000	0.000	0.000	0.000
Co	0.002	0.001	0.001	0.002	0.002	0.002	0.002	0.002	0.002	0.002	0.002
Ca	0.006	0.005	0.005	0.005	0.005	0.005	0.005	0.005	0.005	0.005	0.001
Ni	0.000	0.000	0.001	0.001	0.001	0.001	0.001	0.000	0.001	0.001	0.001
Ti	0.001	0.001	0.001	0.001	0.000	0.001	0.000	0.001	0.001	0.000	0.001
Sc	0.000	0.000	0.000	0.000	0.000	0.000	0.000	0.000	0.000	0.000	0.000
O	4.000	4.000	4.000	4.000	4.000	4.000	4.000	4.000	4.000	4.000	4.000
Fo	**48.942**	**49.240**	**50.358**	**50.214**	**50.315**	**50.591**	**50.326**	**50.151**	**51.905**	**50.395**	**50.254**
Fa	**51.058**	**50.760**	**49.642**	**49.786**	**49.685**	**49.409**	**49.674**	**49.849**	**48.095**	**49.605**	**49.746**

Sample No.	SL-13-34-3.0	SL-13-34-3.0	SL-13-34-3.0	SL-13-34-3.0	SL-13-34-3.0	SL-13-34-3.0	SL-13-34-3.0	SL-13-34-3.0	SL-13-34-3.0	SL-13-34-5.1	SL-13-34-5.1
Spot No.	1	2	3	4	5	6	7	8	9	1	2
SiO_2	33.515	33.588	33.575	33.721	33.47	33.683	33.431	33.134	33.024	33.072	33.013
Al_2O_3	-0.016	-0.017	0.022	-0.021	-0.002	0.015	-0.008	0.016	-0.009	0.029	-0.013
Na_2O	0.005	-0.01	-0.003	-0.001	0.008	0.004	0.008	0.005	0.002	-0.005	-0.011
MgO	16.539	16.413	16.456	16.884	15.526	16.852	16.295	15.636	14.7	14.196	14.273
FeO	48.102	48.444	48.824	48.037	49.783	48.396	48.821	49.639	50.946	50.899	50.904
MnO	1.091	1.107	1.123	1.097	1.107	1.085	1.141	1.133	1.189	1.336	1.314
Cr_2O_3	0.013	0.021	0.018	0.001	-0.017	-0.001	0.005	0.003	-0.003	-0.023	-0.01
CoO											
CaO	0.192	0.201	0.15	0.149	0.154	0.211	0.16	0.146	0.14	0.186	0.196
NiO	-0.012	-0.005	0.002	0.018	-0.025	0.004	0	-0.003	0.005	-0.009	0.007
TiO_2	0.043	0.047	0.065	0.051	0.037	0.03	0.058	0.066	0.016	0.062	0.018
Sc_2O_3	0.013	0.008	0.001	0.014	-0.014	0.002	0	-0.015	-0.008	0.005	-0.014
Total	99.485	99.797	100.233	99.95	100.027	100.281	99.911	99.76	100.002	99.748	99.677
Si	1.007	1.007	1.004	1.007	1.008	1.004	1.004	1.002	1.003	1.008	1.007
Al	-0.001	-0.001	0.001	-0.001	0.000	0.001	0.000	0.001	0.000	0.001	0.000
Na	0.000	-0.001	0.000	0.000	0.000	0.000	0.000	0.000	0.000	0.000	-0.001
Mg	0.745	0.738	0.738	0.756	0.701	0.753	0.734	0.709	0.670	0.649	0.653
Fe	1.205	1.211	1.216	1.195	1.249	1.202	1.222	1.251	1.289	1.292	1.294
Mn	0.028	0.028	0.028	0.028	0.028	0.027	0.029	0.029	0.031	0.034	0.034
Cr	0.000	0.000	0.000	0.000	0.000	0.000	0.000	0.000	0.000	-0.001	0.000
Co	0.000	0.000	0.000	0.000	0.000	0.000	0.000	0.000	0.000	0.000	0.000
Ca	0.006	0.006	0.005	0.005	0.005	0.007	0.005	0.005	0.005	0.006	0.006
Ni	0.000	0.000	0.000	0.000	-0.001	0.000	0.000	0.000	0.000	0.000	0.000
Ti	0.001	0.001	0.001	0.001	0.001	0.001	0.001	0.001	0.000	0.001	0.000
Sc	0.000	0.000	0.000	0.000	0.000	0.000	0.000	0.000	0.000	0.000	0.000

O	4.000	4.000	4.000	4.000	4.000	4.000	4.000	4.000	4.000	4.000	4.000
Fo	**38.230**	**37.882**	**37.760**	**38.750**	**35.954**	**38.529**	**37.531**	**36.183**	**34.183**	**33.423**	**33.542**
Fa	**61.770**	**62.118**	**62.240**	**61.250**	**64.046**	**61.471**	**62.469**	**63.817**	**65.817**	**66.577**	**66.458**

Sample No.	SL-13-34-5.1	SL-13-34-5.1	SL-13-34-5.1	SL-13-34-5.1	SL-13-34-7.0	SL-13-34-7.0	SL-13-34-7.0	SL-13-34-7.0	SL-13-34-7.0	SL-13-34-7.0	SL-13-34-7.0
Spot No.	3	4	5	6	1	2	3	4	5	6	7
SiO_2	32.928	33.093	33.116	33.228	33.371	33.265	33.143	33.388	33.598	33.399	33.365
Al_2O_3	0.009	-0.003	0.015	0.021	-0.083	-0.028	-0.028	-0.076	-0.025	-0.039	0.002
Na_2O	0.003	-0.006	0	-0.016	0.022	0.027	-0.01	-0.004	0.026	0.003	0.032
MgO	14.008	14.279	14.266	14.46	14.868	14.903	14.971	15.893	15.701	15.828	14.926
FeO	51.625	50.955	51.245	50.994	50.135	50.125	50.006	49.152	48.908	49.063	50.357
MnO	1.348	1.26	1.286	1.272	1.491	1.48	1.474	1.438	1.448	1.455	1.501
Cr_2O_3	-0.01	-0.003	0.016	0.015	-0.021	-0.012	0.009	0.015	-0.011	0.006	-0.004
CoO											
CaO	0.166	0.182	0.183	0.155	0.176	0.207	0.202	0.164	0.138	0.177	0.163
NiO	0.003	-0.008	0.023	0.002	-0.008	0.008	-0.003	0.01	0.021	0.031	0.002
TiO_2	0.037	0.053	0.033	0.026	0.019	0.011	0.025	0.001	0.038	0.044	0.003
Sc_2O_3	0.003	-0.005	-0.016	-0.007	-0.004	-0.001	0.006	0.015	0.007	0.012	-0.016
Total	100.12	99.797	100.167	100.15	99.966	99.985	99.795	99.996	99.849	99.979	100.331
Si	1.003	1.008	1.006	1.007	1.010	1.007	1.005	1.005	1.011	1.005	1.007
Al	0.000	0.000	0.001	0.001	-0.003	-0.001	-0.001	-0.003	-0.001	-0.001	0.000
Na	0.000	0.000	0.000	-0.001	0.001	0.002	-0.001	0.000	0.002	0.000	0.002
Mg	0.640	0.652	0.650	0.658	0.675	0.677	0.681	0.718	0.709	0.715	0.676
Fe	1.311	1.293	1.297	1.288	1.265	1.265	1.264	1.233	1.226	1.231	1.266
Mn	0.035	0.032	0.033	0.033	0.038	0.038	0.038	0.037	0.037	0.037	0.038
Cr	0.000	0.000	0.000	0.000	-0.001	0.000	0.000	0.000	0.000	0.000	0.000
Co	0.000	0.000	0.000	0.000	0.000	0.000	0.000	0.000	0.000	0.000	0.000
Ca	0.005	0.006	0.006	0.005	0.006	0.007	0.007	0.005	0.004	0.006	0.005
Ni	0.000	0.000	0.001	0.000	0.000	0.000	0.000	0.000	0.001	0.001	0.000
Ti	0.001	0.001	0.001	0.001	0.000	0.000	0.001	0.000	0.001	0.001	0.000
Sc	0.000	0.000	0.000	0.000	0.000	0.000	0.000	0.000	0.000	0.000	0.000
O	4.000	4.000	4.000	4.000	4.000	4.000	4.000	4.000	4.000	4.000	4.000
Fo	**32.814**	**33.529**	**33.382**	**33.793**	**34.803**	**34.861**	**35.018**	**36.790**	**36.623**	**36.736**	**34.791**
Fa	**67.186**	**66.471**	**66.618**	**66.207**	**65.197**	**65.139**	**64.982**	**63.210**	**63.377**	**63.264**	**65.209**

Sample No.	SL-13-34-7.0	SL-13-34-7.0	SL-13-34-13.3	SL-13-34-13.3	SL-13-34-13.3	SL-13-34-13.3	SL-13-34-13.3	SL-13-34-13.3	SL-13-34-17.4	SL-13-34-17.4	SL-13-34-17.4
Spot No.	8	9	1	2	3	4	5	6	1	2	3
SiO_2	33.173	33.247	33.035	33.301	33.166	33.043	33.076	33.101	33.81	34.044	34.041

Al_2O_3	-0.098	-0.005	-0.037	-0.064	-0.036	-0.043	-0.065	0.016	0.003	0.007	-0.001
Na_2O	0.015	-0.006	0	-0.003	-0.014	-0.003	-0.007	0.004	-0.003	0.003	0
MgO	14.701	14.748	14.199	14.205	14.146	13.727	13.668	13.676	17.202	17.125	17.393
FeO	50.413	50.328	51.354	51.366	51.464	52.09	51.694	51.78	47.644	47.662	47.847
MnO	1.47	1.461	1.383	1.383	1.352	1.456	1.43	1.421	1.196	1.193	1.218
Cr_2O_3	-0.017	0.016	-0.001	0.005	-0.006	0.017	-0.001	-0.009	-0.004	0.009	-0.004
CoO											
CaO	0.087	0.139	0.15	0.148	0.146	0.117	0.112	0.132	0.102	0.098	0.096
NiO	-0.02	-0.007	0.03	0.019	0.017	0.008	0.007	0.021	0.023	0.03	-0.001
TiO_2	0.027	0.039	0.04	0.028	0.024	0.033	0.039	0.038	0.013	0.022	0.015
Sc_2O_3	-0.02	-0.019	0.013	0.001	0.014	-0.019	0.003	0.004	0.016	-0.011	-0.016
Total	99.731	99.941	100.166	100.389	100.273	100.426	99.956	100.184	100.002	100.182	100.588
Si	1.009	1.008	1.005	1.009	1.007	1.006	1.010	1.008	1.007	1.011	1.007
Al	-0.004	0.000	-0.001	-0.002	-0.001	-0.002	-0.002	0.001	0.000	0.000	0.000
Na	0.001	0.000	0.000	0.000	-0.001	0.000	0.000	0.000	0.000	0.000	0.000
Mg	0.670	0.671	0.648	0.646	0.644	0.627	0.626	0.625	0.768	0.763	0.772
Fe	1.277	1.271	1.301	1.297	1.302	1.321	1.315	1.314	1.182	1.180	1.180
Mn	0.038	0.037	0.036	0.035	0.035	0.037	0.037	0.037	0.030	0.030	0.030
Cr	0.000	0.000	0.000	0.000	0.000	0.000	0.000	0.000	0.000	0.000	0.000
Co	0.000	0.000	0.000	0.000	0.000	0.000	0.000	0.000	0.000	0.000	0.000
Ca	0.003	0.005	0.005	0.005	0.005	0.004	0.004	0.004	0.003	0.003	0.003
Ni	0.000	0.000	0.001	0.000	0.000	0.000	0.000	0.001	0.001	0.001	0.000
Ti	0.001	0.001	0.001	0.001	0.001	0.001	0.001	0.001	0.000	0.000	0.000
Sc	-0.001	-0.001	0.000	0.000	0.000	-0.001	0.000	0.000	0.000	0.000	0.000
O	4.000	4.000	4.000	4.000	4.000	4.000	4.000	4.000	4.000	4.000	4.000
Fo	**34.422**	**34.532**	**33.230**	**33.235**	**33.100**	**32.173**	**32.246**	**32.222**	**39.390**	**39.274**	**39.552**
Fa	**65.578**	**65.468**	**66.770**	**66.765**	**66.900**	**67.827**	**67.754**	**67.778**	**60.610**	**60.726**	**60.448**

Sample No.	SL-13-34-17.4	SL-13-34-17.4	SL-13-34-17.4	SL-13-34-17.4	SL-13-34-17.4	SL-13-34-17.4	SL-13-34-19.4	SL-13-34-19.4	SL-13-34-19.4	SL-13-34-19.4	SL-13-34-19.4
Spot No.	4	5	6	7	8	9	1	2	3	4	5
SiO_2	33.668	33.351	33.446	33.615	33.68	33.524	33.406	34.286	34.303	34.42	34.525
Al_2O_3	-0.006	0.01	0.023	-0.018	-0.003	0.016	-0.047	-0.057	-0.043	-0.099	-0.056
Na_2O	0.007	0.014	0	-0.007	-0.014	-0.015	-0.005	0.015	-0.015	0.028	-0.021
MgO	15.876	15.639	15.507	16.602	16.63	16.669	18.648	18.761	18.715	18.882	18.457
FeO	49.324	49.305	49.54	48.397	48.467	48.542	46.347	46.274	46.344	46.129	46.422
MnO	1.359	1.336	1.307	1.31	1.298	1.259	1.082	1.103	1.075	1.092	1.053
Cr_2O_3	-0.008	0.008	-0.008	0.005	-0.012	0.005	-0.008	0.005	-0.009	0	-0.013
CoO											

CaO	0.066	0.082	0.066	0.096	0.097	0.089	0.133	0.133	0.133	0.111	0.13
NiO	0.002	-0.002	0.008	0.02	0.017	-0.012	-0.009	0.009	0.003	0.025	0.032
TiO_2	0.004	0.007	0.024	0.04	0.031	0.027	0.018	0.031	-0.002	0.023	0.031
Sc_2O_3	-0.006	-0.005	-0.002	0.014	0.001	-0.005	0.001	0.001	0.015	-0.002	0.003
Total	100.286	99.745	99.911	100.074	100.192	100.099	99.566	100.561	100.519	100.609	100.563
Si	1.009	1.007	1.008	1.005	1.006	1.003	0.994	1.006	1.007	1.008	1.013
Al	0.000	0.000	0.001	-0.001	0.000	0.001	-0.002	-0.002	-0.001	-0.003	-0.002
Na	0.000	0.001	0.000	0.000	-0.001	-0.001	0.000	0.001	-0.001	0.002	-0.001
Mg	0.714	0.708	0.701	0.745	0.745	0.748	0.833	0.826	0.824	0.830	0.812
Fe	1.232	1.240	1.245	1.206	1.206	1.210	1.150	1.131	1.134	1.126	1.135
Mn	0.034	0.034	0.033	0.033	0.033	0.032	0.027	0.027	0.027	0.027	0.026
Cr	0.000	0.000	0.000	0.000	0.000	0.000	0.000	0.000	0.000	0.000	0.000
Co	0.000	0.000	0.000	0.000	0.000	0.000	0.000	0.000	0.000	0.000	0.000
Ca	0.002	0.003	0.002	0.003	0.003	0.003	0.004	0.004	0.004	0.003	0.004
Ni	0.000	0.000	0.000	0.000	0.000	0.000	0.000	0.000	0.000	0.001	0.001
Ti	0.000	0.000	0.001	0.001	0.001	0.001	0.000	0.001	0.000	0.001	0.001
Sc	0.000	0.000	0.000	0.000	0.000	0.000	0.000	0.000	0.000	0.000	0.000
O	4.000	4.000	4.000	4.000	4.000	4.000	4.000	4.000	4.000	4.000	4.000
Fo	**36.684**	**36.344**	**36.038**	**38.175**	**38.181**	**38.199**	**42.003**	**42.189**	**42.092**	**42.423**	**41.714**
Fa	**63.316**	**63.656**	**63.962**	**61.825**	**61.819**	**61.801**	**57.997**	**57.811**	**57.908**	**57.577**	**58.286**

Sample No.	SL-13-34-19.4	SL-13-34-19.4	SL-13-34-19.4	SL-13-34-19.4	SL-13-34-19.4	SL-13-34-25.7	SL-13-34-25.7	SL-13-34-25.7	SL-13-34-25.7	SL-13-34-25.7	SL-13-34-25.7
Spot No.	6	7	8	9	10	1	2	3	4	5	6
SiO_2	34.31	34.146	34.252	34.281	34.348	34.032	33.945	34.188	34.042	33.868	34.025
Al_2O_3	-0.02	-0.062	-0.069	-0.01	-0.046	-0.009	-0.007	-0.007	0.001	-0.007	0.001
Na_2O	0.018	0.006	-0.017	0.027	-0.015	0.006	-0.007	-0.004	-0.007	0.006	0.007
MgO	18.542	18.564	18.509	18.639	18.409	18.742	18.935	18.976	19.203	19.247	19.209
FeO	46.295	46.735	46.394	46.458	46.34	46.377	45.992	46.306	46.231	46.179	46.242
MnO	1.056	1.126	1.078	1.084	1.093	1.026	1.007	1.046	1.047	1.079	1.083
Cr_2O_3	0.011	0.012	-0.002	0.002	-0.013	-0.007	0.011	0.005	-0.011	-0.007	0.011
CoO											
CaO	0.106	0.129	0.148	0.152	0.127	0.185	0.197	0.171	0.139	0.123	0.16
NiO	0.004	0.022	0	0.03	0.025	-0.011	-0.01	0.005	0.012	0.005	-0.02
TiO_2	0.039	0.029	0.017	0.054	0.029	0.03	0.035	0.034	0.02	0.043	0.03
Sc_2O_3	0.007	0.003	0.002	-0.004	0.031	0.011	0.007	0.015	-0.007	0.021	-0.009
Total	100.368	100.71	100.312	100.713	100.328	100.382	100.105	100.735	100.67	100.557	100.739
Si	1.008	1.003	1.008	1.005	1.010	1.002	1.000	1.001	0.998	0.995	0.997
Al	-0.001	-0.002	-0.002	0.000	-0.002	0.000	0.000	0.000	0.000	0.000	0.000
Na	0.001	0.000	-0.001	0.002	-0.001	0.000	0.000	0.000	0.000	0.000	0.000

Mg	0.818	0.818	0.817	0.820	0.812	0.827	0.837	0.834	0.844	0.848	0.844
Fe	1.134	1.144	1.138	1.135	1.136	1.137	1.130	1.130	1.129	1.130	1.129
Mn	0.026	0.028	0.027	0.027	0.027	0.026	0.025	0.026	0.026	0.027	0.027
Cr	0.000	0.000	0.000	0.000	0.000	0.000	0.000	0.000	0.000	0.000	0.000
Co	0.000	0.000	0.000	0.000	0.000	0.000	0.000	0.000	0.000	0.000	0.000
Ca	0.003	0.004	0.005	0.005	0.004	0.006	0.006	0.005	0.004	0.004	0.005
Ni	0.000	0.001	0.000	0.001	0.001	0.000	0.000	0.000	0.000	0.000	0.000
Ti	0.001	0.001	0.000	0.001	0.001	0.001	0.001	0.001	0.000	0.001	0.001
Sc	0.000	0.000	0.000	0.000	0.001	0.000	0.000	0.000	0.000	0.001	0.000
O	4.000	4.000	4.000	4.000	4.000	4.000	4.000	4.000	4.000	4.000	4.000
Fo	**41.892**	**41.691**	**41.797**	**41.933**	**41.693**	**42.110**	**42.564**	**42.450**	**42.781**	**42.864**	**42.783**
Fa	**58.108**	**58.309**	**58.203**	**58.067**	**58.307**	**57.890**	**57.436**	**57.550**	**57.219**	**57.136**	**57.217**

Sample No.	SL-13-34-25.7	SL-13-34-25.7	SL-13-34-25.7	SL-13-34-28.1	SL-13-34-28.1	SL-13-34-28.1	SL-13-34-28.1	SL-13-34-28.1	SL-13-34-28.1	SL-13-34-28.1	SL-13-34-28.1
Spot No.	7	8	9	1	2	3	4	5	6	7	8
SiO_2	33.671	33.644	33.772	34.168	34.195	34.223	34.388	34.48	34.62	34.056	33.783
Al_2O_3	-0.009	0.011	-0.008	-0.016	-0.006	0.027	0.012	0.024	0.013	-0.005	0.009
Na_2O	0.002	0.002	0.003	-0.004	0.008	-0.017	-0.017	0.014	-0.011	-0.002	0.022
MgO	18.427	18.349	18.734	19.042	18.519	18.891	21.326	21.179	21.384	18.895	18.892
FeO	47.017	47.008	46.9	45.755	46.315	45.673	43.084	43.017	42.608	45.917	45.427
MnO	1.064	1.099	1.084	1.071	1.045	1.052	0.985	0.992	0.975	1.033	1.031
Cr_2O_3	0.001	-0.02	-0.025	0.013	0.001	-0.005	-0.004	-0.012	-0.003	-0.023	0.015
CoO											
CaO	0.14	0.154	0.136	0.157	0.14	0.15	0.15	0.125	0.186	0.113	0.135
NiO	-0.015	0.016	-0.008	0.015	0.024	-0.013	0.015	0.025	0.024	0.002	0.029
TiO_2	0.048	0.015	0.021	0.023	0.05	0.074	0.067	0.059	0.037	0	-0.005
Sc_2O_3	0.008	0.003	-0.002	0.012	0.009	0	0.006	-0.013	0.013	0	-0.007
Total	100.354	100.281	100.607	100.236	100.3	100.055	100.012	99.89	99.846	99.986	99.331
Si	0.996	0.996	0.995	1.004	1.006	1.006	0.998	1.002	1.004	1.004	1.002
Al	0.000	0.000	0.000	-0.001	0.000	0.001	0.000	0.001	0.000	0.000	0.000
Na	0.000	0.000	0.000	0.000	0.000	-0.001	-0.001	0.001	-0.001	0.000	0.001
Mg	0.817	0.815	0.828	0.839	0.818	0.833	0.929	0.923	0.930	0.836	0.841
Fe	1.159	1.160	1.151	1.120	1.136	1.119	1.042	1.041	1.030	1.128	1.123
Mn	0.027	0.028	0.027	0.027	0.026	0.026	0.024	0.024	0.024	0.026	0.026
Cr	0.000	0.000	-0.001	0.000	0.000	0.000	0.000	0.000	0.000	-0.001	0.000
Co	0.000	0.000	0.000	0.000	0.000	0.000	0.000	0.000	0.000	0.000	0.000
Ca	0.004	0.005	0.004	0.005	0.004	0.005	0.005	0.004	0.006	0.004	0.004
Ni	0.000	0.000	0.000	0.000	0.001	0.000	0.000	0.001	0.001	0.000	0.001
Ti	0.001	0.000	0.000	0.001	0.001	0.002	0.001	0.001	0.001	0.000	0.000

Sc	0.000	0.000	0.000	0.000	0.000	0.000	0.000	0.000	0.000	0.000	0.000
O	4.000	4.000	4.000	4.000	4.000	4.000	4.000	4.000	4.000	4.000	4.000
Fo	**41.365**	**41.267**	**41.827**	**42.828**	**41.851**	**42.677**	**47.117**	**46.984**	**47.462**	**42.552**	**42.811**
Fa	**58.635**	**58.733**	**58.173**	**57.172**	**58.149**	**57.323**	**52.883**	**53.016**	**52.538**	**57.448**	**57.189**

Sample No.	SL-13-34-30	SL-13-34-30	SL-13-34-30	SL-13-34-30	SL-13-34-30	SL-13-34-30	SL-13-34-30	SL-13-34-30	SL-13-34-30	SL-13-34-32	SL-13-34-32
Spot No.	1	2	3	4	5	6	7	8	9	1	2
SiO_2	34.889	34.828	34.743	35.172	35.141	35.466	35.316	35.464	35.262	34.031	34.047
Al_2O_3	0.02	-0.002	-0.02	-0.002	0.005	-0.001	-0.016	0.009	0.009	0.009	0.006
Na_2O	-0.007	-0.011	-0.007	0.003	0.014	0.016	-0.009	0.014	0.004	0.016	0.016
MgO	21.141	20.994	20.951	22.321	22.177	22.735	22.536	22.472	22.247	17.695	17.764
FeO	43.163	43.309	43.615	41.849	41.895	41.79	41.837	42.024	41.805	47.55	47.034
MnO	0.948	0.953	0.949	0.936	0.927	0.892	0.886	0.917	0.919	1.164	1.175
Cr_2O_3	0.005	-0.011	-0.01	0	-0.009	-0.012	-0.003	-0.016	-0.001	-0.006	0.005
CoO											
CaO	0.148	0.171	0.182	0.159	0.159	0.185	0.148	0.111	0.129	0.121	0.121
NiO	0.006	0.013	-0.003	0.007	-0.014	0.001	0.028	-0.007	0.004	-0.013	0.008
TiO_2	0.036	0.054	0.034	0.025	0.022	0.046	0.041	0.033	0.051	0.021	0.046
Sc_2O_3	0.001	0.01	0.02	0.009	-0.016	0.009	-0.011	-0.006	0.005	0.017	0.009
Total	100.35	100.308	100.454	100.479	100.301	101.127	100.753	101.015	100.434	100.605	100.231
Si	1.008	1.007	1.005	1.007	1.008	1.007	1.007	1.009	1.009	1.005	1.007
Al	0.001	0.000	-0.001	0.000	0.000	0.000	-0.001	0.000	0.000	0.000	0.000
Na	0.000	-0.001	0.000	0.000	0.001	0.001	0.000	0.001	0.000	0.001	0.001
Mg	0.916	0.911	0.909	0.959	0.954	0.968	0.964	0.959	0.955	0.784	0.788
Fe	1.039	1.044	1.051	0.998	1.002	0.989	0.994	0.996	0.997	1.171	1.160
Mn	0.023	0.023	0.023	0.023	0.022	0.021	0.021	0.022	0.022	0.029	0.029
Cr	0.000	0.000	0.000	0.000	0.000	0.000	0.000	0.000	0.000	0.000	0.000
Co	0.000	0.000	0.000	0.000	0.000	0.000	0.000	0.000	0.000	0.000	0.000
Ca	0.005	0.005	0.006	0.005	0.005	0.006	0.005	0.003	0.004	0.004	0.004
Ni	0.000	0.000	0.000	0.000	0.000	0.000	0.001	0.000	0.000	0.000	0.000
Ti	0.001	0.001	0.001	0.001	0.000	0.001	0.001	0.001	0.001	0.000	0.001
Sc	0.000	0.000	0.001	0.000	0.000	0.000	0.000	0.000	0.000	0.000	0.000
O	4.000	4.000	4.000	4.000	4.000	4.000	4.000	4.000	4.000	4.000	4.000
Fo	**46.855**	**46.597**	**46.371**	**48.981**	**48.792**	**49.476**	**49.228**	**49.046**	**48.925**	**40.114**	**40.470**
Fa	**53.145**	**53.403**	**53.629**	**51.019**	**51.208**	**50.524**	**50.772**	**50.954**	**51.075**	**59.886**	**59.530**

Sample No.	SL-13-34-32	SL-13-34-32	SL-13-34-32	SL-13-34-32	SL-13-34-32	SL-13-34-32	SL-13-34-32	SL-13-34-45	SL-13-34-45	SL-13-34-45	SL-13-34-45
Spot No.	3	4	5	6	7	8	9	1	2	3	4
SiO_2	34.05	34.128	34.519	34.472	34.282	33.992	34.313	34.625	34.68	34.617	34.528

Al_2O_3	-0.009	-0.003	0.005	-0.003	0.008	0.002	0.005	0.035	-0.006	-0.006	0.004
Na_2O	0.003	-0.014	-0.005	0.009	-0.008	-0.006	0.007	0.008	0.014	-0.01	0.017
MgO	17.799	18.85	19.008	19.031	18.58	18.293	18.416	21.062	21.07	21.416	21.375
FeO	47.429	45.614	45.906	45.833	46.178	46.058	46.255	43.186	43.432	43.055	42.734
MnO	1.147	1.102	1.075	1.108	1.127	1.139	1.153	0.983	1.017	1.011	0.979
Cr_2O_3	-0.015	-0.013	0.006	0.005	-0.004	-0.006	0.006	-0.023	-0.008	0.008	-0.004
CoO											
CaO	0.147	0.146	0.142	0.138	0.132	0.112	0.122	0.157	0.139	0.156	0.143
NiO	-0.013	0.007	0.005	0.018	0.001	0.011	-0.006	0.014	-0.014	0.002	0.001
TiO_2	0.026	0.031	0.059	0.049	0.05	0.041	0.031	0.052	0.063	0.043	0.046
Sc_2O_3	-0.002	-0.006	-0.005	0.006	-0.001	-0.006	0	0.009	0.021	-0.009	-0.011
Total	100.562	99.842	100.715	100.666	100.345	99.63	100.302	100.108	100.408	100.283	99.812
Si	1.006	1.006	1.008	1.007	1.008	1.008	1.009	1.004	1.003	1.001	1.002
Al	0.000	0.000	0.000	0.000	0.000	0.000	0.000	0.001	0.000	0.000	0.000
Na	0.000	-0.001	0.000	0.001	0.000	0.000	0.000	0.000	0.001	-0.001	0.001
Mg	0.788	0.834	0.833	0.834	0.819	0.813	0.813	0.916	0.914	0.929	0.931
Fe	1.167	1.121	1.117	1.116	1.131	1.138	1.134	1.043	1.047	1.038	1.034
Mn	0.029	0.027	0.027	0.027	0.028	0.029	0.029	0.024	0.025	0.025	0.024
Cr	0.000	0.000	0.000	0.000	0.000	0.000	0.000	-0.001	0.000	0.000	0.000
Co	0.000	0.000	0.000	0.000	0.000	0.000	0.000	0.000	0.000	0.000	0.000
Ca	0.005	0.005	0.004	0.004	0.004	0.004	0.004	0.005	0.004	0.005	0.004
Ni	0.000	0.000	0.000	0.000	0.000	0.000	0.000	0.000	0.000	0.000	0.000
Ti	0.001	0.001	0.001	0.001	0.001	0.001	0.001	0.001	0.001	0.001	0.001
Sc	0.000	0.000	0.000	0.000	0.000	0.000	0.000	0.000	0.001	0.000	0.000
O	4.000	4.000	4.000	4.000	4.000	4.000	4.000	4.000	4.000	4.000	4.000
Fo	**40.316**	**42.656**	**42.704**	**42.772**	**42.003**	**41.688**	**41.747**	**46.748**	**46.616**	**47.239**	**47.378**
Fa	**59.684**	**57.344**	**57.296**	**57.228**	**57.997**	**58.312**	**58.253**	**53.252**	**53.384**	**52.761**	**52.622**

Sample No.	SL-13-34-45	SL-13-34-45	SL-13-34-45	SL-13-34-45	SL-13-34-45	SL-13-34-45	SL-13-34-45	SL-13-34-49.0	SL-13-34-49.0	SL-13-34-49.0	SL-13-34-49.0
Spot No.	5	6	7	8	9	10	11	1	2	3	4
SiO_2	34.641	34.75	34.872	34.48	34.655	34.958	34.853	34.161	33.963	34.19	34.462
Al_2O_3	-0.01	0.013	-0.007	-0.012	-0.002	0.008	0.008	0.002	0.001	0.009	-0.023
Na_2O	0	0.004	0.001	0.003	-0.003	-0.009	-0.008	0.011	0.009	-0.001	0.028
MgO	21.48	21.375	21.645	20.951	21.083	21.225	20.937	20.684	20.768	20.763	22.27
FeO	42.613	42.887	42.531	43.461	43.124	42.858	43.145	43.398	43.033	43.2	41.128
MnO	0.968	0.996	0.967	1.003	0.995	1.011	1.009	1	0.966	0.969	0.984
Cr_2O_3	-0.002	-0.009	-0.012	0.012	0.015	0.001	0.009	-0.002	-0.003	0.022	0.008
CoO											

CaO	0.136	0.127	0.139	0.123	0.134	0.129	0.155	0.151	0.137	0.118	0.156
NiO	0.001	0.021	0.009	0.011	0.01	-0.015	0	0.016	0.01	0.014	0.001
TiO_2	0.042	0.04	0.014	0.03	0.047	0.05	0.039	0.052	0.038	0.034	0.024
Sc_2O_3	-0.006	0.016	0.002	0.003	0.01	-0.011	0.007	-0.006	0	0.023	-0.011
Total	99.863	100.22	100.161	100.065	100.068	100.205	100.154	99.467	98.922	99.341	99.027
Si	1.004	1.004	1.006	1.002	1.005	1.009	1.009	1.000	0.999	1.001	1.002
Al	0.000	0.000	0.000	0.000	0.000	0.000	0.000	0.000	0.000	0.000	-0.001
Na	0.000	0.000	0.000	0.000	0.000	-0.001	0.000	0.001	0.001	0.000	0.002
Mg	0.934	0.927	0.937	0.913	0.917	0.919	0.909	0.908	0.916	0.912	0.971
Fe	1.029	1.033	1.023	1.053	1.042	1.031	1.041	1.059	1.055	1.054	0.996
Mn	0.024	0.024	0.024	0.025	0.024	0.025	0.025	0.025	0.024	0.024	0.024
Cr	0.000	0.000	0.000	0.000	0.000	0.000	0.000	0.000	0.000	0.001	0.000
Co	0.000	0.000	0.000	0.000	0.000	0.000	0.000	0.000	0.000	0.000	0.000
Ca	0.004	0.004	0.004	0.004	0.004	0.004	0.005	0.005	0.004	0.004	0.005
Ni	0.000	0.000	0.000	0.000	0.000	0.000	0.000	0.000	0.000	0.000	0.000
Ti	0.001	0.001	0.000	0.001	0.001	0.001	0.001	0.001	0.001	0.001	0.001
Sc	0.000	0.000	0.000	0.000	0.000	0.000	0.000	0.000	0.000	0.001	0.000
O	4.000	4.000	4.000	4.000	4.000	4.000	4.000	4.000	4.000	4.000	4.000
Fo	**47.571**	**47.289**	**47.810**	**46.459**	**46.809**	**47.130**	**46.624**	**46.176**	**46.487**	**46.384**	**49.358**
Fa	**52.429**	**52.711**	**52.190**	**53.541**	**53.191**	**52.870**	**53.376**	**53.824**	**53.513**	**53.616**	**50.642**

Sample No.	SL-13-34-49.0	SL-13-34-49.0	SL-13-34-49.0	SL-13-34-53	SL-13-34-53	SL-13-34-53	SL-13-34-53	SL-13-34-53	SL-13-34-53	SL-13-34-53	SL-13-34-58.9
Spot No.	5	6	7	1	2	3	4	5	6	7	1
SiO_2	34.56	34.418	34.514	34.362	35.212	35.088	35.288	35.053	35.214	34.951	35.067
Al_2O_3	-0.026	-0.008	0	-0.02	0.029	0.005	0.003	0.002	0.001	0.006	-0.003
Na_2O	0.014	-0.01	0.001	0	0.017	-0.014	0.006	-0.004	0.002	0.003	0.005
MgO	22.172	22.184	22.166	23.043	23.657	23.723	23.751	23.797	23.759	22.439	22.386
FeO	41.137	41.677	41.178	40.147	39.933	40.166	40.298	40.077	40.274	41.43	41.223
MnO	0.989	0.977	0.964	0.866	0.869	0.844	0.883	0.879	0.876	0.89	0.882
Cr_2O_3	-0.025	0.011	0.001	-0.006	-0.002	0.01	0.005	0.002	-0.016	0.004	-0.009
CoO											
CaO	0.135	0.145	0.149	0.14	0.147	0.133	0.14	0.155	0.116	0.109	0.134
NiO	0	0.011	0.015	0.026	0.007	0.019	0.025	0.015	0.013	0.018	-0.007
TiO_2	0.025	0.049	0.052	0.057	0.054	0.036	0.055	0.033	0.042	0.052	0.051
Sc_2O_3	0	0.009	0.008	-0.01	0.002	0.014	-0.007	-0.005	0.016	-0.004	-0.008
Total	98.981	99.463	99.048	98.605	99.925	100.024	100.447	100.004	100.297	99.898	99.721
Si	1.005	0.998	1.003	0.998	1.004	1.001	1.003	1.000	1.002	1.005	1.009
Al	-0.001	0.000	0.000	-0.001	0.001	0.000	0.000	0.000	0.000	0.000	0.000
Na	0.001	-0.001	0.000	0.000	0.001	-0.001	0.000	0.000	0.000	0.000	0.000

Mg	0.967	0.965	0.966	1.004	1.012	1.015	1.012	1.019	1.014	0.968	0.966
Fe	0.996	1.007	0.997	0.972	0.949	0.955	0.954	0.953	0.955	0.993	0.989
Mn	0.024	0.024	0.024	0.021	0.021	0.020	0.021	0.021	0.021	0.022	0.021
Cr	-0.001	0.000	0.000	0.000	0.000	0.000	0.000	0.000	0.000	0.000	0.000
Co	0.000	0.000	0.000	0.000	0.000	0.000	0.000	0.000	0.000	0.000	0.000
Ca	0.004	0.005	0.005	0.004	0.004	0.004	0.004	0.005	0.004	0.003	0.004
Ni	0.000	0.000	0.000	0.001	0.000	0.000	0.001	0.000	0.000	0.000	0.000
Ti	0.001	0.001	0.001	0.001	0.001	0.001	0.001	0.001	0.001	0.001	0.001
Sc	0.000	0.000	0.000	0.000	0.000	0.000	0.000	0.000	0.000	0.000	0.000
O	4.000	4.000	4.000	4.000	4.000	4.000	4.000	4.000	4.000	4.000	4.000
Fo	**49.243**	**48.930**	**49.211**	**50.815**	**51.606**	**51.530**	**51.477**	**51.663**	**51.501**	**49.365**	**49.431**
Fa	**50.757**	**51.070**	**50.789**	**49.185**	**48.394**	**48.470**	**48.523**	**48.337**	**48.499**	**50.635**	**50.569**

Sample No.	SL-13-34-58.9	SL-13-34-58.9	SL-13-34-58.9	SL-13-34-58.9	SL-13-36-16.6	SL-13-36-16.6	SL-13-36-16.6	SL-13-36-16.6	SL-13-36-16.6	SL-13-36-16.6	SL-13-36-16.6
Spot No.	2	3	4	5	1	2	3	4	5	6	7
SiO_2	34.936	34.782	34.911	34.775	35.24	34.866	34.919	34.979	35.087	34.91	35.067
Al_2O_3	0.016	0.005	-0.005	-0.007	-0.018	-0.002	-0.001	-0.007	0.018	-0.026	-0.005
Na_2O	-0.003	0.017	0.006	0.007	0.003	0.01	0.01	-0.004	-0.006	0.008	-0.002
MgO	22.503	22.151	22.285	21.965	22.043	21.812	21.997	21.896	22.172	21.922	21.941
FeO	41.445	41.911	41.763	42.037	42.267	42.576	42.286	42.589	42.297	42.325	42.051
MnO	0.914	0.946	0.892	0.913	1.044	1.037	0.99	1.031	1.053	1.026	1.005
Cr_2O_3	0.008	0.006	-0.006	0.003	0.003	-0.008	-0.02	0.004	0.003	0.011	0.014
CoO											
CaO	0.114	0.099	0.123	0.114	0.111	0.103	0.147	0.132	0.15	0.153	0.13
NiO	-0.002	-0.003	0.001	-0.018	0.014	0.011	0.013	-0.001	0.021	-0.009	-0.012
TiO_2	0.052	0.021	0.047	0.05	0.036	0.05	0.036	0.034	0.048	0.027	0.029
Sc_2O_3	-0.013	0.009	0.005	-0.002	0.008	0.018	0.001	0.008	0.003	0.009	0.008
Total	99.97	99.944	100.022	99.837	100.751	100.473	100.378	100.661	100.846	100.356	100.226
Si	1.004	1.003	1.005	1.004	1.008	1.003	1.004	1.004	1.004	1.004	1.008
Al	0.001	0.000	0.000	0.000	-0.001	0.000	0.000	0.000	0.001	-0.001	0.000
Na	0.000	0.001	0.000	0.000	0.000	0.001	0.001	0.000	0.000	0.000	0.000
Mg	0.970	0.958	0.962	0.952	0.946	0.941	0.949	0.943	0.951	0.946	0.946
Fe	0.993	1.007	1.001	1.012	1.008	1.021	1.013	1.019	1.008	1.015	1.007
Mn	0.022	0.023	0.022	0.022	0.025	0.025	0.024	0.025	0.025	0.025	0.024
Cr	0.000	0.000	0.000	0.000	0.000	0.000	0.000	0.000	0.000	0.000	0.000
Co	0.000	0.000	0.000	0.000	0.000	0.000	0.000	0.000	0.000	0.000	0.000
Ca	0.004	0.003	0.004	0.004	0.003	0.003	0.005	0.004	0.005	0.005	0.004
Ni	0.000	0.000	0.000	0.000	0.000	0.000	0.000	0.000	0.000	0.000	0.000
Ti	0.001	0.000	0.001	0.001	0.001	0.001	0.001	0.001	0.001	0.001	0.001

Sc	0.000	0.000	0.000	0.000	0.000	0.000	0.000	0.000	0.000	0.000	0.000
O	4.000	4.000	4.000	4.000	4.000	4.000	4.000	4.000	4.000	4.000	4.000
Fo	**49.427**	**48.753**	**48.992**	**48.468**	**48.420**	**47.975**	**48.357**	**48.063**	**48.548**	**48.248**	**48.432**
Fa	**50.573**	**51.247**	**51.008**	**51.532**	**51.580**	**52.025**	**51.643**	**51.937**	**51.452**	**51.752**	**51.568**

Sample No.	SL-13-36-16.6	SL-13-36-16.6	SL-13-36-20.7	SL-13-36-20.7	SL-13-36-20.7	SL-13-36-20.7	SL-13-36-20.7	SL-13-36-20.7	SL-13-36-20.7	SL-13-36-20.7	SL-13-36-20.7
Spot No.	8	9	1	2	3	4	5	6	7	8	9
SiO_2	35.043	35.02	34.948	34.993	35.004	35.055	35.206	35.056	35.08	34.827	34.899
Al_2O_3	0.017	0.016	0.012	-0.002	-0.026	0.001	0.005	-0.01	-0.011	-0.003	-0.006
Na_2O	-0.001	-0.005	0.001	-0.006	-0.004	0.013	0.004	0.004	-0.022	0.004	-0.003
MgO	21.836	21.867	22.282	22.406	22.31	22.143	22.433	22.039	21.547	21.534	21.769
FeO	42.539	42.294	41.932	41.816	41.639	41.708	41.815	42.167	42.471	42.56	41.921
MnO	0.998	0.998	0.949	0.943	0.952	0.964	0.94	0.975	0.973	1.008	0.979
Cr_2O_3	-0.004	-0.003	0.008	0.016	-0.01	0.002	0.004	0.016	0.009	-0.002	0.01
CoO											
CaO	0.114	0.116	0.111	0.121	0.103	0.12	0.114	0.112	0.137	0.128	0.141
NiO	0.003	0.012	-0.002	0.002	0.012	0.022	0.016	0.009	0.006	0.005	0.012
TiO_2	0.056	0.046	0.033	0.023	0.037	0.03	0.038	0.033	0.05	0.039	0.036
Sc_2O_3	-0.008	0.005	0.001	0.008	-0.034	0.012	0.002	-0.014	-0.006	0.018	-0.02
Total	100.593	100.366	100.275	100.32	99.983	100.07	100.577	100.387	100.234	100.118	99.738
Si	1.006	1.007	1.004	1.004	1.007	1.008	1.007	1.007	1.010	1.006	1.009
Al	0.001	0.001	0.000	0.000	-0.001	0.000	0.000	0.000	0.000	0.000	0.000
Na	0.000	0.000	0.000	0.000	0.000	0.001	0.000	0.000	-0.001	0.000	0.000
Mg	0.940	0.943	0.960	0.964	0.963	0.955	0.962	0.949	0.931	0.933	0.944
Fe	1.018	1.013	1.004	1.000	0.998	0.999	0.996	1.009	1.019	1.024	1.010
Mn	0.024	0.024	0.023	0.023	0.023	0.023	0.023	0.024	0.024	0.025	0.024
Cr	0.000	0.000	0.000	0.000	0.000	0.000	0.000	0.000	0.000	0.000	0.000
Co	0.000	0.000	0.000	0.000	0.000	0.000	0.000	0.000	0.000	0.000	0.000
Ca	0.004	0.004	0.003	0.004	0.003	0.004	0.003	0.003	0.004	0.004	0.004
Ni	0.000	0.000	0.000	0.000	0.000	0.001	0.000	0.000	0.000	0.000	0.000
Ti	0.001	0.001	0.001	0.000	0.001	0.001	0.001	0.001	0.001	0.001	0.001
Sc	0.000	0.000	0.000	0.000	-0.001	0.000	0.000	0.000	0.000	0.000	-0.001
O	4.000	4.000	4.000	4.000	4.000	4.000	4.000	4.000	4.000	4.000	4.000
Fo	**48.024**	**48.204**	**48.888**	**49.096**	**49.095**	**48.866**	**49.127**	**48.475**	**47.732**	**47.664**	**48.313**
Fa	**51.976**	**51.796**	**51.112**	**50.904**	**50.905**	**51.134**	**50.873**	**51.525**	**52.268**	**52.336**	**51.687**

Sample No.	SL-13-36-20.7	SL-13-37-7	SL-13-37-7	SL-13-37-7	SL-13-37-7	SL-13-37-7	SL-13-37-7	SL-13-37-7	SL-13-37-7	SL-13-37-7	SL-13-37-7
Spot No.	10	1	2	3	4	5	6	7	8	9	10

SiO_2	34.835	34.749	34.664	34.758	34.659	35.008	34.852	34.882	34.672	34.966	34.982
Al_2O_3	-0.027	-0.007	0.006	0.016	0.01	-0.035	0.007	0	-0.004	-0.021	-0.011
Na_2O	-0.006	0.002	0.003	0	0.007	0.001	0	-0.005	0.004	0.003	0.006
MgO	21.702	22.311	22.061	21.992	21.856	21.755	21.821	21.463	21.328	21.953	21.376
FeO	42.173	41.494	41.604	41.669	42.012	42.02	42.001	42.669	41.703	42.116	42.594
MnO	0.961	0.948	0.936	0.922	0.937	0.972	1.024	0.934	0.916	0.939	0.945
Cr_2O_3	0.012	0.004	-0.003	0.003	0.019	-0.009	0.003	0.015	0.007	0	0
CoO											
CaO	0.123	0.1	0.144	0.12	0.111	0.134	0.104	0.107	0.128	0.129	0.131
NiO	-0.002	0.023	0.021	0.021	0	-0.006	0.022	0.002	-0.021	0.017	0
TiO_2	0.031	0.011	0.015	0.041	0.025	0.033	0.014	0.002	0.024	0.035	0.028
Sc_2O_3	0	0.021	-0.01	-0.006	-0.002	-0.008	-0.024	0.006	-0.001	0.008	0.005
Total	99.802	99.656	99.441	99.536	99.634	99.865	99.824	100.075	98.756	100.145	100.056
Si	1.007	1.004	1.004	1.006	1.004	1.010	1.007	1.008	1.012	1.007	1.010
Al	-0.001	0.000	0.000	0.001	0.000	-0.001	0.000	0.000	0.000	-0.001	0.000
Na	0.000	0.000	0.000	0.000	0.000	0.000	0.000	0.000	0.000	0.000	0.000
Mg	0.941	0.966	0.959	0.955	0.950	0.942	0.946	0.930	0.934	0.948	0.926
Fe	1.016	0.999	1.004	1.005	1.014	1.011	1.011	1.027	1.014	1.010	1.025
Mn	0.024	0.023	0.023	0.023	0.023	0.024	0.025	0.023	0.023	0.023	0.023
Cr	0.000	0.000	0.000	0.000	0.000	0.000	0.000	0.000	0.000	0.000	0.000
Co	0.000	0.000	0.000	0.000	0.000	0.000	0.000	0.000	0.000	0.000	0.000
Ca	0.004	0.003	0.004	0.004	0.003	0.004	0.003	0.003	0.004	0.004	0.004
Ni	0.000	0.001	0.000	0.000	0.000	0.000	0.001	0.000	0.000	0.000	0.000
Ti	0.001	0.000	0.000	0.001	0.001	0.001	0.000	0.000	0.001	0.001	0.001
Sc	0.000	0.001	0.000	0.000	0.000	0.000	-0.001	0.000	0.000	0.000	0.000
O	4.000	4.000	4.000	4.000	4.000	4.000	4.000	4.000	4.000	4.000	4.000
Fo	**48.086**	**49.183**	**48.835**	**48.718**	**48.358**	**48.238**	**48.325**	**47.518**	**47.932**	**48.407**	**47.461**
Fa	**51.914**	**50.817**	**51.165**	**51.282**	**51.642**	**51.762**	**51.675**	**52.482**	**52.068**	**51.593**	**52.539**

Sample No.	SL-13-37-7	SL-13-37-7	SL-13-37-7	SL-13-37-7	SL-13-37-19	SL-13-37-19	SL-13-37-19	SL-13-37-19	SL-13-37-19	SL-13-37-19	SL-13-37-19
Spot No.	11	12	13	14	1	2	3	4	5	6	7
SiO_2	34.733	34.954	34.999	34.93	35.149	35.088	35.024	35.156	35.345	35.194	35.21
Al_2O_3	-0.016	-0.001	0.013	-0.015	-0.021	-0.01	0.004	0.004	-0.006	-0.017	-0.005
Na_2O	-0.001	0.002	0.001	-0.019	-0.003	-0.006	-0.012	0.014	0.005	0.016	-0.003
MgO	22.48	22.335	22.032	22.469	23.223	23.341	23.318	23.617	23.541	23.55	23.366
FeO	41.449	41.521	41.753	41.709	40.335	40.125	40.123	40.315	40.219	40.35	40.351
MnO	0.949	0.918	0.952	0.954	0.849	0.876	0.898	0.844	0.9	0.889	0.874
Cr_2O_3	-0.003	0.003	0.002	-0.014	0.012	-0.006	-0.01	0.008	0.012	0.013	-0.006
CoO											

CaO	0.109	0.124	0.1	0.119	0.155	0.155	0.168	0.159	0.145	0.152	0.138
NiO	0.006	0.005	0.003	0.021	0	-0.021	0.009	0.009	0.01	0.005	0.002
TiO_2	0.025	0.041	0.047	0.042	0.026	0.031	0.023	0.032	0.013	0.019	0.013
Sc_2O_3	0	-0.002	-0.002	-0.004	0.005	-0.009	0.007	0.018	0.017	0.012	0.001
Total	99.731	99.9	99.9	100.192	99.73	99.564	99.552	100.176	100.201	100.183	99.941
Si	1.002	1.006	1.008	1.003	1.007	1.006	1.005	1.002	1.006	1.003	1.006
Al	-0.001	0.000	0.000	-0.001	-0.001	0.000	0.000	0.000	0.000	-0.001	0.000
Na	0.000	0.000	0.000	-0.001	0.000	0.000	-0.001	0.001	0.000	0.001	0.000
Mg	0.973	0.964	0.952	0.968	0.998	1.004	1.003	1.010	1.005	1.007	1.002
Fe	0.996	0.996	1.002	0.998	0.963	0.959	0.959	0.958	0.954	0.959	0.961
Mn	0.023	0.022	0.023	0.023	0.021	0.021	0.022	0.020	0.022	0.021	0.021
Cr	0.000	0.000	0.000	0.000	0.000	0.000	0.000	0.000	0.000	0.000	0.000
Co	0.000	0.000	0.000	0.000	0.000	0.000	0.000	0.000	0.000	0.000	0.000
Ca	0.003	0.004	0.003	0.004	0.005	0.005	0.005	0.005	0.004	0.005	0.004
Ni	0.000	0.000	0.000	0.000	0.000	0.000	0.000	0.000	0.000	0.000	0.000
Ti	0.001	0.001	0.001	0.001	0.001	0.001	0.000	0.001	0.000	0.000	0.000
Sc	0.000	0.000	0.000	0.000	0.000	0.000	0.000	0.000	0.000	0.000	0.000
O	4.000	4.000	4.000	4.000	4.000	4.000	4.000	4.000	4.000	4.000	4.000
Fo	**49.399**	**49.194**	**48.713**	**49.230**	**50.893**	**51.150**	**51.126**	**51.325**	**51.304**	**51.233**	**51.036**
Fa	**50.601**	**50.806**	**51.287**	**50.770**	**49.107**	**48.850**	**48.874**	**48.675**	**48.696**	**48.767**	**48.964**

Sample No.	SL-13-37-19	SL-13-37-25	SL-13-37-25	SL-13-37-25	SL-13-37-25	SL-13-37-25	SL-13-37-25	SL-13-37-25	SL-13-37-25	SL-13-37-25	SL-13-37-25
Spot No.	8	1	2	3	4	5	6	7	8	9	10
SiO_2	35.43	35.455	35.397	35.38	35.378	35.721	35.707	35.29	35.762	35.853	35.842
Al_2O_3	0.013	-0.002	0.016	0	-0.003	-0.008	-0.008	-0.007	0.004	0.005	0.024
Na_2O	-0.021	0.004	0	0.008	0.01	-0.002	0.005	0.003	0.01	0.006	0.012
MgO	23.663	25.599	25.394	25.491	25.433	26.187	26.169	25.703	26.263	26.463	26.311
FeO	40.322	37.736	37.636	37.387	37.544	36.93	36.917	36.915	37.041	36.992	37.036
MnO	0.894	0.828	0.798	0.836	0.828	0.796	0.807	0.812	0.789	0.825	0.794
Cr_2O_3	-0.008	0.01	-0.037	0.026	0.017	0.011	-0.008	-0.001	-0.002	-0.006	0.009
CoO											
CaO	0.155	0.163	0.158	0.176	0.16	0.149	0.15	0.149	0.142	0.111	0.119
NiO	0.019	0.007	-0.004	0.008	-0.015	-0.007	-0.012	0.013	0.007	0.011	0.024
TiO_2	0.034	0.034	0.019	0.05	0.028	0.048	0.039	0.026	0.043	0.045	0.04
Sc_2O_3	0	0.015	-0.008	0.009	0.012	-0.005	0.007	0.011	-0.019	-0.012	-0.008
Total	100.501	99.849	99.369	99.371	99.392	99.82	99.773	98.914	100.04	100.293	100.203
Si	1.006	1.001	1.004	1.002	1.003	1.003	1.004	1.003	1.003	1.002	1.003
Al	0.000	0.000	0.001	0.000	0.000	0.000	0.000	0.000	0.000	0.000	0.001
Na	-0.001	0.000	0.000	0.000	0.001	0.000	0.000	0.000	0.001	0.000	0.001

Mg	1.007	1.084	1.080	1.083	1.081	1.103	1.103	1.095	1.105	1.109	1.104
Fe	0.954	0.888	0.889	0.883	0.887	0.865	0.865	0.874	0.865	0.862	0.864
Mn	0.021	0.020	0.019	0.020	0.020	0.019	0.019	0.020	0.019	0.020	0.019
Cr	0.000	0.000	-0.001	0.001	0.000	0.000	0.000	0.000	0.000	0.000	0.000
Co	0.000	0.000	0.000	0.000	0.000	0.000	0.000	0.000	0.000	0.000	0.000
Ca	0.005	0.005	0.005	0.005	0.005	0.004	0.005	0.005	0.004	0.003	0.004
Ni	0.000	0.000	0.000	0.000	0.000	0.000	0.000	0.000	0.000	0.000	0.001
Ti	0.001	0.001	0.000	0.001	0.001	0.001	0.001	0.001	0.001	0.001	0.001
Sc	0.000	0.000	0.000	0.000	0.000	0.000	0.000	0.000	0.000	0.000	0.000
O	4.000	4.000	4.000	4.000	4.000	4.000	4.000	4.000	4.000	4.000	4.000
Fo	**51.370**	**54.977**	**54.843**	**55.102**	**54.942**	**56.071**	**56.062**	**55.621**	**56.068**	**56.287**	**56.116**
Fa	**48.630**	**45.023**	**45.157**	**44.898**	**45.058**	**43.929**	**43.938**	**44.379**	**43.932**	**43.713**	**43.884**

Sample No.	SL-13-37-25	SL-13-37-27	SL-13-37-27	SL-13-37-27	SL-13-37-27	SL-13-37-27	SL-13-37-27	SL-13-37-27	SL-13-37-27	SL-13-37-27	SL-13-37-27
Spot No.	11	1	2	3	4	5	6	7	8	9	10
SiO_2	35.762	35.372	35.25	35.339	34.995	35.202	35.347	34.937	35.139	35.21	35.204
Al_2O_3	0.005	-0.004	0.009	0.014	-0.005	0.006	-0.032	0	-0.018	0.001	0.004
Na_2O	-0.01	-0.001	-0.008	-0.008	0.006	0.01	0.008	0.005	0.005	-0.001	-0.001
MgO	26.4	23.908	23.812	24.026	23.71	23.802	24.186	23.855	23.951	23.863	23.981
FeO	36.969	40.353	40.27	40.107	39.965	39.973	39.979	39.701	40.04	40.132	39.8
MnO	0.781	0.881	0.846	0.855	0.883	0.879	0.866	0.87	0.894	0.872	0.869
Cr_2O_3	-0.002	0	-0.003	-0.011	-0.001	-0.007	-0.004	-0.009	-0.005	-0.007	0.005
CoO											
CaO	0.126	0.147	0.147	0.126	0.159	0.155	0.143	0.177	0.136	0.135	0.133
NiO	0.001	0.021	0	0.009	0.009	0.024	-0.028	-0.008	0.008	0.009	0.014
TiO_2	0.024	-0.001	0.041	0.046	0.018	0.013	0.017	0.042	0.039	0.045	0.048
Sc_2O_3	0.002	-0.016	-0.013	-0.018	-0.011	0.009	0.002	0.007	0.015	0.011	-0.009
Total	100.058	100.66	100.351	100.485	99.728	100.066	100.484	99.577	100.204	100.27	100.048
Si	1.002	1.003	1.002	1.002	1.001	1.003	1.002	1.000	1.000	1.002	1.002
Al	0.000	0.000	0.000	0.000	0.000	0.000	-0.001	0.000	-0.001	0.000	0.000
Na	-0.001	0.000	0.000	0.000	0.000	0.001	0.000	0.000	0.000	0.000	0.000
Mg	1.110	1.016	1.015	1.022	1.018	1.017	1.028	1.024	1.023	1.018	1.024
Fe	0.863	0.953	0.954	0.948	0.953	0.949	0.944	0.947	0.950	0.951	0.944
Mn	0.019	0.021	0.020	0.021	0.021	0.021	0.021	0.021	0.022	0.021	0.021
Cr	0.000	0.000	0.000	0.000	0.000	0.000	0.000	0.000	0.000	0.000	0.000
Co	0.000	0.000	0.000	0.000	0.000	0.000	0.000	0.000	0.000	0.000	0.000
Ca	0.004	0.004	0.004	0.004	0.005	0.005	0.004	0.005	0.004	0.004	0.004
Ni	0.000	0.000	0.000	0.000	0.000	0.001	-0.001	0.000	0.000	0.000	0.000
Ti	0.001	0.000	0.001	0.001	0.000	0.000	0.000	0.001	0.001	0.001	0.001
Sc	0.000	0.000	0.000	0.000	0.000	0.000	0.000	0.000	0.000	0.000	0.000

O	4.000	4.000	4.000	4.000	4.000	4.000	4.000	4.000	4.000	4.000	4.000
Fo	**56.244**	**51.608**	**51.559**	**51.883**	**51.641**	**51.733**	**52.129**	**51.959**	**51.847**	**51.698**	**52.028**
Fa	**43.756**	**48.392**	**48.441**	**48.117**	**48.359**	**48.267**	**47.871**	**48.041**	**48.153**	**48.302**	**47.972**

Sample No.	SL-13-37-37	SL-13-37-37	SL-13-37-37	SL-13-37-37	SL-13-37-37	SL-13-37-37	SL-13-37-37	SL-13-41-3	SL-13-41-3	SL-13-41-3	SL-13-41-3
Spot No.	1	2	3	4	5	6	7	1	2	3	4
SiO_2	35.304	35.389	35.399	35.34	35.583	35.475	35.835	32.607	32.413	32.513	32.373
Al_2O_3	0.014	-0.007	-0.013	0.012	0.025	-0.002	0.007	-0.004	-0.011	-0.023	-0.017
Na_2O	0.004	0.007	0.015	-0.014	-0.012	-0.002	0.005	0.009	-0.002	-0.012	0.013
MgO	24.525	24.851	24.607	25.168	25.18	25.092	25.124	11.808	11.671	11.735	11.565
FeO	38.85	38.769	38.914	38.239	38.097	38.405	38.241	54.614	54.344	54.51	54.222
MnO	0.835	0.845	0.846	0.824	0.804	0.84	0.862	1.471	1.464	1.501	1.443
Cr_2O_3	0.013	-0.013	0.006	-0.017	0.005	-0.01	0.007	0	0.025	0	0.006
CoO											
CaO	0.146	0.106	0.124	0.145	0.122	0.144	0.129	0.185	0.2	0.19	0.185
NiO	0.005	0.016	0.031	0.01	0.021	0.011	0.021	0.002	0.004	0.002	-0.013
TiO_2	0.03	0.02	0.028	0.046	0.05	0.051	0	0.032	0.043	0.044	0.024
Sc_2O_3	-0.021	-0.008	-0.007	-0.018	0.017	-0.007	-0.002	0.008	0.002	0.007	0.001
Total	99.705	99.975	99.95	99.735	99.892	99.997	100.229	100.732	100.153	100.467	99.802
Si	1.004	1.003	1.004	1.001	1.005	1.003	1.009	1.004	1.004	1.004	1.006
Al	0.000	0.000	0.000	0.000	0.001	0.000	0.000	0.000	0.000	-0.001	-0.001
Na	0.000	0.000	0.001	-0.001	-0.001	0.000	0.000	0.001	0.000	-0.001	0.001
Mg	1.046	1.056	1.047	1.070	1.067	1.064	1.061	0.545	0.542	0.543	0.539
Fe	0.920	0.915	0.920	0.903	0.897	0.905	0.897	1.401	1.403	1.403	1.404
Mn	0.020	0.020	0.020	0.020	0.019	0.020	0.021	0.038	0.038	0.039	0.038
Cr	0.000	0.000	0.000	0.000	0.000	0.000	0.000	0.000	0.001	0.000	0.000
Co	0.000	0.000	0.000	0.000	0.000	0.000	0.000	0.000	0.000	0.000	0.000
Ca	0.004	0.003	0.004	0.004	0.004	0.004	0.004	0.006	0.007	0.006	0.006
Ni	0.000	0.000	0.001	0.000	0.000	0.000	0.000	0.000	0.000	0.000	0.000
Ti	0.001	0.000	0.001	0.001	0.001	0.001	0.000	0.001	0.001	0.001	0.001
Sc	-0.001	0.000	0.000	0.000	0.000	0.000	0.000	0.000	0.000	0.000	0.000
O	4.000	4.000	4.000	4.000	4.000	4.000	4.000	4.000	4.000	4.000	4.000
Fo	**53.190**	**53.571**	**53.232**	**54.227**	**54.332**	**54.045**	**54.183**	**28.015**	**27.880**	**27.928**	**27.742**
Fa	**46.810**	**46.429**	**46.768**	**45.773**	**45.668**	**45.955**	**45.817**	**71.985**	**72.120**	**72.072**	**72.258**

Sample No.	SL-13-41-3	SL-13-41-3	SL-13-41-3	SL-13-41-3	SL-13-41-3	SL-13-41-3	SL-13-41-3	SL-13-41-3	SL-13-41-3	SL-13-41-3	SL-13-41-7.5
Spot No.	5	6	7	8	9	10	11	12	13	14	1
SiO_2	32.096	32.142	32.129	32.342	32.282	32.241	32.479	32.29	32.367	32.124	31.718
Al_2O_3	-0.002	-0.001	0.001	-0.007	-0.01	-0.015	-0.005	-0.016	-0.018	-0.012	-0.002

Na_2O	0.011	-0.01	0.021	0.005	0.005	-0.001	0	0	0.001	0.009	0.007
MgO	11.621	11.306	11.471	11.917	11.927	12.022	12.266	11.659	11.628	11.568	10.47
FeO	54.589	54.727	55.35	54.405	54.483	54.253	53.957	54.766	54.886	54.685	55.698
MnO	1.453	1.456	1.525	1.443	1.456	1.466	1.432	1.491	1.507	1.488	1.544
Cr_2O_3	0.005	0.008	-0.012	-0.003	-0.005	-0.002	0.002	-0.004	0.003	0.003	-0.011
CoO											
CaO	0.162	0.188	0.171	0.166	0.135	0.18	0.16	0.206	0.232	0.223	0.201
NiO	-0.017	-0.019	-0.015	0.007	0	-0.027	-0.016	0.024	-0.018	0.019	0.009
TiO_2	0.035	0.054	0.03	0.032	0.036	0.01	0.014	0.032	0.04	0.026	0.067
Sc_2O_3	-0.003	0.013	0.003	-0.012	-0.001	0.005	-0.002	0.01	-0.017	0.001	0.014
Total	99.95	99.864	100.674	100.295	100.308	100.132	100.287	100.458	100.611	100.134	99.715
Si	0.999	1.002	0.995	1.000	0.999	0.999	1.002	0.999	1.000	0.998	0.997
Al	0.000	0.000	0.000	0.000	0.000	-0.001	0.000	-0.001	-0.001	0.000	0.000
Na	0.001	-0.001	0.001	0.000	0.000	0.000	0.000	0.000	0.000	0.001	0.000
Mg	0.542	0.528	0.533	0.553	0.554	0.559	0.567	0.541	0.539	0.539	0.494
Fe	1.415	1.421	1.429	1.402	1.405	1.400	1.387	1.413	1.413	1.416	1.460
Mn	0.038	0.038	0.040	0.038	0.038	0.038	0.037	0.039	0.039	0.039	0.041
Cr	0.000	0.000	0.000	0.000	0.000	0.000	0.000	0.000	0.000	0.000	0.000
Co	0.000	0.000	0.000	0.000	0.000	0.000	0.000	0.000	0.000	0.000	0.000
Ca	0.005	0.006	0.006	0.006	0.004	0.006	0.005	0.007	0.008	0.007	0.007
Ni	0.000	0.000	0.000	0.000	0.000	-0.001	0.000	0.001	0.000	0.000	0.000
Ti	0.001	0.001	0.001	0.001	0.001	0.000	0.000	0.001	0.001	0.001	0.002
Sc	0.000	0.000	0.000	0.000	0.000	0.000	0.000	0.000	0.000	0.000	0.000
O	4.000	4.000	4.000	4.000	4.000	4.000	4.000	4.000	4.000	4.000	4.000
Fo	**27.703**	**27.106**	**27.169**	**28.278**	**28.266**	**28.513**	**29.037**	**27.704**	**27.607**	**27.577**	**25.282**
Fa	**72.297**	**72.894**	**72.831**	**71.722**	**71.734**	**71.487**	**70.963**	**72.296**	**72.393**	**72.423**	**74.718**

Sample No.	SL-13-41-7.5	SL-13-41-7.5	SL-13-41-7.5	SL-13-41-7.5	SL-13-41-7.5	SL-13-41-7.5	SL-13-41-7.5	SL-13-41-7.5	SL-13-41-12.1	SL-13-41-12.1	SL-13-41-12.1
Spot No.	2	3	4	5	6	7	8	9	1	2	3
SiO_2	31.463	31.398	31.478	31.573	31.246	31.419	31.327	31.53	33.158	33.427	33.272
Al_2O_3	-0.026	-0.002	-0.021	-0.009	-0.039	0	0	-0.003	-0.014	-0.027	-0.003
Na_2O	0.002	0.003	0.006	0.011	0.011	0.01	0.039	-0.015	0.007	-0.003	-0.019
MgO	10.32	9.77	9.928	9.797	9.11	9.725	9.628	9.884	15.274	15.362	15.633
FeO	55.77	56.779	55.819	56.346	57.032	56.675	56.575	56.538	49.63	49.446	49.335
MnO	1.525	1.545	1.556	1.55	1.555	1.53	1.566	1.572	1.418	1.41	1.448
Cr_2O_3	0.005	-0.002	0.005	-0.01	-0.009	-0.005	0.006	-0.005	-0.012	0.004	-0.014
CoO											
CaO	0.177	0.126	0.187	0.181	0.182	0.203	0.204	0.205	0.23	0.277	0.223
NiO	0.006	-0.021	-0.005	0.027	-0.006	-0.019	-0.004	-0.001	-0.021	0.014	-0.003

TiO_2	0.035	0.052	0.049	0.026	0.067	0.034	0.016	0.065	0.022	0.009	0.041
Sc_2O_3	0.008	0.02	0	-0.012	0.025	-0.005	-0.001	0.007	0.005	0.006	-0.003
Total	99.285	99.668	99.002	99.48	99.174	99.567	99.356	99.777	99.697	99.925	99.91
Si	0.996	0.994	1.000	1.000	0.998	0.996	0.996	0.996	1.005	1.009	1.004
Al	-0.001	0.000	-0.001	0.000	-0.001	0.000	0.000	0.000	0.000	-0.001	0.000
Na	0.000	0.000	0.000	0.001	0.001	0.001	0.002	-0.001	0.000	0.000	-0.001
Mg	0.490	0.464	0.473	0.465	0.436	0.462	0.459	0.468	0.694	0.695	0.707
Fe	1.471	1.499	1.478	1.487	1.518	1.497	1.498	1.488	1.253	1.243	1.240
Mn	0.041	0.041	0.042	0.042	0.042	0.041	0.042	0.042	0.036	0.036	0.037
Cr	0.000	0.000	0.000	0.000	0.000	0.000	0.000	0.000	0.000	0.000	0.000
Co	0.000	0.000	0.000	0.000	0.000	0.000	0.000	0.000	0.000	0.000	0.000
Ca	0.006	0.004	0.006	0.006	0.006	0.007	0.007	0.007	0.007	0.009	0.007
Ni	0.000	-0.001	0.000	0.001	0.000	0.000	0.000	0.000	-0.001	0.000	0.000
Ti	0.001	0.001	0.001	0.001	0.002	0.001	0.000	0.002	0.001	0.000	0.001
Sc	0.000	0.001	0.000	0.000	0.001	0.000	0.000	0.000	0.000	0.000	0.000
O	4.000	4.000	4.000	4.000	4.000	4.000	4.000	4.000	4.000	4.000	4.000
Fo	**24.986**	**23.648**	**24.251**	**23.837**	**22.331**	**23.598**	**23.449**	**23.936**	**35.648**	**35.866**	**36.321**
Fa	**75.014**	**76.352**	**75.749**	**76.163**	**77.669**	**76.402**	**76.551**	**76.064**	**64.352**	**64.134**	**63.679**

Sample No.	SL-13-41-12.1	SL-13-41-12.1	SL-13-41-12.1	SL-13-41-45	SL-13-41-45	SL-13-41-45	SL-13-41-45	SL-13-41-45	SL-13-41-45	SL-13-41-45	SL-13-41-45
Spot No.	4	5	6	1	2	3	4	5	6	7	8
SiO_2	33.202	33.108	33.302	33.494	33.425	33.307	33.463	33.226	33.575	32.704	33.071
Al_2O_3	0.005	0	-0.01	-0.015	-0.002	-0.012	-0.002	-0.005	0.002	-0.007	0.008
Na_2O	-0.007	0.009	0.029	-0.001	0.004	0.006	0.004	0.008	-0.006	0.012	-0.013
MgO	15.582	15.579	15.555	16.841	16.919	16.919	16.975	16.914	17.005	16.386	16.37
FeO	49.699	49.798	49.34	48.347	48.166	48.518	48.552	48.212	48.449	48.699	48.905
MnO	1.413	1.399	1.406	1.214	1.23	1.216	1.229	1.201	1.223	1.255	1.27
Cr_2O_3	0.01	0	-0.022	-0.011	0.012	0.002	-0.006	0.003	0.012	-0.002	-0.009
CoO											
CaO	0.149	0.18	0.164	0.184	0.175	0.16	0.175	0.154	0.151	0.174	0.179
NiO	-0.008	0.001	0.022	0.005	0.003	-0.013	-0.014	0.019	0.011	-0.003	0.017
TiO_2	0.037	0.042	0.054	0.048	0.036	0.03	0.027	0.048	0.051	0.03	0.03
Sc_2O_3	0.015	0.004	0.009	-0.008	-0.005	0.002	0.002	0.017	0.003	0.001	0.021
Total	100.097	100.12	99.849	100.098	99.963	100.135	100.405	99.797	100.476	99.249	99.849
Si	1.001	0.999	1.005	1.001	1.000	0.997	0.998	0.997	1.000	0.992	0.996
Al	0.000	0.000	0.000	-0.001	0.000	0.000	0.000	0.000	0.000	0.000	0.000
Na	0.000	0.001	0.002	0.000	0.000	0.000	0.000	0.000	0.000	0.001	-0.001
Mg	0.705	0.705	0.704	0.755	0.759	0.760	0.760	0.761	0.760	0.746	0.740
Fe	1.249	1.252	1.241	1.205	1.201	1.210	1.207	1.206	1.202	1.231	1.228

Mn	0.036	0.036	0.036	0.031	0.031	0.031	0.031	0.030	0.031	0.032	0.032
Cr	0.000	0.000	-0.001	0.000	0.000	0.000	0.000	0.000	0.000	0.000	0.000
Co	0.000	0.000	0.000	0.000	0.000	0.000	0.000	0.000	0.000	0.000	0.000
Ca	0.005	0.006	0.005	0.006	0.006	0.005	0.006	0.005	0.005	0.006	0.006
Ni	0.000	0.000	0.001	0.000	0.000	0.000	0.000	0.000	0.000	0.000	0.000
Ti	0.001	0.001	0.001	0.001	0.001	0.001	0.001	0.001	0.001	0.001	0.001
Sc	0.000	0.000	0.000	0.000	0.000	0.000	0.000	0.000	0.000	0.000	0.001
O	4.000	4.000	4.000	4.000	4.000	4.000	4.000	4.000	4.000	4.000	4.000
Fo	**36.076**	**36.025**	**36.203**	**38.537**	**38.736**	**38.563**	**38.625**	**38.706**	**38.717**	**37.720**	**37.598**
Fa	**63.924**	**63.975**	**63.797**	**61.463**	**61.264**	**61.437**	**61.375**	**61.294**	**61.283**	**62.280**	**62.402**

Sample No.	SL-13-41-45	SL-13-41-63.2	SL-13-41-63.2	SL-13-41-63.2	SL-13-41-63.2	SL-13-41-63.2	SL-13-41-63.2	SL-13-41-63.2	SL-13-41-63.2	SL-13-41-63.2	SL-13-41-68.9
Spot No.	9	1	2	3	4	5	6	7	8	9	1
SiO_2	33.151	33.918	34.185	33.943	34.063	34.162	34.073	34.112	33.828	34.365	34.747
Al_2O_3	-0.017	0.011	-0.016	-0.006	-0.017	-0.002	0.001	0.003	-0.012	-0.03	0.012
Na_2O	-0.001	0.026	-0.011	0.016	0.018	0.009	0.018	-0.003	0.009	0	0.034
MgO	16.561	19.853	20.027	19.714	19.808	19.844	19.791	19.812	19.914	19.932	20.786
FeO	49.062	45.073	44.949	45.017	45.145	45.009	45.192	45.313	45.092	45.152	43.204
MnO	1.276	1.011	1.042	1.039	1.089	1.059	1.056	1.052	1.084	1.069	1.009
Cr_2O_3	0.027	0.012	0.014	0.014	0	-0.008	0.01	-0.02	-0.016	-0.001	-0.008
CoO											
CaO	0.164	0.114	0.152	0.151	0.122	0.112	0.129	0.132	0.141	0.13	0.167
NiO	0.005	0.014	0.022	0.008	0.003	-0.011	-0.009	-0.006	0.012	-0.001	-0.011
TiO_2	0.061	0.024	0.034	0.026	0.035	0.041	0.041	0.049	0.05	0.022	0.013
Sc_2O_3	-0.005	-0.013	0.008	0.004	0.011	-0.02	0.012	0.017	-0.03	0.005	-0.025
Total	100.284	100.043	100.406	99.926	100.277	100.195	100.314	100.461	100.072	100.643	99.928
Si	0.994	0.996	0.998	0.998	0.998	1.000	0.998	0.997	0.994	1.001	1.009
Al	-0.001	0.000	-0.001	0.000	-0.001	0.000	0.000	0.000	0.000	-0.001	0.000
Na	0.000	0.001	-0.001	0.001	0.001	0.001	0.001	0.000	0.001	0.000	0.002
Mg	0.745	0.874	0.877	0.869	0.870	0.871	0.869	0.869	0.877	0.871	0.906
Fe	1.226	1.103	1.094	1.103	1.102	1.098	1.103	1.104	1.104	1.096	1.046
Mn	0.032	0.025	0.026	0.026	0.027	0.026	0.026	0.026	0.027	0.026	0.025
Cr	0.001	0.000	0.000	0.000	0.000	0.000	0.000	0.000	0.000	0.000	0.000
Co	0.000	0.000	0.000	0.000	0.000	0.000	0.000	0.000	0.000	0.000	0.000
Ca	0.005	0.004	0.005	0.005	0.004	0.004	0.004	0.004	0.004	0.004	0.005
Ni	0.000	0.000	0.001	0.000	0.000	0.000	0.000	0.000	0.000	0.000	0.000
Ti	0.001	0.001	0.001	0.001	0.001	0.001	0.001	0.001	0.001	0.000	0.000
Sc	0.000	0.000	0.000	0.000	0.000	-0.001	0.000	0.000	-0.001	0.000	-0.001
O	4.000	4.000	4.000	4.000	4.000	4.000	4.000	4.000	4.000	4.000	4.000

Fo	**37.795**	**44.222**	**44.506**	**44.080**	**44.127**	**44.246**	**44.080**	**44.040**	**44.288**	**44.277**	**46.410**
Fa	**62.205**	**55.778**	**55.494**	**55.920**	**55.873**	**55.754**	**55.920**	**55.960**	**55.712**	**55.723**	**53.590**

Sample No.	SL-13-41-68.9	SL-13-41-68.9	SL-13-41-68.9	SL-13-41-68.9	SL-13-41-68.9	SL-13-41-73	SL-13-41-73	SL-13-41-73	SL-13-41-73	SL-13-41-73	SL-13-41-73
Spot No.	2	3	4	5	6	1	2	3	4	5	6
SiO_2	34.27	35.348	34.773	34.864	35.587	35.036	35.269	35.156	35.392	35.306	35.322
Al_2O_3	-0.003	0.039	-0.01	-0.009	0.024	-0.008	0.031	0.001	0	-0.004	0.008
Na_2O	-0.002	-0.022	0.003	-0.009	0.012	-0.004	-0.004	0.001	0.013	-0.001	0.002
MgO	20.51	21.007	20.99	20.935	21.008	23.593	23.334	23.657	23.704	23.312	23.511
FeO	42.996	43.972	43.871	44.459	44.412	40.447	40.708	40.334	40.392	40.057	40.573
MnO	0.985	1.036	1.049	1.109	1.031	0.866	0.882	0.891	0.841	0.876	0.848
Cr_2O_3	-0.003	0.023	0.012	-0.014	0.007	-0.006	-0.003	-0.015	0.009	0.007	0.003
CoO											
CaO	0.179	0.177	0.136	0.13	0.14	0.147	0.142	0.149	0.116	0.157	0.15
NiO	-0.008	-0.006	-0.013	0.034	0.014	0.007	0.009	0.021	0.002	0.003	0.014
TiO_2	0.005	0.058	0.051	0.057	0.011	0.042	0.018	0.035	0.019	0.009	0.037
Sc_2O_3	0.013	0.007	0.015	-0.004	0.017	0.015	0.024	-0.004	0.01	-0.006	0.009
Total	98.942	101.639	100.877	101.552	102.263	100.135	100.41	100.226	100.498	99.716	100.477
Si	1.007	1.009	1.003	1.001	1.011	1.000	1.004	1.002	1.005	1.010	1.004
Al	0.000	0.001	0.000	0.000	0.001	0.000	0.001	0.000	0.000	0.000	0.000
Na	0.000	-0.001	0.000	-0.001	0.001	0.000	0.000	0.000	0.001	0.000	0.000
Mg	0.904	0.900	0.908	0.902	0.895	1.010	0.997	1.011	1.009	1.000	1.003
Fe	1.053	1.046	1.054	1.064	1.051	0.962	0.966	0.958	0.956	0.955	0.961
Mn	0.024	0.025	0.026	0.027	0.025	0.021	0.021	0.021	0.020	0.021	0.020
Cr	0.000	0.001	0.000	0.000	0.000	0.000	0.000	0.000	0.000	0.000	0.000
Co	0.000	0.000	0.000	0.000	0.000	0.000	0.000	0.000	0.000	0.000	0.000
Ca	0.006	0.005	0.004	0.004	0.004	0.004	0.004	0.005	0.004	0.005	0.005
Ni	0.000	0.000	0.000	0.001	0.000	0.000	0.000	0.000	0.000	0.000	0.000
Ti	0.000	0.001	0.001	0.001	0.000	0.001	0.000	0.001	0.000	0.000	0.001
Sc	0.000	0.000	0.000	0.000	0.000	0.000	0.001	0.000	0.000	0.000	0.000
O	4.000	4.000	4.000	4.000	4.000	4.000	4.000	4.000	4.000	4.000	4.000
Fo	**46.197**	**46.234**	**46.271**	**45.875**	**45.988**	**51.218**	**50.782**	**51.356**	**51.370**	**51.161**	**51.054**
Fa	**53.803**	**53.766**	**53.729**	**54.125**	**54.012**	**48.782**	**49.218**	**48.644**	**48.630**	**48.839**	**48.946**

Sample No.	SL-13-41-73	SL-13-41-73	SL-13-41-73	SL-13-41-73	SL-13-41-73	SL-13-41-73	SL-13-41-91	SL-13-41-91	SL-13-41-91	SL-13-41-91	SL-13-41-91
Spot No.	7	8	9	10	11	12	1	2	3	4	5
SiO_2	35.311	35.316	35.184	35.131	35.107	35.051	35.152	35.116	35.216	35.383	35.461
Al_2O_3	0.001	0.028	0.005	0.005	-0.019	0.002	-0.011	-0.012	0.017	-0.006	-0.018

Na_2O	0.012	0.013	-0.002	0	0.009	-0.008	0.007	0	-0.001	-0.005	-0.011
MgO	23.355	23.633	23.676	23.185	23.448	23.315	24.129	24.139	24.529	24.796	24.98
FeO	40.529	40.271	40.602	40.584	40.665	40.501	39.512	39.37	38.957	38.836	38.837
MnO	0.844	0.88	0.863	0.914	0.912	0.84	0.878	0.874	0.855	0.859	0.831
Cr_2O_3	-0.006	-0.003	0.011	-0.013	-0.002	0.011	0.01	-0.008	-0.02	-0.001	-0.01
CoO											
CaO	0.143	0.156	0.164	0.166	0.158	0.164	0.125	0.118	0.112	0.149	0.135
NiO	0	0.026	-0.013	-0.008	-0.012	-0.01	0.028	0.021	0.01	0.027	0.012
TiO_2	0.043	0.041	0.05	0.015	0.036	0.035	0.035	0.024	0.053	0.022	0.045
Sc_2O_3	0.01	0.014	0.005	0.013	-0.011	-0.003	0.003	-0.007	-0.011	0.011	-0.004
Total	100.242	100.375	100.545	99.992	100.291	99.898	99.868	99.635	99.717	100.071	100.258
Si	1.006	1.004	1.000	1.005	1.002	1.003	1.002	1.002	1.002	1.002	1.002
Al	0.000	0.001	0.000	0.000	-0.001	0.000	0.000	0.000	0.001	0.000	-0.001
Na	0.001	0.001	0.000	0.000	0.000	0.000	0.000	0.000	0.000	0.000	-0.001
Mg	0.998	1.008	1.010	0.995	1.003	1.001	1.031	1.034	1.047	1.053	1.058
Fe	0.962	0.954	0.962	0.967	0.967	0.966	0.938	0.937	0.924	0.916	0.914
Mn	0.020	0.021	0.021	0.022	0.022	0.020	0.021	0.021	0.021	0.021	0.020
Cr	0.000	0.000	0.000	0.000	0.000	0.000	0.000	0.000	0.000	0.000	0.000
Co	0.000	0.000	0.000	0.000	0.000	0.000	0.000	0.000	0.000	0.000	0.000
Ca	0.004	0.005	0.005	0.005	0.005	0.005	0.004	0.004	0.003	0.005	0.004
Ni	0.000	0.001	0.000	0.000	0.000	0.000	0.001	0.000	0.000	0.001	0.000
Ti	0.001	0.001	0.001	0.000	0.001	0.001	0.001	0.001	0.001	0.000	0.001
Sc	0.000	0.000	0.000	0.000	0.000	0.000	0.000	0.000	0.000	0.000	0.000
O	4.000	4.000	4.000	4.000	4.000	4.000	4.000	4.000	4.000	4.000	4.000
Fo	**50.914**	**51.370**	**51.211**	**50.698**	**50.930**	**50.889**	**52.363**	**52.463**	**53.126**	**53.472**	**53.656**
Fa	**49.086**	**48.630**	**48.789**	**49.302**	**49.070**	**49.111**	**47.637**	**47.537**	**46.874**	**46.528**	**46.344**

Sample No.	SL-13-41-91	SL-13-41-91	SL-13-41-91	SL-13-41-91	SL-13-41-109.1	SL-13-41-109.1	SL-13-41-109.1	SL-13-41-109.1	SL-13-41-109.1	SL-13-41-109.1	SL-13-41-109.1
Spot No.	6	7	8	9	1	2	3	4	5	6	7
SiO_2	35.378	35.429	35.385	35.452	35.942	35.885	35.966	35.925	36.016	36.05	35.822
Al_2O_3	-0.018	-0.043	0.011	0.001	-0.017	-0.001	0.001	-0.012	-0.002	0.013	-0.013
Na_2O	0.007	0.018	0.01	0.033	-0.018	0.009	0.017	0.016	0.042	0.016	0.017
MgO	24.762	24.263	24.43	24.39	27.49	27.732	27.602	27.383	27.382	27.371	27.488
FeO	38.946	39.22	39.432	39.077	36.042	35.95	36.201	36.336	36.465	36.254	36.352
MnO	0.844	0.813	0.842	0.811	0.719	0.75	0.696	0.756	0.725	0.749	0.752
Cr_2O_3	0.009	-0.004	-0.016	-0.026	-0.01	0.011	0.001	-0.001	0.016	-0.014	-0.005
CoO											
CaO	0.138	0.131	0.137	0.128	0.119	0.108	0.132	0.14	0.15	0.108	0.1
NiO	0.021	0.01	-0.022	0.008	0.005	0.008	-0.006	0.021	0.025	-0.003	0.005

TiO_2	0.031	0.032	0.015	-0.006	0.02	0.008	0.016	0.021	0.043	0.024	0.058
Sc_2O_3	0.004	-0.027	-0.007	-0.008	-0.004	-0.007	-0.002	0.017	-0.026	-0.007	0.001
Total	100.122	99.842	100.217	99.86	100.288	100.453	100.624	100.602	100.836	100.561	100.577
Si	1.002	1.007	1.003	1.007	0.999	0.996	0.997	0.998	0.998	1.000	0.995
Al	-0.001	-0.001	0.000	0.000	-0.001	0.000	0.000	0.000	0.000	0.000	0.000
Na	0.000	0.001	0.001	0.002	-0.001	0.000	0.001	0.001	0.002	0.001	0.001
Mg	1.052	1.035	1.039	1.039	1.147	1.155	1.148	1.141	1.138	1.139	1.145
Fe	0.919	0.929	0.931	0.925	0.835	0.832	0.836	0.841	0.842	0.838	0.842
Mn	0.020	0.020	0.020	0.019	0.017	0.018	0.016	0.018	0.017	0.018	0.018
Cr	0.000	0.000	0.000	-0.001	0.000	0.000	0.000	0.000	0.000	0.000	0.000
Co	0.000	0.000	0.000	0.000	0.000	0.000	0.000	0.000	0.000	0.000	0.000
Ca	0.004	0.004	0.004	0.004	0.004	0.003	0.004	0.004	0.004	0.003	0.003
Ni	0.000	0.000	-0.001	0.000	0.000	0.000	0.000	0.000	0.001	0.000	0.000
Ti	0.001	0.001	0.000	0.000	0.000	0.000	0.000	0.000	0.001	0.001	0.001
Sc	0.000	-0.001	0.000	0.000	0.000	0.000	0.000	0.000	-0.001	0.000	0.000
O	4.000	4.000	4.000	4.000	4.000	4.000	4.000	4.000	4.000	4.000	4.000
Fo	**53.368**	**52.686**	**52.723**	**52.907**	**57.857**	**58.133**	**57.849**	**57.564**	**57.477**	**57.608**	**57.647**
Fa	**46.632**	**47.314**	**47.277**	**47.093**	**42.143**	**41.867**	**42.151**	**42.436**	**42.523**	**42.392**	**42.353**

Sample No.	SL-13-41-109.1	SL-13-41-109.1	SL-13-41-109.1	SL-13-41-109.1	MW-07-06-3.4	MW-07-06-3.4	MW-07-06-3.4	MW-07-06-3.4	MW-07-06-3.4	MW-07-06-3.4	MW-07-06-3.4
Spot No.	8	9	10	11	1	2	3	4	5	6	7
SiO_2	36.041	35.735	36.007	36.076	32.982	32.883	32.719	32.803	32.789	32.94	33.19
Al_2O_3	-0.009	0.022	-0.003	-0.012	0.019	-0.022	-0.001	-0.023	-0.016	0.011	-0.02
Na_2O	0.014	0.004	0.017	0.014	-0.013	0.015	0.002	0.008	0.01	-0.019	-0.013
MgO	27.439	27.491	27.215	27.23	13.163	13.064	13.208	12.546	12.456	12.782	13.142
FeO	36.405	35.956	36.322	36.35	52.899	52.917	53.145	53.66	53.767	53.542	52.846
MnO	0.725	0.752	0.728	0.789	1.435	1.389	1.385	1.361	1.402	1.376	1.402
Cr_2O_3	-0.02	-0.01	-0.004	-0.007	-0.01	0.006	0.007	-0.002	-0.004	-0.007	0.008
CoO											
CaO	0.132	0.123	0.139	0.137	0.19	0.156	0.183	0.15	0.151	0.14	0.173
NiO	0.009	0.011	0.025	0.024	-0.007	0.014	0.009	0.01	0.017	0.024	-0.015
TiO_2	0.007	0.015	0.026	0.059	0.062	0.042	0.056	0.03	0.004	0.013	0.043
Sc_2O_3	-0.004	-0.009	-0.011	0.017	-0.001	0	0.001	0.016	0.001	-0.008	0.012
Total	100.739	100.09	100.461	100.677	100.719	100.464	100.714	100.559	100.577	100.794	100.768
Si	0.999	0.996	1.001	1.001	1.005	1.005	0.999	1.006	1.006	1.006	1.009
Al	0.000	0.001	0.000	0.000	0.001	-0.001	0.000	-0.001	-0.001	0.000	-0.001
Na	0.001	0.000	0.001	0.001	-0.001	0.001	0.000	0.000	0.001	-0.001	-0.001
Mg	1.141	1.150	1.135	1.133	0.601	0.599	0.605	0.577	0.573	0.585	0.599
Fe	0.841	0.835	0.841	0.840	1.343	1.348	1.352	1.371	1.374	1.362	1.339

Mn	0.017	0.018	0.017	0.019	0.037	0.036	0.036	0.035	0.036	0.036	0.036
Cr	0.000	0.000	0.000	0.000	0.000	0.000	0.000	0.000	0.000	0.000	0.000
Co	0.000	0.000	0.000	0.000	0.000	0.000	0.000	0.000	0.000	0.000	0.000
Ca	0.004	0.004	0.004	0.004	0.006	0.005	0.006	0.005	0.005	0.005	0.006
Ni	0.000	0.000	0.001	0.001	0.000	0.000	0.000	0.000	0.000	0.001	0.000
Ti	0.000	0.000	0.001	0.001	0.001	0.001	0.001	0.001	0.000	0.000	0.001
Sc	0.000	0.000	0.000	0.000	0.000	0.000	0.000	0.000	0.000	0.000	0.000
O	4.000	4.000	4.000	4.000	4.000	4.000	4.000	4.000	4.000	4.000	4.000
Fo	**57.568**	**57.917**	**57.423**	**57.418**	**30.934**	**30.766**	**30.908**	**29.620**	**29.428**	**30.056**	**30.922**
Fa	**42.432**	**42.083**	**42.577**	**42.582**	**69.066**	**69.234**	**69.092**	**70.380**	**70.572**	**69.944**	**69.078**

Sample No.	MW-07-06-3.4	MW-07-06-3.4	MW-07-06-9.4	MW-07-06-9.4	MW-07-06-9.4	MW-07-06-9.4	MW-07-06-9.4	MW-07-06-9.4	MW-07-06-9.4	MW-07-06-13.4	MW-07-06-13.4
Spot No.	8	9	1	2	3	4	5	6	7	1	2
SiO_2	33.037	32.982	32.94	32.955	32.939	33.077	32.717	32.644	32.967	32.852	33.202
Al_2O_3	-0.003	0.003	-0.001	-0.01	-0.018	-0.011	0.001	0.008	-0.016	0.008	-0.003
Na_2O	-0.016	-0.01	0.018	0.03	0.003	-0.002	0.018	0.023	0.016	-0.006	0.003
MgO	13.076	12.997	13.994	13.957	13.893	13.963	13.616	13.555	13.558	14.232	14.048
FeO	53.136	53.044	51.827	51.834	51.848	51.546	51.985	52.455	52.533	50.863	50.952
MnO	1.364	1.361	1.394	1.369	1.331	1.342	1.378	1.378	1.386	1.337	1.335
Cr_2O_3	0.001	0.004	-0.004	0	0	0.004	-0.006	0.006	0.003	-0.004	-0.004
CoO											
CaO	0.167	0.156	0.176	0.171	0.168	0.137	0.176	0.182	0.179	0.16	0.147
NiO	0.028	-0.018	0.004	0.009	0.002	-0.023	0.003	-0.017	0.009	0.01	0.009
TiO_2	0.053	0.031	0.027	0.019	0.016	0.029	0.03	0.033	0.03	0.034	0.051
Sc_2O_3	-0.003	0.003	0.011	-0.008	0.015	-0.003	0.005	-0.017	0.01	-0.007	-0.009
Total	100.84	100.553	100.386	100.326	100.197	100.059	99.923	100.25	100.675	99.479	99.731
Si	1.006	1.007	1.002	1.003	1.004	1.007	1.002	0.999	1.003	1.005	1.012
Al	0.000	0.000	0.000	0.000	-0.001	0.000	0.000	0.000	-0.001	0.000	0.000
Na	-0.001	-0.001	0.001	0.002	0.000	0.000	0.001	0.001	0.001	0.000	0.000
Mg	0.597	0.595	0.639	0.637	0.635	0.638	0.626	0.622	0.619	0.653	0.642
Fe	1.348	1.350	1.314	1.315	1.317	1.308	1.327	1.337	1.332	1.296	1.294
Mn	0.035	0.035	0.036	0.035	0.034	0.035	0.036	0.036	0.036	0.035	0.034
Cr	0.000	0.000	0.000	0.000	0.000	0.000	0.000	0.000	0.000	0.000	0.000
Co	0.000	0.000	0.000	0.000	0.000	0.000	0.000	0.000	0.000	0.000	0.000
Ca	0.005	0.005	0.006	0.006	0.005	0.004	0.006	0.006	0.006	0.005	0.005
Ni	0.001	0.000	0.000	0.000	0.000	-0.001	0.000	0.000	0.000	0.000	0.000
Ti	0.001	0.001	0.001	0.000	0.000	0.001	0.001	0.001	0.001	0.001	0.001
Sc	0.000	0.000	0.000	0.000	0.000	0.000	0.000	0.000	0.000	0.000	0.000
O	4.000	4.000	4.000	4.000	4.000	4.000	4.000	4.000	4.000	4.000	4.000

Fo	**30.698**	**30.606**	**32.706**	**32.645**	**32.538**	**32.777**	**32.040**	**31.747**	**31.720**	**33.496**	**33.168**
Fa	**69.302**	**69.394**	**67.294**	**67.355**	**67.462**	**67.223**	**67.960**	**68.253**	**68.280**	**66.504**	**66.832**

Sample No.	MW-07-06-13.4	MW-07-06-13.4	MW-07-06-13.4	MW-07-06-13.4	MW-07-06-13.4	MW-07-06-13.4	MW-07-06-13.4	MW-07-06-17.4	MW-07-06-17.4	MW-07-06-17.4	MW-07-06-17.4
Spot No.	3	4	5	6	7	8	9	1	2	3	4
SiO_2	32.876	33.534	33.349	33.474	33.501	33.413	33.448	33.439	33.471	33.384	33.34
Al_2O_3	0.017	-0.002	0.022	0.009	-0.014	0.002	-0.001	0.019	0	0.018	-0.003
Na_2O	-0.001	0.003	0.01	0.001	-0.007	0.01	-0.004	-0.008	0.004	0.007	-0.001
MgO	14.006	15.78	15.738	15.728	15.809	15.951	15.649	14.816	14.93	14.569	14.317
FeO	50.999	49.094	49.246	49.28	49.247	48.822	48.929	50.032	50.263	50.306	50.709
MnO	1.32	1.216	1.196	1.246	1.306	1.282	1.278	1.264	1.246	1.303	1.263
Cr_2O_3	-0.004	-0.003	0.014	-0.002	0.011	0.003	-0.009	0.002	0.004	0.004	-0.002
CoO											
CaO	0.164	0.154	0.125	0.125	0.145	0.141	0.162	0.152	0.177	0.147	0.168
NiO	0.006	0.008	0.006	-0.036	0.006	0.016	0	0.005	0.005	0.015	0.019
TiO_2	0.04	0.03	0.052	0.057	0.042	0.034	0.028	0.023	0.026	0.032	0.043
Sc_2O_3	-0.011	-0.01	-0.008	-0.013	-0.009	-0.005	0.003	-0.012	0.004	0.002	0.015
Total	99.412	99.804	99.75	99.869	100.037	99.669	99.483	99.732	100.13	99.787	99.868
Si	1.007	1.009	1.006	1.008	1.007	1.007	1.010	1.013	1.010	1.012	1.012
Al	0.001	0.000	0.001	0.000	0.000	0.000	0.000	0.001	0.000	0.001	0.000
Na	0.000	0.000	0.001	0.000	0.000	0.001	0.000	0.000	0.000	0.000	0.000
Mg	0.643	0.713	0.712	0.710	0.713	0.721	0.709	0.673	0.676	0.663	0.652
Fe	1.301	1.232	1.238	1.236	1.234	1.226	1.232	1.263	1.264	1.271	1.283
Mn	0.034	0.031	0.031	0.032	0.033	0.033	0.033	0.032	0.032	0.033	0.032
Cr	0.000	0.000	0.000	0.000	0.000	0.000	0.000	0.000	0.000	0.000	0.000
Co	0.000	0.000	0.000	0.000	0.000	0.000	0.000	0.000	0.000	0.000	0.000
Ca	0.005	0.005	0.004	0.004	0.005	0.005	0.005	0.005	0.006	0.005	0.005
Ni	0.000	0.000	0.000	-0.001	0.000	0.000	0.000	0.000	0.000	0.000	0.000
Ti	0.001	0.001	0.001	0.001	0.001	0.001	0.001	0.001	0.001	0.001	0.001
Sc	0.000	0.000	0.000	0.000	0.000	0.000	0.000	0.000	0.000	0.000	0.000
O	4.000	4.000	4.000	4.000	4.000	4.000	4.000	4.000	4.000	4.000	4.000
Fo	**33.081**	**36.651**	**36.518**	**36.487**	**36.622**	**37.031**	**36.536**	**34.770**	**34.839**	**34.266**	**33.696**
Fa	**66.919**	**63.349**	**63.482**	**63.513**	**63.378**	**62.969**	**63.464**	**65.230**	**65.161**	**65.734**	**66.304**

Sample No.	MW-07-06-17.4	MW-07-06-17.4	MW-07-06-17.4	MW-07-06-17.4	MW-07-06-17.4	MW-07-06-23.4	MW-07-06-23.4	MW-07-06-23.4	MW-07-06-23.4	MW-07-06-23.4	MW-07-06-23.4
Spot No.	5	6	7	8	9	1	2	3	4	5	6

SiO_2	33.142	33.157	33.443	33.413	33.453	33.066	32.885	32.864	33.048	33.182	32.966
Al_2O_3	-0.008	0.012	0	0.007	-0.011	-0.002	-0.001	-0.013	-0.024	0.007	-0.017
Na_2O	-0.006	-0.007	0.088	0.011	0.006	0.003	0.007	0.015	-0.025	-0.002	-0.009
MgO	14.564	14.411	14.967	14.941	14.813	12.946	12.763	13.043	12.908	13.041	12.869
FeO	50.397	50.627	50.165	50.048	50.252	52.545	52.717	52.406	52.761	52.571	52.582
MnO	1.255	1.237	1.234	1.247	1.249	1.415	1.417	1.394	1.384	1.377	1.45
Cr_2O_3	-0.003	-0.006	0.014	-0.013	-0.021	0.022	0.026	-0.001	0.032	0	-0.012
CoO											
CaO	0.154	0.144	0.168	0.157	0.172	0.145	0.105	0.124	0.137	0.121	0.126
NiO	-0.014	0.008	0.025	-0.002	0.003	-0.008	-0.034	0.01	0.006	-0.008	0.022
TiO_2	0.036	0.046	0.046	0.019	0.024	0.001	0.027	0.044	0.021	0.058	0.034
Sc_2O_3	0.012	0.006	-0.004	0.004	0.014	0.002	0.018	0.001	-0.012	0.004	0
Total	99.529	99.635	100.146	99.832	99.954	100.135	99.93	99.887	100.236	100.351	100.011
Si	1.009	1.009	1.009	1.011	1.012	1.012	1.010	1.009	1.011	1.012	1.011
Al	0.000	0.000	0.000	0.000	0.000	0.000	0.000	0.000	-0.001	0.000	-0.001
Na	0.000	0.000	0.005	0.001	0.000	0.000	0.000	0.001	-0.001	0.000	-0.001
Mg	0.665	0.658	0.677	0.678	0.672	0.594	0.588	0.600	0.592	0.597	0.592
Fe	1.279	1.284	1.262	1.262	1.266	1.340	1.349	1.340	1.345	1.336	1.344
Mn	0.032	0.032	0.031	0.032	0.032	0.037	0.037	0.036	0.036	0.036	0.038
Cr	0.000	0.000	0.000	0.000	-0.001	0.001	0.001	0.000	0.001	0.000	0.000
Co	0.000	0.000	0.000	0.000	0.000	0.000	0.000	0.000	0.000	0.000	0.000
Ca	0.005	0.005	0.005	0.005	0.006	0.005	0.003	0.004	0.004	0.004	0.004
Ni	0.000	0.000	0.001	0.000	0.000	0.000	-0.001	0.000	0.000	0.000	0.001
Ti	0.001	0.001	0.001	0.000	0.001	0.000	0.001	0.001	0.000	0.001	0.001
Sc	0.000	0.000	0.000	0.000	0.000	0.000	0.000	0.000	0.000	0.000	0.000
O	4.000	4.000	4.000	4.000	4.000	4.000	4.000	4.000	4.000	4.000	4.000
Fo	**34.218**	**33.879**	**34.940**	**34.953**	**34.666**	**30.723**	**30.352**	**30.939**	**30.573**	**30.868**	**30.581**
Fa	**65.782**	**66.121**	**65.060**	**65.047**	**65.334**	**69.277**	**69.648**	**69.061**	**69.427**	**69.132**	**69.419**

Sample No.	MW-07-06-23.4	MW-07-06-23.4	MW-07-06-23.4	MW-07-06-36.15	MW-07-06-36.15	MW-07-06-36.15	MW-07-06-36.15	MW-07-06-36.15	MW-07-06-36.15	MW-07-06-36.15	MW-07-06-36.15
Spot No.	7	8	9	1	2	3	4	5	6	7	8
SiO_2	32.879	32.834	32.799	33.013	33.087	33.056	33.03	33.025	33.136	33.054	33.015
Al_2O_3	-0.013	0.011	-0.005	0.013	0.007	-0.014	0.002	0.007	-0.009	-0.001	-0.005
Na_2O	0.016	0.002	-0.013	0.016	0.008	-0.002	0.02	-0.01	-0.002	-0.002	0.001
MgO	12.088	12.265	12.258	15.854	15.918	15.925	15.282	15.341	15.237	15.293	15.295
FeO	53.392	53.412	53.36	49.687	49.43	49.654	50.282	50.1	50.549	50.409	50.484
MnO	1.442	1.438	1.441	1.282	1.312	1.263	1.308	1.268	1.283	1.293	1.298
Cr_2O_3	0.015	-0.018	-0.01	0.004	0.004	-0.005	0.012	0.007	-0.013	0.001	0.017

CoO											
CaO	0.152	0.146	0.128	0.157	0.122	0.143	0.167	0.162	0.162	0.157	0.137
NiO	-0.003	-0.003	0.001	0.025	0.006	0.005	-0.003	0.012	-0.025	-0.003	0.002
TiO_2	0.026	0.035	0.011	0.032	0.025	0.031	0.042	0.028	0.049	0.035	0.039
Sc_2O_3	0.001	-0.015	0.011	-0.007	0.016	0.02	0.001	-0.004	-0.012	0.003	-0.001
Total	99.995	100.107	99.981	100.076	99.935	100.076	100.143	99.936	100.355	100.239	100.282
Si	1.013	1.010	1.011	0.996	0.998	0.997	0.999	1.000	1.000	0.999	0.998
Al	0.000	0.000	0.000	0.000	0.000	0.000	0.000	0.000	0.000	0.000	0.000
Na	0.001	0.000	-0.001	0.001	0.000	0.000	0.001	-0.001	0.000	0.000	0.000
Mg	0.559	0.566	0.567	0.718	0.720	0.720	0.693	0.697	0.690	0.693	0.693
Fe	1.371	1.370	1.370	1.249	1.243	1.248	1.267	1.264	1.272	1.269	1.271
Mn	0.038	0.037	0.038	0.033	0.033	0.032	0.033	0.032	0.033	0.033	0.033
Cr	0.000	0.000	0.000	0.000	0.000	0.000	0.000	0.000	0.000	0.000	0.000
Co	0.000	0.000	0.000	0.000	0.000	0.000	0.000	0.000	0.000	0.000	0.000
Ca	0.005	0.005	0.004	0.005	0.004	0.005	0.005	0.005	0.005	0.005	0.004
Ni	0.000	0.000	0.000	0.001	0.000	0.000	0.000	0.000	-0.001	0.000	0.000
Ti	0.001	0.001	0.000	0.001	0.001	0.001	0.001	0.001	0.001	0.001	0.001
Sc	0.000	0.000	0.000	0.000	0.000	0.001	0.000	0.000	0.000	0.000	0.000
O	4.000	4.000	4.000	4.000	4.000	4.000	4.000	4.000	4.000	4.000	4.000
Fo	**28.953**	**29.245**	**29.254**	**36.481**	**36.695**	**36.600**	**35.362**	**35.533**	**35.173**	**35.320**	**35.289**
Fa	**71.047**	**70.755**	**70.746**	**63.519**	**63.305**	**63.400**	**64.638**	**64.467**	**64.827**	**64.680**	**64.711**

Sample No.	MW-07-06-36.15	MW-07-06-37.5	MW-07-06-37.5	MW-07-06-37.5	MW-07-06-37.5	MW-07-06-37.5	MW-07-06-37.5	MW-07-06-37.5	MW-07-06-37p5_Ol3_spot3	MW-07-06-41	MW-07-06-41
Spot No.	9	1	2	3	4	5	6	7	8	1	2
SiO_2	32.964	33.32	33.241	33.213	33.355	33.497	33.541	33.682	33.395	34.097	34.064
Al_2O_3	0.007	-0.003	-0.004	0.005	-0.006	-0.007	0.01	-0.035	0.007	0.008	-0.004
Na_2O	0.007	-0.003	-0.006	0.01	-0.001	-0.003	0.003	0.017	0.003	0.022	-0.011
MgO	15.172	16.502	16.502	16.577	16.683	16.826	16.501	16.635	16.66	18.245	18.15
FeO	50.222	48.795	48.531	48.507	48.289	48.168	48.614	48.645	48.548	46.533	46.429
MnO	1.3	1.164	1.159	1.184	1.201	1.186	1.237	1.214	1.178	1.017	1.085
Cr_2O_3	0.005	-0.003	-0.002	-0.032	-0.018	-0.003	0.006	0.003	0	0.006	0.008
CoO											
CaO	0.154	0.176	0.191	0.203	0.195	0.178	0.118	0.131	0.101	0.188	0.182
NiO	0.012	0.006	0.031	-0.031	0.019	-0.004	-0.008	-0.009	0.014	-0.008	0.013
TiO_2	0.052	0.031	0.058	0.061	0.035	0.033	0.026	0.021	0.009	0.014	0.05
Sc_2O_3	0.01	0.007	-0.006	-0.003	0.001	-0.016	0.001	0.002	-0.008	-0.011	0.012
Total	99.905	99.992	99.695	99.694	99.753	99.855	100.049	100.306	99.907	100.111	99.978
Si	0.999	1.000	1.000	0.999	1.001	1.003	1.004	1.005	1.002	1.007	1.007

Al	0.000	0.000	0.000	0.000	0.000	0.000	0.000	-0.001	0.000	0.000	0.000
Na	0.000	0.000	0.000	0.001	0.000	0.000	0.000	0.001	0.000	0.001	-0.001
Mg	0.690	0.743	0.745	0.748	0.751	0.756	0.741	0.745	0.749	0.808	0.805
Fe	1.269	1.220	1.217	1.216	1.208	1.202	1.213	1.210	1.213	1.145	1.144
Mn	0.033	0.030	0.029	0.030	0.030	0.030	0.031	0.031	0.030	0.025	0.027
Cr	0.000	0.000	0.000	-0.001	0.000	0.000	0.000	0.000	0.000	0.000	0.000
Co	0.000	0.000	0.000	0.000	0.000	0.000	0.000	0.000	0.000	0.000	0.000
Ca	0.005	0.006	0.006	0.007	0.006	0.006	0.004	0.004	0.003	0.006	0.006
Ni	0.000	0.000	0.001	-0.001	0.000	0.000	0.000	0.000	0.000	0.000	0.000
Ti	0.001	0.001	0.001	0.001	0.001	0.001	0.001	0.000	0.000	0.000	0.001
Sc	0.000	0.000	0.000	0.000	0.000	0.000	0.000	0.000	0.000	0.000	0.000
O	4.000	4.000	4.000	4.000	4.000	4.000	4.000	4.000	4.000	4.000	4.000
Fo	**35.224**	**37.840**	**37.967**	**38.086**	**38.343**	**38.604**	**37.926**	**38.101**	**38.184**	**41.375**	**41.303**
Fa	**64.776**	**62.160**	**62.033**	**61.914**	**61.657**	**61.396**	**62.074**	**61.899**	**61.816**	**58.625**	**58.697**

Sample No.	MW-07-06-41	MW-07-06-41	MW-07-06-41	MW-07-06-41	MW-07-06-41	MW-07-06-41	MW-07-06-41	MW-07-06-41	MW-07-06-41	MW-07-06-41	MW-07-06-41
Spot No.	3	4	5	6	7	8	9	10	11	12	13
SiO_2	34.134	34.072	33.882	33.99	34.07	34.027	34.106	33.915	33.904	33.776	33.592
Al_2O_3	0	-0.005	-0.03	0.003	0.003	-0.017	-0.002	-0.018	-0.008	-0.003	-0.004
Na_2O	-0.009	0.006	0.003	-0.004	0.006	-0.004	-0.01	0.002	-0.002	-0.003	-0.014
MgO	18.22	17.792	17.673	17.917	18.643	18.688	18.55	17.222	17.386	17.404	15.99
FeO	46.613	47.126	47.212	46.837	46.356	46.28	46.207	47.647	47.674	47.84	49.452
MnO	1.059	1.085	1.082	1.086	1.073	1.055	1.098	1.078	1.076	1.1	1.109
Cr_2O_3	-0.011	0.006	0.003	0	-0.012	0.009	-0.025	0	0.001	0.005	0.018
CoO											
CaO	0.179	0.162	0.161	0.172	0.154	0.157	0.201	0.154	0.167	0.149	0.133
NiO	0.015	-0.016	0.004	-0.003	-0.009	0.012	0.003	-0.009	-0.017	-0.018	0.018
TiO_2	0.033	0.003	0.021	0.039	0.04	0.05	0	0.03	0.036	0.016	0.052
Sc_2O_3	-0.006	0.01	0.005	0.007	0.01	-0.029	-0.001	-0.009	-0.012	0.017	0.012
Total	100.227	100.241	100.016	100.044	100.334	100.228	100.127	100.012	100.205	100.283	100.358
Si	1.007	1.008	1.006	1.007	1.003	1.003	1.006	1.009	1.007	1.003	1.006
Al	0.000	0.000	-0.001	0.000	0.000	-0.001	0.000	-0.001	0.000	0.000	0.000
Na	-0.001	0.000	0.000	0.000	0.000	0.000	-0.001	0.000	0.000	0.000	-0.001
Mg	0.806	0.790	0.787	0.796	0.823	0.826	0.821	0.769	0.774	0.776	0.718
Fe	1.146	1.162	1.168	1.156	1.137	1.137	1.135	1.181	1.180	1.184	1.234
Mn	0.026	0.027	0.027	0.027	0.027	0.026	0.027	0.027	0.027	0.028	0.028
Cr	0.000	0.000	0.000	0.000	0.000	0.000	-0.001	0.000	0.000	0.000	0.000
Co	0.000	0.000	0.000	0.000	0.000	0.000	0.000	0.000	0.000	0.000	0.000
Ca	0.006	0.005	0.005	0.005	0.005	0.005	0.006	0.005	0.005	0.005	0.004

Ni	0.000	0.000	0.000	0.000	0.000	0.000	0.000	0.000	0.000	0.000	0.000
Ti	0.001	0.000	0.000	0.001	0.001	0.001	0.000	0.001	0.001	0.000	0.001
Sc	0.000	0.000	0.000	0.000	0.000	-0.001	0.000	0.000	0.000	0.000	0.000
O	4.000	4.000	4.000	4.000	4.000	4.000	4.000	4.000	4.000	4.000	4.000
Fo	**41.300**	**40.461**	**40.256**	**40.778**	**41.992**	**42.091**	**41.949**	**39.416**	**39.629**	**39.571**	**36.790**
Fa	**58.700**	**59.539**	**59.744**	**59.222**	**58.008**	**57.909**	**58.051**	**60.584**	**60.371**	**60.429**	**63.210**

Appendix 9. Mineral chemical data of clinopyroxene determined by electron microprobe. Sample names can be referred to appendix 3.

Sample No.	FD-13-34-5	FD-13-34-5	FD-13-34-5	FD-13-34-5	FD-13-34-5	FD-13-34-18.6	FD-13-34-24	FD-13-34-24	FD-13-34-24	FD-13-34-24	FD-13-34-24	FD-13-34-24
Spot	1	2	3	4	5	1	1	2	3	4	5	6
SiO_2	51.838	51.329	50.939	50.766	50.459	50.002	49.715	50.401	50.923	50.073	49.792	50.322
Al_2O_3	2.321	2.298	2.767	3.045	2.766	3.062	3.166	2.429	2.035	3.028	3.150	2.447
MgO	12.935	12.913	12.814	12.766	12.423	12.764	12.947	13.004	12.779	13.119	12.745	12.675
Na_2O	0.476	0.473	0.429	0.472	0.395	0.438	0.371	0.349	0.385	0.394	0.361	0.346
FeO	10.417	10.414	10.497	10.495	11.383	10.392	10.292	10.256	10.590	10.258	10.908	10.734
MnO	0.269	0.285	0.293	0.291	0.246	0.244	0.267	0.254	0.328	0.250	0.303	0.259
Cr_2O_3	0.025	-0.045	0.016	0.012	0.000	-0.005	-0.016	0.003	0.030	0.025	-0.009	0.003
K_2O	0.001	0.010	0.006	-0.002	0.000	0.009	0.013	0.006	0.001	0.005	0.009	0.005
CaO	21.636	21.570	21.452	21.343	20.989	21.010	21.235	21.494	21.688	21.259	21.128	21.638
NiO	0.013	0.005	0.009	0.010	0.019	0.008	-0.002	0.016	-0.006	-0.003	-0.018	0.006
TiO_2	0.848	0.847	1.003	1.086	1.168	1.047	1.033	0.722	0.529	1.006	1.021	0.741
Sc_2O_3	-0.013	-0.027	-0.061	-0.036	-0.029	-0.054	-0.038	-0.046	-0.032	-0.040	-0.044	-0.009
Total	100.766	100.072	100.164	100.248	99.819	98.917	98.983	98.888	99.250	99.374	99.346	99.167
Si	1.932	1.928	1.912	1.904	1.907	1.900	1.890	1.917	1.933	1.895	1.890	1.914
Al	0.153	0.152	0.183	0.202	0.185	0.205	0.212	0.163	0.136	0.202	0.211	0.164
Mg	0.723	0.727	0.722	0.718	0.704	0.728	0.738	0.742	0.727	0.745	0.726	0.723
Na	0.017	0.017	0.016	0.017	0.014	0.016	0.014	0.013	0.014	0.014	0.013	0.013
Fe	0.323	0.326	0.328	0.328	0.359	0.329	0.326	0.325	0.335	0.323	0.345	0.340
Mn	0.008	0.009	0.009	0.009	0.008	0.008	0.009	0.008	0.011	0.008	0.010	0.008
Cr	0.001	-0.001	0.000	0.000	0.000	0.000	0.000	0.000	0.001	0.001	0.000	0.000
K	0.000	0.000	0.000	0.000	0.000	0.000	0.001	0.000	0.000	0.000	0.000	0.000
Ca	0.864	0.868	0.863	0.858	0.850	0.856	0.865	0.876	0.882	0.862	0.859	0.882
Ni	0.000	0.000	0.000	0.000	0.001	0.000	0.000	0.000	0.000	0.000	-0.001	0.000
Ti	0.024	0.024	0.028	0.031	0.033	0.030	0.029	0.021	0.015	0.029	0.029	0.021
Sc	0.000	-0.001	-0.002	-0.001	-0.001	-0.002	-0.001	-0.002	-0.001	-0.001	-0.001	0.000

O	6.000	6.000	6.000	6.000	6.000	6.000	6.000	6.000	6.000	6.000	6.000	6.000
Mg#	**69.089**	**69.059**	**68.724**	**68.647**	**66.267**	**68.856**	**69.366**	**69.533**	**68.475**	**69.716**	**67.775**	**68.005**
Fe	**16.933**	**16.964**	**17.168**	**17.229**	**18.744**	**17.211**	**16.900**	**16.731**	**17.226**	**16.760**	**17.878**	**17.491**
Ca	**45.219**	**45.175**	**45.109**	**45.048**	**44.436**	**44.738**	**44.832**	**45.083**	**45.358**	**44.658**	**44.522**	**45.333**
Mg	**37.848**	**37.862**	**37.723**	**37.723**	**36.821**	**38.051**	**38.268**	**38.186**	**37.416**	**38.582**	**37.600**	**37.177**

Sample No.	FD-13-34-24	FD-13-34-24	FD-13-34-24	FD-13-34-27.9	FD-13-34-27.9	FD-13-34-27.9	FD-13-34-27.9	FD-13-34-33	FD-13-34-33	FD-13-34-33	FD-13-34-33	FD-13-34-46.1
Spot	7	8	9	1	2	3	4	1	2	3	4	1
SiO_2	51.119	51.218	50.155	51.145	50.557	50.182	51.383	51.365	51.414	50.290	50.200	50.262
Al_2O_3	1.994	1.942	2.774	2.105	2.710	2.731	2.053	2.155	2.149	3.008	2.995	2.957
MgO	12.732	12.671	12.503	13.146	12.999	12.780	13.284	13.320	13.368	12.838	12.909	13.012
Na_2O	0.372	0.382	0.447	0.473	0.408	0.395	0.472	0.467	0.457	0.389	0.465	0.400
FeO	11.239	11.049	10.830	9.826	10.781	10.696	9.767	9.597	9.568	10.743	10.474	10.523
MnO	0.319	0.314	0.322	0.237	0.320	0.307	0.277	0.226	0.215	0.269	0.254	0.257
Cr_2O_3	0.011	0.014	-0.028	-0.035	0.003	-0.031	0.035	0.014	0.019	0.020	-0.041	0.013
K_2O	0.003	0.003	0.004	-0.002	-0.003	-0.003	0.002	0.001	0.000	-0.002	0.004	0.001
CaO	21.760	21.712	21.546	21.867	21.355	21.197	21.878	22.069	21.955	21.224	21.305	21.143
NiO	0.010	-0.008	-0.016	0.002	-0.008	0.002	0.016	0.020	0.006	0.013	-0.004	0.013
TiO_2	0.524	0.536	0.894	0.633	0.902	0.917	0.621	0.717	0.701	1.043	1.041	1.090
Sc_2O_3	-0.030	-0.028	-0.037	-0.045	-0.025	-0.031	-0.043	-0.012	-0.021	-0.035	-0.039	-0.042
Total	100.053	99.805	99.394	99.352	99.999	99.142	99.745	99.939	99.831	99.800	99.563	99.629
Si	1.930	1.936	1.904	1.932	1.905	1.907	1.933	1.927	1.930	1.898	1.898	1.898
Al	0.133	0.130	0.186	0.140	0.180	0.183	0.136	0.143	0.142	0.200	0.200	0.197
Mg	0.721	0.718	0.712	0.745	0.735	0.728	0.749	0.750	0.753	0.727	0.732	0.737
Na	0.014	0.014	0.016	0.017	0.015	0.015	0.017	0.017	0.017	0.014	0.017	0.015
Fe	0.354	0.348	0.343	0.309	0.339	0.339	0.306	0.300	0.299	0.338	0.330	0.331
Mn	0.010	0.010	0.010	0.008	0.010	0.010	0.009	0.007	0.007	0.009	0.008	0.008
Cr	0.000	0.000	-0.001	-0.001	0.000	-0.001	0.001	0.000	0.001	0.001	-0.001	0.000
K	0.000	0.000	0.000	0.000	0.000	0.000	0.000	0.000	0.000	0.000	0.000	0.000
Ca	0.880	0.879	0.877	0.885	0.862	0.863	0.882	0.887	0.883	0.858	0.863	0.855
Ni	0.000	0.000	0.000	0.000	0.000	0.000	0.000	0.001	0.000	0.000	0.000	0.000
Ti	0.015	0.015	0.025	0.018	0.025	0.026	0.018	0.020	0.020	0.030	0.030	0.031
Sc	-0.001	-0.001	-0.001	-0.001	-0.001	-0.001	-0.001	0.000	-0.001	-0.001	-0.001	-0.001
O	6.000	6.000	6.000	6.000	6.000	6.000	6.000	6.000	6.000	6.000	6.000	6.000
Mg#	**67.096**	**67.365**	**67.512**	**70.659**	**68.457**	**68.261**	**70.999**	**71.415**	**71.550**	**68.264**	**68.929**	**68.999**
Fe	**18.088**	**17.887**	**17.743**	**15.950**	**17.492**	**17.548**	**15.802**	**15.492**	**15.468**	**17.571**	**17.142**	**17.215**
Ca	**45.027**	**45.191**	**45.385**	**45.638**	**44.546**	**44.712**	**45.511**	**45.804**	**45.633**	**44.632**	**44.830**	**44.470**
Mg	**36.884**	**36.922**	**36.871**	**38.411**	**37.962**	**37.740**	**38.687**	**38.704**	**38.899**	**37.796**	**38.028**	**38.315**

Sample No.	FD-13-34-46.1	FD-13-34-46.1	FD-13-34-46.1	FD-13-34-46.1	FD-13-34-64.6	FD-13-34-64.6	FD-13-34-64.6	FD-13-34-64.6	FD-13-34-64.6	FD-13-34-79.6	FD-13-34-79.6	FD-13-34-79.6
Spot	2	3	4	5	1	2	3	4	5	1	2	3
SiO_2	50.052	50.321	50.603	50.458	50.790	50.288	50.788	50.619	50.200	50.578	51.220	50.458
Al_2O_3	2.922	2.817	2.730	2.697	2.474	3.032	2.788	2.556	3.010	2.355	1.992	2.360
MgO	13.126	12.776	12.896	12.687	12.134	12.551	12.230	12.267	12.937	12.692	12.614	12.205
Na_2O	0.368	0.492	0.408	0.429	0.350	0.416	0.383	0.352	0.370	0.347	0.289	0.366
FeO	10.487	10.623	10.800	10.926	11.248	10.854	11.049	11.074	10.507	11.853	10.665	12.036
MnO	0.287	0.280	0.251	0.290	0.354	0.305	0.337	0.367	0.255	0.331	0.281	0.345
Cr_2O_3	0.003	-0.008	-0.005	-0.009	0.043	-0.013	0.025	0.014	-0.017	0.000	0.019	-0.008
K_2O	0.004	0.001	0.013	0.004	0.004	0.003	0.001	0.002	0.003	-0.002	0.000	0.004
CaO	21.220	21.208	21.202	21.155	21.642	21.252	21.399	21.628	21.248	20.785	21.825	20.807
NiO	0.013	-0.011	0.003	0.004	-0.017	0.017	-0.013	0.011	-0.006	-0.016	0.014	-0.017
TiO_2	1.075	1.002	0.967	1.060	0.746	1.033	0.928	0.803	1.042	1.029	0.653	1.002
Sc_2O_3	-0.067	-0.033	-0.037	-0.044	-0.032	-0.034	-0.025	-0.026	-0.022	-0.023	-0.030	-0.034
Total	99.490	99.468	99.831	99.657	99.736	99.704	99.890	99.667	99.527	99.929	99.542	99.524
Si	1.894	1.905	1.908	1.908	1.923	1.901	1.916	1.917	1.898	1.913	1.937	1.919
Al	0.195	0.188	0.182	0.180	0.165	0.202	0.186	0.171	0.201	0.157	0.133	0.158
Mg	0.745	0.725	0.730	0.720	0.689	0.712	0.692	0.697	0.734	0.720	0.716	0.696
Na	0.013	0.018	0.015	0.016	0.013	0.015	0.014	0.013	0.014	0.013	0.011	0.013
Fe	0.331	0.335	0.339	0.344	0.355	0.342	0.347	0.350	0.331	0.374	0.336	0.381
Mn	0.009	0.009	0.008	0.009	0.011	0.010	0.011	0.012	0.008	0.011	0.009	0.011
Cr	0.000	0.000	0.000	0.000	0.001	0.000	0.001	0.000	-0.001	0.000	0.001	0.000
K	0.000	0.000	0.001	0.000	0.000	0.000	0.000	0.000	0.000	0.000	0.000	0.000
Ca	0.860	0.860	0.857	0.857	0.878	0.861	0.865	0.878	0.861	0.842	0.884	0.848
Ni	0.000	0.000	0.000	0.000	-0.001	0.001	0.000	0.000	0.000	0.000	0.000	-0.001
Ti	0.031	0.028	0.027	0.030	0.021	0.029	0.026	0.023	0.030	0.029	0.019	0.029
Sc	-0.002	-0.001	-0.001	-0.001	-0.001	-0.001	-0.001	-0.001	-0.001	-0.001	-0.001	-0.001
O	6.000	6.000	6.000	6.000	6.000	6.000	6.000	6.000	6.000	6.000	6.000	6.000
Mg#	**69.259**	**68.403**	**68.247**	**67.639**	**66.007**	**67.547**	**66.582**	**66.599**	**68.908**	**65.840**	**68.040**	**64.605**
Fe	**17.081**	**17.447**	**17.626**	**17.923**	**18.465**	**17.861**	**18.240**	**18.165**	**17.193**	**19.298**	**17.361**	**19.810**
Ca	**44.437**	**44.783**	**44.489**	**44.617**	**45.679**	**44.963**	**45.419**	**45.614**	**44.703**	**43.508**	**45.678**	**44.031**
Mg	**38.482**	**37.769**	**37.885**	**37.460**	**35.855**	**37.176**	**36.341**	**36.220**	**38.105**	**37.194**	**36.961**	**36.159**

Sample No.	FD-13-34-79.6	FD-13-34-79.6	FD-13-34-127.25	FD-13-34-127.25	FD-13-34-127.25	FD-13-34-127.25	FD-13-34-127.25	FD-13-34-127.25	FD-13-34-158.6	FD-13-34-158.6	FD-13-34-158.6	FD-13-34-158.6
Spot	4	5	1	2	3	4	5	6	1	2	3	4
SiO_2	50.196	50.217	50.272	50.121	50.255	49.881	49.829	49.711	51.141	50.167	49.706	49.986
Al_2O_3	2.727	2.602	2.071	2.057	2.145	2.705	2.569	2.549	1.543	1.608	2.459	2.494
MgO	12.831	12.318	11.091	11.063	11.221	11.087	10.970	10.865	11.020	10.413	10.914	11.188

Na_2O	0.368	0.373	0.347	0.332	0.362	0.389	0.355	0.386	0.324	0.368	0.360	0.381
FeO	10.967	11.591	13.624	13.495	13.172	13.798	14.030	13.735	12.969	14.562	13.588	13.272
MnO	0.326	0.339	0.408	0.427	0.424	0.400	0.424	0.400	0.447	0.415	0.374	0.356
Cr_2O_3	0.006	0.011	-0.005	-0.022	-0.009	0.009	-0.003	-0.017	0.000	-0.009	-0.005	-0.008
K_2O	0.001	0.007	0.002	0.008	0.003	0.006	0.003	0.004	0.001	0.000	0.000	0.002
CaO	21.146	20.907	20.859	20.882	20.983	20.824	20.698	20.763	21.603	20.774	20.877	20.843
NiO	-0.009	0.004	-0.005	0.009	0.008	0.011	0.011	-0.003	-0.008	-0.016	0.008	0.008
TiO_2	1.079	1.109	0.897	0.871	0.879	1.091	1.051	1.032	0.460	0.659	0.943	1.022
Sc_2O_3	-0.045	-0.032	-0.015	-0.019	-0.038	-0.023	-0.051	-0.032	-0.048	-0.042	-0.027	-0.022
Total	99.593	99.446	99.546	99.224	99.405	100.178	99.886	99.393	99.452	98.899	99.197	99.522
Si	1.901	1.909	1.927	1.927	1.926	1.902	1.908	1.911	1.957	1.944	1.914	1.914
Al	0.182	0.175	0.140	0.140	0.145	0.182	0.174	0.173	0.104	0.110	0.167	0.168
Mg	0.729	0.702	0.638	0.638	0.645	0.634	0.630	0.626	0.633	0.605	0.630	0.642
Na	0.013	0.014	0.013	0.012	0.013	0.014	0.013	0.014	0.012	0.014	0.013	0.014
Fe	0.346	0.367	0.435	0.432	0.421	0.439	0.448	0.440	0.414	0.470	0.436	0.423
Mn	0.010	0.011	0.013	0.014	0.014	0.013	0.014	0.013	0.014	0.014	0.012	0.012
Cr	0.000	0.000	0.000	-0.001	0.000	0.000	0.000	-0.001	0.000	0.000	0.000	0.000
K	0.000	0.000	0.000	0.000	0.000	0.000	0.000	0.000	0.000	0.000	0.000	0.000
Ca	0.858	0.851	0.857	0.860	0.862	0.851	0.849	0.855	0.886	0.863	0.861	0.855
Ni	0.000	0.000	0.000	0.000	0.000	0.000	0.000	0.000	0.000	0.000	0.000	0.000
Ti	0.031	0.032	0.026	0.025	0.025	0.031	0.030	0.030	0.013	0.019	0.027	0.029
Sc	-0.001	-0.001	-0.001	-0.001	-0.001	-0.001	-0.002	-0.001	-0.002	-0.001	-0.001	-0.001
O	6.000	6.000	6.000	6.000	6.000	6.000	6.000	6.000	6.000	6.000	6.000	6.000
Mg#	**67.804**	**65.670**	**59.438**	**59.606**	**60.527**	**59.123**	**58.462**	**58.744**	**60.466**	**56.277**	**59.113**	**60.276**
Fe	**17.905**	**19.113**	**22.554**	**22.396**	**21.827**	**22.796**	**23.233**	**22.897**	**21.408**	**24.264**	**22.618**	**22.043**
Ca	**44.388**	**44.325**	**44.397**	**44.557**	**44.704**	**44.233**	**44.068**	**44.502**	**45.849**	**44.505**	**44.681**	**44.509**
Mg	**37.707**	**36.562**	**33.049**	**33.048**	**33.469**	**32.971**	**32.699**	**32.602**	**32.743**	**31.231**	**32.701**	**33.448**

Sample No.	FD-13-34-158.6	FD-13-34-158.6	FD-13-34-194.8	FD-13-34-194.8	FD-13-34-194.8	FD-13-34-212.5	FD-13-34-212.5	FD-13-34-212.5	FD-13-34-226.3	FD-13-34-226.3	FD-13-34-226.3	FD-13-34-226.3
Spot	5	6	1	2	3	1	2	3	1	2	3	4
SiO_2	41.572	50.289	50.321	50.379	50.161	50.349	50.512	50.342	50.146	50.205	50.136	50.542
Al_2O_3	10.874	1.919	1.822	1.848	1.765	1.902	1.937	1.945	1.991	1.869	1.934	1.781
MgO	9.546	11.401	11.568	10.718	10.377	11.185	11.126	11.246	11.141	11.277	11.295	11.079
Na_2O	2.117	0.318	0.322	0.327	0.371	0.369	0.393	0.371	0.340	0.396	0.361	0.364
FeO	16.770	13.351	13.394	14.046	14.200	13.375	13.763	13.528	13.373	13.552	13.523	13.720
MnO	0.177	0.376	0.421	0.414	0.369	0.387	0.351	0.377	0.383	0.365	0.336	0.379
Cr_2O_3	0.022	-0.003	-0.025	-0.017	-0.023	-0.008	-0.017	0.011	-0.017	0.000	-0.008	-0.031
K_2O	0.942	0.001	0.002	0.006	0.005	-0.002	0.003	0.003	0.001	-0.002	0.003	0.001

CaO	11.304	20.849	20.580	21.112	21.163	20.879	20.870	20.918	20.972	20.996	20.981	20.942
NiO	0.028	0.008	-0.012	-0.006	0.000	-0.005	0.004	0.021	-0.005	0.009	0.003	0.000
TiO_2	4.324	0.812	0.758	0.531	0.667	0.758	0.749	0.735	0.757	0.748	0.770	0.710
Sc_2O_3	-0.005	-0.037	-0.033	-0.041	-0.031	-0.016	-0.017	-0.048	-0.030	-0.023	-0.046	-0.025
Total	97.671	99.284	99.118	99.317	99.024	99.173	99.674	99.449	99.052	99.392	99.288	99.462
Si	1.640	1.930	1.934	1.940	1.940	1.935	1.934	1.931	1.930	1.928	1.927	1.939
Al	0.757	0.130	0.124	0.126	0.120	0.129	0.131	0.132	0.135	0.127	0.131	0.121
Mg	0.565	0.656	0.667	0.619	0.602	0.645	0.639	0.647	0.643	0.650	0.651	0.638
Na	0.081	0.012	0.012	0.012	0.014	0.014	0.015	0.014	0.013	0.015	0.013	0.014
Fe	0.551	0.427	0.429	0.451	0.458	0.428	0.439	0.432	0.429	0.434	0.433	0.439
Mn	0.006	0.012	0.014	0.013	0.012	0.013	0.011	0.012	0.012	0.012	0.011	0.012
Cr	0.001	0.000	-0.001	-0.001	-0.001	0.000	-0.001	0.000	-0.001	0.000	0.000	-0.001
K	0.047	0.000	0.000	0.000	0.000	0.000	0.000	0.000	0.000	0.000	0.000	0.000
Ca	0.478	0.857	0.847	0.871	0.877	0.860	0.856	0.860	0.865	0.864	0.864	0.861
Ni	0.001	0.000	0.000	0.000	0.000	0.000	0.000	0.001	0.000	0.000	0.000	0.000
Ti	0.128	0.023	0.022	0.015	0.019	0.022	0.022	0.021	0.022	0.022	0.022	0.020
Sc	0.000	-0.001	-0.001	-0.001	-0.001	-0.001	-0.001	-0.002	-0.001	-0.001	-0.002	-0.001
O	6.000	6.000	6.000	6.000	6.000	6.000	6.000	6.000	6.000	6.000	6.000	6.000
Mg#	**50.608**	**60.585**	**60.855**	**57.868**	**56.811**	**60.084**	**59.269**	**59.942**	**59.993**	**59.965**	**60.055**	**59.242**
Fe	**34.587**	**22.003**	**22.074**	**23.223**	**23.632**	**22.161**	**22.703**	**22.299**	**22.144**	**22.273**	**22.231**	**22.645**
Ca	**29.975**	**44.177**	**43.608**	**44.879**	**45.283**	**44.479**	**44.262**	**44.333**	**44.649**	**44.366**	**44.346**	**44.440**
Mg	**35.438**	**33.820**	**34.317**	**31.898**	**31.085**	**33.359**	**33.035**	**33.368**	**33.207**	**33.361**	**33.423**	**32.915**

Sample	FD-13-34-	FD-13-34-	FD-13-34-	FD-13-34-	FD-13-34-	FD-13-34-	FD-13-34-	FD-13-34-	FD-13-34-	FD-13-34-	FD-13-34-	FD-13-34-
No.	226.3	226.3	226.3	226.3	248.5	248.5	248.5	248.5	248.5	248.5	248.5	248.5
Spot	5	6	7	8	1	2	3	4	5	6	7	8
SiO_2	50.225	50.293	50.427	50.310	50.199	50.536	50.459	50.509	50.584	50.537	50.569	50.407
Al_2O_3	1.925	1.806	1.802	2.054	2.319	2.330	2.112	2.104	2.269	2.125	2.318	2.364
MgO	11.110	11.505	11.626	11.517	11.400	11.391	11.271	11.376	11.498	11.168	11.245	11.336
Na_2O	0.362	0.345	0.337	0.356	0.302	0.332	0.348	0.331	0.321	0.345	0.331	0.323
FeO	13.593	13.215	13.396	13.225	12.081	12.163	13.010	12.813	12.695	13.398	12.944	12.565
MnO	0.378	0.361	0.417	0.411	0.395	0.382	0.359	0.353	0.343	0.362	0.363	0.444
Cr_2O_3	0.016	-0.031	0.006	0.031	0.016	-0.027	0.005	0.031	-0.023	0.023	-0.009	0.006
K_2O	0.003	-0.005	0.003	0.003	-0.001	0.003	0.005	0.001	0.007	0.007	0.005	0.001
CaO	21.018	20.407	20.515	20.521	21.204	21.357	21.066	20.873	20.952	20.800	21.263	21.408
NiO	0.006	-0.003	0.001	0.012	0.018	0.006	0.023	-0.003	0.009	-0.028	-0.007	-0.001
TiO_2	0.733	0.754	0.773	0.794	0.768	0.727	0.740	0.736	0.808	0.807	0.765	0.798
Sc_2O_3	-0.036	-0.049	-0.029	-0.043	-0.054	-0.041	-0.068	-0.044	-0.052	-0.023	-0.043	-0.027
Total	99.333	98.598	99.274	99.191	98.647	99.159	99.330	99.080	99.411	99.521	99.744	99.624
Si	1.930	1.940	1.934	1.930	1.929	1.932	1.933	1.936	1.931	1.933	1.928	1.923

Al	0.131	0.123	0.122	0.139	0.157	0.157	0.143	0.142	0.153	0.143	0.156	0.159
Mg	0.641	0.666	0.669	0.663	0.657	0.653	0.648	0.654	0.658	0.641	0.643	0.649
Na	0.013	0.013	0.013	0.013	0.011	0.012	0.013	0.012	0.012	0.013	0.012	0.012
Fe	0.435	0.425	0.428	0.423	0.387	0.387	0.415	0.409	0.404	0.427	0.411	0.400
Mn	0.012	0.012	0.014	0.013	0.013	0.012	0.012	0.011	0.011	0.012	0.012	0.014
Cr	0.000	-0.001	0.000	0.001	0.000	-0.001	0.000	0.001	-0.001	0.001	0.000	0.000
K	0.000	0.000	0.000	0.000	0.000	0.000	0.000	0.000	0.000	0.000	0.000	0.000
Ca	0.866	0.843	0.843	0.843	0.873	0.875	0.864	0.857	0.857	0.852	0.869	0.875
Ni	0.000	0.000	0.000	0.000	0.001	0.000	0.001	0.000	0.000	-0.001	0.000	0.000
Ti	0.021	0.022	0.022	0.023	0.022	0.021	0.021	0.021	0.023	0.023	0.022	0.023
Sc	-0.001	-0.002	-0.001	-0.001	-0.002	-0.001	-0.002	-0.001	-0.002	-0.001	-0.001	-0.001
O	6.000	6.000	6.000	6.000	6.000	6.000	6.000	6.000	6.000	6.000	6.000	6.000
Mg#	**59.534**	**61.045**	**60.971**	**61.052**	**62.943**	**62.766**	**60.928**	**61.511**	**61.981**	**60.006**	**60.994**	**61.889**
Fe	**22.425**	**21.966**	**22.069**	**21.918**	**20.181**	**20.229**	**21.546**	**21.310**	**21.043**	**22.240**	**21.387**	**20.771**
Ca	**44.582**	**43.612**	**43.454**	**43.726**	**45.541**	**45.669**	**44.855**	**44.634**	**44.652**	**44.391**	**45.170**	**45.499**
Mg	**32.992**	**34.422**	**34.476**	**34.356**	**34.278**	**34.102**	**33.599**	**34.056**	**34.305**	**33.369**	**33.443**	**33.730**

Sample No.	FD-13-34-253.1	FD-13-34-253.1	FD-13-34-253.1	FD-13-34-253.1	FD-13-34-253.1	FD-13-34-253.1	FD-13-34-253.1	FD-13-34-253.1	FD-13-34-257.8	FD-13-34-257.8	FD-13-34-257.8	FD-13-34-257.8
Spot	1	2	3	4	5	6	7	8	1	2	3	4
SiO_2	50.500	50.285	50.457	50.594	50.562	50.582	50.200	50.435	50.454	50.440	50.445	51.904
Al_2O_3	2.354	2.336	2.523	2.038	2.187	2.506	2.396	2.446	2.221	2.335	2.351	1.257
MgO	11.397	11.270	11.668	11.204	11.246	11.981	11.896	11.937	10.869	11.091	11.135	11.220
Na_2O	0.357	0.316	0.340	0.346	0.350	0.348	0.349	0.353	0.326	0.305	0.316	0.263
FeO	12.826	12.743	12.445	13.293	12.978	12.210	12.375	12.302	13.458	13.000	12.972	11.932
MnO	0.357	0.369	0.366	0.319	0.330	0.368	0.303	0.323	0.370	0.361	0.370	0.367
Cr_2O_3	0.009	0.019	-0.006	0.008	0.005	-0.011	-0.027	-0.031	-0.009	-0.003	0.019	-0.003
K_2O	-0.003	0.000	0.001	0.001	0.002	0.003	0.006	0.002	0.003	0.002	0.004	0.004
CaO	20.997	21.228	21.129	20.931	21.206	20.962	20.866	20.914	21.135	21.435	21.421	22.485
NiO	0.014	0.003	0.004	-0.007	-0.015	-0.005	-0.007	0.025	0.013	-0.021	-0.020	0.000
TiO_2	0.797	0.818	0.833	0.731	0.717	0.851	0.839	0.855	0.754	0.757	0.750	0.256
Sc_2O_3	-0.026	-0.052	-0.021	-0.047	-0.035	-0.062	-0.064	-0.034	-0.076	-0.042	-0.061	-0.045
Total	99.579	99.335	99.739	99.411	99.533	99.733	99.132	99.527	99.518	99.660	99.702	99.640
Si	1.927	1.925	1.919	1.937	1.932	1.921	1.920	1.920	1.932	1.926	1.926	1.974
Al	0.158	0.158	0.169	0.138	0.147	0.168	0.162	0.164	0.150	0.157	0.158	0.084
Mg	0.652	0.647	0.666	0.643	0.645	0.682	0.682	0.682	0.624	0.635	0.638	0.640
Na	0.013	0.012	0.013	0.013	0.013	0.013	0.013	0.013	0.012	0.011	0.012	0.010
Fe	0.408	0.406	0.394	0.424	0.413	0.386	0.394	0.390	0.430	0.414	0.413	0.378
Mn	0.012	0.012	0.012	0.010	0.011	0.012	0.010	0.010	0.012	0.012	0.012	0.012
Cr	0.000	0.001	0.000	0.000	0.000	0.000	-0.001	-0.001	0.000	0.000	0.001	0.000

K	0.000	0.000	0.000	0.000	0.000	0.000	0.000	0.000	0.000	0.000	0.000	0.000
Ca	0.858	0.871	0.861	0.858	0.868	0.853	0.855	0.853	0.867	0.877	0.876	0.916
Ni	0.000	0.000	0.000	0.000	0.000	0.000	0.000	0.001	0.000	-0.001	-0.001	0.000
Ti	0.023	0.023	0.024	0.021	0.021	0.024	0.024	0.024	0.022	0.022	0.021	0.007
Sc	-0.001	-0.002	-0.001	-0.002	-0.001	-0.002	-0.002	-0.001	-0.003	-0.001	-0.002	-0.001
O	6.000	6.000	6.000	6.000	6.000	6.000	6.000	6.000	6.000	6.000	6.000	6.000
Mg#	**61.530**	**61.419**	**62.792**	**60.272**	**60.934**	**63.850**	**63.374**	**63.591**	**59.246**	**60.563**	**60.709**	**62.861**
Fe	**21.257**	**21.125**	**20.532**	**22.019**	**21.456**	**20.106**	**20.416**	**20.274**	**22.357**	**21.479**	**21.421**	**19.549**
Ca	**44.742**	**45.246**	**44.818**	**44.576**	**45.077**	**44.381**	**44.259**	**44.315**	**45.142**	**45.535**	**45.480**	**47.363**
Mg	**34.000**	**33.629**	**34.650**	**33.405**	**33.467**	**35.513**	**35.326**	**35.411**	**32.501**	**32.985**	**33.098**	**33.088**

Sample No.	FD-13-34-276.5	FD-13-34-276.5	FD-13-34-276.5	FD-13-34-276.5	FD-13-34-276.5	FD-13-34-276.5	FD-13-34-276.5	FD-13-34-276.5	FD-13-34-291.5	FD-13-34-291.5	FD-13-34-291.5	FD-13-34-291.5
Spot	1	2	3	4	5	6	7	8	1	2	3	4
SiO_2	50.992	50.748	50.229	51.215	50.729	50.978	51.139	50.112	51.038	50.786	49.448	51.056
Al_2O_3	2.241	2.402	2.128	1.896	2.227	2.051	2.099	2.896	2.689	2.705	3.511	2.714
MgO	12.439	12.329	11.770	12.144	12.400	12.492	12.509	12.443	12.799	12.691	13.724	12.937
Na_2O	0.348	0.334	0.324	0.332	0.361	0.393	0.349	0.371	0.355	0.343	0.575	0.330
FeO	10.690	10.498	12.020	11.217	10.623	10.648	10.839	10.135	10.609	10.966	10.588	11.094
MnO	0.239	0.272	0.272	0.285	0.274	0.240	0.259	0.231	0.233	0.221	0.226	0.261
Cr_2O_3	0.020	0.046	0.011	-0.003	-0.014	0.002	0.024	0.047	0.012	0.009	-0.005	0.023
K_2O	0.002	0.004	0.002	0.002	0.000	0.003	-0.002	0.000	0.001	-0.001	0.010	0.009
CaO	21.695	21.690	21.385	21.698	21.757	21.750	21.682	21.789	21.628	21.467	1.267	20.920
NiO	0.023	0.022	0.018	0.005	0.020	0.010	0.003	0.021	0.009	0.018	-0.006	0.012
TiO_2	0.680	0.759	0.658	0.558	0.662	0.604	0.607	0.843	0.835	0.819	0.052	0.838
Sc_2O_3	-0.025	-0.050	-0.040	-0.034	-0.051	-0.059	-0.044	-0.020	0.005	-0.049	-0.005	-0.037
Total	99.344	99.054	98.777	99.315	98.988	99.112	99.464	98.868	100.213	99.975	79.385	100.157
Si	1.932	1.928	1.928	1.946	1.931	1.937	1.936	1.907	1.916	1.914	2.171	1.918
Al	0.150	0.161	0.144	0.127	0.150	0.138	0.140	0.194	0.178	0.180	0.272	0.180
Mg	0.707	0.703	0.678	0.692	0.708	0.712	0.711	0.710	0.721	0.717	0.904	0.729
Na	0.013	0.012	0.012	0.012	0.013	0.014	0.013	0.014	0.013	0.013	0.024	0.012
Fe	0.338	0.332	0.385	0.355	0.337	0.337	0.342	0.321	0.332	0.344	0.387	0.347
Mn	0.008	0.009	0.009	0.009	0.009	0.008	0.008	0.007	0.007	0.007	0.008	0.008
Cr	0.001	0.001	0.000	0.000	0.000	0.000	0.001	0.001	0.000	0.000	0.000	0.001
K	0.000	0.000	0.000	0.000	0.000	0.000	0.000	0.000	0.000	0.000	0.001	0.000
Ca	0.881	0.883	0.880	0.883	0.887	0.885	0.880	0.888	0.870	0.867	0.060	0.842
Ni	0.001	0.001	0.001	0.000	0.001	0.000	0.000	0.001	0.000	0.001	0.000	0.000
Ti	0.019	0.022	0.019	0.016	0.019	0.017	0.017	0.024	0.024	0.023	0.002	0.024
Sc	-0.001	-0.002	-0.001	-0.001	-0.002	-0.002	-0.001	-0.001	0.000	-0.002	0.000	-0.001
O	6.000	6.000	6.000	6.000	6.000	6.000	6.000	6.000	6.000	6.000	6.000	6.000

Mg#	**67.685**	**67.886**	**63.802**	**66.087**	**67.753**	**67.863**	**67.504**	**68.846**	**68.470**	**67.566**	**69.998**	**67.732**
Fe	**17.532**	**17.330**	**19.802**	**18.396**	**17.439**	**17.428**	**17.702**	**16.739**	**17.263**	**17.857**	**28.678**	**18.104**
Ca	**45.747**	**46.036**	**45.296**	**45.753**	**45.921**	**45.770**	**45.527**	**46.269**	**45.249**	**44.944**	**4.412**	**43.894**
Mg	**36.721**	**36.634**	**34.902**	**35.850**	**36.640**	**36.803**	**36.772**	**36.992**	**37.488**	**37.199**	**66.910**	**38.002**

Sample No.	FD-13-34-291.5	FD-13-34-291.5	FD-13-34-291.5	FD-13-34-291.5	FD-13-34-295.7	FD-13-34-295.7	FD-13-34-295.7	FD-13-34-316.7	FD-13-34-316.7	FD-13-34-316.7	FD-13-34-321.1	FD-13-34-321.1
Spot	5	6	7	8	1	2	3	1	2	3	1	2
SiO_2	48.510	52.414	51.514	51.423	50.487	51.504	51.218	51.268	50.953	51.089	51.047	51.779
Al_2O_3	3.648	1.431	2.186	2.540	2.914	2.000	2.003	2.004	2.278	1.861	2.540	1.954
MgO	12.572	12.543	12.930	12.506	12.536	12.330	12.994	13.024	12.684	12.419	12.500	12.826
Na_2O	0.261	0.337	0.313	0.329	0.325	0.306	0.391	0.371	0.359	0.403	0.395	0.388
FeO	12.698	9.918	9.415	10.477	10.850	11.224	10.733	10.777	10.442	11.549	11.345	10.799
MnO	0.239	0.240	0.194	0.268	0.296	0.287	0.318	0.303	0.257	0.258	0.285	0.287
Cr_2O_3	0.019	0.002	0.008	0.003	0.031	0.040	0.022	0.035	0.006	-0.038	0.009	0.030
K_2O	0.009	0.004	0.006	0.014	0.004	0.005	-0.001	-0.001	0.002	0.002	0.005	-0.002
CaO	18.594	22.917	22.434	21.775	20.953	21.463	21.235	21.380	21.626	21.361	20.795	21.486
NiO	0.006	0.011	-0.009	0.025	0.010	0.004	0.005	0.012	0.011	0.003	0.020	-0.012
TiO_2	0.693	0.223	0.658	0.784	0.898	0.510	0.652	0.655	0.746	0.596	0.826	0.688
Sc_2O_3	-0.030	-0.045	-0.065	-0.038	-0.047	-0.032	-0.020	-0.053	-0.030	-0.014	-0.034	-0.037
Total	97.219	99.995	99.584	100.106	99.257	99.641	99.550	99.775	99.334	99.489	99.733	100.186
Si	1.886	1.968	1.937	1.930	1.913	1.947	1.935	1.934	1.929	1.940	1.927	1.943
Al	0.250	0.095	0.145	0.168	0.195	0.133	0.134	0.133	0.152	0.125	0.169	0.129
Mg	0.733	0.706	0.729	0.704	0.713	0.699	0.736	0.737	0.720	0.707	0.708	0.722
Na	0.010	0.012	0.011	0.012	0.012	0.011	0.014	0.014	0.013	0.015	0.014	0.014
Fe	0.411	0.310	0.295	0.328	0.343	0.354	0.338	0.339	0.329	0.365	0.357	0.338
Mn	0.008	0.008	0.006	0.009	0.009	0.009	0.010	0.010	0.008	0.008	0.009	0.009
Cr	0.001	0.000	0.000	0.000	0.001	0.001	0.001	0.001	0.000	-0.001	0.000	0.001
K	0.000	0.000	0.000	0.001	0.000	0.000	0.000	0.000	0.000	0.000	0.000	0.000
Ca	0.775	0.922	0.904	0.876	0.851	0.869	0.860	0.864	0.877	0.869	0.841	0.864
Ni	0.000	0.000	0.000	0.001	0.000	0.000	0.000	0.000	0.000	0.000	0.001	0.000
Ti	0.020	0.006	0.019	0.022	0.026	0.014	0.018	0.019	0.021	0.017	0.023	0.019
Sc	-0.001	-0.001	-0.002	-0.001	-0.002	-0.001	-0.001	-0.002	-0.001	0.000	-0.001	-0.001
O	6.000	6.000	6.000	6.000	6.000	6.000	6.000	6.000	6.000	6.000	6.000	6.000
Mg#	**64.056**	**69.479**	**71.198**	**68.240**	**67.529**	**66.413**	**68.545**	**68.507**	**68.617**	**65.935**	**66.480**	**68.131**
Fe	**21.437**	**16.007**	**15.301**	**17.180**	**17.977**	**18.396**	**17.474**	**17.464**	**17.096**	**18.819**	**18.727**	**17.556**
Ca	**40.359**	**47.554**	**46.875**	**45.908**	**44.636**	**45.228**	**44.448**	**44.546**	**45.523**	**44.754**	**44.133**	**44.911**
Mg	**38.204**	**36.439**	**37.824**	**36.912**	**37.387**	**36.376**	**38.078**	**37.990**	**37.380**	**36.427**	**37.140**	**37.533**

Sample No.	FD-13-34-321.1	FD-13-34-321.1	SL-13-34-3.0	SL-13-34-3.0	SL-13-34-3.0	SL-13-34-3.0	SL-13-34-3.0	SL-13-34-3.0	SL-13-34-3.0	SL-13-34-5.1	SL-13-34-5.1	SL-13-34-5.1
Spot	3	4	1	2	3	4	5	6	7	1	2	3
SiO_2	51.596	51.154	51	50.942	49.972	51.095	51.034	51.423	50.758	51.133	51.117	50.945
Al_2O_3	2.035	2.563	2.762	2.752	2.758	2.668	2.579	2.379	2.769	2.728	2.685	2.697
MgO	12.875	12.765	12.667	12.393	12.466	12.479	12.451	12.626	12.23	12.445	12.385	11.903
Na_2O	0.417	0.361	0.437	0.401	0.332	0.363	0.368	0.391	0.376	0.345	0.369	0.438
FeO	10.862	11.475	10.642	10.879	12.161	10.79	10.841	10.479	10.96	10.824	10.725	11.092
MnO	0.315	0.298	0.33	0.324	0.329	0.323	0.307	0.321	0.32	0.335	0.309	0.374
Cr_2O_3	0.036	0.048	0.013	-0.022	-0.008	0.007	0.013	0.016	0.013	-0.007	-0.017	0.002
K_2O	0.002	-0.001										
CaO	21.115	20.643	21.349	21.204	20.116	21.323	21.287	21.479	21.1	21.068	20.963	21.371
NiO	0.022	0.007	0.014	-0.002	-0.003	-0.001	0.011	0.018	-0.02	0.014	-0.015	0.015
TiO_2	0.709	0.820	1.223	1.297	1.254	1.197	1.208	1.108	1.227	1.193	1.241	1.148
Sc_2O_3	-0.015	-0.039	-0.006	-0.004	0.012	-0.006	0.01	0.014	-0.006	-0.003	0.018	0.014
Total	99.969	100.094	100.431	100.164	99.389	100.238	100.109	100.254	99.727	100.075	99.78	99.999
Si	1.940	1.924	1.910	1.914	1.902	1.918	1.919	1.927	1.916	1.921	1.924	1.921
Al	0.135	0.170	0.183	0.182	0.185	0.177	0.171	0.157	0.184	0.181	0.178	0.179
Mg	0.726	0.720	0.712	0.698	0.712	0.702	0.702	0.710	0.692	0.701	0.699	0.673
Na	0.015	0.013	0.016	0.015	0.012	0.013	0.013	0.014	0.014	0.013	0.013	0.016
Fe	0.340	0.360	0.332	0.341	0.386	0.337	0.340	0.327	0.345	0.339	0.336	0.348
Mn	0.010	0.009	0.010	0.010	0.011	0.010	0.010	0.010	0.010	0.011	0.010	0.012
Cr	0.001	0.001	0.000	-0.001	0.000	0.000	0.000	0.000	0.000	0.000	-0.001	0.000
K	0.000	0.000	0.000	0.000	0.000	0.000	0.000	0.000	0.000	0.000	0.000	0.000
Ca	0.851	0.832	0.857	0.854	0.820	0.857	0.857	0.862	0.853	0.848	0.845	0.863
Ni	0.001	0.000	0.000	0.000	0.000	0.000	0.000	0.001	-0.001	0.000	0.000	0.000
Ti	0.020	0.023	0.034	0.037	0.036	0.034	0.034	0.031	0.035	0.034	0.035	0.032
Sc	0.000	-0.001	0.000	0.000	0.000	0.000	0.000	0.000	0.000	0.000	0.001	0.000
O	6.000	6.000	6.000	6.000	6.000	6.000	6.000	6.000	6.000	6.000	6.000	6.000
Mg#	**68.088**	**66.693**	**68.178**	**67.218**	**64.852**	**67.551**	**67.398**	**68.442**	**66.762**	**67.422**	**67.518**	**65.889**
Fe	**17.753**	**18.814**	**17.477**	**17.997**	**20.113**	**17.785**	**17.883**	**17.229**	**18.235**	**17.947**	**17.884**	**18.488**
Ca	**44.370**	**43.515**	**45.078**	**45.100**	**42.775**	**45.189**	**45.147**	**45.405**	**45.137**	**44.912**	**44.943**	**45.799**
Mg	**37.877**	**37.672**	**37.445**	**36.903**	**37.111**	**37.025**	**36.970**	**37.366**	**36.627**	**37.142**	**37.173**	**35.712**

Sample No.	SL-13-34-5.1	SL-13-34-5.1	SL-13-34-5.1	SL-13-34-5.1	SL-13-34-5.1	SL-13-34-7.0	SL-13-34-7.0	SL-13-34-7.0	SL-13-34-7.0	SL-13-34-7.0	SL-13-34-7.0	SL-13-34-7.0
Spot	4	5	6	7	8	1	2	3	4	5	6	7
SiO_2	50.914	51.647	51.162	50.919	50.955	51.533	52.444	52.654	52.123	51.187	51.728	51.465
Al_2O_3	2.699	2.073	2.525	2.688	2.716	2.36	1.518	1.959	2.33	2.842	2.301	2.783
MgO	11.914	11.65	12.427	12.583	12.236	11.952	11.62	11.977	12.352	12.42	12.184	12.649

Na_2O	0.41	0.417	0.34	0.343	0.404	0.373	0.364	0.351	0.361	0.364	0.361	0.349
FeO	11.003	11.447	10.903	10.845	10.919	11.648	12.91	11.542	11.3	10.956	11.494	10.636
MnO	0.328	0.355	0.346	0.324	0.334	0.386	0.42	0.385	0.389	0.386	0.383	0.332
Cr_2O_3	-0.026	-0.01	-0.008	0.014	-0.007	0.004	-0.005	0.003	-0.013	0.005	-0.007	0
K_2O												
CaO	21.22	21.669	20.965	21.053	21.153	21.092	21.412	21.627	21.152	21.061	21.184	21.19
NiO	0.005	0.006	0.01	-0.003	0.011	0.014	0.013	0.018	0.008	0.013	0.004	0.008
TiO_2	1.232	0.789	1.183	1.261	1.239	1.161	0.961	0.765	0.992	1.254	0.953	1.317
Sc_2O_3	-0.001	0.016	0.014	-0.008	0.006	-0.012	0.007	-0.005	-0.008	0.01	-0.001	-0.022
Total	99.698	100.059	99.867	100.019	99.966	100.511	101.664	101.276	100.986	100.498	100.584	100.707
Si	1.923	1.948	1.926	1.915	1.918	1.934	1.956	1.958	1.941	1.916	1.938	1.919
Al	0.180	0.138	0.168	0.178	0.180	0.156	0.100	0.129	0.153	0.188	0.152	0.183
Mg	0.675	0.659	0.702	0.710	0.691	0.673	0.650	0.668	0.690	0.697	0.685	0.707
Na	0.015	0.015	0.012	0.012	0.015	0.014	0.013	0.013	0.013	0.013	0.013	0.013
Fe	0.346	0.360	0.342	0.340	0.343	0.364	0.401	0.358	0.351	0.342	0.359	0.330
Mn	0.010	0.011	0.011	0.010	0.011	0.012	0.013	0.012	0.012	0.012	0.012	0.010
Cr	-0.001	0.000	0.000	0.000	0.000	0.000	0.000	0.000	0.000	0.000	0.000	0.000
K	0.000	0.000	0.000	0.000	0.000	0.000	0.000	0.000	0.000	0.000	0.000	0.000
Ca	0.859	0.876	0.846	0.848	0.853	0.848	0.856	0.862	0.844	0.845	0.850	0.846
Ni	0.000	0.000	0.000	0.000	0.000	0.000	0.000	0.001	0.000	0.000	0.000	0.000
Ti	0.035	0.022	0.033	0.036	0.035	0.033	0.027	0.021	0.028	0.035	0.027	0.037
Sc	0.000	0.001	0.000	0.000	0.000	0.000	0.000	0.000	0.000	0.000	0.000	-0.001
O	6.000	6.000	6.000	6.000	6.000	6.000	6.000	6.000	6.000	6.000	6.000	6.000
Mg#	**66.091**	**64.688**	**67.230**	**67.621**	**66.856**	**64.875**	**61.834**	**65.131**	**66.302**	**67.111**	**65.613**	**68.160**
Fe	**18.421**	**18.991**	**18.103**	**17.907**	**18.156**	**19.323**	**21.041**	**18.950**	**18.607**	**18.142**	**18.948**	**17.537**
Ca	**45.676**	**46.220**	**44.756**	**44.695**	**45.222**	**44.987**	**44.869**	**45.654**	**44.782**	**44.839**	**44.899**	**44.922**
Mg	**35.903**	**34.789**	**37.141**	**37.398**	**36.622**	**35.690**	**34.090**	**35.396**	**36.611**	**37.019**	**36.153**	**37.541**

Sample No.	SL-13-34-7.0	SL-13-34-13.3	SL-13-34-13.3	SL-13-34-13.3	SL-13-34-13.3	SL-13-34-13.3	SL-13-34-13.3	SL-13-34-13.3	SL-13-34-13.3	SL-13-34-13.3	SL-13-34-17.4	SL-13-34-17.4
Spot	8	1	2	3	4	5	6	7	8	9	1	2
SiO_2	51.113	53.171	52.624	52.077	52.053	51.469	52.244	52.028	51.814	51.789	51.746	50.921
Al_2O_3	2.739	1.216	1.875	2.287	2.929	2.915	2.552	2.57	2.864	2.841	2.212	2.818
MgO	12.048	12.489	12.515	11.899	12.96	12.796	12.863	12.614	12.734	12.828	11.865	11.996
Na_2O	0.415	0.296	0.339	0.374	0.374	0.342	0.387	0.388	0.324	0.369	0.415	0.392
FeO	11.505	10.752	10.737	11.302	10.407	10.438	10.684	10.884	10.402	10.315	11.674	10.775
MnO	0.431	0.337	0.327	0.347	0.314	0.32	0.324	0.327	0.329	0.295	0.351	0.322
Cr_2O_3	0.007	-0.004	0.009	-0.015	-0.001	0	-0.005	0.011	-0.009	0.006	0.007	-0.001
K_2O												

CaO	21.214	22.053	21.84	21.716	21.217	21.357	21.164	21.222	21.37	21.31	21.83	21.54
NiO	-0.015	0.021	0.017	0.009	0.002	0.02	-0.008	0.001	-0.007	-0.005	-0.014	-0.001
TiO_2	1.28	0.639	0.677	0.927	1.417	1.409	1.151	1.077	1.375	1.12	0.724	1.195
Sc_2O_3	0.01	0.006	-0.017	0.008	-0.011	0.004	0.003	0.023	0.016	0.011	0.01	-0.017
Total	100.747	100.976	100.943	100.931	101.661	101.07	101.359	101.145	101.212	100.879	100.82	99.94
Si	1.915	1.977	1.958	1.944	1.918	1.911	1.932	1.931	1.919	1.923	1.939	1.918
Al	0.181	0.080	0.123	0.151	0.190	0.191	0.167	0.168	0.187	0.186	0.146	0.187
Mg	0.677	0.697	0.698	0.666	0.716	0.713	0.714	0.702	0.707	0.715	0.667	0.678
Na	0.015	0.011	0.012	0.014	0.013	0.012	0.014	0.014	0.012	0.013	0.015	0.014
Fe	0.359	0.333	0.333	0.351	0.320	0.323	0.329	0.337	0.321	0.319	0.365	0.338
Mn	0.014	0.011	0.010	0.011	0.010	0.010	0.010	0.010	0.010	0.009	0.011	0.010
Cr	0.000	0.000	0.000	0.000	0.000	0.000	0.000	0.000	0.000	0.000	0.000	0.000
K	0.000	0.000	0.000	0.000	0.000	0.000	0.000	0.000	0.000	0.000	0.000	0.000
Ca	0.852	0.879	0.870	0.868	0.838	0.850	0.839	0.844	0.848	0.848	0.877	0.869
Ni	0.000	0.001	0.001	0.000	0.000	0.001	0.000	0.000	0.000	0.000	0.000	0.000
Ti	0.036	0.018	0.019	0.026	0.039	0.039	0.032	0.030	0.038	0.031	0.020	0.034
Sc	0.000	0.000	-0.001	0.000	0.000	0.000	0.000	0.001	0.001	0.000	0.000	-0.001
O	6.000	6.000	6.000	6.000	6.000	6.000	6.000	6.000	6.000	6.000	6.000	6.000
Mg#	**65.337**	**67.646**	**67.722**	**65.459**	**69.151**	**68.815**	**68.425**	**67.597**	**68.785**	**69.122**	**64.657**	**66.711**
Fe	**19.027**	**17.458**	**17.503**	**18.638**	**17.057**	**17.131**	**17.501**	**17.879**	**17.109**	**16.964**	**19.107**	**17.940**
Ca	**45.108**	**46.039**	**45.775**	**46.043**	**44.709**	**45.067**	**44.573**	**44.822**	**45.191**	**45.060**	**45.938**	**46.109**
Mg	**35.865**	**36.502**	**36.722**	**35.320**	**38.234**	**37.802**	**37.926**	**37.298**	**37.700**	**37.975**	**34.955**	**35.951**

Sample No.	SL-13-34-17.4	SL-13-34-17.4	SL-13-34-17.4	SL-13-34-17.4	SL-13-34-17.4	SL-13-34-17.4	SL-13-34-17.4	SL-13-34-19.4	SL-13-34-19.4	SL-13-34-19.4	SL-13-34-19.4	SL-13-34-19.4
Spot	3	4	5	6	7	8	9	1	2	3	4	5
SiO_2	51.448	51.595	51.733	52.22	51.455	51.241	51.326	51.84	51.203	52.471	52.59	52.699
Al_2O_3	2.388	2.729	2.46	2.267	2.722	2.765	2.699	2.765	2.757	2.114	2.355	1.922
MgO	11.841	12.25	12.373	12.817	12.475	12.576	12.555	12.72	12.795	12.551	12.479	12.647
Na_2O	0.371	0.366	0.394	0.34	0.366	0.37	0.376	0.401	0.386	0.424	0.417	0.437
FeO	11.616	10.705	10.865	10.124	10.48	10.556	10.464	10.67	10.436	10.791	11.043	10.99
MnO	0.358	0.317	0.311	0.291	0.316	0.31	0.301	0.299	0.29	0.297	0.363	0.335
Cr_2O_3	0.02	-0.002	0	0.004	-0.014	-0.019	-0.027	0.016	0.003	0.017	-0.012	-0.015
K_2O												
CaO	21.678	21.648	21.579	21.858	21.228	21.301	21.474	21.39	21.254	21.634	21.574	21.344
NiO	0.041	0.019	-0.009	0.007	0.013	0.025	0.007	-0.014	0.007	-0.001	0.016	-0.021
TiO_2	0.763	0.817	0.863	0.74	1.253	1.17	1.216	1.136	1.191	0.84	0.88	0.736
Sc_2O_3	0.01	0.026	0.004	-0.001	-0.004	-0.002	0.019	-0.003	-0.013	0.012	0.004	-0.004
Total	100.534	100.47	100.573	100.667	100.29	100.293	100.41	101.22	100.309	101.15	101.709	101.07
Si	1.933	1.930	1.934	1.943	1.925	1.919	1.920	1.922	1.916	1.948	1.943	1.957

Al	0.158	0.180	0.162	0.149	0.180	0.183	0.178	0.181	0.182	0.138	0.154	0.126
Mg	0.667	0.687	0.694	0.716	0.700	0.706	0.704	0.708	0.718	0.699	0.692	0.705
Na	0.013	0.013	0.014	0.012	0.013	0.013	0.014	0.014	0.014	0.015	0.015	0.016
Fe	0.364	0.334	0.339	0.314	0.327	0.329	0.326	0.330	0.325	0.334	0.340	0.340
Mn	0.011	0.010	0.010	0.009	0.010	0.010	0.010	0.009	0.009	0.009	0.011	0.011
Cr	0.001	0.000	0.000	0.000	0.000	-0.001	-0.001	0.000	0.000	0.000	0.000	0.000
K	0.000	0.000	0.000	0.000	0.000	0.000	0.000	0.000	0.000	0.000	0.000	0.000
Ca	0.873	0.868	0.864	0.872	0.851	0.855	0.861	0.850	0.852	0.860	0.854	0.849
Ni	0.001	0.001	0.000	0.000	0.000	0.001	0.000	0.000	0.000	0.000	0.000	-0.001
Ti	0.022	0.023	0.024	0.021	0.035	0.033	0.034	0.032	0.033	0.023	0.024	0.021
Sc	0.000	0.001	0.000	0.000	0.000	0.000	0.001	0.000	0.000	0.000	0.000	0.000
O	6.000	6.000	6.000	6.000	6.000	6.000	6.000	6.000	6.000	6.000	6.000	6.000
Mg#	**64.725**	**67.318**	**67.211**	**69.501**	**68.180**	**68.198**	**68.351**	**68.212**	**68.817**	**67.675**	**67.041**	**67.441**
Fe	**19.105**	**17.668**	**17.846**	**16.516**	**17.401**	**17.425**	**17.247**	**17.472**	**17.166**	**17.633**	**18.031**	**17.958**
Ca	**45.840**	**45.938**	**45.572**	**45.847**	**45.316**	**45.208**	**45.506**	**45.035**	**44.950**	**45.451**	**45.292**	**44.843**
Mg	**35.055**	**36.393**	**36.582**	**37.637**	**37.283**	**37.367**	**37.248**	**37.493**	**37.884**	**36.916**	**36.677**	**37.199**

Sample No.	SL-13-34-19.4	SL-13-34-19.4	SL-13-34-19.4	SL-13-34-19.4	SL-13-34-25.7	SL-13-34-25.7	SL-13-34-25.7	SL-13-34-25.7	SL-13-34-25.7	SL-13-34-25.7	SL-13-34-25.7	SL-13-34-25.7
Spot	6	7	8	9	1	2	3	4	5	6	7	8
SiO_2	52.268	52.894	52.519	52.961	52.484	51.795	53.061	51.395	51.898	51.764	53.06	52.585
Al_2O_3	2.726	1.658	1.648	2	1.942	1.888	1.619	2.625	2.077	1.922	1.463	1.451
MgO	12.463	12.643	12.571	12.73	12.811	12.612	12.868	12.529	12.576	12.71	12.752	12.708
Na_2O	0.417	0.441	0.411	0.461	0.418	0.393	0.523	0.473	0.408	0.413	0.463	0.46
FeO	10.885	11.08	10.971	11.392	10.775	10.681	10.421	10.766	10.715	10.922	11.038	10.879
MnO	0.327	0.342	0.334	0.379	0.326	0.317	0.345	0.345	0.31	0.322	0.332	0.336
Cr_2O_3	0.006	-0.016	0.014	0.018	0.01	-0.007	-0.008	0.006	0	-0.006	0.019	-0.004
K_2O												
CaO	21.391	21.523	21.37	20.843	21.634	21.751	21.659	21.403	21.786	21.463	21.523	21.549
NiO	-0.001	-0.002	0.013	-0.005	-0.009	-0.008	0.006	-0.013	0.01	-0.003	-0.015	-0.02
TiO_2	1.101	0.711	0.684	0.302	0.824	0.775	0.244	1.132	0.872	0.825	0.681	0.663
Sc_2O_3	0.002	-0.008	0	0.037	-0.001	-0.008	-0.001	-0.006	-0.011	0.002	-0.006	-0.001
Total	101.585	101.266	100.535	101.118	101.214	100.189	100.737	100.655	100.641	100.334	101.31	100.606
Si	1.931	1.962	1.962	1.966	1.948	1.944	1.973	1.921	1.939	1.941	1.967	1.964
Al	0.178	0.109	0.109	0.131	0.127	0.125	0.106	0.173	0.137	0.127	0.096	0.096
Mg	0.691	0.704	0.705	0.709	0.713	0.710	0.718	0.702	0.705	0.715	0.709	0.712
Na	0.015	0.016	0.015	0.017	0.015	0.014	0.019	0.017	0.015	0.015	0.017	0.017
Fe	0.335	0.343	0.342	0.352	0.333	0.334	0.323	0.335	0.334	0.341	0.341	0.339
Mn	0.010	0.011	0.011	0.012	0.010	0.010	0.011	0.011	0.010	0.010	0.010	0.011
Cr	0.000	0.000	0.000	0.001	0.000	0.000	0.000	0.000	0.000	0.000	0.001	0.000

K	0.000	0.000	0.000	0.000	0.000	0.000	0.000	0.000	0.000	0.000	0.000	0.000
Ca	0.847	0.856	0.856	0.829	0.860	0.875	0.863	0.857	0.872	0.862	0.855	0.862
Ni	0.000	0.000	0.000	0.000	0.000	0.000	0.000	0.000	0.000	0.000	0.000	-0.001
Ti	0.031	0.020	0.019	0.008	0.023	0.022	0.007	0.032	0.024	0.023	0.019	0.019
Sc	0.000	0.000	0.000	0.001	0.000	0.000	0.000	0.000	0.000	0.000	0.000	0.000
O	6.000	6.000	6.000	6.000	6.000	6.000	6.000	6.000	6.000	6.000	6.000	6.000
Mg#	**67.330**	**67.255**	**67.347**	**66.793**	**68.154**	**68.004**	**68.970**	**67.687**	**67.873**	**67.686**	**67.527**	**67.769**
Fe	**17.897**	**18.013**	**17.963**	**18.644**	**17.478**	**17.410**	**16.964**	**17.697**	**17.462**	**17.790**	**17.900**	**17.701**
Ca	**45.219**	**44.989**	**44.987**	**43.857**	**45.118**	**45.585**	**45.331**	**45.233**	**45.648**	**44.947**	**44.876**	**45.080**
Mg	**36.884**	**36.998**	**37.049**	**37.500**	**37.404**	**37.005**	**37.705**	**37.070**	**36.890**	**37.263**	**37.224**	**37.219**

Sample No.	SL-13-34-25.7	SL-13-34-28.1	SL-13-34-28.1	SL-13-34-28.1	SL-13-34-28.1	SL-13-34-28.1	SL-13-34-28.1	SL-13-34-28.1	SL-13-34-28.1	SL-13-34-28.1	SL-13-34-30	SL-13-34-30
Spot	9	1	2	3	4	5	6	7	8	9	1	2
SiO_2	51.516	51.247	51.597	51.453	52.37	52.556	51.712	51.727	51.722	51.268	51.253	51.547
Al_2O_3	1.847	2.769	2.718	2.91	1.539	1.676	2.464	2.279	2.191	2.869	3.059	3.092
MgO	12.752	12.408	12.868	12.798	12.811	12.783	12.643	12.881	12.628	12.612	12.59	12.753
Na_2O	0.421	0.409	0.383	0.431	0.47	0.474	0.404	0.392	0.401	0.402	0.388	0.39
FeO	10.651	10.906	10.644	10.791	10.762	10.739	10.89	10.304	10.44	10.232	10.323	10.464
MnO	0.336	0.348	0.313	0.303	0.337	0.334	0.333	0.283	0.302	0.303	0.311	0.293
Cr_2O_3	-0.001	0	-0.016	0.006	-0.017	0.002	-0.002	0.012	0.014	0.005	-0.002	0.008
K_2O												
CaO	21.556	21.39	21.187	21.255	21.585	21.778	21.356	21.476	21.649	21.292	21.409	21.63
NiO	-0.003	-0.001	0.014	-0.017	-0.016	-0.012	-0.006	0.001	0.001	-0.002	0.011	-0.01
TiO_2	0.762	1.318	1.187	1.266	0.673	0.718	1.066	0.955	0.877	1.293	1.246	1.218
Sc_2O_3	0.003	-0.003	0.004	0.006	-0.014	-0.007	0.001	0	0.02	-0.017	0.003	0
Total	99.84	100.791	100.899	101.202	100.5	101.041	100.861	100.31	100.245	100.257	100.591	101.385
Si	1.941	1.914	1.920	1.911	1.958	1.955	1.928	1.934	1.938	1.917	1.912	1.909
Al	0.123	0.182	0.178	0.191	0.102	0.110	0.162	0.150	0.145	0.189	0.201	0.202
Mg	0.721	0.695	0.718	0.713	0.719	0.713	0.707	0.722	0.710	0.708	0.704	0.708
Na	0.015	0.015	0.014	0.015	0.017	0.017	0.015	0.014	0.015	0.015	0.014	0.014
Fe	0.334	0.339	0.330	0.334	0.335	0.333	0.338	0.321	0.326	0.319	0.321	0.323
Mn	0.011	0.011	0.010	0.010	0.011	0.011	0.010	0.009	0.010	0.010	0.010	0.009
Cr	0.000	0.000	0.000	0.000	-0.001	0.000	0.000	0.000	0.000	0.000	0.000	0.000
K	0.000	0.000	0.000	0.000	0.000	0.000	0.000	0.000	0.000	0.000	0.000	0.000
Ca	0.870	0.856	0.845	0.846	0.865	0.868	0.853	0.860	0.869	0.853	0.856	0.858
Ni	0.000	0.000	0.000	-0.001	0.000	0.000	0.000	0.000	0.000	0.000	0.000	0.000
Ti	0.022	0.037	0.033	0.035	0.019	0.020	0.030	0.027	0.025	0.036	0.035	0.034
Sc	0.000	0.000	0.000	0.000	0.000	0.000	0.000	0.000	0.001	-0.001	0.000	0.000
O	6.000	6.000	6.000	6.000	6.000	6.000	6.000	6.000	6.000	6.000	6.000	6.000

Mg#	**68.305**	**67.191**	**68.515**	**68.100**	**68.180**	**68.179**	**67.635**	**69.232**	**68.526**	**68.931**	**68.704**	**68.689**
Fe	**17.370**	**17.955**	**17.436**	**17.645**	**17.478**	**17.391**	**17.822**	**16.864**	**17.113**	**16.966**	**17.060**	**17.090**
Ca	**45.197**	**45.276**	**44.622**	**44.686**	**45.071**	**45.346**	**44.935**	**45.190**	**45.627**	**45.392**	**45.489**	**45.419**
Mg	**37.433**	**36.769**	**37.942**	**37.669**	**37.451**	**37.263**	**37.243**	**37.946**	**37.260**	**37.642**	**37.451**	**37.491**

Sample No.	SL-13-34-30	SL-13-34-30	SL-13-34-30	SL-13-34-30	SL-13-34-32	SL-13-34-32	SL-13-34-32	SL-13-34-45	SL-13-34-45	SL-13-34-45	SL-13-34-45	SL-13-34-45
Spot	3	4	5	6	1	2	3	1	2	3	4	5
SiO_2	51.145	52.048	51.108	51.385	51.285	50.796	51.297	51.745	51.996	52.054	51.718	53.069
Al_2O_3	3.103	2.296	3.084	3.038	3.041	2.998	2.908	2.351	2.3	2.298	2.337	1.756
MgO	12.628	12.448	12.707	12.58	12.641	12.615	12.564	12.792	12.72	12.723	12.764	12.513
Na_2O	0.387	0.372	0.382	0.411	0.355	0.401	0.362	0.417	0.418	0.436	0.407	0.59
FeO	10.443	10.6	10.406	10.474	10.288	10.564	10.803	10.475	10.326	10.442	10.707	9.787
MnO	0.311	0.325	0.271	0.299	0.289	0.328	0.315	0.294	0.296	0.309	0.292	0.323
Cr_2O_3	-0.008	-0.001	-0.006	-0.001	-0.005	-0.015	0	0	-0.006	0.022	-0.007	0
K_2O												
CaO	21.216	21.646	21.439	21.365	21.282	21.354	21.258	21.711	21.752	21.805	21.569	22.439
NiO	-0.009	-0.009	-0.002	-0.005	0.014	-0.002	-0.009	-0.005	0.001	-0.012	0.012	-0.003
TiO_2	1.285	0.599	1.33	1.259	1.235	1.103	1.129	0.875	0.864	0.847	0.873	0.324
Sc_2O_3	0.007	0.011	0.001	-0.014	-0.011	0.005	0.006	0	0.011	0.025	-0.005	0.01
Total	100.508	100.335	100.72	100.791	100.414	100.147	100.633	100.655	100.678	100.949	100.667	100.808
Si	1.910	1.947	1.905	1.913	1.915	1.907	1.916	1.931	1.938	1.936	1.931	1.971
Al	0.204	0.152	0.203	0.200	0.200	0.199	0.192	0.155	0.151	0.151	0.154	0.115
Mg	0.707	0.699	0.711	0.703	0.708	0.711	0.704	0.716	0.711	0.710	0.715	0.697
Na	0.014	0.013	0.014	0.015	0.013	0.015	0.013	0.015	0.015	0.016	0.015	0.021
Fe	0.325	0.330	0.323	0.325	0.320	0.331	0.336	0.326	0.321	0.324	0.333	0.303
Mn	0.010	0.010	0.009	0.009	0.009	0.010	0.010	0.009	0.009	0.010	0.009	0.010
Cr	0.000	0.000	0.000	0.000	0.000	0.000	0.000	0.000	0.000	0.001	0.000	0.000
K	0.000	0.000	0.000	0.000	0.000	0.000	0.000	0.000	0.000	0.000	0.000	0.000
Ca	0.849	0.868	0.856	0.852	0.851	0.859	0.851	0.868	0.869	0.869	0.863	0.893
Ni	0.000	0.000	0.000	0.000	0.000	0.000	0.000	0.000	0.000	0.000	0.000	0.000
Ti	0.036	0.017	0.037	0.035	0.035	0.031	0.032	0.024	0.024	0.024	0.024	0.009
Sc	0.000	0.000	0.000	0.000	0.000	0.000	0.000	0.000	0.000	0.001	0.000	0.000
O	6.000	6.000	6.000	6.000	6.000	6.000	6.000	6.000	6.000	6.000	6.000	6.000
Mg#	**68.520**	**67.885**	**68.731**	**68.374**	**68.864**	**68.249**	**67.673**	**68.732**	**68.918**	**68.683**	**68.212**	**69.709**
Fe	**17.275**	**17.424**	**17.103**	**17.287**	**17.032**	**17.396**	**17.783**	**17.056**	**16.876**	**17.012**	**17.434**	**16.002**
Ca	**45.124**	**45.746**	**45.304**	**45.338**	**45.299**	**45.211**	**44.991**	**45.452**	**45.706**	**45.676**	**45.155**	**47.171**
Mg	**37.601**	**36.830**	**37.593**	**37.374**	**37.669**	**37.392**	**37.227**	**37.492**	**37.419**	**37.312**	**37.411**	**36.827**

Sample No.	SL-13-34-45	SL-13-34-45	SL-13-34-45	SL-13-34-45	SL-13-34-45	SL-13-34-49	SL-13-34-49	SL-13-34-49	SL-13-34-49	SL-13-34-49	SL-13-34-49	SL-13-34-49
Spot	6	7	8	9	10	1	2	3	4	5	6	7
SiO_2	53.113	52.924	52.709	52.417	52.373	50.284	50.309	50.252	50.316	50.708	50.341	51.079
Al_2O_3	1.732	1.672	2.05	2.262	2.018	3.166	2.909	2.991	3.072	2.875	3.09	2.428
MgO	12.444	13.103	12.765	12.803	12.475	12.734	12.632	12.73	12.753	12.857	12.413	12.526
Na_2O	0.594	0.504	0.516	0.495	0.584	0.375	0.496	0.4	0.429	0.406	0.434	0.413
FeO	9.912	10.262	10.097	10.423	10.214	10.467	10.559	10.276	10.159	10.103	10.562	10.573
MnO	0.304	0.325	0.267	0.322	0.29	0.291	0.29	0.309	0.275	0.298	0.323	0.324
Cr_2O_3	0.003	0.001	0.003	0.001	-0.023	-0.001	0.01	-0.002	0.002	-0.002	0.003	0.017
K_2O												
CaO	22.318	21.881	22.147	21.833	22.291	20.918	20.897	21.446	21.218	21.405	21.231	21.409
NiO	-0.002	-0.005	-0.001	-0.003	0.007	-0.021	-0.009	0.009	-0.005	0.002	0.008	-0.001
TiO_2	0.326	0.65	0.682	0.852	0.613	1.19	1.071	1.185	1.202	1.193	1.208	0.891
Sc_2O_3	-0.019	0.021	0.014	0.004	-0.002	0	-0.006	0	-0.008	-0.008	0.001	0.013
Total	100.725	101.338	101.249	101.409	100.84	99.403	99.158	99.596	99.413	99.837	99.614	99.672
Si	1.974	1.958	1.951	1.940	1.950	1.900	1.908	1.898	1.901	1.907	1.902	1.927
Al	0.114	0.109	0.134	0.148	0.133	0.211	0.195	0.199	0.205	0.191	0.206	0.162
Mg	0.694	0.727	0.709	0.711	0.697	0.722	0.719	0.721	0.723	0.725	0.703	0.709
Na	0.021	0.018	0.018	0.018	0.021	0.014	0.018	0.015	0.016	0.015	0.016	0.015
Fe	0.307	0.316	0.311	0.321	0.317	0.330	0.334	0.323	0.320	0.317	0.333	0.332
Mn	0.010	0.010	0.008	0.010	0.009	0.009	0.009	0.010	0.009	0.009	0.010	0.010
Cr	0.000	0.000	0.000	0.000	-0.001	0.000	0.000	0.000	0.000	0.000	0.000	0.001
K	0.000	0.000	0.000	0.000	0.000	0.000	0.000	0.000	0.000	0.000	0.000	0.000
Ca	0.889	0.867	0.878	0.866	0.889	0.847	0.849	0.868	0.859	0.862	0.859	0.865
Ni	0.000	0.000	0.000	0.000	0.000	-0.001	0.000	0.000	0.000	0.000	0.000	0.000
Ti	0.009	0.018	0.019	0.024	0.017	0.034	0.030	0.034	0.034	0.034	0.034	0.025
Sc	-0.001	0.001	0.000	0.000	0.000	0.000	0.000	0.000	0.000	0.000	0.000	0.000
O	6.000	6.000	6.000	6.000	6.000	6.000	6.000	6.000	6.000	6.000	6.000	6.000
Mg#	**69.323**	**69.682**	**69.471**	**68.857**	**68.735**	**68.651**	**68.288**	**69.039**	**69.322**	**69.611**	**67.902**	**68.076**
Fe	**16.248**	**16.557**	**16.405**	**16.937**	**16.654**	**17.363**	**17.550**	**16.911**	**16.821**	**16.626**	**17.544**	**17.434**
Ca	**47.036**	**45.390**	**46.264**	**45.615**	**46.731**	**44.614**	**44.657**	**45.378**	**45.170**	**45.289**	**45.342**	**45.388**
Mg	**36.717**	**38.053**	**37.331**	**37.448**	**36.614**	**38.023**	**37.793**	**37.710**	**38.009**	**38.085**	**37.114**	**37.178**

Sample No.	SL-13-34-49	SL-13-34-49	SL-13-34-53	SL-13-34-53	SL-13-34-53	SL-13-34-53	SL-13-34-53	SL-13-34-53	SL-13-34-53	SL-13-34-53	SL-13-34-53	SL-13-34-53
Spot	8	9	1	2	3	4	5	6	7	8	9	10
SiO_2	50.874	51.055	51.405	51.615	52.541	51.52	51.248	50.863	51.042	51.229	51.159	51.155
Al_2O_3	2.363	2.401	2.89	2.533	1.971	2.621	2.893	3.18	3.179	2.991	3.07	3.233
MgO	12.523	12.44	12.58	13.017	12.922	12.981	12.977	13.085	12.892	12.903	13.015	12.686

Na_2O	0.397	0.409	0.575	0.445	0.513	0.435	0.365	0.381	0.424	0.497	0.431	0.533
FeO	10.546	10.537	9.992	10.022	9.866	10.086	10.079	10.105	10.258	9.848	9.991	9.722
MnO	0.285	0.32	0.269	0.255	0.293	0.291	0.273	0.29	0.289	0.319	0.284	0.267
Cr_2O_3	-0.002	-0.003	-0.002	-0.001	0.006	-0.015	0.004	-0.004	0.009	-0.007	0.022	-0.023
K_2O												
CaO	21.415	21.358	21.685	21.392	21.964	21.653	21.346	21.498	21.404	21.534	21.548	21.652
NiO	0.014	0.012	-0.011	0.014	0.004	-0.031	0.011	0.021	0.005	0.013	0.01	0.015
TiO_2	0.897	0.916	1.064	0.996	0.602	0.958	1.121	1.169	1.261	1.207	1.266	1.214
Sc_2O_3	-0.002	0.001	-0.009	-0.006	-0.005	0.011	-0.011	-0.002	-0.011	-0.005	0.013	0.001
Total	99.31	99.446	100.438	100.282	100.677	100.51	100.306	100.586	100.752	100.529	100.809	100.455
Si	1.927	1.930	1.919	1.928	1.954	1.922	1.915	1.898	1.901	1.910	1.903	1.908
Al	0.158	0.160	0.190	0.167	0.129	0.173	0.191	0.209	0.209	0.197	0.202	0.213
Mg	0.711	0.705	0.705	0.729	0.721	0.726	0.727	0.732	0.720	0.722	0.726	0.710
Na	0.015	0.015	0.021	0.016	0.018	0.016	0.013	0.014	0.015	0.018	0.016	0.019
Fe	0.333	0.332	0.311	0.312	0.306	0.314	0.314	0.314	0.318	0.306	0.310	0.302
Mn	0.009	0.010	0.008	0.008	0.009	0.009	0.009	0.009	0.009	0.010	0.009	0.008
Cr	0.000	0.000	0.000	0.000	0.000	0.000	0.000	0.000	0.000	0.000	0.001	-0.001
K	0.000	0.000	0.000	0.000	0.000	0.000	0.000	0.000	0.000	0.000	0.000	0.000
Ca	0.869	0.865	0.867	0.856	0.875	0.866	0.854	0.859	0.854	0.860	0.859	0.865
Ni	0.000	0.000	0.000	0.000	0.000	-0.001	0.000	0.001	0.000	0.000	0.000	0.000
Ti	0.025	0.026	0.030	0.028	0.017	0.027	0.031	0.033	0.035	0.034	0.035	0.034
Sc	0.000	0.000	0.000	0.000	0.000	0.000	0.000	0.000	0.000	0.000	0.000	0.000
O	6.000	6.000	6.000	6.000	6.000	6.000	6.000	6.000	6.000	6.000	6.000	6.000
Mg#	**68.127**	**68.001**	**69.384**	**70.041**	**70.216**	**69.849**	**69.857**	**69.977**	**69.346**	**70.224**	**70.103**	**70.138**
Fe	**17.397**	**17.448**	**16.511**	**16.441**	**16.078**	**16.456**	**16.555**	**16.485**	**16.821**	**16.208**	**16.346**	**16.097**
Ca	**45.419**	**45.472**	**46.071**	**45.121**	**46.019**	**45.422**	**45.078**	**45.091**	**45.126**	**45.567**	**45.326**	**46.094**
Mg	**37.184**	**37.079**	**37.418**	**38.438**	**37.904**	**38.122**	**38.367**	**38.424**	**38.053**	**38.225**	**38.328**	**37.809**

Sample No.	SL-13-34-58.9	SL-13-34-58.9	SL-13-34-58.9	SL-13-34-58.9	SL-13-34-58.9	SL-13-34-58.9	SL-13-34-58.9	SL-13-34-58.9	SL-13-34-58.9	SL-13-36-16.6	SL-13-36-16.6	SL-13-36-16.6
Spot	1	2	3	4	5	6	7	8	9	1	2	3
SiO_2	51.519	51.51	51.727	51.448	51.558	51.082	52.077	52.116	52.085	52.342	51.693	51.875
Al_2O_3	2.666	2.848	2.834	2.262	2.325	3.203	2.215	2.156	2.222	2.525	2.863	2.817
MgO	12.854	12.856	13.034	13.054	13.261	13.022	13.103	12.929	13.062	12.743	13.038	12.863
Na_2O	0.431	0.41	0.411	0.339	0.348	0.36	0.395	0.433	0.407	0.462	0.418	0.466
FeO	10.282	10.172	10.233	10.702	10.42	10.058	10.144	10.212	10.215	10.428	10.267	10.392
MnO	0.329	0.287	0.272	0.306	0.303	0.28	0.313	0.317	0.306	0.251	0.286	0.328
Cr_2O_3	0.008	0	0.014	-0.007	0.008	0.005	-0.007	0.007	-0.003	-0.012	0.009	0.017
K_2O												

CaO	21.335	21.366	21.314	21.14	21.291	21.347	21.634	21.711	21.611	21.928	21.535	21.495
NiO	-0.011	0.015	-0.017	0.009	0.009	0.001	-0.013	0.02	0.004	-0.004	-0.003	-0.016
TiO_2	1.071	1.119	1.055	1.08	1.06	1.166	0.797	0.677	0.766	0.675	1.115	1.113
Sc_2O_3	0.003	0.008	0.01	-0.001	-0.004	-0.007	0.016	-0.005	0.019	-0.002	-0.008	0.002
Total	100.487	100.591	100.887	100.332	100.579	100.517	100.674	100.573	100.694	101.336	101.213	101.352
Si	1.923	1.919	1.921	1.926	1.924	1.904	1.938	1.943	1.939	1.938	1.915	1.920
Al	0.176	0.187	0.186	0.149	0.153	0.211	0.145	0.142	0.146	0.165	0.187	0.184
Mg	0.720	0.718	0.726	0.733	0.742	0.728	0.732	0.723	0.729	0.708	0.725	0.714
Na	0.016	0.015	0.015	0.012	0.013	0.013	0.014	0.016	0.015	0.017	0.015	0.017
Fe	0.320	0.316	0.317	0.334	0.324	0.312	0.315	0.317	0.317	0.322	0.317	0.321
Mn	0.010	0.009	0.009	0.010	0.010	0.009	0.010	0.010	0.010	0.008	0.009	0.010
Cr	0.000	0.000	0.000	0.000	0.000	0.000	0.000	0.000	0.000	0.000	0.000	0.000
K	0.000	0.000	0.000	0.000	0.000	0.000	0.000	0.000	0.000	0.000	0.000	0.000
Ca	0.853	0.853	0.848	0.848	0.851	0.853	0.863	0.867	0.862	0.870	0.855	0.852
Ni	0.000	0.000	-0.001	0.000	0.000	0.000	0.000	0.001	0.000	0.000	0.000	0.000
Ti	0.030	0.031	0.029	0.030	0.030	0.033	0.022	0.019	0.021	0.019	0.031	0.031
Sc	0.000	0.000	0.000	0.000	0.000	0.000	0.001	0.000	0.001	0.000	0.000	0.000
O	6.000	6.000	6.000	6.000	6.000	6.000	6.000	6.000	6.000	6.000	6.000	6.000
Mg#	**69.233**	**69.465**	**69.630**	**68.707**	**69.612**	**69.974**	**69.925**	**69.502**	**69.712**	**68.746**	**69.566**	**69.021**
Fe	**16.897**	**16.735**	**16.749**	**17.436**	**16.898**	**16.504**	**16.482**	**16.632**	**16.606**	**16.940**	**16.715**	**16.985**
Ca	**45.079**	**45.194**	**44.852**	**44.282**	**44.392**	**45.035**	**45.195**	**45.464**	**45.171**	**45.799**	**45.077**	**45.171**
Mg	**38.023**	**38.071**	**38.399**	**38.282**	**38.709**	**38.461**	**38.322**	**37.904**	**38.223**	**37.261**	**38.208**	**37.844**

Sample No.	SL-13-36-16.6	SL-13-36-16.6	SL-13-36-16.6	SL-13-36-16.6	SL-13-36-16.6	SL-13-36-16.6	SL-13-36-16.6	SL-13-36-20.7	SL-13-36-20.7	SL-13-36-20.7	SL-13-36-20.7	SL-13-36-20.7
Spot	4	5	6	7	8	9	10	1	2	3	4	5
SiO_2	51.208	51.385	51.143	51.742	51.594	52.529	53.207	49.902	51.951	51.655	51.263	52.661
Al_2O_3	3.33	2.736	3.088	2.655	2.955	2.007	1.596	3.378	2.559	2.763	3.179	1.855
MgO	12.803	12.919	12.965	12.813	12.902	12.877	13.184	12.521	12.805	13.104	12.748	12.698
Na_2O	0.456	0.433	0.407	0.417	0.405	0.436	0.416	0.358	0.419	0.359	0.408	0.461
FeO	10.57	10.357	10.476	10.614	10.51	10.499	10.515	12.046	10.215	10.152	10.22	10.196
MnO	0.294	0.289	0.311	0.301	0.293	0.324	0.36	0.312	0.294	0.289	0.291	0.299
Cr_2O_3	-0.002	0.007	0.017	0.024	0.01	-0.011	0.017	0.009	0.01	0.006	0	-0.006
K_2O												
CaO	21.609	21.941	21.526	21.831	21.566	21.925	21.775	19.705	21.559	21.437	21.368	22.165
NiO	-0.008	0.023	0.007	-0.008	0.01	0.012	0.009	0.007	0.014	-0.002	0	-0.006
TiO_2	1.335	1.006	1.138	0.915	1.126	0.64	0.517	1.139	0.962	1.074	1.241	0.553
Sc_2O_3	0.002	0.004	0.012	-0.008	0.003	-0.004	-0.012	0.002	-0.001	-0.02	-0.008	-0.008
Total	101.597	101.1	101.09	101.296	101.374	101.234	101.584	99.379	100.787	100.817	100.71	100.868
Si	1.895	1.911	1.901	1.920	1.911	1.948	1.963	1.895	1.932	1.920	1.909	1.958

Al	0.217	0.180	0.203	0.174	0.193	0.131	0.104	0.226	0.168	0.181	0.209	0.122
Mg	0.711	0.721	0.723	0.713	0.717	0.716	0.730	0.713	0.714	0.730	0.712	0.708
Na	0.016	0.016	0.015	0.015	0.015	0.016	0.015	0.013	0.015	0.013	0.015	0.017
Fe	0.326	0.321	0.325	0.328	0.324	0.324	0.323	0.381	0.317	0.314	0.317	0.316
Mn	0.009	0.009	0.010	0.009	0.009	0.010	0.011	0.010	0.009	0.009	0.009	0.009
Cr	0.000	0.000	0.000	0.001	0.000	0.000	0.000	0.000	0.000	0.000	0.000	0.000
K	0.000	0.000	0.000	0.000	0.000	0.000	0.000	0.000	0.000	0.000	0.000	0.000
Ca	0.857	0.874	0.857	0.868	0.856	0.871	0.861	0.802	0.859	0.854	0.852	0.883
Ni	0.000	0.001	0.000	0.000	0.000	0.000	0.000	0.000	0.000	0.000	0.000	0.000
Ti	0.037	0.028	0.032	0.025	0.031	0.018	0.014	0.032	0.027	0.030	0.035	0.015
Sc	0.000	0.000	0.000	0.000	0.000	0.000	0.000	0.000	0.000	-0.001	0.000	0.000
O	6.000	6.000	6.000	6.000	6.000	6.000	6.000	6.000	6.000	6.000	6.000	6.000
Mg#	**68.556**	**69.186**	**69.018**	**68.483**	**68.844**	**68.825**	**69.296**	**65.169**	**69.291**	**69.910**	**69.186**	**69.152**
Fe	**17.215**	**16.753**	**17.037**	**17.190**	**17.100**	**16.970**	**16.894**	**20.104**	**16.751**	**16.561**	**16.854**	**16.565**
Ca	**45.250**	**45.631**	**45.010**	**45.458**	**45.114**	**45.564**	**44.980**	**42.282**	**45.453**	**44.961**	**45.306**	**46.300**
Mg	**37.534**	**37.615**	**37.953**	**37.352**	**37.786**	**37.465**	**38.127**	**37.614**	**37.796**	**38.478**	**37.841**	**37.135**

Sample No.	SL-13-36-20.7	SL-13-36-20.7	SL-13-36-20.7	SL-13-36-20.7	SL-13-37-7	SL-13-37-7	SL-13-37-7	SL-13-37-7	SL-13-37-7	SL-13-37-7	SL-13-37-7	SL-13-37-7
Spot	6	7	8	9	1	2	3	4	5	6	7	8
SiO_2	51.618	52.143	52.305	52.304	51.097	51.822	52.016	52.227	51.842	52.056	51.081	51.166
Al_2O_3	2.519	2.392	2.394	2.418	3.122	2.371	2.378	2.259	1.636	2.444	3.12	3.265
MgO	12.72	12.846	12.867	12.989	12.776	12.856	12.738	12.864	10.908	12.916	12.955	12.929
Na_2O	0.422	0.433	0.439	0.424	0.427	0.387	0.404	0.484	0.408	0.493	0.431	0.394
FeO	10.381	10.087	10.111	10.193	10.203	10.192	10.518	10.084	12.571	10.154	10.033	10.132
MnO	0.296	0.288	0.286	0.305	0.279	0.293	0.308	0.3	0.946	0.312	0.291	0.274
Cr_2O_3	0.007	0.017	-0.017	0.02	0.004	0.012	-0.002	0.005	-0.014	0.014	-0.008	-0.001
K_2O												
CaO	21.662	21.745	21.702	21.631	21.279	21.523	21.556	21.976	21.983	21.649	21.422	21.377
NiO	0.012	0.007	-0.003	-0.002	0.009	0.001	0.03	-0.008	0.005	0.006	0	-0.014
TiO_2	0.872	0.838	0.819	0.883	1.249	0.901	0.802	0.893	0.522	0.899	1.219	1.229
Sc_2O_3	0.004	-0.014	0.01	-0.013	0.019	-0.002	0.014	0.004	-0.008	-0.004	0.002	0.007
Total	100.513	100.782	100.913	101.152	100.464	100.356	100.762	101.088	100.799	100.939	100.546	100.758
Si	1.928	1.938	1.941	1.937	1.907	1.935	1.937	1.937	1.957	1.933	1.905	1.903
Al	0.166	0.157	0.157	0.158	0.206	0.156	0.156	0.148	0.109	0.160	0.205	0.214
Mg	0.713	0.716	0.716	0.721	0.715	0.720	0.712	0.716	0.618	0.720	0.725	0.721
Na	0.015	0.016	0.016	0.015	0.015	0.014	0.015	0.017	0.015	0.018	0.016	0.014
Fe	0.323	0.312	0.313	0.315	0.317	0.317	0.326	0.312	0.396	0.314	0.312	0.314
Mn	0.009	0.009	0.009	0.010	0.009	0.009	0.010	0.009	0.030	0.010	0.009	0.009
Cr	0.000	0.000	0.000	0.001	0.000	0.000	0.000	0.000	0.000	0.000	0.000	0.000

K	0.000	0.000	0.000	0.000	0.000	0.000	0.000	0.000	0.000	0.000	0.000	0.000
Ca	0.867	0.866	0.863	0.858	0.851	0.861	0.860	0.873	0.889	0.861	0.856	0.852
Ni	0.000	0.000	0.000	0.000	0.000	0.000	0.001	0.000	0.000	0.000	0.000	0.000
Ti	0.024	0.023	0.023	0.025	0.035	0.025	0.022	0.025	0.015	0.025	0.034	0.034
Sc	0.000	0.000	0.000	0.000	0.001	0.000	0.000	0.000	0.000	0.000	0.000	0.000
O	6.000	6.000	6.000	6.000	6.000	6.000	6.000	6.000	6.000	6.000	6.000	6.000
Mg#	**68.804**	**69.626**	**69.611**	**69.639**	**69.268**	**69.424**	**68.553**	**69.662**	**60.966**	**69.601**	**69.918**	**69.668**
Fe	**16.982**	**16.491**	**16.528**	**16.605**	**16.848**	**16.707**	**17.197**	**16.398**	**20.789**	**16.581**	**16.476**	**16.640**
Ca	**45.562**	**45.707**	**45.612**	**45.307**	**45.177**	**45.361**	**45.314**	**45.947**	**46.741**	**45.453**	**45.230**	**45.139**
Mg	**37.456**	**37.802**	**37.860**	**38.088**	**37.975**	**37.932**	**37.488**	**37.654**	**32.470**	**37.965**	**38.294**	**38.221**

Sample No.	SL-13-37-7	SL-13-37-19	SL-13-37-19	SL-13-37-19	SL-13-37-19	SL-13-37-19	SL-13-37-19	SL-13-37-19	SL-13-37-19	SL-13-37-19	SL-13-37-25	SL-13-37-25
Spot	9	1	2	3	4	5	6	7	8	9	1	2
SiO_2	51.176	51.346	51.622	52.639	51.172	51.345	51.482	51.247	51.523	51.128	50.618	51.024
Al_2O_3	3.063	2.709	2.634	1.723	2.905	2.875	2.653	3.236	2.786	3.295	3.153	2.801
MgO	12.925	12.816	12.935	13.074	12.905	12.91	13.087	12.957	12.877	12.774	13.104	13.185
Na_2O	0.419	0.457	0.422	0.415	0.399	0.43	0.389	0.38	0.419	0.396	0.4	0.37
FeO	10.111	10.394	10.303	9.963	10.315	10.27	10.529	10.052	10.448	10.227	10.021	10.351
MnO	0.303	0.284	0.309	0.293	0.281	0.305	0.272	0.286	0.308	0.264	0.263	0.28
Cr_2O_3	-0.008	0.014	0.014	0.006	0.007	-0.01	0.017	0	0.015	-0.018	0.01	0.001
K_2O												
CaO	21.552	21.332	21.397	21.886	21.329	21.309	21.505	21.489	21.2	21.395	21.394	21.374
NiO	0.006	0.005	-0.029	0.008	0	0.035	0.013	-0.014	0.014	0.032	0	0.003
TiO_2	1.177	1.061	1.093	0.604	1.161	1.172	1.085	1.161	1.053	1.233	1.148	0.986
Sc_2O_3	0.01	0.003	0.004	0.018	-0.001	0.013	-0.007	-0.009	-0.004	-0.006	0.017	-0.004
Total	100.734	100.421	100.704	100.629	100.473	100.654	101.025	100.785	100.639	100.72	100.128	100.371
Si	1.906	1.919	1.922	1.958	1.911	1.914	1.914	1.905	1.920	1.904	1.897	1.909
Al	0.201	0.179	0.173	0.113	0.191	0.189	0.174	0.212	0.183	0.217	0.209	0.185
Mg	0.722	0.719	0.723	0.730	0.723	0.722	0.730	0.723	0.720	0.713	0.737	0.740
Na	0.015	0.017	0.015	0.015	0.014	0.016	0.014	0.014	0.015	0.014	0.015	0.013
Fe	0.314	0.324	0.320	0.309	0.321	0.319	0.326	0.311	0.325	0.317	0.313	0.323
Mn	0.010	0.009	0.010	0.009	0.009	0.010	0.009	0.009	0.010	0.008	0.008	0.009
Cr	0.000	0.000	0.000	0.000	0.000	0.000	0.000	0.000	0.000	-0.001	0.000	0.000
K	0.000	0.000	0.000	0.000	0.000	0.000	0.000	0.000	0.000	0.000	0.000	0.000
Ca	0.860	0.854	0.854	0.872	0.854	0.851	0.857	0.856	0.847	0.854	0.859	0.857
Ni	0.000	0.000	-0.001	0.000	0.000	0.001	0.000	0.000	0.000	0.001	0.000	0.000
Ti	0.033	0.030	0.031	0.017	0.033	0.033	0.030	0.032	0.029	0.034	0.032	0.028
Sc	0.000	0.000	0.000	0.001	0.000	0.000	0.000	0.000	0.000	0.000	0.001	0.000
O	6.000	6.000	6.000	6.000	6.000	6.000	6.000	6.000	6.000	6.000	6.000	6.000

Mg#	**69.706**	**68.939**	**69.324**	**70.256**	**69.249**	**69.351**	**69.110**	**69.881**	**68.929**	**69.215**	**70.183**	**69.631**
Fe	**16.552**	**17.070**	**16.864**	**16.164**	**16.919**	**16.862**	**17.055**	**16.478**	**17.161**	**16.841**	**16.397**	**16.813**
Ca	**45.362**	**45.044**	**45.028**	**45.654**	**44.980**	**44.983**	**44.787**	**45.291**	**44.769**	**45.297**	**45.008**	**44.637**
Mg	**38.086**	**37.886**	**38.109**	**38.181**	**38.101**	**38.154**	**38.158**	**38.232**	**38.070**	**37.863**	**38.595**	**38.550**

Sample No.	SL-13-37-25	SL-13-37-25	SL-13-37-25	SL-13-37-25	SL-13-37-25	SL-13-37-25	SL-13-37-25	SL-13-37-27	SL-13-37-27	SL-13-37-27	SL-13-37-27	SL-13-37-27
Spot	3	4	5	6	7	8	9	1	2	3	4	5
SiO_2	50.656	50.71	51.017	51.148	51.491	51.459	51.827	51.452	51.787	51.964	51.708	51.803
Al_2O_3	3.283	3.251	2.956	2.889	2.571	2.798	2.426	2.623	2.372	2.375	2.332	2.373
MgO	13.213	13.106	12.785	12.922	13.074	13.092	13.11	13.166	13.205	13.229	13.107	13.104
Na_2O	0.378	0.354	0.395	0.401	0.451	0.417	0.438	0.447	0.43	0.445	0.455	0.436
FeO	9.881	9.915	10.514	10.326	9.821	9.781	9.746	10.09	10.028	10.048	10.046	9.893
MnO	0.28	0.267	0.267	0.265	0.25	0.272	0.28	0.301	0.27	0.303	0.304	0.27
Cr_2O_3	0.012	0.022	-0.01	0.015	0.006	0.001	0.004	0.011	0.005	-0.002	-0.001	0.003
K_2O												
CaO	21.307	21.43	21.154	21.248	21.826	21.891	21.842	21.73	21.788	21.932	21.694	21.571
NiO	0.006	0.006	0.011	0.016	-0.002	-0.004	-0.003	-0.003	0.015	-0.027	-0.018	-0.019
TiO_2	1.178	1.208	1.151	1.157	0.871	0.95	0.819	1.017	0.837	0.835	0.873	0.873
Sc_2O_3	-0.012	0.017	0.015	0.013	-0.002	-0.009	-0.008	0.005	0.013	0.01	0.017	-0.016
Total	100.182	100.286	100.255	100.4	100.357	100.648	100.481	100.839	100.75	101.112	100.517	100.291
Si	1.895	1.896	1.911	1.912	1.923	1.916	1.931	1.915	1.928	1.927	1.929	1.934
Al	0.217	0.215	0.195	0.191	0.169	0.184	0.160	0.172	0.156	0.155	0.154	0.156
Mg	0.742	0.735	0.718	0.724	0.732	0.731	0.733	0.735	0.737	0.736	0.734	0.734
Na	0.014	0.013	0.014	0.015	0.016	0.015	0.016	0.016	0.015	0.016	0.016	0.016
Fe	0.308	0.309	0.328	0.322	0.306	0.303	0.303	0.313	0.311	0.311	0.312	0.308
Mn	0.009	0.008	0.008	0.008	0.008	0.009	0.009	0.009	0.008	0.010	0.010	0.009
Cr	0.000	0.001	0.000	0.000	0.000	0.000	0.000	0.000	0.000	0.000	0.000	0.000
K	0.000	0.000	0.000	0.000	0.000	0.000	0.000	0.000	0.000	0.000	0.000	0.000
Ca	0.854	0.858	0.849	0.851	0.873	0.873	0.872	0.867	0.869	0.872	0.867	0.863
Ni	0.000	0.000	0.000	0.000	0.000	0.000	0.000	0.000	0.000	-0.001	-0.001	-0.001
Ti	0.033	0.034	0.032	0.032	0.024	0.027	0.023	0.028	0.023	0.023	0.024	0.024
Sc	0.000	0.001	0.000	0.000	0.000	0.000	0.000	0.000	0.000	0.000	0.001	-0.001
O	6.000	6.000	6.000	6.000	6.000	6.000	6.000	6.000	6.000	6.000	6.000	6.000
Mg#	**70.649**	**70.408**	**68.640**	**69.255**	**70.555**	**70.669**	**70.771**	**70.138**	**70.329**	**70.325**	**70.135**	**70.451**
Fe	**16.183**	**16.238**	**17.314**	**16.954**	**15.991**	**15.906**	**15.866**	**16.346**	**16.224**	**16.191**	**16.327**	**16.161**
Ca	**44.866**	**45.125**	**44.789**	**44.855**	**45.692**	**45.771**	**45.717**	**45.261**	**45.321**	**45.438**	**45.331**	**45.307**
Mg	**38.951**	**38.636**	**37.897**	**38.190**	**38.318**	**38.323**	**38.417**	**38.393**	**38.455**	**38.371**	**38.343**	**38.532**

Sample No.	SL-13-37-27	SL-13-37-27	SL-13-37-27	SL-13-37-27	SL-13-37-37	SL-13-37-37	SL-13-37-37	SL-13-37-37	SL-13-37-37	SL-13-37-37	SL-13-37-37	SL-13-37-37
Spot	6	7	8	9	1	2	3	4	5	6	7	8
SiO_2	51.8	51.289	51.153	51.156	51.15	51.747	51.733	51.624	51.231	51.269	50.966	51.19
Al_2O_3	2.347	3.113	3.164	3.14	2.922	2.491	2.611	2.657	3.058	2.735	2.972	3.018
MgO	13.073	12.97	13.051	12.864	12.963	13.233	12.965	13.29	13.054	12.595	13.057	13.079
Na_2O	0.447	0.406	0.393	0.43	0.421	0.399	0.413	0.407	0.463	0.514	0.432	0.458
FeO	10.057	10.364	10.201	10.22	10.167	10.294	10.136	10.115	10.215	10.809	10.277	10.103
MnO	0.291	0.306	0.297	0.285	0.261	0.285	0.288	0.255	0.292	0.282	0.256	0.276
Cr_2O_3	0.015	0.012	0.007	-0.01	-0.004	0.006	0.011	0.006	0.01	0	0.012	0
K_2O												
CaO	21.696	21.556	21.373	21.479	21.55	21.497	21.853	21.419	21.421	21.338	21.446	21.401
NiO	0.006	0	0.018	-0.008	-0.005	-0.002	0.003	-0.032	-0.013	0.001	0	0.02
TiO_2	0.836	1.194	1.273	1.208	1.107	0.973	0.832	1.007	1.12	1.011	1.152	1.134
Sc_2O_3	0.014	0.01	0.007	0.008	0.007	-0.001	-0.008	-0.001	-0.02	0.001	0.018	0.003
Total	100.582	101.22	100.937	100.772	100.539	100.922	100.837	100.747	100.831	100.555	100.588	100.682
Si	1.931	1.903	1.901	1.905	1.909	1.923	1.925	1.920	1.906	1.918	1.903	1.907
Al	0.154	0.204	0.208	0.206	0.192	0.163	0.171	0.174	0.201	0.181	0.196	0.198
Mg	0.731	0.722	0.728	0.718	0.726	0.738	0.724	0.741	0.729	0.707	0.731	0.731
Na	0.016	0.015	0.014	0.015	0.015	0.014	0.015	0.015	0.017	0.019	0.016	0.017
Fe	0.312	0.320	0.316	0.317	0.316	0.319	0.314	0.313	0.317	0.337	0.320	0.314
Mn	0.009	0.010	0.009	0.009	0.008	0.009	0.009	0.008	0.009	0.009	0.008	0.009
Cr	0.000	0.000	0.000	0.000	0.000	0.000	0.000	0.000	0.000	0.000	0.000	0.000
K	0.000	0.000	0.000	0.000	0.000	0.000	0.000	0.000	0.000	0.000	0.000	0.000
Ca	0.867	0.857	0.851	0.857	0.862	0.856	0.871	0.853	0.854	0.855	0.858	0.854
Ni	0.000	0.000	0.001	0.000	0.000	0.000	0.000	-0.001	0.000	0.000	0.000	0.001
Ti	0.023	0.033	0.035	0.034	0.031	0.027	0.023	0.028	0.031	0.028	0.032	0.032
Sc	0.000	0.000	0.000	0.000	0.000	0.000	0.000	0.000	-0.001	0.000	0.001	0.000
O	6.000	6.000	6.000	6.000	6.000	6.000	6.000	6.000	6.000	6.000	6.000	6.000
Mg#	**70.058**	**69.255**	**69.724**	**69.378**	**69.651**	**69.824**	**69.719**	**70.282**	**69.699**	**67.715**	**69.576**	**69.972**
Fe	**16.357**	**16.873**	**16.676**	**16.757**	**16.611**	**16.670**	**16.463**	**16.427**	**16.677**	**17.745**	**16.751**	**16.519**
Ca	**45.370**	**45.120**	**44.922**	**45.279**	**45.268**	**44.758**	**45.634**	**44.723**	**44.963**	**45.038**	**44.942**	**44.989**
Mg	**38.273**	**38.007**	**38.403**	**37.965**	**38.122**	**38.572**	**37.903**	**38.850**	**38.361**	**37.218**	**38.307**	**38.492**

Sample No.	SL-13-41-3	SL-13-41-3	SL-13-41-3	SL-13-41-3	SL-13-41-3	SL-13-41-3	SL-13-41-3	SL-13-41-3	SL-13-41-3	SL-13-41-3	SL-13-41-3	SL-13-41-3
Spot	1	2	3	4	5	6	7	8	9	10	11	12
SiO_2	51.359	51.37	51.517	51.347	51.804	51.691	51.214	51.027	50.616	51.318	51.111	52.509
Al_2O_3	1.516	1.901	1.911	1.912	1.456	1.692	1.858	1.472	1.657	1.577	1.91	1.167
MgO	11.073	11.119	11.143	10.853	10.618	10.823	10.848	9.904	9.619	10.692	11.448	11.174

Na_2O	0.296	0.347	0.338	0.399	0.341	0.359	0.356	0.355	0.321	0.361	0.393	0.356
FeO	14.124	13.353	13.389	13.72	14.484	14.313	13.749	15.664	15.433	14.307	13.021	12.908
MnO	0.483	0.471	0.452	0.473	0.498	0.514	0.463	0.509	0.497	0.485	0.444	0.433
Cr_2O_3	0.002	0.012	0.012	0	-0.009	-0.017	-0.014	0.015	-0.006	0.009	0.003	0.013
K_2O												
CaO	20.753	21.185	21.349	21.349	21.653	21.167	21.34	20.998	21.054	21.107	21.108	21.91
NiO	0.009	0.019	-0.006	0.009	-0.008	0	0.017	0.023	0.006	-0.004	0.019	0.007
TiO_2	0.865	0.992	1.001	0.982	0.657	0.71	1.138	0.967	1.073	0.99	1.169	0.421
Sc_2O_3	0.004	0.003	0.006	0.002	-0.001	-0.008	-0.009	0.029	0.012	0.018	0.023	0.006
Total	100.484	100.772	101.112	101.046	101.493	101.244	100.96	100.963	100.282	100.86	100.649	100.904
Si	1.950	1.940	1.939	1.939	1.954	1.950	1.936	1.946	1.942	1.945	1.931	1.976
Al	0.102	0.127	0.127	0.127	0.097	0.113	0.124	0.099	0.112	0.106	0.127	0.077
Mg	0.631	0.630	0.629	0.615	0.601	0.613	0.615	0.566	0.554	0.608	0.649	0.631
Na	0.011	0.013	0.012	0.015	0.012	0.013	0.013	0.013	0.012	0.013	0.014	0.013
Fe	0.447	0.420	0.420	0.432	0.455	0.450	0.433	0.498	0.494	0.452	0.410	0.405
Mn	0.016	0.015	0.014	0.015	0.016	0.016	0.015	0.016	0.016	0.016	0.014	0.014
Cr	0.000	0.000	0.000	0.000	0.000	-0.001	0.000	0.000	0.000	0.000	0.000	0.000
K	0.000	0.000	0.000	0.000	0.000	0.000	0.000	0.000	0.000	0.000	0.000	0.000
Ca	0.844	0.857	0.861	0.864	0.875	0.856	0.864	0.858	0.866	0.857	0.855	0.883
Ni	0.000	0.001	0.000	0.000	0.000	0.000	0.001	0.001	0.000	0.000	0.001	0.000
Ti	0.025	0.028	0.028	0.028	0.019	0.020	0.032	0.028	0.031	0.028	0.033	0.012
Sc	0.000	0.000	0.000	0.000	0.000	0.000	0.000	0.001	0.000	0.001	0.001	0.000
O	6.000	6.000	6.000	6.000	6.000	6.000	6.000	6.000	6.000	6.000	6.000	6.000
Mg#	**58.526**	**59.982**	**59.969**	**58.744**	**56.888**	**57.647**	**58.681**	**53.230**	**52.872**	**57.359**	**61.279**	**60.910**
Fe	**23.254**	**22.033**	**21.987**	**22.601**	**23.576**	**23.460**	**22.646**	**25.896**	**25.801**	**23.574**	**21.428**	**21.095**
Ca	**43.930**	**44.943**	**45.075**	**45.217**	**45.315**	**44.608**	**45.192**	**44.632**	**45.254**	**44.715**	**44.661**	**46.036**
Mg	**32.815**	**33.024**	**32.938**	**32.181**	**31.109**	**31.932**	**32.162**	**29.472**	**28.945**	**31.711**	**33.911**	**32.869**

Sample No.	SL-13-41-3	SL-13-41-7.5	SL-13-41-7.5	SL-13-41-7.5	SL-13-41-7.5	SL-13-41-7.5	SL-13-41-7.5	SL-13-41-7.5	SL-13-41-7.5	SL-13-41-7.5	SL-13-41-12.1	SL-13-41-12.12
Spot	13	1	2	3	4	5	6	7	8	9	1	2
SiO_2	51.219	50.18	50.081	50.397	51.303	51.387	50.834	50.202	50.617	50.661	51.365	51.547
Al_2O_3	1.98	1.617	1.657	1.354	1.052	1.295	1.228	1.42	1.596	1.41	2.571	2.596
MgO	11.456	9.826	9.51	9.726	10.444	10.469	10.349	9.962	9.596	9.678	13.089	13.188
Na_2O	0.355	0.31	0.3	0.284	0.335	0.347	0.359	0.302	0.301	0.283	0.352	0.315
FeO	13.074	15.327	15.613	15.628	14.436	13.988	14.352	15.166	15.645	15.706	10.592	10.718
MnO	0.44	0.544	0.535	0.606	0.558	0.478	0.549	0.549	0.584	0.559	0.289	0.322
Cr_2O_3	-0.027	-0.003	0.002	-0.003	0.014	-0.009	-0.016	0.002	0	0.012	-0.014	0.005
K_2O												

CaO	21.297	20.729	20.48	20.306	20.938	20.902	20.804	20.432	20.68	20.316	21.317	21.338
NiO	-0.014	0.004	0.011	0.023	-0.009	0.018	0.011	0.023	-0.033	-0.007	-0.023	-0.003
TiO_2	1.141	0.741	0.687	0.771	0.466	0.574	0.569	0.782	0.698	0.709	1.098	1.098
Sc_2O_3	0.012	-0.014	-0.013	-0.005	-0.003	-0.001	-0.012	0.011	0.002	0.006	0.006	-0.022
Total	100.933	99.261	98.863	99.087	99.534	99.448	99.027	98.851	99.686	99.333	100.642	101.102
Si	1.930	1.945	1.950	1.957	1.972	1.971	1.965	1.952	1.954	1.961	1.917	1.916
Al	0.132	0.111	0.114	0.093	0.071	0.088	0.084	0.097	0.109	0.096	0.169	0.170
Mg	0.648	0.571	0.556	0.567	0.602	0.602	0.600	0.581	0.556	0.562	0.733	0.735
Na	0.013	0.012	0.011	0.011	0.012	0.013	0.013	0.011	0.011	0.011	0.013	0.011
Fe	0.411	0.495	0.507	0.506	0.462	0.447	0.462	0.491	0.503	0.507	0.329	0.332
Mn	0.014	0.018	0.018	0.020	0.018	0.016	0.018	0.018	0.019	0.018	0.009	0.010
Cr	-0.001	0.000	0.000	0.000	0.000	0.000	0.000	0.000	0.000	0.000	0.000	0.000
K	0.000	0.000	0.000	0.000	0.000	0.000	0.000	0.000	0.000	0.000	0.000	0.000
Ca	0.860	0.861	0.855	0.845	0.862	0.859	0.861	0.851	0.855	0.843	0.852	0.850
Ni	0.000	0.000	0.000	0.001	0.000	0.001	0.000	0.001	-0.001	0.000	-0.001	0.000
Ti	0.032	0.022	0.020	0.022	0.013	0.017	0.016	0.023	0.020	0.021	0.031	0.031
Sc	0.000	0.000	0.000	0.000	0.000	0.000	0.000	0.000	0.000	0.000	0.000	-0.001
O	6.000	6.000	6.000	6.000	6.000	6.000	6.000	6.000	6.000	6.000	6.000	6.000
Mg#	**61.199**	**53.574**	**52.299**	**52.835**	**56.564**	**57.395**	**56.483**	**54.178**	**52.473**	**52.588**	**68.986**	**68.894**
Fe	**21.406**	**25.688**	**26.435**	**26.380**	**23.998**	**23.428**	**24.029**	**25.546**	**26.291**	**26.509**	**17.206**	**17.318**
Ca	**44.832**	**44.668**	**44.582**	**44.069**	**44.751**	**45.010**	**44.783**	**44.249**	**44.682**	**44.088**	**44.522**	**44.327**
Mg	**33.762**	**29.643**	**28.983**	**29.551**	**31.251**	**31.562**	**31.188**	**30.204**	**29.027**	**29.403**	**38.272**	**38.355**

Sample	SL-13-41-	SL-13-41-	SL-13-41-	SL-13-41-	SL-13-41-	SL-13-41-	SL-13-41-	SL-13-41-	SL-13-41-	SL-13-41-	SL-13-41-	SL-13-41-
No.	12.23	12.34	12.45	12.56	45	45	45	45	45	45	45	45
Spot	3	4	5	6	1	2	3	4	5	6	7	8
SiO_2	51.425	51.319	51.43	51.195	52.225	51.293	50.83	52.055	51.415	52.05	51.933	51.542
Al_2O_3	2.647	1.958	1.999	2.143	1.799	2.477	2.987	1.682	1.604	1.471	1.719	2.414
MgO	13.035	11.565	11.27	11.789	11.698	12.166	12.245	11.422	11.348	11.101	11.737	11.898
Na_2O	0.338	0.324	0.322	0.314	0.365	0.395	0.376	0.345	0.377	0.369	0.4	0.385
FeO	10.524	12.977	13.57	12.801	12.131	11.404	11.205	12.483	12.479	13.145	11.869	11.641
MnO	0.31	0.452	0.461	0.441	0.387	0.352	0.335	0.387	0.384	0.439	0.383	0.379
Cr_2O_3	0.01	-0.006	0	-0.008	-0.017	-0.007	0.01	-0.034	0.012	0.005	-0.004	-0.003
K_2O												
CaO	21.285	21.009	20.84	20.992	21.712	21.405	21.367	21.766	21.85	21.887	21.763	21.682
NiO	-0.006	-0.009	-0.025	-0.007	0.017	0.008	-0.002	0.006	0.011	-0.004	-0.001	0.016
TiO_2	1.129	0.999	0.907	1.031	0.606	1.003	1.239	0.669	0.628	0.598	0.647	0.878
Sc_2O_3	-0.021	0.02	0.003	0.008	0.009	0.004	-0.006	-0.001	-0.009	-0.005	-0.009	0.003
Total	100.676	100.608	100.777	100.699	100.932	100.5	100.586	100.78	100.099	101.056	100.437	100.835
Si	1.918	1.937	1.941	1.929	1.957	1.926	1.906	1.957	1.951	1.960	1.955	1.931

Al	0.174	0.130	0.133	0.142	0.119	0.164	0.198	0.112	0.107	0.098	0.114	0.160
Mg	0.729	0.655	0.638	0.666	0.657	0.685	0.689	0.644	0.646	0.627	0.663	0.669
Na	0.012	0.012	0.012	0.011	0.013	0.014	0.014	0.013	0.014	0.013	0.015	0.014
Fe	0.327	0.408	0.427	0.402	0.379	0.357	0.350	0.391	0.395	0.412	0.372	0.363
Mn	0.010	0.014	0.015	0.014	0.012	0.011	0.011	0.012	0.012	0.014	0.012	0.012
Cr	0.000	0.000	0.000	0.000	-0.001	0.000	0.000	-0.001	0.000	0.000	0.000	0.000
K	0.000	0.000	0.000	0.000	0.000	0.000	0.000	0.000	0.000	0.000	0.000	0.000
Ca	0.850	0.850	0.843	0.847	0.872	0.861	0.858	0.877	0.888	0.883	0.878	0.870
Ni	0.000	0.000	-0.001	0.000	0.001	0.000	0.000	0.000	0.000	0.000	0.000	0.000
Ti	0.032	0.028	0.026	0.029	0.017	0.028	0.035	0.019	0.018	0.017	0.018	0.025
Sc	-0.001	0.001	0.000	0.000	0.000	0.000	0.000	0.000	0.000	0.000	0.000	0.000
O	6.000	6.000	6.000	6.000	6.000	6.000	6.000	6.000	6.000	6.000	6.000	6.000
Mg#	**69.035**	**61.600**	**59.918**	**62.373**	**63.447**	**65.757**	**66.297**	**62.221**	**62.076**	**60.319**	**64.029**	**64.785**
Fe	**17.153**	**21.342**	**22.374**	**20.981**	**19.853**	**18.749**	**18.454**	**20.455**	**20.458**	**21.455**	**19.465**	**19.104**
Ca	**44.605**	**44.423**	**44.178**	**44.238**	**45.686**	**45.247**	**45.245**	**45.856**	**46.055**	**45.931**	**45.888**	**45.749**
Mg	**38.242**	**34.235**	**33.447**	**34.781**	**34.461**	**36.004**	**36.301**	**33.689**	**33.487**	**32.614**	**34.647**	**35.147**

Sample No.	SL-13-41-45	SL-13-41-63.2	SL-13-41-63.2	SL-13-41-63.2	SL-13-41-63.2	SL-13-41-63.2	SL-13-41-63.2	SL-13-41-63.2	SL-13-41-63.2	SL-13-41-63.2	SL-13-41-68.9	SL-13-41-68.9
Spot	9	1	2	3	4	5	6	7	8	9	1	2
SiO_2	51.999	51.688	51.171	51.634	51.785	52.08	52.546	52.015	51.771	51.92	51.834	51.996
Al_2O_3	2.394	2.501	2.42	2.428	2.023	2.511	2.016	2.478	2.545	2.408	2.325	2.438
MgO	11.874	12.62	12.608	12.849	12.746	12.765	12.787	12.68	12.683	12.635	13.163	13.1
Na_2O	0.37	0.395	0.425	0.414	0.404	0.465	0.441	0.372	0.402	0.403	0.329	0.372
FeO	11.845	10.864	10.814	10.62	10.502	10.723	10.591	10.858	10.951	10.836	10.707	10.682
MnO	0.381	0.287	0.339	0.307	0.322	0.312	0.323	0.34	0.31	0.283	0.347	0.306
Cr_2O_3	0.002	0.008	0.01	-0.009	-0.013	-0.01	0.017	-0.016	-0.003	0.021	0	-0.004
K_2O												
CaO	21.94	21.431	21.398	21.616	21.85	21.759	21.823	21.763	21.635	21.674	21.264	21.277
NiO	-0.004	-0.018	0.006	0.006	-0.014	0.007	-0.016	0.003	0.005	0.018	0.014	-0.012
TiO_2	0.87	0.949	0.893	0.902	0.738	1.142	0.72	0.962	0.972	0.972	1.166	1.164
Sc_2O_3	0.015	0.011	0.006	0.009	0.004	-0.027	0.01	-0.002	0.013	-0.002	-0.008	0.011
Total	101.686	100.736	100.09	100.776	100.347	101.727	101.258	101.453	101.284	101.168	101.141	101.33
Si	1.933	1.929	1.925	1.926	1.940	1.924	1.948	1.928	1.923	1.930	1.925	1.926
Al	0.157	0.165	0.161	0.160	0.134	0.164	0.132	0.162	0.167	0.158	0.152	0.159
Mg	0.662	0.706	0.711	0.719	0.716	0.708	0.711	0.705	0.707	0.704	0.733	0.728
Na	0.013	0.014	0.015	0.015	0.015	0.017	0.016	0.013	0.014	0.014	0.012	0.013
Fe	0.367	0.338	0.339	0.330	0.328	0.330	0.327	0.335	0.339	0.336	0.331	0.330
Mn	0.012	0.009	0.011	0.010	0.010	0.010	0.010	0.011	0.010	0.009	0.011	0.010
Cr	0.000	0.000	0.000	0.000	0.000	0.000	0.000	0.000	0.000	0.001	0.000	0.000

K	0.000	0.000	0.000	0.000	0.000	0.000	0.000	0.000	0.000	0.000	0.000	0.000
Ca	0.874	0.857	0.862	0.864	0.877	0.861	0.867	0.864	0.861	0.863	0.846	0.844
Ni	0.000	-0.001	0.000	0.000	0.000	0.000	0.000	0.000	0.000	0.001	0.000	0.000
Ti	0.024	0.027	0.025	0.025	0.021	0.032	0.020	0.027	0.027	0.027	0.032	0.032
Sc	0.000	0.000	0.000	0.000	0.000	-0.001	0.000	0.000	0.000	0.000	0.000	0.000
O	6.000	6.000	6.000	6.000	6.000	6.000	6.000	6.000	6.000	6.000	6.000	6.000
Mg#	**64.342**	**67.647**	**67.727**	**68.532**	**68.599**	**68.181**	**68.486**	**67.763**	**67.582**	**67.730**	**68.875**	**68.823**
Fe	**19.283**	**17.771**	**17.722**	**17.257**	**17.066**	**17.386**	**17.175**	**17.609**	**17.779**	**17.635**	**17.342**	**17.336**
Ca	**45.922**	**45.072**	**45.086**	**45.161**	**45.651**	**45.359**	**45.500**	**45.377**	**45.159**	**45.352**	**44.282**	**44.396**
Mg	**34.795**	**37.158**	**37.192**	**37.582**	**37.283**	**37.254**	**37.325**	**37.014**	**37.063**	**37.013**	**38.376**	**38.268**

Sample No.	SL-13-41-68.9	SL-13-41-68.9	SL-13-41-68.9	SL-13-41-68.9	SL-13-41-68.9	SL-13-41-68.9	SL-13-41-68.9	SL-13-41-73	SL-13-41-73	SL-13-41-73	SL-13-41-73	SL-13-41-73
Spot	3	4	5	6	7	8	9	1	2	3	4	5
SiO_2	51.573	52.511	51.996	51.128	51.448	51.496	51.331	51.829	51.721	51.895	51.104	52.188
Al_2O_3	3.211	2.17	2.4	3.581	2.975	2.967	2.986	2.444	2.442	2.373	3.13	1.984
MgO	12.858	12.772	12.589	12.498	12.461	12.334	12.566	12.959	12.885	12.885	12.898	12.932
Na_2O	0.389	0.421	0.374	0.659	0.443	0.443	0.413	0.406	0.406	0.421	0.419	0.457
FeO	10.83	10.617	10.721	11.447	10.297	10.541	10.321	10.33	10.404	10.346	10.227	10.218
MnO	0.302	0.343	0.292	0.315	0.281	0.316	0.305	0.298	0.311	0.31	0.274	0.309
Cr_2O_3	0.013	-0.009	0.001	0.028	0.022	-0.004	0.007	0.007	0	-0.015	-0.003	0.009
K_2O												
CaO	21.463	21.959	21.852	20.229	21.547	21.431	21.284	22.013	21.918	21.88	21.518	21.808
NiO	0	-0.005	-0.009	0.025	0.013	-0.01	0.027	0.004	0.005	0.002	-0.015	0.001
TiO_2	1.45	0.793	0.848	0.711	1.136	1.073	1.16	0.83	0.836	0.827	1.303	0.7
Sc_2O_3	-0.002	0.022	0.005	0.018	0.007	-0.008	-0.01	-0.01	0.004	0.015	0	0.015
Total	102.087	101.594	101.069	100.639	100.63	100.579	100.39	101.11	100.932	100.939	100.855	100.621
Si	1.899	1.941	1.934	1.910	1.918	1.922	1.918	1.926	1.926	1.931	1.902	1.946
Al	0.209	0.142	0.158	0.236	0.196	0.195	0.197	0.160	0.160	0.156	0.206	0.131
Mg	0.710	0.708	0.702	0.700	0.697	0.691	0.704	0.722	0.720	0.719	0.720	0.723
Na	0.014	0.015	0.013	0.024	0.016	0.016	0.015	0.015	0.015	0.015	0.015	0.016
Fe	0.332	0.327	0.332	0.356	0.320	0.328	0.321	0.320	0.323	0.321	0.317	0.317
Mn	0.009	0.011	0.009	0.010	0.009	0.010	0.010	0.009	0.010	0.010	0.009	0.010
Cr	0.000	0.000	0.000	0.001	0.001	0.000	0.000	0.000	0.000	0.000	0.000	0.000
K	0.000	0.000	0.000	0.000	0.000	0.000	0.000	0.000	0.000	0.000	0.000	0.000
Ca	0.847	0.870	0.871	0.810	0.861	0.857	0.852	0.876	0.874	0.872	0.858	0.871
Ni	0.000	0.000	0.000	0.001	0.000	0.000	0.001	0.000	0.000	0.000	0.000	0.000
Ti	0.040	0.022	0.024	0.020	0.032	0.030	0.033	0.023	0.023	0.023	0.036	0.020
Sc	0.000	0.001	0.000	0.001	0.000	0.000	0.000	0.000	0.000	0.000	0.000	0.000
O	6.000	6.000	6.000	6.000	6.000	6.000	6.000	6.000	6.000	6.000	6.000	6.000

Mg#	**68.123**	**68.408**	**67.883**	**66.276**	**68.536**	**67.806**	**68.667**	**69.307**	**69.033**	**69.152**	**69.420**	**69.495**
Fe	**17.590**	**17.169**	**17.439**	**19.094**	**17.040**	**17.482**	**17.115**	**16.672**	**16.841**	**16.776**	**16.736**	**16.605**
Ca	**44.820**	**45.655**	**45.701**	**43.382**	**45.844**	**45.698**	**45.378**	**45.680**	**45.616**	**45.616**	**45.273**	**45.566**
Mg	**37.591**	**37.176**	**36.860**	**37.524**	**37.117**	**36.820**	**37.507**	**37.648**	**37.543**	**37.608**	**37.992**	**37.829**

Sample No.	SL-13-41-73	SL-13-41-73	SL-13-41-73	SL-13-41-73	SL-13-41-73	SL-13-41-73	SL-13-41-73	SL-13-41-73	SL-13-41-73	SL-13-41-73	SL-13-41-91	SL-13-41-91
Spot	6	7	8	9	10	11	12	13	14	15	1	2
SiO_2	52.053	51.791	52.001	51.801	51.072	52.184	51.362	51.689	51.221	51.76	50.734	51.825
Al_2O_3	2.348	2.427	2.49	2.42	3.147	1.979	2.961	2.578	3.001	2.53	3.279	2.378
MgO	12.879	12.909	12.944	13.006	12.73	12.841	12.721	12.677	12.946	12.81	13.008	13.515
Na_2O	0.407	0.411	0.441	0.427	0.447	0.429	0.441	0.424	0.415	0.416	0.415	0.527
FeO	10.248	10.24	10.187	10.285	10.24	10.192	10.292	10.462	10.283	10.415	10.044	9.403
MnO	0.315	0.318	0.299	0.321	0.287	0.296	0.304	0.29	0.31	0.307	0.245	0.261
Cr_2O_3	-0.013	0.01	-0.013	-0.011	0.008	-0.01	0.003	0.007	-0.013	-0.011	0.001	-0.004
K_2O												
CaO	21.859	21.771	21.743	21.751	21.586	21.867	21.553	21.76	21.45	21.57	21.492	21.923
NiO	0.006	-0.023	0.023	-0.021	0.014	-0.024	-0.009	-0.004	-0.018	-0.017	-0.022	0.012
TiO_2	0.791	0.844	0.907	0.851	1.286	0.714	1.194	0.912	1.235	0.913	1.171	0.828
Sc_2O_3	-0.006	0.008	0.011	0.009	-0.01	0.025	-0.001	-0.02	0.018	-0.007	0.008	0.013
Total	100.887	100.706	101.033	100.839	100.807	100.493	100.821	100.775	100.848	100.686	100.375	100.681
Si	1.936	1.930	1.930	1.928	1.903	1.947	1.912	1.927	1.906	1.929	1.896	1.926
Al	0.154	0.160	0.163	0.159	0.207	0.130	0.195	0.170	0.197	0.166	0.216	0.156
Mg	0.718	0.722	0.721	0.726	0.711	0.719	0.710	0.709	0.723	0.716	0.729	0.753
Na	0.015	0.015	0.016	0.015	0.016	0.015	0.016	0.015	0.015	0.015	0.015	0.019
Fe	0.318	0.318	0.315	0.319	0.318	0.317	0.319	0.325	0.319	0.323	0.313	0.291
Mn	0.010	0.010	0.009	0.010	0.009	0.009	0.010	0.009	0.010	0.010	0.008	0.008
Cr	0.000	0.000	0.000	0.000	0.000	0.000	0.000	0.000	0.000	0.000	0.000	0.000
K	0.000	0.000	0.000	0.000	0.000	0.000	0.000	0.000	0.000	0.000	0.000	0.000
Ca	0.871	0.869	0.865	0.867	0.862	0.874	0.860	0.869	0.855	0.861	0.861	0.873
Ni	0.000	-0.001	0.001	-0.001	0.000	-0.001	0.000	0.000	-0.001	-0.001	-0.001	0.000
Ti	0.022	0.024	0.025	0.024	0.036	0.020	0.033	0.025	0.034	0.026	0.033	0.023
Sc	0.000	0.000	0.000	0.000	0.000	0.001	0.000	-0.001	0.001	0.000	0.000	0.000
O	6.000	6.000	6.000	6.000	6.000	6.000	6.000	6.000	6.000	6.000	6.000	6.000
Mg#	**69.345**	**69.411**	**69.579**	**69.477**	**69.114**	**69.399**	**68.990**	**68.564**	**69.383**	**68.885**	**69.981**	**72.123**
Fe	**16.654**	**16.659**	**16.580**	**16.680**	**16.812**	**16.594**	**16.900**	**17.079**	**16.812**	**17.016**	**16.441**	**15.187**
Ca	**45.673**	**45.538**	**45.499**	**45.353**	**45.567**	**45.774**	**45.502**	**45.671**	**45.089**	**45.311**	**45.232**	**45.524**
Mg	**37.673**	**37.802**	**37.921**	**37.967**	**37.621**	**37.632**	**37.599**	**37.250**	**38.099**	**37.673**	**38.327**	**39.290**

Sample No.	SL-13-41-91	SL-13-41-91	SL-13-41-91	SL-13-41-91	SL-13-41-109.1	SL-13-41-109.1	SL-13-41-109.1	SL-13-41-109.1	SL-13-41-109.1	SL-13-41-109.1	MW-07-06-3.4	MW-07-06-3.4
Spot	3	4	5	6	1	2	3	4	5	6	1	2
SiO_2	52.055	51.511	50.632	51.446	51.563	51.825	51.501	50.559	50.814	50.901	51.676	51.849
Al_2O_3	2.192	2.297	3.366	2.746	2.713	2.718	3.024	3.479	3.089	3.075	1.888	1.612
MgO	13.229	13.298	12.961	13.192	13.136	13.126	13.258	13.222	13.287	13.319	11.633	10.904
Na_2O	0.463	0.415	0.405	0.403	0.448	0.496	0.462	0.395	0.396	0.385	0.386	0.386
FeO	9.729	10.157	10.21	10.12	9.664	9.453	10.018	9.808	10.11	10.087	12.46	13.409
MnO	0.263	0.251	0.261	0.277	0.284	0.248	0.266	0.239	0.303	0.248	0.37	0.367
Cr_2O_3	0.014	-0.012	-0.001	-0.022	0.019	0.006	-0.004	0.005	0.02	0.01	-0.006	0.002
K_2O												
CaO	21.907	21.404	21.515	21.556	21.807	22.123	21.398	21.524	21.462	21.465	21.312	21.637
NiO	0.006	-0.003	-0.001	0.001	0.012	0.004	-0.026	0.007	-0.023	0.017	-0.003	-0.004
TiO_2	0.729	0.961	1.148	1.062	0.924	0.865	1.103	1.124	1.073	1.037	0.828	0.581
Sc_2O_3	-0.01	-0.01	-0.016	0.011	-0.003	-0.007	-0.005	-0.004	0.001	0.019	-0.019	-0.001
Total	100.577	100.269	100.48	100.792	100.567	100.857	100.995	100.358	100.532	100.563	100.525	100.742
Si	1.938	1.926	1.893	1.914	1.920	1.923	1.910	1.889	1.897	1.899	1.947	1.959
Al	0.144	0.152	0.222	0.180	0.178	0.178	0.198	0.229	0.204	0.202	0.126	0.107
Mg	0.739	0.746	0.727	0.736	0.734	0.731	0.737	0.741	0.744	0.745	0.657	0.618
Na	0.017	0.015	0.015	0.015	0.016	0.018	0.017	0.014	0.014	0.014	0.014	0.014
Fe	0.302	0.317	0.318	0.314	0.300	0.292	0.310	0.305	0.315	0.314	0.391	0.422
Mn	0.008	0.008	0.008	0.009	0.009	0.008	0.008	0.008	0.010	0.008	0.012	0.012
Cr	0.000	0.000	0.000	-0.001	0.001	0.000	0.000	0.000	0.001	0.000	0.000	0.000
K	0.000	0.000	0.000	0.000	0.000	0.000	0.000	0.000	0.000	0.000	0.000	0.000
Ca	0.874	0.858	0.862	0.859	0.870	0.880	0.850	0.862	0.859	0.858	0.860	0.876
Ni	0.000	0.000	0.000	0.000	0.000	0.000	-0.001	0.000	-0.001	0.001	0.000	0.000
Ti	0.020	0.027	0.032	0.030	0.026	0.024	0.031	0.031	0.030	0.029	0.023	0.016
Sc	0.000	0.000	-0.001	0.000	0.000	0.000	0.000	0.000	0.000	0.001	-0.001	0.000
O	6.000	6.000	6.000	6.000	6.000	6.000	6.000	6.000	6.000	6.000	6.000	6.000
Mg#	**70.994**	**70.208**	**69.559**	**70.117**	**70.987**	**71.424**	**70.433**	**70.816**	**70.288**	**70.386**	**62.694**	**59.411**
Fe	**15.766**	**16.485**	**16.682**	**16.434**	**15.753**	**15.365**	**16.318**	**16.005**	**16.407**	**16.359**	**20.493**	**22.034**
Ca	**45.645**	**44.665**	**45.198**	**45.006**	**45.704**	**46.232**	**44.812**	**45.158**	**44.780**	**44.759**	**45.067**	**45.713**
Mg	**38.589**	**38.850**	**38.119**	**38.560**	**38.543**	**38.403**	**38.871**	**38.837**	**38.813**	**38.882**	**34.439**	**32.252**

Sample No.	MW-07-06-3.4	MW-07-06-3.4	MW-07-06-3.4	MW-07-06-3.4	MW-07-06-3.4	MW-07-06-3.4	MW-07-06-3.4	MW-07-06-9.4	MW-07-06-9.4	MW-07-06-9.4	MW-07-06-9.4	MW-07-06-9.4
Spot	3	4	5	6	7	8	9	1	2	3	4	5
SiO_2	51.916	52.443	52.663	51.709	51.826	52.962	51.823	51.302	51.149	51.438	51.383	51.395
Al_2O_3	1.805	1.28	1.217	1.97	2.264	1.305	2.365	1.749	1.67	1.452	1.747	2.021
MgO	11.004	11.46	11.474	11.341	11.945	11.987	11.827	10.996	11.04	10.88	11.108	11.344

Na_2O	0.355	0.285	0.306	0.358	0.367	0.29	0.429	0.4	0.383	0.369	0.378	0.387
FeO	13.112	12.301	12.52	12.867	11.841	11.317	11.6	13.01	13.054	13.779	13.057	12.526
MnO	0.396	0.379	0.391	0.399	0.364	0.343	0.351	0.416	0.407	0.441	0.428	0.357
Cr_2O_3	-0.018	-0.002	0	-0.004	0	0.008	0.007	0.011	-0.009	0.017	-0.005	-0.01
K_2O												
CaO	21.727	22.052	22.006	21.318	21.197	22.251	21.204	21.369	21.364	21.185	21.424	21.228
NiO	0.005	-0.018	-0.009	-0.001	0.013	0.021	-0.01	-0.005	0	-0.005	0.013	0.01
TiO_2	0.682	0.428	0.414	0.804	1.032	0.372	1.025	0.732	0.703	0.588	0.721	0.882
Sc_2O_3	0.004	0.007	-0.014	-0.013	0.016	-0.005	0.012	0.005	0.004	-0.007	-0.007	-0.005
Total	100.988	100.615	100.968	100.748	100.865	100.851	100.633	99.985	99.765	100.137	100.247	100.135
Si	1.954	1.973	1.976	1.947	1.939	1.978	1.941	1.951	1.951	1.959	1.949	1.945
Al	0.120	0.085	0.081	0.131	0.149	0.086	0.156	0.117	0.112	0.098	0.117	0.135
Mg	0.621	0.647	0.646	0.641	0.670	0.672	0.664	0.627	0.632	0.621	0.632	0.644
Na	0.013	0.010	0.011	0.013	0.013	0.010	0.016	0.015	0.014	0.014	0.014	0.014
Fe	0.411	0.386	0.391	0.404	0.369	0.352	0.362	0.412	0.415	0.437	0.413	0.395
Mn	0.013	0.012	0.012	0.013	0.012	0.011	0.011	0.013	0.013	0.014	0.014	0.011
Cr	-0.001	0.000	0.000	0.000	0.000	0.000	0.000	0.000	0.000	0.001	0.000	0.000
K	0.000	0.000	0.000	0.000	0.000	0.000	0.000	0.000	0.000	0.000	0.000	0.000
Ca	0.876	0.889	0.885	0.860	0.850	0.891	0.851	0.871	0.873	0.864	0.871	0.861
Ni	0.000	-0.001	0.000	0.000	0.000	0.001	0.000	0.000	0.000	0.000	0.000	0.000
Ti	0.019	0.012	0.012	0.023	0.029	0.010	0.029	0.021	0.020	0.017	0.021	0.025
Sc	0.000	0.000	0.000	0.000	0.001	0.000	0.000	0.000	0.000	0.000	0.000	0.000
O	6.000	6.000	6.000	6.000	6.000	6.000	6.000	6.000	6.000	6.000	6.000	6.000
Mg#	**60.169**	**62.644**	**62.259**	**61.338**	**64.486**	**65.595**	**64.729**	**60.339**	**60.354**	**58.700**	**60.495**	**61.979**
Fe	**21.547**	**20.073**	**20.369**	**21.201**	**19.541**	**18.401**	**19.285**	**21.584**	**21.615**	**22.737**	**21.547**	**20.794**
Ca	**45.905**	**46.266**	**46.031**	**45.162**	**44.976**	**46.516**	**45.323**	**45.580**	**45.481**	**44.946**	**45.457**	**45.309**
Mg	**32.549**	**33.661**	**33.601**	**33.636**	**35.483**	**35.083**	**35.392**	**32.836**	**32.904**	**32.316**	**32.996**	**33.897**

Sample No.	MW-07-06-9.4	MW-07-06-9.4	MW-07-06-9.4	MW-07-06-13.4	MW-07-06-13.4	MW-07-06-13.4	MW-07-06-13.4	MW-07-06-13.4	MW-07-06-13.4	MW-07-06-13.4	MW-07-06-13.4	MW-07-06-13.4
Spot	6	7	8	1	2	3	4	5	6	7	8	9
SiO_2	51.363	51.46	51.443	51.597	51.975	51.637	51.848	51.806	51.651	51.988	52.224	52.09
Al_2O_3	1.975	1.938	2.019	2.177	1.926	1.953	2.014	1.941	1.942	1.692	1.217	2.194
MgO	11.459	11.427	11.362	11.603	11.641	11.738	11.729	11.643	11.447	11.224	11.225	11.813
Na_2O	0.376	0.366	0.363	0.39	0.373	0.407	0.399	0.376	0.377	0.406	0.366	0.422
FeO	12.578	12.756	12.685	12.079	12.106	11.992	12.189	12.091	12.202	12.531	13.017	12.03
MnO	0.353	0.344	0.383	0.374	0.383	0.352	0.361	0.351	0.384	0.386	0.418	0.378
Cr_2O_3	0	0.011	0.005	0.008	-0.005	-0.023	0.004	-0.006	0.013	0	-0.01	0.002
K_2O												

CaO	21.31	21.325	21.29	21.139	21.28	21.173	21.163	21.266	21.231	21.289	21.163	21.181
NiO	-0.01	-0.023	0.002	-0.019	0.033	-0.019	-0.004	-0.001	-0.007	-0.028	-0.019	-0.001
TiO_2	0.8	0.807	0.808	0.983	0.805	0.781	0.904	0.83	0.83	0.711	0.528	0.882
Sc_2O_3	0	0.008	0.011	-0.001	0.014	-0.009	0.005	-0.005	-0.008	0.001	0.013	0.001
Total	100.204	100.419	100.371	100.33	100.531	99.982	100.612	100.292	100.062	100.2	100.142	100.992
Si	1.944	1.944	1.944	1.943	1.954	1.951	1.948	1.952	1.952	1.964	1.978	1.947
Al	0.132	0.129	0.135	0.145	0.128	0.130	0.134	0.129	0.130	0.113	0.081	0.145
Mg	0.650	0.648	0.644	0.655	0.656	0.665	0.661	0.658	0.649	0.636	0.638	0.662
Na	0.014	0.013	0.013	0.014	0.014	0.015	0.015	0.014	0.014	0.015	0.013	0.015
Fe	0.397	0.402	0.399	0.379	0.379	0.378	0.382	0.380	0.384	0.395	0.411	0.375
Mn	0.011	0.011	0.012	0.012	0.012	0.011	0.011	0.011	0.012	0.012	0.013	0.012
Cr	0.000	0.000	0.000	0.000	0.000	-0.001	0.000	0.000	0.000	0.000	0.000	0.000
K	0.000	0.000	0.000	0.000	0.000	0.000	0.000	0.000	0.000	0.000	0.000	0.000
Ca	0.864	0.863	0.862	0.853	0.857	0.857	0.852	0.858	0.860	0.862	0.859	0.848
Ni	0.000	-0.001	0.000	-0.001	0.001	-0.001	0.000	0.000	0.000	-0.001	-0.001	0.000
Ti	0.023	0.023	0.023	0.028	0.023	0.022	0.025	0.023	0.024	0.020	0.015	0.025
Sc	0.000	0.000	0.000	0.000	0.000	0.000	0.000	0.000	0.000	0.000	0.000	0.000
O	6.000	6.000	6.000	6.000	6.000	6.000	6.000	6.000	6.000	6.000	6.000	6.000
Mg#	**62.119**	**61.722**	**61.719**	**63.357**	**63.382**	**63.793**	**63.398**	**63.414**	**62.806**	**61.719**	**60.818**	**63.867**
Fe	**20.755**	**21.000**	**20.964**	**20.084**	**20.036**	**19.873**	**20.144**	**20.021**	**20.302**	**20.848**	**21.540**	**19.876**
Ca	**45.210**	**45.138**	**45.237**	**45.190**	**45.283**	**45.113**	**44.966**	**45.275**	**45.417**	**45.539**	**45.025**	**44.993**
Mg	**34.035**	**33.862**	**33.799**	**34.726**	**34.680**	**35.014**	**34.890**	**34.703**	**34.282**	**33.613**	**33.435**	**35.131**

Sample No.	MW-07-06-17.4	MW-07-06-17.4	MW-07-06-17.4	MW-07-06-17.4	MW-07-06-17.4	MW-07-06-17.4	MW-07-06-17.4	MW-07-06-17.4	MW-07-06-17.4	MW-07-06-23.4	MW-07-06-23.4	MW-07-06-23.4
Spot	1	2	3	4	5	6	7	8	9	1	2	3
SiO_2	51.696	51.381	51.377	51.847	51.693	52.081	52.741	52.203	52.07	51.841	52.17	51.878
Al_2O_3	2.007	1.634	1.449	2.283	2.428	2.028	1.047	1.729	1.759	2.092	1.618	2.057
MgO	11.605	10.407	10.006	11.439	11.796	11.534	11.306	11.668	11.631	10.847	11.345	11.232
Na_2O	0.378	0.363	0.366	0.429	0.421	0.401	0.357	0.387	0.378	0.374	0.362	0.37
FeO	12.649	14.284	14.802	12.124	11.508	12.009	12.255	11.761	11.748	12.874	12.585	12.495
MnO	0.411	0.481	0.479	0.365	0.38	0.351	0.387	0.343	0.357	0.4	0.356	0.382
Cr_2O_3	0.001	-0.001	-0.007	0.01	0.011	0.008	-0.004	-0.003	0.004	-0.004	-0.03	-0.007
K_2O												
CaO	20.878	20.828	20.88	21.294	21.15	21.304	21.958	21.458	21.439	21.365	21.408	21.246
NiO	-0.004	0.001	-0.025	-0.009	0.01	0.002	0.007	0.006	-0.002	0.011	0.021	0.006
TiO_2	0.947	0.938	0.851	1.014	0.971	0.8	0.41	0.623	0.684	0.83	0.56	0.776
Sc_2O_3	0.005	-0.023	0.016	-0.017	0.003	0.018	-0.008	0.009	0.014	0.004	0.002	-0.029
Total	100.573	100.293	100.194	100.779	100.371	100.536	100.456	100.184	100.082	100.634	100.397	100.406
Si	1.946	1.956	1.963	1.944	1.941	1.956	1.986	1.965	1.963	1.954	1.967	1.955

Al	0.133	0.110	0.098	0.151	0.161	0.134	0.070	0.115	0.117	0.139	0.108	0.137
Mg	0.655	0.594	0.573	0.643	0.664	0.650	0.639	0.659	0.658	0.613	0.642	0.635
Na	0.014	0.013	0.014	0.016	0.015	0.015	0.013	0.014	0.014	0.014	0.013	0.013
Fe	0.397	0.453	0.471	0.379	0.360	0.376	0.385	0.369	0.369	0.404	0.395	0.392
Mn	0.013	0.015	0.015	0.012	0.012	0.011	0.012	0.011	0.011	0.013	0.011	0.012
Cr	0.000	0.000	0.000	0.000	0.000	0.000	0.000	0.000	0.000	0.000	-0.001	0.000
K	0.000	0.000	0.000	0.000	0.000	0.000	0.000	0.000	0.000	0.000	0.000	0.000
Ca	0.842	0.850	0.855	0.855	0.851	0.857	0.886	0.866	0.866	0.863	0.865	0.858
Ni	0.000	0.000	-0.001	0.000	0.000	0.000	0.000	0.000	0.000	0.000	0.001	0.000
Ti	0.027	0.027	0.024	0.029	0.027	0.023	0.012	0.018	0.019	0.023	0.016	0.022
Sc	0.000	-0.001	0.001	-0.001	0.000	0.001	0.000	0.000	0.000	0.000	0.000	-0.001
O	6.000	6.000	6.000	6.000	6.000	6.000	6.000	6.000	6.000	6.000	6.000	6.000
Mg#	**62.285**	**56.737**	**54.890**	**62.940**	**64.851**	**63.354**	**62.415**	**64.103**	**64.056**	**60.264**	**61.871**	**61.804**
Fe	**20.949**	**23.888**	**24.811**	**20.176**	**19.201**	**19.961**	**20.144**	**19.487**	**19.499**	**21.504**	**20.791**	**20.815**
Ca	**44.456**	**44.784**	**44.999**	**45.560**	**45.372**	**45.529**	**46.405**	**45.713**	**45.751**	**45.883**	**45.472**	**45.505**
Mg	**34.595**	**31.328**	**30.190**	**34.264**	**35.427**	**34.509**	**33.451**	**34.800**	**34.749**	**32.613**	**33.737**	**33.680**

Sample No.	MW-07-06-23.4	MW-07-06-23.4	MW-07-06-23.4	MW-07-06-36.15	MW-07-06-36.15	MW-07-06-36.15	MW-07-06-36.15	MW-07-06-36.15	MW-07-06-36.15	MW-07-06-36.15	MW-07-06-36.15	MW-07-06-36.15
Spot	4	5	6	1	2	3	4	5	6	7	8	9
SiO_2	51.951	51.939	51.622	33.013	33.087	33.056	33.03	33.025	33.136	33.054	33.015	32.964
Al_2O_3	2.033	1.816	2.327	0.013	0.007	-0.014	0.002	0.007	-0.009	-0.001	-0.005	0.007
MgO	11.361	11.362	11.214	15.854	15.918	15.925	15.282	15.341	15.237	15.293	15.295	15.172
Na_2O	0.384	0.348	0.385	0.016	0.008	-0.002	0.02	-0.01	-0.002	-0.002	0.001	0.007
FeO	11.975	12.129	12.2	49.687	49.43	49.654	50.282	50.1	50.549	50.409	50.484	50.222
MnO	0.376	0.372	0.352	1.282	1.312	1.263	1.308	1.268	1.283	1.293	1.298	1.3
Cr_2O_3	0.016	0.016	0.009	0.004	0.004	-0.005	0.012	0.007	-0.013	0.001	0.017	0.005
K_2O												
CaO	21.259	21.46	21.364	0.157	0.122	0.143	0.167	0.162	0.162	0.157	0.137	0.154
NiO	0.003	-0.009	-0.002	0.025	0.006	0.005	-0.003	0.012	-0.025	-0.003	0.002	0.012
TiO_2	0.765	0.638	0.937	0.032	0.025	0.031	0.042	0.028	0.049	0.035	0.039	0.052
Sc_2O_3	0.018	0.019	0.005	-0.007	0.016	0.02	0.001	-0.004	-0.012	0.003	-0.001	0.01
Total	100.141	100.09	100.413	100.076	99.935	100.076	100.143	99.936	100.355	100.239	100.282	99.905
Si	1.958	1.962	1.944	1.494	1.497	1.495	1.498	1.500	1.500	1.498	1.497	1.499
Al	0.135	0.121	0.155	0.001	0.001	-0.001	0.000	0.001	-0.001	0.000	0.000	0.001
Mg	0.642	0.644	0.633	1.076	1.081	1.081	1.040	1.045	1.035	1.040	1.040	1.035
Na	0.014	0.013	0.014	0.001	0.000	0.000	0.001	0.000	0.000	0.000	0.000	0.000
Fe	0.376	0.382	0.383	1.874	1.864	1.872	1.901	1.896	1.907	1.904	1.907	1.903
Mn	0.012	0.012	0.011	0.049	0.050	0.048	0.050	0.049	0.049	0.050	0.050	0.050
Cr	0.000	0.000	0.000	0.000	0.000	0.000	0.000	0.000	0.000	0.000	0.001	0.000

K	0.000	0.000	0.000	0.000	0.000	0.000	0.000	0.000	0.000	0.000	0.000	0.000
Ca	0.859	0.868	0.862	0.008	0.006	0.007	0.008	0.008	0.008	0.008	0.007	0.008
Ni	0.000	0.000	0.000	0.001	0.000	0.000	0.000	0.000	-0.001	0.000	0.000	0.000
Ti	0.022	0.018	0.026	0.001	0.001	0.001	0.001	0.001	0.002	0.001	0.001	0.002
Sc	0.001	0.001	0.000	0.000	0.001	0.001	0.000	0.000	0.000	0.000	0.000	0.000
O	6.000	6.000	6.000	6.000	6.000	6.000	6.000	6.000	6.000	6.000	6.000	6.000
Mg#	**63.068**	**62.772**	**62.328**	**36.481**	**36.695**	**36.600**	**35.362**	**35.533**	**35.173**	**35.320**	**35.289**	**35.224**
Fe	**20.039**	**20.157**	**20.383**	**63.355**	**63.178**	**63.251**	**64.461**	**64.295**	**64.654**	**64.513**	**64.565**	**64.611**
Ca	**45.740**	**45.854**	**45.892**	**0.257**	**0.200**	**0.234**	**0.275**	**0.267**	**0.266**	**0.258**	**0.225**	**0.255**
Mg	**34.221**	**33.989**	**33.725**	**36.387**	**36.622**	**36.515**	**35.264**	**35.438**	**35.080**	**35.229**	**35.210**	**35.134**

Sample No.	MW-07-06-36.15	MW-07-06-36.15	MW-07-06-36.15	MW-07-06-36.15	MW-07-06-36.15	MW-07-06-36.15	MW-07-06-37.5	MW-07-06-37.5	MW-07-06-37.5	MW-07-06-37.5	MW-07-06-37.5	MW-07-06-37.5
Spot	10	11	12	13	14	15	1	2	3	4	5	6
SiO_2	51.914	52.249	52.556	52.02	52.053	52.494	33.32	33.241	33.213	33.355	33.497	33.541
Al_2O_3	1.816	1.887	1.389	1.561	1.555	1.441	-0.003	-0.004	0.005	-0.006	-0.007	0.01
MgO	11.794	11.664	12.147	11.74	11.612	11.606	16.502	16.502	16.577	16.683	16.826	16.501
Na_2O	0.437	0.622	0.332	0.411	0.437	0.411	-0.003	-0.006	0.01	-0.001	-0.003	0.003
FeO	12.154	11.642	11.55	12.174	12.351	12.439	48.795	48.531	48.507	48.289	48.168	48.614
MnO	0.391	0.381	0.346	0.354	0.381	0.387	1.164	1.159	1.184	1.201	1.186	1.237
Cr_2O_3	-0.007	0.007	0.016	-0.019	0.013	-0.011	-0.003	-0.002	-0.032	-0.018	-0.003	0.006
K_2O												
CaO	21.507	21.74	21.833	21.727	21.628	21.543	0.176	0.191	0.203	0.195	0.178	0.118
NiO	0.005	0.004	-0.01	0.021	0.024	-0.011	0.006	0.031	-0.031	0.019	-0.004	-0.008
TiO_2	0.602	0.607	0.453	0.531	0.584	0.554	0.031	0.058	0.061	0.035	0.033	0.026
Sc_2O_3	0.01	-0.001	0.005	-0.013	0.006	-0.003	0.007	-0.006	-0.003	0.001	-0.016	0.001
Total	100.623	100.802	100.617	100.507	100.644	100.85	99.992	99.695	99.694	99.753	99.855	100.049
Si	1.952	1.957	1.969	1.959	1.959	1.970	1.500	1.500	1.499	1.502	1.505	1.507
Al	0.121	0.125	0.092	0.104	0.103	0.095	0.000	0.000	0.000	0.000	-0.001	0.001
Mg	0.665	0.655	0.683	0.663	0.656	0.653	1.114	1.117	1.122	1.127	1.134	1.112
Na	0.016	0.023	0.012	0.015	0.016	0.015	0.000	0.000	0.000	0.000	0.000	0.000
Fe	0.381	0.363	0.361	0.382	0.387	0.389	1.831	1.825	1.824	1.812	1.803	1.820
Mn	0.012	0.012	0.011	0.011	0.012	0.012	0.044	0.044	0.045	0.046	0.045	0.047
Cr	0.000	0.000	0.000	-0.001	0.000	0.000	0.000	0.000	-0.001	-0.001	0.000	0.000
K	0.000	0.000	0.000	0.000	0.000	0.000	0.000	0.000	0.000	0.000	0.000	0.000
Ca	0.866	0.873	0.877	0.877	0.872	0.866	0.008	0.009	0.010	0.009	0.009	0.006
Ni	0.000	0.000	0.000	0.001	0.001	0.000	0.000	0.001	-0.001	0.001	0.000	0.000
Ti	0.017	0.017	0.013	0.015	0.016	0.016	0.001	0.002	0.002	0.001	0.001	0.001
Sc	0.000	0.000	0.000	0.000	0.000	0.000	0.000	0.000	0.000	0.000	-0.001	0.000
O	6.000	6.000	6.000	6.000	6.000	6.000	6.000	6.000	6.000	6.000	6.000	6.000

Mg#	**63.592**	**64.329**	**65.434**	**63.448**	**62.857**	**62.679**	**37.840**	**37.967**	**38.086**	**38.343**	**38.604**	**37.926**
Fe	**19.913**	**19.215**	**18.785**	**19.879**	**20.228**	**20.382**	**61.982**	**61.839**	**61.709**	**61.461**	**61.217**	**61.954**
Ca	**45.305**	**46.133**	**45.655**	**45.615**	**45.541**	**45.386**	**0.287**	**0.313**	**0.332**	**0.319**	**0.291**	**0.193**
Mg	**34.782**	**34.652**	**35.561**	**34.506**	**34.231**	**34.232**	**37.731**	**37.849**	**37.959**	**38.220**	**38.492**	**37.852**

Sample No.	MW-07-06-37.5	MW-07-06-37.5	MW-07-06-37.5	MW-07-06-37.5	MW-07-06-37.5	MW-07-06-41	MW-07-06-41	MW-07-06-41	MW-07-06-41	MW-07-06-41	MW-07-06-41
Spot	7	8	9	10	11	1	2	3	4	5	6
SiO_2	33.682	33.395	52.549	52.405	52.442	52.129	51.375	51.427	51.94	51.474	51.595
Al_2O_3	-0.035	0.007	1.628	1.68	1.649	1.354	2.186	2.115	1.943	2.252	2.263
MgO	16.635	16.66	12.048	12.071	12.03	11.946	11.793	11.644	12.107	12.118	11.822
Na_2O	0.017	0.003	0.428	0.408	0.411	0.413	0.456	0.463	0.39	0.434	0.476
FeO	48.645	48.548	11.88	11.948	11.93	12.089	11.878	11.851	11.457	11.453	11.398
MnO	1.214	1.178	0.374	0.354	0.365	0.345	0.339	0.377	0.369	0.319	0.344
Cr_2O_3	0.003	0	0.011	0.008	0.006	-0.003	-0.001	-0.001	0.003	0.01	-0.011
K_2O											
CaO	0.131	0.101	21.734	21.629	21.711	21.448	21.267	21.346	21.562	21.232	21.592
NiO	-0.009	0.014	-0.011	0.001	0.02	-0.008	-0.004	-0.003	-0.003	0.013	-0.03
TiO_2	0.021	0.009	0.605	0.654	0.629	0.557	0.869	0.814	0.81	0.889	0.877
Sc_2O_3	0.002	-0.008	-0.002	-0.018	-0.007	0.001	-0.033	-0.005	0.009	-0.001	-0.001
Total	100.306	99.907	101.244	101.14	101.186	100.271	100.125	100.028	100.587	100.193	100.325
Si	1.508	1.502	1.960	1.957	1.958	1.965	1.939	1.943	1.947	1.937	1.940
Al	-0.003	0.001	0.107	0.111	0.109	0.090	0.146	0.141	0.129	0.150	0.150
Mg	1.117	1.124	0.674	0.676	0.674	0.676	0.668	0.660	0.681	0.684	0.667
Na	0.001	0.000	0.015	0.015	0.015	0.015	0.017	0.017	0.014	0.016	0.017
Fe	1.815	1.820	0.369	0.372	0.371	0.380	0.374	0.373	0.358	0.359	0.357
Mn	0.046	0.045	0.012	0.011	0.012	0.011	0.011	0.012	0.012	0.010	0.011
Cr	0.000	0.000	0.000	0.000	0.000	0.000	0.000	0.000	0.000	0.000	0.000
K	0.000	0.000	0.000	0.000	0.000	0.000	0.000	0.000	0.000	0.000	0.000
Ca	0.006	0.005	0.869	0.865	0.868	0.866	0.860	0.864	0.866	0.856	0.870
Ni	0.000	0.001	0.000	0.000	0.001	0.000	0.000	0.000	0.000	0.000	-0.001
Ti	0.001	0.000	0.017	0.018	0.018	0.016	0.025	0.023	0.023	0.025	0.025
Sc	0.000	0.000	0.000	-0.001	0.000	0.000	-0.001	0.000	0.000	0.000	0.000
O	6.000	6.000	6.000	6.000	6.000	6.000	6.000	6.000	6.000	6.000	6.000
Mg#	**38.101**	**38.184**	**64.607**	**64.521**	**64.477**	**64.012**	**64.121**	**63.880**	**65.542**	**65.571**	**65.120**
Fe	**61.766**	**61.714**	**19.314**	**19.433**	**19.399**	**19.764**	**19.650**	**19.668**	**18.791**	**18.911**	**18.859**
Ca	**0.214**	**0.165**	**45.429**	**45.229**	**45.390**	**45.083**	**45.234**	**45.548**	**45.468**	**45.074**	**45.933**
Mg	**38.020**	**38.121**	**35.257**	**35.339**	**35.211**	**35.154**	**35.116**	**34.784**	**35.742**	**36.016**	**35.209**

Appendix 10. Mineral chemical data of plagioclase determined by electron microprobe. Sample names can be referred to appendix 3.

Sample	FD-13-34-5	FD-13-34-5	FD-13-34-5	FD-13-34-5	FD-13-34-5	FD-13-34-5	FD-13-34-5	FD-13-34-5	FD-13-34-18.6	FD-13-34-18.6	FD-13-34-18.6	FD-13-34-18.6
Spot No.	1	2	3	4	5	6	7	8	1	2	3	4
SiO_2	56.066	56.370	55.872	53.918	54.673	54.922	54.703	54.285	55.062	55.252	54.126	56.305
Al_2O_3	27.542	27.510	27.588	28.492	28.634	28.601	28.467	29.066	28.554	28.496	29.034	27.669
MgO	0.010	0.004	0.003	0.508	-0.004	0.010	-0.002	0.004	0.013	0.027	0.023	0.010
Na_2O	5.744	5.825	5.686	4.926	5.133	5.247	5.177	5.017	5.036	5.119	4.787	5.494
FeO	0.198	0.168	0.181	0.497	0.166	0.146	0.197	0.172	0.329	0.315	0.324	0.364
MnO	0.009	-0.007	0.026	0.005	-0.015	-0.007	0.013	-0.018	-0.012	0.007	-0.023	-0.008
K_2O	0.411	0.319	0.399	0.416	0.329	0.318	0.304	0.226	0.665	0.698	0.609	0.847
SrO	0.248	0.302	0.275	0.300	0.319	0.314	0.310	0.322	0.234	0.250	0.247	0.260
BaO	0.305	0.431	0.408	0.225	0.219	0.241	0.237	0.250	0.218	0.192	0.216	0.221
CaO	8.911	8.781	9.009	9.803	10.077	10.022	10.038	10.564	10.369	10.104	10.825	9.247
TiO_2	0.069	0.062	0.084	0.075	0.066	0.077	0.081	0.073	0.074	0.090	0.064	0.040
Total	99.513	99.765	99.531	99.165	99.597	99.891	99.525	99.961	100.542	100.550	100.232	100.449
Si	2.539	2.546	2.533	2.462	2.480	2.484	2.484	2.458	2.481	2.488	2.450	2.533
Al	1.467	1.462	1.471	1.531	1.528	1.522	1.521	1.548	1.514	1.509	1.546	1.465
Mg	0.001	0.000	0.000	0.035	0.000	0.001	0.000	0.000	0.001	0.002	0.002	0.001
Na	0.503	0.509	0.499	0.435	0.451	0.459	0.455	0.440	0.439	0.446	0.419	0.478
Fe	0.007	0.006	0.007	0.019	0.006	0.006	0.007	0.006	0.012	0.012	0.012	0.014
Mn	0.000	0.000	0.001	0.000	-0.001	0.000	0.000	-0.001	0.000	0.000	-0.001	0.000
K	0.024	0.018	0.023	0.024	0.019	0.018	0.018	0.013	0.038	0.040	0.035	0.049
Sr	0.007	0.008	0.007	0.008	0.008	0.008	0.008	0.008	0.006	0.007	0.006	0.007
Ba	0.005	0.008	0.007	0.004	0.004	0.004	0.004	0.004	0.004	0.003	0.004	0.004
Ca	0.432	0.425	0.438	0.480	0.490	0.486	0.488	0.512	0.501	0.487	0.525	0.446
Ti	0.002	0.002	0.003	0.003	0.002	0.003	0.003	0.002	0.003	0.003	0.002	0.001
O	8.000	8.000	8.000	8.000	8.000	8.000	8.000	8.000	8.000	8.000	8.000	8.000
An	**45.057**	**44.611**	**45.602**	**51.065**	**51.045**	**50.414**	**50.820**	**53.095**	**51.183**	**50.062**	**53.594**	**45.821**
Ab	**52.466**	**53.458**	**51.992**	**46.353**	**46.970**	**47.680**	**47.347**	**45.551**	**44.906**	**45.817**	**42.813**	**49.179**
Or	**2.476**	**1.931**	**2.406**	**2.582**	**1.986**	**1.906**	**1.834**	**1.353**	**3.911**	**4.121**	**3.593**	**5.001**

Sample	FD-13-34-18.6	FD-13-34-18.6	FD-13-34-18.6	FD-13-34-24	FD-13-34-24	FD-13-34-24	FD-13-34-24	FD-13-34-24	FD-13-34-24	FD-13-34-24	FD-13-34-24	FD-13-34-27.9
Spot No.	5	6	7	1	2	3	4	5	6	7	8	1
SiO_2	53.895	54.205	55.039	56.012	56.081	55.078	55.036	56.034	55.711	54.497	55.364	54.181
Al_2O_3	29.270	29.087	28.462	28.034	27.760	28.298	28.410	27.631	27.861	28.170	28.437	29.070
MgO	0.020	0.001	0.041	0.010	0.008	0.020	0.001	-0.001	0.007	0.508	0.008	0.014

Na_2O	4.658	4.771	5.000	5.717	5.825	5.354	5.283	5.707	5.540	4.737	5.570	4.834
FeO	0.361	0.318	0.330	0.266	0.209	0.315	0.333	0.222	0.320	0.866	0.249	0.224
MnO	0.000	0.013	0.021	-0.008	-0.009	-0.002	-0.019	0.016	-0.007	-0.013	-0.034	-0.005
K_2O	0.495	0.576	0.738	0.282	0.170	0.337	0.385	0.314	0.421	1.123	0.198	0.379
SrO	0.266	0.259	0.239	0.261	0.235	0.228	0.253	0.297	0.239	0.245	0.250	0.215
BaO	0.179	0.243	0.241	0.281	0.181	0.185	0.119	0.254	0.240	0.169	0.158	0.157
CaO	11.038	10.875	10.163	9.460	9.104	9.959	10.018	9.069	9.428	8.446	9.846	10.834
TiO_2	0.079	0.075	0.057	0.074	0.069	0.069	0.074	0.067	0.067	0.160	0.062	0.069
Total	100.261	100.423	100.331	100.389	99.633	99.841	99.893	99.610	99.827	98.908	100.108	99.972
Si	2.439	2.450	2.485	2.518	2.533	2.493	2.489	2.535	2.519	2.492	2.496	2.453
Al	1.558	1.547	1.512	1.483	1.475	1.507	1.512	1.471	1.482	1.515	1.508	1.549
Mg	0.001	0.000	0.003	0.001	0.001	0.001	0.000	0.000	0.000	0.035	0.001	0.001
Na	0.408	0.417	0.437	0.497	0.509	0.469	0.463	0.500	0.485	0.419	0.486	0.424
Fe	0.014	0.012	0.012	0.010	0.008	0.012	0.013	0.008	0.012	0.033	0.009	0.008
Mn	0.000	0.000	0.001	0.000	0.000	0.000	-0.001	0.001	0.000	-0.001	-0.001	0.000
K	0.029	0.033	0.043	0.016	0.010	0.019	0.022	0.018	0.024	0.066	0.011	0.022
Sr	0.007	0.007	0.006	0.007	0.006	0.006	0.007	0.008	0.006	0.006	0.007	0.006
Ba	0.003	0.004	0.004	0.005	0.003	0.003	0.002	0.004	0.004	0.003	0.003	0.003
Ca	0.535	0.527	0.492	0.456	0.441	0.483	0.486	0.440	0.457	0.414	0.476	0.526
Ti	0.003	0.003	0.002	0.002	0.002	0.002	0.003	0.002	0.002	0.005	0.002	0.002
O	8.000	8.000	8.000	8.000	8.000	8.000	8.000	8.000	8.000	8.000	8.000	8.000
An	**55.074**	**53.890**	**50.626**	**47.010**	**45.912**	**49.715**	**50.039**	**45.913**	**47.288**	**46.049**	**48.878**	**54.121**
Ab	**41.984**	**42.709**	**44.994**	**51.321**	**53.066**	**48.281**	**47.669**	**52.193**	**50.196**	**46.655**	**49.950**	**43.623**
Or	**2.943**	**3.401**	**4.380**	**1.670**	**1.021**	**2.004**	**2.291**	**1.894**	**2.516**	**7.295**	**1.171**	**2.256**

Sample	FD-13-34-27.9	FD-13-34-27.9	FD-13-34-27.9	FD-13-34-27.9	FD-13-34-27.9	FD-13-34-27.9	FD-13-34-27.9	FD-13-34-33	FD-13-34-33	FD-13-34-33	FD-13-34-33	FD-13-34-33
Spot No.	2	3	4	5	6	7	8	1	2	3	4	5
SiO_2	54.209	54.551	54.340	59.571	59.654	54.848	58.115	55.406	56.559	58.052	58.141	58.686
Al_2O_3	28.889	28.896	29.152	25.310	25.158	28.750	26.525	28.197	27.443	26.411	26.416	25.871
MgO	0.039	0.024	0.028	0.034	0.023	0.012	0.017	0.030	0.031	0.022	0.053	0.029
Na_2O	4.910	4.953	4.798	7.128	6.854	5.215	6.642	5.504	5.820	6.558	6.578	6.608
FeO	0.247	0.223	0.280	0.330	0.307	0.404	0.272	0.298	0.308	0.290	0.392	0.306
MnO	0.010	0.021	-0.003	-0.006	-0.014	0.002	-0.017	-0.003	-0.028	0.012	0.022	0.041
K_2O	0.499	0.442	0.360	0.470	0.753	0.252	0.290	0.180	0.411	0.313	0.277	0.358
SrO	0.254	0.254	0.251	0.278	0.242	0.228	0.269	0.297	0.304	0.253	0.273	0.294
BaO	0.180	0.150	0.176	0.136	0.123	0.086	0.122	0.199	0.103	0.122	0.087	0.112
CaO	10.645	10.602	10.841	6.581	6.450	10.416	7.770	9.849	8.992	7.748	7.903	7.203
TiO_2	0.054	0.059	0.071	0.052	0.055	0.073	0.066	0.067	0.072	0.046	0.064	0.057

Total	99.936	100.175	100.294	99.884	99.605	100.286	100.071	100.024	100.015	99.827	100.206	99.565
Si	2.458	2.465	2.453	2.667	2.677	2.473	2.604	2.501	2.547	2.608	2.604	2.638
Al	1.541	1.536	1.548	1.333	1.328	1.525	1.398	1.498	1.454	1.396	1.392	1.368
Mg	0.003	0.002	0.002	0.002	0.002	0.001	0.001	0.002	0.002	0.001	0.004	0.002
Na	0.431	0.433	0.419	0.618	0.595	0.455	0.576	0.481	0.507	0.570	0.570	0.575
Fe	0.009	0.008	0.011	0.012	0.011	0.015	0.010	0.011	0.012	0.011	0.015	0.011
Mn	0.000	0.001	0.000	0.000	-0.001	0.000	-0.001	0.000	-0.001	0.000	0.001	0.002
K	0.029	0.025	0.021	0.027	0.043	0.015	0.017	0.010	0.024	0.018	0.016	0.021
Sr	0.007	0.007	0.007	0.007	0.006	0.006	0.007	0.008	0.008	0.007	0.007	0.008
Ba	0.003	0.003	0.003	0.002	0.002	0.002	0.002	0.004	0.002	0.002	0.002	0.002
Ca	0.517	0.513	0.524	0.316	0.310	0.503	0.373	0.476	0.434	0.373	0.379	0.347
Ti	0.002	0.002	0.002	0.002	0.002	0.002	0.002	0.002	0.002	0.002	0.002	0.002
O	8.000	8.000	8.000	8.000	8.000	8.000	8.000	8.000	8.000	8.000	8.000	8.000
An	**52.936**	**52.809**	**54.375**	**32.876**	**32.694**	**51.726**	**38.630**	**49.230**	**44.971**	**38.803**	**39.287**	**36.813**
Ab	**44.107**	**44.567**	**43.473**	**64.326**	**62.759**	**46.783**	**59.652**	**49.698**	**52.580**	**59.330**	**59.072**	**61.007**
Or	**2.957**	**2.623**	**2.151**	**2.798**	**4.548**	**1.491**	**1.718**	**1.072**	**2.449**	**1.868**	**1.641**	**2.180**

Sample	FD-13-34-33	FD-13-34-33	FD-13-34-33	FD-13-34-33	FD-13-34-33	FD-13-34-33	FD-13-34-46.1	FD-13-34-46.1	FD-13-34-46.1	FD-13-34-46.1	FD-13-34-64.6	FD-13-34-64.6
Spot No.	6	7	8	9	10	11	1	2	3	4	1	2
SiO_2	54.403	54.438	54.507	54.680	56.408	54.751	55.018	55.258	55.405	55.012	54.093	57.188
Al_2O_3	28.609	28.766	28.791	28.802	27.486	28.771	28.564	28.650	28.578	28.906	29.080	27.037
MgO	0.023	0.026	0.017	0.013	0.015	0.029	0.016	0.022	0.029	0.025	0.026	0.034
Na_2O	5.033	4.997	4.971	5.261	5.995	5.158	5.035	5.285	5.225	5.084	4.684	5.746
FeO	0.214	0.227	0.234	0.274	0.270	0.225	0.283	0.258	0.238	0.193	0.325	0.252
MnO	0.013	-0.017	0.021	0.005	-0.003	-0.022	-0.010	-0.003	0.016	0.000	0.003	0.009
K_2O	0.343	0.314	0.375	0.147	0.265	0.358	0.431	0.287	0.439	0.316	0.542	0.856
SrO	0.262	0.306	0.324	0.313	0.301	0.337	0.310	0.285	0.282	0.284	0.245	0.222
BaO	0.157	0.168	0.188	0.179	0.158	0.202	0.226	0.232	0.239	0.232	0.130	0.125
CaO	10.504	10.493	10.495	10.400	9.051	10.402	10.111	10.081	10.029	10.342	10.888	8.658
TiO_2	0.065	0.071	0.068	0.082	0.055	0.071	0.089	0.082	0.080	0.082	0.066	0.050
Total	99.626	99.789	99.991	100.156	100.001	100.282	100.073	100.437	100.560	100.476	100.082	100.177
Si	2.470	2.468	2.468	2.469	2.542	2.471	2.486	2.486	2.491	2.475	2.450	2.570
Al	1.528	1.534	1.533	1.530	1.457	1.528	1.518	1.517	1.511	1.530	1.549	1.430
Mg	0.002	0.002	0.001	0.001	0.001	0.002	0.001	0.001	0.002	0.002	0.002	0.002
Na	0.442	0.438	0.436	0.460	0.523	0.451	0.440	0.460	0.455	0.443	0.411	0.500
Fe	0.008	0.009	0.009	0.010	0.010	0.008	0.011	0.010	0.009	0.007	0.012	0.009
Mn	0.000	-0.001	0.001	0.000	0.000	-0.001	0.000	0.000	0.001	0.000	0.000	0.000
K	0.020	0.018	0.022	0.008	0.015	0.021	0.025	0.016	0.025	0.018	0.031	0.049

Sr	0.007	0.008	0.008	0.008	0.008	0.009	0.008	0.007	0.007	0.007	0.006	0.006
Ba	0.003	0.003	0.003	0.003	0.003	0.004	0.004	0.004	0.004	0.004	0.002	0.002
Ca	0.511	0.510	0.509	0.503	0.437	0.503	0.489	0.486	0.483	0.499	0.528	0.417
Ti	0.002	0.002	0.002	0.003	0.002	0.002	0.003	0.003	0.003	0.003	0.002	0.002
O	8.000	8.000	8.000	8.000	8.000	8.000	8.000	8.000	8.000	8.000	8.000	8.000
An	**52.508**	**52.745**	**52.681**	**51.796**	**44.815**	**51.632**	**51.273**	**50.481**	**50.168**	**51.963**	**54.453**	**43.165**
Ab	**45.449**	**45.375**	**45.076**	**47.332**	**53.622**	**46.250**	**46.123**	**47.807**	**47.215**	**46.145**	**42.317**	**51.750**
Or	**2.043**	**1.881**	**2.243**	**0.872**	**1.563**	**2.117**	**2.604**	**1.712**	**2.617**	**1.892**	**3.230**	**5.085**

Sample	FD-13-34-64.6	FD-13-34-64.6	FD-13-34-64.6	FD-13-34-64.6	FD-13-34-64.6	FD-13-34-79.6	FD-13-34-79.6	FD-13-34-79.6	FD-13-34-79.6	FD-13-34-79.6	FD-13-34-79.6	FD-13-34-79.6
Spot No.	3	4	5	6	7	1	2	3	4	5	6	7
SiO_2	53.881	54.791	56.368	54.903	56.123	57.710	58.033	55.152	54.987	55.116	58.598	55.724
Al_2O_3	29.169	28.405	27.386	28.526	27.755	26.618	26.346	28.454	28.491	28.409	26.207	27.923
MgO	0.025	0.021	0.024	0.036	0.009	0.037	0.028	0.014	0.026	0.025	0.013	0.027
Na_2O	4.621	5.079	5.590	4.996	5.590	6.022	6.141	5.162	5.107	5.020	6.447	5.354
FeO	0.305	0.332	0.289	0.262	0.281	0.330	0.334	0.321	0.275	0.286	0.360	0.272
MnO	0.003	0.000	0.002	0.034	0.006	-0.006	-0.012	0.010	0.009	-0.005	-0.001	0.016
K_2O	0.498	0.596	0.799	0.573	0.555	0.750	0.773	0.500	0.425	0.568	0.850	0.619
SrO	0.237	0.220	0.221	0.249	0.269	0.238	0.241	0.234	0.250	0.221	0.233	0.279
BaO	0.118	0.141	0.171	0.133	0.095	0.096	0.080	0.107	0.118	0.115	0.092	0.136
CaO	11.009	10.232	9.033	10.363	9.374	8.255	8.019	10.150	10.307	10.125	7.588	9.532
TiO_2	0.071	0.074	0.041	0.057	0.062	0.048	0.035	0.072	0.076	0.085	0.033	0.068
Total	99.937	99.891	99.924	100.132	100.119	100.098	100.018	100.176	100.071	99.965	100.420	99.950
Si	2.443	2.482	2.545	2.481	2.528	2.592	2.606	2.489	2.484	2.491	2.620	2.517
Al	1.556	1.514	1.455	1.517	1.471	1.407	1.392	1.511	1.514	1.511	1.379	1.484
Mg	0.002	0.001	0.002	0.002	0.001	0.002	0.002	0.001	0.002	0.002	0.001	0.002
Na	0.406	0.445	0.488	0.437	0.487	0.523	0.534	0.451	0.447	0.439	0.558	0.468
Fe	0.012	0.013	0.011	0.010	0.011	0.012	0.013	0.012	0.010	0.011	0.013	0.010
Mn	0.000	0.000	0.000	0.001	0.000	0.000	0.000	0.000	0.000	0.000	0.000	0.001
K	0.029	0.034	0.046	0.033	0.032	0.043	0.044	0.029	0.025	0.033	0.049	0.036
Sr	0.006	0.006	0.006	0.007	0.007	0.006	0.006	0.006	0.007	0.006	0.006	0.007
Ba	0.002	0.002	0.003	0.002	0.002	0.002	0.001	0.002	0.002	0.002	0.002	0.002
Ca	0.535	0.497	0.437	0.502	0.452	0.397	0.386	0.491	0.499	0.490	0.364	0.461
Ti	0.002	0.003	0.001	0.002	0.002	0.002	0.001	0.002	0.003	0.003	0.001	0.002
O	8.000	8.000	8.000	8.000	8.000	8.000	8.000	8.000	8.000	8.000	8.000	8.000
An	**55.183**	**50.862**	**44.978**	**51.632**	**46.560**	**41.219**	**40.028**	**50.571**	**51.435**	**50.956**	**37.477**	**47.800**
Ab	**41.843**	**45.608**	**50.281**	**44.966**	**50.156**	**54.319**	**55.375**	**46.460**	**46.038**	**45.638**	**57.521**	**48.501**
Or	**2.974**	**3.530**	**4.740**	**3.402**	**3.284**	**4.462**	**4.597**	**2.968**	**2.527**	**3.406**	**5.002**	**3.699**

Sample	FD-13-34-79.6	FD-13-34-79.6	FD-13-34-79.6	FD-13-34-127.25	FD-13-34-127.25	FD-13-34-127.25	FD-13-34-127.25	FD-13-34-127.25	FD-13-34-127.25	FD-13-34-158.6	FD-13-34-158.6	FD-13-34-158.6
Spot No.	8	9	10	1	2	3	4	5	6	1	2	3
SiO_2	56.395	54.833	54.866	58.232	57.276	56.328	57.777	57.260	56.797	58.338	56.908	57.037
Al_2O_3	27.715	28.332	28.338	26.330	26.758	27.555	26.032	26.794	27.243	26.518	27.411	27.099
MgO	0.027	0.022	0.016	0.015	0.014	0.027	0.018	0.027	0.014	0.006	0.028	0.021
Na_2O	5.607	4.919	5.105	6.239	5.932	5.498	5.924	6.029	5.846	6.243	5.744	5.890
FeO	0.297	0.325	0.260	0.253	0.298	0.251	0.251	0.231	0.189	0.241	0.220	0.221
MnO	0.030	0.002	0.016	0.027	-0.003	-0.005	-0.015	0.006	0.023	-0.001	-0.005	-0.027
K_2O	0.583	0.585	0.547	0.952	0.722	0.702	0.972	0.618	0.542	0.741	0.769	0.689
SrO	0.199	0.220	0.222	0.229	0.216	0.229	0.248	0.257	0.284	0.207	0.205	0.202
BaO	0.116	0.093	0.079	0.188	0.183	0.136	0.184	0.174	0.170	0.172	0.175	0.180
CaO	9.309	10.278	10.178	7.677	8.409	9.148	7.798	8.305	8.788	7.830	8.688	8.638
TiO_2	0.090	0.075	0.085	0.048	0.055	0.063	0.054	0.065	0.063	0.057	0.065	0.074
Total	100.368	99.684	99.712	100.190	99.860	99.932	99.243	99.766	99.959	100.352	100.208	100.024
Si	2.533	2.487	2.487	2.612	2.581	2.540	2.616	2.581	2.558	2.609	2.557	2.567
Al	1.465	1.512	1.511	1.390	1.419	1.462	1.386	1.421	1.444	1.395	1.449	1.435
Mg	0.002	0.001	0.001	0.001	0.001	0.002	0.001	0.002	0.001	0.000	0.002	0.001
Na	0.488	0.432	0.448	0.542	0.517	0.480	0.519	0.526	0.510	0.540	0.500	0.513
Fe	0.011	0.012	0.010	0.009	0.011	0.009	0.009	0.009	0.007	0.009	0.008	0.008
Mn	0.001	0.000	0.001	0.001	0.000	0.000	-0.001	0.000	0.001	0.000	0.000	-0.001
K	0.033	0.034	0.032	0.055	0.042	0.040	0.056	0.036	0.031	0.042	0.044	0.040
Sr	0.005	0.006	0.006	0.006	0.006	0.006	0.007	0.007	0.007	0.005	0.005	0.005
Ba	0.002	0.002	0.001	0.003	0.003	0.002	0.003	0.003	0.003	0.003	0.003	0.003
Ca	0.448	0.499	0.494	0.369	0.406	0.442	0.378	0.401	0.424	0.375	0.418	0.416
Ti	0.003	0.003	0.003	0.002	0.002	0.002	0.002	0.002	0.002	0.002	0.002	0.002
O	8.000	8.000	8.000	8.000	8.000	8.000	8.000	8.000	8.000	8.000	8.000	8.000
An	**46.239**	**51.750**	**50.759**	**38.229**	**42.076**	**45.932**	**39.669**	**41.666**	**43.953**	**39.168**	**43.482**	**42.977**
Ab	**50.311**	**44.741**	**45.991**	**56.123**	**53.619**	**49.868**	**54.439**	**54.640**	**52.818**	**56.415**	**51.932**	**52.938**
Or	**3.450**	**3.510**	**3.250**	**5.648**	**4.304**	**4.200**	**5.892**	**3.694**	**3.230**	**4.417**	**4.586**	**4.084**

Sample	FD-13-34-158.6	FD-13-34-158.6	FD-13-34-158.6	FD-13-34-158.6	FD-13-34-158.6	FD-13-34-194.8	FD-13-34-194.8	FD-13-34-194.8	FD-13-34-194.8	FD-13-34-194.8	FD-13-34-194.8	FD-13-34-212.5
Spot No.	4	5	6	7	8	1	2	3	4	5	6	1
SiO_2	59.278	56.994	56.884	56.217	56.668	57.774	57.627	58.792	59.152	58.874	58.451	56.910
Al_2O_3	25.670	27.323	27.386	27.535	27.385	26.659	26.809	25.741	25.708	25.625	26.370	27.010
MgO	0.013	0.017	0.003	0.024	0.017	0.009	0.024	0.005	0.024	0.004	0.016	0.021

Na_2O	6.677	5.754	5.632	5.710	5.780	6.103	6.055	6.533	6.697	6.439	6.447	6.013
FeO	0.248	0.232	0.204	0.300	0.252	0.254	0.289	0.215	0.247	0.225	0.265	0.224
MnO	0.015	0.013	0.026	0.023	0.015	0.020	-0.003	-0.005	-0.001	0.008	-0.009	0.024
K_2O	0.870	0.629	0.710	0.453	0.527	0.848	0.785	0.960	0.882	0.958	0.592	0.619
SrO	0.202	0.255	0.214	0.201	0.216	0.192	0.219	0.200	0.249	0.231	0.240	0.210
BaO	0.156	0.141	0.148	0.153	0.166	0.204	0.215	0.243	0.073	0.138	0.183	0.182
CaO	6.965	8.720	8.822	9.121	8.942	7.947	8.174	7.179	6.940	7.133	7.643	8.568
TiO_2	0.049	0.067	0.055	0.058	0.059	0.065	0.059	0.055	0.040	0.044	0.047	0.056
Total	100.143	100.145	100.084	99.795	100.027	100.075	100.253	99.918	100.011	99.679	100.245	99.837
Si	2.652	2.561	2.558	2.538	2.551	2.595	2.586	2.641	2.649	2.647	2.616	2.566
Al	1.351	1.444	1.449	1.463	1.450	1.409	1.415	1.360	1.355	1.356	1.388	1.433
Mg	0.001	0.001	0.000	0.002	0.001	0.001	0.002	0.000	0.002	0.000	0.001	0.001
Na	0.578	0.500	0.490	0.499	0.504	0.531	0.526	0.568	0.581	0.560	0.558	0.525
Fe	0.009	0.009	0.008	0.011	0.009	0.010	0.011	0.008	0.009	0.008	0.010	0.008
Mn	0.001	0.000	0.001	0.001	0.001	0.001	0.000	0.000	0.000	0.000	0.000	0.001
K	0.050	0.036	0.041	0.026	0.030	0.049	0.045	0.055	0.050	0.055	0.034	0.036
Sr	0.005	0.007	0.006	0.005	0.006	0.005	0.006	0.005	0.006	0.006	0.006	0.005
Ba	0.003	0.002	0.003	0.003	0.003	0.004	0.004	0.004	0.001	0.002	0.003	0.003
Ca	0.334	0.420	0.425	0.441	0.431	0.382	0.393	0.345	0.333	0.344	0.366	0.414
Ti	0.002	0.002	0.002	0.002	0.002	0.002	0.002	0.002	0.001	0.001	0.002	0.002
O	8.000	8.000	8.000	8.000	8.000	8.000	8.000	8.000	8.000	8.000	8.000	8.000
An	**34.715**	**43.899**	**44.461**	**45.661**	**44.685**	**39.770**	**40.773**	**35.673**	**34.547**	**35.833**	**38.225**	**42.484**
Ab	**60.118**	**52.328**	**51.275**	**51.637**	**52.177**	**55.173**	**54.561**	**58.643**	**60.222**	**58.433**	**58.247**	**53.859**
Or	**5.167**	**3.773**	**4.263**	**2.702**	**3.138**	**5.056**	**4.666**	**5.684**	**5.231**	**5.734**	**3.528**	**3.657**

Sample	FD-13-34-212.5	FD-13-34-212.5	FD-13-34-212.5	FD-13-34-212.5	FD-13-34-212.5	FD-13-34-212.5	FD-13-34-212.5	FD-13-34-212.5	FD-13-34-212.5	FD-13-34-212.5	FD-13-34-226.3	FD-13-34-226.3
Spot No.	2	3	4	5	6	7	8	9	10	11	1	2
SiO_2	57.173	57.244	56.906	59.406	58.840	58.599	58.446	59.132	58.155	58.868	56.834	57.034
Al_2O_3	27.050	27.146	27.341	25.131	25.680	25.723	25.773	25.470	26.579	25.624	27.151	26.697
MgO	0.006	0.019	0.007	0.010	0.019	0.024	0.020	0.017	0.011	0.017	0.007	0.002
Na_2O	5.952	5.896	5.775	6.670	6.393	6.421	6.219	5.998	6.157	6.533	5.961	6.131
FeO	0.263	0.251	0.223	0.208	0.231	0.264	0.235	0.259	0.251	0.213	0.205	0.239
MnO	0.030	0.001	-0.008	-0.028	-0.006	-0.022	0.024	-0.021	0.008	0.003	0.009	-0.007
K_2O	0.694	0.791	0.734	1.041	0.930	0.936	1.044	1.226	0.762	1.036	0.599	0.691
SrO	0.229	0.257	0.232	0.248	0.240	0.237	0.229	0.221	0.193	0.264	0.222	0.216
BaO	0.207	0.203	0.187	0.207	0.229	0.129	0.208	0.187	0.116	0.115	0.177	0.157
CaO	8.532	8.511	8.703	6.539	7.106	7.107	7.109	6.757	7.858	6.903	8.624	8.220
TiO_2	0.058	0.063	0.056	0.038	0.058	0.054	0.046	0.055	0.046	0.041	0.053	0.061

Total	100.194	100.382	100.156	99.470	99.720	99.472	99.353	99.301	100.136	99.617	99.842	99.441
Si	2.570	2.569	2.559	2.674	2.646	2.641	2.639	2.664	2.606	2.649	2.562	2.580
Al	1.430	1.433	1.446	1.331	1.358	1.364	1.369	1.350	1.401	1.356	1.440	1.421
Mg	0.000	0.001	0.000	0.001	0.001	0.002	0.001	0.001	0.001	0.001	0.000	0.000
Na	0.518	0.512	0.503	0.581	0.556	0.560	0.543	0.523	0.534	0.569	0.520	0.537
Fe	0.010	0.009	0.008	0.008	0.009	0.010	0.009	0.010	0.009	0.008	0.008	0.009
Mn	0.001	0.000	0.000	-0.001	0.000	-0.001	0.001	-0.001	0.000	0.000	0.000	0.000
K	0.040	0.045	0.042	0.060	0.053	0.054	0.060	0.071	0.044	0.060	0.034	0.040
Sr	0.006	0.007	0.006	0.006	0.006	0.006	0.006	0.006	0.005	0.007	0.006	0.006
Ba	0.004	0.004	0.003	0.004	0.004	0.002	0.004	0.003	0.002	0.002	0.003	0.003
Ca	0.411	0.409	0.419	0.315	0.342	0.343	0.344	0.326	0.377	0.333	0.417	0.398
Ti	0.002	0.002	0.002	0.001	0.002	0.002	0.002	0.002	0.002	0.001	0.002	0.002
O	8.000	8.000	8.000	8.000	8.000	8.000	8.000	8.000	8.000	8.000	8.000	8.000
An	**42.425**	**42.334**	**43.494**	**32.978**	**35.957**	**35.855**	**36.294**	**35.464**	**39.511**	**34.621**	**42.893**	**40.858**
Ab	**53.464**	**52.978**	**52.136**	**60.767**	**58.436**	**58.519**	**57.355**	**56.869**	**55.924**	**59.188**	**53.558**	**55.050**
Or	**4.112**	**4.688**	**4.371**	**6.255**	**5.607**	**5.626**	**6.351**	**7.667**	**4.565**	**6.191**	**3.550**	**4.092**

Sample	FD-13-34-226.3	FD-13-34-226.3	FD-13-34-226.3	FD-13-34-226.3	FD-13-34-226.3	FD-13-34-248.5	FD-13-34-248.5	FD-13-34-248.5	FD-13-34-253.1	FD-13-34-253.1	FD-13-34-253.1	FD-13-34-253.1
Spot No.	3	4	5	6	7	1	2	3	1	2	3	4
SiO_2	57.922	56.283	57.620	57.743	58.019	54.682	55.288	56.101	55.379	54.405	55.259	54.234
Al_2O_3	26.189	27.568	26.295	26.505	26.066	28.418	28.070	27.914	28.480	29.237	28.372	29.090
MgO	0.011	0.019	0.024	0.012	0.025	0.008	0.010	0.000	-0.005	0.007	0.016	0.017
Na_2O	6.146	5.572	6.074	5.907	5.916	5.035	5.196	5.474	5.296	4.717	5.185	4.874
FeO	0.245	0.237	0.245	0.271	0.271	0.230	0.230	0.230	0.214	0.198	0.217	0.303
MnO	0.023	-0.042	0.003	0.010	0.000	0.013	0.015	-0.009	0.021	0.020	0.014	0.017
K_2O	1.053	0.679	0.903	0.996	1.268	0.528	0.556	0.512	0.454	0.400	0.422	0.408
SrO	0.224	0.210	0.228	0.244	0.213	0.273	0.282	0.286	0.265	0.234	0.265	0.274
BaO	0.236	0.172	0.219	0.209	0.242	0.116	0.114	0.130	0.098	0.087	0.122	0.104
CaO	7.598	9.129	7.879	7.896	7.090	10.013	9.749	9.384	10.084	10.916	10.112	10.897
TiO_2	0.070	0.056	0.058	0.068	0.057	0.051	0.038	0.054	0.074	0.049	0.047	0.052
Total	99.717	99.883	99.548	99.861	99.167	99.367	99.548	100.076	100.360	100.270	100.031	100.270
Si	2.612	2.540	2.603	2.600	2.626	2.486	2.507	2.527	2.493	2.454	2.495	2.451
Al	1.390	1.464	1.398	1.404	1.388	1.520	1.497	1.479	1.508	1.552	1.507	1.547
Mg	0.001	0.001	0.002	0.001	0.002	0.001	0.001	0.000	0.000	0.000	0.001	0.001
Na	0.536	0.487	0.531	0.515	0.518	0.443	0.456	0.477	0.461	0.412	0.453	0.426
Fe	0.009	0.009	0.009	0.010	0.010	0.009	0.009	0.009	0.008	0.007	0.008	0.011
Mn	0.001	-0.002	0.000	0.000	0.000	0.000	0.001	0.000	0.001	0.001	0.001	0.001
K	0.061	0.039	0.052	0.057	0.073	0.031	0.032	0.029	0.026	0.023	0.024	0.024

Sr	0.006	0.005	0.006	0.006	0.006	0.007	0.007	0.007	0.007	0.006	0.007	0.007
Ba	0.004	0.003	0.004	0.004	0.004	0.002	0.002	0.002	0.002	0.002	0.002	0.002
Ca	0.367	0.441	0.381	0.381	0.344	0.488	0.474	0.453	0.486	0.528	0.489	0.528
Ti	0.002	0.002	0.002	0.002	0.002	0.002	0.001	0.002	0.002	0.002	0.002	0.002
O	8.000	8.000	8.000	8.000	8.000	8.000	8.000	8.000	8.000	8.000	8.000	8.000
An	**38.075**	**45.637**	**39.539**	**39.973**	**36.759**	**50.731**	**49.243**	**47.197**	**49.941**	**54.817**	**50.607**	**53.978**
Ab	**55.637**	**50.319**	**55.062**	**54.020**	**55.408**	**46.082**	**47.411**	**49.735**	**47.380**	**42.790**	**46.876**	**43.614**
Or	**6.287**	**4.044**	**5.399**	**6.008**	**7.833**	**3.187**	**3.346**	**3.068**	**2.679**	**2.393**	**2.516**	**2.408**

Sample	FD-13-34-253.1	FD-13-34-257.8	FD-13-34-257.8	FD-13-34-257.8	FD-13-34-257.8	FD-13-34-257.8	FD-13-34-257.8	FD-13-34-272.1	FD-13-34-272.1	FD-13-34-272.1	FD-13-34-272.1	FD-13-34-272.1
Spot No.	5	1	2	3	4	5	6	1	2	3	4	5
SiO_2	54.368	55.510	55.555	55.552	55.520	55.339	55.675	56.848	57.388	56.808	57.711	57.007
Al_2O_3	28.959	28.134	28.250	27.980	28.028	28.441	28.328	27.140	27.060	27.386	26.684	27.263
MgO	0.018	0.008	0.001	0.013	0.005	-0.004	-0.009	0.012	0.004	0.001	-0.009	0.012
Na_2O	4.831	5.313	5.360	5.237	5.223	5.436	5.408	6.192	6.253	6.027	6.333	6.234
FeO	0.235	0.230	0.227	0.289	0.195	0.163	0.174	0.235	0.204	0.158	0.168	0.283
MnO	-0.006	0.017	-0.010	0.019	0.016	-0.016	0.006	-0.008	-0.009	0.009	-0.002	0.007
K_2O	0.426	0.547	0.408	0.496	0.522	0.319	0.314	0.284	0.353	0.334	0.293	0.075
SrO	0.300	0.260	0.273	0.274	0.251	0.281	0.298	0.239	0.219	0.227	0.204	0.262
BaO	0.123	0.131	0.138	0.115	0.140	0.122	0.109	0.072	0.085	0.066	0.078	0.086
CaO	10.570	9.789	9.690	9.710	9.748	9.839	9.772	8.645	8.476	8.775	8.143	8.590
TiO_2	0.051	0.049	0.041	0.050	0.051	0.034	0.034	0.042	0.034	0.043	0.036	0.041
Total	99.875	99.988	99.933	99.735	99.699	99.954	100.109	99.701	100.067	99.834	99.639	99.860
Si	2.462	2.507	2.507	2.513	2.512	2.498	2.507	2.563	2.575	2.557	2.596	2.563
Al	1.543	1.495	1.500	1.489	1.492	1.510	1.501	1.439	1.429	1.450	1.412	1.442
Mg	0.001	0.001	0.000	0.001	0.000	0.000	-0.001	0.001	0.000	0.000	-0.001	0.001
Na	0.424	0.464	0.468	0.459	0.457	0.475	0.471	0.540	0.543	0.525	0.551	0.543
Fe	0.009	0.009	0.009	0.011	0.007	0.006	0.007	0.009	0.008	0.006	0.006	0.011
Mn	0.000	0.001	0.000	0.001	0.001	-0.001	0.000	0.000	0.000	0.000	0.000	0.000
K	0.025	0.032	0.024	0.029	0.030	0.018	0.018	0.016	0.020	0.019	0.017	0.004
Sr	0.008	0.007	0.007	0.007	0.007	0.007	0.008	0.006	0.006	0.006	0.005	0.007
Ba	0.002	0.002	0.002	0.002	0.002	0.002	0.002	0.001	0.001	0.001	0.001	0.002
Ca	0.513	0.474	0.469	0.471	0.473	0.476	0.471	0.418	0.408	0.423	0.392	0.414
Ti	0.002	0.002	0.001	0.002	0.002	0.001	0.001	0.001	0.001	0.001	0.001	0.001
O	8.000	8.000	8.000	8.000	8.000	8.000	8.000	8.000	8.000	8.000	8.000	8.000
An	**53.372**	**48.851**	**48.795**	**49.136**	**49.220**	**49.099**	**49.068**	**42.863**	**41.976**	**43.743**	**40.853**	**43.078**
Ab	**44.065**	**47.896**	**48.757**	**47.873**	**47.640**	**49.004**	**49.054**	**55.459**	**55.941**	**54.273**	**57.395**	**56.474**
Or	**2.563**	**3.252**	**2.448**	**2.991**	**3.140**	**1.897**	**1.879**	**1.678**	**2.083**	**1.984**	**1.751**	**0.448**

Sample	FD-13-34-272.1	FD-13-34-272.1	FD-13-34-272.1	FD-13-34-272.1	FD-13-34-272.1	FD-13-34-272.1	FD-13-34-276.5	FD-13-34-276.5	FD-13-34-276.5	FD-13-34-276.5	FD-13-34-276.5	FD-13-34-276.5
Spot No.	6	7	8	9	10	11	1	2	3	4	5	6
SiO_2	57.895	58.688	58.411	54.931	55.826	56.091	53.572	53.343	53.582	53.034	53.169	52.867
Al_2O_3	26.554	26.140	25.941	27.569	27.788	27.616	29.570	29.647	29.555	29.832	29.810	29.915
MgO	0.033	0.027	0.016	0.802	-0.005	0.009	0.029	0.030	0.020	0.022	0.025	0.024
Na_2O	6.383	6.788	6.776	5.490	5.820	5.683	4.555	4.541	4.524	4.340	4.404	4.241
FeO	0.264	0.171	0.206	0.397	0.207	0.288	0.244	0.285	0.236	0.261	0.274	0.297
MnO	0.006	0.012	-0.020	0.015	0.021	0.000	0.023	0.014	-0.021	0.020	-0.007	-0.017
K_2O	0.369	0.256	0.313	0.211	0.183	0.201	0.399	0.382	0.449	0.393	0.283	0.367
SrO	0.255	0.223	0.233	0.261	0.251	0.254	0.172	0.205	0.232	0.254	0.214	0.235
BaO	0.026	0.065	0.055	0.162	0.145	0.166	0.085	0.111	0.102	0.075	0.093	0.085
CaO	8.055	7.393	7.378	9.207	9.315	9.330	11.265	11.438	11.371	11.682	11.719	11.655
TiO_2	0.040	0.044	0.033	0.053	0.031	0.042	0.038	0.047	0.044	0.049	0.046	0.048
Total	99.880	99.807	99.342	99.098	99.582	99.680	99.952	100.043	100.094	99.962	100.030	99.717
Si	2.599	2.629	2.630	2.502	2.525	2.534	2.428	2.419	2.427	2.408	2.411	2.405
Al	1.403	1.378	1.374	1.477	1.479	1.468	1.577	1.582	1.575	1.594	1.590	1.601
Mg	0.002	0.002	0.001	0.055	0.000	0.001	0.002	0.002	0.001	0.001	0.002	0.002
Na	0.555	0.589	0.591	0.484	0.510	0.497	0.400	0.399	0.397	0.381	0.387	0.373
Fe	0.010	0.006	0.008	0.015	0.008	0.011	0.009	0.011	0.009	0.010	0.010	0.011
Mn	0.000	0.000	-0.001	0.001	0.001	0.000	0.001	0.001	-0.001	0.001	0.000	-0.001
K	0.021	0.015	0.018	0.012	0.011	0.012	0.023	0.022	0.026	0.023	0.016	0.021
Sr	0.007	0.006	0.006	0.007	0.007	0.007	0.005	0.005	0.006	0.007	0.006	0.006
Ba	0.000	0.001	0.001	0.003	0.003	0.003	0.002	0.002	0.002	0.001	0.002	0.002
Ca	0.387	0.355	0.356	0.449	0.451	0.452	0.547	0.556	0.552	0.568	0.569	0.568
Ti	0.001	0.001	0.001	0.002	0.001	0.001	0.001	0.002	0.001	0.002	0.002	0.002
O	8.000	8.000	8.000	8.000	8.000	8.000	8.000	8.000	8.000	8.000	8.000	8.000
An	**40.224**	**37.039**	**36.906**	**47.518**	**46.467**	**47.037**	**56.413**	**56.916**	**56.633**	**58.438**	**58.560**	**59.002**
Ab	**57.580**	**61.433**	**61.229**	**51.185**	**52.446**	**51.756**	**41.206**	**40.819**	**40.702**	**39.219**	**39.755**	**38.784**
Or	**2.196**	**1.528**	**1.865**	**1.298**	**1.088**	**1.207**	**2.381**	**2.265**	**2.664**	**2.342**	**1.685**	**2.214**

Sample	FD-13-34-281.05	FD-13-34-281.05	FD-13-34-281.05	FD-13-34-281.05	FD-13-34-281.05	FD-13-34-281.05	FD-13-34-291.05	FD-13-34-291.05	FD-13-34-291.05	FD-13-34-291.05	FD-13-34-291.05	FD-13-34-291.05
Spot No.	1	2	3	4	5	6	1	2	3	4	5	6
SiO_2	54.637	54.008	54.830	55.289	53.015	53.772	54.307	54.279	54.194	54.308	54.624	55.279
Al_2O_3	28.738	29.557	28.678	28.215	29.485	29.688	29.017	28.190	29.066	29.032	28.890	28.333
MgO	0.005	0.017	0.019	0.017	0.179	0.006	0.030	0.591	0.018	0.028	0.033	0.040

Na_2O	5.088	4.706	5.211	5.267	4.429	4.623	4.798	5.088	4.733	4.703	4.880	5.093
FeO	0.203	0.251	0.238	0.240	0.745	0.260	0.226	1.078	0.302	0.234	0.275	0.338
MnO	0.003	-0.001	0.005	-0.008	0.041	-0.023	-0.002	0.044	0.032	0.002	0.003	0.023
K_2O	0.418	0.346	0.197	0.587	0.348	0.181	0.312	0.228	0.503	0.530	0.499	0.576
SrO	0.259	0.289	0.249	0.260	0.251	0.266	0.198	0.211	0.181	0.174	0.175	0.206
BaO	0.097	0.120	0.154	0.148	0.093	0.098	0.094	0.118	0.085	0.086	0.105	0.093
CaO	10.308	11.130	10.221	9.849	11.251	11.408	10.871	9.962	10.854	10.771	10.594	10.130
TiO_2	0.035	0.033	0.023	0.022	0.047	0.035	0.056	0.059	0.063	0.069	0.065	0.047
Total	99.791	100.456	99.825	99.886	99.884	100.314	99.907	99.848	100.031	99.937	100.143	100.158
Si	2.474	2.436	2.480	2.501	2.412	2.428	2.458	2.465	2.453	2.458	2.467	2.494
Al	1.531	1.568	1.526	1.502	1.579	1.577	1.545	1.506	1.548	1.546	1.535	1.504
Mg	0.000	0.001	0.001	0.001	0.012	0.000	0.002	0.040	0.001	0.002	0.002	0.003
Na	0.446	0.411	0.456	0.461	0.390	0.404	0.420	0.447	0.415	0.412	0.427	0.445
Fe	0.008	0.009	0.009	0.009	0.028	0.010	0.009	0.041	0.011	0.009	0.010	0.013
Mn	0.000	0.000	0.000	0.000	0.002	-0.001	0.000	0.002	0.001	0.000	0.000	0.001
K	0.024	0.020	0.011	0.034	0.020	0.010	0.018	0.013	0.029	0.031	0.029	0.033
Sr	0.007	0.008	0.007	0.007	0.007	0.007	0.005	0.006	0.005	0.005	0.005	0.005
Ba	0.002	0.002	0.003	0.003	0.002	0.002	0.002	0.002	0.002	0.002	0.002	0.002
Ca	0.500	0.538	0.495	0.477	0.549	0.552	0.527	0.485	0.526	0.522	0.513	0.490
Ti	0.001	0.001	0.001	0.001	0.002	0.001	0.002	0.002	0.002	0.002	0.002	0.002
O	8.000	8.000	8.000	8.000	8.000	8.000	8.000	8.000	8.000	8.000	8.000	8.000
An	**51.547**	**55.529**	**51.442**	**49.090**	**57.209**	**57.112**	**54.600**	**51.285**	**54.261**	**54.130**	**52.959**	**50.608**
Ab	**45.962**	**42.414**	**47.377**	**47.424**	**40.682**	**41.809**	**43.532**	**47.317**	**42.743**	**42.696**	**44.069**	**45.963**
Or	**2.491**	**2.057**	**1.181**	**3.486**	**2.108**	**1.080**	**1.867**	**1.399**	**2.996**	**3.174**	**2.972**	**3.429**

Sample	FD-13-34-291.05	FD-13-34-295.7	FD-13-34-295.7	FD-13-34-295.7	FD-13-34-295.7	FD-13-34-295.7	FD-13-34-316.7	FD-13-34-316.7	FD-13-34-316.7	FD-13-34-316.7	SL-13-34-3	SL-13-34-3
Spot No.	7	1	2	3	4	5	1	2	3	4	1	2
SiO_2	54.537	54.920	55.560	54.210	54.641	54.812	57.864	57.656	57.470	54.430	53.789	53.499
Al_2O_3	29.065	28.938	28.680	29.029	28.832	28.740	27.590	27.422	26.875	25.720	28.027	28.355
MgO	0.019	0.014	0.017	0.003	0.019	0.021	0.024	0.017	0.313	2.680	0.009	0.003
Na_2O	4.811	4.958	5.087	4.795	4.813	4.898	6.314	6.215	6.951	5.346	5.28	5.125
FeO	0.238	0.326	0.241	0.231	0.258	0.288	0.204	0.221	1.026	1.792	0.143	0.142
MnO	0.017	0.031	-0.048	-0.001	0.035	-0.006	-0.007	0.001	0.094	0.416	-0.021	-0.006
K_2O	0.543	0.411	0.483	0.429	0.428	0.465	0.327	0.420	2.292	0.346		
SrO	0.156	0.238	0.259	0.242	0.222	0.228	0.207	0.191	0.488	0.187	0.354	0.357
BaO	0.048	0.115	0.092	0.108	0.083	0.094	0.059	0.073	0.290	0.051	0.661	0.654
CaO	10.742	10.477	10.143	10.746	10.476	10.431	8.508	8.556	3.952	7.446	10.196	10.478
TiO_2	0.052	0.037	0.061	0.061	0.062	0.069	0.041	0.032	0.032	0.042	0.107	0.12

Total	100.228	100.465	100.575	99.853	99.869	100.040	101.131	100.804	99.783	98.456	98.756	99.065
Si	2.461	2.472	2.493	2.456	2.472	2.476	2.568	2.569	2.603	2.507	2.476	2.460
Al	1.543	1.532	1.514	1.548	1.534	1.527	1.441	1.437	1.432	1.394	1.518	1.534
Mg	0.001	0.001	0.001	0.000	0.001	0.001	0.002	0.001	0.021	0.185	0.001	0.000
Na	0.420	0.432	0.442	0.421	0.421	0.428	0.542	0.536	0.609	0.477	0.470	0.456
Fe	0.009	0.012	0.009	0.009	0.010	0.011	0.008	0.008	0.039	0.069	0.005	0.005
Mn	0.001	0.001	-0.002	0.000	0.001	0.000	0.000	0.000	0.004	0.016	-0.001	0.000
K	0.031	0.024	0.028	0.025	0.025	0.027	0.019	0.024	0.133	0.020	0.000	0.000
Sr	0.004	0.006	0.007	0.006	0.006	0.006	0.005	0.005	0.013	0.005	0.009	0.010
Ba	0.001	0.002	0.002	0.002	0.001	0.002	0.001	0.001	0.005	0.001	0.012	0.012
Ca	0.519	0.505	0.488	0.522	0.508	0.505	0.405	0.408	0.192	0.367	0.503	0.516
Ti	0.002	0.001	0.002	0.002	0.002	0.002	0.001	0.001	0.001	0.001	0.004	0.004
O	8.000	8.000	8.000	8.000	8.000	8.000	8.000	8.000	8.000	8.000	8.000	8.000
An	**53.497**	**52.587**	**50.950**	**53.948**	**53.231**	**52.594**	**41.904**	**42.182**	**20.541**	**42.511**	**51.667**	**53.091**
Ab	**43.281**	**44.955**	**46.160**	**43.486**	**44.178**	**44.612**	**56.177**	**55.351**	**65.265**	**55.136**	**48.333**	**46.909**
Or	**3.222**	**2.458**	**2.891**	**2.566**	**2.591**	**2.794**	**1.919**	**2.467**	**14.194**	**2.354**	**0.000**	**0.000**

Sample	SL-13-34-3	SL-13-34-3	SL-13-34-3	SL-13-34-3	SL-13-34-3	SL-13-34-3	SL-13-34-3	SL-13-34-5.1	SL-13-34-5.1	SL-13-34-5.1	SL-13-34-5.1	SL-13-34-5.1
Spot No.	3	4	5	6	7	8	9	1	2	3	4	5
SiO_2	53.147	55.255	55.998	54.738	56.088	56.361	53.648	54.727	54.594	56.615	55.905	53.504
Al_2O_3	29.075	27.157	26.765	27.796	26.943	26.875	28.639	28.198	28.035	26.638	27.456	28.725
MgO	0.021	0.044	0.005	0.003	0.002	0.003	0.003	0.016	0.006	0.015	0.012	0.01
Na_2O	4.854	5.859	6.257	5.626	6.288	6.34	5.125	5.191	5.323	6.207	5.862	4.87
FeO	0.164	0.203	0.164	0.128	0.106	0.098	0.117	0.16	0.15	0.311	0.126	0.184
MnO	-0.015	-0.009	0.011	0.006	0.01	0.019	-0.008	0.007	-0.011	0.016	-0.002	0.004
K_2O								0.335	0.322	0.429	0.366	0.281
SrO	0.328	0.24	0.229	0.345	0.278	0.296	0.288	0.369	0.365	0.372	0.336	0.344
BaO	0.393	0.255	0.267	0.277	0.337	0.334	0.382	0.372	0.385	0.296	0.324	0.373
CaO	11.203	9.392	8.685	9.719	8.864	8.607	10.62	10.242	10.058	8.39	9.207	10.845
TiO_2	0.111	0.077	0.096	0.096	0.086	0.113	0.102	0.118	0.095	0.081	0.108	0.071
Total	99.465	98.753	98.916	98.997	99.097	99.151	99.097	99.675	99.304	99.284	99.653	99.242
Si	2.430	2.530	2.558	2.503	2.552	2.561	2.456	2.486	2.490	2.570	2.532	2.448
Al	1.564	1.463	1.438	1.495	1.442	1.437	1.543	1.507	1.504	1.422	1.463	1.546
Mg	0.001	0.003	0.000	0.000	0.000	0.000	0.000	0.001	0.000	0.001	0.001	0.001
Na	0.430	0.519	0.553	0.498	0.554	0.558	0.454	0.456	0.470	0.545	0.514	0.431
Fe	0.006	0.008	0.006	0.005	0.004	0.004	0.004	0.006	0.006	0.012	0.005	0.007
Mn	-0.001	0.000	0.000	0.000	0.000	0.001	0.000	0.000	0.000	0.001	0.000	0.000
K	0.000	0.000	0.000	0.000	0.000	0.000	0.000	0.019	0.019	0.025	0.021	0.016

Sr	0.009	0.006	0.006	0.009	0.007	0.008	0.008	0.010	0.010	0.010	0.009	0.009
Ba	0.007	0.005	0.005	0.005	0.006	0.006	0.007	0.007	0.007	0.005	0.006	0.007
Ca	0.549	0.461	0.425	0.476	0.432	0.419	0.521	0.498	0.491	0.408	0.447	0.532
Ti	0.004	0.003	0.003	0.003	0.003	0.004	0.004	0.004	0.003	0.003	0.004	0.002
O	8.000	8.000	8.000	8.000	8.000	8.000	8.000	8.000	8.000	8.000	8.000	8.000
An	**56.095**	**47.016**	**43.451**	**48.883**	**43.831**	**42.906**	**53.426**	**51.163**	**50.146**	**41.713**	**45.506**	**54.287**
Ab	**43.905**	**52.984**	**56.549**	**51.117**	**56.169**	**57.094**	**46.574**	**46.843**	**47.941**	**55.746**	**52.339**	**44.037**
Or	**0.000**	**0.000**	**0.000**	**0.000**	**0.000**	**0.000**	**0.000**	**1.994**	**1.913**	**2.541**	**2.155**	**1.676**

Sample	SL-13-34-5.1	SL-13-34-5.1	SL-13-34-5.1	SL-13-34-5.1	SL-13-34-7	SL-13-34-7	SL-13-34-7	SL-13-34-7	SL-13-34-7	SL-13-34-7	SL-13-34-7	SL-13-34-7
Spot No.	6	7	8	9	1	2	3	4	5	6	7	8
SiO_2	55.77	54.804	54.351	54.709	57.915	55.654	55.442	54.535	53.975	55.118	57.744	55.546
Al_2O_3	27.143	27.785	28.102	27.945	26.974	28.635	28.836	29.787	29.537	28.707	26.983	28.392
MgO	0.008	0.007	0.019	0.004	0.008	0.017	0.011	0.016	0.013	-0.007	0.017	-0.005
Na_2O	5.937	5.444	5.269	5.334	6.59	5.845	5.646	5.279	5.195	5.704	6.728	5.758
FeO	0.164	0.219	0.154	0.148	0.171	0.17	0.185	0.177	0.177	0.184	0.214	0.199
MnO	-0.004	-0.007	-0.004	-0.009	0.003	0.014	-0.02	-0.012	-0.019	0.028	-0.002	0.002
K_2O	0.394	0.424	0.364	0.457	0.763	0.558	0.575	0.344	0.368	0.331	0.681	0.504
SrO	0.348	0.343	0.348	0.302	0.386	0.318	0.353	0.417	0.446	0.366	0.339	0.357
BaO	0.498	0.367	0.376	0.37	0.199	0.292	0.333	0.472	0.554	0.184	0.265	0.303
CaO	8.875	9.813	10.121	10.031	7.467	9.36	9.378	10.084	10.293	9.508	7.344	9.13
TiO_2	0.078	0.115	0.132	0.118	0.059	0.065	0.063	0.119	0.067	0.022	0.053	0.049
Total	99.241	99.4	99.199	99.389	100.536	100.95	100.794	101.202	100.591	100.146	100.368	100.234
Si	2.541	2.500	2.482	2.493	2.591	2.495	2.489	2.444	2.438	2.487	2.588	2.504
Al	1.455	1.491	1.510	1.498	1.420	1.510	1.523	1.570	1.570	1.524	1.423	1.506
Mg	0.001	0.000	0.001	0.000	0.001	0.001	0.001	0.001	0.001	0.000	0.001	0.000
Na	0.523	0.481	0.466	0.470	0.571	0.507	0.490	0.458	0.454	0.498	0.584	0.502
Fe	0.006	0.008	0.006	0.006	0.006	0.006	0.007	0.007	0.007	0.007	0.008	0.007
Mn	0.000	0.000	0.000	0.000	0.000	0.001	-0.001	0.000	-0.001	0.001	0.000	0.000
K	0.023	0.025	0.021	0.027	0.044	0.032	0.033	0.020	0.021	0.019	0.039	0.029
Sr	0.009	0.009	0.009	0.008	0.010	0.008	0.009	0.011	0.012	0.010	0.009	0.009
Ba	0.009	0.007	0.007	0.007	0.003	0.005	0.006	0.008	0.010	0.003	0.005	0.005
Ca	0.433	0.480	0.495	0.490	0.358	0.450	0.451	0.484	0.498	0.460	0.353	0.441
Ti	0.003	0.004	0.005	0.004	0.002	0.002	0.002	0.004	0.002	0.001	0.002	0.002
O	8.000	8.000	8.000	8.000	8.000	8.000	8.000	8.000	8.000	8.000	8.000	8.000
An	**44.222**	**48.694**	**50.421**	**49.631**	**36.818**	**45.473**	**46.283**	**50.344**	**51.168**	**47.054**	**36.161**	**45.351**
Ab	**53.439**	**48.799**	**47.418**	**47.675**	**58.699**	**51.297**	**50.336**	**47.610**	**46.652**	**50.994**	**59.844**	**51.667**
Or	**2.339**	**2.507**	**2.161**	**2.694**	**4.483**	**3.230**	**3.381**	**2.046**	**2.180**	**1.952**	**3.995**	**2.983**

Sample	SL-13-34-7	SL-13-34-7	SL-13-34-7	SL-13-34-7	SL-13-34-13.3	SL-13-34-13.3	SL-13-34-13.3	SL-13-34-13.3	SL-13-34-13.3	SL-13-34-13.3	SL-13-34-13.3	SL-13-34-13.3
Spot No.	9	10	11	12	1	2	3	4	5	6	7	8
SiO_2	55.782	55.634	57.78	56.477	56.154	56.029	54.514	56.055	56.424	54.714	54.86	54.739
Al_2O_3	28.247	28.689	26.772	28.643	28.039	27.988	29.505	28.212	27.922	28.956	28.905	28.8
MgO	0.003	0.007	0.006	0.02	0.01	0.016	0.014	0.002	0.019	0.022	0.015	0.014
Na_2O	5.912	5.682	6.638	6.057	5.887	5.978	5.303	5.773	6.102	5.409	5.491	5.476
FeO	0.227	0.199	0.233	0.206	0.188	0.187	0.185	0.179	0.187	0.203	0.239	0.232
MnO	0.005	0.004	0.018	0.024	-0.008	0.016	0.031	0.002	0.007	0.03	0.012	-0.007
K_2O	0.546	0.541	0.822	0.527	0.463	0.456	0.386	0.441	0.515	0.412	0.312	0.414
SrO	0.354	0.344	0.353	0.342	0.319	0.341	0.358	0.277	0.401	0.316	0.375	0.385
BaO	0.187	0.311	0.263	0.251	0.125	0.163	0.29	0.092	0.126	0.204	0.324	0.371
CaO	8.819	9.328	7.426	9.06	9.119	9.016	10.296	9.332	8.682	10.036	10.001	9.927
TiO_2	0.053	0.078	0.04	0.062	0.044	0.05	0.077	0.065	0.046	0.064	0.098	0.063
Total	100.16	100.806	100.355	101.679	100.358	100.226	100.949	100.412	100.438	100.351	100.631	100.427
Si	2.514	2.495	2.593	2.510	2.524	2.522	2.448	2.516	2.533	2.468	2.470	2.472
Al	1.498	1.514	1.413	1.498	1.482	1.482	1.559	1.490	1.475	1.537	1.531	1.530
Mg	0.000	0.000	0.000	0.001	0.001	0.001	0.001	0.000	0.001	0.001	0.001	0.001
Na	0.516	0.493	0.576	0.521	0.512	0.521	0.461	0.502	0.530	0.472	0.479	0.479
Fe	0.009	0.007	0.009	0.008	0.007	0.007	0.007	0.007	0.007	0.008	0.009	0.009
Mn	0.000	0.000	0.001	0.001	0.000	0.001	0.001	0.000	0.000	0.001	0.000	0.000
K	0.031	0.031	0.047	0.030	0.027	0.026	0.022	0.025	0.030	0.024	0.018	0.024
Sr	0.009	0.009	0.009	0.009	0.008	0.009	0.009	0.007	0.010	0.008	0.010	0.010
Ba	0.003	0.005	0.005	0.004	0.002	0.003	0.005	0.002	0.002	0.004	0.006	0.007
Ca	0.426	0.448	0.357	0.431	0.439	0.435	0.495	0.449	0.418	0.485	0.482	0.480
Ti	0.002	0.003	0.001	0.002	0.001	0.002	0.003	0.002	0.002	0.002	0.003	0.002
O	8.000	8.000	8.000	8.000	8.000	8.000	8.000	8.000	8.000	8.000	8.000	8.000
An	**43.768**	**46.094**	**36.408**	**43.917**	**44.910**	**44.287**	**50.631**	**46.002**	**42.729**	**49.443**	**49.286**	**48.872**
Ab	**53.003**	**50.721**	**58.790**	**53.039**	**52.374**	**53.045**	**47.108**	**51.408**	**54.251**	**48.138**	**48.883**	**48.700**
Or	**3.229**	**3.185**	**4.802**	**3.044**	**2.717**	**2.669**	**2.262**	**2.590**	**3.020**	**2.418**	**1.832**	**2.428**

Sample	SL-13-34-13.3	SL-13-34-17.4	SL-13-34-17.4	SL-13-34-17.4	SL-13-34-17.4	SL-13-34-17.4	SL-13-34-17.4	SL-13-34-17.4	SL-13-34-17.4	SL-13-34-17.4	SL-13-34-17.4	SL-13-34-17.4
Spot No.	9	1	2	3	4	5	6	7	8	9	10	11
SiO_2	55.805	54.616	54.471	54.617	54.425	54.806	55.004	55.127	56.382	55.064	54.522	54.071
Al_2O_3	28.326	27.844	28.112	27.845	28.304	27.946	27.729	27.768	26.665	27.576	27.953	28.167
MgO	0.001	0.018	0.007	0.019	0.027	0.027	0.006	0.024	0.011	0.019	0.027	0.01

Na_2O	5.762	5.407	5.133	5.346	5.112	5.268	5.352	5.491	5.984	5.35	5.322	5.05
FeO	0.202	0.221	0.197	0.212	0.234	0.207	0.216	0.215	0.24	0.237	0.211	0.174
MnO	-0.01	-0.006	0.003	-0.004	0.007	-0.004	0.001	-0.009	0.008	0.018	0.008	0.008
K_2O	0.617	0.33	0.358	0.383	0.392	0.467	0.422	0.362	0.529	0.554	0.493	0.471
SrO	0.344	0.339	0.353	0.335	0.342	0.394	0.317	0.332	0.349	0.37	0.297	0.312
BaO	0.365	0.34	0.366	0.293	0.333	0.35	0.276	0.259	0.215	0.231	0.188	0.184
CaO	9.034	10.035	10.396	10.09	10.491	10.031	9.89	9.852	8.713	9.732	10.125	10.386
TiO_2	0.08	0.104	0.079	0.075	0.066	0.088	0.076	0.09	0.072	0.048	0.07	0.055
Total	100.526	99.192	99.52	99.231	99.791	99.716	99.299	99.545	99.114	99.208	99.224	99.018
Si	2.510	2.493	2.483	2.494	2.475	2.494	2.506	2.506	2.564	2.512	2.489	2.477
Al	1.499	1.495	1.507	1.496	1.514	1.496	1.486	1.485	1.427	1.480	1.501	1.518
Mg	0.000	0.001	0.000	0.001	0.002	0.002	0.000	0.002	0.001	0.001	0.002	0.001
Na	0.502	0.478	0.453	0.472	0.450	0.464	0.472	0.483	0.527	0.472	0.470	0.448
Fe	0.008	0.008	0.007	0.008	0.009	0.008	0.008	0.008	0.009	0.009	0.008	0.007
Mn	0.000	0.000	0.000	0.000	0.000	0.000	0.000	0.000	0.000	0.001	0.000	0.000
K	0.035	0.019	0.021	0.022	0.023	0.027	0.025	0.021	0.031	0.032	0.029	0.028
Sr	0.009	0.009	0.009	0.009	0.009	0.010	0.008	0.009	0.009	0.010	0.008	0.008
Ba	0.006	0.006	0.007	0.005	0.006	0.006	0.005	0.005	0.004	0.004	0.003	0.003
Ca	0.435	0.491	0.508	0.494	0.511	0.489	0.483	0.480	0.425	0.476	0.495	0.510
Ti	0.003	0.004	0.003	0.003	0.002	0.003	0.003	0.003	0.002	0.002	0.002	0.002
O	8.000	8.000	8.000	8.000	8.000	8.000	8.000	8.000	8.000	8.000	8.000	8.000
An	**44.772**	**49.689**	**51.734**	**49.942**	**51.955**	**49.896**	**49.300**	**48.766**	**43.234**	**48.523**	**49.812**	**51.749**
Ab	**51.585**	**48.364**	**46.143**	**47.800**	**45.732**	**47.336**	**48.194**	**49.099**	**53.638**	**48.186**	**47.298**	**45.454**
Or	**3.643**	**1.947**	**2.123**	**2.259**	**2.313**	**2.768**	**2.506**	**2.135**	**3.128**	**3.291**	**2.890**	**2.796**

Sample	SL-13-34-19.4	SL-13-34-19.4	SL-13-34-19.4	SL-13-34-19.4	SL-13-34-19.4	SL-13-34-19.4	SL-13-34-19.4	SL-13-34-19.4	SL-13-34-19.4	SL-13-34-25.7	SL-13-34-25.7	SL-13-34-25.7
Spot No.	1	2	3	4	5	6	7	8	9	1	2	3
SiO_2	57.594	56.94	58.009	54.249	54.444	54.614	54.304	56.54	56.428	56.716	54.712	54.767
Al_2O_3	27.257	27.803	27.331	29.895	29.777	29.711	29.623	27.975	28.029	26.023	27.185	27.367
MgO	0.013	0.017	0.007	0.004	0.014	0.004	0.004	0.025	0.01	0.01	0.002	0.002
Na_2O	6.778	6.594	6.887	5.102	5.166	5.237	5.252	6.243	6.23	6.203	5.434	5.482
FeO	0.593	0.477	0.391	0.149	0.15	0.199	0.152	0.182	0.173	0.15	0.123	0.145
MnO	0.018	0.014	0.004	0.001	-0.001	-0.014	0.011	0.013	-0.011	-0.006	-0.001	-0.007
K_2O	0.126	0.145	0.108	0.397	0.362	0.376	0.278	0.402	0.411	0.481	0.215	0.224
SrO	0.347	0.331	0.336	0.287	0.322	0.271	0.345	0.309	0.252	0.336	0.342	0.384
BaO					0.453	0.484	0.229		0.277	0.472	0.586	0.594
CaO	8.138	8.614	7.936	10.289	10.376	10.24	10.399	8.757	8.87	8.308	10.051	10.148
TiO_2	0.025	0.033	0.022	0.071	0.091	0.101	0.08	0.045	0.083	0.069	0.11	0.09

Total	100.946	101.026	101.16	100.977	101.166	101.205	100.673	100.644	100.732	98.765	98.764	99.219
Si	2.568	2.540	2.577	2.440	2.441	2.446	2.443	2.533	2.527	2.590	2.512	2.506
Al	1.430	1.459	1.429	1.582	1.571	1.566	1.568	1.474	1.477	1.398	1.468	1.473
Mg	0.001	0.001	0.000	0.000	0.001	0.000	0.000	0.002	0.001	0.001	0.000	0.000
Na	0.585	0.569	0.592	0.444	0.448	0.454	0.457	0.541	0.540	0.548	0.483	0.485
Fe	0.022	0.018	0.014	0.006	0.006	0.007	0.006	0.007	0.006	0.006	0.005	0.006
Mn	0.001	0.001	0.000	0.000	0.000	-0.001	0.000	0.000	0.000	0.000	0.000	0.000
K	0.007	0.008	0.006	0.023	0.021	0.022	0.016	0.023	0.023	0.028	0.013	0.013
Sr	0.009	0.009	0.009	0.007	0.008	0.007	0.009	0.008	0.007	0.009	0.009	0.010
Ba	0.000	0.000	0.000	0.000	0.008	0.008	0.004	0.000	0.005	0.008	0.011	0.011
Ca	0.389	0.412	0.378	0.496	0.498	0.491	0.501	0.420	0.426	0.406	0.494	0.497
Ti	0.001	0.001	0.001	0.002	0.003	0.003	0.003	0.002	0.003	0.002	0.004	0.003
O	8.000	8.000	8.000	8.000	8.000	8.000	8.000	8.000	8.000	8.000	8.000	8.000
An	**39.635**	**41.617**	**38.701**	**51.500**	**51.521**	**50.823**	**51.435**	**42.689**	**43.029**	**41.361**	**49.947**	**49.946**
Ab	**59.634**	**57.549**	**60.671**	**46.132**	**46.338**	**46.954**	**46.927**	**54.976**	**54.595**	**55.786**	**48.780**	**48.740**
Or	**0.731**	**0.835**	**0.628**	**2.368**	**2.142**	**2.224**	**1.638**	**2.335**	**2.376**	**2.853**	**1.273**	**1.314**

Sample	SL-13-34-25.7	SL-13-34-25.7	SL-13-34-25.7	SL-13-34-25.7	SL-13-34-25.7	SL-13-34-25.7	SL-13-34-25.7	SL-13-34-28.1	SL-13-34-28.1	SL-13-34-28.1	SL-13-34-28.1	SL-13-34-28.1
Spot No.	4	5	6	7	8	9	10	1	2	3	4	5
SiO_2	56.079	55.101	55.413	53.27	53.774	53.48	59.836	59.082	61.113	55.424	55.135	55.158
Al_2O_3	26.176	25.512	26.49	27.903	27.455	27.786	24.043	24.562	23.339	26.781	26.88	26.995
MgO	0.005	0.45	0.015	0.067	0.017	0.008	0	0.001	0.013	0.003	0.008	0.004
Na_2O	6.018	5.953	5.852	4.747	4.992	4.837	7.981	7.409	8.438	5.852	5.742	5.779
FeO	0.226	1.365	0.213	0.172	0.175	0.15	0.174	0.145	0.198	0.14	0.105	0.173
MnO	0.019	0.086	-0.003	0.014	0.034	0.001	-0.011	-0.022	-0.013	-0.008	0.008	0.002
K_2O	0.342	0.291	0.337	0.337	0.588	0.34	0.168	0.195	0.144	0.283	0.368	0.253
SrO	0.342	0.382	0.355	0.357	0.413	0.311	0.253	0.264	0.253	0.405	0.436	0.416
BaO	0.597	0.631	0.491	0.425	0.592	0.507	0.222	0.27	0.16			
CaO	8.775	8.289	9.24	10.871	10.187	10.843	6.029	6.857	5.283	9.135	9.226	9.381
TiO_2	0.123	0.083	0.11	0.099	0.068	0.127	0.034	0.071	0.081	0.095	0.142	0.112
Total	98.713	98.151	98.52	98.27	98.281	98.389	98.731	98.838	99.004	98.808	98.898	98.79
Si	2.569	2.555	2.546	2.463	2.488	2.470	2.707	2.676	2.749	2.545	2.536	2.531
Al	1.411	1.392	1.432	1.518	1.495	1.510	1.280	1.309	1.235	1.447	1.454	1.457
Mg	0.000	0.031	0.001	0.005	0.001	0.001	0.000	0.000	0.001	0.000	0.001	0.000
Na	0.534	0.534	0.520	0.425	0.447	0.432	0.699	0.650	0.735	0.520	0.511	0.513
Fe	0.009	0.053	0.008	0.007	0.007	0.006	0.007	0.005	0.007	0.005	0.004	0.007
Mn	0.001	0.003	0.000	0.001	0.001	0.000	0.000	-0.001	0.000	0.000	0.000	0.000
K	0.020	0.017	0.020	0.020	0.035	0.020	0.010	0.011	0.008	0.017	0.022	0.015

Sr	0.009	0.010	0.009	0.010	0.011	0.008	0.007	0.007	0.007	0.011	0.012	0.011
Ba	0.011	0.011	0.009	0.008	0.011	0.009	0.004	0.005	0.003	0.000	0.000	0.000
Ca	0.431	0.412	0.455	0.539	0.505	0.537	0.292	0.333	0.255	0.449	0.455	0.461
Ti	0.004	0.003	0.004	0.003	0.002	0.004	0.001	0.002	0.003	0.003	0.005	0.004
O	8.000	8.000	8.000	8.000	8.000	8.000	8.000	8.000	8.000	8.000	8.000	8.000
An	**43.757**	**42.750**	**45.713**	**54.772**	**51.177**	**54.253**	**29.201**	**33.492**	**25.525**	**45.576**	**46.045**	**46.621**
Ab	**54.211**	**55.462**	**52.300**	**43.205**	**45.303**	**43.720**	**69.829**	**65.373**	**73.646**	**52.742**	**51.767**	**51.881**
Or	**2.032**	**1.788**	**1.987**	**2.023**	**3.520**	**2.027**	**0.970**	**1.135**	**0.829**	**1.682**	**2.188**	**1.498**

Sample	SL-13-34-28.1	SL-13-34-28.1	SL-13-34-30	SL-13-34-30	SL-13-34-30	SL-13-34-30	SL-13-34-30	SL-13-34-30	SL-13-34-32	SL-13-34-32	SL-13-34-32	SL-13-34-32
Spot No.	6	7	1	2	3	4	5	6	1	2	3	4
SiO_2	56.409	56.725	54.367	53.844	53.882	54.345	54.215	54.218	54.747	55.361	54.878	57.706
Al_2O_3	26.47	26.508	28.166	28.398	28.559	28.364	28.51	28.304	27.589	27.732	27.877	26.217
MgO	0.007	-0.002	0.016	0.026	0.012	0.016	0.011	0.009	0.011	0.011	0.023	0.017
Na_2O	6.222	6.292	5.275	5.155	5.095	5.28	5.238	5.279	5.548	5.727	5.43	6.595
FeO	0.252	0.169	0.204	0.194	0.189	0.18	0.184	0.167	0.218	0.194	0.213	0.203
MnO	0.006	-0.005	0.006	0.006	0.015	-0.003	0.006	0.008	0.014	0.005	-0.004	-0.015
K_2O	0.291	0.21	0.375	0.345	0.388	0.303	0.295	0.274	0.322	0.357	0.354	0.603
SrO	0.288	0.255	0.322	0.41	0.404	0.368	0.367	0.406	0.303	0.336	0.303	0.31
BaO	0.333	0.452	0.563	0.537	0.513	0.499	0.466	0.509	0.392	0.362	0.33	0.203
CaO	8.646	8.63	10.146	10.393	10.478	10.319	10.428	10.232	9.718	9.698	9.769	7.923
TiO_2	0.069	0.101	0.107	0.096	0.089	0.119	0.088	0.079	0.085	0.074	0.066	0.056
Total	99.003	99.329	99.582	99.366	99.748	99.892	99.798	99.415	98.981	99.782	99.302	99.822
Si	2.569	2.574	2.479	2.462	2.459	2.472	2.466	2.474	2.505	2.510	2.501	2.601
Al	1.419	1.415	1.511	1.528	1.533	1.518	1.526	1.519	1.485	1.479	1.495	1.390
Mg	0.000	0.000	0.001	0.002	0.001	0.001	0.001	0.001	0.001	0.001	0.002	0.001
Na	0.549	0.553	0.466	0.456	0.450	0.465	0.461	0.466	0.491	0.503	0.479	0.575
Fe	0.010	0.006	0.008	0.007	0.007	0.007	0.007	0.006	0.008	0.007	0.008	0.008
Mn	0.000	0.000	0.000	0.000	0.001	0.000	0.000	0.000	0.001	0.000	0.000	-0.001
K	0.017	0.012	0.022	0.020	0.023	0.018	0.017	0.016	0.019	0.021	0.021	0.035
Sr	0.008	0.007	0.009	0.011	0.011	0.010	0.010	0.011	0.008	0.009	0.008	0.008
Ba	0.006	0.008	0.010	0.010	0.009	0.009	0.008	0.009	0.007	0.006	0.006	0.004
Ca	0.422	0.420	0.496	0.509	0.512	0.503	0.508	0.500	0.476	0.471	0.477	0.383
Ti	0.002	0.003	0.004	0.003	0.003	0.004	0.003	0.003	0.003	0.003	0.002	0.002
O	8.000	8.000	8.000	8.000	8.000	8.000	8.000	8.000	8.000	8.000	8.000	8.000
An	**42.733**	**42.625**	**50.423**	**51.665**	**52.015**	**51.038**	**51.517**	**50.919**	**48.291**	**47.379**	**48.845**	**38.545**
Ab	**55.553**	**56.139**	**47.357**	**46.292**	**45.690**	**47.176**	**46.746**	**47.457**	**49.803**	**50.543**	**49.046**	**57.959**
Or	**1.714**	**1.236**	**2.221**	**2.043**	**2.295**	**1.786**	**1.736**	**1.625**	**1.906**	**2.078**	**2.109**	**3.495**

Sample	SL-13-34-32	SL-13-34-32	SL-13-34-32	SL-13-34-32	SL-13-34-32	SL-13-34-45	SL-13-34-45	SL-13-34-45	SL-13-34-45	SL-13-34-45	SL-13-34-45	SL-13-34-45
Spot No.	5	6	7	8	9	1	2	3	4	5	6	7
SiO_2	55.595	60.29	53.813	55.223	53.557	57.434	57.335	57.069	53.604	53.457	55.471	55.4
Al_2O_3	27.191	24.028	28.173	26.96	28.717	26.503	26.961	26.444	29.461	29.155	27.409	27.765
MgO	0.004	0.022	0.022	0.014	0.027	0.004	-0.004	-0.006	0.005	0.014	0.009	0.015
Na_2O	5.702	7.655	5.15	5.816	4.962	6.56	6.356	6.482	4.537	4.593	5.602	5.471
FeO	0.227	0.305	0.217	0.21	0.266	0.16	0.133	0.163	0.16	0.17	0.151	0.185
MnO	0.006	0.013	0.006	0.014	0.006	0.019	-0.004	0.001	0.005	0.011	-0.008	0.014
K_2O	0.559	0.955	0.333	0.422	0.332	0.367	0.377	0.375	0.316	0.343	0.455	0.433
SrO	0.338	0.37	0.34	0.34	0.3	0.253	0.19	0.212	0.335	0.326	0.332	0.385
BaO	0.387	0.181	0.375	0.397	0.306	0.234	0.35	0.214	0.341	0.309	0.678	0.633
CaO	9.168	5.532	10.604	9.141	10.807	8.298	8.604	8.357	11.456	11.385	9.329	9.554
TiO_2	0.07	0.053	0.096	0.074	0.058	0.1	0.079	0.093	0.1	0.086	0.098	0.089
Total	99.287	99.388	99.147	98.637	99.469	99.984	100.394	99.429	100.338	99.873	99.526	100.008
Si	2.534	2.716	2.466	2.533	2.448	2.586	2.572	2.583	2.427	2.432	2.525	2.513
Al	1.458	1.273	1.519	1.455	1.544	1.404	1.423	1.408	1.569	1.561	1.468	1.481
Mg	0.000	0.001	0.002	0.001	0.002	0.000	0.000	0.000	0.000	0.001	0.001	0.001
Na	0.503	0.667	0.457	0.516	0.439	0.572	0.552	0.568	0.398	0.404	0.494	0.480
Fe	0.009	0.011	0.008	0.008	0.010	0.006	0.005	0.006	0.006	0.006	0.006	0.007
Mn	0.000	0.000	0.000	0.001	0.000	0.001	0.000	0.000	0.000	0.000	0.000	0.001
K	0.033	0.055	0.019	0.025	0.019	0.021	0.022	0.022	0.018	0.020	0.026	0.025
Sr	0.009	0.010	0.009	0.009	0.008	0.007	0.005	0.006	0.009	0.009	0.009	0.010
Ba	0.007	0.003	0.007	0.007	0.005	0.004	0.006	0.004	0.006	0.006	0.012	0.011
Ca	0.448	0.267	0.521	0.449	0.529	0.400	0.414	0.405	0.556	0.555	0.455	0.464
Ti	0.002	0.002	0.003	0.003	0.002	0.003	0.003	0.003	0.003	0.003	0.003	0.003
O	8.000	8.000	8.000	8.000	8.000	8.000	8.000	8.000	8.000	8.000	8.000	8.000
An	**45.534**	**26.988**	**52.226**	**45.364**	**53.590**	**40.310**	**41.899**	**40.740**	**57.199**	**56.668**	**46.666**	**47.882**
Ab	**51.158**	**67.461**	**45.820**	**52.140**	**44.449**	**57.566**	**55.913**	**57.082**	**40.921**	**41.298**	**50.622**	**49.532**
Or	**3.308**	**5.551**	**1.954**	**2.495**	**1.962**	**2.124**	**2.187**	**2.178**	**1.880**	**2.034**	**2.712**	**2.586**

Sample	SL-13-34-45	SL-13-34-45	SL-13-34-45	SL-13-34-45	SL-13-34-45	SL-13-34-49	SL-13-34-49	SL-13-34-49	SL-13-34-49	SL-13-34-49	SL-13-34-49	SL-13-34-49
Spot No.	8	9	10	11	12	1	2	3	4	5	6	7
SiO_2	54.485	54.325	54.242	53.779	54.856	56.334	56.977	57.277	55.296	55.266	53.414	54.795
Al_2O_3	28.548	28.662	28.843	29.106	28.358	26.109	25.703	25.057	26.501	26.18	27.822	26.953
MgO	0.003	0.012	0.013	0.007	0.009	0.01	0.019	0.006	0.009	0.003	0.006	0.009

Na_2O	5.196	5.067	5.037	4.793	5.237	6.275	6.504	6.665	5.841	5.866	4.945	5.383
FeO	0.155	0.129	0.141	0.127	0.144	0.199	0.188	0.189	0.142	0.162	0.21	0.221
MnO	0.016	-0.018	0.003	0.004	0.003	-0.001	0.013	0.003	0.014	-0.01	0.011	-0.003
K_2O	0.354	0.368	0.336	0.304	0.321	0.399	0.422	0.376	0.333	0.4	0.298	0.442
SrO	0.381	0.341	0.401	0.307	0.329	0.285	0.318	0.32	0.38	0.329	0.341	0.338
BaO	0.351	0.385	0.27	0.345	0.443	0.393	0.299	0.25	0.365	0.531	0.357	0.375
CaO	10.546	10.636	10.744	11.188	10.38	8.615	8.114	7.717	9.243	9.054	10.872	9.918
TiO_2	0.064	0.107	0.117	0.106	0.093	0.085	0.062	0.056	0.084	0.092	0.089	0.079
Total	100.089	100.134	100.201	100	100.249	98.709	98.639	97.923	98.212	97.858	98.363	98.524
Si	2.470	2.464	2.457	2.440	2.482	2.576	2.602	2.629	2.546	2.555	2.467	2.520
Al	1.522	1.529	1.537	1.554	1.510	1.405	1.381	1.353	1.435	1.424	1.512	1.459
Mg	0.000	0.001	0.001	0.000	0.001	0.001	0.001	0.000	0.001	0.000	0.000	0.001
Na	0.456	0.445	0.442	0.421	0.459	0.555	0.575	0.592	0.520	0.525	0.442	0.479
Fe	0.006	0.005	0.005	0.005	0.005	0.008	0.007	0.007	0.005	0.006	0.008	0.008
Mn	0.001	-0.001	0.000	0.000	0.000	0.000	0.001	0.000	0.001	0.000	0.000	0.000
K	0.020	0.021	0.019	0.018	0.019	0.023	0.025	0.022	0.020	0.024	0.018	0.026
Sr	0.010	0.009	0.011	0.008	0.009	0.008	0.008	0.009	0.010	0.009	0.009	0.009
Ba	0.006	0.007	0.005	0.006	0.008	0.007	0.005	0.004	0.007	0.010	0.006	0.007
Ca	0.512	0.517	0.521	0.544	0.503	0.422	0.397	0.380	0.456	0.449	0.538	0.489
Ti	0.002	0.004	0.004	0.004	0.003	0.003	0.002	0.002	0.003	0.003	0.003	0.003
O	8.000	8.000	8.000	8.000	8.000	8.000	8.000	8.000	8.000	8.000	8.000	8.000
An	**51.813**	**52.581**	**53.074**	**55.363**	**51.328**	**42.177**	**39.841**	**38.194**	**45.777**	**44.984**	**53.929**	**49.175**
Ab	**46.115**	**45.251**	**44.948**	**42.845**	**46.781**	**55.496**	**57.690**	**59.589**	**52.258**	**52.648**	**44.310**	**48.214**
Or	**2.072**	**2.168**	**1.978**	**1.792**	**1.891**	**2.327**	**2.469**	**2.217**	**1.965**	**2.368**	**1.761**	**2.611**

Sample	SL-13-34-49	SL-13-34-49	SL-13-34-53	SL-13-34-53	SL-13-34-53	SL-13-34-53	SL-13-34-53	SL-13-34-53	SL-13-34-58.9	SL-13-34-58.9	SL-13-34-58.9	SL-13-34-58.9
Spot No.	8	9	1	2	3	4	5	6	1	2	3	4
SiO_2	55.901	55.581	53.405	55.771	55.529	53.652	53.766	53.195	53.781	54.778	55.611	53.278
Al_2O_3	26.258	26.294	29.042	27.574	27.727	29.152	28.784	29.229	28.614	27.557	27.038	28.812
MgO	0.007	0.011	-0.002	0.012	0.02	0.007	0.019	0.008	0.017	0.023	0.009	0.001
Na_2O	5.864	5.903	4.764	5.774	5.674	4.767	4.945	4.703	4.917	5.404	5.793	4.739
FeO	0.193	0.228	0.142	0.18	0.175	0.165	0.148	0.186	0.234	0.253	0.247	0.235
MnO	0.005	-0.01	0	0.014	-0.001	0.004	0	-0.003	0.014	0.012	0.012	0.021
K_2O	0.522	0.438	0.192	0.286	0.279	0.232	0.243	0.209	0.416	0.462	0.529	0.447
SrO	0.346	0.333	0.291	0.305	0.37	0.34	0.278	0.333	0.294	0.262	0.297	0.375
BaO	0.523	0.301	0.405	0.607	0.494	0.39	0.415	0.291	0.243	0.212	0.261	0.293
CaO	8.612	9.007	11.249	9.212	9.565	11.299	10.969	11.503	10.893	9.834	9.244	11.111
TiO_2	0.089	0.065	0.097	0.059	0.084	0.071	0.124	0.09	0.038	0.099	0.079	0.064

Total	98.318	98.158	99.62	99.825	100.045	99.999	99.577	99.84	99.44	98.888	99.22	99.386
Si	2.569	2.558	2.435	2.528	2.515	2.436	2.448	2.424	2.454	2.506	2.536	2.438
Al	1.420	1.424	1.558	1.470	1.478	1.557	1.542	1.567	1.536	1.483	1.451	1.551
Mg	0.000	0.001	0.000	0.001	0.001	0.000	0.001	0.001	0.001	0.002	0.001	0.000
Na	0.522	0.526	0.420	0.506	0.497	0.419	0.436	0.415	0.434	0.478	0.511	0.420
Fe	0.007	0.009	0.005	0.007	0.007	0.006	0.006	0.007	0.009	0.010	0.009	0.009
Mn	0.000	0.000	0.000	0.001	0.000	0.000	0.000	0.000	0.001	0.000	0.000	0.001
K	0.031	0.026	0.011	0.017	0.016	0.013	0.014	0.012	0.024	0.027	0.031	0.026
Sr	0.009	0.009	0.008	0.008	0.010	0.009	0.007	0.009	0.008	0.007	0.008	0.010
Ba	0.009	0.005	0.007	0.011	0.009	0.007	0.007	0.005	0.004	0.004	0.005	0.005
Ca	0.424	0.444	0.550	0.447	0.464	0.550	0.535	0.562	0.533	0.482	0.452	0.545
Ti	0.003	0.002	0.003	0.002	0.003	0.002	0.004	0.003	0.001	0.003	0.003	0.002
O	8.000	8.000	8.000	8.000	8.000	8.000	8.000	8.000	8.000	8.000	8.000	8.000
An	**43.436**	**44.606**	**56.011**	**46.099**	**47.476**	**55.972**	**54.325**	**56.811**	**53.737**	**48.812**	**45.449**	**54.993**
Ab	**53.427**	**52.810**	**42.850**	**52.196**	**50.875**	**42.658**	**44.241**	**41.959**	**43.818**	**48.455**	**51.452**	**42.371**
Or	**3.137**	**2.585**	**1.139**	**1.705**	**1.650**	**1.369**	**1.434**	**1.230**	**2.445**	**2.732**	**3.099**	**2.636**

Sample	SL-13-34-58.9	SL-13-34-58.9	SL-13-36-16.6	SL-13-36-16.6	SL-13-36-16.6	SL-13-36-16.6	SL-13-36-16.6	SL-13-36-16.6	SL-13-36-16.6	SL-13-36-20.7	SL-13-36-20.7	SL-13-36-20.7
Spot No.	5	6	1	2	3	4	5	6	7	1	2	3
SiO_2	53.573	53.238	55.974	53.533	56.319	53.493	55.875	54.542	52.482	53.801	53.737	56.151
Al_2O_3	29.154	28.832	27.673	29.396	27.314	29.129	27.453	28.043	28.085	28.834	28.792	27.217
MgO	0.01	0.011	0.012	0.016	0.023	0.014	0.06	0.14	0.506	0.006	0.016	0.005
Na_2O	4.736	4.675	5.597	4.609	5.786	4.615	5.718	5.246	4.628	4.814	4.848	5.824
FeO	0.226	0.237	0.196	0.209	0.226	0.227	0.223	0.631	1.927	0.163	0.176	0.18
MnO	0.018	-0.003	-0.003	0.005	0.003	0.006	0.016	0.031	0.087	0.007	0.01	0.003
K_2O	0.347	0.506	0.64	0.439	0.722	0.372	0.591	0.448	0.352	0.337	0.302	0.407
SrO	0.216	0.286	0.336	0.351	0.316	0.341	0.349	0.326	0.305	0.273	0.258	0.281
BaO	0.177	0.342	0.277	0.329	0.401	0.32	0.484	0.396	0.382	0.28	0.335	0.478
CaO	11.306	11.222	9.553	11.489	9.129	11.292	9.38	10.149	10.341	11.164	11.103	9.077
TiO_2	0.093	0.099	0.092	0.086	0.046	0.094	0.067	0.044	0.084	0.097	0.09	0.085
Total	99.932	99.432	100.396	100.551	100.274	99.897	100.256	100.011	99.231	99.822	99.83	99.704
Si	2.434	2.435	2.523	2.424	2.541	2.433	2.526	2.479	2.424	2.447	2.447	2.544
Al	1.558	1.552	1.468	1.566	1.450	1.559	1.460	1.500	1.526	1.543	1.543	1.451
Mg	0.001	0.001	0.001	0.001	0.002	0.001	0.004	0.010	0.035	0.000	0.001	0.000
Na	0.417	0.414	0.488	0.404	0.505	0.406	0.500	0.462	0.414	0.424	0.427	0.511
Fe	0.009	0.009	0.007	0.008	0.008	0.009	0.008	0.024	0.074	0.006	0.007	0.007
Mn	0.001	0.000	0.000	0.000	0.000	0.000	0.001	0.001	0.003	0.000	0.000	0.000
K	0.020	0.030	0.037	0.025	0.042	0.022	0.034	0.026	0.021	0.020	0.018	0.024

Sr	0.006	0.008	0.009	0.009	0.008	0.009	0.009	0.009	0.008	0.007	0.007	0.007
Ba	0.003	0.006	0.005	0.006	0.007	0.006	0.009	0.007	0.007	0.005	0.006	0.008
Ca	0.550	0.550	0.461	0.557	0.441	0.550	0.454	0.494	0.512	0.544	0.542	0.441
Ti	0.003	0.003	0.003	0.003	0.002	0.003	0.002	0.002	0.003	0.003	0.003	0.003
O	8.000	8.000	8.000	8.000	8.000	8.000	8.000	8.000	8.000	8.000	8.000	8.000
An	**55.764**	**55.362**	**46.768**	**56.490**	**44.659**	**56.257**	**45.950**	**50.344**	**54.083**	**55.099**	**54.910**	**45.198**
Ab	**42.197**	**41.663**	**49.499**	**40.938**	**51.132**	**41.534**	**50.600**	**47.008**	**43.724**	**42.919**	**43.311**	**52.387**
Or	**2.039**	**2.974**	**3.733**	**2.572**	**4.208**	**2.208**	**3.450**	**2.648**	**2.193**	**1.982**	**1.780**	**2.415**

Sample	SL-13-36-20.7	SL-13-36-20.7	SL-13-36-20.7	SL-13-36-20.7	SL-13-36-20.7	SL-13-37-7	SL-13-37-7	SL-13-37-7	SL-13-37-7	SL-13-37-7	SL-13-37-7	SL-13-37-7
Spot No.	4	5	6	7	8	1	2	3	4	5	6	7
SiO_2	58.478	54.408	53.677	54.041	54.887	55.066	54.762	55.255	55.927	56.366	55.871	54.765
Al_2O_3	25.771	28.382	28.854	27.213	28.071	27.97	27.886	27.426	27.217	26.843	27.086	28.137
MgO	0.009	0.012	0.004	0.561	0.01	0.008	0.005	0.012	0.017	0.003	0.012	0.019
Na_2O	6.738	5.224	4.788	5.332	5.313	5.395	5.384	5.55	5.874	6.013	5.954	5.282
FeO	0.221	0.174	0.182	1.541	0.189	0.15	0.169	0.151	0.139	0.161	0.151	0.139
MnO	0.006	-0.023	0.001	0.055	-0.008	0.002	-0.011	-0.005	0.014	0.001	0.003	0.01
K_2O	0.492	0.308	0.261	0.291	0.32	0.337	0.362	0.443	0.455	0.479	0.47	0.364
SrO	0.269	0.308	0.338	0.263	0.371	0.321	0.358	0.308	0.363	0.277	0.351	0.342
BaO	0.278	0.403	0.331	0.331	0.436	0.277	0.537	0.688	0.691	0.716	0.793	0.511
CaO	7.404	10.501	11.221	9.331	10.203	10.018	9.848	9.305	8.968	8.624	8.832	10.094
TiO_2	0.058	0.065	0.096	0.078	0.095	0.07	0.086	0.091	0.118	0.108	0.085	0.092
Total	99.7	99.786	99.858	99.045	99.96	99.596	99.426	99.268	99.859	99.614	99.518	99.791
Si	2.632	2.473	2.444	2.484	2.491	2.500	2.498	2.522	2.538	2.559	2.542	2.489
Al	1.365	1.518	1.545	1.472	1.499	1.494	1.496	1.473	1.453	1.434	1.450	1.504
Mg	0.001	0.001	0.000	0.039	0.001	0.001	0.000	0.001	0.001	0.000	0.001	0.001
Na	0.587	0.460	0.422	0.474	0.467	0.474	0.475	0.490	0.516	0.528	0.524	0.465
Fe	0.008	0.007	0.007	0.059	0.007	0.006	0.006	0.006	0.005	0.006	0.006	0.005
Mn	0.000	-0.001	0.000	0.002	0.000	0.000	0.000	0.000	0.001	0.000	0.000	0.000
K	0.028	0.018	0.015	0.017	0.019	0.020	0.021	0.026	0.026	0.028	0.027	0.021
Sr	0.007	0.008	0.009	0.007	0.010	0.008	0.009	0.008	0.010	0.007	0.009	0.009
Ba	0.005	0.007	0.006	0.006	0.008	0.005	0.010	0.012	0.012	0.013	0.014	0.009
Ca	0.357	0.511	0.547	0.460	0.496	0.487	0.481	0.455	0.436	0.420	0.430	0.492
Ti	0.002	0.002	0.003	0.003	0.003	0.002	0.003	0.003	0.004	0.004	0.003	0.003
O	8.000	8.000	8.000	8.000	8.000	8.000	8.000	8.000	8.000	8.000	8.000	8.000
An	**36.722**	**51.717**	**55.601**	**48.323**	**50.555**	**49.679**	**49.227**	**46.856**	**44.570**	**42.998**	**43.836**	**50.296**
Ab	**60.370**	**46.476**	**42.858**	**49.882**	**47.556**	**48.329**	**48.617**	**50.486**	**52.736**	**54.157**	**53.384**	**47.543**
Or	**2.908**	**1.807**	**1.541**	**1.796**	**1.889**	**1.991**	**2.156**	**2.658**	**2.694**	**2.846**	**2.779**	**2.161**

Sample	SL-13-37-7	SL-13-37-7	SL-13-37-19	SL-13-37-19	SL-13-37-19	SL-13-37-19	SL-13-37-19	SL-13-37-19	SL-13-37-19	SL-13-37-19	SL-13-37-19	SL-13-37-19
Spot No.	8	9	1	2	3	4	5	6	7	8	9	10
SiO_2	54.47	54.657	55.125	55.232	55.309	54.839	54.017	53.999	55.741	54.014	53.8	53.967
Al_2O_3	28.283	27.985	27.927	27.77	27.933	28.256	28.734	28.708	27.577	28.983	28.808	28.833
MgO	0.014	0.002	0.003	0.007	0.01	0.006	0.002	-0.001	0.01	0.009	0.013	0.014
Na_2O	5.195	5.351	5.551	5.693	5.667	5.33	5.035	5.095	5.736	5.088	4.951	5.006
FeO	0.178	0.166	0.169	0.165	0.145	0.14	0.137	0.168	0.149	0.179	0.172	0.164
MnO	-0.014	0.006	-0.005	0.018	0.005	-0.013	0.012	0.006	0.008	-0.01	0.003	-0.012
K_2O	0.353	0.39	0.281	0.261	0.286	0.315	0.298	0.301	0.358	0.296	0.28	0.29
SrO	0.362	0.383	0.327	0.379	0.315	0.341	0.332	0.382	0.329	0.317	0.402	0.354
BaO	0.541	0.566	0.462	0.504	0.538	0.492	0.536	0.488	0.645	0.292	0.251	0.303
CaO	10.286	10.074	9.801	9.667	9.583	10.072	10.694	10.57	9.267	10.985	10.905	10.983
TiO_2	0.109	0.1	0.069	0.096	0.086	0.091	0.075	0.108	0.109	0.084	0.091	0.077
Total	99.795	99.734	99.773	99.756	99.885	99.864	99.891	99.904	99.959	100.123	99.761	100.096
Si	2.478	2.489	2.503	2.507	2.507	2.488	2.457	2.457	2.525	2.446	2.449	2.450
Al	1.514	1.499	1.492	1.483	1.489	1.508	1.537	1.537	1.470	1.544	1.543	1.540
Mg	0.001	0.000	0.000	0.000	0.001	0.000	0.000	0.000	0.001	0.001	0.001	0.001
Na	0.457	0.472	0.488	0.500	0.497	0.468	0.443	0.449	0.503	0.446	0.436	0.440
Fe	0.007	0.006	0.006	0.006	0.005	0.005	0.005	0.006	0.006	0.007	0.007	0.006
Mn	-0.001	0.000	0.000	0.001	0.000	0.000	0.000	0.000	0.000	0.000	0.000	0.000
K	0.020	0.023	0.016	0.015	0.017	0.018	0.017	0.017	0.021	0.017	0.016	0.017
Sr	0.010	0.010	0.009	0.010	0.008	0.009	0.009	0.010	0.009	0.008	0.011	0.009
Ba	0.010	0.010	0.008	0.009	0.010	0.009	0.010	0.009	0.011	0.005	0.004	0.005
Ca	0.501	0.492	0.477	0.470	0.465	0.490	0.521	0.515	0.450	0.533	0.532	0.534
Ti	0.004	0.003	0.002	0.003	0.003	0.003	0.003	0.004	0.004	0.003	0.003	0.003
O	8.000	8.000	8.000	8.000	8.000	8.000	8.000	8.000	8.000	8.000	8.000	8.000
An	**51.197**	**49.859**	**48.608**	**47.710**	**47.533**	**50.170**	**53.086**	**52.502**	**46.207**	**53.510**	**54.032**	**53.913**
Ab	**46.710**	**47.841**	**49.732**	**50.755**	**50.777**	**47.960**	**45.151**	**45.716**	**51.666**	**44.772**	**44.315**	**44.391**
Or	**2.093**	**2.300**	**1.660**	**1.535**	**1.690**	**1.870**	**1.763**	**1.781**	**2.127**	**1.718**	**1.653**	**1.696**

Sample	SL-13-37-19	SL-13-37-25	SL-13-37-25	SL-13-37-25	SL-13-37-25	SL-13-37-25	SL-13-37-25	SL-13-37-25	SL-13-37-25	SL-13-37-27	SL-13-37-27	SL-13-37-27
Spot No.	11	1	2	3	4	5	6	7	8	1	2	3
SiO_2	54.098	54.536	54.307	54.931	54.666	53.336	52.999	53.31	53.861	54.841	54.52	54.886
Al_2O_3	28.729	27.872	28.01	27.489	27.644	28.794	28.9	28.681	28.219	28.112	28.116	28.027
MgO	0.01	0.017	0.017	0.02	0.007	0.015	0.011	0.008	0.019	0.001	0.004	0.006

Na_2O	5.021	5.363	5.293	5.64	5.44	4.895	4.644	4.952	5.168	5.347	5.38	5.471
FeO	0.177	0.172	0.198	0.166	0.204	0.156	0.188	0.165	0.171	0.159	0.145	0.134
MnO	0.012	-0.005	0.007	0.005	0.009	0.004	0.01	0.006	0.01	-0.004	-0.006	-0.004
K_2O	0.29	0.506	0.5	0.54	0.518	0.274	0.272	0.29	0.299	0.349	0.326	0.321
SrO	0.316	0.366	0.352	0.352	0.348	0.338	0.33	0.326	0.364	0.34	0.292	0.344
BaO	0.352	0.522	0.495	0.534	0.515	0.322	0.306	0.325	0.378	0.502	0.416	0.294
CaO	10.886	9.961	10.055	9.528	9.75	10.92	11.307	10.807	10.479	10.028	10.21	10.095
TiO_2	0.05	0.077	0.075	0.089	0.09	0.077	0.1	0.074	0.132	0.082	0.072	0.074
Total	99.973	99.385	99.237	99.386	99.146	99.158	99.013	98.874	99.015	99.758	99.513	99.638
Si	2.457	2.491	2.483	2.510	2.501	2.443	2.431	2.446	2.467	2.492	2.484	2.494
Al	1.535	1.498	1.507	1.478	1.488	1.551	1.559	1.548	1.520	1.503	1.507	1.498
Mg	0.001	0.001	0.001	0.001	0.000	0.001	0.001	0.001	0.001	0.000	0.000	0.000
Na	0.441	0.474	0.468	0.499	0.482	0.434	0.412	0.440	0.458	0.470	0.474	0.481
Fe	0.007	0.007	0.008	0.006	0.008	0.006	0.007	0.006	0.007	0.006	0.006	0.005
Mn	0.000	0.000	0.000	0.000	0.000	0.000	0.000	0.000	0.000	0.000	0.000	0.000
K	0.017	0.030	0.029	0.031	0.030	0.016	0.016	0.017	0.017	0.020	0.019	0.019
Sr	0.008	0.010	0.009	0.009	0.009	0.009	0.009	0.009	0.010	0.009	0.008	0.009
Ba	0.006	0.009	0.009	0.010	0.009	0.006	0.005	0.006	0.007	0.009	0.007	0.005
Ca	0.530	0.487	0.493	0.466	0.478	0.536	0.556	0.531	0.514	0.488	0.498	0.491
Ti	0.002	0.003	0.003	0.003	0.003	0.003	0.003	0.003	0.005	0.003	0.002	0.003
O	8.000	8.000	8.000	8.000	8.000	8.000	8.000	8.000	8.000	8.000	8.000	8.000
An	**53.621**	**49.186**	**49.747**	**46.798**	**48.281**	**54.358**	**56.478**	**53.771**	**51.951**	**49.883**	**50.253**	**49.581**
Ab	**44.677**	**47.838**	**47.306**	**50.042**	**48.663**	**44.017**	**41.903**	**44.509**	**46.283**	**48.048**	**47.835**	**48.540**
Or	**1.702**	**2.977**	**2.947**	**3.160**	**3.056**	**1.625**	**1.619**	**1.719**	**1.766**	**2.069**	**1.912**	**1.878**

Sample	SL-13-37-27	SL-13-37-27	SL-13-37-27	SL-13-37-27	SL-13-37-27	SL-13-37-37	SL-13-37-37	SL-13-37-37	SL-13-37-37	SL-13-37-37	SL-13-37-37	SL-13-37-37
Spot No.	4	5	6	7	8	1	2	3	4	5	6	7
SiO_2	54.792	53.831	53.566	53.622	53.874	53.063	53.152	53.178	54.113	52.848	53.263	53.202
Al_2O_3	28.169	28.585	28.753	28.553	28.48	29.173	29.09	29.089	28.341	29.005	28.66	28.93
MgO	0.005	0.002	0.005	0.02	0.015	0.018	0.025	0.011	0.008	0.008	0.019	0.024
Na_2O	5.334	5.001	4.932	4.99	5.029	4.641	4.719	4.656	5.142	4.55	4.896	4.809
FeO	0.182	0.165	0.155	0.159	0.17	0.228	0.201	0.229	0.228	0.236	0.231	0.229
MnO	-0.012	0.005	0.016	-0.003	0.005	0.01	-0.024	-0.005	0.001	0.002	-0.013	0.001
K_2O	0.353	0.38	0.357	0.374	0.383	0.355	0.373	0.332	0.448	0.414	0.46	0.335
SrO	0.301	0.373	0.329	0.361	0.363	0.365	0.275	0.298	0.384	0.317	0.329	0.308
BaO	0.452	0.396	0.376	0.366	0.37	0.262	0.245	0.283	0.456	0.311	0.312	0.317
CaO	10.214	10.616	10.905	10.697	10.759	11.457	11.259	11.346	10.375	11.491	11.062	11.212
TiO_2	0.109	0.057	0.115	0.055	0.089	0.098	0.113	0.058	0.093	0.108	0.106	0.083

Total	99.802	99.469	99.529	99.224	99.523	99.724	99.427	99.477	99.563	99.325	99.412	99.461
Si	2.486	2.459	2.446	2.455	2.459	2.422	2.428	2.429	2.469	2.422	2.440	2.432
Al	1.504	1.536	1.544	1.538	1.529	1.566	1.563	1.563	1.521	1.564	1.544	1.556
Mg	0.000	0.000	0.000	0.001	0.001	0.001	0.002	0.001	0.001	0.001	0.001	0.002
Na	0.468	0.442	0.436	0.442	0.444	0.410	0.417	0.412	0.454	0.404	0.434	0.426
Fe	0.007	0.006	0.006	0.006	0.006	0.009	0.008	0.009	0.009	0.009	0.009	0.009
Mn	0.000	0.000	0.001	0.000	0.000	0.000	-0.001	0.000	0.000	0.000	-0.001	0.000
K	0.020	0.022	0.021	0.022	0.022	0.021	0.022	0.019	0.026	0.024	0.027	0.020
Sr	0.008	0.010	0.009	0.010	0.010	0.010	0.007	0.008	0.010	0.008	0.009	0.008
Ba	0.008	0.007	0.007	0.007	0.007	0.005	0.004	0.005	0.008	0.006	0.006	0.006
Ca	0.497	0.519	0.533	0.525	0.526	0.560	0.551	0.555	0.507	0.564	0.543	0.549
Ti	0.004	0.002	0.004	0.002	0.003	0.003	0.004	0.002	0.003	0.004	0.004	0.003
O	8.000	8.000	8.000	8.000	8.000	8.000	8.000	8.000	8.000	8.000	8.000	8.000
An	**50.389**	**52.808**	**53.879**	**53.069**	**53.000**	**56.539**	**55.660**	**56.301**	**51.368**	**56.876**	**54.081**	**55.236**
Ab	**47.536**	**44.939**	**44.019**	**44.720**	**44.752**	**41.373**	**42.143**	**41.736**	**45.990**	**40.683**	**43.239**	**42.798**
Or	**2.075**	**2.252**	**2.102**	**2.211**	**2.248**	**2.087**	**2.197**	**1.963**	**2.643**	**2.442**	**2.680**	**1.966**

Sample	SL-13-41-3	SL-13-41-3	SL-13-41-3	SL-13-41-3	SL-13-41-3	SL-13-41-3	SL-13-41-3	SL-13-41-7.5	SL-13-41-7.5	SL-13-41-7.5	SL-13-41-7.5	SL-13-41-7.5
Spot No.	1	2	3	4	5	6	7	1	2	3	4	5
SiO_2	55.887	56.912	57.501	58.36	58.967	57.867	58.538	61.632	61.967	61.46	61.88	61.707
Al_2O_3	27.082	26.647	26.083	25.673	25.137	25.561	25.549	22.785	22.798	23.235	22.945	23.221
MgO	0	0.002	0	0.011	0.006	0.078	0.007	0.007	0.004	0.004	0	0.014
Na_2O	6.008	6.344	6.535	7.052	7.132	6.742	6.968	8.499	8.663	8.341	8.448	8.43
FeO	0.162	0.135	0.176	0.187	0.213	0.376	0.17	0.129	0.164	0.149	0.196	0.192
MnO	0.013	0.009	0.003	0	0.006	0.008	-0.004	-0.004	-0.007	0.006	0.007	-0.004
K_2O	0.471	0.495	0.644	0.533	0.531	0.535	0.608	0.325	0.486	0.432	0.64	0.555
SrO	0.261	0.269	0.27	0.188	0.256	0.242	0.283	0.082	0.081	0.058	0.135	0.141
BaO	0.452	0.401	0.473	0.382	0.278	0.433	0.47	-0.005	0.01	0.053	0.008	0.025
CaO	8.804	8.233	7.702	7.196	6.787	7.172	7.25	4.916	4.579	4.98	4.735	4.969
TiO_2	0.114	0.076	0.062	0.107	0.035	0.085	0.092	0.023	0.015	0.021	0.034	0.023
Total	99.336	99.453	99.536	99.739	99.4	99.127	99.897	98.397	98.742	98.754	99.037	99.258
Si	2.544	2.577	2.605	2.630	2.661	2.626	2.635	2.780	2.785	2.765	2.778	2.765
Al	1.450	1.420	1.390	1.361	1.334	1.365	1.353	1.209	1.206	1.230	1.212	1.224
Mg	0.000	0.000	0.000	0.001	0.000	0.005	0.000	0.000	0.000	0.000	0.000	0.001
Na	0.529	0.556	0.573	0.615	0.623	0.592	0.607	0.742	0.754	0.726	0.734	0.731
Fe	0.006	0.005	0.007	0.007	0.008	0.014	0.006	0.005	0.006	0.006	0.007	0.007
Mn	0.001	0.000	0.000	0.000	0.000	0.000	0.000	0.000	0.000	0.000	0.000	0.000
K	0.027	0.029	0.037	0.031	0.031	0.031	0.035	0.019	0.028	0.025	0.037	0.032

Sr	0.007	0.007	0.007	0.005	0.007	0.006	0.007	0.002	0.002	0.002	0.004	0.004
Ba	0.008	0.007	0.008	0.007	0.005	0.008	0.008	0.000	0.000	0.001	0.000	0.000
Ca	0.429	0.399	0.374	0.348	0.328	0.349	0.350	0.238	0.221	0.240	0.228	0.239
Ti	0.004	0.003	0.002	0.004	0.001	0.003	0.003	0.001	0.001	0.001	0.001	0.001
O	8.000	8.000	8.000	8.000	8.000	8.000	8.000	8.000	8.000	8.000	8.000	8.000
An	**43.545**	**40.591**	**37.989**	**34.983**	**33.428**	**35.881**	**35.260**	**23.799**	**22.007**	**24.219**	**22.810**	**23.822**
Ab	**53.680**	**56.501**	**58.227**	**61.930**	**63.456**	**60.930**	**61.217**	**74.326**	**75.210**	**73.278**	**73.517**	**73.007**
Or	**2.776**	**2.908**	**3.785**	**3.087**	**3.116**	**3.189**	**3.523**	**1.875**	**2.783**	**2.503**	**3.673**	**3.170**

Sample	SL-13-41-7.5	SL-13-41-7.5	SL-13-41-7.5	SL-13-41-7.5	SL-13-41-12.1	SL-13-41-12.1	SL-13-41-12.1	SL-13-41-12.1	SL-13-41-12.1	SL-13-41-12.1	SL-13-41-12.1	SL-13-41-12.1
Spot No.	6	7	8	9	1	2	3	4	5	6	7	8
SiO_2	61.993	61.643	61.424	61.531	56.009	55.939	55.154	56.23	53.952	55.564	54.757	54.794
Al_2O_3	22.744	23.07	23.073	22.987	26.906	27.093	27.421	26.752	28.56	27.35	27.863	27.983
MgO	-0.001	-0.005	-0.001	0.004	0.024	0.025	0.032	0.034	0.032	0.035	0.034	0.018
Na_2O	8.389	8.29	8.292	8.253	5.896	5.912	5.619	6.124	5.014	5.685	5.281	5.369
FeO	0.212	0.151	0.201	0.181	0.332	0.313	0.314	0.314	0.295	0.278	0.279	0.247
MnO	-0.005	-0.002	-0.005	-0.009	0	-0.001	0.002	0.015	0.006	0.018	-0.004	-0.004
K_2O	0.709	0.705	0.63	0.656	0.381	0.365	0.386	0.312	0.309	0.351	0.334	0.342
SrO	0.144	0.14	0.152	0.142	0.384	0.395	0.343	0.412	0.403	0.437	0.397	0.434
BaO	0.044	0.008	0.016	0.016	0.46	0.256	0.257	0.272	0.435	0.314	0.348	0.414
CaO	4.722	4.856	4.987	4.887	9.028	9.284	9.625	8.793	10.662	9.386	10.168	10.019
TiO_2	0.03	0.059	0.018	0.012	0.095	0.134	0.102	0.085	0.054	0.1	0.074	0.102
Total	98.992	98.895	98.77	98.641	99.484	99.693	99.262	99.434	99.698	99.513	99.581	99.745
Si	2.785	2.771	2.767	2.773	2.546	2.537	2.515	2.556	2.459	2.526	2.494	2.492
Al	1.202	1.220	1.223	1.219	1.439	1.445	1.471	1.430	1.531	1.463	1.493	1.497
Mg	0.000	0.000	0.000	0.000	0.002	0.002	0.002	0.002	0.002	0.002	0.002	0.001
Na	0.729	0.721	0.723	0.720	0.519	0.519	0.496	0.539	0.442	0.500	0.466	0.473
Fe	0.008	0.006	0.008	0.007	0.013	0.012	0.012	0.012	0.011	0.011	0.011	0.009
Mn	0.000	0.000	0.000	0.000	0.000	0.000	0.000	0.001	0.000	0.001	0.000	0.000
K	0.041	0.040	0.036	0.038	0.022	0.021	0.022	0.018	0.018	0.020	0.019	0.020
Sr	0.004	0.004	0.004	0.004	0.010	0.010	0.009	0.011	0.011	0.012	0.010	0.011
Ba	0.001	0.000	0.000	0.000	0.008	0.005	0.005	0.005	0.008	0.006	0.006	0.007
Ca	0.227	0.234	0.241	0.236	0.440	0.451	0.470	0.428	0.521	0.457	0.496	0.488
Ti	0.001	0.002	0.001	0.000	0.003	0.005	0.003	0.003	0.002	0.003	0.003	0.003
O	8.000	8.000	8.000	8.000	8.000	8.000	8.000	8.000	8.000	8.000	8.000	8.000
An	**22.788**	**23.491**	**24.072**	**23.750**	**44.842**	**45.513**	**47.565**	**43.471**	**53.077**	**46.757**	**50.572**	**49.783**
Ab	**73.135**	**72.445**	**72.304**	**72.452**	**52.903**	**52.355**	**50.162**	**54.692**	**45.090**	**51.159**	**47.448**	**48.192**
Or	**4.077**	**4.064**	**3.623**	**3.798**	**2.255**	**2.132**	**2.273**	**1.838**	**1.833**	**2.083**	**1.979**	**2.025**

Sample	SL-13-41-12.1	SL-13-41-12.1	SL-13-41-12.1	SL-13-41-12.1	SL-13-41-12.1	SL-13-41-12.1	SL-13-41-12.1	SL-13-41-12.1	SL-13-41-12.1	SL-13-41-45	SL-13-41-45	SL-13-41-45
Spot No.	9	10	11	12	13	14	15	16	17	1	2	3
SiO_2	55.293	54.724	54.062	54.262	54.132	54.313	56.634	57.053	56.901	54.638	54.038	54.728
Al_2O_3	27.538	27.963	28.072	28.339	28.157	28.085	26.577	26.267	26.326	30.219	30.011	29.825
MgO	0.018	0.016	0.021	0.025	0.029	0.012	0.012	0.002	0.012	0.013	0.024	0.01
Na_2O	5.693	5.429	5.17	5.081	4.951	5.123	6.119	6.344	6.366	5.003	4.937	5.152
FeO	0.232	0.234	0.481	0.231	0.224	0.238	0.23	0.228	0.224	0.174	0.181	0.217
MnO	0.006	0.003	0.008	-0.002	0.005	-0.003	-0.01	-0.005	0.013	0.007	0.005	0.012
K_2O	0.241	0.245	0.231	0.493	0.536	0.484	0.491	0.479	0.366	0.317	0.343	0.357
SrO	0.421	0.415	0.309	0.388	0.334	0.352	0.349	0.299	0.305	0.394	0.376	0.353
BaO	0.295	0.386	0.207	0.222	0.288	0.247	0.3	0.26	0.236	0.215	0.333	0.264
CaO	9.725	10.141	10.483	10.595	10.455	10.387	8.521	8.194	8.353	11.468	11.351	11.172
TiO_2	0.09	0.093	0.072	0.053	0.113	0.057	0.048	0.057	0.048	0.071	0.083	0.077
Total	99.679	99.661	99.163	99.756	99.262	99.24	99.196	99.18	99.156	102.528	101.677	102.164
Si	2.514	2.490	2.473	2.470	2.475	2.480	2.572	2.590	2.584	2.421	2.417	2.434
Al	1.473	1.497	1.511	1.518	1.514	1.509	1.420	1.403	1.407	1.575	1.579	1.560
Mg	0.001	0.001	0.001	0.002	0.002	0.001	0.001	0.000	0.001	0.001	0.002	0.001
Na	0.501	0.478	0.458	0.448	0.438	0.453	0.538	0.557	0.560	0.429	0.427	0.443
Fe	0.009	0.009	0.018	0.009	0.009	0.009	0.009	0.009	0.008	0.006	0.007	0.008
Mn	0.000	0.000	0.000	0.000	0.000	0.000	0.000	0.000	0.000	0.000	0.000	0.000
K	0.014	0.014	0.013	0.029	0.031	0.028	0.028	0.028	0.021	0.018	0.020	0.020
Sr	0.011	0.011	0.008	0.010	0.009	0.009	0.009	0.008	0.008	0.010	0.010	0.009
Ba	0.005	0.007	0.004	0.004	0.005	0.004	0.005	0.005	0.004	0.004	0.006	0.005
Ca	0.474	0.494	0.514	0.517	0.512	0.508	0.415	0.399	0.406	0.545	0.544	0.532
Ti	0.003	0.003	0.002	0.002	0.004	0.002	0.002	0.002	0.002	0.002	0.003	0.003
O	8.000	8.000	8.000	8.000	8.000	8.000	8.000	8.000	8.000	8.000	8.000	8.000
An	**47.915**	**50.103**	**52.160**	**52.036**	**52.177**	**51.375**	**42.267**	**40.515**	**41.170**	**54.914**	**54.894**	**53.444**
Ab	**50.670**	**48.454**	**46.470**	**45.079**	**44.635**	**45.773**	**54.831**	**56.664**	**56.680**	**43.277**	**43.130**	**44.521**
Or	**1.415**	**1.442**	**1.369**	**2.885**	**3.187**	**2.852**	**2.902**	**2.822**	**2.149**	**1.809**	**1.976**	**2.035**

Sample	SL-13-41-45	SL-13-41-45	SL-13-41-45	SL-13-41-45	SL-13-41-45	SL-13-41-45	SL-13-41-63.2	SL-13-41-63.2	SL-13-41-63.2	SL-13-41-63.2	SL-13-41-63.2	SL-13-41-63.2
Spot No.	4	5	6	7	8	9	1	2	3	4	5	6
SiO_2	55.665	55.257	55.463	54.523	55.875	56.258	56.628	57.372	57.278	55.21	55.35	54.397
Al_2O_3	28.583	29.803	28.96	29.058	28.602	27.973	27.428	26.656	26.473	28.097	27.92	28.648
MgO	0.01	0.022	0.019	0.011	0.01	0.007	0.012	0.026	0.02	0.01	0.008	0.018

Na_2O	5.664	5.395	5.509	5.289	5.766	5.919	6.007	6.377	6.239	5.522	5.565	5.157
FeO	0.159	0.153	0.212	0.164	0.163	0.172	0.193	0.248	0.271	0.201	0.214	0.194
MnO	0.025	-0.004	-0.009	-0.01	-0.008	-0.004	0	0.006	-0.007	-0.006	0.008	0.015
K_2O	0.413	0.352	0.393	0.354	0.452	0.443	0.631	0.792	0.706	0.511	0.546	0.451
SrO	0.416	0.351	0.387	0.387	0.365	0.356	0.312	0.292	0.324	0.341	0.401	0.351
BaO	0.415	0.293	0.242	0.37	0.515	0.322	0.434	0.294	0.177	0.397	0.285	0.355
CaO	10.182	10.847	10.453	10.65	9.753	9.517	8.741	8.195	8.146	9.869	9.645	10.548
TiO_2	0.073	0.069	0.1	0.068	0.11	0.05	0.074	0.068	0.079	0.09	0.082	0.082
Total	101.594	102.535	101.723	100.872	101.609	101.011	100.453	100.342	99.716	100.238	100.026	100.234
Si	2.486	2.446	2.472	2.455	2.494	2.519	2.547	2.580	2.587	2.497	2.506	2.464
Al	1.502	1.552	1.519	1.539	1.502	1.474	1.451	1.410	1.407	1.495	1.487	1.527
Mg	0.001	0.001	0.001	0.001	0.001	0.000	0.001	0.002	0.001	0.001	0.001	0.001
Na	0.490	0.462	0.475	0.461	0.498	0.513	0.523	0.555	0.545	0.483	0.488	0.452
Fe	0.006	0.006	0.008	0.006	0.006	0.006	0.007	0.009	0.010	0.008	0.008	0.007
Mn	0.001	0.000	0.000	0.000	0.000	0.000	0.000	0.000	0.000	0.000	0.000	0.001
K	0.024	0.020	0.022	0.020	0.026	0.025	0.036	0.045	0.041	0.029	0.032	0.026
Sr	0.011	0.009	0.010	0.010	0.009	0.009	0.008	0.008	0.008	0.009	0.011	0.009
Ba	0.007	0.005	0.004	0.007	0.009	0.006	0.008	0.005	0.003	0.007	0.005	0.006
Ca	0.487	0.514	0.499	0.514	0.466	0.457	0.421	0.395	0.394	0.478	0.468	0.512
Ti	0.002	0.002	0.003	0.002	0.004	0.002	0.002	0.002	0.003	0.003	0.003	0.003
O	8.000	8.000	8.000	8.000	8.000	8.000	8.000	8.000	8.000	8.000	8.000	8.000
An	**48.704**	**51.622**	**50.079**	**51.634**	**47.099**	**45.893**	**42.966**	**39.669**	**40.212**	**48.252**	**47.399**	**51.703**
Ab	**48.942**	**46.382**	**47.678**	**46.321**	**50.300**	**51.561**	**53.339**	**55.763**	**55.636**	**48.771**	**49.404**	**45.663**
Or	**2.354**	**1.996**	**2.243**	**2.045**	**2.601**	**2.545**	**3.696**	**4.568**	**4.152**	**2.977**	**3.197**	**2.634**

Sample	SL-13-41-63.2	SL-13-41-63.2	SL-13-41-63.2	SL-13-41-68.9	SL-13-41-68.9	SL-13-41-68.9	SL-13-41-68.9	SL-13-41-68.9	SL-13-41-68.9	SL-13-41-68.9	SL-13-41-68.9	SL-13-41-68.9
Spot No.	7	8	9	1	2	3	4	5	6	7	8	9
SiO_2	55.463	54.808	55.298	56.443	55.4	56.103	55.646	55.147	55.905	54.928	56.09	55.173
Al_2O_3	27.954	28.433	28.088	27.432	27.997	27.504	28.712	28.18	27.64	28.548	28.89	29.099
MgO	0.012	0.013	0.012	0.016	0.015	0.013	0.014	0.021	0.016	0.04	0.018	0.016
Na_2O	5.653	5.437	5.546	6.232	5.533	5.891	5.484	5.385	5.738	5.323	5.715	5.321
FeO	0.197	0.198	0.19	0.207	0.245	0.255	0.239	0.261	0.253	0.286	0.256	0.216
MnO	0.021	0.002	-0.004	0.004	0.006	0.004	0.011	0.009	0.012	0.007	0.009	0.005
K_2O	0.496	0.436	0.462	1.13	0.687	0.649	0.58	0.581	0.676	0.46	0.577	0.486
SrO	0.395	0.346	0.317	0.331	0.317	0.333	0.309	0.345	0.356	0.358	0.345	0.335
BaO	0.363	0.387	0.371	0.19	0.42	0.217	0.2	0.183	0.307	0.295	0.348	0.334
CaO	9.626	10.189	9.987	7.964	9.462	9.095	10.101	10.058	9.212	10.314	9.438	10.285
TiO_2	0.081	0.044	0.079	0.065	0.12	0.044	0.068	0.07	0.064	0.076	0.063	0.082

Total	100.263	100.29	100.357	100.011	100.209	100.107	101.375	100.229	100.192	100.652	101.748	101.352
Si	2.506	2.479	2.497	2.549	2.505	2.533	2.486	2.492	2.525	2.476	2.495	2.468
Al	1.486	1.513	1.492	1.457	1.490	1.461	1.509	1.498	1.469	1.514	1.512	1.531
Mg	0.001	0.001	0.001	0.001	0.001	0.001	0.001	0.001	0.001	0.003	0.001	0.001
Na	0.494	0.476	0.485	0.545	0.484	0.515	0.474	0.471	0.502	0.464	0.492	0.461
Fe	0.007	0.007	0.007	0.008	0.009	0.010	0.009	0.010	0.010	0.011	0.009	0.008
Mn	0.001	0.000	0.000	0.000	0.000	0.000	0.000	0.000	0.000	0.000	0.000	0.000
K	0.029	0.025	0.027	0.065	0.040	0.037	0.033	0.034	0.039	0.026	0.033	0.028
Sr	0.010	0.009	0.008	0.009	0.008	0.009	0.008	0.009	0.009	0.009	0.009	0.009
Ba	0.006	0.007	0.007	0.003	0.007	0.004	0.003	0.003	0.005	0.005	0.006	0.006
Ca	0.466	0.494	0.483	0.385	0.458	0.440	0.484	0.487	0.446	0.498	0.450	0.493
Ti	0.003	0.001	0.003	0.002	0.004	0.001	0.002	0.002	0.002	0.003	0.002	0.003
O	8.000	8.000	8.000	8.000	8.000	8.000	8.000	8.000	8.000	8.000	8.000	8.000
An	**47.120**	**49.629**	**48.584**	**38.720**	**46.667**	**44.344**	**48.800**	**49.116**	**45.195**	**50.367**	**46.153**	**50.229**
Ab	**49.987**	**47.840**	**48.738**	**54.734**	**49.296**	**51.886**	**47.861**	**47.503**	**50.854**	**46.957**	**50.485**	**46.943**
Or	**2.893**	**2.530**	**2.678**	**6.546**	**4.037**	**3.770**	**3.339**	**3.380**	**3.952**	**2.676**	**3.362**	**2.828**

Sample	SL-13-41-68.9	SL-13-41-73	SL-13-41-73	SL-13-41-73	SL-13-41-73	SL-13-41-73	SL-13-41-73	SL-13-41-91	SL-13-41-91	SL-13-41-91	SL-13-41-91	SL-13-41-91
Spot No.	10	1	2	3	4	5	6	1	2	3	4	5
SiO_2	55.746	53.365	55.324	53.393	58.868	58.996	58.747	56.502	55.44	54.607	53.618	53.198
Al_2O_3	28.302	28.754	27.449	28.887	25.3	25.16	25.324	27.016	27.568	28.11	28.592	28.644
MgO	0.01	0.015	0.024	0.018	0.021	-0.003	0.015	0.005	0.006	0.017	0.013	0.005
Na_2O	5.668	4.76	5.583	4.851	7.07	7.228	7.081	6.195	5.887	5.528	4.954	4.927
FeO	0.231	0.216	0.238	0.216	0.151	0.162	0.134	0.139	0.158	0.145	0.211	0.245
MnO	-0.006	0.007	0.016	0.005	0.008	-0.01	-0.018	-0.007	0.004	-0.014	-0.006	-0.014
K_2O	0.551	0.332	0.492	0.327	0.768	0.496	0.491				0.319	0.408
SrO	0.315	0.321	0.36	0.362	0.255	0.231	0.29	0.294	0.347	0.325	0.279	0.337
BaO	0.419	0.383	0.534	0.321	0.213	0.206	0.199	0.204	0.251	0.394	0.274	0.408
CaO	9.558	11.213	9.302	11.05	6.737	6.825	7.166	8.795	9.467	9.989	10.9	10.83
TiO_2	0.079	0.083	0.118	0.119	0.083	0.065	0.052	0.083	0.087	0.082	0.091	0.087
Total	100.901	99.512	99.61	99.638	99.523	99.436	99.503	99.499	99.394	99.245	99.172	99.214
Si	2.503	2.440	2.520	2.438	2.654	2.660	2.648	2.560	2.521	2.490	2.452	2.442
Al	1.495	1.547	1.471	1.552	1.342	1.334	1.343	1.440	1.475	1.508	1.538	1.547
Mg	0.001	0.001	0.002	0.001	0.001	0.000	0.001	0.000	0.000	0.001	0.001	0.000
Na	0.493	0.421	0.492	0.429	0.617	0.631	0.618	0.543	0.518	0.488	0.438	0.438
Fe	0.009	0.008	0.009	0.008	0.006	0.006	0.005	0.005	0.006	0.006	0.008	0.009
Mn	0.000	0.000	0.001	0.000	0.000	0.000	-0.001	0.000	0.000	-0.001	0.000	-0.001
K	0.032	0.019	0.029	0.019	0.044	0.029	0.028	0.000	0.000	0.000	0.019	0.024

Sr	0.008	0.008	0.009	0.010	0.007	0.006	0.008	0.008	0.009	0.009	0.007	0.009
Ba	0.007	0.007	0.010	0.006	0.004	0.004	0.004	0.004	0.004	0.007	0.005	0.007
Ca	0.460	0.549	0.454	0.541	0.325	0.330	0.346	0.427	0.461	0.488	0.534	0.533
Ti	0.003	0.003	0.004	0.004	0.003	0.002	0.002	0.003	0.003	0.003	0.003	0.003
O	8.000	8.000	8.000	8.000	8.000	8.000	8.000	8.000	8.000	8.000	8.000	8.000
An	**46.730**	**55.490**	**46.571**	**54.696**	**32.986**	**33.337**	**34.884**	**44.006**	**47.096**	**50.007**	**53.882**	**53.570**
Ab	**50.060**	**42.553**	**50.494**	**43.376**	**62.533**	**63.777**	**62.268**	**55.994**	**52.904**	**49.993**	**44.239**	**44.025**
Or	**3.210**	**1.958**	**2.935**	**1.929**	**4.480**	**2.887**	**2.848**	**0.000**	**0.000**	**0.000**	**1.879**	**2.405**

Sample	SL-13-41-91	SL-13-41-91	SL-13-41-91	SL-13-41-91	SL-13-41-109.1	SL-13-41-109.1	SL-13-41-109.1	SL-13-41-109.1	SL-13-41-109.1	SL-13-41-109.1	SL-13-41-109.1	SL-13-41-109.1
Spot No.	6	7	8	9	1	2	3	4	5	6	7	8
SiO_2	53.416	54.782	54.592	54.956	55.455	55.5	55.611	53.981	54.377	54.206	54.366	54.507
Al_2O_3	28.786	27.546	27.645	27.619	27.477	27.474	27.574	28.65	28.36	28.527	28.573	28.366
MgO	0.012	0.009	0.01	0.02	0.003	0.007	0.006	0.029	0.022	0.034	0.041	0.007
Na_2O	4.883	5.409	5.42	5.464	6.053	6.069	6.035	5.327	5.503	5.353	5.464	5.541
FeO	0.27	0.289	0.324	0.282	0.149	0.19	0.153	0.201	0.256	0.196	0.236	0.181
MnO	0.006	0.002	0.008	-0.007	0.007	-0.013	0.011	0.018	-0.008	-0.007	-0.003	0.02
K_2O	0.407	0.573	0.557	0.569								
SrO	0.351	0.387	0.335	0.356	0.379	0.411	0.398	0.299	0.373	0.337	0.335	0.3
BaO	0.419	0.466	0.44	0.413	0.454	0.532	0.312	0.393	0.295	0.361	0.399	0.472
CaO	10.924	9.622	9.75	9.661	9.379	9.368	9.398	10.553	10.435	10.572	10.37	10.242
TiO_2	0.102	0.097	0.069	0.103	0.114	0.08	0.096	0.085	0.079	0.079	0.07	0.04
Total	99.62	99.231	99.158	99.504	99.581	99.769	99.59	99.705	99.754	99.894	100.042	99.819
Si	2.441	2.506	2.499	2.506	2.521	2.521	2.522	2.458	2.472	2.465	2.467	2.478
Al	1.547	1.482	1.489	1.482	1.469	1.468	1.471	1.535	1.517	1.526	1.526	1.517
Mg	0.001	0.001	0.001	0.001	0.000	0.000	0.000	0.002	0.002	0.002	0.003	0.000
Na	0.432	0.479	0.480	0.482	0.532	0.534	0.530	0.470	0.484	0.471	0.480	0.487
Fe	0.010	0.011	0.012	0.011	0.006	0.007	0.006	0.008	0.010	0.007	0.009	0.007
Mn	0.000	0.000	0.000	0.000	0.000	0.000	0.000	0.001	0.000	0.000	0.000	0.001
K	0.024	0.033	0.033	0.033	0.000	0.000	0.000	0.000	0.000	0.000	0.000	0.000
Sr	0.009	0.010	0.009	0.009	0.010	0.011	0.010	0.008	0.010	0.009	0.009	0.008
Ba	0.007	0.008	0.008	0.007	0.008	0.009	0.006	0.007	0.005	0.006	0.007	0.008
Ca	0.535	0.472	0.478	0.472	0.457	0.456	0.457	0.515	0.508	0.515	0.504	0.499
Ti	0.003	0.003	0.002	0.004	0.004	0.003	0.003	0.003	0.003	0.003	0.002	0.001
O	8.000	8.000	8.000	8.000	8.000	8.000	8.000	8.000	8.000	8.000	8.000	8.000
An	**53.999**	**47.928**	**48.256**	**47.804**	**46.171**	**46.077**	**46.296**	**52.305**	**51.212**	**52.228**	**51.234**	**50.574**
Ab	**43.603**	**48.671**	**48.459**	**48.841**	**53.829**	**53.923**	**53.704**	**47.695**	**48.788**	**47.772**	**48.766**	**49.426**
Or	**2.397**	**3.401**	**3.285**	**3.355**	**0.000**	**0.000**	**0.000**	**0.000**	**0.000**	**0.000**	**0.000**	**0.000**

Sample	SL-13-41-109.1	SL-13-41-109.1	SL-13-41-109.1	SL-13-41-109.1	MW-07-06-3.4	MW-07-06-3.4	MW-07-06-3.4	MW-07-06-3.4	MW-07-06-3.4	MW-07-06-3.4	MW-07-06-3.4	MW-07-06-3.4
Spot No.	9	10	11	12	1	2	3	4	5	6	7	8
SiO_2	55.914	54.078	53.366	54.145	58.584	57.819	57.457	58.839	59.121	59.768	59.256	58.941
Al_2O_3	27.44	28.774	28.92	28.385	25.453	26.011	26.031	24.112	24.643	24.204	25.018	24.958
MgO	0.016	0.019	0.027	0.019	0.009	0.011	0.014	0.011	-0.003	0.031	0.003	0.01
Na_2O	6.024	5.197	4.995	5.324	6.651	6.279	6.26	5.929	6.59	6.535	6.832	6.98
FeO	0.169	0.148	0.21	0.192	0.232	0.223	0.22	0.17	0.134	0.227	0.225	0.213
MnO	0.011	0.005	-0.003	0.018	-0.001	-0.006	0.016	0.013	0.007	0.009	-0.003	0.002
K_2O					0.834	0.729	0.746	3.087	1.792	2.509	0.864	0.819
SrO	0.338	0.294	0.375	0.28	0.48	0.396	0.391	0.369	0.327	0.329	0.409	0.426
BaO	0.367	0.347	0.307	0.381	0.399	0.407	0.439	2.645	1.392	1.771	0.486	0.422
CaO	9.154	10.723	11.139	10.463	7.24	7.847	7.906	5.045	5.96	5.232	6.629	6.689
TiO_2	0.08	0.091	0.114	0.136	0.055	0.062	0.077	0.159	0.127	0.124	0.05	0.091
Total	99.735	99.838	99.716	99.413	99.98	99.768	99.537	100.302	100.059	100.739	99.63	99.525
Si	2.534	2.457	2.436	2.469	2.640	2.611	2.603	2.690	2.677	2.700	2.669	2.662
Al	1.463	1.538	1.553	1.523	1.349	1.382	1.387	1.297	1.313	1.286	1.326	1.326
Mg	0.001	0.001	0.002	0.001	0.001	0.001	0.001	0.001	0.000	0.002	0.000	0.001
Na	0.528	0.457	0.441	0.470	0.580	0.549	0.549	0.525	0.578	0.571	0.596	0.610
Fe	0.006	0.006	0.008	0.007	0.009	0.008	0.008	0.006	0.005	0.009	0.008	0.008
Mn	0.000	0.000	0.000	0.001	0.000	0.000	0.001	0.001	0.000	0.000	0.000	0.000
K	0.000	0.000	0.000	0.000	0.048	0.042	0.043	0.180	0.104	0.145	0.050	0.047
Sr	0.009	0.008	0.010	0.007	0.013	0.010	0.010	0.010	0.009	0.009	0.011	0.011
Ba	0.007	0.006	0.005	0.007	0.007	0.007	0.008	0.047	0.025	0.031	0.009	0.007
Ca	0.444	0.522	0.545	0.511	0.350	0.380	0.384	0.247	0.289	0.253	0.320	0.324
Ti	0.003	0.003	0.004	0.005	0.002	0.002	0.003	0.005	0.004	0.004	0.002	0.003
O	8.000	8.000	8.000	8.000	8.000	8.000	8.000	8.000	8.000	8.000	8.000	8.000
An	**45.688**	**53.319**	**55.247**	**52.105**	**35.756**	**39.121**	**39.327**	**25.960**	**29.800**	**26.125**	**33.145**	**32.993**
Ab	**54.312**	**46.681**	**44.753**	**47.895**	**59.337**	**56.549**	**56.252**	**55.113**	**59.524**	**58.947**	**61.708**	**62.194**
Or	**0.000**	**0.000**	**0.000**	**0.000**	**4.908**	**4.330**	**4.421**	**18.927**	**10.676**	**14.927**	**5.147**	**4.813**

Sample	MW-07-06-3.4	MW-07-06-3.4	MW-07-06-3.4	MW-07-06-3.4	MW-07-06-3.4	MW-07-06-3.4	MW-07-06-3.4	MW-07-06-9.6	MW-07-06-9.6	MW-07-06-9.6	MW-07-06-9.6	MW-07-06-9.6
Spot No.	9	10	11	12	13	14	15	1	2	3	4	5
SiO_2	59.306	59.058	58.185	59.194	58.252	58.521	58.046	58.141	58.011	58.324	57.803	57.914
Al_2O_3	24.958	25.13	25.944	24.935	25.563	25.394	25.764	25.927	25.786	25.449	25.893	25.671
MgO	0.009	0.007	0.015	0.015	0.014	0.012	0.004	-0.001	0.021	0.013	0.01	0.019

Na_2O	6.99	6.947	6.639	7.025	6.67	6.769	6.624	6.656	6.75	6.966	6.794	6.783
FeO	0.186	0.207	0.162	0.177	0.217	0.227	0.212	0.19	0.181	0.225	0.2	0.152
MnO	0.005	0.007	-0.002	-0.017	0.025	-0.008	-0.002	-0.008	0.011	-0.014	0.012	0.006
K_2O	0.875	0.781	0.632	0.831	0.674	0.704	0.597	0.708	0.765	0.663	0.571	0.587
SrO	0.382	0.387	0.403	0.35	0.399	0.393	0.369	0.378	0.41	0.427	0.39	0.376
BaO	0.49	0.402	0.257	0.373	0.494	0.483	0.539	0.42	0.411	0.439	0.491	0.468
CaO	6.464	6.847	7.653	6.533	7.199	7.191	7.548	7.371	7.292	7.145	7.495	7.421
TiO_2	0.085	0.061	0.03	0.072	0.06	0.047	0.063	0.054	0.04	0.046	0.08	0.041
Total	99.85	99.804	99.916	99.499	99.538	99.751	99.709	99.852	99.674	99.649	99.729	99.435
Si	2.671	2.659	2.619	2.670	2.634	2.641	2.622	2.621	2.622	2.635	2.613	2.623
Al	1.322	1.331	1.374	1.323	1.360	1.348	1.369	1.375	1.371	1.353	1.377	1.368
Mg	0.001	0.000	0.001	0.001	0.001	0.001	0.000	0.000	0.001	0.001	0.001	0.001
Na	0.609	0.605	0.578	0.613	0.584	0.591	0.579	0.581	0.590	0.609	0.594	0.595
Fe	0.007	0.008	0.006	0.007	0.008	0.009	0.008	0.007	0.007	0.008	0.008	0.006
Mn	0.000	0.000	0.000	-0.001	0.001	0.000	0.000	0.000	0.000	-0.001	0.000	0.000
K	0.050	0.045	0.036	0.048	0.039	0.041	0.034	0.041	0.044	0.038	0.033	0.034
Sr	0.010	0.010	0.011	0.009	0.010	0.010	0.010	0.010	0.011	0.011	0.010	0.010
Ba	0.009	0.007	0.005	0.007	0.009	0.009	0.010	0.007	0.007	0.008	0.009	0.008
Ca	0.312	0.330	0.369	0.316	0.349	0.348	0.365	0.356	0.353	0.346	0.363	0.360
Ti	0.003	0.002	0.001	0.002	0.002	0.002	0.002	0.002	0.001	0.002	0.003	0.001
O	8.000	8.000	8.000	8.000	8.000	8.000	8.000	8.000	8.000	8.000	8.000	8.000
An	**32.105**	**33.684**	**37.516**	**32.320**	**35.903**	**35.498**	**37.320**	**36.421**	**35.750**	**34.822**	**36.653**	**36.425**
Ab	**62.716**	**61.738**	**58.792**	**62.782**	**60.092**	**60.362**	**59.163**	**59.411**	**59.781**	**61.328**	**60.020**	**60.142**
Or	**5.178**	**4.578**	**3.691**	**4.898**	**4.005**	**4.141**	**3.517**	**4.168**	**4.469**	**3.850**	**3.327**	**3.433**

Sample	MW-07-06-9.6	MW-07-06-9.6	MW-07-06-9.6	MW-07-06-9.6	MW-07-06-9.6	MW-07-06-13.4	MW-07-06-13.4	MW-07-06-13.4	MW-07-06-13.4	MW-07-06-13.4	MW-07-06-13.4	MW-07-06-13.4
Spot No.	6	7	8	9	10	1	2	3	4	5	6	7
SiO_2	57.47	57.388	59.004	58.999	58.577	59.437	58.894	58.889	55.648	56.669	57.198	57.15
Al_2O_3	26.067	26.182	25.595	25.571	25.448	24.668	24.954	24.985	27.035	26.242	25.957	25.907
MgO	0.011	0.004	0.015	0.008	0.01	0.008	0.02	0.007	0.006	0.013	0.014	0.007
Na_2O	6.601	6.545	7.113	7.075	7.003	7.14	6.98	6.907	5.761	6.325	6.387	6.472
FeO	0.166	0.17	0.283	0.256	0.276	0.202	0.19	0.244	0.188	0.189	0.161	0.285
MnO	0.008	0.024	-0.002	-0.003	0	0	-0.01	0.017	0.001	-0.005	0.008	0
K_2O	0.557	0.536	0.623	0.613	0.609	0.866	0.798	0.844	0.416	0.491	0.515	0.506
SrO	0.376	0.398	0.396	0.386	0.31	0.384	0.369	0.387	0.37	0.422	0.437	0.361
BaO	0.337	0.433	0.404	0.422	0.373	0.277	0.307	0.333	0.458	0.405	0.377	0.455
CaO	7.729	7.926	6.874	6.964	7.015	6.307	6.685	6.716	9.02	8.178	7.714	7.813
TiO_2	0.04	0.08	0.033	0.048	0.044	0.066	0.049	0.072	0.107	0.073	0.107	0.11

Total	99.364	99.673	100.326	100.306	99.649	99.239	99.145	99.431	99.043	99.076	98.819	98.969
Si	2.604	2.596	2.644	2.644	2.642	2.683	2.664	2.662	2.541	2.583	2.604	2.601
Al	1.390	1.393	1.349	1.348	1.350	1.310	1.328	1.329	1.452	1.407	1.390	1.387
Mg	0.001	0.000	0.001	0.001	0.001	0.001	0.001	0.000	0.000	0.001	0.001	0.000
Na	0.579	0.573	0.617	0.614	0.611	0.624	0.611	0.604	0.509	0.558	0.563	0.570
Fe	0.006	0.006	0.011	0.010	0.010	0.008	0.007	0.009	0.007	0.007	0.006	0.011
Mn	0.000	0.001	0.000	0.000	0.000	0.000	0.000	0.001	0.000	0.000	0.000	0.000
K	0.032	0.031	0.036	0.035	0.035	0.050	0.046	0.049	0.024	0.029	0.030	0.029
Sr	0.010	0.010	0.010	0.010	0.008	0.010	0.010	0.010	0.010	0.011	0.012	0.010
Ba	0.006	0.008	0.007	0.007	0.007	0.005	0.005	0.006	0.008	0.007	0.007	0.008
Ca	0.375	0.384	0.330	0.334	0.339	0.305	0.324	0.325	0.441	0.399	0.376	0.381
Ti	0.001	0.003	0.001	0.002	0.001	0.002	0.002	0.002	0.004	0.002	0.004	0.004
O	8.000	8.000	8.000	8.000	8.000	8.000	8.000	8.000	8.000	8.000	8.000	8.000
An	**38.042**	**38.876**	**33.588**	**34.012**	**34.402**	**31.166**	**33.021**	**33.250**	**45.275**	**40.508**	**38.831**	**38.857**
Ab	**58.692**	**57.991**	**62.785**	**62.421**	**62.039**	**63.735**	**62.283**	**61.772**	**52.237**	**56.595**	**58.080**	**58.145**
Or	**3.267**	**3.132**	**3.627**	**3.567**	**3.558**	**5.099**	**4.697**	**4.979**	**2.488**	**2.898**	**3.089**	**2.998**

Sample	MW-07-06-13.4	MW-07-06-13.4	MW-07-06-13.4	MW-07-06-13.4	MW-07-06-13.4	MW-07-06-13.4	MW-07-06-13.4	MW-07-06-13.4	MW-07-06-17.4	MW-07-06-17.4	MW-07-06-17.4	MW-07-06-17.4
Spot No.	8	9	10	11	12	13	14	15	1	2	3	4
SiO_2	56.256	55.806	58.898	59.119	58.317	57.955	57.876	59.069	57.177	55.634	57.799	56.188
Al_2O_3	26.745	26.984	25.004	24.976	25.634	25.655	25.534	24.798	26.071	27.34	25.851	26.827
MgO	0.009	0.023	0.014	-0.001	0.017	0.006	0.015	0.001	0.003	-0.001	0.007	-0.001
Na_2O	6.017	5.721	6.895	6.933	6.621	6.49	6.51	6.917	6.446	5.593	6.645	5.858
FeO	0.193	0.286	0.173	0.185	0.2	0.185	0.193	0.195	0.239	0.143	0.132	0.176
MnO	-0.001	-0.004	-0.001	-0.003	0.004	0.007	-0.001	-0.011	0.009	0.002	-0.006	-0.002
K_2O	0.405	0.408	0.903	0.912	0.81	0.73	0.793	0.956	0.511	0.375	0.44	0.553
SrO	0.399	0.426	0.346	0.313	0.33	0.378	0.303	0.337	0.336	0.297	0.363	0.359
BaO	0.445	0.442	0.367	0.297	0.26	0.321	0.402	0.256	0.37	0.344	0.308	0.493
CaO	8.733	9.081	6.744	6.663	7.33	7.614	7.494	6.541	7.898	9.536	7.666	8.782
TiO_2	0.106	0.129	0.062	0.057	0.057	0.079	0.067	0.052	0.107	0.081	0.091	0.081
Total	99.315	99.311	99.44	99.471	99.643	99.441	99.223	99.111	99.247	99.375	99.242	99.198
Si	2.559	2.542	2.662	2.668	2.632	2.624	2.627	2.674	2.597	2.530	2.616	2.557
Al	1.431	1.446	1.330	1.326	1.361	1.366	1.363	1.321	1.393	1.463	1.377	1.436
Mg	0.001	0.002	0.001	0.000	0.001	0.000	0.001	0.000	0.000	0.000	0.000	0.000
Na	0.530	0.504	0.603	0.606	0.578	0.569	0.572	0.606	0.567	0.492	0.582	0.516
Fe	0.007	0.011	0.007	0.007	0.008	0.007	0.007	0.007	0.009	0.005	0.005	0.007
Mn	0.000	0.000	0.000	0.000	0.000	0.000	0.000	0.000	0.000	0.000	0.000	0.000
K	0.024	0.024	0.052	0.053	0.047	0.042	0.046	0.055	0.030	0.022	0.025	0.032

Sr	0.011	0.011	0.009	0.008	0.009	0.010	0.008	0.009	0.009	0.008	0.010	0.009
Ba	0.008	0.008	0.006	0.005	0.005	0.006	0.007	0.005	0.007	0.006	0.005	0.009
Ca	0.426	0.443	0.327	0.322	0.355	0.369	0.364	0.317	0.384	0.465	0.372	0.428
Ti	0.004	0.004	0.002	0.002	0.002	0.003	0.002	0.002	0.004	0.003	0.003	0.003
O	8.000	8.000	8.000	8.000	8.000	8.000	8.000	8.000	8.000	8.000	8.000	8.000
An	**43.480**	**45.629**	**33.262**	**32.865**	**36.187**	**37.679**	**37.101**	**32.421**	**39.194**	**47.475**	**37.962**	**43.859**
Ab	**54.117**	**51.928**	**61.432**	**61.775**	**59.048**	**58.017**	**58.221**	**61.933**	**57.785**	**50.300**	**59.442**	**52.850**
Or	**2.403**	**2.443**	**5.307**	**5.360**	**4.765**	**4.304**	**4.678**	**5.646**	**3.021**	**2.224**	**2.596**	**3.291**

Sample	MW-07-06-17.4	MW-07-06-17.4	MW-07-06-17.4	MW-07-06-17.4	MW-07-06-17.4	MW-07-06-23.4	MW-07-06-23.4	MW-07-06-23.4	MW-07-06-23.4	MW-07-06-23.4	MW-07-06-23.4	MW-07-06-23.4
Spot No.	5	6	7	8	9	1	2	3	4	5	6	7
SiO_2	56.729	56.575	58.253	58.535	57.789	59.583	58.842	59.44	58.046	57.68	57.778	59.249
Al_2O_3	26.383	26.869	25.728	25.449	25.852	24.736	25.298	24.785	25.988	26.086	25.971	24.741
MgO	0.008	0.006	0.01	-0.004	0.001	0.011	0.005	0.012	0.008	0.014	0.011	0.004
Na_2O	6.186	6.009	6.644	6.733	6.502	7.162	6.855	7.046	6.613	6.472	6.658	7.003
FeO	0.184	0.175	0.163	0.154	0.13	0.247	0.201	0.225	0.178	0.194	0.188	0.191
MnO	-0.002	0.007	-0.001	0.019	-0.005	0.008	0	-0.023	0.022	-0.019	0.009	0.007
K_2O	0.568	0.539	0.67	0.679	0.584	0.66	0.703	0.778	0.43	0.434	0.371	0.939
SrO	0.389	0.419	0.349	0.314	0.34	0.288	0.334	0.286	0.323	0.354	0.334	0.393
BaO	0.498	0.467	0.303	0.287	0.233	0.13	0.162	0.183	0.259	0.257	0.193	0.479
CaO	8.304	8.653	7.545	7.118	7.692	6.526	7.133	6.583	7.761	7.963	7.9	6.407
TiO_2	0.106	0.086	0.055	0.058	0.059	0.022	0.037	0.047	0.058	0.091	0.068	0.066
Total	99.374	99.815	99.751	99.325	99.176	99.361	99.726	99.357	99.706	99.539	99.404	99.461
Si	2.579	2.561	2.627	2.645	2.618	2.683	2.651	2.679	2.616	2.606	2.610	2.677
Al	1.411	1.431	1.365	1.353	1.378	1.311	1.341	1.314	1.378	1.387	1.380	1.315
Mg	0.001	0.000	0.001	0.000	0.000	0.001	0.000	0.001	0.001	0.001	0.001	0.000
Na	0.544	0.527	0.580	0.589	0.570	0.624	0.598	0.615	0.577	0.566	0.582	0.612
Fe	0.007	0.007	0.006	0.006	0.005	0.009	0.008	0.008	0.007	0.007	0.007	0.007
Mn	0.000	0.000	0.000	0.001	0.000	0.000	0.000	-0.001	0.001	-0.001	0.000	0.000
K	0.033	0.031	0.039	0.039	0.034	0.038	0.040	0.045	0.025	0.025	0.021	0.054
Sr	0.010	0.011	0.009	0.008	0.009	0.008	0.009	0.007	0.008	0.009	0.009	0.010
Ba	0.009	0.008	0.005	0.005	0.004	0.002	0.003	0.003	0.005	0.005	0.003	0.008
Ca	0.404	0.420	0.365	0.345	0.373	0.315	0.344	0.318	0.375	0.385	0.382	0.310
Ti	0.004	0.003	0.002	0.002	0.002	0.001	0.001	0.002	0.002	0.003	0.002	0.002
O	8.000	8.000	8.000	8.000	8.000	8.000	8.000	8.000	8.000	8.000	8.000	8.000
An	**41.200**	**42.943**	**37.085**	**35.431**	**38.205**	**32.227**	**35.045**	**32.528**	**38.384**	**39.477**	**38.784**	**31.755**
Ab	**55.443**	**53.870**	**58.992**	**60.542**	**58.339**	**63.890**	**60.840**	**62.892**	**59.082**	**57.960**	**59.046**	**62.700**
Or	**3.358**	**3.187**	**3.924**	**4.027**	**3.456**	**3.883**	**4.115**	**4.580**	**2.534**	**2.564**	**2.170**	**5.545**

Sample Spot No.	MW-07-06-23.4 8	MW-07-06-23.4 9	MW-07-06-23.4 10	MW-07-06-23.4 11	MW-07-06-23.4 12	MW-07-06-23.4 13	MW-07-06-23.4 14	MW-07-06-23.4 15	MW-07-06-36.15 1	MW-07-06-36.15 2	MW-07-06-36.15 3	MW-07-06-36.15 4
SiO_2	59.463	55.607	56.985	56.638	57.831	56.377	55.082	55.175	56.972	57.169	56.379	57.684
Al_2O_3	24.507	27.393	26.674	27.026	25.938	26.7	27.718	27.527	26.272	27.723	26.894	25.787
MgO	0.007	0.013	0.01	0.017	0.012	0.006	0.01	0.015	0.009	0.01	0.011	-0.003
Na_2O	7.094	5.722	6.263	6.048	6.669	5.962	5.404	5.474	6.655	6.021	6.468	7.124
FeO	0.226	0.202	0.178	0.238	0.204	0.239	0.184	0.187	0.166	0.154	0.183	0.166
MnO	-0.009	0.008	0.002	-0.006	-0.016	0.017	0.003	0.007	-0.001	0.001	-0.011	0.012
K_2O	0.992	0.458	0.401	0.341	0.526	0.546	0.467	0.46	0.234	0.188	0.175	0.163
SrO	0.339	0.295	0.272	0.359	0.303	0.403	0.321	0.344	0.305	0.309	0.302	0.374
BaO	0.489	0.42	0.293	0.32	0.267	0.367	0.33	0.377	0.352	0.246	0.138	0.457
CaO	6.159	9.306	8.621	8.936	7.768	8.655	9.756	9.745	8.137	8.923	8.741	7.536
TiO_2	0.037	0.089	0.052	0.052	0.055	0.119	0.083	0.111	0.059	0.092	0.073	0.058
Total	99.285	99.557	99.755	99.918	99.522	99.458	99.362	99.388	99.177	100.852	99.336	99.363
Si	2.689	2.527	2.574	2.556	2.613	2.562	2.508	2.513	2.587	2.550	2.556	2.613
Al	1.304	1.465	1.417	1.435	1.379	1.427	1.485	1.475	1.404	1.455	1.434	1.375
Mg	0.000	0.001	0.001	0.001	0.001	0.000	0.001	0.001	0.001	0.001	0.001	0.000
Na	0.621	0.503	0.548	0.528	0.583	0.524	0.476	0.483	0.585	0.520	0.568	0.625
Fe	0.009	0.008	0.007	0.009	0.008	0.009	0.007	0.007	0.006	0.006	0.007	0.006
Mn	0.000	0.000	0.000	0.000	-0.001	0.001	0.000	0.000	0.000	0.000	0.000	0.000
K	0.057	0.027	0.023	0.020	0.030	0.032	0.027	0.027	0.014	0.011	0.010	0.009
Sr	0.009	0.008	0.007	0.009	0.008	0.011	0.008	0.009	0.008	0.008	0.008	0.010
Ba	0.009	0.007	0.005	0.006	0.005	0.007	0.006	0.007	0.006	0.004	0.002	0.008
Ca	0.298	0.453	0.417	0.432	0.376	0.421	0.476	0.476	0.396	0.427	0.425	0.366
Ti	0.001	0.003	0.002	0.002	0.002	0.004	0.003	0.004	0.002	0.003	0.002	0.002
O	8.000	8.000	8.000	8.000	8.000	8.000	8.000	8.000	8.000	8.000	8.000	8.000
An	**30.557**	**46.096**	**42.234**	**44.090**	**38.000**	**43.112**	**48.599**	**48.287**	**39.814**	**44.562**	**42.363**	**36.584**
Ab	**63.579**	**51.201**	**55.426**	**53.906**	**58.934**	**53.647**	**48.629**	**48.998**	**58.822**	**54.319**	**56.627**	**62.474**
Or	**5.864**	**2.703**	**2.341**	**2.005**	**3.066**	**3.241**	**2.772**	**2.716**	**1.364**	**1.119**	**1.011**	**0.943**

Sample Spot No.	MW-07-06-36.15 5	MW-07-06-36.15 6	MW-07-06-36.15 7	MW-07-06-36.15 8	MW-07-06-36.15 9	MW-07-06-37.5 1	MW-07-06-37.5 2	MW-07-06-37.5 3	MW-07-06-37.5 4	MW-07-06-37.5 5	MW-07-06-37.5 6	MW-07-06-37.5 7
SiO_2	57.857	57.875	57.705	58.048	57.973	56.016	56.636	56.325	63.142	62.805	63.288	64.605
Al_2O_3	25.954	25.533	25.861	25.933	26.074	26.656	26.862	26.836	22.413	22.547	22.323	21.227
MgO	0.011	0.062	0.01	-0.002	0.015	0.028	0.006	0.012	0.002	0.015	0.011	0.769

Na_2O	7.112	7.32	7.079	7.075	7.046	6.331	6.412	6.279	9.019	9.066	9.06	10.001
FeO	0.158	0.222	0.163	0.147	0.185	0.19	0.163	0.17	0.166	0.214	0.174	0.899
MnO	-0.003	0.013	0.016	0.012	0.003	0	-0.014	0	0.006	0.011	-0.004	0.014
K_2O	0.17	0.175	0.205	0.201	0.218	0.365	0.382	0.342	0.694	0.642	0.724	0.059
SrO	0.372	0.322	0.317	0.252	0.315	0.309	0.324	0.316	0.19	0.235	0.227	0.321
BaO	0.372	0.514	0.387	0.312	0.398	0.349	0.363	0.453	0.189	0.234	0.191	-0.011
CaO	7.57	7.094	7.486	7.565	7.478	8.49	8.566	8.586	3.594	3.628	3.489	1.949
TiO_2	0.068	0.08	0.08	0.061	0.066	0.05	0.067	0.09	0.042	0.062	0.061	-0.006
Total	99.627	99.205	99.29	99.606	99.764	98.797	99.758	99.4	99.458	99.443	99.527	99.832
Si	2.612	2.625	2.613	2.617	2.612	2.559	2.562	2.558	2.818	2.807	2.822	2.862
Al	1.378	1.362	1.378	1.376	1.382	1.433	1.429	1.434	1.177	1.186	1.171	1.106
Mg	0.001	0.004	0.001	0.000	0.001	0.002	0.000	0.001	0.000	0.001	0.001	0.051
Na	0.621	0.643	0.620	0.617	0.614	0.560	0.561	0.552	0.779	0.784	0.782	0.858
Fe	0.006	0.008	0.006	0.006	0.007	0.007	0.006	0.006	0.006	0.008	0.006	0.033
Mn	0.000	0.000	0.001	0.000	0.000	0.000	-0.001	0.000	0.000	0.000	0.000	0.001
K	0.010	0.010	0.012	0.012	0.013	0.021	0.022	0.020	0.040	0.037	0.041	0.003
Sr	0.010	0.008	0.008	0.007	0.008	0.008	0.008	0.008	0.005	0.006	0.006	0.008
Ba	0.007	0.009	0.007	0.006	0.007	0.006	0.006	0.008	0.003	0.004	0.003	0.000
Ca	0.366	0.345	0.363	0.365	0.361	0.416	0.415	0.418	0.172	0.174	0.167	0.093
Ti	0.002	0.003	0.003	0.002	0.002	0.002	0.002	0.003	0.001	0.002	0.002	0.000
O	8.000	8.000	8.000	8.000	8.000	8.000	8.000	8.000	8.000	8.000	8.000	8.000
An	**36.712**	**34.561**	**36.485**	**36.750**	**36.539**	**41.696**	**41.574**	**42.220**	**17.351**	**17.467**	**16.840**	**9.703**
Ab	**62.306**	**64.423**	**62.325**	**62.087**	**62.192**	**56.168**	**56.217**	**55.776**	**78.657**	**78.850**	**78.996**	**89.947**
Or	**0.982**	**1.016**	**1.190**	**1.163**	**1.269**	**2.136**	**2.209**	**2.004**	**3.992**	**3.683**	**4.164**	**0.350**

Sample	MW-07-06-37.5	MW-07-06-37.5	MW-07-06-41	MW-07-06-41	MW-07-06-41	MW-07-06-41	MW-07-06-41	MW-07-06-41	MW-07-06-41	MW-07-06-41	MW-07-06-41	MW-07-06-41
Spot No.	8	9	1	2	3	4	5	6	7	8	9	10
SiO_2	67.396	67.603	56.144	56.099	55.933	55.301	55.441	55.44	54.371	54.459	54.517	55.917
Al_2O_3	20.181	20.025	26.967	26.952	26.829	27.264	27.505	27.178	28.083	28.006	27.845	27.047
MgO	-0.003	-0.004	0.019	0.018	0.023	0.014	0.019	0.005	0.017	0.023	0.017	0.017
Na_2O	11.429	11.496	6.111	6.001	6.081	5.698	5.765	5.821	5.352	5.38	5.451	5.891
FeO	0.028	0.019	0.206	0.189	0.173	0.174	0.171	0.152	0.199	0.183	0.212	0.168
MnO	0.02	0.002	-0.02	-0.007	-0.015	0.009	0.009	0.007	-0.011	0.002	-0.017	0.007
K_2O	0.059	0.048	0.338	0.355	0.367	0.411	0.379	0.415	0.338	0.324	0.34	0.432
SrO	0.195	0.148	0.363	0.342	0.349	0.34	0.302	0.353	0.348	0.403	0.384	0.375
BaO	-0.029	-0.005	0.237	0.293	0.301	0.516	0.476	0.519	0.365	0.359	0.402	0.401
CaO	0.56	0.423	8.776	8.883	8.872	9.262	9.288	9.196	10.14	10.002	9.986	8.957
TiO_2	0.011	-0.011	0.068	0.078	0.096	0.071	0.085	0.077	0.073	0.12	0.071	0.082

Total	99.833	99.746	99.246	99.074	99.038	99.08	99.481	99.109	99.293	99.282	99.159	99.336
Si	2.958	2.968	2.552	2.551	2.550	2.527	2.522	2.531	2.483	2.487	2.492	2.544
Al	1.042	1.034	1.442	1.442	1.439	1.466	1.472	1.460	1.509	1.504	1.497	1.448
Mg	0.000	0.000	0.001	0.001	0.002	0.001	0.001	0.000	0.001	0.002	0.001	0.001
Na	0.971	0.977	0.538	0.528	0.537	0.504	0.508	0.514	0.473	0.475	0.482	0.519
Fe	0.001	0.001	0.008	0.007	0.007	0.007	0.006	0.006	0.008	0.007	0.008	0.006
Mn	0.001	0.000	-0.001	0.000	-0.001	0.000	0.000	0.000	0.000	0.000	-0.001	0.000
K	0.003	0.003	0.020	0.021	0.021	0.024	0.022	0.024	0.020	0.019	0.020	0.025
Sr	0.005	0.004	0.010	0.009	0.009	0.009	0.008	0.009	0.009	0.011	0.010	0.010
Ba	0.000	0.000	0.004	0.005	0.005	0.009	0.008	0.009	0.007	0.006	0.007	0.007
Ca	0.026	0.020	0.427	0.433	0.433	0.453	0.453	0.450	0.496	0.489	0.489	0.437
Ti	0.000	0.000	0.002	0.003	0.003	0.002	0.003	0.003	0.003	0.004	0.002	0.003
O	8.000	8.000	8.000	8.000	8.000	8.000	8.000	8.000	8.000	8.000	8.000	8.000
An	**2.632**	**1.991**	**43.407**	**44.092**	**43.717**	**46.206**	**46.086**	**45.512**	**50.171**	**49.744**	**49.343**	**44.532**
Ab	**97.038**	**97.740**	**54.601**	**53.808**	**54.129**	**51.351**	**51.674**	**52.041**	**47.836**	**48.336**	**48.656**	**52.909**
Or	**0.330**	**0.269**	**1.992**	**2.100**	**2.155**	**2.443**	**2.241**	**2.447**	**1.993**	**1.920**	**2.002**	**2.559**

Sample	MW-07-06-41	MW-07-06-41	MW-07-06-41	MW-07-06-41	MW-07-06-41
Spot No.	11	12	13	14	15
SiO_2	55.185	55.876	55.083	54.704	54.677
Al_2O_3	27.448	27.234	27.584	27.925	27.383
MgO	0.008	0.01	0.013	0.008	0.017
Na_2O	5.677	5.875	5.591	5.471	5.598
FeO	0.168	0.182	0.18	0.182	0.158
MnO	0.003	0.005	-0.003	0.001	-0.004
K_2O	0.401	0.508	0.34	0.328	0.334
SrO	0.354	0.4	0.37	0.326	0.362
BaO	0.416	0.489	0.376	0.378	0.367
CaO	9.416	8.923	9.673	9.819	9.498
TiO_2	0.092	0.093	0.057	0.1	0.07
Total	99.138	99.576	99.159	99.2	98.538
Si	2.518	2.538	2.512	2.496	2.512
Al	1.474	1.455	1.480	1.499	1.480
Mg	0.001	0.001	0.001	0.001	0.001
Na	0.501	0.517	0.493	0.483	0.498
Fe	0.006	0.007	0.007	0.007	0.006
Mn	0.000	0.000	0.000	0.000	0.000
K	0.023	0.029	0.020	0.019	0.020
Sr	0.009	0.011	0.010	0.009	0.010

Ba	0.007	0.009	0.007	0.007	0.007
Ca	0.460	0.434	0.473	0.480	0.468
Ti	0.003	0.003	0.002	0.003	0.002
O	8.000	8.000	8.000	8.000	8.000
An	**46.732**	**44.302**	**47.938**	**48.868**	**47.470**
Ab	**50.897**	**52.693**	**50.054**	**49.187**	**50.541**
Or	**2.371**	**3.005**	**2.008**	**1.945**	**1.989**

Appendix 10. Mineral chemical data of biotite determined by electron microprobe. Sample names can be referred to appendix 3.

Sample	SL-13-34-3.0	SL-13-34-3.0	SL-13-34-3.0	SL-13-34-3.0	SL-13-34-3.0	SL-13-34-3.0	SL-13-34-5.1	SL-13-34-5.1	SL-13-34-5.1	SL-13-34-17.4	SL-13-34-17.4	SL-13-34-17.4
Spot	1	2	3	4	5	6	1	2	3	1	2	3
SiO_2	35.319	35.539	35.101	34.273	34.278	35.425	35.186	34.402	34.155	35.173	35.424	35.525
Al_2O_3	13.457	13.510	13.519	13.707	13.807	13.186	13.423	13.421	13.503	14.012	13.942	13.939
Na_2O	0.546	0.518	0.572	0.562	0.562	0.535	0.434	0.419	0.408	0.174	0.138	0.170
MgO	11.327	11.310	11.505	9.906	10.199	10.862	11.021	8.961	8.109	12.922	12.806	13.081
F	0.142	0.276	0.438	0.113	0.182	0.229	0.420	0.249	0.231	1.046	1.018	1.215
CaO	0.024	0.012	0.029	0.017	0.017	0.021	0.018	0.021	0.005	0.064	0.028	0.043
TiO_2	7.349	6.888	7.022	7.997	7.412	6.861	6.946	7.000	7.075	4.350	4.690	4.407
Cl	0.046	0.046	0.039	0.045	0.054	0.054	0.070	0.066	0.057	0.074	0.072	0.068
FeO	17.484	17.754	17.614	18.973	18.850	18.701	17.911	20.769	22.299	17.165	16.917	16.657
MnO	0.069	0.094	0.086	0.082	0.101	0.060	0.110	0.119	0.134	0.154	0.108	0.096
BaO	1.151	1.062	1.698	2.580	2.662	0.719	1.355	1.806	2.063	1.388	1.510	1.484
K_2O	8.746	8.617	8.392	7.934	7.927	8.590	8.577	8.348	8.250	8.697	8.990	9.048
SrO	0.051	0.048	0.040	0.045	0.042	0.057	0.022	0.063	-0.004	0.006	0.039	-0.004
Cr_2O_3	-0.011	-0.016	-0.009	0.003	-0.011	-0.002	-0.010	-0.006	-0.012	0.008	0.000	0.009
Total	95.700	95.658	96.046	96.237	96.082	95.298	95.483	95.638	96.273	95.233	95.682	95.738
Si	2.705	2.724	2.696	2.652	2.659	2.731	2.717	2.697	2.682	2.729	2.736	2.744
Al	1.213	1.218	1.222	1.248	1.260	1.196	1.219	1.238	1.248	1.279	1.267	1.267
Na	0.081	0.077	0.085	0.084	0.084	0.080	0.065	0.064	0.062	0.026	0.021	0.025
Mg	1.301	1.300	1.326	1.150	1.187	1.256	1.276	1.054	0.955	1.504	1.484	1.515
F	0.034	0.067	0.106	0.028	0.045	0.056	0.102	0.062	0.057	0.256	0.248	0.296
Ca	0.002	0.001	0.002	0.001	0.001	0.002	0.001	0.002	0.000	0.005	0.002	0.004
Ti	0.422	0.396	0.405	0.464	0.431	0.397	0.402	0.412	0.417	0.253	0.272	0.255
Cl	0.006	0.006	0.005	0.006	0.007	0.007	0.009	0.009	0.008	0.010	0.009	0.009
Fe	1.116	1.134	1.127	1.224	1.219	1.202	1.152	1.357	1.459	1.110	1.089	1.072
Mn	0.004	0.006	0.006	0.005	0.007	0.004	0.007	0.008	0.009	0.010	0.007	0.006
Ba	0.035	0.032	0.051	0.078	0.081	0.022	0.041	0.056	0.064	0.042	0.046	0.045
K	0.855	0.843	0.823	0.784	0.785	0.845	0.845	0.835	0.827	0.861	0.887	0.892

Sr	0.002	0.002	0.002	0.002	0.002	0.003	0.001	0.003	0.000	0.000	0.002	0.000
Cr	-0.001	-0.001	-0.001	0.000	-0.001	0.000	-0.001	-0.001	-0.001	0.001	0.000	0.001
O	11.000	11.000	11.000	11.000	11.000	11.000	11.000	11.000	11.000	11.000	11.000	11.000

Sample	SL-13-34-32	SL-13-34-32	SL-13-34-32	SL-13-34-32	SL-13-34-32	SL-13-34-32	SL-13-34-45	SL-13-34-45	SL-13-34-45	SL-13-34-53	SL-13-34-53	SL-13-34-53
Spot	1	2	3	4	5	6	1	2	3	1	2	3
SiO_2	35.536	35.501	35.776	34.921	34.821	34.854	35.875	35.734	35.486	35.612	35.738	36.070
Al_2O_3	13.958	14.092	13.981	13.774	13.707	13.843	13.387	13.350	13.453	13.637	13.715	13.551
Na_2O	0.399	0.381	0.416	0.395	0.409	0.423	0.605	0.654	0.641	0.584	0.575	0.606
MgO	13.400	13.212	13.366	11.563	11.414	11.355	11.766	11.837	11.817	13.891	14.027	14.285
F	0.789	0.965	0.779	0.630	0.531	0.759	0.781	0.748	0.813	0.389	0.598	0.484
CaO	0.008	-0.001	0.016	0.030	0.045	0.039	7.650	7.632	7.762	7.479	7.595	7.330
TiO_2	6.386	6.360	6.316	7.289	7.462	7.382	0.012	0.012	0.005	0.012	-0.007	0.012
Cl	0.048	0.044	0.052	0.049	0.052	0.045	0.001	0.015	0.003	-0.022	0.001	0.018
FeO	15.037	15.088	15.125	17.112	17.188	17.557	17.144	17.064	17.100	13.204	13.184	12.947
MnO	0.074	0.078	0.128	0.098	0.101	0.124	0.108	0.086	0.107	0.054	0.050	0.072
BaO	1.783	1.698	1.786	2.042	2.205	2.249	0.949	1.172	1.163	1.785	1.841	1.315
K_2O	8.937	8.914	8.935	8.567	8.533	8.520	8.832	8.756	8.751	8.534	8.446	8.563
SrO	0.035	0.020	-0.004	0.047	0.024	0.020	0.011	0.016	0.038	0.021	0.010	0.017
Cr_2O_3	-0.020	-0.003	0.002	-0.013	-0.014	0.000	0.005	0.009	-0.013	0.004	-0.003	0.001
Total	96.370	96.349	96.674	96.504	96.478	97.170	97.161	97.138	97.169	95.204	95.782	95.286
Si	2.700	2.701	2.709	2.678	2.673	2.667	2.775	2.769	2.754	2.760	2.758	2.779
Al	1.248	1.261	1.245	1.243	1.238	1.246	1.218	1.217	1.228	1.243	1.245	1.228
Na	0.059	0.056	0.061	0.059	0.061	0.063	0.091	0.098	0.096	0.088	0.086	0.090
Mg	1.527	1.508	1.518	1.330	1.314	1.303	1.365	1.376	1.375	1.615	1.624	1.651
F	0.189	0.232	0.186	0.153	0.129	0.183	0.191	0.183	0.199	0.095	0.146	0.118
Ca	0.001	0.000	0.001	0.002	0.004	0.003	0.634	0.634	0.645	0.621	0.628	0.605
Ti	0.364	0.363	0.359	0.419	0.430	0.424	0.001	0.001	0.000	0.001	0.000	0.001
Cl	0.006	0.006	0.007	0.006	0.007	0.006	0.000	0.002	0.000	-0.003	0.000	0.002
Fe	0.952	0.956	0.954	1.093	1.100	1.119	1.105	1.102	1.106	0.853	0.848	0.831
Mn	0.005	0.005	0.008	0.006	0.007	0.008	0.007	0.006	0.007	0.004	0.003	0.005
Ba	0.053	0.051	0.053	0.061	0.066	0.067	0.029	0.036	0.035	0.054	0.056	0.040
K	0.867	0.866	0.864	0.839	0.836	0.832	0.872	0.866	0.867	0.844	0.832	0.842
Sr	0.002	0.001	0.000	0.002	0.001	0.001	0.000	0.001	0.002	0.001	0.000	0.001
Cr	-0.002	0.000	0.000	-0.001	-0.001	0.000	0.000	0.001	-0.001	0.000	0.000	0.000
O	11.000	11.000	11.000	11.000	11.000	11.000	11.000	11.000	11.000	11.000	11.000	11.000

Sample	SL-13-34-58.9	SL-13-34-58.9	SL-13-34-58.9	SL-13-34-58.9	SL-13-36-16.6	SL-13-36-16.6	SL-13-36-16.6	SL-13-36-20.7	SL-13-36-20.7	SL-13-36-20.7	SL-13-36-20.7	SL-13-37-7
Spot	1	2	3	4	1	2	3	1	2	3	4	1
SiO_2	34.789	35.180	33.309	33.243	36.461	36.499	36.228	36.341	35.851	35.872	36.319	34.552
Al_2O_3	13.467	13.460	13.795	13.815	13.855	14.030	14.049	14.057	13.799	13.978	13.760	13.789
Na_2O	0.273	0.296	0.211	0.183	0.445	0.431	0.586	0.578	0.558	0.658	0.346	0.498
MgO	10.152	10.392	6.992	6.367	13.943	14.581	13.803	14.340	13.313	13.502	13.827	11.895
F	0.409	0.340	0.177	0.202	0.910	0.950	1.014	0.706	0.488	0.430	0.539	0.637
CaO	7.476	7.559	5.833	5.848	7.506	7.255	7.575	6.435	7.465	6.860	6.734	8.081
TiO_2	0.039	0.040	0.065	0.055	0.055	0.043	0.046	0.055	0.025	0.044	0.010	0.024
Cl	-0.022	-0.004	-0.003	0.012	0.018	0.013	0.015	-0.025	0.021	0.020	0.008	-0.022
FeO	19.408	19.098	24.884	25.879	14.316	13.440	14.321	14.233	14.915	14.903	14.446	15.616
MnO	0.128	0.123	0.157	0.162	0.078	0.102	0.101	0.066	0.088	0.083	0.077	0.113
BaO	1.144	0.988	0.987	1.119	1.040	1.002	1.532	1.551	1.576	1.547	0.803	3.046
K_2O	9.047	9.101	9.018	8.965	9.074	9.207	8.742	8.568	8.636	8.451	9.224	8.166
SrO	0.039	-0.008	0.013	-0.014	0.068	0.027	0.028	0.011	-0.003	0.022	0.009	0.006
Cr_2O_3	-0.010	0.009	-0.007	0.008	0.001	0.000	0.016	-0.023	0.004	0.011	-0.003	-0.023
Total	96.401	96.648	95.506	95.905	97.813	97.626	98.109	96.928	96.779	96.411	96.132	96.429
Si	2.745	2.757	2.714	2.712	2.765	2.760	2.749	2.767	2.753	2.755	2.783	2.716
Al	1.250	1.241	1.322	1.326	1.236	1.248	1.254	1.259	1.247	1.263	1.241	1.275
Na	0.042	0.045	0.033	0.029	0.065	0.063	0.086	0.085	0.083	0.098	0.051	0.076
Mg	1.202	1.222	0.855	0.779	1.586	1.654	1.571	1.638	1.534	1.555	1.590	1.403
F	0.102	0.084	0.046	0.052	0.218	0.227	0.243	0.170	0.118	0.104	0.130	0.158
Ca	0.632	0.635	0.509	0.511	0.610	0.588	0.616	0.525	0.614	0.564	0.553	0.681
Ti	0.002	0.002	0.004	0.003	0.003	0.002	0.003	0.003	0.001	0.003	0.001	0.001
Cl	-0.003	-0.001	0.000	0.002	0.002	0.002	0.002	-0.003	0.003	0.003	0.001	-0.003
Fe	1.276	1.247	1.690	1.760	0.905	0.847	0.906	0.903	0.955	0.954	0.923	1.023
Mn	0.009	0.008	0.011	0.011	0.005	0.007	0.006	0.004	0.006	0.005	0.005	0.008
Ba	0.035	0.030	0.032	0.036	0.031	0.030	0.046	0.046	0.047	0.047	0.024	0.094
K	0.911	0.910	0.938	0.934	0.878	0.889	0.847	0.833	0.847	0.828	0.902	0.819
Sr	0.002	0.000	0.001	-0.001	0.003	0.001	0.001	0.000	0.000	0.001	0.000	0.000
Cr	-0.001	0.001	-0.001	0.001	0.000	0.000	0.001	-0.002	0.000	0.001	0.000	-0.002
O	11.000	11.000	11.000	11.000	11.000	11.000	11.000	11.000	11.000	11.000	11.000	11.000

Sample	SL-13-37-7	SL-13-37-7	SL-13-37-7	SL-13-37-7	SL-13-37-19	SL-13-37-19	SL-13-37-19	SL-13-37-27	SL-13-37-27	SL-13-37-27	SL-13-41-73	SL-13-41-73
Spot	2	3	4	5	1	2	3	1	2	3	1	2
SiO_2	34.982	36.083	36.053	36.378	34.845	35.145	34.722	35.461	35.067	34.876	36.575	36.596
Al_2O_3	13.648	13.518	13.327	13.247	13.997	13.990	13.947	13.942	13.936	13.657	13.737	13.717
Na_2O	0.453	0.453	0.348	0.333	0.587	0.574	0.605	0.773	0.732	0.751	0.667	0.652

MgO	12.214	13.001	12.032	12.277	13.140	13.499	13.215	13.451	13.459	13.221	14.656	14.693
F	0.817	0.604	0.654	0.588	0.659	0.764	0.717	0.957	1.049	0.833	1.098	0.910
CaO	7.970	7.429	7.257	7.525	8.004	7.901	8.011	8.352	8.164	8.079	6.905	6.908
TiO_2	0.034	0.011	0.015	0.040	-0.006	-0.006	0.007	0.019	0.028	0.030	0.067	0.032
Cl	0.010	0.015	0.003	0.017	-0.026	0.005	0.014	0.000	-0.008	0.003	0.024	0.015
FeO	15.327	15.004	17.236	16.726	13.535	13.460	13.679	13.865	13.889	14.187	13.236	13.128
MnO	0.112	0.093	0.121	0.108	0.087	0.077	0.073	0.054	0.069	0.116	0.074	0.075
BaO	2.389	0.773	0.667	0.240	2.905	2.818	2.886	2.508	2.562	2.508	0.052	0.054
K_2O	8.396	9.023	9.077	9.212	8.172	8.224	8.121	8.156	8.147	8.047	9.043	8.961
SrO	0.027	0.016	-0.016	-0.014	0.044	0.003	0.026	0.041	0.015	-0.008	0.009	0.009
Cr_2O_3	-0.004	-0.017	0.011	0.013	0.008	0.006	0.013	-0.018	0.014	-0.006	0.009	0.001
Total	96.412	96.028	96.834	96.738	95.966	96.474	96.059	97.585	97.153	96.322	96.204	95.788
Si	2.737	2.784	2.786	2.798	2.719	2.725	2.711	2.724	2.711	2.718	2.786	2.790
Al	1.256	1.227	1.212	1.199	1.285	1.276	1.281	1.260	1.268	1.252	1.231	1.230
Na	0.069	0.068	0.052	0.050	0.089	0.086	0.091	0.115	0.110	0.113	0.098	0.096
Mg	1.434	1.505	1.395	1.416	1.538	1.570	1.548	1.550	1.561	1.546	1.674	1.680
F	0.202	0.147	0.160	0.143	0.162	0.187	0.177	0.232	0.256	0.205	0.264	0.219
Ca	0.668	0.614	0.601	0.620	0.669	0.656	0.670	0.687	0.676	0.675	0.563	0.564
Ti	0.002	0.001	0.001	0.002	0.000	0.000	0.000	0.001	0.002	0.002	0.004	0.002
Cl	0.001	0.002	0.000	0.002	-0.003	0.001	0.002	0.000	-0.001	0.000	0.003	0.002
Fe	0.999	0.965	1.110	1.072	0.880	0.870	0.890	0.887	0.895	0.921	0.840	0.834
Mn	0.007	0.006	0.008	0.007	0.006	0.005	0.005	0.004	0.005	0.008	0.005	0.005
Ba	0.073	0.023	0.020	0.007	0.089	0.086	0.088	0.076	0.078	0.077	0.002	0.002
K	0.839	0.889	0.896	0.905	0.814	0.814	0.810	0.800	0.804	0.801	0.879	0.872
Sr	0.001	0.001	-0.001	-0.001	0.002	0.000	0.001	0.002	0.001	0.000	0.000	0.000
Cr	0.000	-0.002	0.001	0.001	0.001	0.001	0.001	-0.002	0.001	-0.001	0.001	0.000
O	11.000	11.000	11.000	11.000	11.000	11.000	11.000	11.000	11.000	11.000	11.000	11.000

Sample	SL-13-41-73	FD-13-34-24	FD-13-34-24	FD-13-34-24	FD-13-34-24	FD-13-34-24	FD-13-34-24	FD-13-34-24	FD-13-34-158.6	FD-13-34-158.6	FD-13-34-158.6	FD-13-34-158.6
Spot	3	1	2	3	4	5	6	7	1	2	3	4
SiO_2	36.559	36.486	36.361	36.037	35.983	34.964	34.991	34.898	35.623	35.86	35.294	36.01
Al_2O_3	13.807	12.951	13.042	13.253	13.469	13.127	13.094	13.111	13.192	13.227	12.849	13.206
Na_2O	0.697	0.715	0.699	0.634	0.655	0.479	0.46	0.513	0.427	0.437	0.322	0.385
MgO	14.904	15.203	15.03	13.715	13.983	10.373	10.351	10.072	11.246	11.395	9.611	11.613
F	1.262	1.326	1.439	1.61	1.394	1.223	1.087	1.232	0.984	1.092	0.827	1.003
CaO	6.949	0.047	0.009	0.042	0.036	0.018	0.019	0.039	0.008	0.018	0.025	0.025
TiO_2	0.050	5.157	5.201	5.636	4.948	6.012	6.084	5.792	5.589	5.635	5.88	6.179
Cl	0.008	0.06	0.05	0.047	0.05	0.095	0.091	0.105	0.079	0.071	0.08	0.085
FeO	12.644	14.648	14.769	15.695	15.302	19.612	19.711	20.392	18.955	18.394	20.648	18.127

MnO	0.052	0.128	0.089	0.119	0.097	0.16	0.161	0.167	0.127	0.109	0.127	0.112
BaO	0.070	0.66	0.711	0.719	0.738	0.684	0.676	0.744	0.519	0.504	0.528	0.537
K_2O	8.938	8.893	8.877	8.849	8.871	8.795	8.753	8.672	8.98	8.862	8.977	9.123
SrO	0.045	0.015	-0.035	0.052	0.086	0.001	0.027	0.027	0.038	-0.01	0.046	0.003
Cr_2O_3	-0.009	-0.001	-0.014	0.006	-0.017	-0.024	0.025	0.015	-0.007	0.007	-0.014	0.016
Total	96.007	96.307	96.261	96.452	95.622	95.56	95.564	95.833	95.809	95.615	95.235	96.446
Si	2.786	2.761	2.757	2.747	2.756	2.738	2.736	2.737	2.759	2.771	2.771	2.757
Al	1.238	1.153	1.164	1.189	1.214	1.209	1.205	1.210	1.202	1.203	1.187	1.189
Na	0.103	0.105	0.103	0.094	0.097	0.073	0.070	0.078	0.064	0.065	0.049	0.057
Mg	1.704	1.726	1.710	1.568	1.607	1.218	1.214	1.185	1.306	1.321	1.132	1.334
F	0.304	0.317	0.345	0.388	0.337	0.302	0.268	0.305	0.241	0.267	0.205	0.242
Ca	0.567	0.004	0.001	0.003	0.003	0.002	0.002	0.003	0.001	0.001	0.002	0.002
Ti	0.003	0.293	0.296	0.322	0.284	0.353	0.357	0.341	0.325	0.327	0.346	0.355
Cl	0.001	0.008	0.006	0.006	0.006	0.013	0.012	0.014	0.010	0.009	0.011	0.011
Fe	0.803	0.924	0.933	0.997	0.977	1.280	1.284	1.333	1.223	1.185	1.351	1.157
Mn	0.003	0.008	0.006	0.008	0.006	0.011	0.011	0.011	0.008	0.007	0.008	0.007
Ba	0.002	0.020	0.021	0.021	0.022	0.021	0.021	0.023	0.016	0.015	0.016	0.016
K	0.869	0.859	0.859	0.861	0.867	0.879	0.874	0.868	0.888	0.874	0.900	0.892
Sr	0.002	0.001	-0.002	0.002	0.004	0.000	0.001	0.001	0.002	0.000	0.002	0.000
Cr	-0.001	0.000	-0.001	0.001	-0.002	-0.002	0.002	0.001	-0.001	0.001	-0.001	0.001
O	11.000	11.000	11.000	11.000	11.000	11.000	11.000	11.000	11.000	11.000	11.000	11.000

Sample	FD-13-34-158.6	FD-13-34-33	FD-13-34-33	FD-13-34-33	FD-13-34-33	MW-07-06-3.4	MW-07-06-3.4	MW-07-06-3.4	MW-07-06-3.4	MW-07-06-13.4	MW-07-06-13.4	MW-07-06-13.4
Spot	5	1	2	3	4	1	2	3	4	1	2	3
SiO_2	35.86	36.896	36.928	37.174	37.057	33.394	33.594	33.348	33.458	34.498	34.591	34.186
Al_2O_3	13.024	13.906	13.721	13.798	13.708	13.545	13.758	13.622	13.789	13.33	13.644	13.382
Na_2O	0.387	0.97	1.014	0.947	0.992	0.554	0.564	0.523	0.458	0.539	0.339	0.526
MgO	11.362	16.132	16.137	16.442	16.289	8.529	8.889	8.397	8.691	10.22	10.585	9.55
F	0.917	1.575	1.546	1.407	1.47	0.537	0.688	0.509	0.767	0.594	0.583	0.455
CaO	0.023	0.012	0.026	0.021	0.011	-0.004	0.012	0.023	-0.01	0.026	0.045	0.02
TiO_2	6.154	6.926	6.787	6.743	6.5	7.555	7.073	7.381	6.984	7.369	6.189	7.496
Cl	0.072	0.014	0.014	0.022	0.021	0.085	0.101	0.109	0.135	0.103	0.114	0.109
FeO	18.124	11.592	11.409	11.514	11.374	21.191	21.032	21.592	21.354	19.107	19.311	20.051
MnO	0.097	0.04	0.072	0.061	0.085	0.148	0.134	0.147	0.132	0.121	0.11	0.171
BaO	0.475	0.849	0.719	0.744	0.685	3.903	3.842	3.704	3.627	2.08	2.17	2.226
K_2O	9.038	8.585	8.754	8.628	8.681	7.673	7.575	7.734	7.793	8.378	8.57	8.254
SrO	-0.003	0.033	0.032	0.029	0.03	-0.013	0.031	0.031	0.006	0.02	0.009	0.053
Cr_2O_3	0.021	-0.02	-0.006	-0.005	0.022	0.017	0.008	-0.016	-0.013	-0.001	0.006	-0.014

Total	95.565	97.524	97.149	97.517	96.936	97.114	97.301	97.104	97.171	96.384	96.266	96.465
Si	2.767	2.717	2.728	2.729	2.738	2.632	2.640	2.631	2.639	2.679	2.692	2.665
Al	1.182	1.205	1.192	1.191	1.192	1.256	1.272	1.264	1.279	1.218	1.249	1.227
Na	0.058	0.138	0.145	0.135	0.142	0.084	0.086	0.080	0.070	0.081	0.051	0.079
Mg	1.315	1.782	1.788	1.810	1.805	1.008	1.048	0.994	1.028	1.190	1.236	1.117
F	0.223	0.366	0.361	0.326	0.343	0.134	0.171	0.127	0.191	0.146	0.143	0.112
Ca	0.002	0.001	0.002	0.002	0.001	0.000	0.001	0.002	-0.001	0.002	0.004	0.002
Ti	0.356	0.383	0.376	0.371	0.360	0.447	0.417	0.437	0.413	0.429	0.361	0.438
Cl	0.009	0.002	0.002	0.003	0.003	0.011	0.013	0.015	0.018	0.014	0.015	0.014
Fe	1.165	0.711	0.702	0.704	0.700	1.392	1.377	1.420	1.403	1.236	1.253	1.303
Mn	0.006	0.002	0.004	0.004	0.005	0.010	0.009	0.010	0.009	0.008	0.007	0.011
Ba	0.014	0.025	0.021	0.021	0.020	0.121	0.118	0.115	0.112	0.063	0.066	0.068
K	0.890	0.807	0.826	0.808	0.819	0.772	0.760	0.779	0.785	0.831	0.852	0.822
Sr	0.000	0.001	0.001	0.001	0.001	-0.001	0.001	0.001	0.000	0.001	0.000	0.002
Cr	0.002	-0.002	-0.001	0.000	0.002	0.002	0.001	-0.002	-0.001	0.000	0.001	-0.001
O	11.000	11.000	11.000	11.000	11.000	11.000	11.000	11.000	11.000	11.000	11.000	11.000

Sample	MW-07-06-17.4	MW-07-06-17.4	MW-07-06-17.4	MW-07-06-17.4	MW-07-06-23.4	MW-07-06-23.4	MW-07-06-23.4	MW-07-06-23.4	MW-07-06-23.4	MW-07-06-23.4	MW-07-06-23.4	MW-07-06-23.4
Spot	1	2	3	4	1	2	3	4	5	6	7	8
SiO_2	35.146	34.335	34.095	33.996	34.984	35.013	34.874	34.206	34.423	34.4	34.47	34.708
Al_2O_3	13.196	13.395	13.359	13.59	13.457	13.529	13.572	13.525	13.558	13.485	13.555	13.701
Na_2O	0.477	0.63	0.552	0.625	0.425	0.419	0.408	0.488	0.469	0.485	0.433	0.385
MgO	10.452	9.936	9.789	9.989	10.695	10.422	10.29	9.98	9.976	9.923	9.374	10.235
F	0.415	0.682	0.462	0.674	0.605	0.666	0.58	0.651	0.556	0.707	0.704	0.688
CaO	0.021	0.015	-0.009	0.007	0.013	0.014	0.005	-0.007	0.003	0.004	0.013	0.016
TiO_2	7.012	7.641	7.789	7.786	6.817	6.95	6.819	7.344	7.325	7.365	7.339	6.769
Cl	0.078	0.088	0.078	0.079	0.105	0.087	0.096	0.093	0.083	0.078	0.084	0.076
FeO	19.013	19.067	19.017	18.69	18.524	19.183	19.374	19.468	19.488	19.692	20.526	19.506
MnO	0.149	0.104	0.107	0.099	0.117	0.127	0.149	0.126	0.111	0.144	0.14	0.115
BaO	1.239	2.907	3.252	3.56	1.876	1.948	1.988	3.083	2.961	3.094	2.495	2.47
K_2O	8.687	7.908	7.906	7.706	8.61	8.553	8.654	8.081	8.159	8.065	8.306	8.442
SrO	0.014	0.037	0.04	0.039	0.015	0.049	0.002	0.044	0.003	0.034	0.04	0.048
Cr_2O_3	0.03	-0.006	-0.007	-0.005	0.008	-0.018	-0.002	-0.003	-0.013	-0.018	0.017	0.017
Total	95.929	96.739	96.43	96.835	96.251	96.942	96.809	97.079	97.102	97.458	97.496	97.176
Si	2.716	2.670	2.661	2.648	2.706	2.699	2.695	2.660	2.669	2.667	2.672	2.684
Al	1.200	1.225	1.227	1.245	1.225	1.227	1.234	1.237	1.237	1.230	1.236	1.246
Na	0.071	0.095	0.083	0.094	0.064	0.063	0.061	0.073	0.070	0.073	0.065	0.058

Mg	1.212	1.159	1.146	1.167	1.241	1.205	1.193	1.164	1.160	1.154	1.090	1.187
F	0.101	0.167	0.114	0.166	0.148	0.162	0.142	0.160	0.136	0.173	0.172	0.168
Ca	0.002	0.001	-0.001	0.001	0.001	0.001	0.000	-0.001	0.000	0.000	0.001	0.001
Ti	0.406	0.446	0.456	0.455	0.396	0.402	0.395	0.428	0.426	0.428	0.427	0.393
Cl	0.010	0.012	0.010	0.010	0.014	0.011	0.013	0.012	0.011	0.010	0.011	0.010
Fe	1.225	1.235	1.237	1.213	1.194	1.232	1.248	1.262	1.259	1.272	1.326	1.257
Mn	0.010	0.007	0.007	0.007	0.008	0.008	0.010	0.008	0.007	0.009	0.009	0.008
Ba	0.038	0.089	0.100	0.109	0.057	0.059	0.060	0.094	0.090	0.094	0.076	0.075
K	0.857	0.785	0.788	0.766	0.850	0.842	0.854	0.802	0.808	0.798	0.822	0.833
Sr	0.001	0.002	0.002	0.002	0.001	0.002	0.000	0.002	0.000	0.002	0.002	0.002
Cr	0.003	-0.001	-0.001	0.000	0.001	-0.002	0.000	0.000	-0.001	-0.002	0.002	0.002
O	11.000	11.000	11.000	11.000	11.000	11.000	11.000	11.000	11.000	11.000	11.000	11.000

Sample	MW-07-06-23.4	MW-07-06-41	MW-07-06-41	MW-07-06-41
Spot	9	1	2	3
SiO_2	34.61	35.206	35.106	35.08
Al_2O_3	13.657	13.106	13.016	12.956
Na_2O	0.489	0.626	0.63	0.639
MgO	9.716	11.433	11.292	11.605
F	0.579	0.849	0.658	0.75
CaO	0.027	0.042	0.031	0.036
TiO_2	7.175	7.278	7.146	7.098
Cl	0.09	0.071	0.071	0.062
FeO	19.77	17.476	17.499	17.491
MnO	0.129	0.119	0.109	0.114
BaO	2.455	1.585	1.502	1.56
K_2O	8.22	8.423	8.263	8.316
SrO	-0.001	0.044	0.019	0.045
Cr_2O_3	-0.027	-0.004	0	0.012
Total	96.889	96.254	95.342	95.764
Si	2.683	2.709	2.719	2.710
Al	1.245	1.187	1.186	1.178
Na	0.073	0.093	0.094	0.096
Mg	1.130	1.320	1.312	1.345
F	0.142	0.206	0.161	0.183
Ca	0.002	0.003	0.003	0.003
Ti	0.417	0.420	0.415	0.411
Cl	0.012	0.009	0.009	0.008
Fe	1.277	1.121	1.129	1.126

Mn	0.008	0.008	0.007	0.007
Ba	0.075	0.048	0.046	0.047
K	0.813	0.827	0.817	0.820
Sr	0.000	0.002	0.001	0.002
Cr	-0.003	0.000	0.000	0.001
O	11.000	11.000	11.000	11.000

Appendix 12. Mineral chemical data of alkali feldspar determined by electron microprobe. Sample names can be referred to appendix 3.

Sample	SL-13-34-5.1	SL-13-34-5.1	SL-13-34-5.1	SL-13-34-5.1	SL-13-34-5.1	SL-13-34-5.1	SL-13-34-17.4	SL-13-34-17.4	SL-13-34-17.4	SL-13-34-32	SL-13-34-32	SL-13-34-32
Spot	1	2	3	4	5	6	1	2	3	1	2	3
SiO_2	57.532	58.105	57.651	56.262	57.908	57.771	57.71	57.369	57.14	58.136	58.095	57.542
Al_2O_3	21.188	21.242	21.284	20.671	21.221	21.311	20.926	20.952	20.802	21.1	21	20.891
Na_2O	2.863	2.866	2.91	2.606	3.197	3.295	2.591	2.66	2.348	3.321	3.298	2.681
MgO	0.007	0.005	0.006	0.562	-0.007	-0.004	-0.014	-0.002	0.003	0.003	-0.003	-0.007
CaO	1.191	1.103	1.265	0.735	1.166	1.163	0.623	0.725	0.339	1.032	0.929	0.526
TiO_2	0.32	0.324	0.315	0.326	0.335	0.338	0.356	0.375	0.421	0.356	0.309	0.329
FeO	0.086	0.056	0.046	1.015	0.093	0.075	0.093	0.066	0.105	0.18	0.108	0.122
MnO	0.003	-0.018	0.005	0.031	0.008	-0.015	-0.008	0.014	0.005	0.009	0.014	0.003
BaO	6.618	6.434	6.703	7.19	6.61	6.685	7.644	7.94	8.654	6.767	6.786	7.26
K_2O	8.728	8.852	8.561	8.542	8.364	8.025	9.277	8.923	9.322	8.194	8.243	9.232
SrO	0.391	0.4	0.41	0.407	0.41	0.462	0.406	0.382	0.511	0.408	0.475	0.503
Cr_2O_3	0.005	-0.008	-0.025	-0.008	-0.013	0.003	-0.011	-0.04	0.003	-0.019	-0.006	-0.02
Total	98.911	99.26	99.075	98.274	99.331	99.196	99.424	99.401	99.626	99.432	99.235	99.219
Si	2.782	2.791	2.781	2.761	2.785	2.782	2.794	2.787	2.788	2.791	2.797	2.795
Al	1.205	1.200	1.208	1.194	1.201	1.207	1.192	1.198	1.194	1.192	1.189	1.194
Na	0.268	0.266	0.272	0.248	0.298	0.307	0.243	0.250	0.222	0.309	0.307	0.252
Mg	0.001	0.000	0.000	0.041	-0.001	0.000	-0.001	0.000	0.000	0.000	0.000	-0.001
Ca	0.062	0.057	0.065	0.039	0.060	0.060	0.032	0.038	0.018	0.053	0.048	0.027
Ti	0.012	0.012	0.011	0.012	0.012	0.012	0.013	0.014	0.015	0.013	0.011	0.012
Fe	0.003	0.002	0.002	0.042	0.004	0.003	0.004	0.003	0.004	0.007	0.004	0.005
Mn	0.000	-0.001	0.000	0.001	0.000	-0.001	0.000	0.001	0.000	0.000	0.001	0.000
Ba	0.125	0.121	0.127	0.138	0.124	0.126	0.145	0.151	0.165	0.127	0.128	0.138
K	0.539	0.543	0.527	0.535	0.514	0.493	0.573	0.553	0.581	0.502	0.507	0.572
Sr	0.011	0.011	0.011	0.012	0.011	0.013	0.011	0.011	0.014	0.011	0.013	0.014
Cr	0.000	0.000	-0.001	0.000	0.000	0.000	0.000	-0.002	0.000	-0.001	0.000	-0.001
O	8.000	8.000	8.000	8.000	8.000	8.000	8.000	8.000	8.000	8.000	8.000	8.000

Sample	SL-13-34-32	SL-13-34-32	SL-13-34-32	SL-13-34-58.9	SL-13-34-58.9	SL-13-34-58.9	SL-13-37-19	SL-13-37-19	SL-13-37-19	SL-13-37-19	SL-13-37-19	SL-13-37-19
Spot	4	5	6	1	2	3	1	2	3	4	5	6
SiO_2	56.71	56.603	57.013	58.784	58.525	58.374	57.207	57.324	56.984	56.613	57.05	57.416
Al_2O_3	21.033	20.744	21.134	21.044	21.04	21.046	21.674	21.727	21.49	21.482	21.411	21.56
Na_2O	2.556	2.248	2.382	2.268	2.321	2.493	4.114	4.127	3.738	3.565	4.028	4.318
MgO	-0.009	-0.008	-0.01	-0.004	0.003	0.005	-0.003	-0.004	-0.013	-0.001	-0.012	-0.003
CaO	0.561	0.449	0.52	0.253	0.294	0.287	0.357	0.35	0.377	0.427	0.367	0.397
TiO_2	0.385	0.379	0.373	1.026	1.132	1.344	1.031	1.153	0.684	0.492	0.765	0.926
FeO	0.096	0.082	0.085	0.077	0.134	0.063	0.108	0.069	0.102	0.116	0.158	0.162
MnO	0.005	0.006	0.018	0.009	0.003	-0.004	0.002	0.02	-0.006	-0.005	0.013	0
BaO	8.298	8.513	8.574	5.909	5.656	5.532	8.488	8.403	9.193	9.674	9.003	8.532
K_2O	9.177	9.347	9.101	10.154	10.08	9.846	6.409	6.333	6.868	7.029	6.527	6.353
SrO	0.45	0.516	0.463	0.361	0.339	0.411	0.366	0.372	0.383	0.316	0.374	0.371
Cr_2O_3	-0.007	-0.021	-0.011	-0.03	0.008	-0.006	-0.012	-0.033	-0.025	-0.02	-0.016	-0.044
Total	99.185	98.846	99.719	99.807	99.547	99.422	99.729	99.853	99.741	99.729	99.716	100.02
Si	2.773	2.784	2.777	2.804	2.797	2.790	2.752	2.752	2.760	2.757	2.760	2.758
Al	1.210	1.200	1.211	1.181	1.183	1.184	1.227	1.227	1.225	1.231	1.219	1.218
Na	0.242	0.214	0.225	0.209	0.215	0.231	0.383	0.383	0.350	0.336	0.377	0.401
Mg	-0.001	-0.001	-0.001	0.000	0.000	0.000	0.000	0.000	-0.001	0.000	-0.001	0.000
Ca	0.029	0.024	0.027	0.013	0.015	0.015	0.018	0.018	0.020	0.022	0.019	0.020
Ti	0.014	0.014	0.014	0.037	0.041	0.048	0.037	0.042	0.025	0.018	0.028	0.033
Fe	0.004	0.003	0.003	0.003	0.005	0.003	0.004	0.003	0.004	0.005	0.006	0.006
Mn	0.000	0.000	0.001	0.000	0.000	0.000	0.000	0.001	0.000	0.000	0.001	0.000
Ba	0.159	0.164	0.163	0.110	0.106	0.103	0.160	0.158	0.174	0.184	0.170	0.160
K	0.573	0.587	0.566	0.618	0.615	0.601	0.394	0.388	0.425	0.437	0.403	0.390
Sr	0.013	0.015	0.013	0.010	0.009	0.011	0.010	0.010	0.011	0.009	0.010	0.010
Cr	0.000	-0.001	0.000	-0.001	0.000	0.000	0.000	-0.001	-0.001	-0.001	-0.001	-0.002
O	8.000	8.000	8.000	8.000	8.000	8.000	8.000	8.000	8.000	8.000	8.000	8.000

Sample	SL-13-37-19	SL-13-37-19	SL-13-37-19	SL-13-37-19	SL-13-37-19	SL-13-37-27	SL-13-37-27	SL-13-37-27	SL-13-41-3	SL-13-41-3	SL-13-41-12.1	SL-13-41-12.1
Spot	7	8	9	10	11	1	2	3	1	2	1	2
SiO_2	57.693	57.014	57.376	56.557	56.059	57.843	57.716	58.215	61.017	60.026	57.298	56.856
Al_2O_3	21.69	21.566	21.754	21.563	21.2	21.578	21.605	21.692	20.063	21.056	21.573	21.02
Na_2O	4.515	3.96	4.368	3.993	3.235	4.334	4.263	4.493	4.13	4.236	3.428	2.908
MgO	-0.004	-0.003	0.013	0.001	-0.016	0.011	0.007	0.001	-0.007	-0.006	-0.013	-0.002
CaO	0.354	0.425	0.356	0.396	0.434	0.299	0.344	0.297	0.173	0.263	0.344	0.361
TiO_2	1.119	0.843	1.248	0.858	0.192	1.489	1.316	1.58	0.715	1.378	1.414	0.521

FeO	0.151	0.114	0.117	0.14	0.089	0.097	0.097	0.092	0.117	0.089	0.101	0.069
MnO	-0.014	0.014	-0.01	0.005	0.021	0.013	-0.013	0.007	-0.018	-0.011	0.013	-0.002
BaO	8.146	8.792	8.056	8.775	10.488	6.948	7.205	6.6	3.498	4.568	7.27	8.503
K_2O	6.017	6.682	6.198	6.515	7.5	6.375	6.486	6.228	8.801	7.588	7.466	8.412
SrO	0.358	0.389	0.36	0.448	0.406	0.414	0.425	0.423	0.268	0.247	0.294	0.381
Cr_2O_3	-0.003	-0.027	-0.009	-0.008	-0.031	-0.014	-0.015	-0.014	0.001	-0.037	0.019	-0.042
Total	100.074	99.692	99.831	99.275	99.578	99.358	99.331	99.56	98.683	99.384	99.219	99.017
Si	2.757	2.754	2.748	2.747	2.759	2.760	2.760	2.762	2.873	2.817	2.756	2.778
Al	1.219	1.225	1.226	1.232	1.227	1.212	1.215	1.211	1.111	1.163	1.221	1.208
Na	0.418	0.370	0.405	0.375	0.308	0.400	0.395	0.413	0.376	0.385	0.319	0.275
Mg	0.000	0.000	0.001	0.000	-0.001	0.001	0.001	0.000	0.000	0.000	-0.001	0.000
Ca	0.018	0.022	0.018	0.021	0.023	0.015	0.018	0.015	0.009	0.013	0.018	0.019
Ti	0.040	0.031	0.045	0.031	0.007	0.053	0.047	0.056	0.025	0.049	0.051	0.019
Fe	0.006	0.005	0.005	0.006	0.004	0.004	0.004	0.004	0.005	0.003	0.004	0.003
Mn	-0.001	0.001	0.000	0.000	0.001	0.001	-0.001	0.000	-0.001	0.000	0.001	0.000
Ba	0.152	0.166	0.151	0.167	0.202	0.130	0.135	0.123	0.064	0.084	0.137	0.163
K	0.367	0.412	0.379	0.404	0.471	0.388	0.396	0.377	0.529	0.455	0.458	0.525
Sr	0.010	0.011	0.010	0.013	0.012	0.011	0.012	0.012	0.007	0.007	0.008	0.011
Cr	0.000	-0.001	0.000	0.000	-0.001	-0.001	-0.001	-0.001	0.000	-0.001	0.001	-0.002
O	8.000	8.000	8.000	8.000	8.000	8.000	8.000	8.000	8.000	8.000	8.000	8.000

Sample	SL-13-41-12.1	MW-07-06-3.4	MW-07-06-3.4	MW-07-06-3.4	MW-07-06-3.4	MW-07-06-3.4	MW-07-06-3.4	MW-07-06-3.4	MW-07-06-3.4	MW-07-06-3.4	MW-07-06-13.4	MW-07-06-13.4
Spot	3	1	2	3	4	5	6	7	8	9	1	2
SiO_2	57.776	58.228	59.021	58.472	56.83	58.365	56.567	56.293	56.536	58.222	56.918	55.89
Al_2O_3	21.341	20.817	20.976	20.698	21.222	21.122	21.295	21.437	21.372	20.996	21.296	21.133
Na_2O	3.331	3.323	3.748	3.325	2.924	3.648	3.094	2.864	2.935	3.113	3.52	3.016
MgO	0.006	-0.009	-0.002	-0.005	-0.003	0.01	0.008	0.002	-0.013	-0.011	-0.009	-0.012
CaO	0.357	0.543	0.801	0.549	0.533	0.85	0.699	0.471	0.608	0.451	0.893	0.584
TiO_2	1.003	0.354	0.32	0.378	0.435	0.326	0.44	0.456	0.501	0.351	0.384	0.416
FeO	0.083	0.076	0.058	0.206	0.047	0.078	0.079	0.074	0.053	0.1	0.091	0.072
MnO	0.011	0.003	-0.006	-0.002	0.003	-0.006	-0.008	-0.007	0.01	-0.012	-0.009	0.003
BaO	7.409	7.656	6.752	7.471	9.406	7.418	9.207	9.971	9.67	7.934	8.498	9.496
K_2O	7.83	8.275	7.816	8.389	8.031	7.649	7.84	8.078	7.942	8.432	7.314	7.885
SrO	0.386	0.454	0.52	0.569	0.561	0.454	0.525	0.546	0.512	0.542	0.499	0.598
Cr_2O_3	-0.018	-0.016	-0.014	-0.028	-0.012	-0.006	-0.023	0.006	-0.015	-0.018	-0.02	-0.023
Total	99.473	99.714	100.071	100.058	99.944	99.871	99.742	100.132	100.001	100.163	99.317	99.087
Si	2.776	2.805	2.811	2.808	2.767	2.795	2.758	2.749	2.755	2.800	2.765	2.754

Al	1.206	1.180	1.175	1.169	1.216	1.190	1.222	1.232	1.225	1.188	1.217	1.225
Na	0.310	0.310	0.345	0.309	0.276	0.338	0.292	0.271	0.277	0.290	0.331	0.288
Mg	0.000	-0.001	0.000	0.000	0.000	0.001	0.001	0.000	-0.001	-0.001	-0.001	-0.001
Ca	0.018	0.028	0.041	0.028	0.028	0.044	0.037	0.025	0.032	0.023	0.046	0.031
Ti	0.036	0.013	0.011	0.014	0.016	0.012	0.016	0.017	0.018	0.013	0.014	0.015
Fe	0.003	0.003	0.002	0.008	0.002	0.003	0.003	0.003	0.002	0.004	0.004	0.003
Mn	0.000	0.000	0.000	0.000	0.000	0.000	0.000	0.000	0.000	0.000	0.000	0.000
Ba	0.139	0.144	0.126	0.140	0.179	0.139	0.176	0.191	0.184	0.149	0.162	0.183
K	0.480	0.509	0.475	0.514	0.499	0.468	0.488	0.504	0.494	0.518	0.454	0.496
Sr	0.011	0.013	0.014	0.016	0.016	0.013	0.015	0.015	0.014	0.015	0.014	0.017
Cr	-0.001	-0.001	-0.001	-0.001	0.000	0.000	-0.001	0.000	-0.001	-0.001	-0.001	-0.001
O	8.000	8.000	8.000	8.000	8.000	8.000	8.000	8.000	8.000	8.000	8.000	8.000

Sample	MW-07-06-13.4	MW-07-06-13.4	MW-07-06-13.4	MW-07-06-13.4	MW-07-06-13.4	MW-07-06-17.4	MW-07-06-17.4	MW-07-06-17.4	MW-07-06-17.4	MW-07-06-17.4	MW-07-06-17.4
Spot	3	4	5	6	7	1	2	3	4	5	6
SiO_2	55.732	58.204	58.306	56.552	57.298	60.025	59.905	59.793	59.64	59.39	59.128
Al_2O_3	21.262	20.797	20.418	21.468	21.381	20.781	20.186	19.992	20.468	20.575	20.466
Na_2O	3.242	2.98	3.114	3.276	3.557	3.965	3.244	3.306	3.569	3.368	3.525
MgO	-0.018	-0.001	-0.018	-0.003	0.005	0	-0.009	0.001	0.002	0	0.002
CaO	0.695	0.346	0.42	0.872	1.148	1.129	0.334	0.332	0.658	0.496	0.543
TiO_2	0.455	0.339	0.329	0.427	0.365	0.252	0.226	0.203	0.278	0.268	0.271
FeO	0.066	0.392	0.064	0.073	0.182	0.074	0.095	0.078	0.096	0.084	0.09
MnO	0.018	-0.005	0.004	-0.006	0.006	0.004	0.003	0.003	0.011	0.009	-0.008
BaO	9.736	7.868	7.317	9.033	7.662	5.039	5.707	5.74	5.68	6.131	6.217
K_2O	7.346	8.746	8.735	7.405	7.256	8.045	9.478	9.277	8.565	8.767	8.564
SrO	0.499	0.507	0.474	0.541	0.531	0.423	0.383	0.359	0.466	0.452	0.473
Cr_2O_3	-0.026	-0.025	0.011	-0.015	-0.008	-0.011	-0.002	-0.015	-0.023	-0.017	-0.009
Total	99.006	100.169	99.103	99.567	99.346	99.802	99.501	99.005	99.457	99.655	99.235
Si	2.746	2.803	2.821	2.753	2.767	2.832	2.855	2.862	2.840	2.835	2.832
Al	1.233	1.178	1.162	1.229	1.215	1.154	1.132	1.126	1.147	1.155	1.153
Na	0.309	0.278	0.292	0.309	0.333	0.362	0.299	0.306	0.329	0.311	0.327
Mg	-0.001	0.000	-0.001	0.000	0.000	0.000	-0.001	0.000	0.000	0.000	0.000
Ca	0.037	0.018	0.022	0.045	0.059	0.057	0.017	0.017	0.034	0.025	0.028
Ti	0.017	0.012	0.012	0.016	0.013	0.009	0.008	0.007	0.010	0.010	0.010
Fe	0.003	0.016	0.003	0.003	0.007	0.003	0.004	0.003	0.004	0.003	0.004
Mn	0.001	0.000	0.000	0.000	0.000	0.000	0.000	0.000	0.000	0.000	0.000
Ba	0.188	0.148	0.139	0.172	0.145	0.093	0.106	0.108	0.106	0.115	0.117
K	0.462	0.538	0.539	0.460	0.447	0.485	0.577	0.567	0.521	0.534	0.524
Sr	0.014	0.014	0.013	0.015	0.015	0.012	0.011	0.010	0.013	0.012	0.013

Cr	-0.001	-0.001	0.000	-0.001	0.000	0.000	0.000	-0.001	-0.001	-0.001	0.000
O	8.000	8.000	8.000	8.000	8.000	8.000	8.000	8.000	8.000	8.000	8.000

Curriculum vitae

Mr. Yonghua Cao (Ph.D.)

Born in June, 1987

Education Since 2005

2012-January, 2017

● Ph.D. candidate at Department of Earth Sciences, Western University, Canada.

2009-2011

● M.Sc. at School of Geosciences and Info-Physics, Central South University (CSU), China.

2005-2009

● B.Sc. at School of Geosciences and Environmental Engineering, Central South University (CSU), China.

Courses taken at Western University

● Graduate Seminar, 86/100

● Advance mineral deposit geochemistry, 88/100

● Best practices in exploration drilling, 90/100

Teaching Experiences

● Earth Rocks (Teaching assistant, 2012)

● Life on Planet Earth (Teaching assistant, 2013)

● Catastrophic Events in Earth History (Teaching assistant, 2014-15)

● bSEM training (serve as the bSEM technician, 2013-present)

Research Experiences

2013-present

● Cu-Pd mineralization and exploration geochemistry of the northeastern portion of the Coldwell Complex, Ontario, Canada. **(Ph.D. thesis, funded by NSERC and China Scholarship Council).**

2012-2013

● Mineralization in the Young-Davidson gold deposit, Matachewan, Ontario, Canada.

2009-2011

● Characteristics of Ore-forming Fluids and Mineralization in the Dehelongwa Cu (Au) deposit, Tongren, Qinghai Province. **(M.Sc. thesis)**

●Evaluation of prospecting target in Kusilapu Copper-Lead-Zinc Metallogenic Belt, West Kunlun, Xinjiang, China.

2008-2009

● Characteristics of ore-bearing sedimentary rocks in the Saishitang Copper Mine Area, Qinghai, China. **(B.Sc. thesis).**

2007-2008

●Leader of Innovative Experimental project funded by Central South University, title of the project is "Geological Characteristics and Genesis of Yixingzai Au deposit, Sanxi, China".

Main Articles

(1) Published journal and conference papers

● Yonghua Cao, Robert Linnen, David Good, Iain Samson, Rachel Epstein. 2016. The application of portable XRF and benchtop SEM-EDS to Cu- Pd exploration in the Coldwell Alkaline Complex, Ontario, Canada. Geochemistry: Exploration, Environment, Analysis, 16, 193-212.

●Yonghua Cao, Robert Linnen, David Good, Iain Samson: Advancing Field Portable Techniques in Exploration by Combining pXRF and Benchtop SEM (bSEM): A Case Study of the Igneous Stratigraphy and Cu-Pd Mineralization of the

Eastern Gabbro of the Coldwell Alkaline Complex, Ontario, Canada. In Mineral Resources in a Sustainable World, 13th SGA Biennial Meeting, Nancy, France. A.-S. André-Mayer, M. Cathelineau, P. Muchez, E. Pirard and S. Sindern eds., v. 3, 901-904.

(2) Conference abstracts

●Yonghua Cao, Robert Linnen, David Good, Iain Samson: Igneous stratigraphy and Cu-Pd mineralization at Area 41 within the Eastern Gabbro of the Coldwell Alkaline Complex, Canada. GAC-MAC2016 Whitehorse; 06/2016.

● Yonghua Cao, Robert Linnen, David Good, Iain Samson: The application of pXRF and benchtop SEM (bSEM) to characterize the igneous stratigraphy and Cu-Pd mineralization in the Eastern Gabbro, Coldwell Alkaline Complex. 2015 Joint Assembly; 05/2015.

●Yonghua Cao, Robert Linnen, David Good, Iain Samson, Matthew Brzozowski: The study on the igneous stratigraphy and mineralization at the Eastern Gabbro, Coldwell Complex: a combination of the benchtop SEM and pXRF. Mineral Exploration Roundup; 01/2015.

●Yonghua Cao, Robert Linnen, David Good, Charles Wu, Iain Samson: Application of pXRF to Cu grade estimation and igneous stratigraphy characterization: A case study at the north edge of the Eastern Gabbro, Coldwell Alkaline Complex, Canada. GAC-MAC; 05/2014.

●Yonghua Cao, Robert Linnen, David Good, Iain Samson: Application of pXRF to Cu grade estimation and igneous stratigraphy characterization: A case study at the north edge of the Eastern Gabbro, Coldwell Alkaline Complex, Canada. PDAC-SEG students mineral Colloquium; 03/2014.

(3) Papers in preparation

● Yonghua Cao, Robert Linnen, David Good, Iain Samson. Igneous stratigraphy and Cu-Pd mineralization at Area 41 within the Eastern Gabbro, Coldwell Alkaline Complex, Canada. (In preparation, to be submitted to <Economic Geology>).

● Yonghua Cao, Robert Linnen, David Good, Iain Samson. Characteristics and development of the Layered Series in the Eastern Gabbro, Coldwell Alkaline Complex, Ontario, Canada: constrains from geochemical modelling. (In preparation, to be submitted to <Journal of petrology>).

Other Activities

● Structure Economic Geology in Mineral Exploration workshop, Western University, 2013.

● Gocad 3D modeling workshop, Western University, 2015.

● Leapfrog 3D modeling short course, Western University, 2016.

● SEG student membership, 2013-2016

● APGO student membership, 2013-2015

● GAC student membership, 2013-2016

● CIM student membership, 2013-2016

Honors and Scholarships

● 'China Scholarship Council' scholarship (2012-2016).

● Mineral Deposit Division (MDD) grant (2016).

● Teaching assistantship (2012-2016)

● Research assistantship (2014-2017)

● Won the best M.Sc. thesis prize at CSU (2011).

● Scholarship of Academic Excellence for three years (2006~2008).

● Won the first Prize of undergraduate thesis Design (2009).

● Received "excellent graduate" prize at CSU (2009).

● Chinese National Endeavor Fellowship (2007).

● Chinese National scholarship (2006).

Computer Skills

● Fluent in Photoshop, IoGas, AutoCAD, Grapher, CorelDraw, ∑-plot, Microsoft Office (Word/Excel/PowerPoint), Igpet

● 3D modelling programs: Gocad, Leapfrog, MapInfo (discover 3D)

Language

● Chinese (mother language)

● Fluent in English (written, speaking, listening)

License

X-ray Fluorescence Operator, Ontario Driver's license (G2)